SECTION A

JOURNAL OF RESEARCH

of the NATIONAL BUREAU OF STANDARDS

JNBAAR 80A(2) 143–387 March–April 1976

U.S. DEPARTMENT OF COMMERCE / National Bureau of Standards

Physics and Chemistry

Journal of Research

of the

National Bureau of Standards

A. Physics and Chemistry

Mar.-Apr. • 1976

VOLUME • 80A

NUMBER • 2

Editor: C. W. Beckett

Associate Editor: D. D. Wagman

Publication dates:
Feb. 1, Apr. 1, June 1, Aug. 1, Oct. 1, Dec. 1, 1976

J. Res. Nat. Bur. Stand. (U.S.), A

JOURNAL OF RESEARCH

The National Bureau of Standards Journal of Research reports research and development in the fields of activity shown at right. Also included from time to time are survey articles on topics closely related to the Bureau's scientific and technical program.

The Journal is published in two separate sections as follows:

A. Physics and Chemistry

Contains papers of interest primarily to scientists working in these fields. Issued six times a year. Annual subscription: domestic, $17.00; foreign $21.25. Single copy, varies.

B. Mathematical Sciences

Presents studies and compilations designed mainly for the mathematician and the theoretical physicist. Issued quarterly. Annual subscription: domestic, $9.00; foreign, $11.25 Single copy, $2.25.

U.S. DEPARTMENT OF COMMERCE
Elliot L. Richardson, Secretary
NATIONAL BUREAU OF STANDARDS
Ernest Ambler, Acting Director

The National Bureau of Standards [1] was established by an act of Congress March 3, 1901. The Bureau's overall goal is to strengthen and advance the Nation's science and technology and facilitate their effective application for public benefit. To this end, the Bureau conducts research and provides: (1) a basis for the Nation's physical measurement system, (2) scientific and technological services for industry and government, (3) a technical basis for equity in trade, and (4) technical services to promote public safety. The Bureau consists of the Institute for Basic Standards, the Institute for Materials Research, the Institute for Applied Technology, the Institute for Computer Sciences and Technology, and the Office for Information Programs.

THE INSTITUTE FOR BASIC STANDARDS provides the central basis within the United States of a complete and consistent system of physical measurement; coordinates that system with measurement systems of other nations; and furnishes essential services leading to accurate and uniform physical measurements throughout the Nation's scientific community, industry, and commerce. The Institute consists of the Office of Measurement Services, the Office of Radiation Measurement and the following Center and divisions:

Applied Mathematics — Electricity — Mechanics — Heat — Optical Physics — Center for Radiation Research: Nuclear Sciences; Applied Radiation — Laboratory Astrophysics [2] — Cryogenics [2] — Electromagnetics [2] — Time and Frequency [2].

THE INSTITUTE FOR MATERIALS RESEARCH conducts materials research leading to improved methods of measurement, standards, and data on the properties of well-characterized materials needed by industry, commerce, educational institutions, and Government; provides advisory and research services to other Government agencies; and develops, produces, and distributes standard reference materials. The Institute consists of the Office of Standard Reference Materials, the Office of Air and Water Measurement, and the following divisions:

Analytical Chemistry — Polymers — Metallurgy — Inorganic Materials — Reactor Radiation — Physical Chemistry.

THE INSTITUTE FOR APPLIED TECHNOLOGY provides technical services to promote the use of available technology and to facilitate technological innovation in industry and Government; cooperates with public and private organizations leading to the development of technological standards (including mandatory safety standards), codes and methods of test; and provides technical advice and services to Government agencies upon request. The Institute consists of the following divisions and Centers:

Standards Application and Analysis — Electronic Technology — Center for Consumer Product Technology: Product Systems Analysis; Product Engineering — Center for Building Technology: Structures, Materials, and Life Safety; Building Environment; Technical Evaluation and Application — Center for Fire Research: Fire Science; Fire Safety Engineering.

THE INSTITUTE FOR COMPUTER SCIENCES AND TECHNOLOGY conducts research and provides technical services designed to aid Government agencies in improving cost effectiveness in the conduct of their programs through the selection, acquisition, and effective utilization of automatic data processing equipment; and serves as the principal focus within the executive branch for the development of Federal standards for automatic data processing equipment, techniques, and computer languages. The Institute consists of the following divisions:

Computer Services — Systems and Software — Computer Systems Engineering — Information Technology.

THE OFFICE FOR INFORMATION PROGRAMS promotes optimum dissemination and accessibility of scientific information generated within NBS and other agencies of the Federal Government; promotes the development of the National Standard Reference Data System and a system of information analysis centers dealing with the broader aspects of the National Measurement System; provides appropriate services to ensure that the NBS staff has optimum accessibility to the scientific information of the world. The Office consists of the following organizational units:

Office of Standard Reference Data — Office of Information Activities — Office of Technical Publications — Library — Office of International Relations — Office of International Standards.

[1] Headquarters and Laboratories at Gaithersburg, Maryland, unless otherwise noted; mailing address Washington, D.C. 20234.
[2] Located at Boulder, Colorado 80302.

Order all publications from the Superintendent of Documents
U.S. Government Printing Office, Washington, D.C. 20402

The Secretary of Commerce has determined that the publication of this periodical is necessary in the transaction of the public business required by law of this Department. Use of funds for printing this periodical has been approved by the Director of the Office of Management and Budget through June 30, 1976.

JOURNAL OF RESEARCH of the National Bureau of Standards—A. Physics and Chemistry
Vol. 80A, No. 2, March–April 1976

Extinction Coefficients of NO_2 and N_2O_4*

Arnold M. Bass, Albert E. Ledford, Jr., and Allan H. Laufer

Institute for Materials Research, National Bureau of Standards, Washington, D.C. 20434

(December 31, 1975)

The extinction coefficient of NO_2 has been measured in the spectral range 185 to 410 nm as a function of temperature between 235 and 298 K. In order to correct for the effect of the dimer absorption, the extinction coefficient of N_2O_4 has also been measured. The effect of a decrease in temperature upon the NO_2 absorption is a reduction in the extinction coefficient of approximately 10 percent in the range 320 to 380 nm.

Key words: Absorption: extinction coefficients; N_2O_4; NO_2; spectra; temperature effects.

1. Introduction

The absorption of solar radiation by NO_2 is of prime importance in the chemical processes which may occur in the troposphere and stratosphere. The photodissociation of NO_2 is an important source of oxygen $O(^3P)$ atoms in the atmosphere. At all wavelengths shorter than the dissociation limit, 398 nm, absorption of light by NO_2 results in dissociation of the molecule with the formation of an oxygen atom. The fate of the O atom, ultimately $O(^3P)$ in large part, is to react with O_2 resulting in O_3, the chemistry and physics of which are crucial to the dynamics of the stratosphere. A determination of the atom yield in the atmosphere depends on a knowledge of the NO_2 absorption cross-section, concentration and quantum yield of dissociation, and the solar flux over the wavelength range 185–410 nm.

The measurements on NO_2 reported in the previously published literature have been made at room temperature. Considerations of the photochemistry of NO_2 in the stratosphere require a knowledge of the extinction coefficients at ambient stratospheric conditions—low temperature and low pressure. Extrapolation of data obtained at room temperature to stratospheric temperature requires a knowledge of the states involved in the absorption. If any of the absorption is attributable to "hot-bands" the relative importance of such absorption will decrease markedly with decreasing temperature. Since the details of the transitions involved in the NO_2 absorption spectrum over this wavelength range are not entirely understood, we have undertaken to determine the experimental behavior of the extinction coefficient as a function of temperature.

The measurement of the extinction coefficient of NO_2 at any temperature is severely complicated by the presence of its dimer, N_2O_4. The equilibrium mole fraction of N_2O_4 is a function of both temperature and pressure. It is well known that low pressures minimize the N_2O_4 contribution. However, as the temperature of a mixture is reduced, the mole fraction of N_2O_4 increases. It is a relatively simple matter to determine the concentration ratio (NO_2/N_2O_4) based upon thermodynamic considerations [1].[1] While concentration corrections to the measured absorption may be small, a possibly greater error would result from the absorption by N_2O_4 if the extinction coefficient of N_2O_4 is large compared to that of NO_2. It was imperative, therefore, to measure the extinction coefficient of N_2O_4.

Hall and Blacet [2] have reported values of the extinction coefficients for N_2O_4. Their experiments, however, were not performed under conditions where N_2O_4 formation was favored, i.e., low temperature and high pressure.

Three previous photoelectric measurements of the ultraviolet absorption cross-sections for NO_2 have been reported. Nakayama et al. [3] examined the region from 108–270 nm with a spectral resolution of 0.02 nm. Corrections for the overlapping absorption by the dimer, N_2O_4, were made at five selected wavelengths between 190 and 240 nm by making measurements at several pressures, and extrapolating to zero pressure. Hall and Blacet [2] made measurements from 240–500 nm with an average spectral band width of 0.4 nm on three mixtures each of which contained appreciable N_2O_4. By using the equilibrium expression of Verhoek and Daniels [4] and Beer's law, they were able to determine the extinction coefficients for

* Work supported in part by the Climatic Impact Assessment Program, Office of the Secretary, Department of Transportation, and by the National Aeronautics and Space Administration.

[1] Figures in brackets indicate the literature references at the end of this paper.

both NO_2 and N_2O_4. Johnston and Graham [5], in connection with a study of the absorption by nitric acid vapor, determined the NO_2 extinction coefficient at low pressures and with a long optical path over the wavelength range 185–420 nm. Because of the low pressures used, the N_2O_4 was negligible.

2. Experimental Detail

All measurements were made with a 0.75 m Fastie-Ebert monochromator equipped with a 2400 groove/mm grating. With 10 μ slits, the spectral resolution was 0.01 nm. The actual measurements were made at intervals of 0.125 nm with a spectral resolution of 0.015 to 0.04 nm. The light source for the absorption studies was either a low-pressure hydrogen discharge for the region 185–360 nm, or, in the region above 360 nm, a quartz-iodine incandescent lamp. The entire gas handling system was fabricated of stainless steel and monel to minimize surface decomposition of the NO_2. Pressures were measured by means of a capacitance manometer.

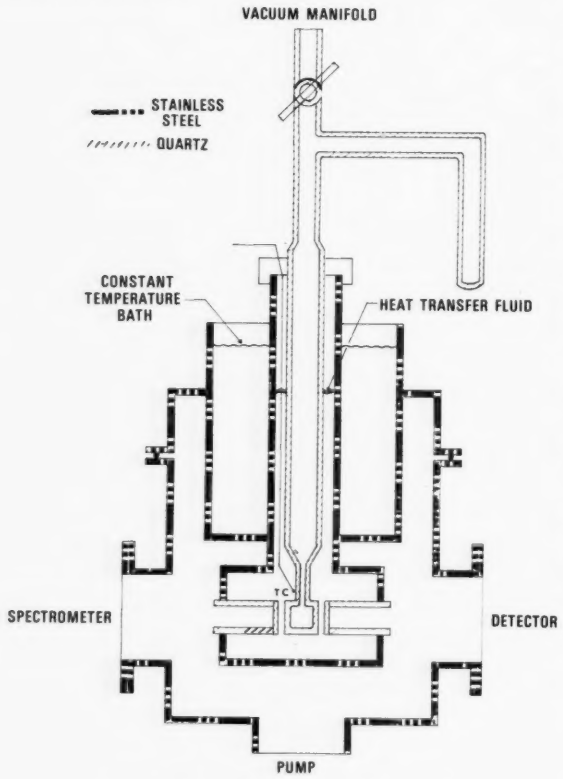

FIGURE 1. *Cell used to measure* ϵ (N_2O_4).

Experimental: N_2O_4

Two distinct, separate measurements were made; one involving the spectrum of N_2O_4 and the other of NO_2. The spectrum of the former was obtained by using a low-temperature cell which has been previously described [6]. A Pyrex [2] tube was sealed to one of several fused silica absorption cells of path lengths between 0.1 mm and 5.0 mm. The Pyrex portion was equipped with a side-arm which could be used as a cold trap. Purified NO_2 was distilled into the cell through polytetrafluoroethylene vacuum valves. This cell was immersed in another cell fabricated of stainless steel, shown in figure 1. The heat transfer fluid was either methanol or 2,2,2-trifluoroethanol, both of which possess excellent light transmission properties at wavelengths as low as 185 nm at low temperature. Constant temperature was attained using either *n*-pentanoic acid slush (240 K) or CCl_4 slush (250 K). At these temperatures and at the pressures used, the $NO_2-N_2O_4$ equilibrium mixture remains gaseous. The absorption cell temperature was measured with a chromel-constantan thermocouple which was in contact with the cell. As may be seen in figure 1, the surrounding volume was evacuated thereby eliminating the problem of frost formation on the fused silica windows.

In a typical experiment, the transmitted light intensity was determined through both the cooled absorption cell and optical system. Then NO_2 was condensed into the side-arm of the absorption cell. Removal of the cold trap permitted the $NO_2 - N_2O_4$ mixture to vaporize once again and fill the entire cold absorption cell. The material was allowed to equilibrate thermally and then the transmitted intensity was measured. The system was assumed to be in equilibrium when the measured absorption at any given wavelength remained invariant with time.

To describe adequately the ratio of NO_2/N_2O_4, determination of both the temperature and pressure in the absorption cell are required. The temperature determination is straightforward. The pressure in the absorption cell could not be monitored during the course of an experiment (see fig. 2). Furthermore, portions of the cell were usually at two different temperatures during any particular measurement, i.e., room and some reduced temperature. As a consequence of these two factors, the pressure and hence the concentration of both monomer and dimer in the cold portion of the cell was determined by calculation based upon the conservation of N atoms in the system. The details of the calculation are shown in appendix A. The calculation does require knowledge of the temperature variation of K_p which was derived from Chao et al. [1], and is partially described in appendix B.

Experimental: NO_2

In order to minimize the effect of the N_2O_4; the NO_2 absorption measurements required low pressures and, therefore, long path lengths for which a variable temperature stainless steel cell was constructed (fig. 2). The cell was approximately 50 cm long and by

[2] Trade names used in this paper do not imply recommendation or endorsement by the National Bureau of Standards.

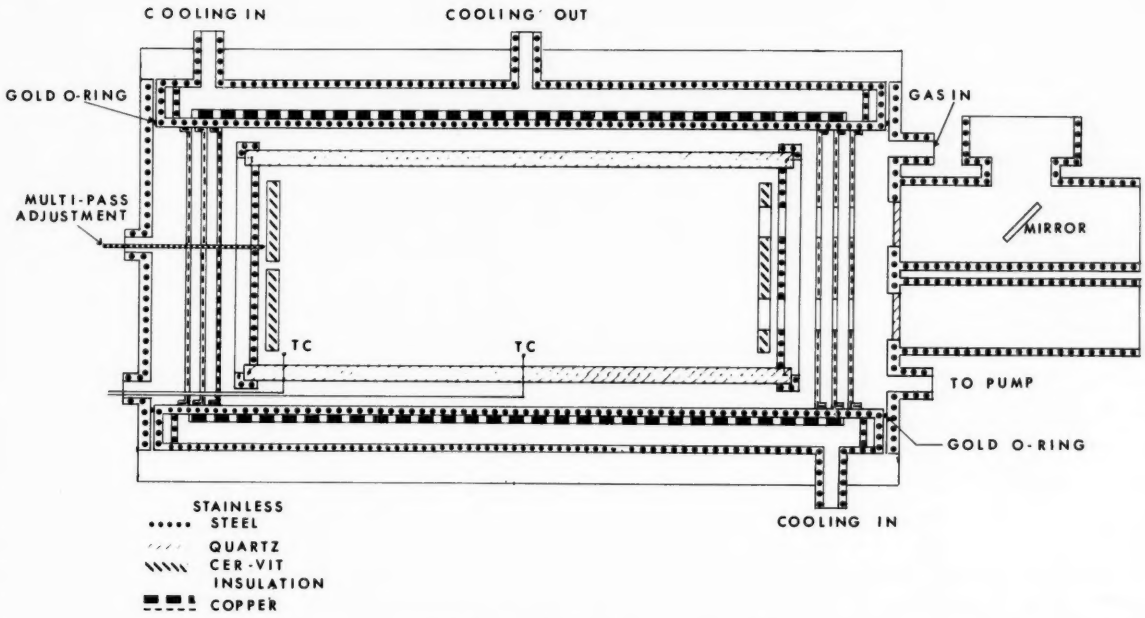

FIGURE 2. *Multiple-pass low-temperature cell.*

using the multiple-pass design of White [7a] and Bernstein and Herzberg [7b] path lengths up to a maximum of 10 meters could be used. Since the cell was also to be used at low temperatures, the multiple-reflection mirrors were connected to each other by rigid fused silica rods to insure that the path length between the mirrors remained fixed as the cell temperature was changed. The arrangement also permitted adjustment of the optics on the bench and insertion, as a unit, into the cell.

The ends of the cell were thermally isolated from the environment by gold-plated copper radiation shields. The multiple-reflection mirrors were made of a low thermal expansion material and were aluminized and overcoated with magnesium fluoride. Temperature control was obtained by circulation of a refrigerated fluid, usually methanol, through the outer jacket of the cell. Further, the outer surface of the cell was coated with copper using a "flame-spraying" process to further insure uniformity of temperature along the cell. The gas sample temperature was measured by means of three calibrated chromel-constantan thermocouples inside the cell. At a cell termperature of 220 K the temperature variation of the sample over the length of the cell was approximately 1 °C.

Care was taken to avoid the use, as far as possible, of any materials which would be subject to corrosion by NO_2. The vacuum seals were made by compressed gold O-rings. Two layers of aluminized-mylar were wrapped around the outer shell to provide insulation of the cell from room temperature.

The absorption cells were placed in the exit beam of the monochromator. Immediately in front of the cell, a sapphire plate was used to split the light beam so that a portion of the signal illuminated a 13-stage photomultiplier tube. The signal measured by this photomultiplier monitored the variation of the light source. Corrections for changes in the incident light signal were applied in the data reduction process. A second photomultiplier tube recorded the light flux transmitted through the absorption cell.

In all experiments, data acquisition was automated by photon counting equipment in conjunction with a stepping motor control for the monochromator wavelength drive. The operation of the equipment has been previously described [8].

The procedure used in a typical NO_2 measurement involved a scan over the wavelength region to be examined, with the cell evacuated. The ratio of the incident signal to the transmitted signal (through the multpile-reflection cell) as a function of wavelength was determined. Then the cell was filled with a known pressure of NO_2 as measured with a capacitance manometer and the scan repeated. The data were reduced by computer calculation after corrections were made for both the concentration and absorption due to N_2O_4.

The NO_2 was obtained commercially and purified by reaction with excess O_2. When cooled to − 78 °C, a pure white solid was obtained which, following thorough pumping, was warmed, distilled through P_2O_5 and subsequently stored in the dark in a glass bulb. NO, a probable impurity, was absent in a 1 torr [3] sample of NO_2 as indicated by the absence of absorption of the strong (A − X) system at 226 nm.

[3] 1 Torr = 133.3 Pa.

TABLE 1. *Experimental conditions for measurement of* N_2O_4 *absorption*

Wavelength (nm)	Pathlength (nm)	Temp. (K)	Sample pressure (Torr)	Mole fraction (N_2O_4)	Spectrum Band (nm)
185–215	0.5	250	25(4)	0.80	0.04
185–215	.095	299	117	.38	.04
195–225	.5	252	32(2)	.79	.04
215–245	.5	253	29(2)	.78	.04
215–245	.095	299	150(2)	.42	.04
225–250	.5	251	47(2)	.84	.04
245–275	.502	299	414	.58	.04
245–275	5.01	251	31(2)	.80	.04
275–305	0.502	298	443	.60	.04
275–305	5.01	253	31(2)	.78	.04
305–335	0.502	298	500	.62	.04
305–335	5.01	253	35(2)	.80	.04
335–365	0.502	274	140	.72	.02
335–365	.502	299	405	.58	.02
335–365	5.01	253	39(2)	.80	.02
345–375	0.502	299	420	.59	.02
350–380	.502	296	405	.62	.02
350–380	5.01	274	113(2)	.70	.02
380–410	0.502	296	500	.65	.02
380–410	5.01	274	114	.70	.02

A minimum of 0.005 torr NO would be observable under these conditions. To minimize errors in the determination of the extinction coefficients of both N_2O_4 and NO_2, the following procedure was followed. Initial measurements were performed at low pressure over the complete wavelength region. Under these conditions, the concentration of N_2O_4 was minimal and a correction due to its concentration, but not its absorption, could be made. The values obtained are an upper limit for ϵNO_2 since some of the absorption is undoubtedly due to N_2O_4. The next series of experiments involved measurement of the N_2O_4 absorption as previously described. Here again, a correction due to the presence of NO_2 could be made; both as to its concentration and absorption. In the region where the relative values of $\epsilon(NO_2)$ and $\epsilon(N_2O_4)$ are about equal, the correction is less than 1%. At shorter wavelengths, where $\epsilon(N_2O_4) \gg \epsilon(NO_2)$, an error in the latter has but a small effect on the determination of the former. With an adequate determination of $\epsilon(N_2O_4)$, an accurate value of $\epsilon(NO_2)$ was readily obtainable.

3. Results and Discussion

3.1. N_2O_4

The extinction coefficient ϵ is defined by the Lambert-Beer equation: $I/I_0 = \exp(-\epsilon px)$ where I and I_0 are the transmitted and incident light intensities, p the pressure in atmospheres at 273 K,[4] and x the path length in cm.

The N_2O_4 absorption measurements were performed at − 23 °C at pressures of about 30 torr and at room temperature at high pressures (117–500 torr). Under these conditions, the mole fraction of N_2O_4 represents between 40–80 percent of the sample. The actual experimental conditions are shown in table 1.

The results, which are shown in figures 3 and 4 and in table 3, were obtained at low and room temperature but have been corrected to the equivalent pressure at 273 K and represent the non-weighted average of at least 2 and usually 3 values at each wavelength. No temperature effect on the spectrum was observed. The data, then, represent the extinction coefficient of N_2O_4. There have been only two reported examinations of the N_2O_4 spectrum with which our results may be compared. In the shorter wavelength region, (185–240 nm) an approximate value for $\epsilon(N_2O_4) = 950$ atm^{-1} cm^{-1} at 197 nm has been reported as the maximum value [3] which is to be compared to our value of ~ 1180 atm^{-1} cm^{-1} at 197 nm. Since the previous work is, in reality, an estimate and was obtained in systems with low N_2O_4 concentrations (~ 3 percent in measurements at 195 nm), the discrepancy of 20 percent is small. Of greater significance is the observation that the maximum absorption appears in the present work not at 197 nm, but at ~ 190 nm. Any rationale for the discrepancy would, of course, be speculative, but it should perhaps be noted that the values for ϵ (NO_2) determined by Nakayama et al. [3], in the region below 200 nm are significantly greater than determined in the present work. It is possible that the absorption, incorrectly attributed to NO_2, was in fact due to N_2O_4 whose concentration could have been incorrectly determined.

The N_2O_4 data with which we have the widest correspondence are those of Hall and Blacet [2]. The results of both sets of data have the same general shape with the first maximum at ~ 340 nm and a second, less pronounced, in the vicinity of ~ 265 nm. At shorter wavelengths, the absorption increases sharply to what appears to be another maximum in

[4] In computing ϵ, the experimental pressures have been converted to the equivalent values at 273 K. To convert to absorption cross sections (cm^2 molecule^{-1}), multiply ϵ by 3.72×10^{-20}.

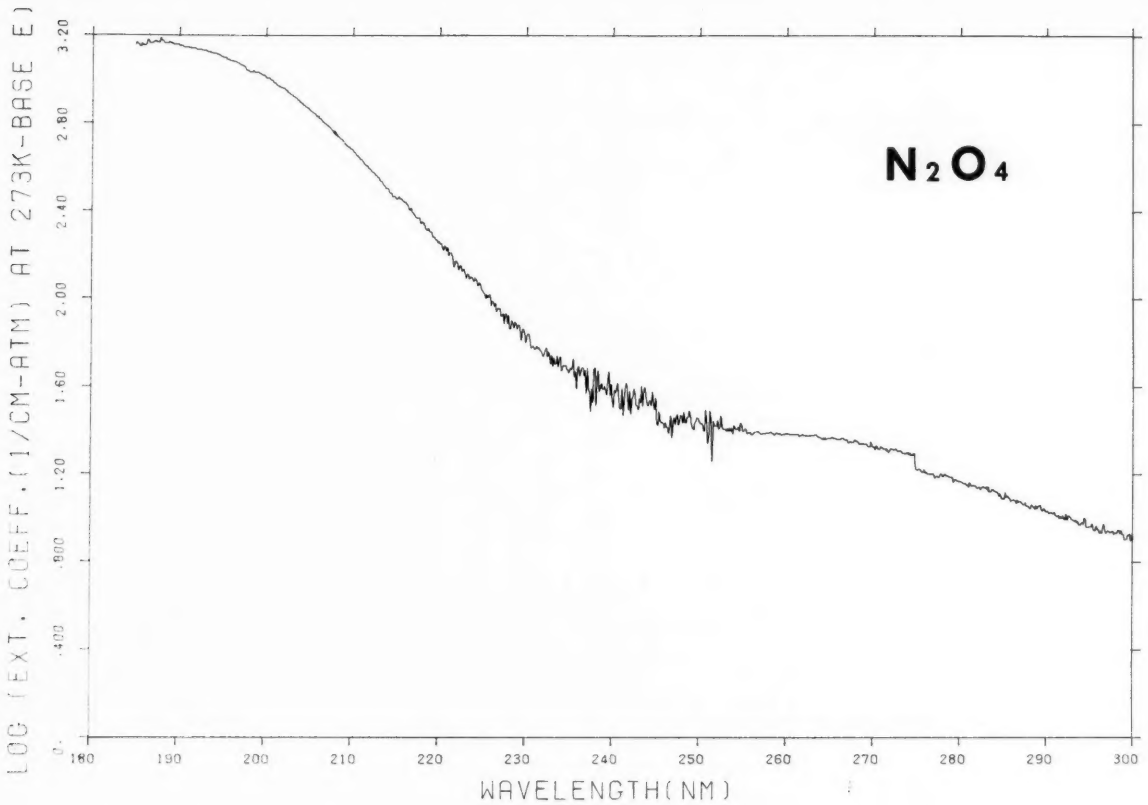

FIGURE 3. *Common logarithm of the extinction coefficients of* N_2O_4, *180–300 nm,* ϵ *in* cm^{-1} *(atm at 273 K)*$^{-1}$ *base* e.

[Plot is a computer reconstruction of averaged data. See text.]

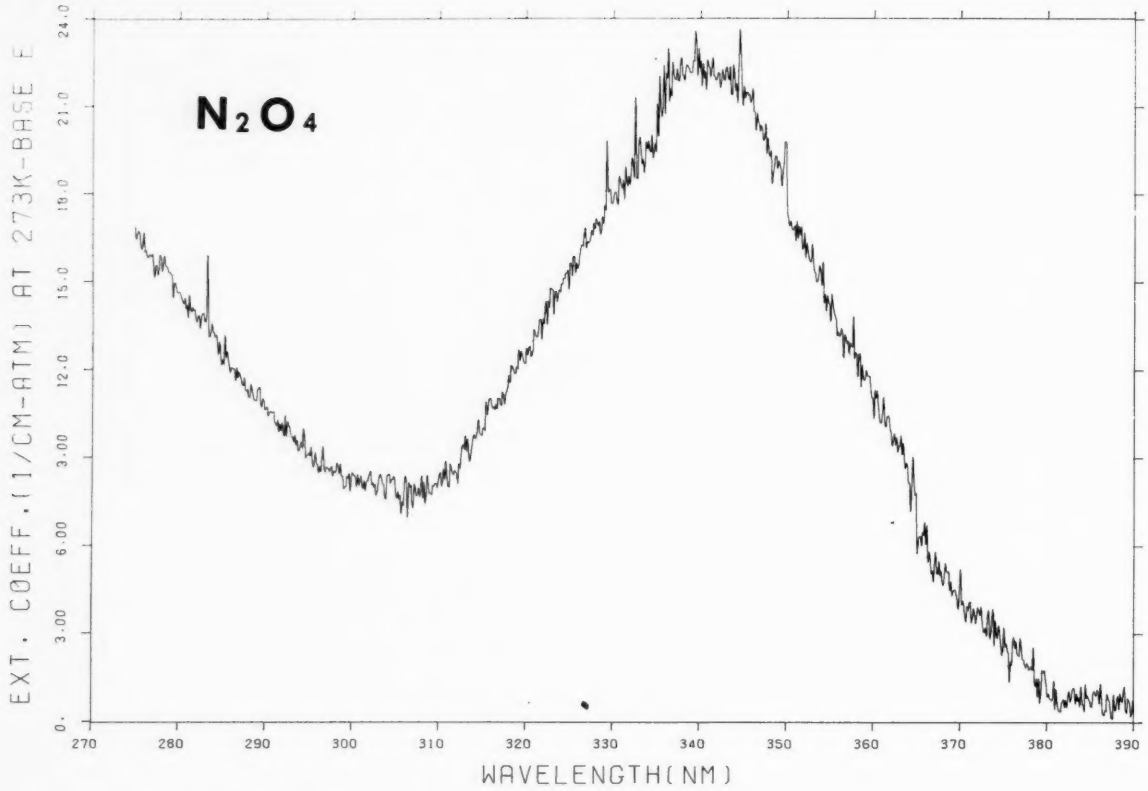

FIGURE 4. *The extinction coefficients of* N_2O_4, *270–390 nm,* ϵ *in* cm^{-1} *(atm at 273 K)*$^{-1}$ *base* e.

[Plot is a computer reconstruction of averaged data. See text.]

the region of ~ 190 nm. The apparent discontinuity amounting to ~ 20 percent in the value of ϵ at 275 nm is an artifact and is caused by the method used to collect the data, i.e., the wavelenth overlap between successive determinations was not sufficient to eliminate the error at that point. The difference at 275 nm is a likely indication of the maximum error due to all causes in our determination of the extinction coefficient.

Hall and Blacet indicate the absence of structure in the spectrum of N_2O_4. Since the error in our determination is probably of the order of 20 percent, it is uncertain whether the features observed in the region between 275–390 nm are indeed resolved structure or simply indicative of the "noise" in the experiment. In any case, no obvious regular pattern is apparent. It is important to note the large value of the extinction coefficient at short wavelengths, which indicates that extreme care is required to account adequately for N_2O_4 absorption in any measurement of the NO_2 spectrum.

Although the general shape of the absorption curve agrees well with that of Hall and Blacet, the differences between the two measurements are not constant over the complete wavelength region. Between 260 and 335 nm, the two sets of measurements lie within 10 percent of each other but outside of these limits (i.e., 240–260 and 335–390 nm) the difference is closer to 20 percent. The explanation for this discrepancy may lie in the fact that in our experiments, the ratio of N_2O_4/NO_2 was usually close to 4 while those of Hall reached a maximum of 1.3. Thus, the correction due to NO_2 absorption is larger in Hall's work than in ours.

3.2. NO_2

The room temperature absorption spectrum of NO_2 is shown in figures 5 and 6 and in table 3. The spectrum shown has been corrected for the contribution of N_2O_4 to the measured pressure. The N_2O_4 mole fraction was obtained from the calculated value of the equilibrium constant, K_p, based upon spectroscopic and thermodynamic considerations [1]. At the pressures used, usually less than about 0.1 torr, the correction due to N_2O_4 concentration was less than about 0.1 percent. Similarly, a correction for the absorption due to N_2O_4 could be made using the measured values for $\epsilon(N_2O_4)$. In particular, at shorter wave-

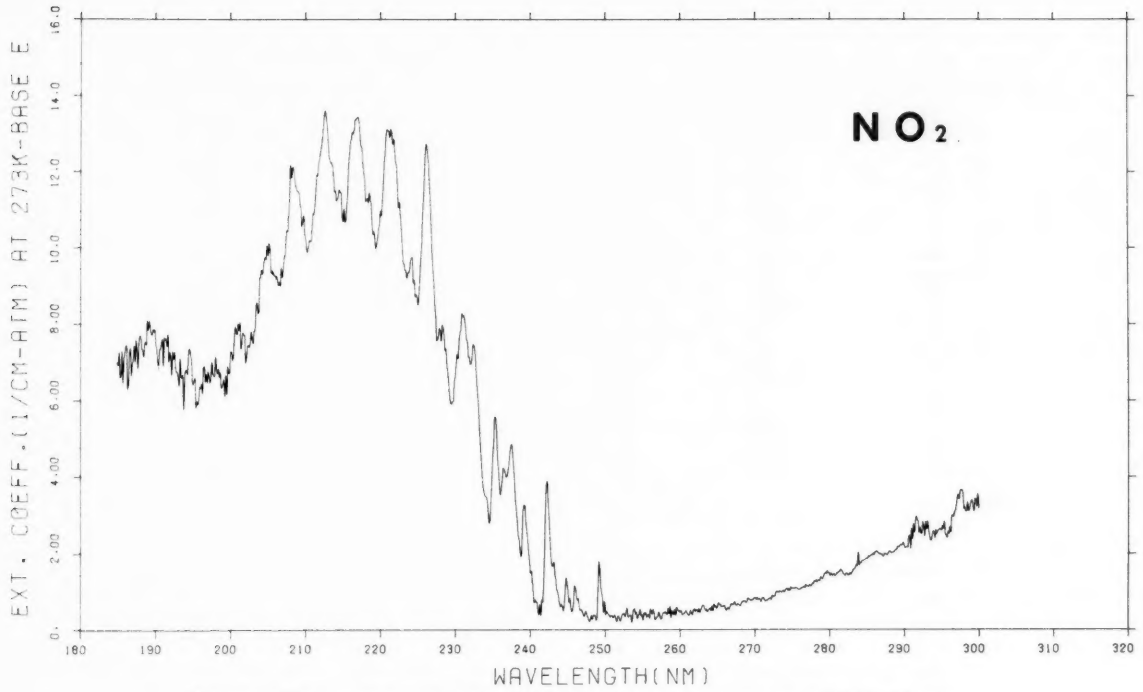

FIGURE 5. *The extinction coefficients of* NO_2, *180–300 nm,* ϵ *in* cm^{-1} *(atm at 273 K)*$^{-1}$ *base* e.
[Plot is a computer reconstruction of averaged data. See text.]

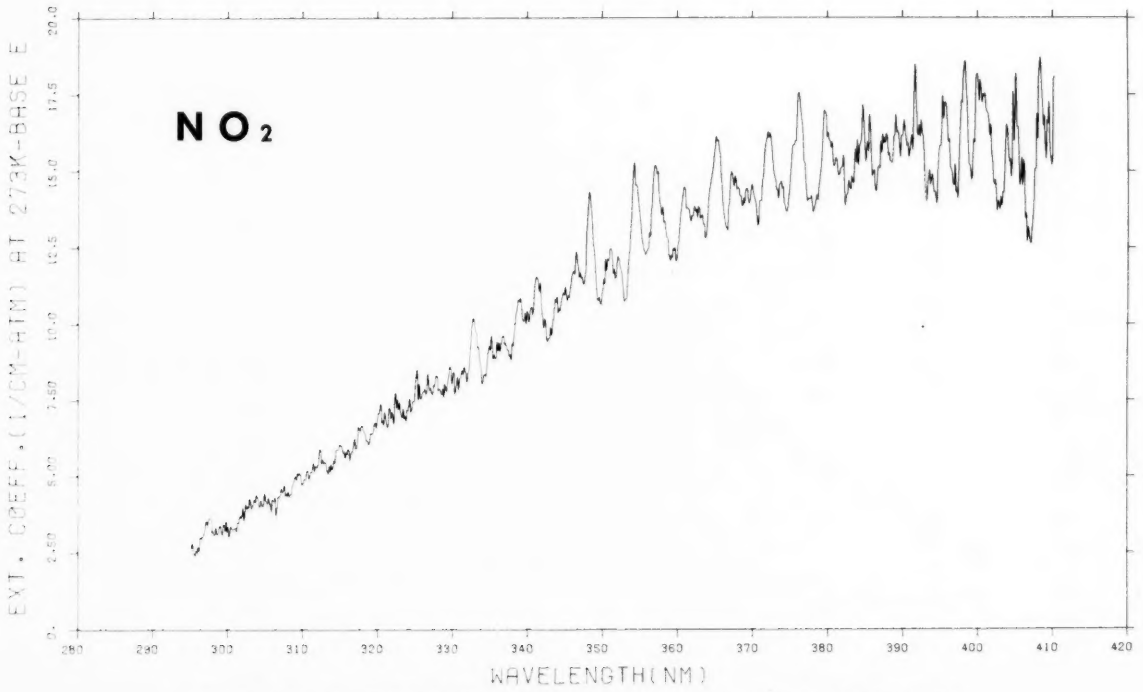

FIGURE 6. *The extinction coefficients of* NO_2, *290–410 nm,* ϵ *in* cm^{-1} *(atm at 273 K)*$^{-1}$ *base* e.
[Plot is a computer reconstruction of averaged data. See text.]

TABLE 2. *Experimental conditions for* NO_2 *measurements*

Wavelength (nm)	Path length (cm)	Sample pressure (torr)	Spectral band pass (nm)	Temperature
185–215	618	[a]0.100(3)	0.050	298 K
185–215	1017	.030, .040	.040	298 K
210–245	618	.090, .160, .254	.030	298 K
210–245	1017	.040, .050	.025	298 K
235–265	618	.150, .200, .350	.025	298 K
235–265	1017	.050, .060	.025	298 K
260–290	618	.280, .380, .600	.025	298 K
260–290	1017	.200, .450	.025	298 K
290–320	618	.100, .150, .250(6)	.025	298 K
310–340	1017	.050(2)	.025	298 K
320–350	618	.070, .110(6)	.025	298 K
350–380	618	.050, .100(6)	.020	298 K
350–380	219	.100(3)	.015	298 K
380–410	618	.050(3)	.015	298 K
290–350	618	.050, .070(9)	.025	235 K
320–350	618	.050, .070(3)	.025	235 K
350–380	618	.050(6)	.015	235 K
380–410	618	.030, .050(6)	.015	235 K

[a] Value in parentheses indicates number of runs at specified pressure.

lengths where N_2O_4 exhibits a very large absorption, the correction assumes more significant proportions. The experimental conditions are summarized in table 2.

The appearance of the spectrum and positions of the absorption peaks agree well with the data in the published literature [2, 3, 5]. The major difference between the present and previously published work is related to the spectral band-pass used. The larger amount of structure evident in figures 5 and 6 as compared to previous work is a consequence of the greater resolving power in the present experiments.

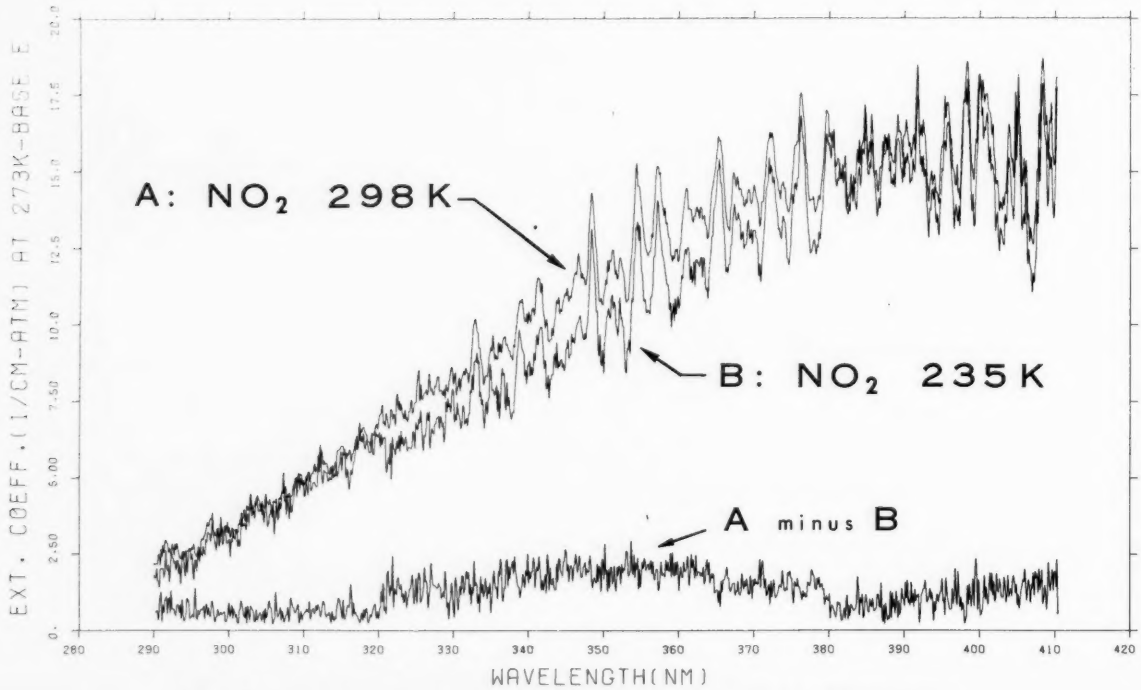

FIGURE 7. *Effect of temperature upon* $\epsilon(NO_2)$, *290–410 nm,* ϵ *in* cm^{-1} *(atm at 273 K)*$^{-1}$ *base* e.

[Plot is a computer reconstruction of averaged data. See text.]

Bayes [9] has carefully reexamined the data of Hall and Blacet [2] and presented the values in tabular form at 0.5 nm intervals. Over the range from 250 to 410 nm our values for the extinction coefficients are 10–20 percent lower than those of Hall and Blacet. Comparison with Johnston [5] indicates good agreement (within 10 percent) over the range from 245–410 nm. Although the present values are slightly lower than those of Johnston, the latter are also lower than those of Hall and Blacet. At shorter wavelengths (245–190 nm) the agreement between Johnston and us is not quite so good, but generally it is within 15 percent. Presumably the discrepancy may be attributed to the methods used to correct for the N_2O_4 absorption.

A comparison between the room-temperature and low temperature (235 K) absorption spectrum is shown in figure 7. It is clear that the discernible effect is no greater than about 10 percent and appears between 320–380 nm. It is apparent that no single feature is removed at low temperature but rather a reduction in the underlying continuum is noticed.

It may be argued that the difference spectrum is an artifact due to the incorrect numerical adjustment of the spectrum caused by the presence of N_2O_4 at low temperature. However, although N_2O_4 does have a broad absorption peak in this region (figure 4) the appearance of a "temperature effect" at 360 nm and no observable effect at $\sim$ 290 nm where the N_2O_4 absorption is similar to that at 310 or 360 nm would rule out this interpretation.

We have attempted to estimate the possible sources of error in our measurements. The wavelength scale of the monochromator has been calibrated with the known emission lines of Hg and is accurate to about 0.02 nm. Inaccuracies in the pressure measurements were of the order of 1 percent and were limited to the accuracy in reading the analog output from the manometer. Significantly larger errors may result from the intensity measurement and in particular, the ratio of I/I_0 although each individual measurement is probably accurate to within 5 percent of the "true" value. Errors in the N_2O_4 measurement may be more significant. For example, at a pressure of $\sim$ 30 torr at a temperature of $\sim$ 250 K, a one degree temperature error results in a 1.25-percent error in the N_2O_4 mole fraction. The method used to determine the concentration in the absorption cell involves the temperature of the cell so that an error in temperature is manifested in several ways and results in an overall N_2O_4 concentration which is only accurate to $\pm$ 5 percent. In all experiments, scatter between runs amounted to 10 percent or less. Consideration of those factors suggest the final value for ϵ (N_2O_4) is probably correct to within $\pm$ 20 percent, and for ϵ (NO_2) to within $\pm$ 10 percent.

Table 3 lists the extinction coefficients of NO_2 and N_2O_4 corrected to the equivalent pressure at 273 K.

TABLE 3. *Extinction coefficients of* NO_2 *and* N_2O_4, *180–410 nm at 298 K and 235 K,* ϵ *in* cm^{-1} *(atm at 273 K)*$^{-1}$ *base* e

Wavelength (nm)	Ext. coeff. NO_2 298 K	Ext. coeff. NO_2 235 K	Ext. coeff. N_2O_4	Wavelength (nm)	Ext. coeff. NO_2 298 K	Ext. coeff. NO_2 235 K	Ext. coeff. N_2O_4
185.000	6.99		1435.12	188.750	7.55		1454.37
185.125	6.90		1489.56	188.875	7.44		1493.62
185.250	7.28		1446.73	189.000	8.11		1465.15
185.375	6.60		1455.49	189.125	7.83		1463.46
185.500	6.63		1413.05	189.250	8.10		1461.20
185.625	7.31		1415.12	189.375	7.88		1440.60
185.750	6.43		1471.03	189.500	7.78		1448.38
185.875	7.12		1428.93	189.625	7.70		1445.53
186.000	7.23		1421.68	189.750	7.88		1459.83
186.125	7.43		1445.05	189.875	7.79		1435.95
186.250	7.46		1441.26	190.000	7.87		1443.90
186.375	6.27		1515.10	190.125	7.43		1418.47
186.500	6.45		1519.66	190.250	7.36		1438.68
186.625	7.28		1460.57	190.375	7.00		1427.96
186.750	7.39		1473.96	190.500	6.84		1415.87
186.875	6.64		1457.69	190.625	7.36		1397.85
187.000	7.02		1476.38	190.750	7.36		1417.17
187.125	7.05		1494.71	190.875	7.49		1405.36
187.250	7.45		1493.05	191.000	7.63		1401.97
187.375	6.99		1502.92	191.125	6.89		1400.23
187.500	7.60		1474.22	191.250	7.66		1385.26
187.625	7.30		1478.17	191.375	7.61		1397.96
187.750	6.82		1472.67	191.500	7.62		1382.16
187.875	7.52		1558.19	191.625	7.41		1390.34
188.000	7.71		1509.11	191.750	7.76		1383.04
188.125	7.68		1495.25	191.875	6.99		1383.01
188.250	7.34		1496.28	192.000	7.28		1381.11
188.375	7.33		1456.37	192.125	7.13		1362.83
188.500	7.13		1472.65	192.250	6.64		1373.01
188.625	7.48		1476.16	192.375	7.30		1376.83

TABLE 3. *Extinction coefficients of* NO_2 *and* N_2O_4, *180–410 nm at 298 K and 235 K,* ϵ *in* cm^{-1} *(atm at 273 K)*$^{-1}$ *base* e—Continued

Wavelength (nm)	Ext. coeff. NO_2 298 K	Ext. coeff. NO_2 235 K	Ext. coeff. N_2O_4	Wavelength (nm)	Ext. coeff. NO_2 298 K	Ext. coeff. NO_2 235 K	Ext. coeff. N_2O_4
192.500	7.08		1364.96	200.375	7.04		1013.74
192.625	7.28		1374.45	200.500	7.19		1016.60
192.750	6.86		1352.88	200.625	7.65		995.60
192.875	6.74		1363.21	200.750	7.96		991.83
193.000	6.73		1347.79	200.875	7.75		985.55
193.125	6.61		1350.68	201.000	7.73		966.78
193.250	6.36		1343.91	201.125	8.03		962.74
193.375	7.12		1329.56				
193.500	6.60		1331.66	201.250	7.84		952.24
193.625	6.58		1342.98	201.375	8.07		939.16
				201.500	7.34		932.56
193.750	6.69		1322.65	201.625	7.59		927.16
193.875	5.76		1312.04	201.750	7.80		927.35
194.000	6.65		1314.07	201.875	7.70		919.00
194.125	6.81		1318.37	202.000	7.72		918.44
194.250	6.81		1325.53	202.125	6.95		913.48
194.375	6.67		1298.82	202.250	7.16		908.92
194.500	7.21		1307.81	202.375	7.45		893.77
194.625	7.38		1289.91				
194.750	7.21		1287.15	202.500	7.45		893.91
194.875	7.09		1273.11	202.625	7.40		874.78
				202.750	7.50		866.46
195.000	6.51		1269.54	202.875	7.83		860.91
195.125	6.40		1259.85	203.000	7.59		850.68
195.250	6.54		1256.52	203.125	7.48		849.85
195.375	6.61		1256.33	203.250	7.84		839.54
195.500	5.80		1251.84	203.375	7.83		830.97
195.625	5.99		1232.64	203.500	8.43		827.94
195.750	5.89		1239.66	203.625	8.59		820.62
195.875	6.04		1221.63				
196.000	6.36		1215.02	203.750	8.26		806.66
196.125	6.31		1218.30	203.875	8.33		802.67
				204.000	9.22		789.38
196.250	6.45		1215.61	204.125	9.23		783.10
196.375	6.16		1206.04	204.250	9.43		779.09
196.500	6.87		1209.04	204.375	9.29		764.28
196.625	6.92		1199.03	204.500	9.51		766.24
196.750	6.47		1190.28	204.625	9.68		755.55
196.875	6.70		1182.31	204.750	9.76		748.27
197.000	6.46		1180.36	204.875	9.67		742.25
197.125	6.78		1166.57				
197.250	6.61		1157.68	205.000	10.08		739.04
197.375	6.45		1154.93	205.125	9.77		726.37
				205.250	10.13		719.61
197.500	6.63		1148.60	205.375	9.94		712.35
197.625	7.03		1139.64	205.500	9.33		706.30
197.750	6.69		1111.14	205.625	9.42		699.53
197.875	6.65		1099.47	205.750	9.14		696.19
198.000	6.62		1108.31	205.875	8.95		687.54
198.125	7.16		1083.49	206.000	8.98		676.20
198.250	6.77		1076.57	206.125	9.14		687.38
198.375	6.69		1095.03				
198.500	6.86		1077.86	206.250	9.26		661.62
198.625	6.60		1105.59	206.375	9.14		660.08
				206.500	9.00		657.77
198.750	6.75		1079.75	206.625	9.11		644.67
198.875	6.32		1089.15	206.750	8.98		638.26
199.000	6.35		1076.41	206.875	9.50		627.86
199.125	6.49		1074.24	207.000	9.20		625.71
199.250	6.57		1081.82	207.125	9.43		618.75
199.375	6.10		1061.40	207.250	9.74		614.16
199.500	6.69		1062.31	207.375	9.80		606.47
199.625	6.14		1049.95				
199.750	6.91		1042.97	207.500	10.23		602.78
199.875	6.72		1048.94	207.625	10.46		590.97
				207.750	10.42		585.00
200.000	6.72		1030.98	207.875	10.99		575.64
200.125	7.30		1011.94	208.000	11.36		499.61
200.250	7.26		1025.08	208.125	12.20		564.13

TABLE 3. *Extinction coefficients of* NO_2 *and* N_2O_4, *180–410 nm at 298 K and 235 K,* ϵ *in* cm^{-1} *(atm at 273 K)*$^{-1}$ *base e*—Continued

Wavelength (nm)	Ext. coeff. NO_2 298 K	Ext. coeff. NO_2 235 K	Ext. coeff. N_2O_4	Wavelength (nm)	Ext. coeff. NO_2 298 K	Ext. coeff. NO_2 235 K	Ext. coeff. N_2O_4
208.250	11.82		558.14	216.250	12.87		277.77
208.375	12.10		552.35	216.375	13.05		270.61
208.500	12.13		546.85	216.500	13.00		266.72
208.625	11.87		540.10	216.625	13.08		255.81
				216.750	13.39		254.71
208.750	11.66		533.24	216.875	13.37		261.66
208.875	11.55		530.16	217.000	13.43		249.59
209.000	11.48		523.04	217.125	13.45		244.93
209.125	11.49		513.46	217.250	13.30		242.00
209.250	11.44		506.32	217.375	13.01		237.84
209.375	11.15		500.45				
209.500	11.02		493.22	217.500	12.66		233.99
209.625	10.53		491.29	217.625	12.66		236.10
209.750	10.74		488.43	217.750	12.22		233.91
209.875	10.87		481.50	217.875	11.98		232.83
				218.000	11.75		219.62
210.000	10.34		479.60	218.125	11.20		225.42
210.125	10.20		473.98	218.250	11.30		222.08
210.250	9.96		467.10	218.375	11.29		220.51
210.375	9.86		461.92	218.500	11.17		210.23
210.500	10.06		453.41	218.625	11.47		205.43
210.625	10.20		449.39				
210.750	10.17		443.48	218.750	11.23		205.34
210.875	10.19		441.01	218.875	11.18		211.63
211.000	10.58		433.79	219.000	10.53		201.90
211.125	10.92		430.67	219.125	10.34		201.07
				219.250	10.44		199.81
211.250	10.87		425.20	219.375	10.20		190.04
211.375	11.11		417.67	219.500	9.96		191.92
211.500	11.43		412.24	219.625	10.14		189.35
211.625	11.92		405.19	219.750	10.26		184.20
211.750	11.89		406.99	219.875	10.52		184.96
211.875	12.25		400.57				
212.000	12.34		392.69	220.000	10.64		179.65
212.125	12.52		388.81	220.125	10.99		182.78
212.250	12.65		382.41	220.250	10.83		177.87
212.375	12.85		378.31	220.375	11.24		178.31
				220.500	11.66		170.95
212.500	13.14		375.68	220.625	12.26		165.77
212.625	13.47		372.30	220.750	12.53		174.80
212.750	13.63		365.72	220.875	12.97		171.59
212.875	13.44		363.96	221.000	13.13		164.99
213.000	13.21		358.44	221.125	13.08		171.63
213.125	12.84		354.46				
213.250	12.41		347.51	221.250	13.04		156.75
213.375	12.28		342.43	221.375	12.89		163.22
213.500	12.23		340.95	221.500	13.14		161.85
213.625	12.25		333.78	221.625	13.02		156.90
				221.750	12.71		149.78
213.750	12.11		327.59	221.875	12.88		138.57
213.875	11.77		325.05	222.000	12.53		149.25
214.000	11.46		318.52	222.125	12.23		148.80
214.125	11.51		320.46	222.250	12.16		144.25
214.250	11.22		316.63	222.375	11.49		134.67
214.375	11.30		305.72				
214.500	11.35		302.35	222.500	11.04		142.57
214.625	11.55		305.19	222.625	11.21		141.75
214.750	11.45		291.06	222.750	10.87		132.37
214.875	11.44		294.52	222.875	10.53		136.72
				223.000	10.07		134.86
215.000	10.81		295.14	223.125	9.59		129.75
215.125	10.67		287.13	223.250	9.57		123.02
215.250	11.05		285.43	223.375	9.40		130.14
215.375	10.66		288.95	223.500	9.40		129.51
215.500	10.72		293.68	223.625	9.19		122.44
215.625	11.11		284.66				
215.750	11.43		287.52	223.750	9.35		125.91
215.875	12.18		281.27	223.875	9.34		124.61
216.000	12.46		278.41	224.000	9.40		122.33
216.125	12.79		274.74	224.125	9.63		119.06

TABLE 3. *Extinction coefficients of* NO_2 *and* N_2O_4, *180–410 nm at 298 K and 235 K,* ϵ *in* cm^{-1} *(atm at 273 K)*$^{-1}$ *base* e—Continued

Wavelength (nm)	Ext. coeff. NO_2 298 K	Ext. coeff. NO_2 235 K	Ext. coeff. N_2O_4
224.250	9.76		125.55
224.375	9.74		122.10
224.500	9.07		119.00
224.625	9.17		113.73
224.750	8.70		119.06
224.875	8.78		115.24
225.000	8.71		110.60
225.125	8.49		108.02
225.250	8.77		106.09
225.375	9.20		104.94
225.500	9.68		100.06
225.625	10.04		104.52
225.750	10.91		100.81
225.875	11.30		104.02
226.000	11.99		104.88
226.125	12.56		92.47
226.250	12.75		97.89
226.375	12.50		95.76
226.500	12.28		91.87
226.625	11.77		95.83
226.750	11.24		86.61
226.875	10.61		90.89
227.000	9.89		89.88
227.125	9.44		90.61
227.250	9.04		82.91
227.375	8.47		84.62
227.500	8.20		86.00
227.625	7.55		76.59
227.750	7.60		85.84
227.875	7.69		85.22
228.000	7.90		76.98
228.125	7.82		85.19
228.250	7.54		72.86
228.375	8.00		74.00
228.500	7.88		80.39
228.625	7.69		77.17
228.750	7.30		73.80
228.875	7.35		79.25
229.000	6.90		76.46
229.125	6.73		72.83
229.250	6.43		76.44
229.375	6.08		76.10
229.500	5.91		69.57
229.625	5.91		64.62
229.750	5.98		73.00
229.875	6.00		72.98
230.000	6.52		68.66
230.125	6.64		62.98
230.250	6.97		68.12
230.375	7.23		69.95
230.500	7.08		68.89
230.625	7.55		63.53
230.750	7.78		59.49
230.875	7.86		61.43
231.000	8.30		60.82
231.125	8.19		58.75
231.250	8.23		59.75
231.375	8.10		61.43
231.500	7.88		59.29
231.625	7.57		60.42
231.750	7.54		58.54
231.875	7.12		57.57
232.000	7.14		56.50
232.125	6.93		54.46
232.250	6.98		56.54
232.375	7.16		58.55
232.500	7.48		60.39
232.625	7.43		54.39
232.750	7.25		57.91
232.875	6.93		54.77
233.000	6.42		50.30
233.125	6.11		56.00
233.250	5.67		49.04
233.375	5.12		54.58
233.500	4.69		50.31
233.625	4.29		51.51
233.750	3.85		55.63
233.875	3.67		48.91
234.000	3.55		53.60
234.125	3.48		55.17
234.250	3.47		46.90
234.375	3.38		49.60
234.500	3.09		50.23
234.625	2.78		49.48
234.750	2.89		50.28
234.875	3.38		47.36
235.000	3.98		47.37
235.125	4. 9		45.90
235.250	4.94		49.00
235.375	5.59		47.79
235.500	5.54		49.24
235.625	5.19		54.10
235.750	4.47		44.08
235.875	4.19		46.98
236.000	3.78		38.78
236.125	3.51		48.57
236.250	3.71		49.89
236.375	3.93		44.55
236.500	4.24		47.09
236.625	4.19		49.03
236.750	4.10		48.72
236.875	3.98		44.72
237.000	4.01		47.77
237.125	4.15		36.85
237.250	4.28		48.97
237.375	4.59		38.62
237.500	4.80		37.57
237.625	4.87		30.41
237.750	4.60		39.40
237.875	4.26		33.52
238.000	3.87		47.94
238.125	3.42		49.02
238.250	3.09		32.33
238.375	2.85		43.17
238.500	2.45		37.64
238.625	2.37		47.79
238.750	2.08		39.67
238.875	1.90		41.41
239.000	2.26		38.66
239.125	3.06		38.97
239.250	3.26		40.21
239.375	3.25		37.98
239.500	2.84		36.42
239.625	2.61		43.61
239.750	2.36		47.05
239.875	2.01		36.11
240.000	1.80		41.15

TABLE 3. *Extinction coefficients of* NO_2 *and* N_2O_4, *180–410 nm at 298 K and 235 K,* ϵ *in* cm^{-1} *(atm at 273 K)*$^{-1}$ *base e*—Continued

Wavelength (nm)	Ext. coeff. NO_2 298 K	Ext. coeff. NO_2 235 K	Ext. coeff. N_2O_4	Wavelength (nm)	Ext. coeff. NO_2 298 K	Ext. coeff. NO_2 235 K	Ext. coeff. N_2O_4
240.125	1.48		34.54	248.000	.21		29.57
240.250	1.55		31.80	248.125	.27		28.83
240.375	1.27		38.66	248.250	.39		27.03
240.500	1.00		37.36	248.375	.27		30.55
240.625	0.70		38.91	248.500	.39		27.08
240.750	.81		41.61	248.625	.38		27.21
240.875	.72		35.66				
241.000	.71		31.30	248.750	.39		29.19
241.125	.52		31.71	248.875	.23		29.13
				249.000	.37		31.09
241.250	0.38		39.45	249.125	1.05		29.11
241.375	0.68		29.13	249.250	1.81		26.61
241.500	0.37		34.54	249.375	1.52		25.46
241.625	0.80		39.27	249.500	1.09		25.22
241.750	0.71		41.75	249.625	.94		27.21
241.875	1.09		37.20	249.750	.80		27.91
242.000	2.00		30.89	249.875	.44		28.75
242.125	3.14		38.31				
242.250	3.80		29.58	250.000	.76		28.27
242.375	3.90		35.10	250.125	.38		27.43
				250.250	.50		26.99
242.500	3.23		36.23	250.375	.44		27.05
242.625	2.85		39.33	250.500	.40		26.52
242.750	2.24		36.16	250.625	.38		24.83
242.875	1.82		32.52	250.750	.33		25.06
243.000	1.66		32.31	250.875	.38		31.50
243.125	1.69		30.95	251.000	.37		26.77
243.250	1.80		35.41	251.125	.31		21.71
243.375	1.45		33.41				
243.500	1.33		40.46	251.250	.34		24.06
243.625	1.03		32.10	251.375	.40		31.14
				251.500	.30		27.51
243.750	1.00		38.57	251.625	.19		17.90
243.875	0.85		39.85	251.750	.35		27.87
244.000	.69		36.30	251.875	.37		26.29
244.125	.59		33.61	252.000	.24		26.27
244.250	.69		32.40	252.125	.23		26.16
244.375	.63		34.62	252.250	.33		27.98
244.500	.48		34.25	252.375	.42		25.36
244.625	.65		32.48				
244.750	1.03		37.99	252.500	.42		26.20
244.875	1.37		33.69	252.625	.44		29.44
				252.750	.33		26.10
245.000	1.17		31.13	252.875	.47		25.12
245.125	1.02		35.69	253.000	.59		25.42
245.250	0.71		27.16	253.125	.32		25.64
245.375	.84		26.32	253.250	.36		24.76
245.500	.59		30.89	253.375	.39		25.62
245.625	.46		27.72	253.500	.38		24.86
245.750	.55		27.15	253.625	.18		25.98
245.875	.70		27.21				
246.000	1.17		26.99	253.750	.39		24.78
246.125	1.09		25.54	253.875	.54		25.80
				254.000	.56		24.06
246.250	0.88		27.48	254.125	.40		26.61
246.375	.77		25.67	254.250	.47		25.59
246.500	.82		25.90	254.375	.28		25.23
246.625	.59		24.13	254.500	.39		25.51
246.750	.50		26.35	254.625	.42		26.08
246.875	.54		29.55	254.750	.56		24.79
247.000	.49		23.02	254.875	.35		27.30
247.125	.43		27.13				
247.250	.34		28.88	255.000	.39		26.45
247.375	.40		26.56	255.125	.24		24.75
				255.250	.45		25.10
247.500	0.50		29.13	255.375	.40		25.00
247.625	.39		29.85	255.500	.46		25.41
247.750	.32		26.45	255.625	.32		24.07
247.875	.26		28.03	255.750	.38		24.56

TABLE 3. *Extinction coefficients of* NO_2 *and* N_2O_4, *180–410 nm at 298 K and 235 K,* ϵ *in* cm^{-1} *(atm at 273 K)*$^{-1}$ *base* e—Continued

Wavelength (nm)	Ext. coeff. NO_2 298 K	Ext. coeff. NO_2 235 K	Ext. coeff. N_2O_4	Wavelength (nm)	Ext. coeff. NO_2 298 K	Ext. coeff. NO_2 235 K	Ext. coeff. N_2O_4
255.875	.41		24.66	263.750	.47		23.32
256.000	.29		24.48	263.875	.52		23.32
256.125	.56		23.86	264.000	.56		23.12
				264.125	.57		22.96
256.250	.47		24.02	264.250	.49		22.74
256.375	.40		24.53	264.375	.64		23.00
256.500	.55		24.53	264.500	.49		29.56
256.625	.42		25.04	264.625	.69		22.66
256.750	.26		24.64	264.750	.61		22.97
256.875	.29		24.81	264.875	.63		23.15
257.000	.36		24.31				
257.125	.35		24.29	265.000	.55		23.17
257.250	.48		23.92	265.125	.66		23.22
257.375	.38		24.40	265.250	.72		23.03
				265.375	.66		23.57
257.500	.27		24.23	265.500	.67		23.00
257.625	.31		24.22	265.625	.60		23.08
257.750	.41		24.32	265.750	.63		22.87
257.875	.46		24.59	265.875	.61		22.79
258.000	.44		24.21	266.000	.64		22.71
258.125	.48		24.42	266.125	.58		22.82
258.250	.42		24.65				
258.375	.40		24.79	266.250	0.50		23.02
258.500	.58		24.11	266.375	.56		22.77
258.625	.42		24.34	266.500	.60		23.23
				266.625	.53		22.96
258.750	.63		23.69	266.750	.59		22.98
258.875	.30		24.23	266.875	.69		22.58
259.000	.51		24.58	256.000	.65		22.57
259.125	.47		24.19	267.125	.68		22.82
259.250	.38		24.00	267.250	.67		21.90
259.375	.56		24.52	267.375	.75		22.22
259.500	.37		23.90				
259.625	.61		23.88	267.500	.65		22.42
259.750	.55		23.98	267.625	.64		22.00
259.875	.47		24.28	267.750	.68		22.30
				267.875	.67		22.31
260.000	0.51		23.93	268.000	.64		22.79
260.125	.46		24.42	268.125	.63		22.32
260.250	.51		23.98	268.250	.71		22.18
260.375	.38		24.37	268.375	.75		22.16
260.500	.41		23.86	268.500	.75		21.57
260.625	.43		24.12	268.625	.75		21.98
260.750	.46		24.17				
260.875	.52		24.10	268.750	.77		21.63
261.000	.44		24.28	268.875	.72		21.87
261.125	.41		23.84	269.000	.75		21.67
				269.125	.84		21.68
261.250	.38		24.02	269.250	.81		21.60
261.375	.41		23.91	269.375	.80		21.65
261.500	.53		24.13	269.500	.77		21.02
261.625	.42		23.37	269.625	.80		21.26
261.750	.39		23.86	269.750	.78		21.11
261.875	.54		23.90	269.875	.82		22.32
262.000	.55		24.15				
262.125	.48		23.64	270.000	.84		21.25
262.250	.53		23.60	270.125	.84		20.97
262.375	.54		23.71	270.250	.80		20.92
				270.375	.85		20.35
262.500	.45		23.56	270.500	.80		21.48
262.625	.57		23.57	270.625	.82		20.83
262.750	.45		23.80	270.750	.80		20.45
262.875	.54		23.95	270.875	.73		20.72
263.000	.60		23.63	271.000	.82		21.23
263.125	.65		23.85	271.125	.85		20.90
263.250	.63		23.53				
263.375	.55		24.09	271.250	.84		20.63
263.500	.50		23.91	271.375	.76		20.60
263.625	.55		23.83	271.500	.76		20.74

TABLE 3. *Extinction coefficients of* NO_2 *and* N_2O_4, *180–410 nm at 298 K and 235 K,* ϵ *in* cm^{-1} *(atm at 273 K)*$^{-1}$ *base* e—Continued

Wavelength (nm)	Ext. coeff. NO_2 298 K	Ext. coeff. NO_2 235 K	Ext. coeff. N_2O_4
271.625	.78		20.73
271.750	.78		14.99
271.875	.81		20.03
272.000	.83		20.23
272.125	.85		20.82
272.250	.79		20.67
272.375	.92		20.43
272.500	.86		20.48
272.625	.89		20.76
272.750	.89		20.63
272.875	1.00		20.17
273.000	1.02		20.08
273.125	.99		20.34
273.250	.98		20.08
273.375	1.02		20.09
273.500	1.00		19.69
273.625	.98		19.69
273.750	1.02		19.66
273.875	1.05		19.49
274.000	.98		19.82
274.125	1.05		19.96
274.250	1.08		19.38
274.375	1.08		19.83
274.500	1.03		19.25
274.625	1.08		16.36
274.750	1.03		19.73
274.875	1.13		19.72
275.000	1.08		16.89
275.125	1.09		16.43
275.250	1.09		16.63
275.375	1.08		16.75
275.500	1.11		16.64
275.625	1.10		16.29
275.750	1.07		16.09
275.875	1.06		16.24
276.000	1.06		16.70
276.125	1.07		16.00
276.250	1.11		16.08
276.375	1.10		15.83
276.500	1.12		15.82
276.625	1.14		15.92
276.750	1.10		15.93
276.875	1.19		15.84
277.000	1.14		15.95
277.125	1.15		15.57
277.250	1.13		15.12
277.375	1.19		15.57
277.500	1.15		15.56
277.625	1.15		15.20
277.750	1.23		15.45
277.875	1.20		15.93
278.000	1.29		15.82
278.125	1.26		15.32
278.250	1.31		15.67
278.375	1.24		15.92
278.500	1.31		15.52
278.625	1.29		15.50
278.750	1.28		15.46
278.875	1.40		15.31
279.000	1.35		15.30
279.125	1.32		15.24
279.250	1.41		15.22
279.375	1.48		14.44
279.500	1.50		14.97
279.625	1.47		14.97
279.750	1.55		14.76
279-875	1.48		14.61
280.000	1.49		14.66
280.125	1.41		14.63
280.250	1.49		14.51
280.375	1.42		14.42
280.500	1.43		14.32
280.625	1.47		14.25
280.750	1.42		14.46
280.875	1.44		14.07
281.000	1.50		14.23
281.125	1.48		13.76
281.250	1.52		14.58
281.375	1.52		14.02
281.500	1.59		13.97
281.625	1.55		14.15
281.750	1.52		14.02
281.875	1.47		14.07
282.000	1.44		13.75
282.125	1.41		13.61
282.250	1.49		13.86
282.375	1.47		13.84
282.500	1.43		13.39
282.625	1.43		13.83
282.750	1.49		13.93
282.875	1.45		13.95
283.000	1.50		13.64
283.125	1.54		13.62
283.250	1.60		13.89
283.375	1.60		15.94
283.500	1.65		13.11
283.625	1.72		13.15
283.750	1.67		13.30
283.875	2.04		13.61
284.000	1.68		13.26
284.125	1.77		13.25
284.250	1.76		13.10
284.375	1.81		13.21
284.500	1.82		12.93
284.625	1.83		12.50
284.750	1.85		13.00
284.875	1.88		12.48
285.000	1.88		12.14
285.125	1.86		12.37
285.250	1.94		12.16
285.375	1.91		13.22
285.500	1.95		12.38
285.625	1.97		12.63
285.750	1.95		12.34
285.875	2.01		12.12
286.000	1.96		11.89
286.125	2.05		12.10
286.250	2.05		12.02
286.375	2.06		12.05
286.500	2.02		11.94
286.625	1.98		11.60
286.750	2.00		12.10
286.875	1.97		11.71
287.000	1.98		11.93
287.125	1.93		11.79
287.250	1.93		11.67
287.375	2.01		11.48

TABLE 3. *Extinction coefficients of* NO_2 *and* N_2O_4, *180–410 nm at 298 K and 235 K,* ϵ *in* cm^{-1} *(atm at 273 K)*$^{-1}$ *base* e—Continued

Wavelength (nm)	Ext. coeff. NO_2 298 K	Ext. coeff. NO_2 235 K	Ext. coeff. N_2O_4	Wavelength (nm)	Ext. coeff. NO_2 298 K	Ext. coeff. NO_2 235 K	Ext. coeff. N_2O_4
287.500	1.98		11.44	295.375	2.84	1.64	9.39
287.625	1.98		11.77	295.500	2.50	2.29	8.94
287.750	1.95		11.29	295.625	2.46	2.31	8.65
287.875	2.00		11.25	295.750	2.39	1.92	8.82
288.000	2.06		11.33	295.875	2.58	2.28	9.21
288.125	2.05		11.05	296.000	2.50	2.76	8.77
288.250	2.01		11.06	296.125	2.70	2.20	8.75
288.375	2.02		11.52				
288.500	2.03		11.30	296.250	2.53	2.56	8.45
288.625	2.04		11.09	296.375	2.98	2.53	8.74
				296.500	3.00	2.40	8.50
288.750	2.07		10.95	296.625	2.94	2.77	8.94
288.875	2.10		11.43	296.750	3.08	2.52	9.42
289.000	2.12		10.93	296.875	3.12	2.45	8.70
289.125	2.18		11.31	297.000	3.27	2.98	8.47
289.250	2.16		11.38	297.125	3.44	2.89	8.71
289.375	2.18		11.42	297.250	3.55	3.24	8.64
289.500	2.23		10.88	297.375	3.39	3.15	8.59
289.625	2.22		10.71				
289.750	2.21		11.04	297.500	3.62	3.13	8.52
289.875	2.30		10.93	297.625	3.67	2.89	8.64
				297.750	3.65	3.15	8.72
290.000	2.20	1.82	10.62	297.875	3.59	3.86	8.35
290.125	2.13	1.70	10.70	298.000	3.15	3.10	8.56
290.250	2.17	1.72	10.74	298.125	3.21	2.96	8.48
290.375	2.17	2.04	10.40	298.250	3.08	2.83	8.55
290.500	2.15	1.60	10.56	298.375	3.10	2.60	8.84
290.625	2.45	1.60	10.59	298.500	3.34	3.07	8.66
290.750	2.48	1.39	10.52	298.625	3.09	3.37	8.42
290.875	2.10	2.02	10.38				
291.000	2.66	2.01	10.59	298.750	3.12	2.72	8.81
291.125	2.37	2.01	10.20	298.875	3.26	2.96	8.35
				299.000	3.38	3.74	8.35
291.250	2.79	2.01	10.15	299.125	3.39	3.01	7.91
291.375	2.53	1.72	10.07	299.250	3.19	2.78	8.01
291.500	2.83	1.91	10.32	299.375	3.07	3.01	8.02
291.625	2.97	2.64	9.86	299.500	3.43	3.34	8.37
291.750	2.85	2.06	10.17	299.625	3.40	3.18	8.27
291.875	2.82	1.94	9.90	299.750	3.20	2.84	8.48
292.000	2.52	2.16	10.23	299.875	3.56	2.85	7.82
292.125	2.69	1.56	9.87				
292.250	2.52	2.04	9.73	300.000	3.15	2.93	8.32
292.375	2.50	2.62	10.48	300.125	3.37	2.98	8.51
				300.250	3.01	2.37	8.37
292.500	2.84	2.36	9.70	300.375	3.17	2.99	8.39
292.625	2.69	2.33	10.26	300.500	3.38	2.86	8.29
292.750	2.43	2.17	10.07	300.625	3.27	3.32	7.99
292.875	2.84	2.27	10.01	300.750	3.25	3.03	8.45
293.000	2.62	1.96	9.80	300.875	3.29	2.96	8.02
293.125	2.85	2.30	9.68	301.000	3.30	3.27	8.21
293.250	2.63	2.27	9.66	301.125	3.28	3.25	8.41
293.375	2.49	1.84	9.52				
293.500	2.34	2.16	9.80	301.250	3.18	2.72	8.00
293.625	2.33	1.50	9.42	301.375	3.49	2.99	7.93
				301.500	3.50	2.71	8.23
293.750	2.46	2.20	9.61	301.625	3.65	3.05	7.84
293.875	2.59	2.50	9.21	301.750	3.71	3.87	8.20
294.000	2.55	2.36	9.27	301.875	3.64	3.38	8.21
294.125	2.38	2.02	9.43	302.000	3.73	3.51	8.30
294.250	2.62	1.76	9.56	302.125	3.98	3.41	8.45
294.375	2.50	2.54	9.28	302.250	3.55	3.54	8.56
294.500	2.60	1.86	10.03	302.375	3.86	3.25	8.05
294.625	2.61	2.43	9.69				
294.750	2.65	2.69	8.96	302.500	4.10	3.70	8.15
294.875	2.62	2.66	9.11	302.625	3.93	3.84	7.97
				302.750	4.03	3.42	8.09
295.000	2.60	2.29	9.10	302.875	3.97	4.19	7.68
295.125	2.72	2.51	9.17	303.000	4.28	4.50	7.86
295.250	2.63	2.01	9.04	303.125	4.11	3.73	8.14

TABLE 3. *Extinction coefficients of* NO_2 *and* N_2O_4, *180–410 nm at 298 K and 235 K,* ϵ *in* cm^{-1} *(atm at 273 K)*$^{-1}$ *base* e—Continued

Wavelength (nm)	Ext. coeff. NO_2 298 K	Ext. coeff. NO_2 235 K	Ext. coeff. N_2O_4
303.250	3.93	3.85	8.35
303.375	4.06	3.96	8.45
303.500	4.13	3.65	8.26
303.625	4.23	4.11	8.07
303.750	4.15	4.34	8.08
303.875	4.42	4.12	7.61
304.000	4.29	3.90	7.57
304.125	4.23	3.95	8.37
304.250	4.01	3.91	8.43
304.375	4.02	4.15	8.45
304.500	4.24	3.79	8.10
304.625	4.02	4.01	8.26
304.750	4.04	3.50	8.23
304.875	4.13	3.94	8.38
305.000	4.45	4.48	8.18
305.125	4.20	3.69	7.75
305.250	4.17	3.38	7.60
305.375	4.08	3.53	7.86
305.500	4.32	3.81	7.55
305.625	4.09	3.82	7.73
305.750	4.11	4.11	7.05
305.875	3.83	3.69	7.51
306.000	4.25	4.02	7.35
306.125	4.19	3.13	8.07
306.250	4.17	3.69	8.40
306.375	4.32	4.10	8.08
306.500	3.69	3.88	6.92
306.625	3.98	3.60	8.17
306.750	4.31	3.74	7.98
306.875	4.32	4.21	8.07
307.000	4.39	3.96	7.43
307.125	4.46	4.50	7.26
307.250	4.61	4.56	8.12
307.375	4.48	5.19	7.92
307.500	4.53	4.23	7.68
307.625	4.73	4.40	7.78
307.750	4.35	3.78	7.98
307.875	4.45	4.38	7.65
308.000	4.35	4.07	7.87
308.125	4.51	3.63	8.40
308.250	4.33	4.44	7.59
308.375	4.39	3.85	8.17
308.500	4.42	3.90	7.40
308.625	4.67	4.29	7.66
308.750	4.78	4.42	8.42
308.875	4.86	4.93	7.96
309.000	4.94	4.99	7.76
309.125	5.01	4.35	7.78
309.250	4.88	4.87	7.71
309.375	5.12	5.17	8.05
309.500	5.03	4.59	8.02
309.625	5.12	5.00	8.11
309.750	5.06	4.76	8.12
309.875	4.78	4.83	7.95
310.000	4.72	4.91	8.20
310.125	4.78	4.37	8.39
310.250	4.91	4.41	8.51
310.375	4.90	5.06	8.00
310.500	4.97	4.60	8.20
310.625	5.18	4.41	8.65
310.750	5.19	5.06	8.22
310.875	4.90	5.02	8.91
311.000	5.05	4.56	8.31
311.125	5.15	4.64	8.01
311.250	5.15	4.82	7.97
311.375	5.24	4.85	8.81
311.500	5.47	4.85	8.60
311.625	5.15	4.73	8.45
311.750	5.34	4.69	8.40
311.875	5.32	4.77	8.58
312.000	5.27	5.75	8.49
312.125	5.40	5.17	8.43
312.250	5.61	6.10	8.08
312.375	5.92	5.29	8.81
312.500	5.80	5.03	8.61
312.625	5.40	4.77	9.07
312.750	5.56	5.25	9.41
312.875	5.42	5.19	9.44
313.000	5.47	5.15	9.26
313.125	5.45	5.15	9.79
313.250	5.28	4.88	9.21
313.375	5.15	4.89	9.67
313.500	5.08	5.04	9.08
313.625	5.37	4.94	8.85
313.750	5.13	4.92	9.16
313.875	5.42	5.31	9.42
314.000	5.22	4.96	9.68
314.125	5.30	5.13	9.81
314.250	5.52	5.03	9.64
314.375	5.41	5.43	9.74
314.500	5.88	5.01	9.90
314.625	5.91	5.14	10.31
314.750	5.92	5.36	9.62
314.875	5.95	5.49	9.78
315.000	6.05	5.89	9.74
315.125	6.01	5.20	10.01
315.250	6.02	5.85	10.04
315.375	5.90	5.74	9.90
315.500	5.77	5.96	10.93
315.625	5.82	5.29	10.44
315.750	5.60	4.97	10.81
315.875	5.81	5.26	11.01
316.000	5.73	5.04	11.03
316.125	5.92	4.60	10.79
316.250	5.84	4.95	10.67
316.375	5.50	5.26	10.75
316.500	5.80	5.08	10.61
316.625	5.78	5.45	10.84
316.750	5.93	5.54	10.65
316.875	6.03	5.74	11.04
317.000	6.26	6.00	10.98
317.125	5.91	6.39	10.85
317.250	5.92	5.94	10.76
317.375	6.32	6.28	11.25
317.500	6.63	6.83	11.10
317.625	6.56	6.18	10.81
317.750	6.48	6.36	11.20
317.875	6.64	6.15	11.28
318.000	6.67	6.47	11.43
318.125	6.52	6.04	11.83
318.250	6.46	5.93	11.54
318.375	6.40	6.23	12.15
318.500	6.17	6.13	12.07
318.625	6.18	6.02	12.00
318.750	6.15	5.82	11.86
318.875	6.04	5.81	12.11
319.000	6.22	5.85	12.01
319.125	6.42	6.49	12.70

201-606 O - 76 - 2

TABLE 3. *Extinction coefficients of* NO_2 *and* N_2O_4, *180–410 nm at 298 K and 235 K,* ϵ *in* cm^{-1} *(atm at 273 K)*$^{-1}$ *base* e—Continued

Wavelength (nm)	Ext. coeff. NO_2 298 K	Ext. coeff. NO_2 235 K	Ext. coeff. N_2O_4
319.250	6.38	5.77	12.30
319.375	6.41	5.74	12.65
319.500	6.55	6.23	11.87
319.625	6.70	6.51	12.51
319.750	6.77	6.34	12.34
319.875	6.57	6.40	12.21
320.000	6.82	6.31	12.20
320.125	7.08	6.50	12.76
320.250	7.06	5.98	12.49
320.375	7.16	6.44	12.76
320.500	7.41	6.06	12.81
320.625	6.75	6.32	12.43
320.750	6.86	6.29	12.52
320.875	6.66	6.35	12.67
321.000	7.13	5.52	13.40
321.125	6.91	5.15	13.21
321.250	6.77	5.51	13.10
321.375	6.59	5.67	13.13
321.500	6.70	5.41	13.36
321.625	7.26	6.16	13.72
321.750	7.18	4.92	13.73
321.875	6.87	6.35	13.01
322.000	7.12	5.94	13.74
322.125	6.98	5.91	13.55
322.250	6.69	5.73	13.99
322.375	7.48	6.01	14.37
322.500	7.76	6.22	13.52
322.625	7.21	5.94	14.37
322.750	7.54	6.40	14.11
322.875	7.17	5.84	14.80
323.000	7.44	6.56	14.73
323.125	7.11	6.09	14.70
323.250	7.03	6.34	13.87
323.375	6.91	6.03	14.69
323.500	7.24	6.12	14.68
323.625	6.89	6.37	14.29
323.750	6.98	6.12	14.57
323.875	6.80	5.86	14.74
324.000	7.19	6.02	14.64
324.125	7.15	5.97	14.93
324.250	7.34	5.98	14.92
324.375	7.57	5.93	15.12
324.500	7.09	6.06	15.09
324.625	7.19	6.54	15.30
324.750	7.45	6.42	15.29
324.875	7.46	5.95	15.41
325.000	7.49	6.83	14.69
325.125	8.04	6.65	15.64
325.250	8.26	6.55	15.62
325.375	8.53	6.94	15.17
325.000	7.48	6.78	15.88
325.625	8.05	7.24	15.84
325.750	7.55	6.61	15.28
325.875	7.56	6.30	15.66
326.000	7.74	5.86	15.42
326.125	7.79	6.41	15.58
326.250	7.77	6.34	15.90
326.375	7.89	6.71	16.15
326.500	7.68	7.16	16.27
326.625	7.83	6.86	16.19
326.750	8.42	7.21	16.55
326.875	7.95	5.93	16.85
327.000	7.82	6.32	16.12
327.125	7.93	6.63	16.39
327.250	7.73	6.47	16.32
327.375	7.68	6.42	16.40
327.500	8.00	6.77	16.53
327.625	7.95	6.77	16.76
327.750	8.17	6.97	16.55
327.875	8.32	6.96	17.02
328.000	8.27	7.03	16.79
328.125	7.80	6.60	17.16
328.250	7.87	7.03	17.01
328.375	7.85	6.91	16.90
328.500	7.72	6.65	17.06
328.625	7.68	6.81	16.58
328.750	7.90	6.14	16.77
328.875	7.58	6.36	17.23
329.000	8.06	7.51	16.96
329.125	7.86	7.15	17.62
329.250	7.78	7.62	17.42
329.375	8.10	7.32	19.84
329.500	8.26	7.44	18.03
329.625	8.50	7.12	18.14
329.750	8.63	7.63	18.13
329.875	8.43	7.92	17.65
330.000	8.03	7.82	17.69
330.125	8.36	6.80	17.84
330.250	8.45	7.07	18.05
330.375	7.66	6.86	18.07
330.500	7.93	7.49	17.72
330.625	8.01	7.08	17.60
330.750	8.28	7.02	18.63
330.875	7.82	6.87	18.44
331.000	8.20	6.59	18.24
331.125	8.28	6.71	18.17
331.250	8.37	7.38	18.49
331.375	8.50	7.32	17.78
331.500	8.33	6.74	18.95
331.625	8.60	6.84	18.44
331.750	8.43	6.95	18.24
331.875	8.39	6.68	18.62
332.000	8.08	7.10	18.29
332.125	8.44	7.12	18.71
332.250	8.50	7.86	19.26
332.375	8.99	7.76	18.98
332.500	9.39	8.38	18.52
332.625	9.94	7.84	21.33
332.750	10.05	8.80	18.52
332.875	10.20	8.83	18.51
333.000	10.02	8.76	19.72
333.125	9.77	9.10	19.97
333.250	9.70	8.70	19.45
333.375	9.21	8.83	19.00
333.500	9.23	7.64	19.20
333.625	8.83	7.80	18.70
333.750	8.69	7.38	19.17
333.875	8.46	7.57	19.80
334.000	8.01	6.98	19.54
334.125	8.14	6.60	19.83
334.250	8.35	7.20	19.48
334.375	8.33	7.51	19.42
334.500	8.29	7.05	20.05
334.625	8.56	7.56	19.20
334.750	9.00	7.62	19.44
334.875	9.11	8.74	19.74

TABLE 3. *Extinction coefficients of* NO_2 *and* N_2O_4, *180–410 nm at 298 K and 235 K,* ϵ *in* cm^{-1} *(atm at 273 K)*$^{-1}$ *base e*—Continued

Wavelength (nm)	Ext. coeff. NO_2 298 K	Ext. coeff. NO_2 235 K	Ext. coeff. N_2O_4	Wavelength (nm)	Ext. coeff. NO_2 298 K	Ext. coeff. NO_2 235 K	Ext. coeff. N_2O_4
335.000	9.28	8.43	19.41	343.000	9.53	8.22	22.29
335.125	9.12	7.82	21.11	343.125	9.90	8.38	22.36
335.250	9.67	7.89	19.94	343.250	9.62	8.37	21.97
335.375	9.17	7.83	22.06	343.375	9.99	8.88	21.88
335.500	8.83	7.66	20.92	343.500	10.19	9.06	22.37
335.625	9.01	7.79	20.62	343.625	10.54	8.55	21.41
335.750	8.85	8.03	20.97				
335.875	8.89	7.15	22.42	343.750	10.82	9.45	21.37
336.000	9.43	7.86	20.71	343.875	10.69	8.53	22.45
336.125	9.09	6.92	22.15	344.000	10.91	8.79	22.08
				344.125	10.33	8.61	21.51
336.250	9.40	7.49	21.95	344.250	10.52	8.84	21.78
336.375	9.06	8.12	23.00	344.375	10.41	8.87	21.09
336.500	9.32	8.59	21.15	344.500	10.64	8.58	22.41
336.625	9.53	8.33	21.60	344.625	10.82	8.74	23.66
336.750	9.60	8.43	21.34	344.750	10.93	8.46	24.97
336.875	9.62	7.53	22.54	344.875	11.03	8.68	21.63
337.000	9.31	7.17	22.03				
337.125	9.37	8.14	21.91	345.000	10.94	9.21	20.99
337.250	9.24	7.33	21.89	345.125	11.22	9.25	21.71
337.375	9.13	7.64	22.30	345.250	10.92	9.54	21.27
				345.375	10.74	8.87	21.47
337.500	9.12	7.24	21.85	345.500	10.95	9.01	21.50
337.625	8.93	7.83	21.85	345.625	10.86	9.05	21.34
337.750	8.98	6.90	22.51	345.750	11.11	9.72	21.43
337.875	8.81	7.16	22.68	345.875	11.30	9.41	21.10
338.000	9.35	7.10	22.03	346.000	11.54	9.57	21.28
338.125	9.27	7.54	22.05	346.126	11.67	9.36	21.63
338.250	9.69	8.11	21.86				
338.375	9.89	8.58	22.30	346.250	11.72	9.74	20.79
338.500	10.34	9.12	22.43	346.375	11.61	9.93	20.78
338.625	10.48	9.29	22.33	346.500	12.06	10.05	20.14
				346.625	12.36	10.10	20.80
338.750	10.70	9.85	22.27	346.750	11.99	10.22	20.43
338.875	10.80	9.64	22.14	346.875	11.83	10.32	20.36
339.000	10.72	9.45	22.15	347.000	11.50	9.94	20.12
339.125	10.85	9.19	22.16	347.125	11.68	9.80	20.35
339.250	10.55	9.12	22.57	347.250	11.48	9.57	20.14
339.375	10.22	9.04	22.53	347.375	11.53	9.48	19.81
339.500	10.08	8.32	23.61				
339.625	10.10	8.52	23.11	347.500	11.29	9.71	19.93
339.750	10.37	8.04	22.01	347.625	11.32	9.50	20.43
339.875	9.99	8.67	23.01	347.750	11.59	9.89	19.36
				347.875	11.82	10.09	19.93
340.000	10.43	8.69	22.27	348.000	12.96	10.69	19.36
340.125	10.30	8.82	22.55	348.125	13.46	11.51	19.25
340.250	10.04	8.33	21.67	348.250	13.84	12.39	19.51
340.375	10.35	8.63	22.49	348.375	14.33	13.15	18.33
340.500	10.53	8.33	21.93	348.500	14.05	12.55	18.73
340.625	10.55	8.55	22.20	348.625	13.68	12.14	18.94
340.750	10.28	9.10	21.55				
340.875	10.55	8.81	22.61	348.750	13.15	11.77	19.32
341.000	11.20	9.30	22.36	348.875	12.56	11.21	19.27
341.125	11.41	9.68	22.28	349.000	12.40	10.40	18.85
				349.125	11.84	10.46	19.15
341.250	11.55	9.31	21.98	349.250	11.22	9.31	18.96
341.375	11.48	9.68	22.34	349.375	10.78	8.94	18.84
341.500	11.37	9.86	22.68	349.500	10.75	9.70	18.24
341.625	11.03	9.92	22.02	349.625	10.88	8.72	18.79
341.750	11.37	9.92	21.98	349.750	10.68	8.64	19.04
341.875	10.62	9.52	21.87	349.875	10.63	9.18	19.80
342.000	10.30	8.92	21.98				
342.125	10.19	8.55	22.16	350.000	11.02	8.37	19.75
342.250	9.85	8.85	22.09	350.125	11.13	9.52	17.34
342.375	10.20	7.89	21.61	350.250	11.46	9.67	17.16
				350.375	11.29	10.24	16.88
342.500	9.94	7.92	21.88	350.500	12.13	10.32	17.08
342.625	9.46	8.36	22.28	350.625	11.72	10.55	16.84
342.750	9.42	7.56	21.90	350.750	12.14	10.27	16.74
342.875	9.52	8.22	21.87	350.875	12.05	10.17	16.79

TABLE 3. *Extinction coefficients of* NO_2 *and* N_2O_4, *180–410 nm at 298 K and 235 K,* ϵ *in* cm^{-1} *(atm at 273 K)*$^{-1}$ *base* e—Continued

Wavelength (nm)	Ext. coeff. NO_2 298 K	Ext. coeff. NO_2 235 K	Ext. coeff. N_2O_4	Wavelength (nm)	Ext. coeff. NO_2 298 K	Ext. coeff. NO_2 235 K	Ext. coeff. N_2O_4
351.000	12.15	10.84	16.91	358.750	12.80	10.46	12.20
351.125	12.46	11.00	16.36	358.875	12.23	10.72	11.68
				359.000	12.24	9.87	11.63
351.250	12.44	10.50	17.09	359.125	12.04	10.43	11.75
351.375	12.04	10.76	16.45	359.250	12.26	10.70	12.00
351.500	11.63	10.56	16.90	359.375	12.14	10.09	11.77
351.625	11.80	9.91	16.57	359.500	12.47	10.87	11.76
351.750	11.46	9.88	16.90	359.625	12.40	10.32	11.81
351.875	11.53	9.60	16.08	359.750	12.49	10.65	11.39
352.000	11.93	10.10	16.18	359.875	12.03	10.95	11.04
352.125	12.21	10.91	16.68				
352.250	12.14	10.15	15.79	360.000	12.13	10.48	11.05
352.375	11.92	10.25	16.35	360.125	12.57	10.66	10.31
				360.250	12.68	11.16	11.33
352.500	11.78	9.94	16.04	360.375	13.15	11.61	11.02
352.625	11.66	9.90	15.78	360.500	13.54	11.49	11.31
352.750	11.31	9.20	15.67	360.625	13.77	12.05	10.81
352.875	10.90	8.48	15.66	360.750	14.06	12.32	10.34
353.000	10.72	8.39	16.31	360.875	14.28	12.49	10.17
353.125	10.80	9.24	15.70	361.000	14.48	12.25	10.27
353.250	10.81	9.18	15.36	361.125	14.38	12.53	10.57
353.375	11.27	9.51	15.26				
353.500	11.77	9.02	14.97	361.250	13.74	12.50	11.09
353.625	12.21	10.40	15.04	361.375	13.80	12.11	10.12
				361.500	13.75	11.44	10.05
353.750	12.49	10.88	15.25	361.625	13.73	11.92	10.41
353.875	13.05	10.74	15.57	361.750	13.48	11.34	10.45
354.000	13.55	12.05	15.34	361.875	13.31	11.47	10.34
354.125	14.32	12.30	14.85	362.000	13.55	12.07	9.99
354.250	14.99	13.19	15.69	362.125	13.50	11.22	9.82
354.375	15.28	13.10	14.26	362.250	13.69	12.13	9.38
354.500	14.51	13.38	14.60	362.375	13.86	12.14	9.67
354.625	14.55	12.73	13.98				
354.750	14.48	13.27	14.55	362.500	13.66	11.98	9.86
354.875	14.14	12.44	14.27	362.625	13.73	12.03	9.41
				362.750	13.43	11.86	9.73
355.000	13.79	11.74	14.20	362.875	13.85	12.18	9.17
355.125	13.43	11.62	13.63	363.000	13.77	12.22	9.41
355.250	13.11	10.92	14.61	363.125	13.41	11.52	9.42
355.375	12.75	10.74	14.17	363.250	13.49	12.20	9.79
355.500	12.59	10.85	13.98	363.375	13.57	12.14	9.08
355.625	12.41	10.47	13.82	363.500	13.22	11.27	9.51
355.750	12.34	10.36	13.73	363.625	13.24	11.11	8.96
355.875	12.24	10.49	13.14				
356.000	12.38	10.41	13.32	363.750	12.78	11.18	8.61
356.125	12.43	10.33	13.13	363.875	12.85	10.81	8.85
				364.000	13.10	11.78	8.67
356.250	12.55	10.91	13.20	364.125	13.58	12.07	8.11
356.375	12.99	10.92	13.45	364.250	14.09	12.42	8.15
356.500	12.84	11.22	13.20	364.375	14.40	12.90	7.13
356.625	13.69	12.25	12.40	364.500	14.55	12.89	7.95
356.750	13.88	12.23	13.24	364.625	14.77	13.77	9.05
356.875	14.65	12.84	13.07	364.750	14.96	13.89	8.09
357.000	15.00	13.19	12.88	364.875	15.15	14.03	7.71
357.125	15.18	14.09	13.00				
357.250	15.12	13.89	12.54	365.000	15.54	14.44	7.80
357.375	14.89	13.30	12.94	365.125	15.75	15.05	5.71
				365.250	16.15	15.06	6.23
357.500	14.98	12.92	12.83	365.375	15.97	15.42	6.33
357.625	14.25	12.67	12.77	365.500	16.01	14.60	6.34
357.750	13.94	12.27	13.83	365.625	15.68	14.63	5.98
357.875	13.82	12.19	12.36	365.750	15.55	14.10	6.47
358.000	13.54	12.02	12.60	365.875	14.85	13.40	6.35
358.125	13.84	11.73	12.50	366.000	14.51	13.00	6.82
358.250	13.29	11.55	11.74	366.125	13.91	12.28	6.03
358.375	13.35	11.28	12.56				
358.500	13.05	11.31	12.55	366.250	13.57	11.69	6.71
358.625	12.82	11.09	11.39	366.375	13.35	11.87	5.42

TABLE 3. *Extinction coefficients of* NO_2 *and* N_2O_4, *180–410 nm at 298 K and 235 K,* ϵ *in* cm^{-1} (*atm at 273 K*)$^{-1}$ *base* e—Continued

Wavelength (nm)	Ext. coeff. NO_2 298 K	Ext. coeff. NO_2 235 K	Ext. coeff. N_2O_4	Wavelength (nm)	Ext. coeff. NO_2 298 K	Ext. coeff. NO_2 235 K	Ext. coeff. N_2O_4
366.500	13.17	11.66	5.81	374.500	13.68	12.10	3.30
366.625	13.11	11.97	5.56	374.625	13.65	11.92	3.03
366.750	13.03	11.98	5.05	374.750	13.81	12.34	2.66
366.875	13.82	12.62	5.17	374.875	14.11	12.62	2.25
367.000	13.94	12.62	4.76				
367.125	14.60	13.27	5.35	375.000	14.39	13.43	2.49
367.250	14.99	13.64	5.82	375.125	14.91	14.27	3.24
367.375	14.89	13.96	5.06	375.250	15.32	13.92	2.54
				375.375	15.78	14.48	2.67
367.500	14.67	13.58	5.03	375.500	15.86	14.64	2.39
367.625	14.47	13.38	5.49	375.625	15.85	14.35	2.32
367.750	14.85	13.44	4.97	375.750	15.99	14.78	1.35
367.875	14.65	13.67	5.15	375.875	15.99	14.79	2.08
368.000	14.36	13.42	4.78	376.000	16.76	15.70	1.93
368.125	14.45	13.38	4.64	376.125	17.48	16.52	2.71
368.250	14.40	12.73	4.93				
368.375	14.16	12.88	5.43	376.250	17.57	16.81	2.91
368.500	14.18	13.06	5.13	376.375	17.34	16.24	2.49
368.625	13.87	12.45	5.08	376.500	16.93	16.05	2.76
				376.625	16.65	15.62	2.32
368.750	13.83	12.61	5.13	376.750	16.33	15.47	2.24
368.875	14.10	12.61	4.47	376.875	15.28	14.38	2.23
369.000	13.93	12.70	4.81	377.000	15.24	13.86	2.87
369.125	14.27	13.30	4.28	377.125	14.69	13.40	2.43
369.250	14.42	13.43	4.48	377.250	14.21	12.97	2.11
369.375	14.39	12.79	4.51	377.375	13.99	12.60	2.09
369.500	14.05	12.88	4.49				
369.625	13.91	13.11	4.32	377.500	14.08	12.29	1.94
369.750	14.06	12.60	4.15	377.625	14.06	12.39	1.82
369.875	14.31	13.08	3.82	377.750	14.08	12.51	2.01
				377.875	14.19	12.68	1.88
370.000	14.57	13.08	4.39	378.000	13.91	12.78	1.76
370.125	14.35	13.05	5.23	378.125	13.63	12.51	1.85
370.250	14.19	12.81	3.98	378.250	13.76	12.26	1.89
370.375	14.07	12.78	4.15	378.375	13.88	12.60	1.74
370.500	13.93	12.40	3.95	378.500	14.04	12.50	2.56
370.625	13.67	11.54	3.65	378.625	14.21	13.04	1.38
370.750	13.17	12.00	3.40				
370.875	13.34	11.35	3.96	378.750	14.04	12.77	1.20
371.000	14.01	11.92	3.77	378.875	14.42	13.10	1.50
371.125	14.02	12.43	4.09	379.000	14.70	13.60	.83
				379.125	14.96	13.81	1.51
371.250	14.01	12.85	4.10	379.250	15.31	14.71	.62
371.375	14.66	13.16	3.35	379.375	15.84	15.00	.99
371.500	14.83	13.92	3.56	379.500	16.53	15.60	1.78
371.625	15.40	14.42	3.89	379.625	17.00	16.22	1.68
371.750	15.80	14.57	3.68	379.750	16.90	16.15	1.76
371.875	15.98	14.69	3.33	379.875	16.82	15.81	1.47
372.000	16.08	15.46	3.64				
372.125	16.29	14.87	3.92	380.000	16.09	15.93	1.23
372.250	16.06	15.19	3.76	380.125	16.25	15.64	.84
372.375	16.26	15.03	3.62	380.250	15.99	15.38	.99
				380.375	15.96	16.29	.79
372.500	16.06	14.60	3.96	380.500	15.73	15.97	.76
372.625	15.80	14.83	3.40	380.625	15.97	16.38	.71
372.750	15.32	14.47	3.04	380.750	15.37	15.17	.84
372.875	14.96	14.04	3.05	380.875	15.13	14.67	1.45
373.000	14.79	13.79	3.22	381.000	15.22	14.49	.42
373.125	14.69	13.56	2.89	381.125	15.43	14.79	1.15
373.250	14.35	13.06	3.59				
373.375	14.37	13.13	3.83	381.250	15.36	14.67	.63
373.500	14.06	12.88	2.80	381.375	15.03	15.25	.42
373.625	14.54	12.77	3.07	381.500	14.83	14.73	.35
				381.625	14.91	14.76	.34
373.750	14.58	13.20	3.50	381.750	15.08	15.24	.61
373.875	14.68	13.56	3.87	381.875	15.10	14.58	.73
374.000	14.41	13.35	2.56	382.000	15.15	14.99	.78
374.125	14.46	13.28	3.47	382.125	15.52	14.81	.48
374.250	13.93	12.83	2.97	382.250	14.73	13.77	.78
374.375	13.85	12.15	2.82	382.375	13.83	13.70	.48

TABLE 3. *Extinction coefficients of* NO_2 *and* N_2O_4, *180–410 nm at 298 K and 235 K,* ϵ *in* cm^{-1} *(atm at 273 K)*$^{-1}$ *base* e—Continued

Wavelength (nm)	Ext. coeff. NO_2 298 K	Ext. coeff. NO_2 235 K	Ext. coeff. N_2O_4	Wavelength (nm)	Ext. coeff. NO_2 298 K	Ext. coeff. NO_2 235 K	Ext. coeff. N_2O_4
382.500	14.16	13.56	.88	390.500	16.07	15.25	
382.625	14.22	13.96	1.08	390.625	15.79	15.21	
382.750	14.30	13.65	.67	390.750	15.93	14.57	
382.875	14.70	14.94	.85	390.875	15.42	14.76	
383.000	14.44	14.45	1.10	391.000	15.67	14.67	
383.125	14.39	13.98	1.17	391.125	15.94	15.41	
383.250	14.83	14.88	1.07				
383.375	14.62	14.10	.61	391.250	16.19	15.05	
383.500	14.58	13.91	.99	391.375	15.67	14.94	
383.625	15.27	13.72	.71	391.500	16.73	15.80	
				391.625	17.68	16.79	
383.750	15.72	14.60	.84	391.750	18.49	17.50	
383.875	15.23	14.96	.52	391.875	17.17	17.14	
384.000	16.04	15.17	1.24	392.000	16.26	15.83	
384.125	15.16	14.48	.59	392.125	16.14	15.18	
384.250	15.78	14.80	.57	392.250	16.51	15.48	
384.375	15.89	15.71	.34	392.375	16.10	14.95	
384.500	15.96	15.70	1.31				
384.625	16.28	15.51	.80	392.500	16.68	15.53	
384.750	17.18	16.21	.91	392.625	16.22	14.79	
384.875	16.58	16.91	.79	392.750	16.13	15.06	
				392.875	15.64	14.96	
385.000	15.97	15.55	0.69	393.000	14.66	13.86	
385.125	15.28	14.91	.52	393.125	14.47	13.53	
385.250	15.68	14.86	.53	393.250	13.98	12.81	
385.375	15.97	15.30	.99	393.375	14.57	13.79	
385.500	15.60	15.07	1.07	393.500	14.76	13.72	
385.625	16.87	16.03	0.91	393.625	15.04	14.33	
385.750	16.40	15.90	.90				
385.875	15.36	14.96	1.12	393.750	14.53	14.43	
386.000	14.80	14.90	1.00	393.875	14.78	14.05	
386.125	14.98	14.46	.61	394.000	14.90	14.49	
				394.125	14.53	13.69	
386.250	15.03	14.06	1.33	394.250	14.28	13.30	
386.375	14.43	13.49	0.69	394.375	14.31	13.61	
386.500	14.30	13.74	.25	394.500	14.07	13.15	
386.625	14.66	14.13	.22	394.625	13.91	12.88	
386.750	15.11	13.76	.41	394.750	15.00	13.89	
386.875	15.16	14.75	.36	394.875	15.62	14.13	
387.000	15.06	15.00	.99				
387.125	15.98	15.36	.78	395.000	15.83	15.10	
387.250	15.58	15.58	.71	395.125	15.83	14.98	
387.375	16.22	15.54	.41	395.250	16.27	15.99	
				395.375	17.46	15.94	
387.500	15.89	15.62	.12	395.500	16.70	15.62	
387.625	16.08	15.96	.15	395.625	17.21	16.42	
387.750	15.91	15.65	.96	395.750	17.25	16.58	
387.875	16.24	16.09	.36	395.875	17.07	16.60	
388.000	16.07	14.98	.47	396.000	16.52	16.03	
388.125	15.49	15.31	.76	396.125	15.92	15.44	
388.250	15.60	14.57	.90				
388.375	15.30	14.76	.41	396.250	16.05	14.89	
388.500	15.29	14.51	1.00	396.375	15.10	14.48	
388.625	15.24	14.91	0.72	396.500	15.03	14.02	
				396.625	14.91	13.09	
388.750	15.53	14.45	.68	396.750	14.53	13.71	
388.875	16.11	15.45	.99	396.875	14.53	13.93	
389.000	16.19	16.01	1.22	397.000	15.23	13.51	
389.125	16.86	16.08	0.38	397.125	14.29	13.34	
389.250	16.24	15.96	.30	397.250	14.43	13.89	
389.375	16.31	15.85	.82	397.375	14.07	13.17	
389.500	16.22	15.05	.71				
389.625	15.85	15.03	.57	397.500	14.88	14.46	
389.750	15.43	14.58	.17	397.625	15.97	15.27	
389.875	16.17	15.60	.39	397.750	16.66	16.13	
				397.875	17.32	17.31	
390.000	16.13	14.77	.76	398.000	17.22	17.33	
390.125	16.29	15.46		398.125	17.97	17.71	
390.250	16.68	15.25		398.250	18.39	17.13	
390.375	16.26	15.59		398.375	18.60	17.99	

TABLE 3. *Extinction coefficients of* NO_2 *and* N_2O_4, *180–410 nm at 298 K and 235 K,* ϵ *in* cm^{-1} *(atm at 273 K)*$^{-1}$ *base* e—Continued

Wavelength (nm)	Ext. coeff. NO_2 298 K	Ext. coeff. NO_2 235 K	Ext. coeff. N_2O_4	Wavelength (nm)	Ext. coeff. NO_2 298 K	Ext. coeff. NO_2 235 K	Ext. coeff. N_2O_4
398.500	17.87	16.56		404.375	15.40	13.80	
398.625	17.27	16.39		404.500	14.78	13.39	
				404.625	15.40	14.40	
398.750	15.94	15.39		404.750	17.60	16.29	
398.875	15.20	14.20		404.875	15.95	15.34	
399.000	15.15	13.66					
399.125	14.83	14.27		405.000	16.99	16.02	
399.250	14.68	13.17		405.125	18.17	17.67	
399.375	15.41	13.25		405.250	16.44	17.02	
399.500	16.05	14.44		405.375	16.42	15.29	
399.625	15.92	15.48		405.500	15.58	14.35	
399.750	17.30	15.85		405.625	14.50	13.05	
399.875	18.09	17.51		405.750	14.72	13.33	
				405.875	15.44	13.63	
400.000	18.17	17.91		406.000	14.49	13.25	
400.125	17.89	17.91		406.125	15.36	14.61	
400.250	17.27	16.78					
400.375	17.98	17.08		406.250	14.93	13.63	
400.500	17.61	16.01		406.375	13.42	11.96	
400.625	17.21	16.43		406.500	13.62	12.46	
400.750	17.51	16.30		406.625	12.67	11.98	
400.875	17.44	16.66		406.750	13.17	11.87	
401.000	17.54	16.92		406.875	12.85	11.68	
401.125	17.02	15.86		407.000	12.71	11.02	
				407.125	12.60	11.68	
401.250	16.92	15.24		407.250	13.09	11.36	
401.375	16.87	15.82		407.375	13.42	11.90	
401.500	16.64	14.97					
401.625	16.15	15.23		407.500	13.89	12.23	
401.750	16.53	15.13		407.625	15.06	14.05	
401.875	15.56	14.85		407.750	15.08	13.26	
402.000	15.35	14.52		407.875	16.88	15.77	
402.125	14.69	13.02		408.000	16.03	14.65	
402.250	14.55	13.49		408.125	17.93	16.15	
402.375	14.71	13.68		408.250	18.42	17.77	
				408.375	18.71	17.86	
402.500	14.31	12.83		408.500	18.01	16.73	
402.625	13.66	12.37		408.625	17.29	16.21	
402.750	14.02	13.16					
402.875	13.91	13.03		408.750	16.47	16.01	
403.000	13.72	12.85		408.875	16.82	15.83	
403.125	14.17	12.63		409.000	15.86	13.82	
403.250	13.85	12.58		409.125	15.37	14.08	
403.375	14.31	13.62		409.250	16.66	15.58	
403.500	14.26	13.28		409.375	16.54	15.05	
403.625	15.02	13.42		409.500	17.27	15.47	
				409.625	15.76	14.67	
403.750	15.98	15.11		409.750	15.41	13.72	
403.875	16.54	15.45		409.875	15.17	13.44	
404.000	16.31	15.15					
404.125	15.64	14.74		410.000	15.52	14.31	
404.250	15.28	13.87		410.125	17.96	15.82	
				410.250	18.08	17.75	

4. Appendix A

Consider a volume, V, in which is measured a certain pressure, P_T, of an $NO_2-N_2O_4$ equilibrium mixture at temperature T. The number of nitrogen atoms is $N=(V/RT)\ (P_1+2P_2)$ where P_1 and P_2 refer to the pressure of monomer and dimer, respectively. If we follow the procedure utilized in the experiments, the gas is now transferred completely to the cell with volume, V', and subsequently vaporized. A fraction (f) of the cell is maintained at a reduced temperature, T^* and the remainder at T. The number of nitrogen atoms in the warm fraction is then

$$N=\frac{(1-f)V'}{RT}\ (P_1'+2P_2') \tag{1}$$

while the number in the cold portion is:

$$N=\frac{fV'}{RT^*}\ (P_1^*+2P_2^*). \tag{2}$$

Since the number of N atoms is conserved:

$$(3)\quad \frac{V'}{R}\left[\left(\frac{1-f}{T}\right)(P_1'+2P_2')+\frac{f}{T^*}(P_1^*+2P_2^*)\right]=\frac{V}{RT}(P_1+2P_2).$$

If we set $(1-f)/T=a$ and $f/T^*=b$, eq (3) reduces to:

$$(4)\quad aP'[X_1'+2(1-X_1')]+bP^*[X_1^*+2(1-X_1^*)]=\frac{V}{V'}\frac{1}{T}(P_1+2P_2)$$

where X_1 is the mole fraction of NO_2. Since the volume ratio, V/V', may be measured, the RHS of eq (4) is known. Recognizing that the pressure throughout the cell is constant, $P'=P^*$, and eq (4) may be solved by iteration. An initial estimate is made of the total pressure in the absorption cell and then using the equilibrium constant, K_p, appropriate to the temperature (either room or reduced), a new pressure may be obtained. The process is continued until successive calculations yield similar results. Typical values for our apparatus are $V/V'=8.9$ and $f=0.5$.

5. Appendix B

Chao et al. [1] calculated the thermodynamic properties of NO_2 and N_2O_4. The method involved a statistical thermodynamic calculation based upon a rigid rotor and harmonic oscillator model. Equilibrium constants were obtained from the thermodynamic functions; from a least squares fit the following empirical relationship was obtained.

$$(1)\quad \log_{10}K_{eq}=0.3199+2.945\times10^{-5}T-2768.85/T+5.841484\log T-7.89560\,[(1+100/T)\log(1+T/100)]$$

Chao et al., note the standard deviation between log K calculated from (1) versus that from thermodynamic functions is 0.00055, and agreement between log K from (1) and experimental measurements is excellent.

The equilibrium constants used here have been compared with those derivable from the molecular parameters used in the JANAF Thermochemical Tables.[5] Chao's expression (1) yields K_p uniformly 4 percent higher than the JANAF value. K_p from (1) is also in good agreement with the experimental K_p's reported by Vosper,[6] agreeing within 4 percent below 290 K. In both cases the agreement is well within the accuracy of the available thermochemical and molecular data.

6. References

[1] Chao, J., Wilhoit, R. C., Zwolinski, B. J., Thermodynamic Properties of Nitrogen Oxides and Their Mixtures, Thermodynamic Research Center, Texas A & M University, June 9, 1972, Typescript.

[2] Hall, T. C., Jr., and Blacet, F. E., J. Chem. Phys. **20,** 1745 (1952).

[3] Nakayama, T., Kitamura, M. Y., and Watanabe, K., J. Chem. Phys. **30,** 1180 (1959).

[4] Verhoek, F. H., and Daniels, F., J. Am. Chem. Soc. **53,** 1250 (1931).

5] Johnston, H., and Graham, R., J. Phys. Chem. **77,** 62 (1973). H. Johnston and R. Graham, Can. J. Chem. **52,** 1415 (1974).

[6] Laufer, A. H., and Keller, R. A., J. Am. Chem. Soc. **93,**61 (1971).

[7] (a) White, J. U., J. Opt. Soc. Am. **32,** 285 (1942); (b) Bernstein, H. J., and Herzberg, G., J. Chem. Phys. **16,** 30 (1948).

[8] Bass, A. M., and Laufer, A. H., J. Photochem. **2,** 465 (1973/74).

[9] Bayes, K. D., private communication.

[5] JANAF Thermochemical Tables, D. R. Stull and H. Prophet, eds., 2nd Edition, NSRDS–NBS **37,** June, 1971.

[6] A. J. Vosper, J. Chem. Soc. A325, 1970.

(Paper 80A2–884)

JOURNAL OF RESEARCH of the National Bureau of Standards—A. Physics and Chemistry
Vol. 80A, No. 2, March–April 1976

A Study of the Chemiluminescence of the $Pb + O_3$ Reactions*

M. J. Kurylo, W. Braun, S. Abramowitz, and M. Krauss

Institute for Materials Research, National Bureau of Standards, Washington, D.C. 20234

(December 8, 1975)

The chemiluminescent reaction of $Pb + O_3$ has been studied using both "cold" and vibrationally excited O_3. Emission from new states *a* and *b* has been observed in addition to the A and B states. The reaction of vibrationally excited O_3 with Pb to yield PbO(A) appears to be faster than that using "cold" O_3.

Key words: Chemiluminescence; electronic states; gas kinetics; laser enhanced reactions; O_3; PbO.

1. Introduction

The results of our recent studies on laser enhanced reactions have shown that vibrational energy in a reactant molecule can reappear as excitation in a product species. For example, emissions from both NO_2^* and SO_2^* produced in the reactions of NO and SO with O_3 were observed to shift to shorter wavelength when the O_3 was vibrationally excited using a CO_2 laser [1, 2].[1] Because of the spectroscopic complexities of the triatomic molecules, NO_2 and SO_2, our intention in the present study was to investigate a chemiluminescent reaction producing a diatomic product which would be, in principle, easier to characterize spectroscopically. The metal atom-oxidant systems represent a class of such reactions. A significant number of these have been investigated to date because of their potential as chemical lasers. We report herein some observations on the reaction

$$Pb + O_3 \rightarrow PbO + O_2. \qquad (1)$$

While the information obtained from studying the infrared laser-enhanced reaction component is minimized by the overall reaction complexity, it does nevertheless provide some additional insight into this reaction system. This information coupled with new high pressure spectroscopic results complement the detailed low pressure investigation by Oldenborg, Dickson, and Zare (ODZ) [3].

*This work was supported in part by the U.S. Air Force Office of Scientific Research.

[1] Figures in brackets indicate the literature references at the end of this paper.

2. Experimental Detail

The furnace, reaction cell, fast flow pumping system, CO_2 laser, and spectrometer are shown schematically in figure 1. Lead vapor, produced from a resistively heated crucible containing lead metal enters the glass reaction chamber in an Ar diluent stream. The effluent from a commercial O_3 generator, consisting of 4 percent O_3 in O_2 is mixed with Ar and flows past the cell windows (to eliminate window deposits) into the cell. There it diffusively mixes with the lead-argon flow. The temperature of the crucible (as measured by a thermocouple probe) ranges from 900–1000 K while the temperature in the flame reaction zone varies from 500–600 K. The total pressure in the cell varies from 1 to 5 torr (1 torr = 133.3 Pa) with the flow through the furnace being anywhere from 20 to 50 percent of the total flow.

The 0.5 cm diameter beam from a CO_2 laser tuned to the 9.6 μm P(30) transition is square wave chopped and traverses the flame exciting ν_3, the asymmetric stretching mode of O_3 (1043 cm^{-1}). The chemiluminescence from the $Pb + O_3$ reaction is monitored through a spectrometer-photomultiplier assembly. The photomultiplier output is fed through a series of pulse amplifiers and voltage discriminator into a dual counter, one channel of which records the "laser-on" signal and the other the "laser-off". A printout from these counters is synchronized with the spectrometer wavelength-scan-drive thereby facilitating the recording of the modulation spectrum vs wavelength. The normal spectral ("laser-off") emission is automatically obtained from the "laser-off" counter.

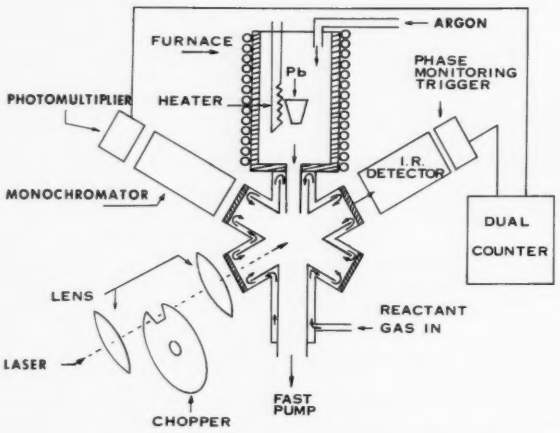

FIGURE 1. *Schematic of the chemiluminescent flow reaction apparatus.*

3. Results

In contrast to the spatially sharp diffusion flame observed for the $Ba + O_3$ (or N_2O) reaction, the $Pb + O_3$ flame is quite diffuse (apparently reaction limited). It is brightest in the high temperature zone at the furnace nozzle, diminishes with decreasing temperature (increasing distance from the nozzle), and persists for some two to three feet into the pumping system. These observations suggest a reaction rate for $Pb + O_3$ which is considerably slower than gas kinetic. The spectrum which we observe at several torr total pressure partly resembles the low pressure spectrum obtained by ODZ and reproduced by us in a similar quasi-beam apparatus. The short wavelength end of the more complete spectrum (fig. 2) can be identified from

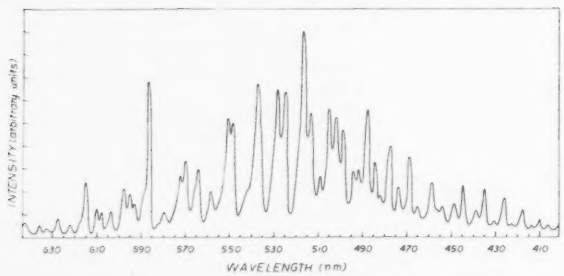

FIGURE 2. *Chemiluminescence spectrum for the* $Pb(v) + O_3$ *reaction.*

the low (submicron) pressure spectrum in that it is less diffuse. The long wavelength portion between 480 nm and 595 nm is almost entirely the new *a* state recently characterized by ODZ. At still longer wavelengths, our spectrum differs from that of ODZ in that we observe a series of strong lines which do not agree with $a \rightarrow X$, $A \rightarrow X$, or $B \rightarrow X$, but rather appear to originate from a new state observed via six weak lines by ODZ and identified as *b* by them. This *b* state is seen more intensely in our high pressure spectrum. This series of lines in our spectrum can be fit to the expression:

$$\nu(v',\ v'') = 16315 + 441.0v' - \{717.7v'' - 3.53v''^2\}$$

where the lower state constants have been taken from Rosen's compendium [4]. The spectral constants given here and in tables 1 and 2 for the *a*, A, and B state are not as well determined as previous values given in references [1] and [4].

TABLE 1. *Observed band heads and assignments in* cm^{-1}

ν(obs)	ν(calc)	assignment
24143	24116	B (4,0)
23590	23640	B (3,0)
23392	23402	B (4,1)
23170	23157	B (2,0)
22957	22926	B (3,1)
22636	22665	B (1,0)
22457	22443	B (2,1)
22178	22166	B (0,0)
21954	21951	B (1,1)
21636	21660	*b* (12,0)
21474	21452	B (0,1)
21169	21211	*b* (11,0)
21079	21065	B (5,5)
20877	20870	*a* (11,0)
20721	20745	B (0,2)
20614	20616	B (4,5)
20442	20445	*a* (10,0)
20338	20314	*b* (9,0)
20149	20156	*a* (11,1)
20024	20014	*a* (9,0)
19904	19867	*b* (8,0)
19743	19731	*a* (10,1)
19585	19578	*a* (8,0)
19467	19449	*a* (11,2)
19128	19138	*a* (7,0)
19015	19023	*a* (10,2)
18688	18692	*a* (6,0)
18515	18530	*b* (5,0) Sh.
18305	18323	*a* (10,3)
18238	18241	*a* (5,0)
17986	17978	*a* (6,1)
17790	17785	*a* (4,0)
17615	17630	*a* (10,4)
17535	17527	*a* (5,1)
17319	17325	*a*(3,0)
17212	17199	*b* (2,0)
17108	17052	*b* (8,4)
17033	17108	*b* (5,2)
16915	16853	*b* (6,3)
16858	16859	*a* (2,0)
16773	16757	*b* (1,0)
16614	16664	*b* (4,2)
16488	16485	*b* (2,1)
16434	16367	*b* (10,5)
16297	16315	*b* (0,0)
16215	16220	*b* (3,2)
16108	16160	*b* (6,4)
15773	15778	*b* (2,2)
15623	15601	*b* (0,1)
15672	15715	*b* (5,4)
15363	15335	*b* (1,2)

The calculated ν have been generated from a least-squares treatment of the observed data using Rosen's constants for the X state. The generating equations are:

a. $\nu_{(v',\,v'')} = 15912 + 478.4\,v' - 2.5\,v'^2 - \{717.7\,v'' - 3.53\,v''^2\}$
b. $\nu_{(v',\,v'')} = 16315 + 441.0\,v' - \{717.7\,v'' - 3.53\,v''^2\}$
B. $\nu_{(v',\,v'')} = 22166 + 502.0\,v' - 3.8\,v'^2 - \{717.7\,v'' - 3.53\,v''^2\}$

TABLE 2. *Observed band heads for the modulated spectrum* (A → X) *in cm*$^{-1}$

ν(obs)	ν(calc)	v'	v''
17592	17599.3	0	3
18319	18299.3	0	2
19015	19006.4	0	1
19708	19720.6	0	0
18005	18041.	1	3
18748	18741.	1	2
17765	17789.3	2	4
18470	18482.3	2	3
19216	19182.4	2	2
19885	19889.5	2	1
20644	20603.6	2	0
18925	18923.2	3	3
19611	19623.3	3	2
20350	20330.4	3	1
17972	17984.9	4	5
18642	18670.8	4	4
19384	19363.8	4	3
20064	20063.8	4	2
20773	20770.9	4	1
21463	21485.1	4	0
19826	19803.9	5	3
20517	20504.	5	2
21191	21211.1	5	1
18783	18864.8	6	5
19554	19550.7	6	4
20226	20243.7	6	3
20947	20943.8	6	2
21737	21650.9	6	1
20024	19990.1	7	4
18403	18392.5	8	7
19015	19064.3	8	6
20434	20429.1	8	4
18854	18831.	9	7
19497	19502.9	9	6
17940	17946.8	10	9
18573	18604.5	10	8
19271	19269.2	10	7
19964	19941.1	10	6
20584	20619.9	10	5
21350	21305.9	10	4

The calculated ν have been generated from a least-squares treatment of the data using Rosen's constants for the X state. The generating equation is:

$$\nu(v', v'') = 19721 + 441.9\, v' - 0.20\, v'^2 - \{717.7\, v'' - 3.53\, v''^2\}$$

A definite vibrational assignment for an electronic state, for which a rotational analysis has not been observed, requires the measurement of a vibrational isotope shift. Lacking data of this type one tries to assign band heads such that both (0, v'') and (v', 0) levels are observed. The assignment hypothesized by ODZ on the basis of six observed transitions in a (v', 0) transition has placed T_{00} of the b state about one vibrational quanta above T_{00} of the a state. In this study 20 band heads have been observed that can be assigned to b state. In addition to the (v', 0) band heads, other bands have been observed with $v''=1$, 2, 3, 4, 5. The hypothesis regarding the separation of the a and B states is supported by arguments given later.

Although considerable intensity is observed for B − X transition, the zeroth level of this state lies very close to the thermodynamic threshold for the reaction

$$Pb(J=0) + O_3 \rightarrow PbO(B) + O_2.$$

The dissociation energy (D_0°) of PbO is given by Rosen [4] as 30,920 ± 500 cm^{-1}. Using $\Delta Hf°$(298 K) of O_3 and O as 34.1 and 59.5 kcal/mol as recommended by Wagman et al. [5], one computes 22036 cm^{-1} for the exothermicity of the reaction.

$$Pb\,(J=0) + O_3 \rightarrow PbO(X'\Sigma^+) + O_2$$

This to be compared to 22174 cm^{-1} of the $\nu_{(0,0)}$ level of the B state. Oldenborg and Zare have suggested that production of this state results from reaction of Pb ($J=1$) present in their experiments due to an electric discharge in their furnace. The strong B → X emission observed in our high pressure experiment was found to vary markedly with the oven temperature. The observed B → X emission increase over that emission from either a or b → X with increasing temperature obeyed an Arrhenius-type formulation with an activation energy of some 10 kcal (i.e. nearly equal to the energy difference between $J=0$ and $J=1$ multiplet components of Pb). This observation suggests that Pb ($J=1$) is produced thermally in our furnace as opposed to its possible production via secondary processes, e. g.

$$PbO^* + Pb\,(J=0) \rightarrow PbO + Pb\,(J=1).$$

If PbO(B) is indeed produced through reaction of Pb ($J=1$) with ozone, the rate of this reaction must be extremely fast to compete with the deactivation process

$$Pb\,(J=1) + O_2 \rightarrow Pb\,(J=0) + O_2$$

since the deactivation proceeds with a high rate constant and the O_2 pressure is twenty times that of O_3 under our usual experimental conditions.

Part of the modulation spectrum is reproduced in figure 3. This spectrum, which has been smoothed,

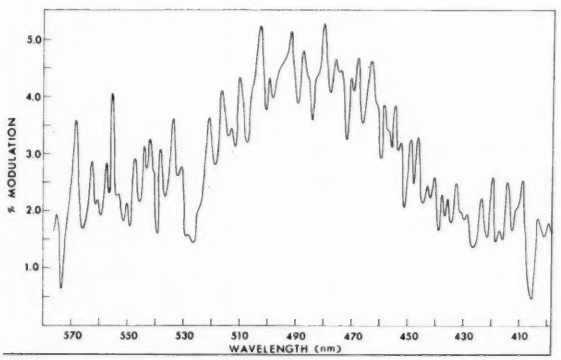

FIGURE 3. *Smoothed modulation spectrum (the component of the emission which varies with laser excitation of* O_3*) of the* Pb(v) + O_3 *reaction.*

represents only that component of the chemiluminescent emission which varies with the laser excitation of O_3 (i.e. only that component which either increases or decreases due to a change in reaction rate with reactant vibrational excitation). Thus, if the emission originated only from a single electronic state, the modulation spectrum would appear as a quasi-continuum with possibly some small structure due to sharp changes in population of one vibrational line relative to an adjacent one. The large amount of structure in figure 3 indicates the presence of emission from at least two electronic states. One might speculate that at the longer wavelength, where the normal spectrum consists mainly of a and b emission lines, this modulation structure could reveal an increase or decrease of b emission lines relative to a emission lines (or vice versa). However, the peaks (or valleys) in the modulation spectrum do not agree well with either a or b state emission lines. More surprisingly, they agree much better with $A \rightarrow X$ transitions. We therefore tentatively identify the modulation spectrum as a quasi continuum due to $a \rightarrow X$ and $b \rightarrow X$ emissions at long wavelengths (possibly some $B \rightarrow X$ short wavelength) with structure due to $A \rightarrow X$ emission lines superimposed throughout the entire wavelength range. This suggests that vibrational excitation in O_3 increases the production of the a, b, and possibly the B state of the PbO all to some small degree, while increasing A state production most significantly. We must emphasize, however, that the assignment of A state responsibility for structure in the modulation spectrum is tentative since the modulation data are difficult to obtain, require long integration times, and should be obtained in the low (submicron) pressure region where only the a and B states have been observed. Nevertheless, we can speculate on the production of PbO (A) in the laser excited reaction. It is possible that as a result of laser excitation of O_3 forming $O_3\dagger$ the reaction with Pb ($J=1$) now produces PbO (B) in higher vibrational levels. These can then be collisionally transferred to the A state which is seen in emission. A second equally likely possibility is that the vibrational energy in O_3 increases the rate of A state production directly at the expense of one or more of the other reaction channels.

From the numerical value of the percent modulation in the laser experiments (i.e. the continuum region assigned to a and b state enhancement) we can calculate a rate constant enhancement of approximately a factor of two. This is obtained by comparing the percent modulation of both the $Pb+O_3\dagger$ and $NO+O_3\dagger$ reactions in this apparatus under identical experimental conditions.

We can obtain a very rough estimate of the quantum yield of a and b state production in the following manner. First we assume the reaction of O_3 with Pb ($J=1$) funnels entirely into PbO (B), (i.e. quantum yield of unity). From figure 2 we see that the $a+b$ emission intensity is comparable to the intensity of PbO (B). However, at the oven temperature of 1000 K only 1 part of 10^5 of the Pb atoms are in $J=1$. This would imply a quantum yield of $a+b$ due to Pb ($J=0$) of about 10^{-5} assuming Pb ($J=0$) and Pb ($J=1$) reacted with O_3 with the same rate constant. The observation of the decay of chemiluminescence over several feet in our flow tube points to a slow rate of reaction for Pb ($J=0$) while the fact that the reaction of Pb ($J=1$) must compete favorably with its deactivation channels speaks for a very fast (collision frequency) rate of reaction for Pb ($J=1$). Assuming a reaction efficiency of 10^{-2} for the Pb ($J=0$) reaction in the spectrometer observation zone increases the quantum yield for $a+b$ state production by a factor of 100 to 10^{-3}. We compare this to the ODZ upper limit of 10^{-2} obtained under the assumption of a fast reaction rate for Pb ($J=0$). A slower reaction rate would unfortunately raise their quantum yield (in greater disagreement with our 10^{-3} estimate). However, our observation of a large luminescent region is not necessarily contradictory to ODZ's estimate of a fast reaction rate because of the different temperature regions of the two studies. In the quasi-beam configuration, Pb exits the furnace at very high temperature (> 1000 K) and collides with O_3 with much higher kinetic energy than in our high pressure experiments (kinetic energy of 600 K at the nozzle tip and decreasing rapidly to 400 K downstream of the mixing zone).

4. Analysis and Conclusions

Oldenborg et al. identify the two (0^-, 1) components of the $^3\Sigma^+$ as b and a, respectively. This energy ordering is consistent with the present observations including an analysis of the relative intensities of the a and b transitions. A theoretical analysis can also be made of the spin-spin splitting constant of the $^3\Sigma$ state which shows that the 0^- component must be at a higher energy than the 1 component. The spin-spin splitting for a molecule containing a heavy atom is dominated by the second-order spin-orbit coupling to nearby electronic states. Spin-orbit coupling will occur for $\Delta\Omega=0$ and couple the 0^- component to $^3\pi(0^-)$, $^1\Sigma^-(0^-)$ and the 1 component to $^3\pi(1)$, $^3\Sigma^-(1)$, $^1\pi(1)$. Note that there is no first-order spin-orbit coupling between the $^3\Sigma^+(1)$ and $^3\Delta(1)$ states. Using a hamiltonian of the form

$$\sum_i \mathbf{l}_i \cdot \mathbf{s}_i,$$

the spin-orbit interaction is reduced [6] to the one-electron spin-orbit integrals given in table 3.

TABLE 3. *Molecular spin-orbit interactions*

$\Omega = o^-$	
$^3\Sigma^+ - {}^3\pi$	$-1/2\sqrt{2} < \pi \\| \sigma >$
$^3\Sigma^+ - {}^1\Sigma^-$	$-1/2 < \pi \\| \pi > + 1/2 < \pi^* \\| \pi^* >$
$\Omega = 1$	
$^3\Sigma^+ - {}^3\pi$	$1/2\sqrt{2} < \pi \\| \sigma >$
$^3\Sigma^+ - {}^1\pi$	$-1/2\sqrt{2} < \pi \\| \sigma >$
$^3\Sigma^+ - {}^3\Sigma^-$	$-1/2 < \pi \\| \pi > -1/2 < \pi^* \\| \pi^* >$

Interaction with the $^3\pi$ state shifts both components

equally and can be ignored. The $^1\pi(1)$ interaction is small both because the σ and π orbitals are primarily localized on the oxygen atom, and there is a large energy separation between the $^1\pi$ and $^3\Sigma^-$ states. The spin-spin splitting constant is dominated by the difference between the $^3\Sigma^-(1)$ and $^1\Sigma^-(0^-)$ interactions. From table 3 we see that the $^3\Sigma^-$ interaction is necessarily the largest term. This demonstrates that the $^3\Sigma^-(1)$ component is lower in enrgy than $^3\Sigma^-(0)$.

Quantitative estimates of the spin-spin splitting cannot be made from molecular spin-orbit parameters since little is known for the PbO excited states. Using the atomic spin-orbit parameter [6], assuming atomic populations by comparing calculations on PbO [7] and CO [8], and excitation energies for the perturbing states [9], a spin-spin splitting of about 1000 cm^{-1} is obtained. This qualitatively confirms the analysis of the emission spectrum and the assignment of the *a* and *b* states. Assuming that the molecular integrals will scale with the atomic spin-orbit parameters, the splitting in the case of SnO would be an order of magnitude less than the value for PbO while GeO is about two orders of magnitude less.

There are two mechanisms which could give intensity to the dipole forbidden $b \rightarrow X$ transition, spin-rotation and electronic rotational coupling. For large spin-spin splitting the spin-rotation coupling between the *a* and *b* states is negligible even for *J* as large as 100 (one expects the most probable value of *J* to be 24 for $T = 500$ K).

The electronic-rotation coupling matrix elements between a $^3\Sigma^+$ and $^3\pi$ state are given by Kovacs [11]. The coupling is proportional to $4B^2J(J+1)/\Delta E$ for the Hund's case *a* representation where ΔE is the difference in the electronic energies and *B* is the rotational constant. Since $\Delta E \sim 5000$ cm^{-1} and $T \sim 500$ K, this coupling is significant but can only be ascertained quantitatively if the complete mixing between $^3\Sigma^+$ and $^3\pi$ states is considered. It is likely that the *b* state transition probability would increase with temperature.

Since all the observed transitions to the ground state ultimately derive their intensity from spin-orbit mixing to the higher singlet excited states, it is well to remember that the transitions between $^3\pi$ and $^3\Sigma^+$ states are electric-dipole allowed and should have significant intensity even though they are in the infrared (~ 5000 cm^{-1}).

The present results point to a slow overall reaction of Pb ($J = 0$) with O_3 as well as a small quantum yield for production of PbO excited electronic states. Since the reactant states can couple to only one final product state, adiabatically this must be PbO (X) and O_2 (X). Excited PbO states are the result of a nonadiabatic transition. The enhanced reactivity of Pb ($J = 1$) into the excited B state reflects the additional channels that are now available but the population yield of the various excited states remains puzzling.

Our observations at high pressure are somewhat different from those of Oldenborg et al. In particular, we find more intensity in the *b* state than they did. Their observations were made before collisions took place. In the present case many collisions can occur before the emitted light is observed. Two general explanations can be advanced for the different observations. The effective rotational temperatures can be very different. Pressure effects can also be important both by collisionally deactivating other excited states into the *b* state or by collisionally inducing the radiative transition.

Finally, we note that the enhancement or even initial formation of the A state by laser excitation of the ozone is not understood. In order to further unravel these questions, additional experiments must be carried out in conjunction with a more extensive theoretical investigation of the Group IV oxides.

5. References

[1] Braun, W., Kurylo, M. J., Kaldor, A., and Wayne, R. P., J. Chem. Phys. **61**, 461 (1974).

[2] Kaldor, A., Braun, W., and Kurylo, M. J., J. Chem. Phys. **61**, 2496 (1974).

[3] Oldenborg, R. C., Dickson, C. R., and Zare, R. N., J. Mol. Spectroscopy, **58**, 283 (1975).

[4] Rosen, B., ed., Spectroscopic Data Relative to Diatomic Molecules (Pergamon Press, New York, 1970).

[5] Wagman, D. D., Evans, W. H., Parker, V. B., Halow, I., Bailey, S. M., and Schumm, R. H., Selected Values of Chemical Thermodynamic Properties, Nat. Bur. Stand. (U.S.), Tech. Note 270–3, 266 pages (Jan. 1968).

[6] Field, R. W., and Lefebvre-Brion, H., Acta Phys. Hung. **35**, 51 (1974).

[7] Lawrence, G. M., Astrophys. J. **148**, 261 (1967).

[8] Schwenzer, G. M., Liskow, D. H., Schaefer, H. F., Bagus, P. S., Liu, B., McLean, A. D., and Yoshimine, M., J. Chem. Phys. **58**, 3181 (1973).

[9] Huo, W. M., J. Chem. Phys. **45**, 1554 (1966).

[10] Barrow, R. F., Deutsch, J. L., and Travis, D. N., Nature **191**, 374 (1961).

[11] Kovacs, I., Rotational Structure in the Spectra Diatomic Molecules (American Elsevier Publ., New York, 1969).

(Paper 80A2–885)

JOURNAL OF RESEARCH of the National Bureau of Standards—A. Physics and Chemistry
Vol. 80A, No. 2, March–April 1976

Structure- and Solvent-Property Relationships for the Electronic Energies of Charge-Transfer Complexes Between Certain Benzene Derivatives *

Harold Argentar **

Institute for Materials Research, National Bureau of Standards, Washington, D.C. 20234

(November 26, 1975)

A chemical model is proposed for describing charge-transfer complexes between aromatic amines and electron-accepting benzene derivatives containing a group having a double- or triple-bond conjugated with the benzene ring. According to this model, an electron migrates from the nitrogen atom of the amine to one of the atoms of the multiple-bonded group during charge-transfer interaction.

Structure-property relationships were derived for correlating: (1), the transition energies of the complexes; (2), the ionization, or oxidation, potentials of the amines, and (3), the electron affinities or reduction potentials of the electron acceptors, with the electron-donating abilities of the substituents of the various compounds. Transition energies calculated from reported spectroscopic data for these complexes were correlated using equations derived in this study. Similarly correlated were reported data for the above properties of the amine and electron acceptor.

Equations were derived for correlating the effect of variation in solvent on the transition energies of the complexes. Correlation of reported spectroscopic data indicated that the greatest effect is caused by variation in the refractive index; of secondary importance was the change in dielectric constant.

Key words: Aromatic amine; benzene derivative; charge-transfer complex; dental materials; electron affinity; electron spin resonance spectroscopy; extrathermodynamic relationships; ionization potential; linear free-energy relationship; polarography; solvatochromic relationship; ultraviolet and visible spectroscopy.

1. Introduction

A number of reports on investigations of electron donor-acceptor (EDA) complexes in which aromatic amines function as the electron donor and other benzene derivatives function as the electron acceptor have appeared in the last twenty years [1–24].[1] (In this investigation, the term "aromatic amine" is limited to aniline and its derivatives, while compounds like benzylamine and naphthylamine are excluded.) Figure 1 shows the structures of the components of the complex discussed.

Practical application of the complexes between aromatic amines and electron-accepting benzene derivatives have been quite diverse in materials science and applied chemistry. In one investigation, the complexes were prepared for the purpose of obtaining materials with a greater mechanical strength than that possessed by the isolated components of the complex [17, 18, 21]. In other cases, the complexes were used as a tool for studying certain biochemical processes and in an analytical procedure [11, 13, 23, 24]. In some instances, complexes between aniline derivatives and other aromatic compounds have been shown to have undesirable properties, e.g., a considerable amount of color when present in otherwise acceptable composite filling materials designed for use in dentistry [25, 26].

Although such donor-acceptor complexes are of fundamental interest and have practical utility, an overall view of the physiochemical properties of these complexes as they vary with the natures of the substituents of the electron-donating amine and the electron acceptor and of the solvent has apparently not heretofore been undertaken. If a quantitative relationship between a measured physical property and structural and solvent parameters were effected, then a complex could be designed having the value of the physical property optimized over all possible variations in structure.

One of the most important properties of these complexes is the appearance of an intermolecular electronic

[1] Figures in brackets indicate the literature references at the end of this paper.

* This investigation was supported, in part, by Research Grant DE02494–09 to the American Dental Association Health Foundation from the National Institute of Dental Research and is part of the dental research program conducted by the National Bureau of Standards in cooperation with the American Dental Association Health Foundation. This paper is adapted from a thesis submitted to the American University, Washington, D.C., in partial fulfillment of the requirements for the M.S. Degree in Chemistry, April 1975.

** Research Associate, American Dental Association Health Foundation Research Unit at the National Bureau of Standards, Washington, D.C. 20234.

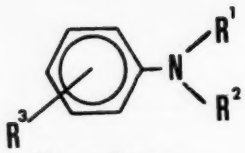

Electron-Donating
Aromatic Amine

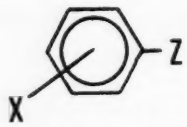

Electron-Accepting
Benzene Derivative

FIGURE 1. *Components of the Electron Donor-Acceptor Complex Studied in This Investigation.*

R^1 and R^2 are either H or $CR'R''R'''$, where R', R'' or R''' is any atom or group of atoms that is sufficiently small to allow for coplanarity of the benzene ring and the nitrogen substituent.
R^3 is any substituent in the *meta*- or *para*-position; if in the *ortho*-position, the substituent must be small enough to allow for coplanarity of the benzene ring and the nitrogen substituents.
Z is a group of atoms containing a double- or triple-bond conjugated with the benzene ring.
X is any substituent, and X may be repeated so that multiply-substituted compounds are considered.

charge-transfer (*c-t*) transition observable by ultraviolet or visible light spectroscopy [1, 4]. The term "charge-transfer complexes" has therefore been applied to these complexes as well as to others that exhibit this phenomenon [27]. "The property of charge-transfer complexes which is normally most readily, and certainly most frequently, measured is the energy of the (usually lowest) intermolecular charge-transfer transition of the complex in solution" [28]. This energy, E_{ct}, is readily obtained by spectroscopic measurements using the relationship [29]:

$$E_{ct} = N_0 h \nu_{\max}^{ct} = N_0 hc/\lambda_{\max}^{ct}, \qquad (1)$$

where E_{ct} is the *c-t* transition energy per mole of the complex, N_0 is Avogadro's number, h is Planck's constant, $\nu_{\max}^{ct}$ is the frequency at which the differential absorption of the complex is a maximum [5], c is the speed of light in a vacuum and $\lambda_{\max}^{ct}$, the wavelength corresponding to $\nu_{\max}^{ct}$. The differential absorption is obtained by measuring the absorption of the complex relative to the sum of the absorptions of the individual components rather than to the absorption of the solvent as in the usual case [26].

It must be clearly realized that in addition to the charge-transfer transition occurring in a thermodynamically stable donor-acceptor complex, charge-transfer transitions may occur during a random encounter of the donor and acceptor. Orgel and Mulliken have referred to this phenomenon as "contact charge-transfer" [30]. If only contact charge-transfer occurs in a given material, then the experimentally determined thermodynamic formation constant for the hypothetical complex assumed to be present would be found to be essentially zero. For economy of words, both stable complexes and those interactions demonstrating charge-transfer transitions will be referred to as "charge-transfer complexes", or simply, "complexes". The results obtained in this investigation are thus not necessarily related to the thermodynamics of EDA complex formation and should be kept separate.

The principal purposes of this investigation were: (1), to derive equations suitable for correlating the electronic transition energies of complexes (in solution) between aromatic amines and compounds from one class of electron-accepting benzene derivatives with the properties of the substituents of the two compounds and the nature of the solvent and (2), to use these relationships for correlating previously reported transition energies (or transition energies calculated from previously reported frequencies, or wavelengths, at which maximum spectroscopic absorption occurs) of the complexes. The electron acceptors considered here are exemplified by aryl-substituted nitrobenzenes, cyanobenzenes, and benzoates, i.e., compounds in which an electron-accepting group possesses a double- or triple-bond that is conjugated with the benzene ring. This class contains those benzene derivatives that most readily accept electrons, e.g., 1,3,5-trinitrobenzene and 1,2,4,5-tetracyanobenzene.

In the course of this investigation, comparable equations were derived for correlating the ionization potentials, or oxidation potentials, of the aromatic amines and the electron affinities, or reduction potentials, of the aromatic compounds possessing a common electron-accepting group with structures in the respective series of compounds.

2. Transition Energies and the Natures of the Electron Donor and Acceptor—An Overview

Several equations have been derived relating the *c-t* transition energy to the natures of the donor and acceptor [31 and references contained therein]. The

simplest equation and probably the first to be derived is:

$$E_{ct} = N_0(IP - EA + C), \quad (2)$$

where IP is the ionization potential of the electron donor, EA is the electron affinity of the acceptor and C is a collective term for the solvation, polarization, and nonbonding contributions to the energy [32, 33]. As originally conceived, N_0 in eq (2) is absent and thus the energy computed is for one molecule of complex. As will be seen shortly, use of N_0 provides for the calculation of the energy on a molar basis, which is more convenient for correlation of chemical data.

3. Identification of the Reaction Sites of the Electron Donor and Acceptor

It will become apparent from the next section that, in order for the transition energies to be correlatable by the usual structure-property relationships, it is necessary to identify the reaction sites in the electron donor and acceptor and to determine if they remain the same as the structures of the reactant molecules change.

The first (and most generally accepted) hypotheses to be published regarding the locations of reaction sites in various molecules forming charge-transfer complexes were those by Mulliken in 1952 [34]. He considered electron transfer from an aliphatic amine to involve the non-bonded electrons on the nitrogen atom and therefore designated this class of compounds as n-donors. Similarly, if electron transfer to a vacant orbital of an electron acceptor occurred, then the acceptor was labeled a v-acceptor. However, on the basis of theoretical considerations, he concluded that *all* aromatic compounds donate or accept an electron during charge-transfer complexation primarily, if not solely, at the π-electron system of the benzene ring. That is to say, there is no one single reaction site although, of course, one location may be somewhat more reactive than another. He thus designated these compounds as π-donors or π-acceptors.

This assumption with respect to the nature of aromatic electron acceptors has been used in several studies on charge-transfer complexes [26, 33]. However, Tsubomara concluded that in charge-transfer complexes of aniline derivatives with an iodine molecule that the amine can function as an n-donor [35].

In order to reach a definite conclusion as to whether the aromatic amines and acceptors in this study involve the π-system or n-electrons or v-orbitals, direct experimental evidence is required. Unfortunately, this is not available. However, indirect evidence has been obtained that can be used to provide a reasonable assumption concerning the locations of the reaction sites. Recently, Janzen reviewed the literature on the electron spin resonance spectra of free radicals formed from benzene derivatives on gaining or losing an electron [36]. He indicated that an aromatic amine cation radical has the odd electron primarily located on the nitrogen atom. Likewise, an anion radical formed from a substituted nitrobenzene, cyanobenzene, or other benzene derivative possessing a group having one double- or triple-bond conjugated with the benzene ring generally has the odd electron on the atom on the group adjacent to the benzene ring, i.e., α-atom, although in some cases, the odd electron may reside on the β-atom.

Another approach for obtaining the location of the odd electron in aromatic radical anions has been reviewed by Hayon and Simic [37]. In water, anion radicals produced from the reaction of electrons (generated in pulse radiolysis of the solvent) with various compounds are basic and can protonate. Protonation of the anion radicals derived from benzoic and terephthalic acids and those from benzoyl esters occurs at the carboxyl group and not in the aromatic ring. Consistent with this is that protonation of anion radicals formed from nitrobenzene and aryl substituted nitrobenzenes takes place at the nitro group. In addition, the protonated anion radicals of benzaldehyde, acetophenone and benzophenone produced indirectly exist as α-hydroxyalkyl radicals. Consequently, in anion radicals of these highly electrophilic compounds, the odd electron is localized on the substituent and not the ring.

Meisel and Nata [38] have very recently stated that "electron transfer to a nitro compound and from its radical anion is expected to involve the nitro group as the main site of the transfer." Their experimental results were consistent with this assumption.

Based on all these considerations, it will be assumed that the charge-transfer complex between an aromatic amine and a benzene derivative containing a group having a double- or triple-bond conjugated with the ring is as shown in figure 2. That is to say, electron transfer occurs between the nitrogen atom of the aniline derivative and one of the atoms of the group containing the multiple-bond, i.e., n-v complexation, in Mulliken's terminology.

4. Transition Energies and Extrathermodynamic Relationships

In order to correlate the thermodynamic properties (e.g., equilibrium constants and enthalpy) or the kinetic data (e.g., rate constants and activation energies) with chemical structure for reactions of a series of closely related compounds in which the reaction site is held constant and various nonreacting atoms or groups of atoms are substituted in the molecule, chemists have utilized the concept of the "extrathermodynamic relationship" [39, 40 and references therein]. (Since one major use of this concept is in correlating the free energy changes in a group of compounds during reaction, the term "linear free-energy relationship" has also been applied but it is probably best to use this terminology in its more restrictive sense.)

According to this treatment of the data, each substituent has a numerical value, i.e., sigma value, that reflects the ability of the substituent to donate elec-

201-606 O - 76 - 3

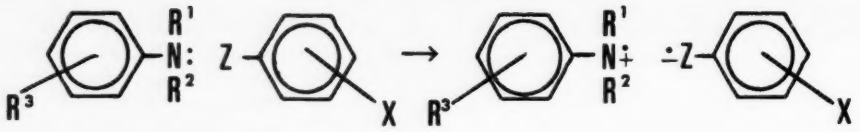

FIGURE 2. *The formation and structure of the aromatic amine charge-transfer complex of benzene derivatives containing an electron-accepting group.*

Not depicted are the canonical structures showing the resonance stabilizing of the electronic charge by the aromatic rings.

trons to the reaction site and which is independent of the reaction conditions, e.g., temperature and solvent. The sigma value will, however, depend on: (a) in aromatic compounds, the position of the substituent in relationship to the reacting site, i.e., *ortho*, *meta*, or *para* (abbreviated as *o*, *m*, *p*, respectively); (b) the nature of the intervening atoms, i.e., aliphatic versus aromatic molecule; and (c) in some rather unusual circumstances in aromatic molecules, if direct conjugation with the reacting site occurs.

In the usual case, i.e., the reaction of *meta*- and *para*-substituted benzoic acid, the relationship is generally given as

$$\log K/K^0 = \rho\sigma, \tag{3}$$

where K is the reaction rate, or equilibrium constant; K^0 is the corresponding value for the compound in the series chosen as the standard; ρ is a parameter that depends on the reaction and the reaction conditions, and reflects the relative sensitivity of the reaction rate or equilibrium constant to variations in the substituent constant σ ("sigma") previously described. The standard compound is benzoic acid and σ for the aromatic hydrogen atoms is defined as zero.

For *ortho*-substituted derivatives, two effects come into play: (1) the ability of the substituent to donate electrons, and (2) the steric interaction of the substituent on the reaction site [41]. This site generally is a group of atoms that requires a specific geometrical relationship with respect to the plane of the aromatic ring. If the substituent is small or is sufficiently flexible that no steric hindrance results, then $\sigma_o - \sigma_p$ is approximately constant, as in one series of benzoic acid derivatives [41]. If the substituent is so large that it interferes with the reacting site then no simple relationship between these σ values is possible. This latter case is beyond the scope of this investigation.

For reaction of aromatic compounds, e.g., phenols and anilines, in which a negative charge that is in direct conjugation with the substituent in the *para*-position is created or destroyed, the appropriate equation is:

$$\log K/K^0 = \rho\sigma^-. \tag{4}$$

(For most substituents, the values of σ and σ^- are equal.)

For reactions of aromatic compounds, e.g. benzylic carbonium ions, in which a positive charge that is in direct conjugation with the *meta*- or *para*-substituent is generated or eliminated, the appropriate equation is:

$$\log K/K^0 = \rho\sigma^+. \tag{5}$$

For reactions in the aliphatic series, in which the substituent is bridged by methylene groups to the reacting site, the appropriate equation is:

$$\log K/K^0 = \rho\sigma^*. \tag{6}$$

Tables of the values of the substituent constants have been compiled and are readily available [41, 42].

A heuristic approach will be used to derive the corresponding relationships involving charge-transfer energies. It has previously been shown for a series of methine dyestuffs formed from an organic acid that the low level transition energies ($\lambda_{max} \sim 450$–600 nm), which have been assigned to an intramolecular *c-t* process, of the dyes vary with the logarithms of the ionization constants, K_A, of the parent acids by the relationship [43, 44]:

$$N_0 h\nu_{max} - 2.303\ RT \log K_A = \text{constant}, \tag{7}$$

where ν_{max} is the frequency at which the spectroscopic absorption of the dye is maximum, R is the gas constant and T is the absolute temperature. Solving eq (7) for $\log K_A$ gives:

$$\log K_A = \frac{N_0 h\nu_{max}}{2.303\ RT} - \frac{\text{const}}{2.303\ RT}. \tag{8}$$

Assuming that K_A can be correlated with the electron-donating ability of a substituent by one of the previous equations, eqs (3)–(6), gives:

$$\frac{N_0 h\nu_{max}}{2.303\ RT} - \frac{N_0 h\nu^0_{max}}{2.303\ RT} = \rho\sigma^x, \tag{9}$$

where ν^0_{max} corresponds to K^0_A and σ^x represents σ, σ^- etc. as the case may be.

In the charge-transfer complexes considered in this investigation, it was hypothesized that electron loss occurs at the nitrogen atom of the aromatic amine and electron acceptance occurs at the multiple-bond conjugated with the benzene ring of the second compound (see previous section). For such complexes

TABLE 1. *Measured physiochemical properties of electron donors, acceptors and donor acceptor complexes and their associated energy and extrathermodynamic* (ET) *function of their energy*

Material investigated	Property measured	Symbol	Associated energy, E (J/mol$^-$)[a]	ET function symbol [b]
Electron donor	Ionization potential	IP	$N_0(IP)$	pP_I
	Polarographic half-wave potential, oxidation	$E^{ox}_{1/2}$	$FE^{ox}_{1/2}$	[c] pE
Electron acceptor	Electron affinity	EA	$N_0(EA)$	pA_E
	Polarographic half-wave potential, reduction	$E^{red}_{1/2}$	$FE^{red}_{1/2}$	[c] pE
EDA complex	Frequency at maximum absorption in the ultraviolet or visible spectrum	ν^{ct}_{max}	[d] $N_0h\nu^{ct}_{max}$	pE_T
	Wavelength at maximum absorption in the ultraviolet or visible spectrum	λ^{ct}_{max}	[d] N_0hc/λ^{ct}_{max}	pE_T

[a] Meaning of symbols: N_0, Avogardro's number (6.023×10^{23} molecules/mol); h, Planck's constant (6.626×10^{-34} Js); c, the speed of light in a vacuum (2.998×10^8 m/s); F, Faraday's constant (9.649×10^4 J/V).

[b] The ET function equals $E/2.303RT$, where E is the energy (or free energy) associated with a given process; R is the gas constant [8.314 J/(mol − K)]; T is the temperature (K).

[c] See ref. [48].

[d] See ref. [29].

[e] All values of physical constants taken from "ASTM Metric Practice Guide", NBS Handbook 102 (1967).

between one series of aromatic compounds in which only one type of substituent is varied, e.g., the nitrogen substituent of the amine or the aryl substituent a nitrobenzene, and the second aromatic compound kept constant, it is reasonable to assume that an equation similar in form to Equation (9) is applicable. This is so because in both cases, the reaction sites are fixed and in varying the substituents, families of compounds are obtained. Therefore, the appropriate equation for correlating the *c-t* transition energies of the EDA complexes in this investigation with substituent electron-donating abilities is obtained by replacing ν_{max} with ν^{ct}_{max}, giving

$$\frac{N_0h\nu^{ct}_{max}}{2.303\,RT} - \frac{N_0h(\nu^{ct}_{max})^0}{2.303\,RT} = \rho\sigma^x. \qquad (9')$$

In the only investigation in which a comparable equation was applied, the *c-t* transition energies of 1-alkylpyridinium iodides with various substitutents in the 3- and 4-positions of the pyridinium ring were correlated by assuming that the 3- and 4-positions were comparable to the *meta*- and *para*-positions, respectively, of a benzene derivative [45–47]. Although used in the form:

$$\frac{E_TX - E_T}{2.303\,RT} = \rho\sigma^-, \qquad (9'A)$$

where E_TX is the transition energy of the substituted compound and E_T, that of the parent, it is written in the abstract of ref. [46] and in ref. [47] as:

$$\frac{E_T}{2.303\,RT} = \rho\sigma. \qquad (9'B)$$

(When the σ and σ^- values differed, Kosower used the σ^- values and referred to them as "resonance" σ values.) A value of −13.4 was reported for ρ [45–47].

Because the term for the equilibrium free-energy change or its analog in kinetic or spectroscopic data can be put into the form $\Delta G/2.303RT$, where ΔG represents the free-energy change or the kinetic or spectroscopic counterpart thereof, in extrathermodynamic relationships [39, 40], it will be useful to denote this function of G simply as pG. This expression will be called "the extrathermodynamic function" of G. This convention follows the concept discussed by Sillen [48] in that instead of the electrical potential e of a half-cell, sometimes the dimensionless quantity pE is used, which is defined by:

$$pE = \frac{eF}{RT\ln 10} = \frac{eF}{2.303\,RT}, \qquad (10)$$

where F is Faraday's constant.

Thus eq (9′) can be written as:

$$pE_T - pE^0_T = \rho\sigma^x. \qquad (9'C)$$

This function of the transition energy as well as others to be discussed for extrathermodynamic relationships is given in table 1.

It has been shown previously that if the extrathermodynamic relationship is fitted in the forms indicated in eqs (3)–(6), (9)–(9′C), infinite statistical weight is placed on the measured value of the parent compound [49, 50]. To avoid this, it was proposed that the regression line fitting the data not be forced to go through the origin, i.e., that there be an intercept calculated from the data [49, 50]. Therefore, the extrathermody-

TABLE 2. *Characteristics of amine systems correlated in this investigation*

Regression number	Parent amine [a]	Substituents	Electron acceptor	Solvent	Temperature	Ref.
1.	*N*,N-Dimethylaniline	*N*-CH_3; *N*,*N*-$(CH_3)_2$; *N*,*N*-$(C_2H_5)_2$; *N*,*N*-$(n\text{-}C_3H_7)_2$; *N*,*N*-$(n\text{-}C_4H_9)_2$	2,4,6-trinitrotoluene	cyclohexane	18–20° [b]	[1]
2.	*N*,*N*-Dimethylaniline	H; *N*-CH_3; *N*-C_2H_5; *N*-$(n\text{-}C_3H_7)$; *N*-$(iso\text{-}C_3H_7)$; *N*-$(n\text{-}C_4H_9)$; *N*,*N*-$(CH_3)_2$; *N*,*N*-$(C_2H_5)_2$; *N*,*N*-$(n\text{-}C_3H_7)_2$; *N*,*N*-$(n\text{-}C_4H_9)_2$	1,3,5-trinitrobenzene	……do……	……do……	[1]
3. a.	*N*,*N*-Dimethylaniline	H; *p*-CH_3; *p*-$NHCOCH_3$; *p*-NH_2; *p*-I; *p*-Br; *p*-Cl; *p*-OCH_3	trinitrobenzene	chloroform	not reported [d]	[14]
b.	……do……	([c])	……do……	……do……	…… do……	[14]
4. a.	Aniline	H; *m*-NO_2; *p*-NO_2; *m*-CH_3; *p*-CH_3 *m*-NH_2, *p*-NH_2; *p*-OCH_3	……	vacuum	not reported [e]	[58]
b.	……do……	([c])	……	……do……	…… do……	[58]
5. a.	*N*,*N*-Dimethylaniline	H; *m*-OCH_3; *p*-OCH_3; 3,4-$(OCH_3)_2$; 3,5-$(OCH_3)_2$; *p*-$N(CH_3)_2$	……	acetonitrile (Ag^0/0.01M Ag^+)	room temperature	[61]
b.	……do……	([c])	……	……do……	……do……	[61]
6.	*N*,*N*-Dimethylaniline	H; *p*-OCH_3; *p*-CH_3; *p*-NO_2; *p*-Cl	……	acetonitrile (satd. calomel electrode)	not reported [f]	
7.	*N*,*N*-Dimethylaniline	H; *m*-CH_3; 3,5-$(CH_3)_2$	tetracyanoethylene	chloroform	24°	[67]
8.	*N*,*N*-Dimethylaniline	H; *p*-CH_3; *p*-C_2H_5; *p*-*iso*-C_3H_7; *p*-*t*-C_4H_9; *p*-F; *p*-Cl; *p*-Br; *p*-I	……do……	……do……	……do……	[67]

[a] The parent compound is that compound in the family taken as the standard; the intercept in the regression results shown in table 3 is an estimate of the extrathermodynamic function of the energy under consideration involving this compound.

[b] Since most of the values were obtained at 20°, this temperature was used.

[c] Same as above except NH_2 or $N(CH_3)_2$ substituent(s) omitted.

[d] In all cases, unless otherwise indicated, when no temperature is reported, a temperature of 25° was used.

[e] In literature available from the manufacturer, 250° was recommended as the operating temperature. This temperature was used.

[f] Seo, E. T., Nelson, R. F., Fritsch, J. M., Marcoux, L. S., Leedy, D. W., Adams, R. N., J. Am. Chem. Soc. **88**, 3498 (1966).

namic relationships should (and will in this investigation) be expressed in the general form

$$pE_T = pE_T^0 + \rho\sigma^x, \qquad (9'D)$$

where both pE_T^0 and ρ are obtained by least-squares fitting the equation.

5. Ionization Potential of Amines and Extrathermodynamic Relationships

The effect of the amine structure on the *c-t* transition energy of the complex is probably due primarily to variations in the ionization potential of the amine donor as indicated in eq. (2). Therefore, the correlation of the ionization potential of the amine with structure is an important area of inquiry.

Effect of Varying the Nitrogen Substituents

For aromatic amines, two separate structural changes are possible: nitrogen substitution and ring (aryl) substitution. The effect of substituents on the ionization potentials of aliphatic amines is highly correlated with that of alkyl free radicals [51]. Thus a straight line is obtained if the ionization potentials of aliphatic amines with the formula $R^1R^2R^3N$ is plotted against those of the corresponding methyl free radical, i.e., $R^1R^2R^3C\cdot$ [51]. In addition the ionization potentials of these latter free radicals are approximately linearly related to the sum of the σ^* constants, $\Sigma\sigma^*$, of the substituents on the carbon atom possessing the odd electron [51]. However, Poldoja [52] proposed that for such systems hyperconjugation effects must be considered and proposed the equation:

$$IP = H(n) + \alpha n_1 + a\Sigma\sigma^*, \qquad (11)$$

where $H(n)$ are the intercepts, which may vary with the number of protons on the atom possessing the odd electron; n_1 is the number of protons on the carbon atom of the alkyl substituent next to the atom with the odd electron, and α and a are parameters obtained by least-squares fitting the equation.

To obtain the corresponding extrathermodynamic relationship, eq (11) is substituted into eq (2) and C is assumed to be linearly related to the ionization potential, giving:

$$E_{ct} = N_0[H'(n) + \alpha' n_1 + a'\Sigma\sigma^* - EA]. \qquad (12)$$

Therefore:

$$pE_T = \frac{E_{ct}}{2.303\,RT} = H''(n) + \alpha'' n_1 + \rho\Sigma\sigma^*, \qquad (12')$$

where the value of EA is contained in the intercepts $H''(n)$.

The data of Foster and Hammick [1] for complexes of *N*-substituted anilines with 1,3,5-trinitrobenzene in cyclohexane were fitted by eq (12′) (the contribution of the aromatic portion of the amine to $\Sigma\sigma^*$ was ignored since it was constant throughout this series) using indicator variables [53] to obtain the intercepts $H''(n)$ and the results are shown in table 3. (In what follows, whenever no reference is indicated after it is mentioned that data were correlated, the correlation was performed by the author. The results in the tables were obtained by the author). Since $H''(n)$ are not significantly different for the various amines (95% confidence level) [53] and α'' is negligible, the regression was repeated using the relationship:

$$pE_T = pE_T^0 + \rho\Sigma\sigma^*. \qquad (13)$$

The results are shown in table 3. An analysis of variance [54] infers (at the 95 percent confidence level) that the goodness-of-fit eq (13) is consistent with that of eq (12′) and, therefore, eq (13) describes the data adequately.

An implicit assumption made in the derivation and use of eq (13) is that the substituent produces no steric interference with the benzene ring. Just as *ortho*-substituents that are bulky can cause serious problems in correlating thermodynamic data (sec. 4), some nitrogen substituents may also prove to be anomalous. Hickinbottom [55] found that tertiary aromatic amines such as *N*-methyl-*N*-*t*-butylaniline and *N*-methyl-*N*-*t*-amylaniline are as unreactive with nitrous acid as is *N*,*N*-dimethyl-*o*-toluidine, which possesses a bulky methyl substituent in the *ortho*-position, although other tertiary aromatic amines possessing an unsubstituted *para*-position are generally quite reactive in forming the *p*-nitroso derivative [56]. Primary alkyl substituents such as CH_2R, where R may be any atom or group of atoms, attached to the nitrogen atom produce no apparent steric problems in aniline derivatives with no *ortho*-substituents. If the alkyl substituent is secondary, it is not known if steric interference with the ring occurs. A further discussion may be found under "*Ortho Substitution*" below.

Effect of Varying the Ring (Aryl) Substituents

Although few investigations on the effect of varying the nitrogen substituent have been made, a number of them have indicated the effect of ring substitution. Since the ionization potentials of alkyl free radicals are linearly related to the ionization potential of the corresponding substituted aliphatic amines [51], it would not be surprising to find that the ionization potentials of aryl-substituted benzylic free radicals are linearly related to those of the correspondingly ring-substituted anilines possessing nitrogen substituents held constant throughout the series under comparison. However, the correspondence does not appear to have been made previously.

In the case of *meta*- and *para*-substituted benzylic free radicals, the ionization potential is linearly related to σ^+ of the ring substituent [57]. Crable and Kearns [58] found that for *para*-substituted anilines,

TABLE 3. *Extrathermodynamic relationships of electron-donating aromatic amines*

Regression number	*ET* function [a]	Substituent location	Substituent parameter or indicator variable	Slope [b]	Intercept [b]	S [c]	N [d]
1.	pE_T	Nitrogen	σ^*	6.9 ±2.3	48.53 ±0.57	1.24	5
2.a	pE_T	Nitrogen	σ^*	12.5 ±5.6	42.3 ±5.4	0.32	10
			[e] x_1	1.7 ±4.5			
			[f] x_2	2.7 ±4.6			
			[g] n_1	−0.36 ±0.61			
2.b	pE_T	Nitrogen	σ^*	9.81 ±0.30	44.55 ±0.13	.36	10
3.a	pE_T	Aryl	σ^+	3.99 ±0.26	42.64 ±0.15	.36	8
3.b	pE_T	Aryl	σ^+	3.78 ±0.40	42.63 ±0.16	.37	7
4.a	pP_I	Aryl	σ^+	6.04 ±0.60	80.04 ±0.39	1.09	8
4.b	pP_I	Aryl	σ^+	6.41 ±0.12	80.273 ±0.067	0.16	6
5.a	pE	Aryl	σ^+	5.70 ±0.65	8.41 ±0.53	1.02	6
5.b	pE	Aryl	σ^+	5.0 ±1.2	8.29 ±0.59	1.09	5
6	pE	Aryl	σ^+	7.56 ±0.88	13.40 ±0.46	1.02	5
7	pE_T	Aryl	σ^+	20.174 ±0.074	31.1956 ±0.0063	0.0069	3
8	pE_T	Aryl	σ^+	−1.3 ±1.6	30.21 ±0.34	.91	9

[a] Defined in table 1.
[b] Least-squares estimate of the coefficient ±its standard error.
[c] Standard error of regression.
[d] Number of measurements.
[e] Indicator variable set equal to *zero* in the case of primary amine; set equal to *one* otherwise.
[f] Indicator variable set equal to *one* in the case of tertiary amine; set equal to *zero* otherwise.
[g] Number of hydrogen atoms on the α-carbon atom of the nitrogen substituent.

the ionization potential is linearly related to σ^+. A plot of their data (not shown) for *meta*- and *para*-substituted anilines shows that by excluding the *meta*- and *para*-amino substituted compounds, the correlation between ionization potential and σ^+ is quite good. This plot indicates that the maximum deviation (if the amino substituents are ignored) is approximately 0.02 electron volts which is in agreement with the finding that the average deviation between determinations for the same compound was approximately 0.03 electron volts.

The corresponding extrathermodynamic relationship is given by (see table 1):

$$pP_I = \frac{N_0(IP)}{2.303RT} = pP_I^0 + \rho\sigma^+. \qquad (14)$$

The results of correlating the data by eq (14) are given in table 3. In this case, two results are shown, one including all the data and one in which the amino substituent values are excluded. A test for outliers [59] (95% confidence interval) indicates that the amino substituted compounds come from a population different from the others. This lack of agreement for the amino substituents has been found in correlating the effect that aryl substituents have on the electron spin resonance spectra of *N,N*-dimethylanilinium radical cation [36], a topic that will be discussed below.

Polarography of Aromatic Amines

An indirect method for assessing the relative ionization potentials of aromatic amines involves polarography. According to Foster [60] "polarographic oxidations may provide, by their experimentally determined half-wave oxidation potentials $E_{1/2}^{ox}$, a measure of the ionization potential of a compound." If certain requirements are met, then the following equation holds:

$$E_{1/2}^{ox} = IP + \Delta F_{solv} + \text{constant}, \qquad (15)$$

where "ΔF_{solv} is the difference in solvation-energy between the compound and its positive ion. If it is assumed that, for a series of compounds, variations in IP are much greater than ΔF_{solv}, then $E_{1/2}^{ox}$ may be used as a measure of the electron-donating ability of a donor. Because of this restriction it is obviously advisable to compare compounds which are chemically related" [60]. Correlation of the polarographic half-wave potentials of a series of aryl singly and multiply substituted *N,N*-dimethylanilines in acetonitrile [61] with $\Sigma\sigma^+$ of the substituents gives results shown in table 3. In this case, the *p*-dimethylamino group gives a result consistent with other substituents. In contrast to this, Lagutskaya and Dadali [62] discuss their own and previous efforts to correlate the half-wave potentials of aromatic amines dissolved in aqueous solutions of various pH with σ and σ^- values of the substituents and remark that a poor correlation is obtained. No mention of σ^+ values was made. According to Zuman [63], who has probably succeeded more than anyone else in correlating polarographic data, in describing the reactivity of benzene derivatives, the use of σ^+ is needed "in those so far rare examples in which the reaction constant ρ is negative," which in Zuman's terminology indicates polarographic oxidation. (Zuman employs a sign convention opposite the one in this paper.)

Electron Spin Resonance Spectroscopy

A practical way to evaluate the effects of substituents on the properties of free radicals is through the

use of electron spin resonance (ESR) spectroscopy [36]. From observed coupling constants, a measure of the electronic spin density of the atom possessing an odd electron is ascertainable. Janzen correlated the nitrogen ESR hyperfine coupling constants of *meta*- and *para*-substituted *N, N*-dimethylanilinium cation radical against σ^+ and obtained a good correlation if the amino groups were excluded [36]. The only substituents to be at a considerable distance from the regression line were *m*-OH, *m*-CO_2H and *m*-$CO_2C_2H_5$. He also obtained ESR data for substituted nitrobenzene anion radicals to be discussed in section 6.

Ortho Substitution

In the case of *ortho* substitution both electron-donating ability and a steric effect of the substituent may play a role, as discussed in section 4. This steric effect causes the reacting site, in this case, the amino group, to be out of the plane of the benzene ring [64]. A similar effect occurs when a dialkylamino group acts as a substituent [65]. Since the steric effect depends on the sizes of the aryl and the nitrogen substituents, it would be difficult, if not impossible, to correlate such data with respect to substituent constants and it will not be attempted in this investigation.

A simple rule to predict if steric interference preventing the coplanarity of the aromatic ring and the nitrogen substituents is absent is an adaptation of "the rule of six" [66]. In a secondary or tertiary aromatic amine, consider each of the atoms attached to the benzene ring at the *ortho*-position as number 1. A count of the attached atoms in succession shows that the atoms attached to the α-carbon of each of the nitrogen substituents are number 6. If the number 1 atoms and two of the number 6 atoms in each substituent are hydrogen (or are absent as in the case of the secondary amine), molecular scale models indicate that steric interference is absent, no matter the rest of the molecule. Otherwise, steric interference may be present.

Spectroscopic Evaluation

The only previous investigation in which spectroscopic data of EDA complexes of aryl-substituted anilines with another benzene derivative were correlated against σ^+ of the substituent is that of Kravtsov and Faingor [14], who correlated the frequencies of the absorption maxima of complexes of *para*-substituted *N, N*-dimethylanilines with trinitrobenzene in chloroform versus σ^+ of the *para*-substituents. The extrathermodynamic relationship for their data is given in table 3.

Finally, it should be noted that Farrell and Newton proposed that the charge-transfer transition energies of the aniline complexes of tetracyanoethylene in chloroform be used to assess the ionization potentials of the amines [67]. However, the slope obtained from their data for *para*-substituted *N, N*-dimethylanilines (summarized in table 3) is inconsistent with that from the data of another investigation [14] and with the slopes from the extrathermodynamic relationships correlating ionization potential data [58]. The reason may be as follows. In the case of complexes of aromatic amines with other aromatic compounds, the amine is assumed to act as an *n*-donor with the electrons primarily of the nitrogen atom involved in the complexation. On the other hand, it has been shown that tetracyanoethylene reacts with aromatic amines at the *para*-position by, according to one hypothesis, first forming a π-complex, then a σ-complex and finally a new compound [68]. Thus the ionization potentials calculated from the transition energies of these latter complexes are not readily related to those obtained by other means.

6. Electron Affinities of Electron Acceptors and Extrathermodynamic Relationships

Previously Reported Correlations

In comparison with studies on electron-donating aromatic amines, no exact relationship has apparently been published that correlates the *c-t* transition energies of complexes with the substituents of the electron acceptor if the acceptor is a benzene derivative.

However, approximate techniques have been derived. Lepley and Thelman [33] noted that the electron affinity of an electron acceptor generally increases with the number of strong electron withdrawing substituents and the location of these substituents in the acceptor structure. Based on the previous investigation of Hammond [69], who correlated the frequencies of the charge-transfer absorption peaks of complexes of mono-substituted *p*-benzophenones with hexamethylbenzene with σ_p of the benzophenone substituent, Lepley and Thelman postulated that the electron affinity of a benzene derivative could be related to σ_p of the substituent but they did not report any mathematical relationship. Argentar and Bowen used the sum of the σ_p values of the substituents of aromatic compounds functioning as electron acceptors, the geometry being ignored, in correlating the *c-t* transition energies of complexes of *N, N*-dimethyl-*p*-toluidine by a linear regression [26]. In these cases, the electron acceptors were assumed to function as π-acceptors.

According to Kosower (mentioned above in section 4) the *c-t* transition energies of 1-alkyl, 3- and 4-substituted pyridinium iodides, which form a charge-transfer complex by themselves, can be correlated with the σ^- values of the ring-substituents by assuming that the 3- and 4-positions of the pyridinium ring are analogous to the *meta*- and *para*-positions of an aromatic compound, respectively [45–47].

Determination of the Exact Extrathermodynamic Relationship

Before attempting to derive the extrathermodynamic relationship for the substituent effect on the electron

TABLE 4. *Characteristics of electron acceptor systems correlated in this investigation*

Regression number	Parent electron acceptor [a]	Substituents	Electron donor	Solvent	Temperature	Ref.
1.	nitrobenzene	H; *p*-Cl; *m*-NO_2; *o*-NO_2; *p*-NO_2; 3-NO_2-4-F; 3-NO_2-2,4-F_2; 3,5-$(NO_2)_2$	.....	acetonitrile (satd. calomel electrode)	25°	[75]
2.	do.	H; *p*-Cl; *m*-NO_2; *p*-NO_2; 3,5-$(NO_2)_2$	*N*,*N*,*N*,*N*-tetramethyl-*p*-phenylenediamine	methylene chloride	room temperature [b]	[75]
3.	methyl benzoate	*o*-CO_2CH_3; *m*-CO_2CH_3; *p*-CO_2CH_3; 2,3,5,6-Cl_4-4-CO_2CH_3; *p*-CO_2H	.....	dimethyl formamide (satd. calomel electrode)	not reported	[74]
4.	methyl benzoate	H; *o*-CO_2CH_3; *m*-CO_2CH_3; *p*-CO_2CH_3; 2,3,5,6-Cl_4-4-CO_2CH_3	.....	gas phase	180–270° [c]	[74]

[a] The parent compound is that compound in the family taken as the standard; the intercept in the regression results shown in table 5 is an estimate of the value of the ET function of the energy under consideration involving this compound.

[b] In all cases, when the temperature was not reported, 25° was used in the calculation of the ET function.

[c] The average temperature of 193°C was used.

acceptor, the correct set of "sigma" values for the substituent must be established. Since there is no precedent for this, the correlation of ESR data as previously stated in the case of aromatic amines (sec. 4) furnishes this information indirectly. Janzen [36] showed that for *meta*- and *para*-substituted nitrobenzene anion radicals the nitrogen hyperfine coupling constants form two lines when correlated with σ^- of the substituent. Most of the values fall on one line. However, the unsubstituted compound and the two dinitro compounds form a second line, which intersects the first at the value of the unsubstituted nitrobenzene. This was explained by assuming that the second nitro group has more than just a minor perturbing influence on the nitro group that has gained an electron. The use of σ^- has also been reported by others in correlating the coupling constants of nitrobenzene anion radicals [70 and references therein]. The assumption that the logarithms of the coupling constants are correlated with the substituent constants [71] requires that new ad hoc substituent constants be defined and is therefore to be avoided.

Polarography of Electron Acceptors

Analogous to the situation regarding aromatic amines discussed in (sec. 4), polarographic measurements provide a relative measure of the electron affinity. "By analogy with one-electron oxidation potentials . . . determinations of polarographic one-electron reduction potentials, E_1^{red}, whilst not directly measuring E, nevertheless provide one of the few independent experimental estimates of E which are available for a range of acceptor species [72]." In this quotation, E is the electron affinity. "Within experimental error, the reduction potential (E_1^{red}) is equal to the half-wave potential ($E_{1/2}^{red}$). For measurements against a standard calomel electrode:

$$E_{1/2}^{red} = E_1^{red} = E - \Delta F_{solv} - \varphi_{Hg} - E_{Hg:Hg^{++}} \qquad (16)$$

where ΔF_{solv} is the difference in solvation energy between the compound and its negative ion, and represents mainly the solvation of the anion. φ_{Hg} is the work function [for the half-reaction:][2] e^- (in Hg) $\rightarrow$ $Hg_{liq} + e^-$ (equal to 4.54 eV) and $E_{Hg:Hg^{++}}$ is the absolute value of the calomel electrode (equal to 0.53 V). For two different acceptors A_1 and A_2, is ΔF_{solv} is assumed to be constant, then [72]"

$$EA(A_1) - EA(A_2) = E_1(A_1) - E_1(A_2) \qquad (17)$$

In discussing substituent effects on the polargraphic reduction potentials of aromatic compound containing a reducible group having a double bond conjugated with the benzene ring, Zuman indicated that σ^- should be the preferable substituent constant for correlating the data [73]. However, in some instances, experimental evidence was available for preferring σ over σ^- [73]. In no instance was there mentioned an equation of the form shown as Equation (9′D) although linear structure-property equations were used for treating this type of data.

The electron affinities and polarographic half-wave potentials of several aryl substituted methyl benzoates have been measured [74]. However, there was no mention of correlating the data with the substituent parameters. These are correlated here and the results given in table 5. In this set of data and the following, the σ^- value of the *ortho*-substituent is set equal to σ_p. In one previous investigation where steric factors were not important, $\sigma_o - \sigma_p$ was approximately constant (as discussed in sec. 3).

Peover has determined the half-wave reduction potentials of a number of substituted nitrobenzenes [75]. The result of correlating the data by an extrathermodynamic relationship is given in table 5. Although *ortho*-substituents are apparently well-behaved in these instances, further investigation is needed to determine the limitations in assuming that σ_o^- equals σ_p.

Spectroscopic Evaluation

In apparently the only investigation of its type, Peover obtained the *c-t* transition energies of complexes of substituted nitrobenzenes with *N,N,N,N*-tetramethylphenylenediamine and correlated the energies with the polarographic half-wave reduction potentials of the electron acceptor [75]. No correlation of the energies directly with substituent parameters was reported. The results of correlating the calculated pE_T values versus σ^- of the *meta*- or *para*-substituent is given in table 5.

7. Effect of Solvent on the C-T Transition Energy—Solvatochromic Relationships

The most popular equation for correlating the effect of solvent on the transition energy of charge-transfer complexes is that due to McRae [76] as reviewed by Mataga and Kubota [77]. This is given as:

$$\Delta\nu_{abs} = \nu_{abs} - \nu_{abs}^{g}$$

$$= (A + B + C)\left[\frac{n^2-1}{2n^2+1}\right] + E_{abs}\left[\frac{D-1}{D+2} - \frac{n^2-1}{n^2+2}\right] + F_{abs}\left[\frac{D-1}{D+2} - \frac{n^2-1}{n^2+2}\right]^2 \qquad (18)$$

where $\Delta\nu_{abs}$ is the difference in the frequency at which maximum absorption occurs in solution relative to that of the complex in vacuum (gas phase); A, B, C, E_{abs}, and F_{abs} are constants dependent only on the solute; n and D are the refractive index and dielectric constant of the solvent, respectively.

In general, the quadratic term is negligibly small [78] so that this equation is approximately:

[2] Author's editorial change.

TABLE 5. *Extrathermodynamic relationships for aryl-substituted nitrobenzenes and methyl benzoates*

Regression number	ET [a] function	Substituent location	Substituent parameter	Slope [a]	Intercept [a]	S [a]	N [a]
1.	pE	Aryl	σ^-	-6.40 ± 0.31	19.62 ± 0.27	0.38	8
2.	pE_T	Aryl	σ^-	-12.10 ± 0.35	50.93 ± 0.35	.43	5
3.	pE	Aryl	σ^-	5.9 ± 1.9	59.8 ± 1.9	2.25	4
4.	pA_E	Aryl	σ^-	2.8 ± 1.1	4.0 ± 1.0	1.58	5

[a] For explanation of terms, see table 2 footnotes.

$$\nu_{abs} = \nu^g_{abs} + C_1\left[\frac{n^2-1}{2n^2+1}\right] + C_2\left[\frac{D-1}{D+2} - \frac{n^2-1}{n^2+2}\right] \quad (18')$$

This equation has also been expressed as:

$$\Delta h\nu_{ct} = (AL_0 + B)\left[\frac{n^2-1}{2n^2+1}\right] + C\left[\frac{D-1}{D+2} - \frac{n^2-1}{n^2+2}\right]. \quad (19)$$

In this form Aihara et al. [78] correlated the solvent effects of the naphthalene-tetracyanoethylene and pyrene-tetracyanoethylene complexes, obtaining two straight lines, with hydrocarbons and halogenated hydrocarbons forming one series and carbonyl-containing compounds forming a second.

Emslie and Foster [8] correlated the frequencies of the ultraviolet absorption peaks of four complexes, of which two were of the aniline-substituted benzene type, against Kosower's Z value [79] of the solvent. This value is the transition energy (in kcal/mol) of the charge-transfer complex, 1-ethyl-4-carbomethoxypyridinium iodide, dissolved in the solvent. They obtained two sets of straight lines depending on whether the solvents contained hydroxyl groups. Some nucleophilic solvents, e.g., acetone, did not fit the correlation.

Moriguchi et al. [80] correlated the solvent effects on the hexamethylbenzene-chloranil and hexamethylbenzene-tetracyanoethylene complexes and obtained linear relationships between ν^{ct}_{max} and n, $(n^2-1)/(2n^2+1)$ or Kosower's Z value. They also showed that an excellent correlation (correlation coefficient = 0.999) existed between $(n^2-1)/(2n^2+1)$, $(n^2-1)/(n^2+2)$ and n for the common solvents tested.

Koppel and Palm [81] have suggested the use of a multiparameter solvent effect relationship:

$$A = Ao + yY + pP + eE + bB \quad (20)$$

where A is the measured property or a simple mathematical function thereof; Y is the polarity of the solvent, $(D-1)/(D+2)$ or $(D-1)/(2D+1)$; P is the polarizability, $(n^2-1)/(n^2+2)$; E is the electrophilic solvation power, which is based on Dimroth's solvent polarity parameter, E_T [82] and which is used in this case primarily to measure the ability of the solvent to hydrogen-bond to the solute; B is the nucleophilic solvating power (Lewis basicity) defined as $\nu^0_{OD} - \nu_{OD}$ where ν_{OD} is the infrared stretching frequency of a hydrogen-bond donor group (e.g., the OD band of monomeric CH_3OD) in the gas phase and ν_{OD} is the corresponding value in the solvent; and A_0, Y, p, e and b are empirical constants obtained by least-squares fitting the equation. For solvatochromic shifts in electronic spectra, the functions $(D-1)/(D+2)$ and $(n^2-1)/(n^2+2)$ were preferred.

In correlating the transition energies of N-phenyl pyridinium betaine (E_T parameters) and the charge-transfer bands of 1-ethyl-4-carbomethoxypyridinium iodide complexes (Z parameter), the values of y, p, and e are not substantially different for the two sets of data [81]. Interestingly, statistical analysis [54] infers that in both cases p is not significantly different from zero at the 95 percent confidence level, indicating that for these systems, the refractive index is unimportant.

In order to obtain the relevant solvatochromic relationship, the pE_T values calculated from the spectroscopic data for the complexes of N,N-dimethylaniline with 1,3,5-trinitrobenzene or 1,2,4,5-tetracyanobenzene studied by Emslie and Foster [8] were correlated using a simplified form of Koppel's equation in which the B term was eliminated. This deletion was made because there are few solvents for which this value is known. Furthermore, this term was found necessary in very few previous cases [81]. Values of n, D, and E with the following exceptions were taken from the compilation of Koppel [81]; the refractive index of chloroform was taken as 1.4459 [83] and the values of E for chloroform, 1,1-dichloroethane and 1,1,2,2-tetrachloroethane were taken as 3.04, 3 and 3, respectively. The results are shown in table 4.

Statistical analysis [54] implies (at the 95 percent confidence level) that only the coefficient for the refractive index term is significant different from zero in the case in which 1,3,5-trinitrobenzene is the electron acceptor and that the coefficients for both refractive index and dielectric constant terms are significantly different from zero in the second case. Further analysis [84] indicates (at the 95 percent confidence level) that the intercepts and the corresponding slopes in the two cases are not significantly different from each other.

Since the standard errors of regression in the two cases are not significantly different from each other (at the 95 percent confidence level) [85] the data for

TABLE 6. *Solvatochromic relationships* (pE_T *versus solvent properties*) *of electron donor-acceptor complexes of* N,N-*dimethylaniline with two benzene derivatives*

Regression number	Electron acceptor[a]	Solvent parameter or indicator variable	Slope[b]	Intercept[b]	S^b	N^b
1.a	1,3,5-trinitrobenzene	[c]Y	−0.65 ± 0.55	56.1 ± 1.3	0.44	20
		[d]P	−43.5 ± 5.0			
		[e]E	0.016 ± 0.032			
1.b	Same data as in 1.a	Y	−0.47 ± 0.40	56.2 ± 1.2	0.44	20
		P	−44.1 ± 4.8			
2.a	1,2,4,5-tetracyanobenzene	Y	−2.03 ± 0.81	53.6 ± 1.8	0.65	20
		P	−42.9 ± 7.3			
		E	0.035 ± 0.047			
2.b	Same data as in 2.a	Y	−1.62 ± 0.59	53.8 ± 1.8	0.64	20
		P	−44.1 ± 7.0			
3.a	1,3,5-trinitrobenzene and 1,2,4,5-tetracyanobenzene	[f]X	−2.39 ± 0.47	56.2 ± 1.1	0.54	40
		Y	−0.47 ± 0.49			
		XY	−1.15 ± 0.69			
		P	−44.1 ± 4.2			
3.b	Same data as in 3.a	X	−3.13 ± 0.18	56.6 ± 1.1	0.55	40
		Y	−1.04 ± 0.36			
		P	−44.1 ± 4.3			

[a] All raw data from ref. [8]. (The data for the solvent decanol was omitted because its E value is unknown.)
[b] For explanation of term, see Table 2 footnotes.
[c] The polarity of the solvent, estimated by $(D-1)/(D+2)$, where D is the dielectric constant at 20 °C.
[d] The polarizability of the solvent, estimated by $(n^2-1)/(n^2+2)$, where n is the refractive index at 20 °C.
[e] The electrophilic solvation power, which measures the ability of the solvent to hydrogen-bond to the solute.
[f] An indicator variable set equal to zero for the complex of 1,3,5-trinitrobenzene and to one, otherwise.
The use of these terms is explained in the text.
No temperature for the determination of the raw data was reported by the investigators. Since the solvent parameters, Y and P, were determined at 20 °C, pE_T was calculated using this temperature.

the two complexes may be pooled and fitted by the equation

$$pE_T = pE_T^0 + \Delta pE_T X + y\left[\frac{D-1}{D+2}\right] + \Delta yX\left[\frac{D-1}{D+2}\right] + p\left[\frac{n^2-1}{n^2+2}\right] \qquad (20)$$

where pE_T^0 is the intercept, which estimates the extrathermodynamic function of the *c-t* transition energy of the trinitrobenzene complex in a vacuum; X is an indicator variable set equal to *zero* in the case of the trinitrobenzene complex and to *one* otherwise, and ΔpE_T^0 and Δy, which are obtained by least-squares fitting of the equation, are the differences in the pE_T^0 and y values for the trinitrobenzene and tetracyanobenzene complexes respectively. These results are given in table 6. Statistical analysis [53] implies that (at the 95 percent confidence level) y and Δy are not significantly different from zero. Repeating the regression after eliminating the Δy term gives the final result shown in table 4. This correlation indicates that the effect of solvent on the *c-t* transition energies of the two complexes is parallel.

A correlation in which the y term was eliminated (not shown) indicates that the slopes of the dielectric constant terms are significantly different for the two complexes, and that the slope of the dielectric constant term for the trinitrobenzene complex is zero. Although this latter correlation is consistent with the data, the closeness of the slopes of the refractive index term in the two cases tends to persuade one that the slopes of the dielectric constant term should also be similar. More data on the transition energies of other complexes in this series in various solvents is required before it can be decided definitely that the solvent effects on this type of complex are indeed the same in all cases, i.e., that y and p always have the same values (within experimental error) as those found in this investigation.

These results along with those of Koppel [81] indicate that in correlating the charge-transfer transition energies of complexes between species that are uncharged in the ground state, the refractive index term is of primary importance; with species that are charged, the dielectric constant term is of supreme importance.

8. Summary and Conclusions

The mathematical relationships for the variations in the charge-transfer transition energy of a complex between an aromatic amine and a benzene derivative

possessing an electron-accepting group may be summarized as follows:

For changes only in

1. Nitrogen substituent of the amine

$$pE_T = pE_T^0 + \rho\Sigma\sigma^* \tag{22}$$

2. Aryl substituent of the amine

$$pE_T = pE_T^0 + \rho\Sigma\sigma^+ \tag{23}$$

3. Substituent of the electron-accepting benzene derivative (with the electron-accepting group kept constant)

$$pE_T = pE_T^0 + \rho\Sigma\sigma^- \tag{24}$$

4. Solvent

$$pE_T = pE_T^0 + a\left[\frac{n^2-1}{n^2+2}\right] + b\left[\frac{D-1}{D+2}\right]. \tag{25}$$

In these four equations, pE_T is the extrathermodynamic function of the charge-transfer transition energy defined as $E_{ct}/2.303RT$, where E_{ct} is the transition energy (equal to $N_0 h\nu_{max}^{ct}$, where N_0 is Avogadro's number, h is Planck's constant, and ν_{max}^{ct} is the frequency in the ultraviolet or visible spectrum at which the differential absorption of the complex is maximum), R is the ideal gas constant and T is the temperature (K); σ^*, σ^+, and σ^- are the appropriate substituent parameters available in the literature; n and D are the refractive index and dielectric constant of the solvent, respectively, and pE_T^0, ρ, a and b are parameters obtained by least-squares fitting the line. For this system, a is much greater than b.

For changes, either in the nitrogen substituent of the amine or in the aryl substituent of either compound, the implicit assumption is that the substituent does not prevent coplanarity of the reacting group and the benzene ring. In addition, anomalous results may possibly occur if: for the amine, the σ_p^+ value of the aryl substituent is approximately equal to, or less than, the σ_p^+ value of the substituted amino group, which acts as the electron source; and for the electron acceptor, the σ_p^- value of the substituent is approximately equal to, or greater than, the σ_p^- value of the electron-accepting group of the parent compound.

The extrathermodynamic relationships for the electron-donating ability of the amine in the charge-transfer process with respect to variation in the aryl substituent is

$$pE_D = pE_D^0 + \rho\Sigma\sigma^+ \tag{26}$$

where pE_D is the extrathermodynamic function of the ionization potential, IP, or of the polarographic oxidation half-wave potential, $E_{1/2}^{ox}$, of the electron donor equal to $N_0(IP)/2.303RT$ or $FE_{1/2}^{ox}/2.303RT$, respectively.

The corresponding relationship for the electron-accepting ability of the electron acceptor with respect to variations in the nonreacting substituent is

$$pE_A = pE_A^0 + \rho\Sigma\sigma^- \tag{27}$$

where pE_A is the extrathermodynamic function of the electron affinity, EA, or of the polarographic reduction half-wave potential, $E_{1/2}^{red}$, of the electron acceptor equal to $N_0(EA)/2.303RT$ or $FE_{1/2}^{red}/2.303RT$, respectively.

The same requirements of coplanarity and of the restrictions on the magnitudes of the sigma values of the substituent mentioned for the c-t transition energy of a complex hold in the above cases also.

Note added in proof: After the present investigation was completed, Davidson [86] proposed that the mechanism illustrated in figure 2 was the first step in the photoreaction of aromatic nitrocompounds with N-alkylanilines to yield primary aromatic amines.

The author wishes to thank M. H. Aldrich and P. F. Waters of the American University for their helpful discussions.

9. References

[1] Foster, R., and Hammick, D. L., J. Chem. Soc. 2685 (1965).
[2] Dale, B., Foster, R., and Hammick, D. L., J. Chem. Soc. 3986 (1954).
[3] Ross, S. D., Bassin, M., and Kuntz, I., J. Am. Chem. Soc. **76,** 4176 (1954).
[4] Bier, A., Rec. Trav. Chim. Pays-Bas **75,** 866 (1956).
[5] Foster, R., Tetrahedron, **10,** 96 (1960).
[6] Beukers, R., and Szent-Gyorgyi, A., Rec. Trav. Chim. Pays-Bas **81,** 255 (1962).
[7] Foster, R., and Thomson, T. J., Trans. Faraday Soc. **59,** 2287 (1963).
[8] Emslie, P. H., and Foster, R., Rec. Trav. Chim. Pays-Bas **84,** 255 (1965).
[9] Foster, R., and Fyfe, C. A., Trans. Faraday Soc. **61,** 1626 (1965).
[10] Iwatha, S., Tanaka, J., and Nagakura, S., J. Am. Chem. Soc., **88,** 894 (1966).
[11] Carrion, J. P., Donzel, B., Deranleau, D., Esko, K., Mosser, P., and Schwyzer, R., in Peptides. Beyerman, H. C., Vande Linde, A. R. C., and Maasen van den Brink, W., eds., (North-Holland Publishing Co., Amsterdam—The Netherlands, 1967), p. 177.
[12] Beaumont, T. G., and Davis, K. M. C., J. Chem. Soc. (B), 1131 (1967).
[13] Carrion, J. P., Deranleau, D. A., Donzel, B., Esko, K., Moser, P., and Schwyzer, R., Helv. Chim. Acta. **51,** 459 (1968).
[14] Kravtsov, D. N., and Faingor, B. A., Izv. Akad. Nauk SSR, Ser. Khim. 289 (1968); Chem Abstr. **69,** 66717v (1968).
[15] Beaumont, T. S., and Davis, K. M. C., Nature, **218,** 865 (1968).
[16] Anikeev, V. S., Polle, E. G., and Tronov, B. V., Zh. Obshch. Khim, **38,** 1127 (1968); J. Gen. Chem. USSR, **38,** 1081 (1968).
[17] Sulzberg, T., and Cotter, R. J., Macromolecules **1,** 554 (1968).
[18] Sulzberg, T., and Cotter, R. J., Macromolecules **2,** 146 (1969).
[19] Foster, R., Organic Charge-Transfer Complexes (Academic Press, New York, N.Y., 1969), pp. 200, 201.
[20] Foster, R., and Morris, J. W., J. Chem. Soc. (B), 703 (1970).
[21] Sulzberg, T., and Cotter, R. J., J. Polym. Sci. Part A-1, **8,** 2747 (1970).

[22] Barlatier, A., Meyer, R., and Vincent, E. J., C. R. Acad. Sci. Paris, Serie C, 273, 789 (1971).
[23] Sharma, J. P., Z. Phys. Chem. (Leipzig), 249, 408 (1972).
[24] Sharma, J. P., and Tiwari, R. D., Microchem. J. 17, 151 (1972).
[25] Barton, J. A., Jr., Burns, C. L., Chandler, H. H., and Bowen, R. L., J. Dent. Res. **52**, 731 (1973).
[26] Argentar, H., and Bowen, R. L., J. Dent Res. **54**, 588 (1975).
[27] Foster, R., Organic Charge-Transfer Complexes (Academic Press, New York, N.Y., 1969), p. 3.
[28] Foster, R., Organic Charge-Transfer Complexes (Academic Press, New York, N.Y., 1969), p. 37.
[29] Herzberg, G., Atomic Spectra and Atomic Structure (Dover Publications, New York, N.Y., 1944), pp. 8, 9.
[30] Orgel, L. E., and Mulliken, R. S., J. Am. Chem. Soc. **79**, 4839 (1957).
[31] Foster, R., Organic Charge-Transfer Complexes (Academic Press, New York, N.Y., 1969), pp. 23–27, 43, 44.
[32] McConnell, H., Ham, J. S., and Platt, J. P., J. Phys. Chem. **21**, 66 (1953).
[33] Lepley, A. R., and Thelman, J. P., Tetrahedron **22**, 101 (1966).
[34] Mulliken, R. S., J. Phys. Chem. **56**, 801 (1952).
[35] Tsubomura, H., J. Am. Chem. Soc. **82**, 40 (1960).
[36] Janzen, E. G., Accounts Chem. Res. **2**, 279 (1969).
[37] Havon, E., and Simic, M., Accounts Chem. Res. **7**, 114 (1974).
[38] Meisel, D., and Neta, P., J. Am. Chem. Soc. **97**, 5198 (1975).
[39] Wold, S., Chem. Scr. **5**, 97 (1974).
[40] Wells, P. R., Chem. Rev. **63**, 171 (1963).
[41] Jungers, J. C., and Sajus, L., Rev. Inst. Fr. Petrole Ann. Combust Liquides **22**, 1699 (1967).
[42] Leffler, J. E., and Grunwald, E., Rates and Equilibria of Organic Reactions (John Wiley and Sons, Inc., New York, N.Y.), pp. 173, 204, 211, 222 (1963).
[43] Scheibe, G., and Brueck, D., Z. Elektrochem. **54**, 403 (1950).
[44] Leffler, J. E., and Grunwald, E., Rates and Equilibria of Organic Reactions (John Wiley and Sons, Inc., New York, N.Y., 1963), pp. 258–261.
[45] Kosower, E. M., and Skorcz, J. A., in Advances in Molecular Spectroscopy, Vol. 1, Mangini, A., ed. (Pergamon Press, 1962), p. 413.
[46] Kosower, E. M., Hofmann, D., and Wallenfells, K., J. Am. Chem. Soc. **84**, 2755 (1962).
[47] Kosower, E. M. in Progress in Physical Organic Chemistry, Vol. 3, Cohen, S. G., Streitwieser, A., Jr., and Taft, R. W., eds. (Interscience Publishers, New York, N.Y., 1965), p. 81.
[48] Sillen, L. G., Lange, P. W. and Gabrielson, C. O., Problems in Physical Chemistry (Prentice-Hall, Inc., Englewood Cliffs, N.J., 1952), p. 174.
[49] Wold, S., Chem. Scr. **2**, 49 (1972).
[50] Wold, S., Acta Chem. Scand. **27**, 3602 (1973).
[51] Streitwieser, A., Jr., in Progress in Physical Organic Chemistry, Vol. I, Cohen, S. G., Streitwieser, A., Jr., and Taft, R. W., eds. (Interscience Publishers, New York, N.Y., 1963), p. 1.
[52] Poldoja, P. K., and Palm, V. A., Reakts. Sponobnost Org. Soedin. **4**, 768 (1967); Org. Reactiv. (USSR), **4**, 320 (1967).
[53] Neter, J., and Wasserman, W., Applied Linear Statistical Models (Richard D. Irwin, Inc., Homewood, Ill., 1974), pp. 297–312.
[54] Afifi, A. A., and Azen, S. P., Statistical Analysis: A Computer Oriented Approach (Academic Press, Inc., New York, N.Y., 1972), pp. 108–113, 146–151.
[55] Hickinbottom, W. J., J. Chem. Soc. 946 (1933).
[56] Mueller, E., Methoden Der Organischen Chemie (Houben-Weyl) Georg Thieme Verlag, Stuttgart, Germany, pp. 1040–1043. 4th Edition. Vol. 10, Part 1 (1971).
[57] Harrison, A. G., Kebarle, P., and Lossing, R. P., J. Am. Chem. Soc. **83**, 777 (1961).
[58] Crable, G. F., and Kearns, G. L., J. Phys. Chem. **66**, 436 (1962).
[59] Tietjen, G., private communication.
[60] Foster, R., Organic Charge-Transfer Complexes (Academic Press, New York, N.Y., 1969), pp. 49–40.
[61] Zweig, A., Lancaster, J. E., Neglia, M. T., and Jura, W. H., J. Am. Chem. Soc. **86**, 4130 (1964).
[62] Lagutskaya, L. I. and Dadali, V. A., Reakts. Sposobnost Org. Soedin., **4**, 588 (1967); Org. Reactiv. (USSR), **4**, 241 (1967).
[63] Zuman, P., Substituent Effects in Organic Polarography, (Plenum Press, New York, N.Y., 1967), p. 43.
[64] Andrews, L. J., Chem. Rev. **54**, 713 (1954).
[65] Geske, D. H., in Progress in Physical Organic Chemistry, Vol. 4, Streitwieser, A., Jr., and Taft, R. W., eds., (Interscience Publishers, New York, N.Y., 1967), p. 125.
[66] Gould, E. S., Mechanism and Structure in Organic Chemistry, (Holt, Rinehart and Winston, New York, N.Y., 1959), p. 323.
[67] Farrell, P. G., and Newton, J., J. Phys. Chem., **69**, 3506 (1965).
[68] Sulzberg, T. and Cotter, R. J., Macromolecules **2**, 150 (1969).
[69] Hammond, P. R., J. Chem. Soc. **471** (1964).
[70] Shein, S. M., Starichenko, V. F., Katkova, N. M., and Anufrienko, V. F., Reakts. Sposobnost Org. Soedin. **6**, 692 (1969); Org. Reactiv. (USSR), **6**, 294 (1969).
[71] Bowers, K. W. in Radical Ions, Kaiser, E. T. and Kevan, L., Eds. (Interscience Publishers, New York, N.Y., Chapter 5, 1968).
[72] Foster, R., Organic Charge-Transfer Complexes (Academic Press, New York, N.Y., 1969), p. 51.
[73] Zuman, P., Substituent Effects in Organic Polarography, (Plenum Press, New York, N.Y., 1967), pp. 34, 35, 72–4.
[74] Kuhn, W. F., Levins, R. J., and Lilly, A. C., Jr., J. Chem. Phys. **49**, 5550 (1968).
[75] Peover, M. E., Trans. Faraday Soc. **60**, 479 (1964).
[76] McRae, E. G., J. Phys. Chem. **61**, 562 (1967).
[77] Mataga, N., and Kubota, T., Molecular Interactions and Electronic Spectra (Marcel Dekker, Inc., New York, N.Y. 1970), pp. 251, 371–410.
[78] Aihara, J., Tsuda, M., and Inokuchi, H., Bull. Chem. Soc. Jap. **42**, 1824 (1969).
[79] Kosower, E. M., J. Amer. Chem. Soc. **80**, 3253 (1958).
[80] Moriguchi, I, Fushimi, S. and Kaneniwa, N., Chem. Pharm. Bull. **19**, 2132 (1971).
[81] Koppel, I. A., and Palm, V. A. in Advances in Linear Free Energy Relationships", Chapman, N. B., and Shorter, J., eds. (Plenum Press, New York, N.Y., Chapter 5, 1972).
[82] Dimroth, K., Reichardt, C., Siepmann, T., and Bholmann, F., Justus Liebigs Ann. Chem. **661**, 1 (1963).
[83] Weast, R. C., Handbook of Chemistry and Physics, 50th Ed. (The Chemical Rubber Co., Cleveland, Ohio, P. C–369, 1969–1970.
[84] Bowen, R. L., and Argentar, H., J. Appl. Poly. Sci. **17**, 2213 (1973).
[85] Afifi, A. A., and Azen, S. P., Statistical Analysis: A Computer oriented Approach (Academic Press, Inc., New York, N.Y., 1972), pp. 64–65.
[86] Davidson, R. S., in Molecular Association, Vol. 1, Foster, R., Ed. (Academic Press, New York, N.Y., 1975), p. 215.

(Paper 80A2-886)

JOURNAL OF RESEARCH of the National Bureau of Standards—A. Physics and Chemistry
Vol. 80A, No. 2, March–April 1976

Bidirectional Reflectometry. Part I.

A High Resolution Laser Bidirectional Reflectometer With Results on Several Optical Coatings

Jack J. Hsia and Joseph C. Richmond
Institute for Basic Standards, National Bureau of Standards, Washington, D.C. 20234

(February 2, 1976)

A laser-source bidirectional reflectometer that is fully automated and has angular resolution on the order of one degree has been designed and built. The direction of incidence and viewing can be independently varied over an entire hemisphere except for directions more than 77.5° from the normal, and the two directions must be at least 2.5° apart. Bidirectional reflectances for 15 samples of black and white coatings are presented.

Key words: Barium sulphate; bidirectional reflectance; bidirectional reflectometer; black coating; gonioreflectometer; magnesium oxide; mu sulphur; reflectance; reflectometer; sodium chloride.

1. Introduction

The bidirectional reflectance distribution function (BRDF), f_r, has been defined [1, 2][1] as a quantity that describes the detailed reflectance properties of a sample.

$$f_r(\theta_i; \phi_i; \theta_r, \phi_r) = dL_r(\theta_i, \phi_i; \theta_r, \phi_r; E_i)/dE_i(\theta_i, \phi_i)\,[sr^{-1}]$$

The angle θ is measured from the surface normal to the given direction, and ϕ is the azimuth angle from a reference direction on the sample to the given direction. The subscripts i and r refer to incident and reflected flux, respectively. f_r is the quotient $dL_r(\theta_r, \phi_r)/dE_i(\theta_i, \phi_i)$ of the radiance dL_r, in the direction (θ_r, ϕ_r) due to irradiance dE_i in the direction (θ_i, ϕ_i), over all possible combinations of the directions (θ_i, ϕ_i) of incidence and (θ_r, ϕ_r) reflection.

The reflectance of a material under any geometrical conditions of irradiation and viewing can be computed from f_r by integrating over the solid angles of incidence and collection.

$$\rho(\omega_i; \omega_r; L_i) = \frac{\int_{\omega_i}\int_{\omega_r} f_r(\theta_i, \phi_i; \theta_r, \phi_r) L_i(\theta_i, \phi_i) \cos\theta_i \cos\theta_r \, d\omega_r d\omega_i}{\int_{\omega_i} L_i(\theta_i, \phi_i) \cos\theta_i \, d\omega_i}$$

or, if L_i is constant over the solid angle ω_i

$$\rho(\omega_i, \omega_r) = \frac{\int_{\omega_i}\int_{\omega_r} f_r(\theta_i, \phi_i, \theta_r, \phi_r) \cos\theta_i \cos\theta_r \, d\omega_r \, d\omega_i}{\int_{\omega_i} \cos\theta_i \, d\omega_i} \tag{1.1}$$

Because of the importance of the BRDF in evaluating geometrically different types of reflectance, and in estimating errors due to flux losses in instruments designed to measure directional-hemispherical reflectance, equipment for its evaluation was designed and built. The average BRDF is computed from bidirectional reflectance by dividing by $\cos\theta_r \, \Delta\omega_r$, the projected solid angle over which reflected flux is collected in the measurement. Several criteria for such equipment were established before attempting to design the equipment. These included the following:

1. Incident radiation to consist of a highly collimated beam of monochromatic radiation, with provision for control of polarization.
2. Solid angle of collector to be small, on the order of one degree square, in order to achieve good angular resolution in the reflected beam.
3. Angles of incidence (θ_i, ϕ_i) and reflection (θ_r, ϕ_r) to be known to better than 1°.
4. Both angle of incidence and angle of reflection to be variable over nearly a complete hemisphere.

[1] Figures in brackets indicate the literature references at the end of this paper.

5. Increments between successive points of measurement to be variable.

6. Random error of measurement not to exceed 1 percent of the measured value, and bias not to exceed 1 percent of the measured value or 0.005 in reflectance, whichever is larger.

7. Automatic preprogrammed operation of the equipment, and on-line processing of the data with an electronic digital computer.

A 10-mW helium-neon laser with Brewster angle windows was selected as a source, to meet the requirements for a highly collimated, intense monochromatic incident beam. It can be operated at 0.6328, 1.15, and 3.39 μm by use of cavity mirrors coated for operation at those wavelengths.

The requirement for automatic preprogrammed operation and computer processing of data is necessitated by the volume of data required. Evaluation of BRDF for points 1° apart over the hemisphere involves 400,000,000 data points. At 5° intervals, the number of data points is still over 1,600,000 points. Fortunately, most of the materials of interest are essentially isotropic in reflectance, that is, the bidirectional reflectance is essentially independent of the azimuth angle of incidence, ϕ_i. For such materials, the directions of incidence for measurements at 5° intervals can be reduced from about 1250 to 18. Measurements in which the directions of incidence and reflection coincide, and those in which either direction is 80° or more from the normal, are difficult to make. By eliminating such measurements, the number of directions of incidence can be reduced to 16, and the total number of data points for complete evaluation to less than 20,000. By limiting the directions of reflectance to points lying in the plane of incidence, or in a few planes at fixed angles to the plane of incidence, the number of data points can be reduced to about 500 for each plane.

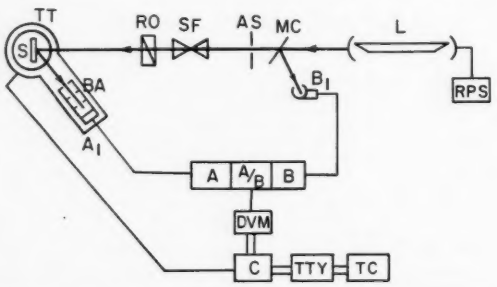

FIGURE 2.1. *Schematic diagram of bidirectional reflectometer.*

RPS: Regulated power supply	L: Laser
MC: Mirror chopper	AS: Aperture stop
SF: Spatial filter	RO: Rotator
S: Sample holder	TT: Turntables
BA: Baffles	A_1, B_1: Detectors A and B
A: Amplifier A	B: Amplifier B
A/B: Ratiometer	DVM: Digital voltmeter
C: Controller	TTY: Teletypewriter
TC: Time-shared computer	

Due to a shift in priorities, part of the equipment has been disassembled and the instrument described here is no longer in operating condition. The preliminary results obtained in this study are being published to make available the data obtained, and to give others the benefit of our experience in designing and operating the equipment.

2. Bidirectional Reflectometer

As shown in figure 2.1, the beam was chopped by a mirror chopper, which directed the beam alternately along two paths. The beam reflected by the chopper went directly to a monitor detector. The beam passed by the chopper went through an aperture, spatial filter, polarization rotator and onto the sample. The sample was rotated about three axes by stepping motors to control the angles of incidence and viewing. The reflected flux was received by a baffled detector. The signals from the two detectors were separately amplified, and the ratio of the two signals was recorded by the data acquisition system.

2.1. Source

The source was a He-Ne continuous wave gas laser. Three pairs of interchangeable reflectors were provided to permit operation of the laser at 0.6328, 1.15, and 3.39 micrometers, respectively. The laser was used in the multimode confocal configuration. The multimode operation has the advantage of high amplitude stability. The confocal configuration makes alignment of the reflectors less critical. The laser beam was polarized and highly collimated with beam diameter about 2 mm. The current was supplied by a high voltage power supply. The nominal output of the He-Ne laser was given by the manufacturer as 10 milliwatts at 0.6328 μm.

2.2. Mirror Chopper

The mirror chopper served two purposes: to direct the laser beam along two separate paths, and to modulate both of these beams so that phase-locked ac amplifiers could be used to amplify the signals, and thus reduce the random fluctuation of the two signals by reducing the effect of background. The double beam system [3], in which the signals from the two detectors were separately amplified, and the ratio of the two signals was used as a measure of the bidirectional reflectance, automatically compensated for the slight (about 2 percent) fluctuation in the laser output.

2.3. Aperture

An aperture with about 2 mm diameter was placed between the laser and the chopper. The aperture diameter was just larger than that of the laser beam to block light other than the main beam.

2.4. Spatial Filter

The spatial filter consisted of two lenses and one 20 μm diameter pinhole. The pinhole could be adjusted horizontally and vertically by means of micrometer

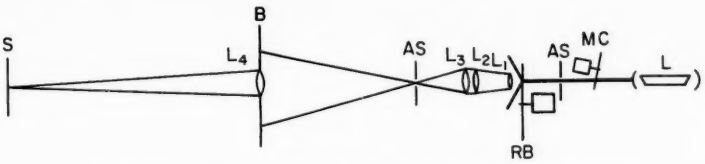

FIGURE 2.2. *Schematic diagram of unpolarized laser light source arrangement.*

L:	Laser
AS:	Aperture stop
RB:	Rotating blade with drafting film; rotation speed 1800 rpm with motor shaft to light beam distance of 7 cm.
L_1, L_2, L_3, and L_4:	Lenses
B:	Baffle
S:	Sample
MC:	Mirror chopper

screws. The first lens focused the collimated laser beam onto the pinhole and the second lens converted the diverging beam from the pinhole into a collimated beam. The purpose was to further filter out the scattered light, and produce a highly collimated beam.

2.5. Rotator

The rotator unit contained two quartz, quarter-wave plates. The first plate could be rotated manually so that its plane of retardation could be set at 45 degrees from the plane of polarization of the laser, to produce a circularly polarized beam. The light beam, after passing through the first plate, was found to have 1.5 percent polarization. The second quarter-wave plate could be used to convert the circularly polarized beam back to a plane polarized beam. The plane of polarization could be varied by rotation of the second quarter-wave plane, which was accomplished by means of a stepping motor.

An attempt was made to generate an unpolarized light beam from the polarized laser beam. A blade made of K & E Herculene drafting film was inserted in the light beam after the aperture and rotated at 1800 rpm. This is an optically inhomogeneous film that transmits a large fraction of the incident beam. Because of the finite size of the inhomogenieties in the material, the plane polarized and well-collimated laser beam is broken up into a diffuse beam with more-or-less random polarization in which the direction of the plane of polarization varies with position in the field. By rotating the film, these variations are constantly changing at a rapid rate, and the time-averaged residual polarization over the field is uniform not only from point to point, but for the same point from time to time. Lenses were then used to focus the beam onto the sample as shown in figure 2.2. The light beam, after passing through the rotating blade, was found to have 20 percent residual polarization.

2.6. Sample Holder and Turntable

The sample holder was made of aluminum alloy with a 38.1 mm diameter open space in the center. The front side tapered 10° toward the edge of the opening and was painted with matte black paint. The back side of the holder had three protrusions against which the sample surface was clamped. The three protrusions were located on a circle of 63.5 mm diameter. The axis (A) of rotation of the holder was in the sample-surface plane formed by the tips of these three protrusions. This axis (A) was normal to and rotated about a horizontal gimbal axis (B). The sample holder and gimbal were also mounted on a turntable which rotated around a vertical axis (C), as shown in figure 2.3.

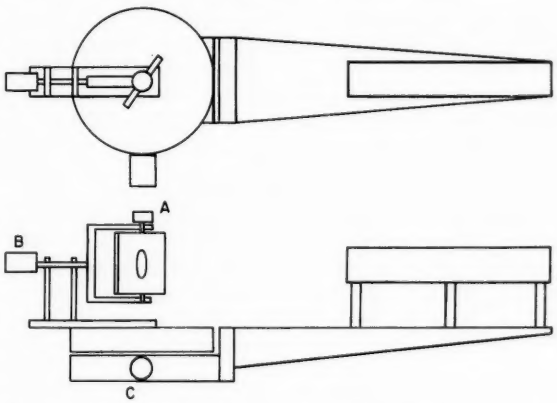

FIGURE 2.3A. *Schematic drawing of sample holder and turntables.*

A, B, and C are stepping motors.

The relations of the azimuthal and polar angles relative to the sample surface with angles about these three axes will be discussed in section 3.

2.7. Stepping Motors and Control

The sample holder was rotated about each of the three respective axes by a separate stepping motor, through a motor controller. Instructions to the control could be typed manually on a Teletype, fed into the Teletype as pre-punched paper tape, or supplied through an acoustic coupler by an on-line time-shared

201-606 O - 76 - 4

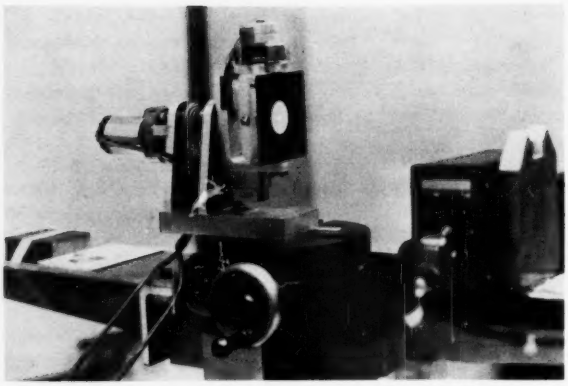

FIGURE 2.3B. *Photograph of sample holder.*

computer. Rotation about the vertical axis (C) was controlled to 0.045° (200 steps/rev. gear ratio 40/1), and that about the other axes (A & B) to 0.1° (48 steps/rev. gear ratio 75/1).

2.8. Detectors

Two lead sulfide detectors were used, one to monitor the laser beam, and the other to measure the light reflected from or incident on the sample. Both were 10×10 mm in size, and were operated with a 180 V dc bias. The sample detector was mounted on an arm attached to a turntable so that it could be rotated about the vertical axis C, in the horizontal plane of the horizontal axis B, at a distance of 940 mm from the intersection of axes B and C, as shown in figure 2.3. The detector thus subtended a plane angle of 0.61°, or a solid angle of 1.132×10^{-4} sr, at this point of intersection. Baffles, with apertures selected to confine the field of view of the detector to an area about the point of intersection slightly larger than the exposed area of the sample, were placed in front of the detector to block scattered light from reaching the detector.

2.9. Averaging Spheres

Two averaging spheres, 76.2 mm in diameter, were used; one in front of the monitor detector, and one in front of the sample detector when measuring incident light. The inside of each sphere was coated with barium sulfate. Each sphere was so constructed that the area irradiated by the beam being measured was not viewed by the detector. The transmittance (or efficiency) of the sample detector averaging sphere was measured, using the double-sphere method, and found to be 0.72 percent. The calculated transmittance was 0.82 percent.

2.10. Double-Detector and Amplifier System

The double-detector system was used to make the measurement independent of the output level of the laser. The laser beam was chopped by the mirror chopper at 33.9 Hz. During the first half of each cycle, the beam was incident on the sample. During the second half, the beam was reflected by the chopper blade into a small averaging sphere. The radiance of the averaging sphere wall was measured by the monitor detector, whose signal was then fed into a phase sensitive synchronous preamplifier and amplifier. The signal from the sample detector was amplified by an identical amplifier. The outputs of the two amplifiers were then fed into a ratioing multiplexer whose output was proportional to the ratio of the two signals. The resulting signal was then fed into a digital voltmeter.

2.11. Data Acquisition and Data Processing

The signal from the digital voltmeter was printed by the Teletype. In our experiments the stepping motors were controlled by the controller which accepted commands from the Teletype through prepunched paper tape. During the scan, each time that the stepping motors finished their rotation, the controller signaled the acquisition system to record ten data points. The signal from the digital voltmeter was printed by the Teletype and also fed into the on-line time-shared computer to process the data.

3. Azimuth and Polar Angles

The reflectometer controls the directions of incidence and viewing in terms of the angular position of the sample relative to the three axes of rotation of the sample holder. In order to convert the coordinates of these directions from the instrument angles into the more common polar and azimuth angles of the directions of incidence and viewing, relative to the sample normal and a fixed azimuth reference on the sample, it is necessary to transform the axes from those of the instrument to those of the sample.

The instrument axes are A, B, and C, and the corresponding angles about the respective axes are a, b, c. The pairs A and B and B and C are each mutually perpendicular, and all three meet at the origin, which lies in the plane of the sample surface. The C axis is vertical, and its positive direction is up from the origin; the B axis is horizontal, rotates about the C axis and always coincides with the direction of viewing. Its positive direction is from the origin to the detector. The A axis is normal to and rotates about the B axis. Its positive direction is from the origin to the stepping motor that rotates the sample about that axis.

Angle ϕ_0 is the angle between the positive A axis and the fixed azimuth reference mark on the sample. This angle remains fixed once the sample is mounted in the sample holder. Angle a is measured about the A axis from the positive B axis to the sample normal. Angle b is measured about the B axis from the positive C axis to the positive A axis. Angle c is measured about the C axis from the direction of incidence to the positive B axis. Each angle is positive in the counterclockwise direction, when

viewed from the positive direction of the respective axis of rotation toward the origin.

The desired parameters are θ_i, ϕ_i, θ_r, ϕ_r. (See fig. 3.1.)

θ_i is the polar angle between the sample normal and the direction of incidence.

ϕ_i is the azimuth angle between the reference line on the sample surface and the direction of incidence.

θ_r is the polar angle between the sample normal and the direction of viewing.

ϕ_r is the azimuth angle between the reference line and the direction of viewing.

The laser, and hence the direction of incidence, remains fixed. The detector rotates about the sample in the horizontal plane, and the direction of viewing always coincides with axis B.

The azimuth angle, ϕ_r, between the reference line and the direction of viewing remains fixed once the sample is mounted in the sample holder. During design of the sample holder inclusion of provision for rotating the sample in its own plane was considered. Since most of the materials of interest are essentially isotropic, equipment to provide such rotation is complex and somewhat bulky, and the space available for such equipment is small, it was decided that inclusion of this equipment was not justified.

The sample holder permits measurement of bi-directional reflectance at all angles of incidence where $\theta_i \leq 80°$ and the direction of incidence is not closer than 2.5° to the direction of viewing, and at all angles of viewing where $\theta_r \leq 80°$ at a single value of ϕ_r. Since the beams of incident and reflected flux are of very small angular size, no error is introduced in the measured reflectance by interchanging the directions of incidence, θ_i, ϕ_i and reflectance, θ_r, ϕ_r. In this way it is possible to obtain data over nearly a complete hemisphere of angles of viewing for all angles of incidence, θ_i, within a fixed azimuth plane. The location of the fixed azimuth plane can be changed, if desired, between series of measurements by manually rotating the sample in the holder.

When angles a, b, and c are zero, the B axis will coincide with the sample normal, the direction of incidence and the direction of viewing, and the C and A axes will coincide. As the sample is rotated about the several axes, its normal will move away from its zero position as follows: with $a=b=0$, the normal will move from its zero position by angle c; as b is changed, the plane containing the sample normal rotates about axis B by angle b; when $b=c=0$, the sample normal moves away from its zero position by angle a.

Since the direction of viewing coincides with the B axis, its direction is independent of angles b and c.

$$\theta_r = a. \tag{3.1}$$

For the same reason, ϕ_r, the azimuth angle of the direction of viewing will be independent of angles a, b, and c.

$$\phi_r = 90° - \phi_0. \tag{3.2}$$

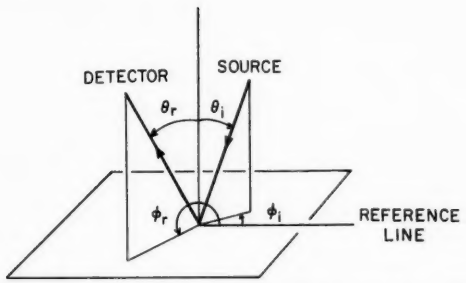

FIGURE 3.1. *Coordinate system related to sample surface.*

The equations for angles θ_i and ϕ_i are more complex. Several equations can be set up relating θ_i to a, b, and c. When $b=0$, $\theta_i = c + a$. When $b=0$ and $a=-c$, $\theta_i = 0$. When $c=a=0$, $\theta_i = 0$, regardless of b. When $b=90°$, $\cos\theta_i = \cos a \cos c$. When $a=0$, $\theta_i = |c|$. Hence,

$$\cos\theta_i = \cos a \cos c - \sin a \cos b \sin c. \tag{3.3}$$

Equations can also be derived relating ϕ_i to a, b, c, ϕ_0 and θ_i. When $\theta_i = 0$, ϕ_i is indeterminate. When $a=0$, ϕ_i is independent of c and θ_i, and $\phi_i = [(c/|c|) \cdot 90°] - b - \phi_0$. When $b = (c/|c|) \cdot 90°$, $\phi_i = -\phi_0$. The final equations are:

$$\begin{aligned} \phi_i &= \phi_0' - \phi_0 \\ \cos\phi_0' &= \frac{\sin b - \sin c}{\sin\theta_i}. \end{aligned} \tag{3.4}$$

Figure 3.2 shows the physically impractical conditions of angles a, b, and c. When $a=30°$, for example, and b and c lie in the shaded area of the figure, the incident beam will be on the back of the sample. Only one quarter of the possible combinations of b and c in figure 3.2 is enough to give all the polar and azimuth angles needed. Figures 3.3, 3.4, 3.5, and 3.6 show the relations between θ (i.e., θ_i), ϕ (i.e., ϕ_i), and b, c when $a=0°$, 30°, 60°, and 80° respectively. ϕ_r equals 90° when $\phi_0=0$. Thus when $\phi_i=-90°$, the measurement is made in the plane of incidence.

4. Alignment

Alignment of the optical system involved the following steps: (1) leveling the laser beam to establish a level plane of reference for alignment of other optical elements; (2) leveling the sample holder and centering it in the laser beam; check to see that axis C is vertical, axis B is horizontal and in a horizontal plane through the laser beam, axis A is perpendicular to axis B and in a vertical plane through axis C, and that the three axes intersect at the point where the laser beam hits the sample; (3) establish the zero angular position about each axis; (4) align detector and detector baffle; and (5) position and align other optical elements: chopper, spatial filter, polarization rotator and aperture.

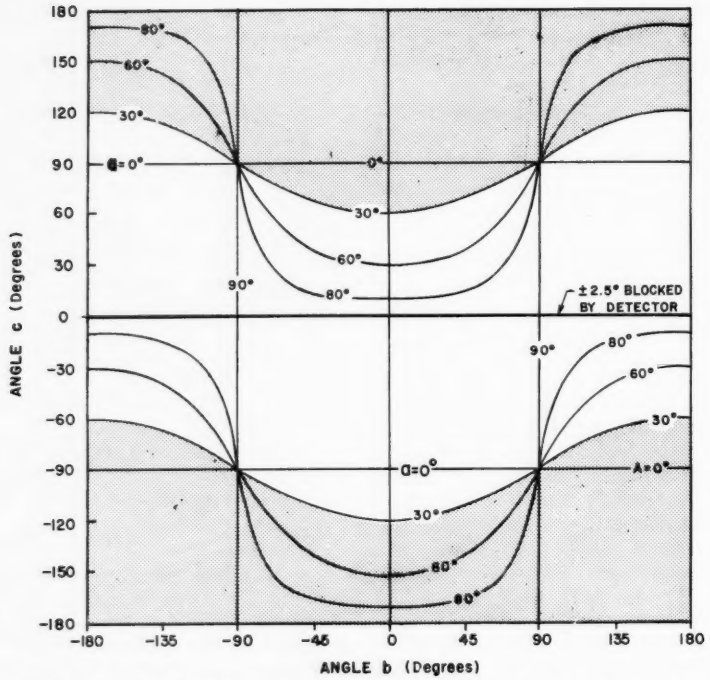

FIGURE 3.2. *Physically impractical conditions of angles* a, b, *and* c, *indicated by shaded portion.*

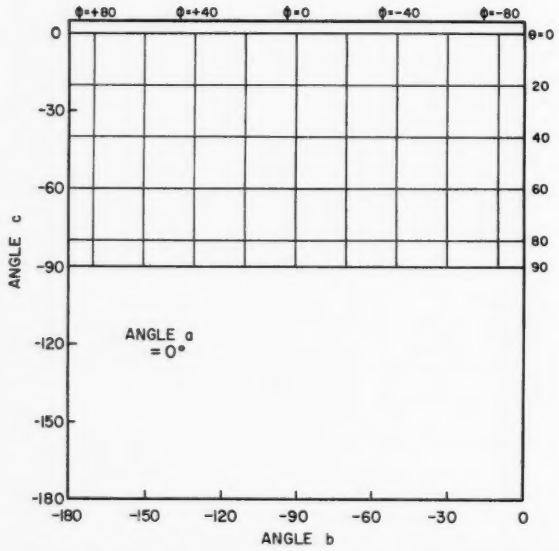

FIGURE 3.3. *Relations between* θ, ϕ *and* b, c *when* a = *0 degrees.*

$\theta_r = a, \phi_r = +90°, \theta_i = \theta, \phi_i = \phi$.

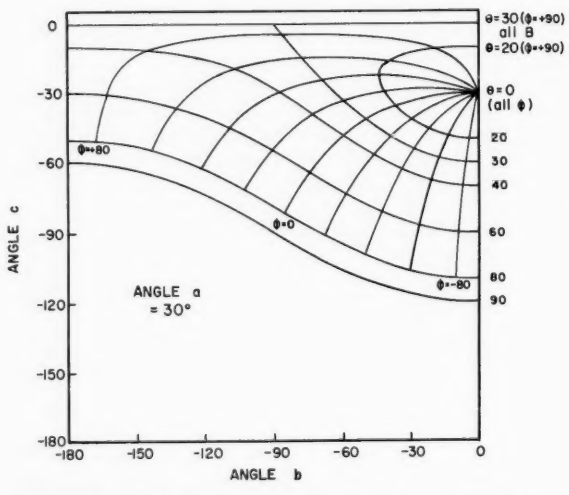

FIGURE 3.4. *Relations between* θ, ϕ *and* b, c *when* a = *30 degrees.*

$\theta_r = a, \phi_r = +90°, \theta_i = \theta, \phi_i = \phi$.

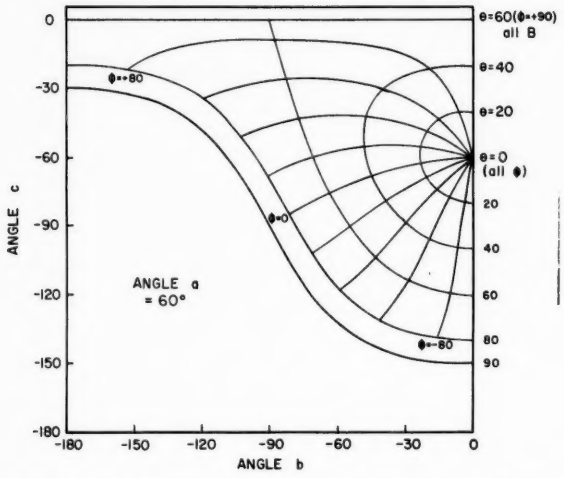

FIGURE 3.5. *Relations between* θ, ϕ *and* b, c *when* a = *60 degrees.*
$\theta_r = a, \phi_r = +90°, \theta_i = \theta, \phi_i = \phi$.

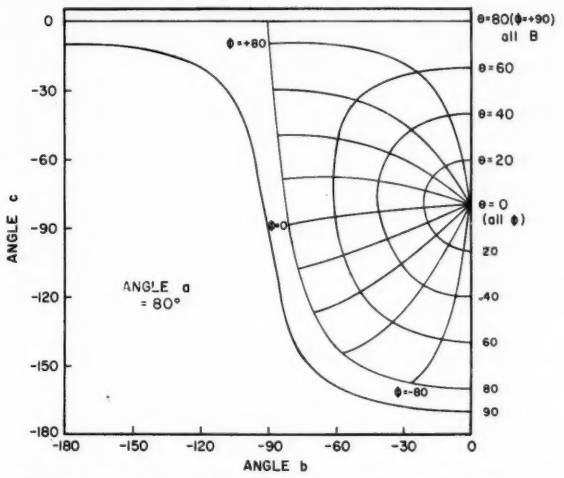

FIGURE 3.6. *Relations between* θ, ϕ *and* b, c *when* a = *80 degrees.*
$\theta_r = a, \phi_r = +90°, \theta_i = \theta, \phi_i = \phi$.

4.1. Leveling Laser Beam

Since the laser beam remained fixed in position, and served as the reference for alignment of the rest of the optical system, it was carefully leveled. A high-sensitivity machinists' level was used to level the base on which the laser tube is mounted, which approximately leveled the beam. A surveyor's level was then set up so that, when level, its crosshairs were in the horizontal plane containing the laser beam. The level was then sighted in turn on the two bright spots produced by the front and rear laser beams on the end walls of the laboratory, about 5 m apart. The level of the laser was adjusted until the crosshairs of the level telescope were well centered on each of the two bright spots. The level plane thus established became the reference plane for alignment of the other elements of the system, and the level was left in place until alignment was completed.

4.2. Positioning Sample Holder

The sample holder consisted of two separate parts, which were mounted on a different table from that on which the laser was mounted. Part one consisted of two rotary milling machine heads mounted one above the other so that their axes of rotation coincided. Two arms, each about 110 cm long, were attached to opposite sides of the bottom rotary head. One supported the detector and its baffles, and the other supported counterweights, so that the entire rotating head was approximately balanced. The upper rotary head supported part two, which was a mount for a horizontal shaft (axis *B*) with a yoke attached to one end holding a second shaft (axis *A*) normal to the first shaft.

Part one of the sample holder was clamped in place on the supporting table, which was of such height that the center of the sample, when the sample is mounted in the holder, would be approximately centered on the laser beam. Part two of the sample holder was placed in position, and a card with crossed vertical and horizontal lines was centered in the sample holder. The table was adjusted until the laser beam was centered on the crossed lines. A small graduated cylinder was placed near the end of the detector support arm, and filled with water until the meniscus was in the reference plane. The surveyor's level was sighted on the meniscus, as the arm was rotated about the *C* axis, and the level of the table was adjusted until the meniscus remained in the reference plane at all positions of the arm. This showed that the *C* axis was vertical. The position of the laser beam was again checked on the crossed lines, the card was removed and the laser beam was found to be well centered on the end of the horizontal shaft (*B* axis). A plane mirror was mounted in the sample holder, angle *c* was set at about 40°, and angle *a* was adjusted until the bright spot on the wall formed by the laser beam after reflection from the mirror, remained stationary while angle *b* was varied from 0° to 180°. This showed the sample to be normal to axis *B*. Angle *c* was then changed until the laser beam was reflected back along its path, and the sample holder was shimmed until the sample was normal to the laser beam. The plane mirror was replaced with the card with crossed lines, and the card was adjusted until the laser beam was centered on the crossed lines. Angle *b* was varied from 0° to 360° to check that the cross was at axis *B*. The position of the crossed lines relative to axis *C* was checked by rotating the sample from 0° to +80° and −80° about axis *C* and adjusting the position of part two of the sample holder until the laser beam was well centered on the crossed lines in all positions. Part two of the sample holder was then clamped in position.

The position of axis A relative to axis C was checked by rotating the holder about axis B until axis A was approximately horizontal, then rotating the sample from 0° to +80° about axis A. The position of axis A was adjusted by shifting shaft B along its axis of rotation until the laser beam was well centered on the crossed lines in all positions. Axis B was then fixed in this position.

The above adjustments positioned the various parts of the sample holder relative to the laser beam and to each other so that the laser beam was centered on the point on the sample surface where the three axes of rotation intersected.

4.3. Setting Zeros on Each Axis of Rotation

The zero position of each axis was established with a plane mirror in the sample holder. Angle a was adjusted as before until the sample was normal to axis B. This was the zero position of angle a. Angle c was then adjusted until the sample was normal to the laser beam. This was the zero position of angle c. Angle c was then set at about 10°, 40°, 75°, −40°, and −75°, and at each setting a horizontal reference line was drawn on the laboratory wall at a height where the laser spot was bisected by the line. The position of each reference line was checked with the level, to make sure that it was in the reference plane. Angle c was then reset at zero, and angles a and b were adjusted to center the laser spot on one of the reference marks with angle a at about ±40°. This was the zero position of angle b.

The reference marks on the laboratory wall could be used for a quick check to see that axis C was vertical, and to check the zero position of angle b.

4.4. Aligning Detector Baffles

The detector baffle consisted of several sections of 6 cm i.d. brass tubing of 1.5 mm wall thickness, 5, 10, or 25 cm long. The ends of each tube were squared and smoothed on a lathe. A shoulder 1 mm deep of outside diameter just under 6 cm, was machined on each side of each diaphragm plate, so that it fits snugly into the end of a tube, and could be used as a coupling between tubes. A circular aperture was machined in the center of each plate. The plate was tapered evenly on both sides from about 3 mm from its outer edge to the edge of the aperture, so that the thickness at the edge of the aperture was about 0.25 mm, and the edge of the aperture was rounded. Aperture plates with apertures of various diameters from 1 mm to 6 cm were prepared. The detector was mounted at the center of one face of a brass block of outer diameter such as to fit snugly into the baffle tubing, and the leads were passed through holes in the block. The insides of the tubes, the diaphragms and the end of the block on which the detector was mounted were painted with a diffusely reflecting black paint.

The detector and baffles, in the form of a tube 6 cm in diameter and 75 cm long, rested in four V-blocks mounted on the detector arm of the sample holder. The V-blocks were aligned by use of a 25 cm section of baffle tubing with 2 mm diaphragms in each end. The tube was supported by the first two V-blocks, with angle c set at the zero position, and the position of the blocks was adjusted until the laser beam was well centered in the two apertures. The tube was then moved to the second and third V-blocks, and the third block adjusted, then to the third and fourth V-blocks, and the fourth block adjusted. The V-blocks were clamped in position after adjustment.

The detector baffle consisted of lengths of 10, 25, 25, 10, and 5 cm of tubing, with baffle plates at the front end and acting as a coupling between successive tubes. The size of the apertures was graduated for 3 cm at the front end to 1.4 cm in front of the detector so that the view of the detector was restricted to essentially the 3.8 cm hole in the sample holder. The detector was mounted 94 cm from the point where the axes crossed.

4.5. Aligning Optical Elements

The mirror chopper consisted of a single sheet of plate glass, cut to have six blades and six spaces, then coated with vacuum deposited aluminum to form a first surface mirror. It is necessary, in order for the reflections from the six blades to coincide, that the mirror be mounted on its rotating shaft so that the plane of the reflecting surfaces is normal to the axis of rotation. Such alignment is difficult to achieve by mechanical means.

The mirror chopper was adjusted until it was nearly normal to the shaft on which it was mounted. The chopper was set in position to reflect the laser beam onto a wall about 3 m away. The position of the beam when reflected by each blade in turn was recorded on a piece of paper. These points fell on a circle. The position of the chopper blade on the shaft was shifted, and the points recorded, until the diameter of the circle had been reduced to about 1 mm. The chopper was then positioned about 18 cm in front of the laser mirror, tilted slightly so that the laser beam was reflected slightly downward to a plane mirror, which reflected it to the entrance aperture of the averaging sphere in front of the reference detector. The plane mirror was adjusted to center the beam in the aperture.

The spatial filter consisted of a microscope objective lens which focused the laser beam onto a 20 μm aperture and a second microscope objective which recollimated the beam emerging from the aperture. The aperture was in a magnetized steel mount which was held magnetically in contact with the aperture plate and with horizontal and vertical micrometer screws. In order to avoid deviation or displacement of the laser beam, it was necessary that the beam be accurately centered on each of the lenses and the aperture. The filter was mounted on a micromanipulator which provided vertical and horizontal adjustment in a plane normal to the laser beam.

The lenses and aperture were removed from the filter, and it was approximately centered and aligned by eye. The aperture was then inserted, and approximately centered in the laser beam. A piece of white cardboard was mounted a few cm behind the aperture, and was uniformly but faintly illuminated by light passing through the aperture. The first lens was then inserted, and brought toward focus, until the card was dark on one side. The aperture was then moved perpendicular to the laser beam toward the light side of the card until the circle of light was again uniform. This process was repeated until the laser beam was fully focused on the aperture, which was indicated by a marked increase in brightness on the card. The focus adjustment was critical, and the focus could be destroyed by movement of only a few micrometers of either the lens or aperture. The second lens was then inserted and the laser beam was recollimated to form a uniform bright spot about 2 mm in diameter on the sample. However, this spot was no longer centered on the crossed lines, but deviated from the cross by several cm. The aperture was removed from the filter, leaving the micrometer screws set at the focus position, and the filter was adjusted in angle and position, until the beam was again centered on the cross. The aperture was then replaced, but was no longer in the focus position, and had to be realigned. The readings on the two micrometer screws were recorded, and the aperture was scanned in a raster pattern over an area about 0.25 mm square about the former focus position, until some light could be seen coming through the filter, after which the aperture was moved toward the light side of the pattern until the focus position was again attained.

The polarization rotator consisted of two 8-mm diameter quartz quarter-wave plates, each mounted in a holder that permitted it to rotate in its own plane. When the plane of retardation of the first filter was at 45° to the plane of polarization of the beam, it converted the plane-polarized beam into a circularly polarized beam. This first plate could be rotated manually. The second plate converted the circularly polarized beam back into a plane-polarized beam whose plane of polarization rotated with the plate. This plate was rotated by a stepping motor in synchronization with that used to rotate the sample about axis B. This arrangement maintained the angle between the plane of polarization and the plane of incidence constant as the sample was rotated to change the plane of incidence. The holder for the second plate could easily be removed so that the circularly polarized beam could be used when an unpolarized incident beam was desired.

Alignment and adjustment of the rotator involved mounting the two plates so that the beam was well centered on each plate, and was incident at an angle about 1° off normal, so that interreflections between the plates themselves or other optical elements would be avoided, and adjustment of the angular position of the plane of retardation of each plate. The holder was constructed so that the two plates were mounted at an angle of about 1° to each other. After the holder was properly positioned, the second plate was removed, a rotatable polarizing filter was placed in the beam, and the beam was directed to an averaging sphere in front of a detector. The first plate was positioned so that its plane of retardation was at approximately 45° to the plane of polarization of the laser beam on the basis of the marked position on the plate of the plane of polarization. The residual polarization was measured as the difference between the high and low readings of the detector as the polarizing filter was rotated, divided by the sum of the two readings. Fine adjustments were made in the angular position of the first plate until the residual polarization reached a minimum, which was about 1.5 percent. The second plate was then inserted in its holder, and its angular position adjusted until the plane of polarization was vertical. Angle b was then set at zero, and the stepping motors that drove the sample about axis B and the polarizing filter, respectively were synchronized.

The final step was to insert an aperture, about 2.5 mm in diameter, into the beam between the laser and the chopper. The aperture was placed so that the beam was well centered, and did not touch the edge of the aperture at any point.

5. Errors

The possible sources of error associated with reflectance measurements are listed and discussed below.

5.1. Solid Angle of Viewing

For a small solid angle, the following expression can be used

$$\omega = h \cdot w/l^2$$

where ω is the solid angle subtended by an area with height h and width w and placed l distance away. The error caused by the uncertainties Δh, Δw, and Δl in determining h, w, and l can be expressed as

$$\frac{\Delta\omega}{\omega} = \left[\left(\frac{\Delta h}{h} \right)^2 + \left(\frac{\Delta w}{w} \right)^2 + 2 \left(\frac{\Delta l}{l} \right)^2 \right]^{1/2} \quad (5.1)$$

h and w can be measured to 0.025 mm and l to 1 mm. With $h = w = 10$ mm and $l = 940$ mm, $\Delta\omega/\omega = 0.005$. The uncertainty in the size of the solid angle subtended by the detector contributes no error to the measured bidirectional reflectance. However, when the bidirectional reflectance is converted to average bidirectional reflectance distribution function (BRDF) the uncertainty in the size of the solid angle contributes directly to the uncertainty in the average BRDF. With a diffuse sample, the measured average BRDF will have an uncertainty of 0.5 percent of its own value.

5.2. Incident Level

The irradiance received by the detector from the laser source is six to seven orders of magnitude higher than that from some of the black coatings.

The incident light is measured by using a 3-inch-diameter averaging sphere in front of the detector and the diffuse light reflected from the sample is viewed by the detector directly. The signal produced by the laser source would be

$$S_0 = I_0 \cdot T_0 \cdot G_0 \tag{5.2}$$

and the signal produced by the sample would be

$$S_s = I_0 \cdot \rho \cdot G_s \tag{5.3}$$

where I_0 is the total power in the beam from the source; T_0 is the transmittance of the averaging sphere; ρ is the bidirectional reflectance of the sample; and G_0 and G_s are the gains used for measuring the source and sample, respectively.

Combining equation (5.2) and (5.3), the reflectance is expressed as

$$\rho = \frac{S_s}{S_0}(T_0 \cdot G) \tag{5.4}$$

where

$$G = G_0/G_s$$

The contribution of T_0 and G to the uncertainty of the reflectance can be written as

$$\frac{\Delta\rho}{\rho} = \left[\left(\frac{\Delta T_0}{T_0} \right)^2 + \left(\frac{\Delta G}{G} \right)^2 \right]^{1/2}. \tag{5.5}$$

The transmittance of the averaging sphere (sphere A) was determined by employing another averaging sphere (sphere B) of the same size and construction. A signal was first obtained when both spheres were used with sphere B over the detector and sphere A over sphere B. The signal with just sphere B over the detector was then measured. The ratio of these two signals yielded the transmittance of sphere A. Some uncertainties are involved in the measurements. The interreflection between these spheres, although it existed, was very small. The directly irradiated area on the wall of sphere B was larger in the first measurement than that in the second measurement. The uncertainty of the transmittance T_0 of sphere A is thus dependent on the variation of the reflectance of the directly irradiated portion of the wall of sphere B, which is estimated to be 2 percent of its value.

The true ratio of the gains used was determined by feeding a signal from a square wave generator through an attenuator to the preamplifier of amplifier A (fig. 1). The method of determination was designed so that the ratio thus measured was independent of the accuracy of the attenuator. The uncertainty of the ratio was about 0.22 percent of its value. From equation (5.5), the uncertainty in the measurement of the incident level is about 2.2 percent of its value.

5.3. Angular Position

In the plane of incidence and assuming $\phi_0 = 0$, equations (3.1) to (3.5) can be rewritten as

$$\theta_r = a$$
$$\phi_r = +90°$$
$$\theta_i = |\, c + a \,|$$
$$\phi_i = -90°.$$

From section 2.7, a is controlled to 0.1° and c to 0.045°. Thus, $\Delta\theta_r = 0.1°$ and $\Delta\theta_i \simeq 0.15°$. For a diffuse sample, the contribution to the uncertainty of the reflectance would be negligible.

5.4. Linearity

Nonlinearity within one gain setting of amplifier A was determined to be less than 0.2 percent.

5.5. Stability

The measurement is made independent of the fluctuations in the laser source by using the monitor detector. However variations in the gain of the measuring and monitor receiver systems should be considered. The detector is slightly temperature sensitive. The temperature of the laboratory is controlled within one degree. The instability of the detection system is estimated to cause uncertainty in reflectance of 0.2 percent of its value.

5.6. Polarization

For samples with random roughness distribution, the use of circularly polarized light to replace unpolarized light should not contribute any error to the reflectance determination.

5.7. Random Error

The noise is higher for lower reflectance samples. For a sample with 10^{-3} percent reflectance, the noise is 0.1 percent of its value. For a sample with 2×10^{-4} percent reflectance, the noise is 1 percent of its value and for a sample with 2×10^{-5} reflectance, the noise is 10 percent of its value. The error due to these noise levels could be reduced by taking more data.

5.8. Error Budget

For relative measurements the first two factors (solid angle and incident level) could be ignored. Thus for the absolute and relative measurement with reflectance less than 10^{-3} percent, the error budgets are as follows:

	Absolute (% of its value)	Relative (% of its value)
Solid angle	0.5	
Incident level	2.2	
Angular position	–	–
Linearity	0.2	0.2
Stability	0.2	0.2
Polarization	–	–
Random noise	0.1–10	0.1–10
	3.2–13.1%	0.5–10.4%

5.9. Performance Tests

Figure 5.1 shows the angular resolution attained with the instrument. The specular peak reflected by a piece of polished black glass was measured. For the circularly polarized beam the half-height width of the peak is about 0.7 degree, and with the mylar sheet depolarizer the half-height width is about two degrees because the incident beam is convergent.

The accuracy of the specular measurements is shown in figure 5.2. The absolute reflectance of a piece of polished black glass was measured as a function of angle of incidence. The reflectance was obtained as the ratio of the measured reflected and incident fluxes. The value obtained at 7.5 degrees from the normal was used to compute the index of refraction of the glass, which was in turn used to compute the Fresnel reflectance at the other angles of incidence. The difference between the measured and computed values is shown as the dotted line, and does not exceed 0.02 percent in absolute reflectance.

6. Results

Data for 15 samples of coated metal are shown in figures 6.1 through 6.16. All data were taken at 0.6328 μm in the plane of incidence, at angles of incidence varying from 2.5° to 77.5° from normal at increments of 5°, and at angles of reflection from − 77.5° to + 77.5°, again at increments of 5°. The directions of incidence are defined as postive, hence reflection in a negative direction is forward scattering, and reflection in a positive direction is backscattering.

In order to permit easy comparison of the effects of (1) variations in direction of reflection, (2) variation in direction of incidence, and (3) method of applying a coating, the data were treated in two ways. First, each measured bidirectional reflectance was divided by the cosine of the angle of reflection, θ_r, measured from the normal to the surface to the direction of reflection, in order to show the deviation of the bidirectional reflectance from that of a perfect lambertian diffuser, for which $\rho/(\cos\theta_r)$ would be constant for all angles of reflection. Second, a separate curve was drawn for each direction of incidence. In order to minimize overlap of these curves, the zero line for the incidence at 2.5° from normal was selected to place the curve near the bottom of the graph. The zero line for each succeeding curve was displaced upwards, by an amount indicated on the right hand margin of the graph. Hence for materials that are very good diffusers, the different curves will be essentially flat and parallel, while retroreflectors will exhibit peaks near the direction of incidence, and specular reflectors will exhibit peaks in the specular direction.

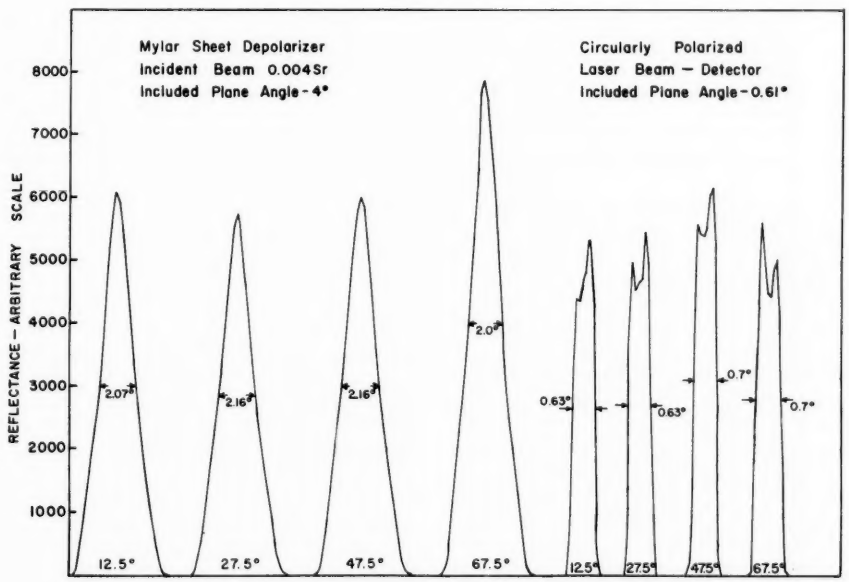

FIGURE 5.1. *Results of angular resolution tests.*

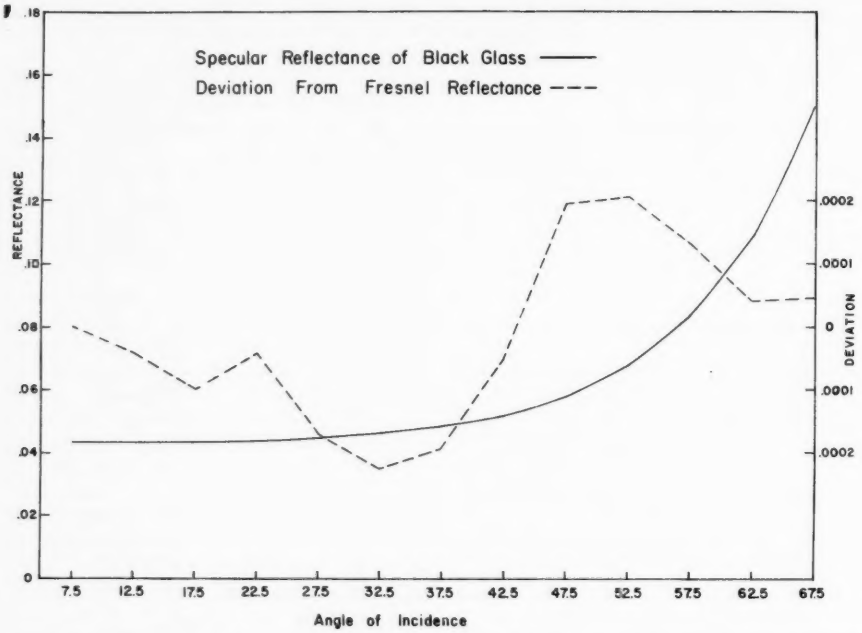

FIGURE 5.2. *Measured reflectance of black glass compared to reflectance computed from Fresnel's equation.*

The major interest in this study was to develop a method of evaluating bidirectional reflectance, and particularly to study the variations in bidirectional reflectance with directions of incidence and reflection. The coatings chosen for measurement were optical coatings that are either highly absorbant, primarily for use in reducing stray radiation in optical systems, and those that are highly reflecting and good diffusers, for use as integrating sphere coatings.

Since the variations in bidirectional reflectance are of primary interest, the data are plotted in arbitrary units. However, a conversion factor to absolute units is indicated on each figure. The bidirectional reflectance, even of the high-reflectance coatings, is necessarily low, because of the very small solid angle of collection. For many of the coatings, the relative directional hemispherical reflectance was computed from the measured bidirectional reflectance, and plotted as a function of angle of incidence. This graph is shown as an insert in the main figure.

The bidirectional reflectance of Thomas Parsons Optical Black [2] applied by brushing is shown in figure 6.1. This coating is very diffuse at angles of incidence within about 30° of normal, and becomes increasingly specular [3] at increasing angles of incidence beyond 30°. There is no indication of retroreflectance. The same coating applied by spraying, figure 6.2, is a pronounced retroreflector, and somewhat less specular.

The Eppley Laboratory purchased the rights to this coating from Thomas Parsons in England. Their version of Parsons Optical Black, when applied by brushing, shows in figure 6.3 a slight tendency toward retroreflectance, but in general appears quite similar to the original. When applied by spraying, the Eppley coating shows significantly reduced retroreflection and somewhat greater specular reflection at large angles of incidence, as shown in figure 6.4, compared to the original.

3M Nextel black is very diffuse in reflectance at angles of incidence of 45° or less from normal. At angles of incidence greater than 45° from normal it becomes increasingly specular with an increase in the angle of incidence. There is no pronounced retroreflection.

The data for black velvet cloth, shown in figure 6.6, were taken with a plane polarized incident beam. In all other cases the incident beam was either circularly polarized, or depolarized. The data on black velvet cloth are shown for their general interest. The black velvet is an excellent diffuser, becoming somewhat specular and retroreflective at angles of incidence beyond about 60° from the normal.

In the measurements on sprayed barium sulphate, figure 6.7, the incident beam was depolarized by use of the spinning drafting film sheet (see para. 2.5). Sprayed barium sulphate is a good diffuser at angles of incidence less than about 50° from normal. It

[2] The proprietary coatings measured in this study are identified by manufacturer and trade name for the convenience of the reader. Such identification does not constitute endorsement of the coatings by the National Bureau of Standards.

[3] But not at the normal angle for specular reflection. See discussion at end of this section.

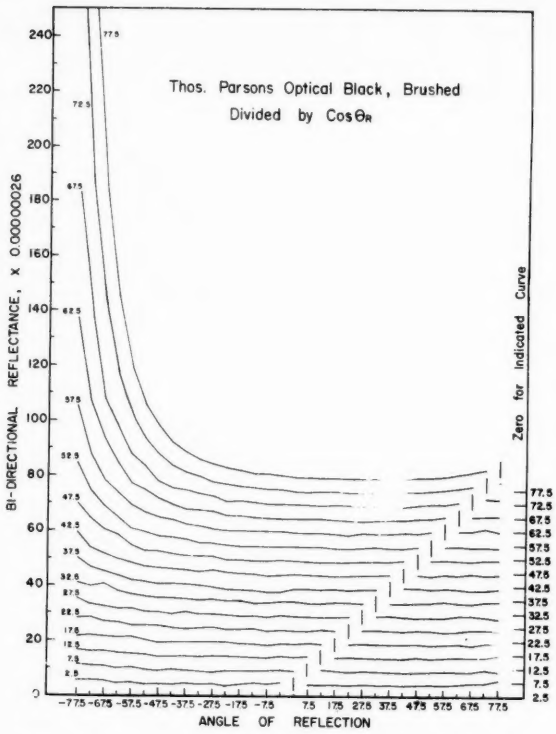

FIGURE 6.1. *Bidirectional reflectance of brushed Thomas Parsons optical black.*

For BRDF multiply scale values by 0.0023.

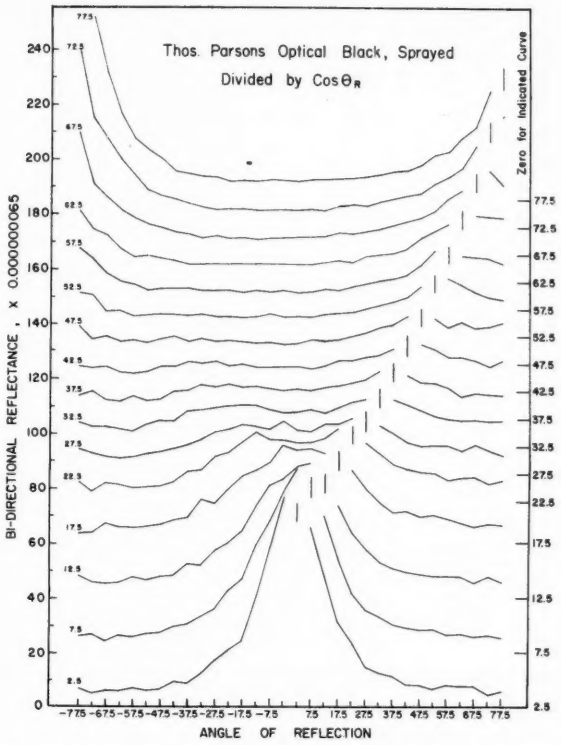

FIGURE 6.2. *Bidirectional reflectance of sprayed Thomas Parsons optical black.*

For BRDF multiply scale values by 0.00057.

becomes slightly retroreflective at angles of incidence greater than about 15° from normal, and somewhat specular at angles of incidence greater than about 50° from normal. Even at 77.5° from normal, the retroreflectance is relatively small, but the specular reflection is quite pronounced. The scatter in the data is attributed to roughness of the sprayed coating. The pressed barium sulphate, figure 6.8, is similar to the same coating applied by spraying, but the scatter in the data is greatly reduced, probably because of the smoother surface.

Sodium chloride, figure 6.9, is an excellent diffuser, showing essentially no specular or retroreflectance at directions of incidence less than about 65° from the normal, and the specular and retroreflectance even at 77.5° from normal is low compared to that of barium sulphate.

Mu sulfur, figure 6.10, is also a good diffuser, but becomes somewhat retroreflective at angles of incidence beyond about 15° from normal, and slightly specular at angles of incidence beyond about 65° from normal.

Smoked magnesium oxide, figure 6.11, is somewhat inferior to barium sulphate and sodium chloride as a diffuser, particularly at angles of incidence near normal. It shows significant fall-off in back reflection with increasing angle of viewing at all directions of incidence.

Sprayed Mautz black, figure 6.12, is a good diffuser at near normal incidence, but becomes increasingly specular with increasing angle of incidence beyond about 10° from normal, and a slight retroreflector at angles of incidence near grazing. The same coating when brushed, figure 6.13, becomes even more specular, especially at near grazing angles.

Sprayed Catalac black, figures 6.14 and 6.15, shows significant specular reflection even at near-normal directions of incidence, and is very specular at near grazing angles. This coating shows about the same pattern when brushed, figure 6.16.

It should be noted that the specular peak of the diffusely reflecting coatings tends to occur at an angle of reflection greater than the angle of mirror reflection, and for some coatings at an angle of reflection beyond 77.5° from normal. This tendency has been noted by previous workers in the field. [4]

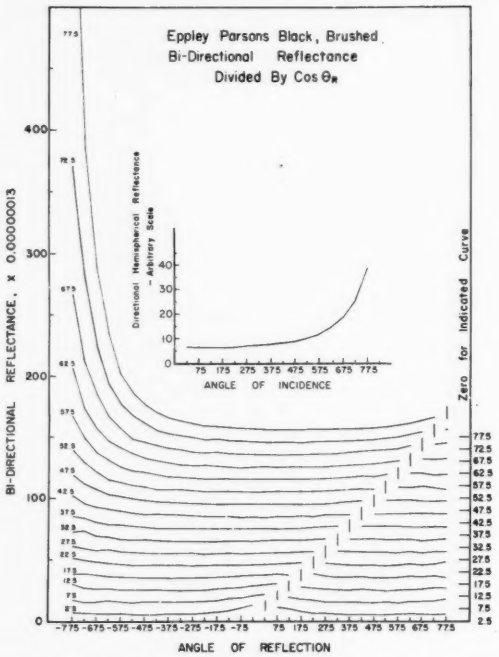

FIGURE 6.3. *Bidirectional reflectance of brushed Eppley Parsons optical black.*

For BRDF multiply scale values by 0.00115.

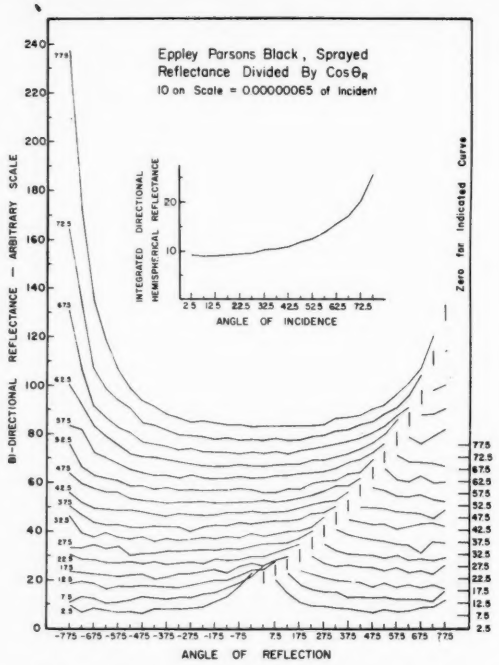
Eppley Parsons Black, Sprayed
Reflectance Divided By Cos θR
10 on Scale = 0.00000065 of Incident
BI-DIRECTIONAL REFLECTANCE — ARBITRARY SCALE
INTEGRATED DIRECTIONAL HEMISPHERICAL REFLECTANCE
ANGLE OF INCIDENCE
Zero for Indicated Curve
ANGLE OF REFLECTION

FIGURE 6.4. *Bidirectional reflectance of sprayed Epply Parsons optical black.*

For BRDF multiply scale values by 0.00057.

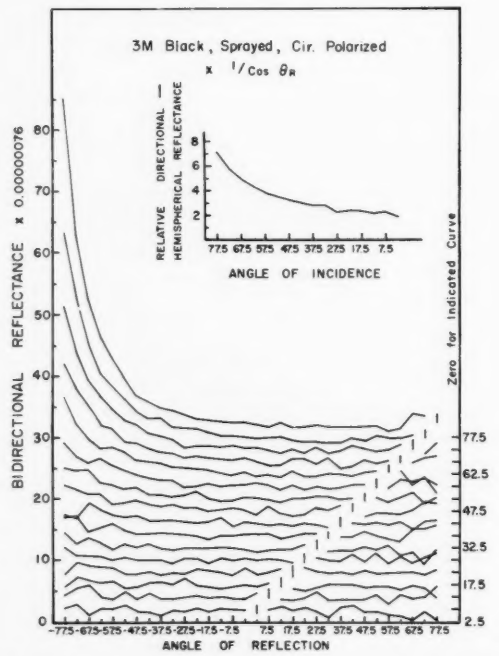

FIGURE 6.5. *Bidirectional reflectance of sprayed 3M black.*

For BRDF multipy scale values by 0.0067.

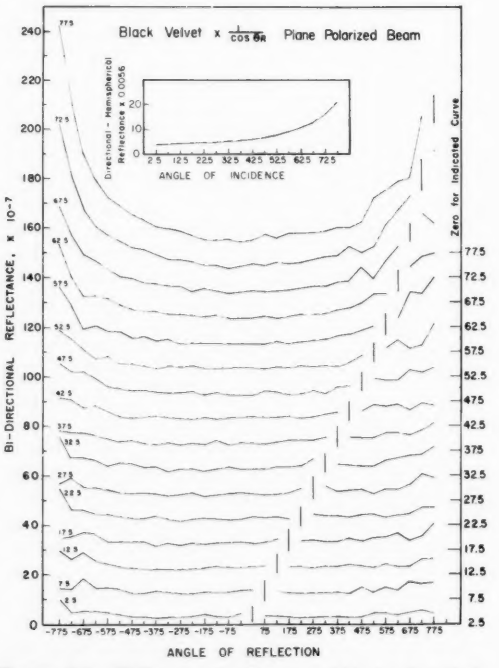
Black Velvet x 1/cos θR Plane Polarized Beam
BI-DIRECTIONAL REFLECTANCE, x 10⁻⁷
Directional - Hemispherical Reflectance x 0.0056
ANGLE OF INCIDENCE
Zero for Indicated Curve
ANGLE OF REFLECTION

FIGURE 6.6. *Bidirectional reflectance of black velvet cloth.*

The incident beam was polarized normal to the plane of incidence. For BRDF multiply scale values by 0.00088.

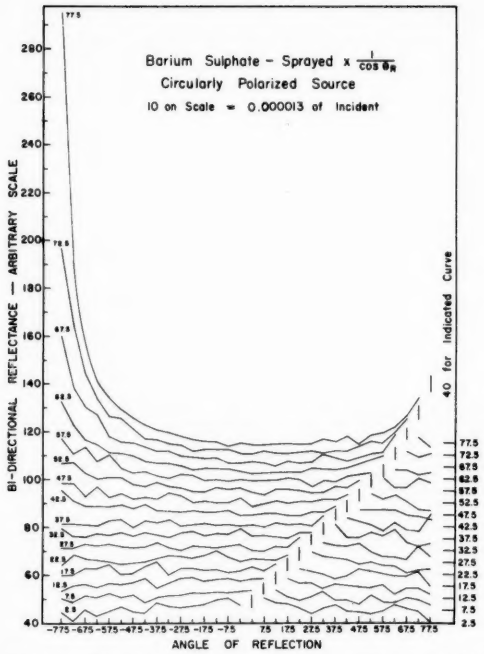
Barium Sulphate – Sprayed x 1/cos θR
Circularly Polarized Source
10 on Scale = 0.000013 of Incident
BI-DIRECTIONAL REFLECTANCE – ARBITRARY SCALE
40 for Indicated Curve
ANGLE OF REFLECTION

FIGURE 6.7. *Bidirectional reflectance of sprayed barium sulphate.*

For BRDF multiply scale value by 0.0115.

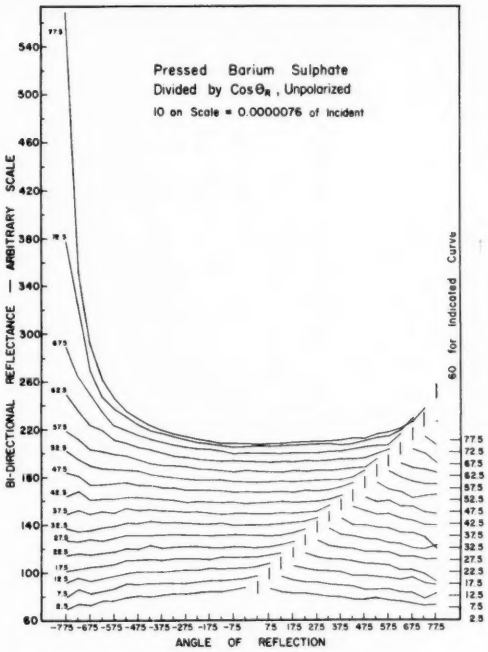
Pressed Barium Sulphate
Divided by Cos θR, Unpolarized
10 on Scale = 0.0000076 of Incident
BI-DIRECTIONAL REFLECTANCE – ARBITRARY SCALE
60 for Indicated Curve
ANGLE OF REFLECTION

FIGURE 6.8. *Bidirectional reflectance of pressed barium sulphate.*

For BRDF multiply scale values by 0.0067.

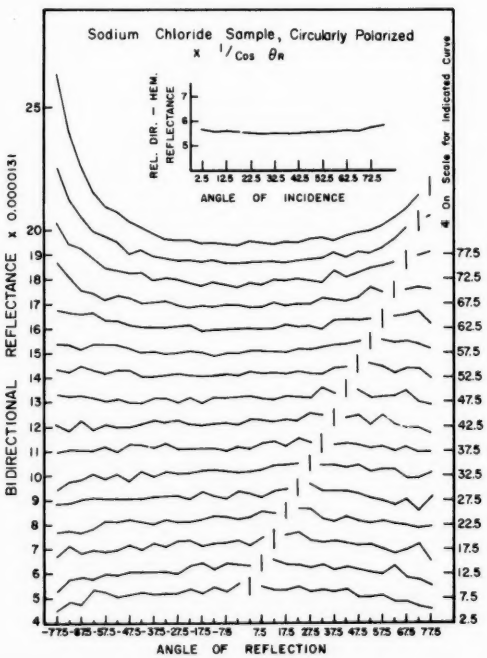
Sodium Chloride Sample, Circularly Polarized
x 1/Cos θR
REL. DIR. – HEM. REFLECTANCE
ANGLE OF INCIDENCE
BIDIRECTIONAL REFLECTANCE x 0.0000131
40 On Scale for Indicated Curve
ANGLE OF REFLECTION

FIGURE 6.9. *Bidirectional reflectance of sprayed sodium chloride.*

For BRDG multiply scale values by 0.116.

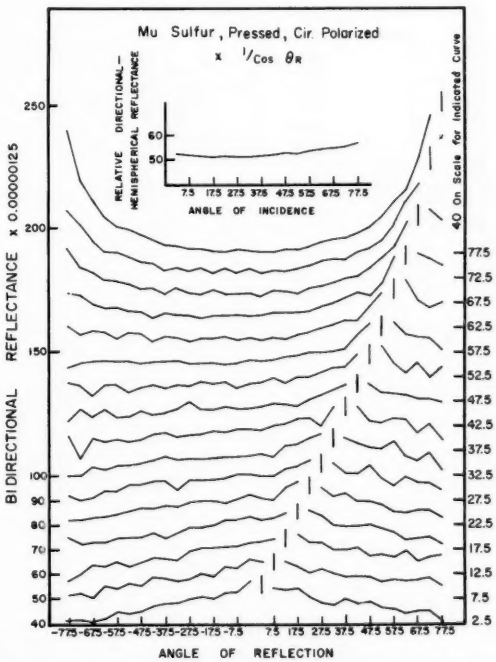
Mu Sulfur, Pressed, Cir. Polarized
x 1/Cos θR
RELATIVE DIRECTIONAL – HEMISPHERICAL REFLECTANCE
ANGLE OF INCIDENCE
BIDIRECTIONAL REFLECTANCE x 0.00000125
40 On Scale for Indicated Curve
ANGLE OF REFLECTION

FIGURE 6.10. *Bidirectional reflectance of pressed Mu sulfur.*

For BRDF multiply scale values by 0.011.

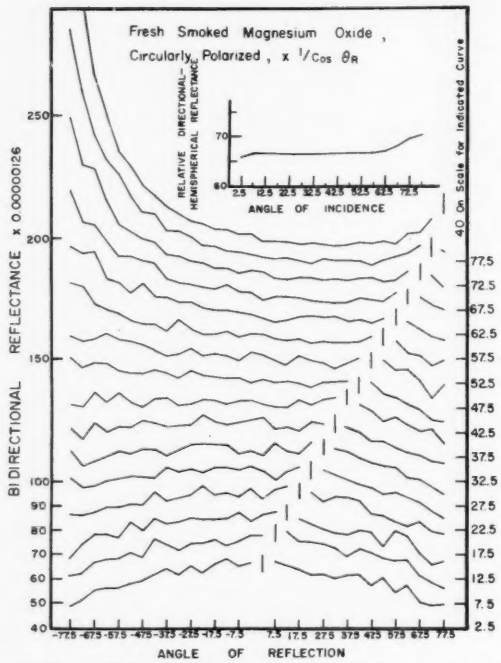
Fresh Smoked Magnesium Oxide,
Circularly Polarized, x 1/Cos θR
RELATIVE DIRECTIONAL – HEMISPHERICAL REFLECTANCE
ANGLE OF INCIDENCE
BIDIRECTIONAL REFLECTANCE x 0.00000126
40 On Scale for Indicated Curve
ANGLE OF REFLECTION

FIGURE 6.11. *Bidirectional reflectance of smoked magnesium oxide.*

For BRDG multiply scale values by 0.011.

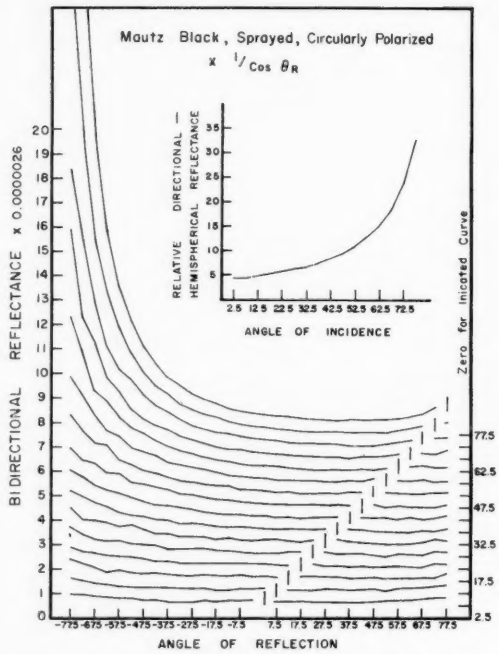

FIGURE 6.12. *Bidirectional reflectance of sprayed Mautz black.*

For BRDF multiply scale values by 0.023.

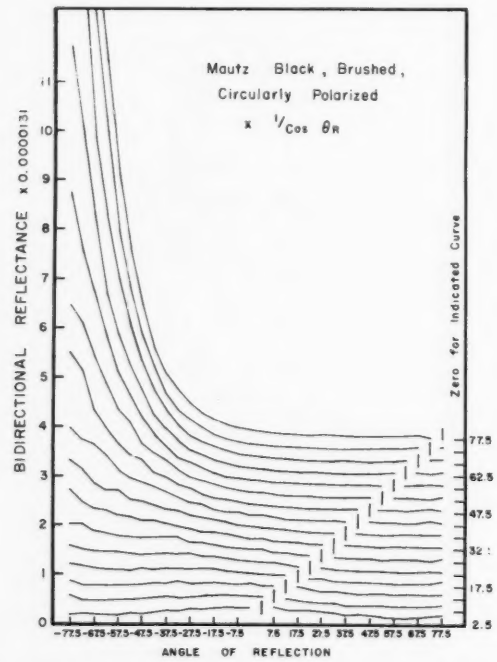

FIGURE 6.13. *Bidirectional reflectance of brushed Mautz black.*

For BRDF multiply scale values by 0.116.

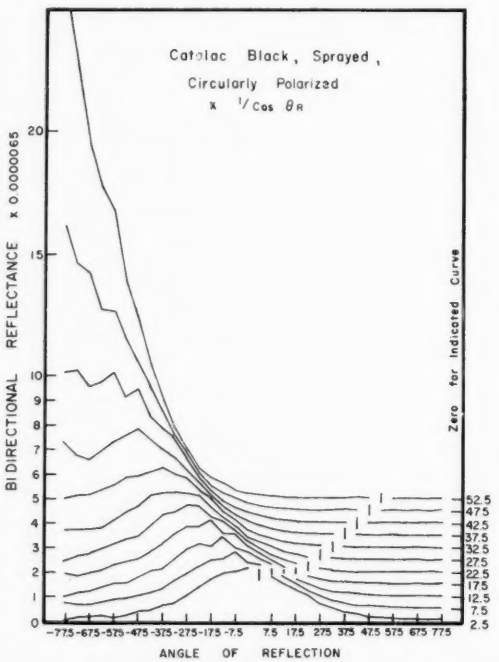

FIGURE 6.14. *Bidirectional reflectance of sprayed Catalac black.*

For BRDF multiply scale values by 0.057.

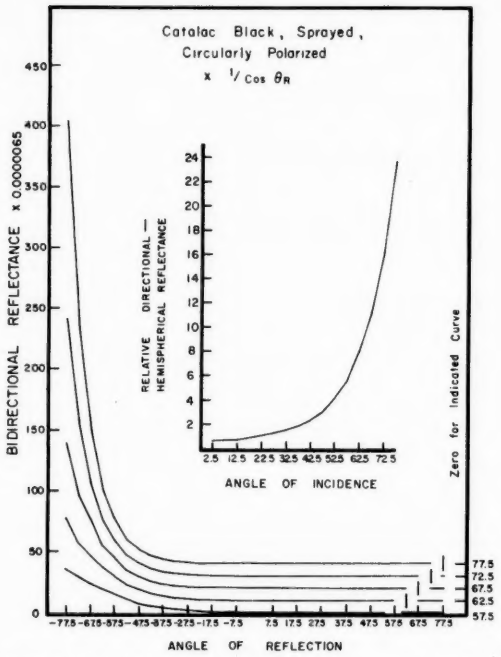

FIGURE 6.15. *Bidirectional reflectance of sprayed Catalac black.*

For BRDF multiply scale values by 0.057.

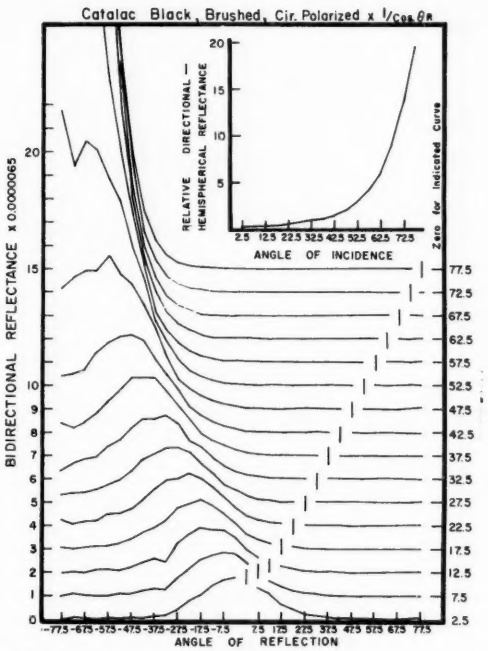
Catalac Black, Brushed, Cir. Polarized x 1/Cos θR
BIDIRECTIONAL REFLECTANCE x 0.0000065
RELATIVE DIRECTIONAL — HEMISPHERICAL REFLECTANCE
ANGLE OF INCIDENCE
Zero for Indicated Curve
ANGLE OF REFLECTION

FIGURE 6.16. *Bidirectional reflectance of brushed Catalac black.*

For BRDF multiply scale values by 0.057.

7. Conclusion

This paper has described the design, construction and alignment of a laser source bidirectional reflectometer that is fully automated and has angular resolution on the order of one degree. The directions of incidence and viewing can be independently varied over an entire hemisphere except for directions more than 77.5° from the normal, and the two directions must be at least 2.5° apart. Error analyses has been performed. Bidirectional reflectance for 15 samples of black and white coatings are presented.

It is clear in retrospect that many of the design features and procedures could be improved: (1) kinematic design to allow simpler alignment procedure; (2) designs that can measure liquid and loose powder sample; (3) designs that can measure bidirectional transmittance over an entire hemisphere; (4) better attenuation method to obtain higher accuracy in absolute reflectance determination; and (5) tunable laser or continuous wavelength source to allow wider wavelength range.

An extensive bibliography on scattering by reflection from surfaces, in which the papers are classified by subject matter, immediately follows this paper.

8. References

[1] Nicodemus, F. E., Richmond, J. C., Hsia, J. J., Venable, W. H., Jr., Ginsberg, I. W., and Limperis, T., Geometrical considerations and nomenclature for reflectance, to be published as NBS Monograph.

[2] Venable, W. H., Jr., and Hsia, J. J., Describing spectrophotometric measurements, Nat. Bur. Stand. (U.S.), Tech. Note 594–9, 50 pages (Nov. 1974).

[3] Kneissl, G. J., and Richmond, J. C., A Laser-Source Integrating Sphere Reflectometer, Nat. Bur. Stand. (U.S.), Tech. Note 439, 72 pages (Feb. 1968).

[4] Torrance, K. E., and Sparrow, E. M., Theory for off-specular reflection from roughened surfaces, J. Opt. Soc. Am. **57**(9), 1105 (1967).

(Paper 80A2–887)

JOURNAL OF RESEARCH of the National Bureau of Standards—A. Physics and Chemistry
Vol. 80A, No. 2, March–April 1976

Bidirectional Reflectometry. Part II. Bibliography on Scattering by Reflection from Surfaces

Joseph C. Richmond and Jack J. Hsia

Institute for Basic Standards, National Bureau of Standards, Washington, D.C. 20234

(February 2, 1976)

In connection with the work on development of a high resolution laser source bidirectional reflectometer, a large number of papers were collected dealing with various aspects of the geometrical distribution of the radiant energy reflected from surfaces of different types.

Each paper has been classified into one or more classes on the basis of its technical content. There are eight general classes, with several subclasses in some of the general classes.

Because of the interest in this field, the bibliography is being published as a service to the public.

Key words: Bibliography; emittance; heat transfer; measurement techniques; periodic surfaces; polarization; random surfaces; reflectance; reflectance of coherent radiation; scattering; scattering theory; surface roughness; transmittance.

A large number (371) of papers was collected, dealing with various aspects of the geometrical distribution of the radiant energy scattered by reflection from surfaces, and particularly from rough surfaces. These papers were referred to during the development of a high-resolution laser-source bidirectional reflectometer.

Each paper is classified in the Bibliography into one or more of thirteen subject categories on the basis of its technical content. A key to the symbols used in the bibliography is given in table 1.

In addition, each paper by number has been classified in a second system, consisting of eight primary classes, with several subclasses in several of the primary classes, in table 2.

The bibliography, while extensive, is by no means complete. Few additions have been made since about 1972. However, it is sufficiently extensive to be of significant help to workers in the field, and particularly to those just beginning work in the field.

The references from archival journals should be available in any good technical library. Most of the reports that have not been published in the archival literature are available from the National Technical Information Service. Most of these are identified by an AD number, or other identifying number by which they can be ordered.

Copies of all papers listed are on file in the Radiometric Physics Section of the National Bureau of Standards, and may be read at NBS if not otherwise available.

TABLE 1. *Subject Categories*

Symbol	
R	Reflectance
Em	Emittance
T	Transmittance
S	Scattering
P	Polarization
Ma	Mathematics
H	Heat Transfer Between Rough Surfaces
Ex	Experimental
Th	Theoretical
Su	Survey
L	Laser
SM	Surface Roughness Measurement
Ap	Apparatus

TABLE 2. *Primary Classes*

NOMENCLATURE AND APPLICATION

8, 42, 50, 52, 97, 101, 102, 113, 125, 132, 141, 143, 144, 154, 155, 180, 195, 216, 237, 238, 243, 275, 314, 315, 327, 341, 345

SURFACE ROUGHNESS MEASUREMENT

3, 12, 13, 16, 36, 61, 64, 65, 66, 69, 73, 80, 87, 95, 98, 99, 111, 115, 127, 133, 135, 136, 149, 157, 162, 171, 176, 190, 226–232, 245, 247, 255, 257, 258, 262, 265, 267, 277, 281, 286, 308, 312, 331, 347, 359, 361–365

THEORY (RANDOM DISTRIBUTION SURFACE ROUGHNESS)

201-606 O - 76 - 5

SMALL FACETS SURFACE ASSUMPTION

18–21, 41, 77, 137, 138a, 181, 198, 210, 217, 223, 241, 261, 280, 292, 306, 321, 326, 328, 330

KIRCHHOFF-HUYGENS SOLUTION

9, 11, 32, 34, 36, 54, 81, 82, 90, 91, 92, 114, 116, 121, 137, 140, 150, 153, 160, 166, 178, 179, 254, 263, 264, 268, 299, 304, 311

OTHERS

10, 23, 24, 25, 32, 53, 67, 70, 76, 79, 84, 88, 89, 96, 105, 108, 109, 112, 119, 120, 123, 126, 128, 134, 146, 159, 170, 183, 184, 185, 193, 194, 199, 202, 205, 211, 223, 233, 242, 244, 274, 291, 301, 303, 307, 313, 328, 339, 342, 343

THEORY (PERIODIC DISTRIBUTION SURFACE ROUGHNESS)

CONTINUOUS SURFACES (SINUSOIDAL, GRATING, V-GROOVE, etc.)

1, 5, 6, 7, 14, 17, 22, 29, 32, 49, 51, 55, 59, 60, 114, 142, 156, 161, 167, 168, 169, 188, 209, 213, 214, 215, 219, 233, 234, 284, 353, 367, 370

SPHERES AND DISTRIBUTION

37–40, 43, 44, 56, 57, 104, 158, 177, 187, 207, 246, 248, 272, 332, 334, 335, 337, 352, 355, 356, 366

CYLINDERS AND DISTRIBUTION

56, 68, 110, 147, 164, 174, 220, 222, 239, 250, 289, 293, 294, 332, 333, 336, 338, 340, 349, 350, 351

SHADOWING AND POLARIZATION

28, 30, 57, 62, 74, 103, 117, 118, 119, 122, 124, 129, 138a, 202, 203, 204, 210, 224, 225, 252, 253, 260, 261, 279, 287, 292, 298, 317, 348, 367, 368

EXPERIMENTAL DATA (ON RANDOM DISTRIBUTION SURFACES)

COHERENT SOURCE

15, 75, 84, 85, 131, 189, 191, 192, 194, 208, 283

INCOHERENT SOURCE

4, 26, 27, 33, 35, 45–48, 58, 70, 72, 73, 93, 102, 106, 130, 139, 145, 151, 163, 165, 212, 218, 221, 240, 251, 256, 259, 261, 270, 271, 273, 276, 278, 285, 295, 296, 297, 300, 309, 310, 316–318, 320, 323, 324, 325, 329, 346, 354, 357

EXPERIMENTAL DATA (ON PERIODIC DISTRIBUTION SURFACES)

78, 86, 94, 168, 197, 201, 285, 370, 371

GONIOREFLECTOMETER

COHERENT SOURCE

15, 71, 78, 84, 85, 131, 180, 191, 192, 194, 201, 206, 208, 283

INCOHERENT SOURCE

4, 35, 45, 47, 48, 58, 73, 83, 106, 139, 145, 163, 196, 197, 212, 218, 221, 235, 259, 295, 297, 300, 320, 323, 354, 371

R, Th — 1. Adorjan, A. S. and Wierum, F. A., Radiative properties of rough surfaces, AIAA Paper No. 70–862, AIAA 5th Thermophysics Conference, June 1970.

Em, Th — 2. Agababov, S. G., Effect of roughness of the surface of a solid body on its radiation properties and methods for their experimental determination, High Temp. **6** (1), 76–85 (1968).

SM — 3. Agababov, S. G. and Eksler, L. I., Influence of the geometric characteristics of the relief of the surface of a solid on its radiation properties (determination of the roughness factor), High Temp. **9** (3), 475–479 (1971).

R, Ex — 4. Agnew, J. T. and McQuistan, R. B., Experiments concerning infrared diffuse reflectance standards in the range 0.8 to 20.0 microns, J. Opt. Soc. Am. **43** (11), 999–1007 (1953).

S, R, Th — 5. Aksenov, V. I., On the scattering of electromagnetic waves from sinusoidal and trochoidal surfaces of finite conductivity, Radio Eng. & Electron. **3** (4), 1–10 (1958).

S, Ex, Ap — 6. Aksenov, V. I., Experimental investigation of electromagnetic wave scattering from periodically uneven surfaces, Radio Eng. & Electron. (USSR) **5** (5) 113–129 (1960).

S, Th — 7. Aksenov, V. I., Utilization of Kirchhoff's approximation in the problem of the scattering of radio waves by periodically rough surfaces with finite conductivity, Radio Eng. & Electron. **3,** 307–314 (Mar. 1961).

H — 8. Amar, R. C. and Edwards, D. K., Reflection and transmission by rough-walled passages, AIAA Paper No. 72-303, 1–9, AIAA 7th Thermophysics Conference, San Antonio, Tex., Apr. 10–12, 1972.

R, Th — 9. Ament, W. S., Toward a theory of reflection by a rough surface, Proc. IRE **41,** 142–146 (Jan. 1953).

R, S, Th — 10. Ament, W. S., Forward- and back-scattering from certain rough surfaces, IRE Trans. **AP-4** (3), 369–373 (July 1956).

R, S, Th — 11. Ament, W. S., Reciprocity and scattering by certain rough surfaces, IRE Trans. on Antennas and Propagation **AP-8** (2), 167–174 (Mar. 1960).

SM — 12. American Standard, Surface texture-surface roughness, waviness and lay – ASA B46.1–1962, UDC 621.9.015 – American Society of Mechanical Engineers.

SM — 13. Armand, G., Lapujoulade, J., and Paigne, J., A theoretical relationship between the leakage of gases through the interface of two metals in contact and their superficial micro-geometry, Vacuum **14,** 53–57 (1964).

S, Th — 14. Artmann, K., Zur Theorie der anomalen reflexion von optischen strichgittern, Z. Physik **119,** 529–567 (1942).

Ap, Ex(L) — 15. Bair, M. E., Carmer, D. C., and Stewart, S. R., A gonioreflectometer facility using coherent and incoherent sources, Tech. Rept. AFAL-TR-70–161, p. 1–30. Infrared and Optics Lab., Univ. of Michigan, Ann Arbor, Mich. (Aug. 1970).

SM 16. Barash, V. Ya. and Uspenskii, Yu. P., Test metrological characteristics of surface-roughness measuring instruments, Measurement Tech. No. 2, 273–274 (Feb. 1969). (Translated from Izmeritel'naya Tekhnika, No. 2, 83, Feb. 1969).

S, Th 17. Baret, J. F. and Mann, J. A., Role of high-order grating effects in the scattered irradiance of corrugated surfaces, Appl. Opt. **10** (5), 1174–1176 (1971).

R, Th, Ex 18. Barkas, W. W., Analysis of light scattered from a surface of low gloss into its specular and diffuse components, Proc. Phys. Soc. (London) **51**, 274–295 (1939).

R, S, Th 19. Barrick, D. E., Rough surface scattering based on the specular point theory, IEEE Trans. Antennas and Propagation **AP–16**, 449–454 (1968).

R, Th 20. Barrick, D. E., Relationship between slope probability density function and the physical optics integral in rough surface scattering, Proc. IEEE **56**, No. 10, 1728–1729 (Oct. 1968).

R, S, Th 21. Barrick, D. E., Correction to "Rough surface scattering based on the specular point theory", IEEE Trans. on Antennas and Propagation **AP–17** (1), 81 (1969).

S, Th 22. Barrick, D. E., Low-frequency scatter from a semi-elliptic groove in a ground plane, J. Opt. Soc. Am. **60** (5), 625–634 (May 1970).

S, Th 23. Barrick, D. E. and Peake, W. H., Scattering from surfaces with different roughness scales: analysis and interpretation, Rept. No. BAT–197A–10–3, Battelle Memorial Institute, Columbus, Ohio (1967). AD–662 751.

S, Th 24. Bass, F. G., On the theory of combination scattering of waves on a rough surface, AFCRL No. 511, 1–12, 1961. (Translated from Izvestiia VUZ, Radiofizika, **4** (1), 58–66, 1961). AD–262 417.

S, Th 25. Bass, F. G. and Bocharov, V. G., On the theory of scattering of electromagnetic waves from a statistically uneven surface, Radio Eng. & Electron. (USSR), **3** (2), 251–258 (1958).

Su(Th) R, T, Ex 26. Beaglehole, D. and Hunderi, O., Study of the interaction of light with rough metal surfaces. I. Experiment, Phys. Rev. B **2** (2), 309–321 (1970).

S, Ex 27. Beard, C. I., Coherent and incoherent scattering of microwaves from the ocean, IRE Trans. on Antennas and Propagation **AP-9** (5), 470–483 (Sept. 1961).

P, Th 28. Beckmann, P., The depolarisation of electromagnetic waves scattered from rough surfaces, Acta Technica No. 6, 511–523 (1961).

S, R, Th 29. Beckmann, P., The scattering of waves by a periodic surface, Czech. J. Phys. **B11**, 863–870 (1961).

R, S, Th 30. Beckmann, P., Shadowing of random rough surfaces, IEEE Trans. on Antennas and Propagation **AP–13**, 384–388 (May 1965).

S, R, Th 31. Beckmann, P., Scattering from rough surfaces for finite distances between transmitter and receiver, Rept. No. D1–82–0657, 1–39, Boeing Scientific Research Labs., Seattle, Wash., Geoastrophysics Lab. (Oct. 1967). AD–666 593.

R, Th, Su 32. Beckmann, P. and Spizzichino, A., The scattering of electromagnetic waves from rough surfaces, Vol. **4**, International Series of Monographs on Electromagnetic Waves (Pergamon Press, Macmillan, New York, N.Y. 1963).

R, Ex 33. Bennett, H. E., Specular reflectance of aluminized ground glass and the height distribution of surface irregularities, J. Opt. Soc. Am. **53** (12), 1389–1394 (1963).

R, Th 34. Bennett, H. E., Influence of surface roughness, surface damage, and oxide films on emittance, NASA SP–55, Symposium on Thermal Radiation of Solids (S. Katzoff, Ed.) pp. 145–152, NASA (1965).

Ex, R 35. Bennett, H. E., Measurement of Light scattered from very smooth surfaces, Preprint of a paper presented at the Optical Society of America 1970 Annual Meeting, Sept. 28–Oct. 2, held at Hollywood, Fla.

R, Th, Ex 36. Bennett, H. E. and Porteus, J. O., Relation between surface roughness and specular reflectance at normal incidence, J. Opt. Soc. Am. **51** (2), 123–129 (Feb. 1961).

R, Th 37. Berreman, D. W., Anomalous reststrahl structure from slight surface roughness, Phys. Rev. **163** (3), 855–864 (Nov. 1967).

R, Th 38. Berreman, D. W., Resonant reflectance anomalies: effect of shapes of surface irregularities, Preprint of 1969 spring meeting, Optical Society of America, San Diego, Calif., March 1969.

R, Th 39. Berreman, D. W., Reflectance and ellipsometry of slightly tarnished, dirty or rough surfaces, Bell Telephone Lab. Inc., Murray Hill, N.J., Preprint of paper ThG 17, Optical Society of America Annual Meeting, Chicago, Ill., Oct. 21–24, 1969.

R, Th 40. Barreman, D. W., Reflectance and ellipsometry when submicroscopic particles bestrew a surface, J. Opt. Soc. Am. **60** (4), 499–505 (Apr. 1970).

R, Th 41. Berry, E. M., Diffuse reflection of light from a matt surface, J. Opt. Soc. Am. **7**, 627–633 (1923).

H, Th 42. Bevans, J. T. and Edwards, D. K., Radiation exchange in an enclosure with directional wall properties, ASME Paper No. 64–WA/HT–52, 1–21, 1964 ASME Winter Annual Meeting, New York, N.Y.

R, Th 43. Biot, M. A., On the reflection of electromagnetic waves on a rough surface, J. Appl. Phys. **27** (9), 998 (Sept. 1956).

R, Th 44. Biot, M. A., Some new aspects of the reflection of electromagnetic waves on a rough surface, J. Appl. Phys. **28** (12), 1455–1463 (Dec. 1957).

R, Th, Ex 45. Birkebak, R. C., Monochromatic directional distribution of reflected thermal radiation from roughened surfaces, Ph. D. Dissertation, University of Minnesota, Minneapolis, Minn., 1962.

R, Ex 46. Birkebak, R. C., Dawson, J. P., McCullough, B. A., and Wood, B. E., Hemispherical reflectance of

metal surfaces as a function of wavelength and surface roughness, Int. J. Heat Mass Transfer **10**, 1225–1232 (1967).

R, Th, Ex 47. Birkebak, R. C. and Eckert, E. R. G., Effects of roughness of metal surfaces on angular distribution of monochromatic reflected radiation, J. Heat Transf., Trans. ASME **C87**, 85–93 (1965).

R, Ex 48. Birkebak, R. C., Sparrow, E. M., Eckert, E. R. G., and Ramsey, J. W., Effect of surface roughness on the total hemispherical and specular reflectance of metallic surfaces, J. Heat. Transf., Trans. ASME **C86(2)**, 193–199 (May 1964).

Em, Th, Ex 49. Black, W. Z. and Schoenhals, R. J., A study of directional radiation properties of specially prepared V-groove cavities, Trans. ASME (J. Heat Transf.) **90C** (4), 420–428 (Nov. 1968).

H, Ex 50. Black, W. Z. and Schoenhals, R. J., An experimental study of radiation heat transfer from parallel plates with direction-dependent properties, ASME Paper No. 70–HT/SpT–1, 1–6 (1970).

R, Th 51. Blakely, J. M. and Olson, D. L., Intensity distribution from a sinusoidal grating and application to diffusion measurements, Appl. Phys. **39** (7), 3476–3479 (June 1968). AD–682 663.

H, Th 52. Bobco, R. P., A script-F matrix formulation for enclosures with arbitrary surface emission and reflection characteristics, ASME Paper No. 70–HT/SpT–3, 1–8 (1970).

S, Th 53. Bocharov, V. G. and Bass, F. G., On the scattering of electromagnetic waves from a statistically inhomogeneous surface, Radio Eng. & Electron. (USSR), **3** (4), 184–187 (1958).

R, Th 54. Boerner, W. M., Compatibility studies. Vol. IV. appendix 3, Scattering of a beam with finite beam width from an impedance surface, Rept. No. 68–16, pp. 1–208, School of Electrical Engineering, Pennsylvania Univ. (Feb. 1968). AD–829 846.

R, Th 55. Bonzel, H. P. and Gjostein, N. A., Diffraction theory of sinusoidal gratings and application to in situ surface self-diffusion measurements, J. Appl. Phys. **39** (7), 3480–3491 (June 1968).

S, Th 56. Bowman, J. J., Senior, T. B. A., and Uslenghi, P. L. E., Electromagnetic and acoustic scattering by simple shapes, Wiley Interscience Div. (John Wiley and Sons, Inc., New York, N.Y., 1970). AD–699 859.

R, Th 57. Brand, K. W. and Spagnolo, F. A., Lambert diffuse reflection from general quadric surfaces, Rept. No. RE–278J, 1–30, Grumman Aircraft Engineering Corp., Bethpage, N.Y., Research Dept. (Jan. 1967). AD–805 421.

R, Ex 58. Brandenburg, W. M. and Neu, J. T., Undirectional reflectance of imperfectly diffuse surfaces, J. Opt. Soc. Am. **56** (1), 97–103 (Jan. 1966).

S, Th 59. Brekhovskikh, L. M., Diffraction of waves on a rough surface I. General theory, Zhurnal Eksperimental'nol I Theoreticheskoi Fiziki (J. Exptl. Theo. Phys. USSR) **23**, 275–288 (1952). Translated by Goss, R. N., U.S. Naval Electronics Lab., San Diego, Calif., in Three papers on diffraction of waves from a rough surface. pp. 1–22a.

S, Th 60. Brekhovskikh, L. M., Diffraction of waves on a rough surface II. Applications of the general theory, Zhurnal Eksperimental'nol I Theoreticheskoi (J. Exptl. Theo. Phys. USSR) **23**, 289–304 (1952). Translated by Goss, R. N., U.S. Naval Electronics Lab., San Diego, Calif., In Three papers on diffraction of waves from a rough surface. pp. 23–38g.

SM 61. Broadston, J. A., Education for surface texture assessment, Proceedings 1967–68 of International Conference on Properties and Metrology of Surfaces, Vol. **182**, Part 3K. Institution of Mechanical Engineers, London (Millson, R. J., Ed.).

R, Th 62. Brockelman, R. A. and Hagfors, T., Note on the effect of shadowing on the backscattering of waves from a random rough surface, IEEE Trans. on Antennas and Propagation, **AP–14**, 621–629 (Sept. 1966).

S, Ex 63. Bruehlman, R. J., Thomas, L. W., and Gonick, E., Effect of particle size and pigment volume concentration on hiding power of titanium oxide, (E. I. du Pont de Nemours and Co., Inc.), Official Digest, 252–267 (Feb. 1961).

SM 64. Bryan, J., Resume and critique of papers in part eight, International Research in Production Engineering, pp. 647–658 (1963). Published by ASME.

SM 65. Bryan, J. B. and Mohl, O., Microinterferometric scanning for full surface metrology, ASME Paper No. 64–WA/PROD–15, 1–7, Winter Annual Meeting, New York, N.Y., Nov. 29–Dec. 4, 1964 of ASME.

SM 66. Bufalini, J. J., An Investigation of methods of determining surface roughness of metals, Master Thesis, Dept. of Chemistry, Univ. of Arkansas (1958).

R, Th 67. Bullington, K., Reflection coefficients of irregular terrain, Proc. IRE **42**, 1258–1262 (Aug. 1954).

S, Th 68. Burke, J. E. and Twersky, V., On Scattering of waves by an elliptic cylinder and by a semielliptic protuberance on a ground plane, J. Opt. Soc. Am. **54** (6), 732–744 (June 1964).

SM 69. Butler, R. D. and Pope, R. J., Surface roughness and lubrication in sheet metal working, pp. 162–170, PMS* Proceedings, 1967–68.

Em 70. Caren, R. P. and Liu, C. K., Thermal radiation from a microscopically roughened dielectric surface, J. Heat Transfer, 73–79 (Feb. 1972).

Ap(L) 71. Carpenter, R. L. and Dalton, W. A. J., A laser bidirectional reflectometer, Rept. MDC 69–023, pp. 1–10, McDonnell Aircraft Company, McDonnell Douglas Corp. (1969).

R, Ex 72. Chaabane, G., Pieroway, C., and Francis, J., Reflectance measurements of dielectric coatings on a conductor substrate, AIAA Paper No. 71–448 AIAA 6th Thermophysics Conference, Tullahoma, Tenn., Apr. 26–28, 1971.

SM 73. Chamberlin, J. L., Centerline correction for precision roughness specimens, J. Res. Nat. Bur.

Stand. (U.S.) **69C** (Eng. & Instr.), No. 4, 303–305 (Oct.–Dec. 1965).

R, P — 74. Chen, Hsi-Shu, and Nagaraja, C. R., Polarization of light on reflection by some natural surfaces, Brit. J. Appl. Phys. (J. Phys. D.) **1**, Ser. 2, 1191–1200 (1968).

S, P, Ex(L) — 75. Cheo, P. K. and Renau, J., Wavelength dependence of total and depolarized back-scattered laser light from rough metallic surfaces, J. Opt. Soc. Am. **59** (7), 821–826 (1969).

S, Th — 76. Chia, R. C., The theory of radar scatter from the ocean, Rept. No. CRES-TR-112-1, 1–125, Kansas Univ. Lawrence center for Research (Oct. 1968). AD-849 139.

R, Th — 77. Christie, A. W., The luminous directional reflectance of snow, J. Opt. Soc. Am. **43**, 621–622 (1953).

R(Ex)L, Th — 78. Christie, F. A. and Devriendt, A. B., Bidirectional reflectance from surfaces formed by the ruling of orthogonal parallel V-grooves, AIAA Paper No. 72–55, 1–9, AIAA 10th Aerospace Sciences Meeting, San Diego, Calif., Jan. 17–19, 1972.

S, Th — 79. Chu, C. M. and Churchill, S. W., Multiple scattering by randomly distributed obstacles—Methods of solution, IRE Trans. **AP-4** (2), 142–148 (Apr. 1956).

SM — 80. Chunin, B. A., Measuring depth of point defects in polished surfaces by means a linnik microinterferometer, Measurement Tech. No. 2, 276–277 (Feb. 1969). Translated from Izmeritel'naya Tekhnika, No. 2, 84–85 (Feb. 1969).

R, Th — 81. Clarke, R. H., Theoretical characteristics of radiation reflected obliquely from a rough conducting surface, Proc. IEE **110** (1), 91–100 (Jan. 1963).

R, Th, Ex — 82. Clarke, R. H. and Hendry, G. O., Prediction and measurement of the coherent and incoherent power reflected from a rough surface, IEEE Trans. on Antennas and Propagation, **AP-12** (3), 353–363 (1964).

R, Ap — 83. Comstock, D. F., Reflectance measurement by three-dimensional goniometry, Preprint (Appl. Opt.) (Arthur D. Little, Inc., 1968).

R, Th, Ex(L) — 84. Condie, M. A., An experimental investigation of the statistics of diffusely reflected coherent light, Tech. Report No. AFAL-TR-66-387, Oct. 1966.

R, Th, Ex — 85. Considine, P. S., Cronin, D. J., and Reynolds, G. O., Angular dependence of radiance of rough surfaces in imaging systems, J. Opt. Soc. Am. **56** (7), 877–883 (July 1966).

S, P, Ex — 86. Cooke, D. D. and Kerker, M., Light scattering from long thin glass cylinders at oblique incidence, J. Opt. Soc. Am. **59** (1), 43–48 (1969).

S(L), Th — 87. Crane, R. B., Use of a laser-produced speckle pattern to determine surface roughness, J. Opt. Soc. Am. **60** (12), 1658–1663 (Dec. 1970).

R, Th — 88. Crowell, J. and Ritchie, R. H., Surface-plasmon effect in the reflectance of a metal, J. Opt. Soc. Am. **60** (6), 794–799 (June 1970).

S, Th(L) — 89. Dainty, J. C., Some statistical properties of random speckle patterns in coherent and partially coherent illumination, Optica Acta **17** (10), 761–772 (1970).

R, Th — 90. Daniels, F. B., Radar determination of the scattering properties of the moon, Nature **187** No. 4735, 399 (July 1960).

R, Th — 91. Davies, H., The reflection of electromagnetic waves from a rough surface, Proc. Inst. Elec. Engr. **101**, 118 (1954).

R, Th — 92. Davies, H., The reflection of electromagnetic waves from a rough surface, Proc. IEE **101**, 209–214 (1954).

R, Ex — 93. Davies, J. M. and Zagieboylo, W., An integrating sphere system for measuring average reflectance and transmittance, Appl. Opt. **4** (2), 167–174 (1965).

R, Ex — 94. Drummeter, L. F., Jr., and Fowler, W. B., Some angular reflectance properties of light-trapping surfaces, NRL Report No. 5753, 1–14, U.S. Naval Research Lab. (1962). AD-276 052.

SM — 95. Dunin-Barkovsky, I. V., Analysis of surface irregularities by the spectral method, pp. 211–215, PMS* Proceedings, 1967–68.

R, Su — 96. Dunn, S. T., A possible approach to evaluation of flux scattered by roughened surfaces, AIAA 3rd Aerospace Sciences Meeting, AIAA Paper No. 66–20 (Jan. 1966).

R, Em Su(Ex) — 97. Dunn, S. T., Richmond, J. C., and Parmer, J. F., Survey of infrared measurement techniques and computational methods in radiant heat transfer, J. Spacecraft and Rockets, 962–975 (July 1966).

SM — 98. Dupuy, M. O., High-precision optical profilometer for the study of micro-geometrical surface defects, pp. 255–259, PMS* Proceedings, 1967–68.

SM — 99. Eberle, O. A., Graphical method for statistical assessment of surface roughness comparison specimens, pp. 368–396, PMS* Proceedings, 1967–68.

R, Su — 100. Edward, D. K., Radiative transfer characteristics of materials, J. Heat Transfer, Trans. ASME **C91**, 1–15 (1969).

H, Th — 101. Edwards, D. K. and Bertak, I. V., Imperfect reflections in thermal radiation transfer, AIAA Paper No. 70–860, AIAA 5th Thermophysics Conference, June 1970.

R, Em, Th, Ex — 102. Edwards, D. K. and Catton, I., Radiation characteristics of rough and oxidized metals, Symposium on Thermophysical properties, held at Purdue Univ., 1965, pp. 189–199.

P(L), Ex — 103. Egan, W. G. and Hallock, H. B., Coherence-polarization, 1–38, Grumman Aircraft Engineering Corp., Bethpage, N.Y., Research Dept. (Mar. 1969). AD-849 398.

S, R, Th — 104. Erma, V. A., Exact solution for the scattering of electromagnetic waves from bodies of arbitrary shape. III. obstacles with arbitrary electromagnetic properties, Phys. Rev. **179** (5), 1238–1246 (1969).

S, Ex(L)Th — 105. Estes, L. E., Narducci, L. M., and Tuft, R. A.,

Scattering of light from a rotating ground glass, J. Opt. Soc. Am. **61** (10), 1301–1306 (Oct. 1971).

R, Ex, Ap 106. Euler, J., Reflexionsmessungen an gesandetem aluminium, Z. Angen Physik **1** (12), 569–573 (1949).

R, Th 107. Evans, L. B., Chu, C. M., and Churchill, S. W., The effect of anisotropic scattering on radiant transport J. Heat Transfer Trans. ASME **C87** (3), 381–387 (1965).

S, R, Th 108. Fante, R. L., Discussion of a model for rough surface scattering, IEEE Trans. on Antennas and Propagation, **AP-13** (4), 652–653 (1965).

R, Th 109. Fedders, P. A., Surface roughness and the absorption of electromagnetic waves in simple metals, Phys. Rev. **181** (3), 1053–1058 (1969).

S, Th 110. Felsen, L. B., Comment on the paper, The scattering of electromagnetic waves by a corrugated sheet, by T. B. A. Senior, Can. J. Phys. **37**, 1563–1565 (1959).

SM 111. Felstead, E. B., Additional optical data processing techniques for surface roughness studies, Proc. IEEE **57** (3), 343–344 (Mar. 1969).

R, Th 112. Fenstermaker, C. A. and McCrackin, F. L., Errors arising from surface roughness in ellipsometric measurement of the refractive index of a surface, Surface Sci. **16**, 85–96 (1969).

H 113. Fischer, W. D. and Hering, R. G., Radiant heat transfer between nongray directional surfaces, AIAA Paper No. 72-306, 1–7, AIAA 7th Thermophysics Conference, San Antonio, Tex., Apr. 10–12, 1972.

R, S, Su 114. Friedhoffer, J. A., Scattering of electromagnetic waves by rough surfaces, Rept. No. BRL–MR–1805, 1–29, Ballistic Research Labs., Aberdeen Proving Ground, Md. (Nov. 1966). AD–813 377.

SM 115. Funai, A. I. and Rolling, R. E., Inspection techniques for characterization of smooth, rough, and oxidized surfaces, AIAA Progress in Aeronautics and Astronautics: Thermophysics of Spacecraft and Planetary Bodies (G. B. Heller, ed.), **20**, 41–64 (Academic Press, New York, N.Y., 1967).

R, S, Th 116. Fung, A. K., Theory of radar scatter from rougl surfaces, bistatic and monostatic, with application to lunar radar return, J. Geophys. Res. **69** (6), 1063–1073 (Mar. 1964).

S, P, Th 117. Fung, A. K., Scattering and depolarization of EM waves from a rough surface, Proc. IEEE **54**, 395–396 (1966).

P, Th 118. Fung, A. K., Character of wave depolarization by a perfectly conducting rough surface and its application to earth and moon experiments, Planet. Space Sci. **15**, 1337–1347 (1967), Pergamon Press Ltd., Printed in Northern Ireland.

R, S, P, Th 119. Fung, A. K. and Chan, H. L., Backscattering of waves by composite rough surfaces, IEEE Trans. on Antennas and Propagation **AP-17** (5), 590–597 (1969).

S, Th 120. Fung, A. K. and Chan, H. L., On the integral for backscattering from a randomly rough surface, Proc. IEEE **59** (8), 1280–1281 (Aug. 1971).

S Th 121. Fung, A. K. and Moore, R. K., The correlation function in Kirchoff's method of solution of scattering of waves from statistically rough surfaces, J. Geophys. Res. **71** (12), 2939–2943, June 15, 1966.

S, P, Th 122. Fung, A. K., Moore, R. K., and Parkins, B. E., Notes on backscattering and depolarization by gently undulating surfaces, J. Geophys. Res. **70** (6), 1559–1562, Mar. 15, 1965.

S, Th(L) 123. Gabor, D., Laser speckle and its elimination, IBM J. Res. & Develop. **14** (5), 509–514 (1970).

S, P, Th 124. George, J. L., Back-scattering of circularly polarized waves from slightly rough surfaces, Rept. No. 1179–1, Antenna Lab. Ohio State Univ. Research Foundation, pp. 1–11 (Apr. 1961). AD–407 424.

Su 125. Ginsberg, I. W., Limperis, T., Nicodemus, F. E., and Richmond, J. C., Geometrical considerations in reflectance nomenclature, to be published as Nicodemus, F. E., Richmond, J. C., Hsia, J. J., Venable, W. H., Jr., Ginsberg, I. W. and Limperis, T. Geometrical considerations and nomenclature for reflectance. NBS Monograph.

S, Th. 126. Goldfischer, L. I., Autocorrelation function and power spectral density of laser-produced speckle patterns, J. Opt. Soc. Am. **55** (3), 247–253 (Mar. 1965).

SM 127. Gorodinskii, G. M., Device for the production inspection of the surface roughness of plate glass, Measurement Techniques No. 4, 413–415 (July-Aug. 1958).

R, Th, Ex 128. Gorodinskii, G. M., The statistical interference of light upon reflection from matte-glass surfaces, Opt. Spectrosc. **15**, 57–60 (1963).

P, Ex 129. Gorodinskii, G. M., Polarizing properties of frosted glass surfaces in the case of reflection, Opt. Spectrosc. **16**, 59–60 (1964).

R, Ex 130. Gorton, A. F., Reflection from, and transmission through, rough surfaces, Phys. Rev. **7** (1), 66–78 (1916).

S, Ex(L) 131. Gould, G., et al., Coherent detection of light scattered from a diffusely reflecting surface, Appl. Opt. **3**, 648–649 (1964).

S 132. Gravatt, C. C., Jr., The applications of light scattering Appl. Spectroscopy **25** (5), 509–517 (1971).

SM 133. Green, E., Review of surface texture measurement and the associated metrological problems, pp. 330–343, PMS* Proceedings, 1967–68.

S, Th, Ex(L) 134. Greenwood, D. P. and Powers, E. J., Determination of surface-height power spectral density from a laser-scattering measurement, J. Opt. Soc. Am. **61** (11), 1589 (Nov. 1971).

SM 135. Greenwood, J. A. and Williamson, J. B. P., Contact of nominally flat surfaces, Proc. Roy. Soc. **A295**, 300–319 (1965).

SM 136. Guentert, O. J., Development of surface measurement system, Raytheon Co. Waltham, Mass., Research Div. Rept. No. S–815, 1–40 (Sept. 1965). AD–472 415.

R, S, Th 137. Hagfors, T., Relationship of geometric optics and and auto-corelation approaches to the analysis of lunar and planetary radar echoes, J. Geophys. Res. **71,** 379–383 (Jan. 1966).

S, Th 138. Hansen, J. E. and Cheyney, H., Theoretical spectral scattering of clouds in the near infrared, J. Geophys. Res. **74** (13), 3337–3346 (1969).

R, Th 138a. Hapke, B. W., A theoretical photometric function for the lunar surface, J. Geophys. Res. **68** (15), 4571–4586 (1963).

R, S, Ex 139. Harten, H., Zur Streureflexion an matten Oberflächen, Z. Physik **126,** 27–34 (1949).

S, Th 140. Hayre, H. S. and Moore, R. K., Theoretical scattering coefficient for near vertical incidence from contour maps, J. Res. Nat. Bur. Stand. (U.S.), **65D** (Radio Prop.) No. 5, 427–432 (Sept.–Oct. 1961).

H 141. Hering, R. G. and Fischer, W. D., Radiant heat transfer between nongray surfaces, AIAA Paper No. 71–464 AIAA 6th Thermophysics Conference, Tullahoma, Tenn., Apr. 26–28, 1971.

R, Th 142. Hering, R. G. and Smith, T. F., Apparent radiation properties of a rough surface, AIAA Paper No. 69–622, AIAA 4th Thermophysics Conference, June 1969.

H, Th 143. Hering, R. G. and Smith, T. F., Surface roughness effects on equilibrium temperature of interacting surfaces, AIAA Paper No. 70–817, AIAA 5th Thermophysics Conference, June 1970.

H, Th 144. Hering, R. G. and Smith, T. F., Surface roughness effects on radiant energy interchange, ASME Paper No. 70–HT/SpT–2, 1–9 (1970).

R, Th, Ex 145. Herold, L. M. and Edwards, D. K., Bidirectional reflectance characteristics of rough, sintered-metal, and wire-screen surface systems, AIAA Paper No. 66–19, AIAA 3rd Aerospace Sciences Meeting, Jan. 1966.

S, Th, Ex 146. Hiatt, R. E., Senior, T. B. A. and Weston, V. H., A study of surface roughness and its effect on the backscattering cross section of spheres, Proc. IRE **48** (12), 2008–2016 (Dec. 1960).

S, Th 147. Hills, N. L. and Karp, S. N., Semi-infinite diffraction gratings.I., Commun. Pure Appl. Math. **18** (1/2), 203–233 (Feb.–May 1965). AD–617 220.

Em, Ex 148. Hires, R. G. and Evans, R. C., Study of surfaces designed to increase thermal radiation, Report No. TG–618, Applied Physics Laboratory, Johns Hopkins University, Silver Spring, Md. (Nov. 1964). AD–459 468.

SM 149. Hodgkinson, I. J., A simple scatter method for optical surface roughness and slope measurements. Roughness of polished fused silica, J. Phys. E (Sci. Instrum.) **3** (5), 341–342 (May 1970).

S, Th 150. Hoffman, W. C., Scattering of electromagnetic waves from rough surfaces, Quart. Appl. Math. **13,** 291–304 (Oct. 1955).

S, Ex 151. Hottel, H. C., Sarofim, A. F., Dalzell, W. H. and Vasalos, I. A., Optical properties of coatings: effect of pigment concentration, AIAA Journal, 1395–1398 (Oct. 1971).

S, Ex, Th 152. Hottel, H. C., Sarofim, A. F., Vasalos, I. A. and Dalzell, W. H., Multiple scatter: comparison of theory with experiment, ASME Paper No. 69–WA/HT–44, 1–7, ASME Winter Annual Meeting, Nov. 16–20, 1969.

R, Th 153. Houchens, A. and Hering, R. G., Bidirectional reflectance of rough metal surfaces, AIAA Progress in Aeronautics and Astronautics: Thermophysics of Spacecraft and Planetary Bodies (G. B. Heller, ed.) **20,** 65–89 (Academic Press, New York, N.Y., 1967).

H 154. Houchens, A. F., Hering, R. G. and Savage, L. D., Roughness effects on radiant heat transfer between interacting surfaces, AIAA Paper No. 72–305, AIAA 7th Thermophysics Conference, San Antonio, Tex., Apr. 10–12, 1972.

H 155. Howell, J. R. and Durkee, R. E., Comparison of analysis and experiment for radiative transfer between surfaces with collimated incident radiation, ASME Paper No. 70–HT/SpT–23, Am Soc. Mech. Engr. (1970).

R, Em, Th 156. Howell, J. R. and Perlmutter, M., Directional behavior of emitted and reflected energy from a specular, gray, asymmetric groove, NASA TND–1874 (1963).

SM 157. Hsia, J. J. G., Electrolytic preparation of reproducible metallic surfaces, Master thesis, Dept. of Mechanical Engineering, Purdue Univ., 1964.

Ma 158. Hufford, G., An integral equation approach to the problem of wave propagation over an irregular surface, Quart. Appl. Math. **9,** (4), 391–403 (1952).

R(Th) 159. Hunderi, O. and Beaglehole, D., Study of the interaction of light with rough metal surfaces. II. Theory, Phys. Rev. B **2** (2), 321–329 (1970).

S, Th 160. Isakovich, M. A., Scattering of waves from a statistically rough surface, Zhurnal Eksperimental'noi I Theoreticheskoi Fiziki (J. Exptl. Theo. Phys. USSR) **23,** 305–314 (1952). Translated by Goss, R. N., U.S. Naval Electronics Lab., San Diego, Calif., in Three papers on diffraction of waves from a rough surface. pp. 39–52c.

R, Th 161. Itoh, T. and Mittra, R., An Analytical study of the echelette grating with application to open resonators, IEEE Tran. on Microwave Theory and Techniques **VMTT–17** (6), 319–327 (June 1969). AD–696 236.

SM 162. Janssen, J. E. and Schmidt, R. N., The measurement of total surface area, NASA SP–55, Symposium on Thermal Radiation of Solids (S. Katzoff, ed.), pp. 179–181, NASA (1965).

S, Ex, Ap 163. Johnson, M. C., Vacuum ultraviolet scattering distributions, Appl. Opt. **7** (5), 879–881 (1968).

S, Th 164. Jones, A. R., Scattering of focused electromagnetic waves by infinite cylinders, J. Phys. A (Gen. Phys.) Great Britain Ser. 2, **2,** 311–322, 1969.

S, Th, Ex 165. Judd, D. B., Optical specification of light scatter-

ing materials, J. Res. Nat. Bur. Stand. (U.S.) **19**, 287–317 (Sept. 1937). RP1026.

Ma — 166. Kac, M., On the average number of real roots of a random algebraic equation, Bull. Math. Soc. **49**, 314–320 (1943).

R, Th — 167. Kalhor, H. A. and Neureuther, A. R., Numerical method for the analysis of diffraction gratings, J. Opt. Soc. Am. **61** (1), 43–48 (1971).

Em, Th, Ex, Ap — 168. Kanayama, K., Apparent directional emittances of V- groove and circular -groove rough surfaces, Heat Transfer-Japanese Res. **1** (1), 11–22 (Jan.–Mar. 1972).

S(L), Ex — 169. Karinskii, S. S., Komarov, V. G. and Mondikov, V. D., Scattering of light by elastic surface waves, JETP Letters **9** (7), 225–226, 1969. (Original ZhETF Pis. Red. **9** (7), 380–383, 1969.)

R, Th — 170. Kaufman, D. E., A vector solution for electromagnetic wave scattering from a rough surface of arbitrary dielectric constant, Radio Sci. **6** (1), 7–20 (1971).

R, Ex, SM — 171. Keegan, H. J., Schleter, J. C., Weidner, V. R., Spangenberg, D. B., Strang, A. G. and Chamberlin, J. L., Effect of surface texture on diffuse spectral reflectance, NASA SP–55, Symposium on Thermal Radiation of Solids (S. Katzoff, ed.) pp. 165–177, NASA (1965).

R, Ex — 172. Kelly, F. J. and Moore, D. G., A test of analytical expressions for the thermal emissivity of shallow cylindrical cavities, Appl. Opt. **4** (1), 31–40 (1965).

S, Su — 173. Kerker, M., The scattering of light and other electromagnetic radiation (Academic Press, New York, 1969).

S, Th — 174. Kerker, M., Cooke, D. D. and Carlin, J. M., Light scattering from infinite cylinders, the dielectric-needle limit, J. Opt. Soc. Am. **60** (9), 1236–1239 (Sept. 1970).

R, Th — 175. Kholopov, G. K., Calculation of emissivities of non-diffuse cavity-type sources, Soviet J. Opt. Technology **35** (1), 1–6 (1968).

SM — 176. Kimoto, S. and Russ, J. C., The characteristic and applications of the scanning electron microscope, Am Scientists **57** (1), 112–133 (1969).

S, Th — 177. King, R. W. P. and Harrison, C. W. Jr., Scattering by imperfectly conducting spheres, IEEE Trans. on Antennas and Propagation **AP–19** (2), 197–207 (1971).

R, Th, Su — 178. Kirtikos, H., Lang, K. C. and Boerner, W., et al, Investigation of rough earth propagation models, RADC–TR–67–531, 10–18 (Oct. 1967). AD–822 904.

R, S, Th — 179. Kivelson, M. and Moszkowski, S., Reflection of electromagnetic waves from a rough surface, J. Appl. Phys. **36**, 3609–3612 (1966).

Ap — 180. Kneissl, G. J. and Richmond, J. C., A laser-source integrating sphere reflectometer, Nat. Bur. Stand. (U.S.), Tech. Note 439, 54–63 (Feb. 1968).

S, Th — 181. Kodis, R. D., A note on the theory of scattering from an irregular surface, IEEE Trans. on Antennas and Propagation, **AP–14**, 77–82 (Jan. 1966).

S, Th, Ex — 182. Kozlov, V. P. and Federova, E. O., Reflection of light from a scattering medium, Soviet J. Opt. Technology **34** (1), 1–6 (1967).

S, Th — 183. Kroll, N. M. and Kelly, P. L., Temporal and spatial gain in stimulated light scattering, Phys. Rev. A **4** (2), 763–776 (1971).

S, Th — 184. Kubelka, P., New contributions to the optics of intensely light-scattering materials. Part I, J. Opt. Soc. Am. **38** (5), 448–457 (May 1948).

T, S, Th — 185. Kurtz, C. N., Transmittance characteristics of surface diffusers and the design of nearly band-limited binary diffusers, J. Opt. Soc. Am. **62** (8), 982–989 (Aug. 1972).

R, Ex — 186. Lagrone, A. H. and Tolbert, C. W., Reflection studies of millimeter and centimeter radio waves for Gulf of Mexico paths, Rept. No. EERL–64, 1–38, Texas Univ. Austin Electrical Engineering Research Lab. (Oct. 1952). AD–494 931.

S, Th — 187. Lam, J., Scattering by an expanding conducting sphere, J. Math. Phys. (Cambridge) **47** (2), 199–212 (1968).

S, Th — 188. Lang, K. C., Diffraction of electromagnetic waves by a moving impedance wedge, Radio Sci. **6** (6), 655–663 (1971).

S(L) — 189. Langmuir, R. V., Scattering of laser light, Appl. Phys. Letters **2** (2), 29–30 (January 15, 1963).

SM — 190. Latanision, R. M., Characterization of metal surfaces, RIAS Tech. Rept. 71–08c, Research Institute for Advanced Studies, Martin Marietta Co., Baltimore, Md. (1971). AD–722 013.

R, Ex, Th — 191. Latta, M. R., The scattering of 10.6 micron radiation from ground glass surfaces, Preprint of 1969 spring meeting. Optical Society of America, San Diego, Calif., March 1969.

R, Th Ex(L) — 192. Leader, J. C., Bidirectional scattering of electromagnetic waves from rough surfaces, MDC 70–022, McDonnell Aircraft Co., St. Louis, Mo. (1970).

S, Th — 193. Leader, J. C., Multiple scattering of electromagnetic waves from rough surfaces, MDC 70–037, McDonnell Aircraft Co., St. Louis, Mo. (1970).

S, Th, Ex(L) — 194. Leader, J. C., Hemispherical scattering of electromagnetic waves from rough surfaces, McDonnell Aircraft Co. Rept. No. MCAIR 72–037 (1972).

L — 195. Libenson, M. N., Romanov, G. S., and Imas Ya. A., Temperature dependence of the optical constants of a metal in heating by laser radiation, Soviet Physics-Technical Physics **13** (7), 925–928 (Jan. 1969). Translated from Zhurnal Tekhnicheskoi Fiziki **38** (7), 1116–1119 (July 1968).

Ap — 196. Lindberg, R. W., A specular gonioreflectometer, Proc. 21st Inst. Soc. Am. Conf., N.Y. 1966, **21** pt. 1, Paper No. 12.6–3–66.

R, Ex — 197. Loehrlein, J. E., Winter, E. R. F., and Viskanta, R., Measurement of bidirectional reflectance using a photographic technique, AIAA Paper No. 70–859, AIAA 5th Thermophysics Conference, June 1970.

R, Th — 198. Longuet-Higgins, M., Reflection and refraction of a random moving surface—II: Number of specular points on a Gaussian surface, J. Opt. Soc. Am. **50**, 845–850 (1960).

R, Th — 199. Look, D. C. Jr. and Love, T. J., Investigation of the effects of surface roughness upon reflectance, AIAA Paper No. 70–820, AIAA 5th Thermophysics Conference, June 1970.

Em, Th — 200. Love, T. J. and Turner, W. D., Directional emittance from emitting, absorbing, and scattering media, AIAA Paper No. 69–625, AIAA 4th Thermophysics Conference, June 1969.

S, Ex — 201. Lundberg, J. L., Light scattering from large fibers at normal incidence, J. Colloid and Interface Sci. **29** (3), 565–583, 1969.

S, Th — 202. Lynch, P. J., Curvature corrections to rough-surface scattering at high frequencies, J. Acoust. Soc. Am. **47** (3) part 2, 804–815 (1970).

S, Th — 203. Lynch, P. J. and Wagner, R. J., Energy conservation for rough-surface scattering, J. Acoust. Soc. Am. **47** (3) part 2, 816–821 (1970).

R, Th — 204. Lynch, P. J. and Wagner, R. J., Rough-surface Scattering: Shadowing, multiple scatter, and energy conservation, J. Math. Phys. **11** (10), 3032–3042 (1970).

R, T, Th — 205. Marathay, A. S., Heiko, L. and Zuckerman, J. L., Study of rough surfaces by light scattering, Appl. Opt. **9** (11), 2470–2476 (1970).

R, Ex(L) — 206. Massey, G. A., Photomixing with diffusely reflected light, Appl. Opt. **4** (7), 781–784 (July 1965).

S, Th — 207. Mautz, J. R. and Harrington, R. F., Radiation and scattering from bodies of revolution, Appl. Sci. Res. **20**, 405–435 (June 1969).

R, Ex, Ap(L) — 208. Maxwell, J. R., Target signature analysis center: DATA compilation eleventh supplement. Vol. 1: Bidirectional reflectance: Definition, discussion, and utilization., Report No. AFAL–TR–72–226, Target signature analysis center, infrared and optics Division, Willow Run Laboratories, The University of Michigan, Ann Arbor, Mich. (Oct. 1972).

S, Th — 209. McClellan, R. P. and Stroke, G. W., Solution of the non-homogeneous Helmholtz equation for optical gratings with perfectly conducting boundaries, J. Math. Phys. **45**, 383–390 (1967).

P, Th — 210. McCoyd, G. C., Polarization properties of a simple dielectric rough-surface model, J. Opt. Soc. Am. **57** (11), 1345–1350 (1967).

S, Th — 211. McIvor, I. K., Two-dimensional scattering of a plane compressional wave by surface imperfections, Bull. Seismol. Soc. Am. **59** (3), 1349–1364 (June 1969). AD–692 601.

R, Ex — 212. McNicholas, H. J., Absolute methods in reflectometry, J. Res. Nat. Bur. Stand. (U.S.), **1**, 29–73 (1928). RP3.

R, Th — 213. Meecham, W. C., A method for the calculation of the distribution of energy reflected from a periodic surface, IRE Trans. on Antennas and Propagation **AP–4** (3), 581 (July 1956).

R, Th — 214. Meecham, W. C., Variational method for the calculation of the distribution of energy reflected from a periodic surface. I., J. Appl. Phys. **27** (4), 361–367 (1956).

R, Th — 215. Meecham, W. C., Fourier transform method for the treatment of the problem of the reflection of radiation from irregular surfaces, J. Acoust. Soc. Am. **28** (3) 370–377 (1956).

S, R, Th — 216. Merriam, R. L. and Viskanta, R., Radiative characteristics of absorbing, emitting, and scattering media on opaque substrata, J. Spacecraft **5** (10), 1210–1215 (1968).

R, Th, Ex — 217. Middleton, W. E. Knowles and Mungal, A. G., The luminous directional reflectances of snow, J. Opt. Soc. Am. **42** (8), 572–579 (1952).

R, Ex — 218. Middleton, W. E. Knowles and Wyszecki, G., Colors produced by reflection at grazing incidence from rough surfaces, J. Opt. Soc. Am. **47** (11), 1020–1023 (1957).

S, R, Th — 219. Miles, J. W., On nonspecular reflection at a rough surface, J. Acous. Soc. Am. **26**, 191–199 (Mar. 1954).

S, Th — 220. Millar, R. F., Rayleigh Hypothesis in scattering problems, Electronics Letters **5** (17), 416–418, 1969.

R, Ap — 221. Miller, E. R. and Vun Kannon, R. S., Development and use of a bidirectional spectroreflectometer, AIAA Paper No. 67–313, AIAA Thermophysics Specialist Conference, New Orleans, La. (Apr. 17–20, 1967).

S, Th — 222. Mittra, R. and Wilton, D. R., Anumerical approach to the determination of electromagnetic scattering characteristics of perfect conductors, Proc. IEEE **57** (11), 2064–2065 (Nov. 1969).

R, Th — 223. Mitzner, K. M., Theory of the scattering of electromagnetic waves by irregular interfaces, Rept. No. TR 30, pp. 1–131, Antenna Lab. Calif. Inst. Tech. (Jan. 1964). AD–436 811.

P, Th — 224. Mitzner, K. M., Change in polarization on reflection from a tilted plane, Radio Science **1** (1), 27–29 (Jan. 1966).

R, P, Th — 225. Monroe, R. L., Approximate step-function response of a horizontally polarized electromagnetic wave reflected at an imperfectly conducting surface, J. Appl. Phys. **41** (12), 4820–4822 (1970).

SM — 226. Moody, J. C., Measurement of ultrafine surface finishes, Rept. No. SC–DC–67–1425, pp. 1–17, Sandia Corp. Albuquerque, N. Mex. (Mar. 1967).

SM — 227. Motycka, J., Proposed interferometric method of measurement of roughness and autocorrelation function in smooth-finished surfaces, Appl. Opt. **8** (7), 1435–1438 (1969).

SM — 228. Munnerlyn, C. R. and Latta, M., Rough surface interferometry using a CO_2 laser source, Appl. Opt. **7** (9), 1858–1859 (1968).

SM 229. Munnerlyn, C. R., Givens, N. P., Hopkins, R. E., Interferometric measurements of optically rough surfaces, preprint of 1969 IEEE Conference on Laser Engineering and Applications, Washington, D.C., May 1969.

R, Th 230. Nagata, K., Yoshida, N., and Nishiwaki, J., Ensemble-averaged coherence function of light reflected from rough surface: determination of its correlation length, Japanese J. Appl. Phys. **9** (5), 505–515 (1970).

SM 231. Nara, J., Profile analyzer, Bull. Japan Soc. Prec. Engg. **3** (3), 59–61 (1969). (Also in Bull. Natl. Res. Lab. Metrology, Japan, No. 19, 18–20, Oct. 1969).

SM 232. Nara, J., Two-dimensional representation of surface roughness, Bull. Natl. Res. Lab. Metrology (Japan) No. 19, pp. 7–17 (Oct. 1969). (C.I.R.P. Vol. **XVII**, 485–495, Pergamon Press Ltd. 1969).

R, Th 233. Nelson, H. F., Ray reflection from rough dielectric surfaces, AA & ES 66–5, Purdue University, 1–142 (1966).

R, Th 234. Nelson, H. F. and Goulard, R., Reflection from a dielectric surface, J. Opt. Soc. Am. **57** (6), 769–771 (1967).

R, Ex 235. Neu, J. T. and Dummer, R. S., Theoretical and practical implications of the bidirectional reflectance of spacecraft surfaces, Paper No. 68–26, AIAA 6th Aerospace Sciences Meeting New York, N.Y. Jan. 22–24, 1968.

Em, Th 236. Nevskii, A. S. and Il'chukova, L. V., Effect of macroscopic roughness on the character of the emission from a surface, High Temp. **6** (6), 990–994 (1968).

R, Th 237. Nicodemus, F. E., Directional reflectance and emissivity of an opaque surface, Appl. Opt. **4** (7), 767–773, 818 (1965).

R 238. Nicodemus, F. E., Reflectance nomenclature and directional reflectance and emissivity, Appl. Opt. **9** (6), 1474–1475 (June 1970).

S, Th 239. Olaofe, G. O., Scattering by an arbitrary configuration of parallel circular cylinders, J. Opt. Soc. Am. **60** (9), 1233–1236 (Sept. 1970).

S(L) 240. Oliver, B. M., Sparkling spots and random diffraction, Proc. IEEE **51**, 220–221 (1963).

R, Th 241. Ornstein, L. S., and Van der Burg, A., Reflectivity of corrugated surfaces, Physica **IV** (11), 1181–1189 (1937).

S, Th 242. Parkins, B. E., Scattering from time-varying rough surfaces, Rept. No. TR–3, 1–18, Bell Telephone Labs., Inc., Whippany, N.J. (Sept. 1966). AD–656 549.

R, Em, Th 243. Parmer, J. F., and Wiebelt, J. A., The thermal radiation characteristics of specular walled grooves in the solar space environment, AIAA 4th Aerospace Sciences Meeting, Los Angeles, Calif., AIAA Paper No. 66–459 (June 1966).

S, Th 244. Peake, W. H., Barrick, D. E., Fung, A. K., and Chan, H. L., Comments on Backscattering of waves by composite rough surfaces, IEEE Trans. on Antennas and Propagation **AP–18** (5), 716–726 (Sept. 1970).

SM 245. Peklenik, J., New developments in surface characterization and measurements by means of random process analysis pp. 108–126, PMS* Proceedings 1967–68.

S, Th 246. Pimenov, Yu. V., and Kravtsova, G. V., Diffraction of a plane electromagnetic wave by an ideally conducting spherical segment, Radio Eng. **24** (2), 101–106, 1969.

SM 247. Piper, B., and Callis, W. P., Surface-finish measurement on non-ferrous materials, American Machinist Special Rept. No. 476, 105–120 (1959).

S, Th 248. Plonus, M. A., Scattering from small obstacles on an infinite conducting plane, Rept. 7741–3–T, 1–60, University of Michigan, Ann Arbor, Mich. (Dec. 1966). AD–814 843.

R, Th 249. Polgar, L. G., and Howell, J. R., Directional radiative characteristics of conical cavities and their relation to lunar phenomena, AIAA Progress in Aeronautics and Astronautics: Thermophysics and Temperature Control of Spacecraft and Entry Vehicles (G. B. Heller, ed.), (Vol. **18**, pp. 311–323, Academic Press, New York, N.Y., 1966).

S, Th 250. Pollon, G. E., Statistical parameters for scattering from randomly oriented arrays, cylinders, and plates, IEEE Trans. on Antennas and Propagation **AP–18** (1), 68–75 (Jan. 1970).

R, P, Ex 251. Polyanskii, V. K., Kovalskii, L. V., and Milovidova, T. I., Specular reflection from a mat surface with coarse microtopography, Opt. Spectrosc. **25** (5), 415–416 (1968).

P, Ex, Ap 252. Polyanskii, V. K., and Rvachev, V. P., On the reflection of light from rough surfaces, Opt. Spectrosc. **20** (4), 391–394 (1966).

R, P 253. Polyanskii, V. K., and Rvachev, V. P., Light reflection from rough surfaces, Report No. RSIC–588 (Opt. Spectrosc. **20** (4), 701–708, 1966) AD–641 140.

R, Th 254. Porteus, J. O., Relation between the height distribution of a rough surface and the reflectance at normal incidence, J. Opt. Soc. Am. **53** (12), 1394–1402 (Dec. 1963).

SM 255. Posey, C. J., Measurement of surface roughness, Mech. Eng. **68** (4), 305–306, 338 (April 1966).

R, Ex, Th 256. Pouey, M., and Fabre, D., Quelques experiences de diffusion du rayonnement ultraviolet par des surfaces rugueuses, Optica Acta **16** (4), 471–481, 1969.

SM 257. Reason, R. E., The application of an electronic computer to the study of surface measurement, Automatisme **9** (5), (May 1964).

SM 258. Reason, R. E., Workshop requirements of surface measurement, pp. 299–305, PMS* Proceedings 1967–68.

R, S, Ex(L) 259. Renau, J. and Collinson, J. A., Measurements of electromagnetic backscattering from known, rough surfaces, The Bell Syst. Tech. Journal, **44** (10), 2203–2226 (Dec. 1965).

S, P, Ex 260. Renau, J., Cheo, P. K., and Cooper, H. G., Depolarization of linearly polarized EM waves backscattered from rough metals and inhomogeneous dielectrics, J. Opt. Soc. Am. **57** (4), 459–466 (1967).

R, P, Th, Ex 261. Rense, W. A., Polarization studies of light diffusely reflected from ground and etched glass surfaces, J. Opt. Soc. Am. **40**, 55–59 (1950).

SM 262. Ribbens, W. B., Interferometric surface roughness measurement, Appl. Opt. **8** (11), 2173–2176 (1969).

Ma 263. Rice, S., Mathematical analysis of random noise, I & II, Bell Sys. Tech. J. **23**, 282–332 (1944); III & IV, Bell Sys. Tech. J. **24**, 45–156 (1945).

R, Th 264. Rice, S. O., Reflection of electromagnetic waves from slightly rough surfaces, Comm. Pure Appl. Math. **4**, 351–378 (1951).

SM 265. Richards, P.J., Review of methods of measurement and assessment of surface form and texture, pp. 453–465, PMS* Proceedings 1967–68.

R, Th 266. Richmond, J. C., Effect of surface roughness on emittance of nonmetals, AIAA Thermophysics Specialist Conference, Monterey, Calif., AIAA Paper No. 65–675 (Sept. 1965). J. Opt. Soc. Am. **56** (2), 253–254 (Feb. 1966).

SM 267. Richmond, J. C. and Francisco, A. C., Use of plastic replicas in evaluating surface texture of enamels, J. Res. Nat. Bur. Stand. (U.S.), **42**, 449–460 (May 1949). RP1985.

R, Th 268. Rolling, R. E., The effect of slight surface roughness on emittance, NASA SP–55, Symposium on Thermal Radiation of solids (S. Katzoff, ed.), pp. 153–155, NASA (1965).

Em, Ex 269. Rolling, R. E., Effect of surface roughness on the spectral and total emittance of platinum, AIAA Paper No. 67–320, AIAA Thermophysics Specialist Conference, New Orleans, La. (Apr. 1967).

R, Ex, Th 270. Rolling, R. E. and Funai, A. I., Investigation of the effect of surface condition on the emittance and reflectance of opaque materials, Quarterly Progress Reports, 1963, Contract No. AF 33 (657)–11281, task No. 736001, Aerospace Science Laboratory, Lockheed Missiles and Space Co., Palo Alto, Calif., 1963.

Em, P, Ex 271. Rolling, R. E. and Funai, A. I., Investigation of the effect of surface conditions on the radiant properties of metals, Part II, Measurements on roughened platinum and oxidized stainless steel, AFML–TR–64–363 (Apr. 1964).

S, Th 272. Ross, R. A., Small-angle scattering by a finite cone, IEEE Trans., on Antennas and Propagation **AP–17** (2), 241–242 (1969).

R, Ex 273. Rouse, J. W., Jr., Wavelength dependence of backscatter from rough surface, Tech. Rept. RSC–12, Remote Sensing Center, Texas A. & M. Univ., 1–21 (Sept. 1970).

S, Th 274. Rousseau, M., Statistical properties of optical fields scattered by random media. Application to rotating ground glass, J. Opt. Soc. Am. **61** (10), 1307–1316 (Oct. 1971).

S, H 275. Roux, J. A., Radiative heat transfer of coatings on a cryogenic surface, AEDC–TR–71–90, 1–205, Von Karman Gas Dynamics Facility, Arnold Engineering Development Center, Air Force Systems Command, Arnold Air Force Station, Tenn. (Apr. 1971).

R, Ex 276. Russell, D. A., The spectral reflectance of rough surfaces in the infrared, Master's thesis, Dept. of Mechanical Engineering, Univ. of Calif. at Berkeley (1961).

SM 277. Sadowski, A., Trends and actual state of Polish scientific research work in the field of surface metrology, pp. 229–240, PMS* Proceedings, 1967–68.

R, Ex, Th 278. Safwat, H. H. and Parmer, J. F., Effect of surface roughness on specular and diffuse reflectance components of carbon steel in visible wavelength range, ASME Paper No. 69–WA/HT–42, ASME Winter Annual Meeting, Nov. 1969.

S, Th 279. Sancer, M. I., Shadow-corrected electromagnetic scattering from a randomly rough surface, IEEE Trans. on Antennas and Propagation **AP–17** (5), 557–585 (1969).

R, Th 280. Schmidt, R. N., Infrared diffuse reflector coating, Honeywell Doc. 12041–QR2, 1967.

SM 281. Schneider, E. J., Surface finish testing. The present state of the art and its future, Engis Equipment Co. Morton Grove, Ill. (Sept. 15, 1969).

Em, Th 282. Schocken, K., The angular distribution of infrared radiation, Rept. No. DA TN–3–60, Research Projects Laboratory, George C. Marshall Space Flight Center (Feb. 1960).

R(L), Ex, Ap 283. Seaney, R. J., The angular backscattering characteristics of plane surfaces illuminated by carbon dioxide laser radiation, R.A.R.D.E. Memorandum 3/69 Royal Armament Research and Development Establishment (Feb. 1969). AD–850 443.

S, Th 284. Senior, T.B.A., The scattering of electromagnetic waves by a corrugated sheet, Can. J. Phys. **37** (7), 787–797, 1572 (1959).

S, Th, Ex 285. Senior, T. B. A., Surface roughness and tolerances in model scattering experiments, IEEE Trans. on Antennas and Propagation **AP–13** (4), 620–636 (1965).

SM 286. Sharman, H. B., Influence of sample size and the relationships between the common surface texture parameters, pp. 416–424 PMS* Proceedings 1967–68.

R, Th 287. Shaw, L., Comments on 'Shadowing of random surfaces', IEEE Trans. on Antennas and Propagation (Communications) **AP–14**, 253 (Mar. 1966).

R, Ex 288. Shelley, R., Sea surface forward scattering at low grazing angles, Navy Electronics Lab., San Diego Calif., Rept. No. NEL–1338, 1–30 (Nov. 1965). AD–480 126.

S, Th 289. Shubert, H. A., Plane wave diffraction by thick dielectric gratings and zone phase plates, Tech. Rept. No. 77, 1–149, Illinois Univ. Urbana

Engineering Experiment Station (June 1964). AD-603 026.

Em, Ex 290. Siegfried, R. G. and Birkebak, R. D., A comparative study of the total directional emittance of a dielectric and a metal as a function of surface roughness, AIAA 3rd Thermophysics Conference, Los Angeles, Calif., AIAA Paper No. 68-778 (June 1968).

R, Th 291. Simmons, E. L., An equation relating the diffuse reflectance of weakly absorbing powdered sample to the fundamental optical parameters, Optica Acta **18** (1), 59-68 (1971).

P, Th 292. Sirohi, R. S., Optical constants of rough surface by ellipsometry, Brit. J. Appl. Phys. **3** (9), 1407-1409 (1970).

S, Th 293. Sledge, O. D., The scattering of a plane electromagnetic wave by a linear array of center loaded cylinders, Rept. No. NRL-6681, 1-45, Naval Research Lab., Wash. D.C. (June 1968). AD-672 182.

S, R, Th 294. Sledge, O. D., Scattering of a plane electromagnetic wave by a linear array of cylindrical elements, IEEE Trans. on Antennas and Propagation **AP-17** (2), 169-174 (1969).

R, Ex 295. Smith, A. M. and Muller, P. R., Super- and subspecular maxima in the angular distribution of polarized radiation reflected from roughened dielectric surfaces, AEDC-TR-70-286, Von Karman Gas Dynamics Facility, Arnold Engineering Development Center, Air Force Systems Command, Arnold Air Force Station, Tenn. (1971).

T (Ex, Th) 296. Smith, A. M. and Muller, P. R., Anomalous refraction maxima in the bidirectional transmittances of roughened dielectric surfaces, AIAA Paper No. 72-302, 1-11, AIAA 7th Thermophysics Conference, San Antonio, Tex. Apr. 10-12, 1972.

R, Ex 297. Smith, A. M., Muller, P. R., Frost, W., and Hsia, Han M., Super- and sub-specular maxima in the angular distribution of polarized radiation reflected from roughened dielectric surfaces, AIAA Paper No. 70-861, AIAA 5th Thermophysics Conference, June 1970.

S, Th 298. Smith, B. G., Geometrical shadowing of a random rough surface, IEEE Trans. Antennas and Propagation **AP-15**, 668-671 (Sept. 1967).

R, Th 299. Smith, T. F., and Hering, R. G., Bidirectional reflectance of a randomly rough surface, AIAA Paper No. 71-465, AIAA 6th Thermophysics Conference, Tullahoma, Tenn., Apr. 26-28, 1971.

R, Su, Th, Ex, Ap 300. Smith, T. F., and Hering, R. G., Surface roughness effects on bidirectional reflectance, Tech. Rept. No. ME-TR-661-2, Heat Transfer Laboratory, University of Illinois, Urbana, Ill. (June 1972).

R, Th, Ex 301. Solesvik, A., Effective reflectivity and angular distribution of light reflected from sea water with surface waves, Norwegian Defense Research Establishment, Rept. No. Teknisk notat E-118 (Sept. 1966). AD-815 675.

R, Ex, Su 302. Sparrow, E. M., and Cess, R. D., Radiation Heat Transfer, pp. 60-63 (Wadsworth Publishing Co., Belmont, Calif., 1966).

R, Th 303. Spencer, D. E., and Gaston, E. A., The numerical ranges of diffuse and specular reflectance, Dept. of Mathematics U-9, The University of Connecticut, Storrs, Conn. (1973). Unpublished report.

R, Th 304. Spetner, L. M., Discussion of H. Davies' The reflection of electromagnetic waves from a rough surface, Proc. IEE, Pt. III, **102**, 148 (1955).

R, S, Th 306. Spetner, L. M., A statistical model for forward scattering of waves off a rough surface, IRE Trans. on Antennas and Propagation **AP-6** (1), 88-94 (Jan. 1958).

S, Th, Ex 307. Sporton, T. M., The scattering of coherent light from a rough surface, Brit. J. Appl. Phys. (J. Phys. D), Ser. 2, **2** (7), 1027-1034 (1969).

SM 308. Spragg, R. C., Accurate calibration of surface texture and roundness measuring instruments, pp. 397-405, PMS* Proceeding, 1967-68.

Ex, R 309. Stanford, J. L., Ashley, E. J., and Bennett, H. E., Roughness-induced absorption in metallic mirrors, Preprint of a paper presented at the Optical Society of America 1970 Annual Meeting, Sept. 28-Oct. 2, Held at Hollywood, Fla.

R, Ex 310. Stevison, D. F., Effect of surface roughness on the reflectance of refractory metals, AFML-TR-66-232 (Dec. 1966).

S, Th 311. Stogryn, A., Electromagnetic scattering from rough, finitely conducting surfaces, Radio Sci. **2**, 415-428 (1967).

SM 312. Strang, A. G., and Ogborn, F., Measurement of surface roughness of electrodeposited and electropolished surfaces by means of the microinterferometer, NBS Handbook 77, Vol. III: Precision Measurement and Calibration—Optics, Metrology and Radiation, 324/1-335/12 (1961).

S, Th 313. Swift, C. T., A note on scattering from a slightly rough surface, IEEE Tran. on Antennas and Propagation **AP-19** (4), 561-562 (July 1971).

H 314. Toor, J. S. and Viskanta, R., Experiment and Analysis of directional effects on radiant heat transfer, J. Heat Transfer, 459-466 (Nov. 1972).

H 315. Toor, J. S., Viskanta, R., and Winter, E. R. F., An experimental and analytical study of real surface effects on radiant heat transfer, Heat Transfer Laboratory Rept., Mechanical Engineering School, Purdue University (May 1971).

R, Ex 316. Toporets, A. S., Specular reflection from a rough surface, Opt. Spectrosc. **16**, 54-58 (1964).

P, Ex 317. Toporets, A. S. and Mazurenko, M. M., Depolarization of light upon diffuse reflection, Soviet J. Opt. Tech. **35** (1), 81-83 (1968).

R, P, Ex 318. Toporets, A. S., Specular reflection of polarized light from rough surfaces, Soviet J. Opt. Technology **35** (4), 419-422 (1968).

R, Ex 319. Toporets, A. S., Specular reflection of light from a rough surface, Opt. Spectrosc. **24** (1), 62-64 (Jan. 1968).

R, Th, Ex 320. Torrance, K. E., Off-specular peaks and angular

distribution of reflected thermal radiation, Ph. D. dissertation, University of Minnesota, Minneapolis, Minn., March 1966.

R, P, Th 321. Torrance, K. E., Theoretical polarization of off-specular reflection peaks, J. Heat Transf., Trans. ASME **C91** (2), 287–290 (1969).

R, Ex 322. Torrance, K. E. and Sparrow, E. M., Discussion of Effects of roughness of metal surfaces on angular distribution of monochromatic radiation, J. Heat Trans. ASME **C87,** 93 (1965).

R, Ex 323. Torrance, K. E., and Sparrow, E. M., Biangular reflectance of an electric nonconductor as a function of wavelength and surface roughness, J. Heat Transf., Trans. ASME **C87,** 283–291 (1965).

R, Ex 324. Torrance, K. E. and Sparrow, E. M., Off-specular peaks in the directional distribution of reflected thermal radiation, J. Heat Transf. Trans. ASME **C88,** 223–230 (1966).

R, P, Ex 325. Torrance, K. E., Sparrow, E. M., and Birkebak, R. C., Polarization, directional distribution, and off-specular peak phenomena in light reflected from roughened surfaces, J. Opt. Soc. Am. **56** (7), 916–925 (1966).

R, Th 326. Torrance, K. E. and Sparrow, E. M., Theory for off-specular reflection from roughened surfaces, J. Opt. Soc. Am. **57** (9), 1105–1114 (1967).

H, Th 327. Treat, C. H., Directional effects in radiant heat transfer between pairs of simply arranged surfaces, Ph. D. Dessertation, Univ. of New Mexico, Albuquerque, N. Mex., 1–154 (Jan. 1968).

R, Th 328. Treat, C. H. and Wildin, M. W., Investigation of a model for bidirectional reflectance of rough surfaces, AIAA Paper No. 69–64, AIAA 7th Aerospace Sciences Meeting, New York City, N.Y., Jan. 20–22, 1969.

R, Ex 329. Trotter, A. P., Diffused reflection and transmission of light, Illuminating Engineer **12,** 243–267 (Sept. 1919).

R, Th 330. Trowbridge, T. S. and Reitz, K. P., New ray optics model for the directional distribution of light reflected from a rough surface, Naval Missile Center, Point Mugu, Calif. (1973). Unpublished report.

SM 331. Trumpold, H., Limits of application of the interference methods for surface measurements, pp. 241–254, Proceedings PMS * 1967–68.

R, Th 332. Twersky, V., On the nonspecular reflection of electromagnetic waves, J. Appl. Phys. **22** (6), 825–835 (Jan. 1951).

S, Th 333. Twersky, V., Multiple scattering of radiation by an arbitrary planar configuation of parallel cylinders and by two parallel cylinders, J. Appl. Phys. **23** (4), 407–414 (1952).

R, S, Th 334. Twersky, V., Reflection coefficients for certain rough surfaces, J. Appl. Phys. **24** (5), 659–660 (1953).

S, Th 335. Twersky, V., Scattering theorems for bounded periodic structures, J. Appl. Phys. **57** (10), 1118–1122 (Oct. 1956).

S, Th 336. Twersky, V., On the scattering of waves by an infinite grating, IRE Trans. on Antennas and Propagation **AP-4** (3), 330–345 (July 1956).

R, S, Th 337. Twersky, V., On scattering and reflection of electromagnetic waves by rough surfaces, IRE Trans. on Antennas and Propagation **AP-5** (1), 81–90 (Jan. 1957).

S, Th 338. Twersky, V., Scattering by quasiperiodic and quasirandom distributions, IRE Trans. on Antennas and Propagation **AP-7** (Special Supplement) 307–319 (Dec. 1959).

S, Th 339. Twersky, V., Multiple scattering of waves and optical phenomena, J. Opt. Soc. Am. **52** (2), 145–171 (Feb. 1962).

S, Th 340. Twersky, V., On scattering of waves by the infinite grating of circular cylinders, IRE Trans. on Antennas and Propagation **AP-10** (6), 737–765 (Nov. 1962).

Su 341. Ulrich, J., Unusual reconnaissance concepts Vol. **III:** A bibliography of recent contributions on electromagnetic and acoustic scattering, Tech. Rept. AFAL-TR-65-331, Vol. **III,** Willow Run Lab., Institute of Science and Technology, University of Michigan, Ann Arbor, Mich. (Jan. 1966).

R, Th 342. Valenzuela, G. R., The effective reflection coefficients in forward scatter from a dielectric slightly rough surface, Proc. IEEE (U.S.) **58** (8), 1279 (1970).

S, Th 343. Venable, W. H., Jr., Effects upon radiant intensity measurements due to scattering by optical elements, Appl. Opt. **9** (3), 609–615 (Mar. 1970).

R, Th 344. Vincent, R. K., and Hunt, G. R., Infrared reflectance from mat surfaces, Appl. Opt. **7** (1), 53–59 (Jan. 1968).

H, Th, Ex 345. Viskanta, R., Schornhorst, J. R., and Toor, J. S., Analysis and experiment of radiant heat exchange between simply arranged surfaces, Tech. Note May 65–June 67, 1–131, Purdue Univ. Lafayette Indiana, School of Mechanical Engineering (June 1967). AD-655 335.

R, Ex 346. Voishvillo, N. A., Reflection of light by a rough glass surface at large angles of incidence of the illuminating beam, Opt. Spectrosc. **22** (6), 517–520 (June 1967).

SM 347. Von Weingraber, H., Optical methods for surface finish evaluation, International Research in Production Engineering, pp. 659–666 (1963). Published by ASME.

R, S, Th 348. Wagner, R., Shadowing of randomly rough surfaces, J. Acoust. Soc. Am. **41** (1), 138–147 (1967).

S, Th 349. Wait, J. R., Reflection at arbitrary incidence from a parallel wire grid, Appl. Sci. Res. **B4,** 393–400 (1954–55).

S, Th 350. Wait, J. R., On the theory of reflection from a wire grid parallel to an interface between homogeneous media (I), Appl. Sci. Res. **B6,** 259–275 (1957).

S, Th 351. Wait, J. R., On the theory of reflection from a wire grid parallel to an interface between homo-

geneous media (II), Appl. Sci. Res. **B7**, 355–360 (1958–59).

R, Th — 352. Wait, J. R., Guiding of electromagnetic waves by uniformly rough surfaces Part I & II, IRE Trans. on Antennas and Propagation **AP–7** (Special Supplement), 154–168 (Dec. 1959).

S, Th — 353. Wait, J. R., Pertubation analysis for reflection from two-dimensional periodic sea-waves, Radio Sci. **6** (3), 387–391 (1971).

R(Ex) — 354. Walter, F. E. and Wiebelt, J. A., An investigation of bi-directional reflectance from randomly rough engineering surfaces, AIAA Paper No. 72–308, 1–9, AIAA 7th Thermophysics Conference, San Antonio, Tex., Apr. 10–12, 1972.

S, Th, Ex — 355. Waterman, P. C., Matrix formulation of bistatic electromagnetic scattering, Rept. No. MTR–543, ESD–TR–67–629, 1–26, Mitre Corp. Bedford, Mass. (May 1968). AD–669 093.

S, Th — 356. Waterman, P. C. and McCarthy, C. V., Numerical solution of electromagnetic scattering problems, Rept. No. MTP–74, 1–132, Mitre Corp. Bedford, Mass. (June 1968). AD–685 715.

R, Ex — 357. Weaver, J. H., Recent advances in optical properties of oxide and intermetallic coatings, AFML–TR–65–29, 220–235 (1965).

S, Th — 358. Weston, V. H., Boerner, W. M., and Hodgins, D. R., Inverse scattering investigation, Quarterly Rept. No. ESD–TR–67–517, Dept. of Electrical Engineering, Radiation Lab., Univ. of Michigan, 1968.

SM — 359. White, E. W., McKinstry, H. A., and Diness, A., Quantitative surface finish characterization by CESEMI, Preprint of paper presented at the Symposium on the Science of Ceramic Machining and Surface Finishing, Nov. 2–4, 1970. Held at the National Bureau of Standards, Gaithersburg, Md.

SM — 360. White, E. W., McKinstry, H. A. and Diness, A., Quantitative surface finish characterization by CESEMI, Tech. Rept. No. 4, Office of Naval Research, Metallyrgy Program; Material Research Lab. The Pennsylvania State University, University Park, Pa. (1971). AD–719 925.

SM — 361. Whitehouse, D. J., and Reason, R. E., The equation of the mean line of surface texture found by an electric wave filter, Rank Taylor Hobson, Leicester, Great Britain (1965).

SM — 362. Whitehouse, D. J., Improved type of wavefilter for use in surface-finish measurement, pp. 306–318, PMS* Proceedings, 1967–68.

SM — 363. Whitehouse, D. J., Discussion, pp. 498–502, PMS* Proceedings, 1967–68.

SM — 364. Williamson, J. B. P., Microtopography of surfaces, pp. 21–30, PMS* Proceedings, 1967–68.

SM — 365. Wolff, H., Surface testing using the Hommel tester type T, pp. 279–298, PMS* Proceedings, 1967–68.

S, Th — 366. Yen, J. L., Multiple scattering and wave propagation in periodic structures, IRE Trans. on Antennas and Propagation **AP–10** (6), 769–775 (Nov. 1962).

R, Th — 367. Zaki, K. A., and Neureuther, A. R., Scattering from a perfectly conducting surface with a sinusoidal height profile: TE polarization, IEEE Trans. on Antennas and Propagation **AP–19** (2), 208–214 (1971).

R, Th — 368. Zhitomirskii, I. S., Chebanova, R. S., Shakhnovich, M. I., Effect of self-shadowing on the coefficient of reflection from the cleaved surfaces of a monocrystal, Opt. Spectrosc. **19** (3), 229–232 (Sept. 1965).

Em, Th — 369. Zhulev, Yu. G., Radiative power of a toothed surface, (Translated from) Teplofizika Vysokikh Temperatur **3** (2), 321–323 (Mar.–Apr. 1965).

R, Th, Ex — 370. Zipin, R. B., The apparent thermal radiation properties of an isothermal V-groove with specularly reflecting walls, J. Res. Nat. Bur. Stand. (U.S.), **70C** (Eng. & Instr.), No. 4, 275–280 (Oct–Dec. 1966).

R, Th, Ex — 371. Zipin, R. B., A preliminary investigation of the bidirectional spectral reflectance of V-grooved surfaces, Appl. Opt. **5** (12), 1954–1957 (1966).

*Properties and Metrology of Surface—Proceedings 1967–68, Vol. **82**, part 3k, Presented at International Conference organized by the Institution of Mechanical Engineers at Oxford, 1st to 4th April 1968.

(Paper 80A2–888)

JOURNAL OF RESEARCH of the National Bureau of Standards—A. Physics and Chemistry
Vol. 80A, No. 2, March–April 1976

Energy Levels, Classified Lines, and Zeeman Effect of Neutral Thorium

Romuald Zalubas

Institute for Basic Standards, National Bureau of Standards, Washington, D.C. 20234

(December 3, 1975)

A list of about 9500 classified lines of Th I in the range 2345–29 662 Å is given. Lines in the range 2345–9239 A were observed and measured at NBS. Zeeman effect data for 2281 lines are listed. Lists of 254 even and 322 odd levels including their g values are presented. Among them there are 72 new levels, which were not contained in earlier publications.

Key words: Energy levels; thorium; Th I; wavelengths; Zeeman-effect of Th I

1. Introduction

A review of early research on the spectra of neutral and singly ionized thorium has been given by Zalubas [1960].[1] In the meantime light sources and spectrographs have been improved and more standard wavelengths of thorium have become available. Their development is described by Giacchetti, Stanley, and Zalubas [1970]. Therefore, at NBS I undertook a new observation and description of Th I and Th II in order to expand the analyses of these spectra. A complete line list of about 35 000 Th I and Th II lines will be published separately. That list will include all available thorium standards and will be useful for users of thorium standards. Zalubas and Corliss have published a list of classified lines in Th II [1974].

In the present paper I will review only the work on finding the energy levels and g factors of Th I.

2. Wavelengths and Classified Lines

New observations were taken on the NBS 10.7 meter Eagle spectrograph in the range 2000–12 000 Å. Electrodeless lamps and sliding sparks were used as light sources for the separation of Th I and Th II. Professor S. P. Davis supplied some spectrograms for range 2600–4500 Å produced on the Czerny-Turner spectrograph at the University of California. I measured wavelengths in the 2800–12 000 Å observation range. Stronger lines were measured on 3 to 6 plates, weaker lines (below intensity 5) on 2 to 3 plates. Small numbers of lines of intensity 1 are included which were measured only once. The wavelengths in the range 2000–2800 Å were measured only once. Internal thorium standards from Giachetti [1966], and Giacchetti, Stanley, and Zalubas [1970] were used.

All classified lines fit the energy level scheme to within ± 0.05 cm^{-1}. More than 60 percent of them do not exceed ± 0.02 cm^{-1}.

The consistency of wavelengths in this list can be demonstrated by the following test. The average absolute value of the difference between observed and calculated wavelengths expressed in cm^{-1} was 0.008 for 50 lines around each of the wavelengths 3000, 4000, 5000, 6000, and 8000 Å.

At the Laboratoire Aimé Cotton, Orsay, France wavelengths of Th I and Th II lines in the range 9239–29 662 Å were recorded by means of Fourier transform spectroscopy. The list of 3100 lines, including classified lines of Th I and Th II, was published by Giacchetti, Blaise, Corliss, and Zalubas [1974]. The average deviation between the observed and calculated wavenumbers from this list is less than 0.002 cm^{-1}.

These two lists combined together have around 35 000 lines and excel earlier observations in accuracy and extent. In order to have all classified lines of Th I at hand, the 1900 Th I lines measured by Fourier transform spectroscopy are taken from Giacchetti et al. [1974] and incorporated in table 4.

Table 4 contains about 9500 classified lines in the wavelength range 2345–29 662 Å. For the wavelength range 2345–9239 Å visually estimated relative intensities on an arbitrary scale from 1 to 5000 are given for electrodeless lamp and sliding spark. For the wavelength range 9239–29 662 Å only the electrodeless lamp intensity on a scale 0 to 9 is given. The letter symbols are used to describe the character of lines;

[1] Dates enclosed in brackets indicate literature references at the end of this paper.

b—blend (two wavelengths measured), d—double (one wavelength measured), h—hazy, l—shaded to longer wavelength, r—reversed, s—shaded to shorter wavelength, and w—wide. In column 4 the wavenumber is given in vacuum in units of cm^{-1}. In the fifth and sixth columns the classification of a line is given by rounded-off values of the energy levels responsible for the transition, with their J-values as subscripts and a superscript degree symbol to indicate odd parity.

3. Zeeman Effect and g-Factors

B. E. Moore [1909] observed the splittings of thorium lines in the magnetic field in the range 3002–4721 Å. He observed mostly Th II lines and at that time of course did not derive J and g values.

Lier [1939] observed the Zeeman effect of 40 lines of Th I in the range 3427–6182 Å. Fifteen of these lines had resolved ZE patterns. These data were used by Schuurmans [1946], who derived g factors for all levels he found. Charles [1958] furnished ZE data for 46 lines in the range 3041–6457 Å.

In the final list I used g factors derived from my observations. I have measured ca. 2281 Zeeman patterns in a magnetic field of 2.4 teslas, produced by the electromagnet at Argonne National Laboratory. From completely resolved patterns I derived J values and g values, and from partly resolved patterns I obtained Δg, or p, or n, or a combination of these. Δg is the difference between two g values for that line. The distance from the no-field position to the most distant p component (parallel polarization) is denoted by p, and n is the distance from no-field position to the strongest n component (normal polarization). All these measurements are given in Lorentz units. The type of Zeeman pattern is described by the following numbers: 1 indicates that the n pattern shades out, 2 indicates that the n pattern shades in, 3 indicates that the n pattern is symmetrical, $J_1 = J_2$, and the p pattern shades in, and 7 indicates that the pattern is either triplet or unresolved. The values of g derived from my measurements or measured Δg, p, and n are given in table 3.

Values of g factors for the energy levels are derived from various numbers of patterns, from 60 for one level to only one for some levels. Therefore, the g-values are given with three, two, or one decimal digits. The estimated error is not greater than 2 in the last digit.

4. Energy Levels

In previous papers on Th I [Zalubas, 1959, 1968] I gave an account of the earlier analyses of Th I. Here I will give just the total number of levels contributed by those early investigators that have proved to be real. Schuurmans [1946] found 29 energy levels and properly identified the five lowest levels. Stukenbroeker and McNally [1953] contributed 7 levels. Charles [1958] found 2 levels. Steers [1967], using his far infrared observations, found 13 levels. Giacchetti and Blaise [1970] found 10 levels. The remaining levels were found by the present author. Now the total number of known even levels is 254, and 322 odd levels. There are 72 levels given here for the first time.

Th I has two very distinct systems of levels, which I have connected. One system starts with the ground state $6d^27s^2\ ^3F_2$. The other starts 7795 cm^{-1} above ground state with the $5f6d7s^2\ ^3H^\circ_4$ level.

For energy level searches I treated the two systems separately. In such searches, I used a set of programs called COMBO, written by J. Tech for the analysis of spectra. The numbers of combinations and the available ZE data were the critical factors in establishing new energy levels. I have not included levels which can be found by intercombinations between high odd levels, and high even levels, despite the fact that some chains are long. Some of them may be confirmed later by theoretical calculations and extension of the analysis. Even levels are given in table 1 and odd levels in table 2.

The uncertainty of the level values for levels below 15 000 is 0.001 cm^{-1}, and the uncertainties of most of the high levels do not exceed 0.005 cm^{-1}. Levels given with two decimal places have uncertainties of 0.01 to 0.02 cm^{-1}.

I have identified the lowest levels by using g values, and by comparison of the levels with calculations for the $6d^27s^2$ and $6d^37s$ configurations by Trees [1960]. For the low odd levels I made preliminary identifications using Martin's [1963] Ce I identifications, and also Klinkenberg's [1950] Th III identifications. Later I used Sugar's [1968] preliminary calculations for the $5f6d7s^2$ and $5f6d^27s$ configurations. Giacchetti and Blaise [1970] identified the ^5F, ^5G, ^5H, ^5I terms of the $5f5d7s7p$ configuration. In addition, Brewer [1971] identified 14 465 as $^5G^\circ_2$ of $6d^27s7p$, and 18 431 as $^3F_3$ of $5f7s^27p$. No attempt has been made to identify the terms or configurations of the high energy levels.

5. Ionization Energy

Ionov and Mittsev [1961] derived the ionization energy of Th I as 6.95 ± 0.06 eV, and Smith and Hertel [1969] as 7.5 ± 0.3 eV by the surface ionization method. Avni and Klein [1973] got 7.4 ± 0.3 eV for the ionization energy from measurements in a d.c. arc plasma, using the Saha equations. Meggers, Corliss, and Scribner [1961] estimated this energy to be about 50 000 cm^{-1}. Rauh and Ackermann [1973] obtained an ionization potential of 6.0 ± 0.1 eV from an ionization efficiency curve and from the appearance potential by electron impact. The best value of 49 000 ± 1000 cm^{-1} (6.08 ± 0.12 eV) was obtained by Sugar [1973] utilizing interpolated spectral properties of actinide atoms.

TABLE 1. *Even energy levels of* Th I

Configuration	Term	J	Level (cm^{-1})	g	Configuration	Term	J	Level (cm^{-1})	g
$6d^2\ 7s^2$	^3F	2	0.000	0.736			2	24671.898	1.118
$6d^2\ 7s^2$	^3P	0	2558.058		$5f\ 6d7s7p$	^5F	3	24915.019	1.183
$6d^2\ 7s^2$	^3F	3	2869.260	1.084	$5f\ 6d7s7p$	^5H	4	25405.160	0.918
$6d^2\ 7s^2$	^3P	2	3687.988	1.254			2	25890.390	1.113
$6d^2\ 7s^2$	^3P	1	3865.476	1.478			4	25923.018	0.96
$6d^2\ 7s^2$	^3F	4	4961.660	1.212			1	26111.536	0.374
$6d^3(^4F)7s$	^5F	1	5563.143	0.065			4	26255.580	1.032
$6d^3(^4F)7s$	^5F	2	6362.397	1.011			5	26380.537	1.049
$6d^2\ 7s^2$	^1D	2	7280.125	1.188			3	26796.070	0.814
$6d^3(^4F)7s$	^5F	3	7502.290	1.250			4	26971.459	1.036
$6d^2\ 7s^2$	^1G	4	8111.005	1.067	$5f\ 6d7s7p$	^5I	6	26997.242	1.11
$6d^3(^4F)7s$	^5F	4	8800.251	1.310			3	27044.218	1.17
$6d^3(^4F)7s$	^5F	5	9804.808	1.366	$5f\ 6d7s7p$	^5G	5	27191.358	1.116
$6d^3(^4P)7s$	^5P	1	11601.032	2.398			3	27343.737	0.690
$6d^3(^4P)7s$	^5P	2	11802.934	1.713			4	27495.586	0.998
$6d^3(^2G)7s$	^3G	3	12847.971	1.388			4	27521.523	0.925
$6d^3(^4P)7s$	^5P	3	13088.564	1.050			2	27566.853	0.811
$6d^3(^2G)7s$	^3G	4	13297.436	0.992			5	27591.803	1.10
$6d^3(^4F)7s$	^3F	2	13847.774	0.932			3	27612.267	0.928
$6d^3(^2D2)7s$	^3D	1	13962.523	0.753			3	27980.683	1.030
$6d^3(^2G)7s$	^3G	5	14204.268	1.144			5	28034.004	1.074
$6d^3(^2P)7s$	^3P	0	14226.823				4	28227.932	1.128
$6d^3(^2H)7s$	^3H	4	15493.222	0.914			2	28273.215	0.848
$6d^3(^2D2)7s$	^3D	2	15863.892	1.05			5	28342.498	1.101
$6d^3(^4F)7s$	^3F	3	15970.099	1.200			3	28358.393	1.190
$6d^2\ 7s^2$	^1S	0	16351.942				2	28531.046	0.910
$6d^3(^2H)7s$	^3H	6	16554.245	1.17			4	28562.659	1.033
$6d^3(^4P)7s$	^3P	1	17073.814	1.28			2	28679.257	0.97
$6d^3(^2H)7s$	^3H	5	17166.108	1.11			4	28845.562	0.98
$6d^3(^2D2)7s$	^3D	3	17398.399	1.19			2	28882.455	0.860
$6d^3(^4F)7s$	^3F	4	17959.898	1.17			3	28934.903	1.031
$5f\ 6s^2\ 7p$	^3G	3	18431.685				4	29104.006	0.996
$6d^3(^2P)7s$	^3P	2	18549.409	1.2			5	29141.525	1.07
$6d^3(^2P)7s$	^3P	1	18574.613	1.37			2	29418.388	1.042
		2	18699.627				1	29422.086	1.104
$6d^3(^4P)7s$	^3P	2	19273.284	1.180			6	29552.52	1.18
$6d^3(^2F)7s$	^3F	4	19532.421	1.20			2	29650.955	0.84
$6d^3(^2F)7s$	^3F	3	19713.035	1.1			5	29684.194	1.175
$6d^3(^2F)7s$	^3F	2	20054.776	0.88			4	29756.400	1.090
$6d^3(^2H)7s$	^1H	5	21143.425	1.03			3	29835.046	1.065
		2	21575.040	1.19			4	29849.160	1.03
		3	21594.676	1.035			1	29961.798	1.339
$5f\ 6d7s7p$	^5I	4	22098.187	0.742			3	30011.343	1.070
		1	22401.215	1.180			4	30014.330	
		3	22637.461	1.128			2	30132.640	0.75
		4	23032.983	1.084			1	30286.898	0.624
$5f\ 6d7s7p$	^5G	2	22988.523	0.625			6	30372.711	1.15
$5f\ 6d7s7p$	^5G	3	23201.985	0.946			5	30508.001	1.11
$5f\ 6d7s7p$	^5I	5	23277.380	1.006			2	30544.560	0.970
$5f\ 6d7s7p$	^5F	1	23769.872	0.468			4	30552.501	1.19
$5f\ 6d7s7p$	^5F	2	23990.407	0.875			3	30651.163	1.057
$5f\ 6d7s7p$	^5G	4	24032.222	1.091	$5f\ 6d7s7p$	^5I	7	30726.784	
$5f\ 6d7s7p$	^5H	3	24399.112	0.832			2	30758.008	0.984
		1	24627.874	0.504			1	30889.931	0.734
		3	24664.727	0.895			6	30930.435	1.2

201-606 O - 76 - 6

TABLE 1. *Even energy levels of* Th I—continued

Configuration	Term	J	Level (cm^{-1})	g	Configuration	Term	J	Level (cm^{-1})	g
		3	30964.652	1.15			5	35216.987	1.177
		1	31095.84	1.327			5	35300.91	0.87
		3	31141.795	1.096			3	35405.303	1.067
		2	31245.890	1.336			1	35421.028	1.164
		3	31265.632	1.075			3	35440.891	1.07
		5	31271.000	1.084			3	35576.514	1.192
		4	31326.971	1.15			5	35582.288	1.15
		1	31429.253	1.294			4	35633.866	1.120
		3	31537.237	0.900			4	35794.375	1.144
		5	31626.821	1.111			6	35799.978	1.075
		3	31774.590	1.05			3	35831.292	1.190
		4	31793.697	1.090			2	35877.81	1.412
		3	31929.499	1.14			2	36047.30	0.83
		4	31995.652	0.92			4	36089.691	1.09
		4	32012.954	1.2			5	36133.494	1.041
		2	32041.231	1.08			5	36210.789	1.0
		5	32201.997	1.052			4	36297.296	1.128
		5	32293.919	1.186			3	36336.196	1.10
		4	32458.177	1.132			2	36485.388	1.275
		3	32551.611	1.25			3	36515.98	0.834
		5	32737.014	1.136			2	36653.567	1.203
		4	32781.597	1.083			6	36748.997	1.13
		3	32796.121	1.156			3	36775.361	0.97
		5	32963.392	1.20			5	36781.317	1.118
		6	33068.085	1.07			3	36808.30	1.094
		3	33099.412	1.337			2	36818.110	0.95
		5	33214.534	1.028			4	36885.289	1.048
		1	33273.846	1.380			4	37085.86	1.20
		2	33309.040	1.002			2	37094.849	1.155
		1	33390.746	0.704			3	37131.059	0.88
		3	33408.661	1.113			5	37211.68	1.03
		4	33418.121	1.121			4	37303.438	1.02
		4	33459.180	0.95			3	37307.14	0.995
		4	33527.562	1.15			6	37332.502	1.00
		3	33564.851	1.1			3	37404.631	1.3
		2	33606.291	1.417			3	37521.509	1.127
		2	33689.043	1.0			3	37688.21	1.238
		2	33721.308	1.159			6	37742.28	1.1
		1	33773.617	1.410			2	37748.043	0.99
		4	33831.881	1.15			2	37784.402	1.02
		3	34167.473	1.041			4	37819.119	1.04
		1	34298.062	0.931			5	37890.46	0.97
		4	34301.432	0.905			4	37892.823	0.86
		6	34407.566	1.19			4	37992.254	1.01
		3	34431.335	1.047			2	38097.10	
		2	34444.594	1.102			5	38106.740	1.16
		4	34447.172	1.11			3	38145.74	1.07
		5	34460.873	1.175			4	38186.12	0.95
		3	34707.730	1.165			4	38366.571	1.042
		5	34849.054	1.111			3	38382.14	1.0
		4	34873.350	1.11			3	38529.930	1.0
		3	34874.059	1.095			2	38602.98	1.1
		1	35046.030	0.4			4	38700.25	1.2
		3	35089.394	1.184			3	38734.401	1.10
		2	35149.75	1.09			4	38760.633	1.05

TABLE 1. *Even energy levels of* Th I – continued

Configuration	Term	J	Level (cm^{-1})	g	Configuration	Term	J	Level (cm^{-1})	g
		2	38807.67	1.02					
		5	38953.228	1.1					
		4	38956.877	1.05					
		3	39010.164						
		3	39174.919	1.03					
		5	39252.291	1.05					
		4	39283.816	1.02					
		3	39321.807	1.01					
		5	39351.78	1.07					
		4	39520.19	1.0					
		2	39680.452	0.99					
		5	39694.33	1.006					
		3	39837.63	0.95					
		4	40052.463	0.94					
		3	40200.428	1.02					
		4	40426.73	1.01					
		3	40493.279	1.08					
		5	40582.766						
		2	40611.670	1.0					
		4	40701.33	1.07					
		2	40886.99	1.2					
		4	41230.973	1.05					
		5	41356.165	1.0					
		3	41361.409	0.91					
		2	41578.403	0.86					
		3	41686.69	1.1					
		5	41712.85	1.10					
		4	41755.863	1.09					
		2	42027.37	1.019					
		3	42286.444	0.95					
		5	42635.880						
		5	43857.368	1.05					
		6	43937.23	1.16					
		6	44437.81	1.12					

TABLE 2. *Odd energy levels of* Th I

Configuration	Term	J	Level (cm^{-1})	g	Configuration	Term	J	Level (cm^{-1})	g
$5f\,6d7s^2$	$^3H°$	4	7795.270	0.863			3	21165.099	1.306
$5f\,6d7s^2$	$^3F°$	2	8243.597	0.778			2	21252.603	0.668
$5f\,6d7s^2$	$^1G°$	4	10414.133	0.986			4	21539.593	1.154
$5f\,6d7s^2$	$^3G°$	3	10526.540	0.869			1	21668.958	1.585
$6d7s^2\ 7p$	$^3F°$	2	10783.153	0.732	$6d^3\ 7p$	$^5G°$	2	21738.052	0.529
$5f\,6d7s^2$	$^3H°$	5	11197.027	1.034			3	21890.134	0.942
$5f\,6d7s^2$	$^3F°$	3	11241.728	1.004			4	21902.272	0.984
$5f\,6d7s^2$	$^3D°$	1	11877.836	0.726			3	22141.606	1.095
$5f\,6d7s^2$	$^1D°$	2	12114.365	0.970			4	22163.133	0.992
$5f\,6d7s^2$	$^3G°$	4	13175.113	1.084			2	22248.950	1.141
$6d7s^2\ 7p$	$^3F°$	3	13945.308	1.116			3	22338.996	1.017
$5f\,6d7s^2$	$^3D°$	2	14032.084	1.125			1	22396.827	1.527
$5f\,6d7s^2$	$^3F°$	4	14206.916	1.167			5	22399.400	0.935
$5f\,6d7s^2$	$^3P°$	1	14243.992	1.200			2	22508.048	1.384
$5f\,6d7s^2$	$^3P°$	0	14247.307				3	22669.890	1.233
$6d^2\ 7s7p$	$^5G°$	2	14465.220	0.810			3	22855.301	1.133
$5f\,6d7s^2$	$^3H°$	6	14481.873	1.170			1	22877.519	0.615
$5f\,6d7s^2$	$^3D°$	3	15166.899	1.064			5	22877.583	1.198
$5f\,6d7s^2$	$^3G°$	5	15490.075	1.19			5	23015.155	1.08
$5f\,6d^2\ 7s$	$^5H°$	3	15618.985	0.600			1	23049.461	1.363
$6d^2\ 7s7p$	$^5F°$	1	15736.968	0.388			2	23093.984	1.321
$6d^2\ 7s7p$	$^5F°$	2	16217.482	1.070			4	23113.549	1.040
$5f\,6d^2\ 7s$	$^5H°$	4	16346.648	0.880			6	23306.831	1.1
$5f\,6d^2\ 7s$	$^5I°$	4	16783.847	0.712			0	23410.201	
$5f\,6d7s^2$	$^3P°$	2	17224.302	1.040			1	23481.375	0.843
$6d^2\ 7s7p$	$^3D°$	1	17354.638	0.507			3	23521.050	1.078
$6d^2\ 7s7p$	$^5F°$	3	17411.223	1.134			2	23603.522	1.379
$5f\,6d^2\ 7s$	$^5H°$	5	17501.174	1.004			5	23609.172	0.99
$6d^2\ 7s7p$	$^3D°$	2	17847.078	1.162			4	23655.141	1.2
$5f\,6d^2\ 7s$	$^5I°$	5	18011.379	0.996			1	23741.076	0.769
$6d7s^2\ 7p$	$^3F°$	4	18053.617	1.2			2	23752.688	1.112
$6d^2\ 7s7p$	$^3D°$	3	18069.066	1.136			4	23916.899	1.25
$6d^2\ 7s7p$	$^3P°$	0	18382.825				6	24084.943	1.211
$6d^2\ 7s7p$	$^3P°$	1	18614.338	1.380			2	24182.432	1.252
$6d^2\ 7s7p$	$^5F°$	4	18809.886	1.15			4	24202.565	1.376
		3	18930.293	0.970			4	24259.777	1.044
		2	19039.154	1.090			5	24274.716	
$5f\,6d^2\ 7s$	$^5H°$	6	19227.334	1.08			2	24307.749	1.518
		3	19503.144	1.086			2	24381.336	1.253
$6d^2\ 7s7p$	$^3P°$	2	19516.981	1.361			3	24421.060	1.16
$5f\,5d7s^2$	$^1H°$	5	19588.362	1.16			3	24561.653	1.177
		1	19817.182	1.572			5	24701.047	1.150
		4	19948.396	1.281			3	24769.718	1.141
$5f\,6d^2\ 7s$	$^5I°$	6	19986.166	1.2			1	24838.924	0.770
		3	20214.931	1.182			6	24850.30	
		5	20322.267	1.06			1	24880.220	0.78
		1	20423.495	1.433			3	24981.111	1.075
		2	20522.715	0.815			2	25306.763	1.166
		0	20543.845				3	25321.922	1.386
		4	20566.625	1.233			4	25355.576	0.98
		0	20724.396				3	25442.686	1.091
		1	20737.288	1.363			1	25526.314	1.066
$5f\,6d^2\ 7s$	$^5I°$	7	20867.975	1.2			4	25575.046	1.05
		2	20922.123	1.170			5	25690.475	1.209
$6d^2\ 7s7p$	$^5F°$	5	21077.152	1.252			2	25703.403	1.177

TABLE 2. *Odd energy levels of* Th I – continued

Configuration	Term	J	Level (cm^{-1})	g	Configuration	Term	J	Level (cm^{-1})	g
		5	25753.940	1.15			3	29744.522	1.148
		1	25809.306	1.568			2	29853.148	0.910
		4	25877.502	1.041			4	29881.457	1.165
		3	26036.352	0.954			3	30017.100	1.129
		4	26048.543	1.116			4	30160.006	1.11
		3	26096.986	1.001			2	30208.582	1.095
		2	26113.270	0.979			3	30255.452	1.082
		1	26287.049	0.710			1	30281.011	1.471
		2	26363.104	1.036			5	30517.108	1.18
		4	26384.927	1.060			4	30517.390	1.455
		3	26508.031	1.074			2	30553.291	1.042
		5	26645.412	1.1			0	30613.62	
		2	26651.831	1.102			1	30723.82	1.06
		4	26790.430	1.139			3	30761.719	1.192
		3	26878.162	0.903			5	30788.179	1.19
		0	26882.511				2	30812.991	0.929
		3	26995.777	1.166			1	30928.742	0.976
		2	27061.417	0.987			3	30990.520	1.097
		1	27087.981	1.162			4	31019.110	1.19
		3	27260.171	1.105			2	31075.91	1.326
		4	27266.028	1.150			5	31141.255	0.947
		1	27297.579	0.6			4	31194.703	0.730
		3	27317.393	1.087			3	31283.117	1.11
		2	27447.746	1.07			3	31523.937	1.108
		3	27670.964	1.219			2	31599.274	1.216
		2	27674.327	1.090			4	31671.155	1.18
		2	27784.368	0.860			1	31712.73	1.175
		5	27852.743	1.259			5	31716.592	1.14
		4	27948.610	1.263			3	31780.865	1.175
		1	28024.691	1.030			2	31870.097	0.944
		4	28140.870	1.222			4	31953.464	1.073
		2	28347.551	1.543			5	32023.60	1.16
		1	28372.707	1.805			1	32080.416	0.795
		4	28480.159	1.02			2	32160.486	1.080
		2	28513.300	1.100			3	32197.119	1.138
		3	28589.314	1.179			3	32285.180	1.12
		1	28649.145	1.091			4	32294.089	1.16
		2	28673.429	1.130			4	32439.049	1.141
		3	28676.243	1.093			2	32503.62	1.200
		4	28680.738	1.192			2	32575.427	0.716
		3	28884.958	1.180			1	32650.907	1.14
		2	28917.957	0.945			1	32665.561	0.82
		4	28932.654	1.111			3	32754.504	1.12
		5	29050.740	1.12			4	32862.480	1.16
		1	29157.095	0.876			2	32954.59	1.114
		3	29157.879	1.210			3	33043.332	1.134
		1	29197.326	1.141			1	33161.77	1.332
		2	29197.906	1.38			4	33270.547	1.170
		2	29252.790	0.978			3	33294.928	1.10
		4	29310.020				2	33297.133	1.26
		2	29419.232	1.680			2	33427.039	0.80
		1	29640.260	0.952			4	33560.06	1.18
		3	29686.370	1.260			3	33591.166	1.010
		5	29711.622	1.2			1	33662.23	1.018
		5	29733.325	1.18			2	33718.42	1.064

TABLE 2. *Odd energy levels of* Th I – continued

Configuration	Term	J	Level (cm^{-1})	g	Configuration	Term	J	Level (cm^{-1})	g
		2	33734.706	1.302			3	37159.544	1.00
		4	33799.730	1.15			2	37234.01	1.10
		3	33800.621	1.10			5	37571.34	1.044
		5	33844.960	1.118			4	37605.73	1.13
		3	33967.906	0.794			1	37616.308	
		4	34001.333	1.078			3	37656.975	1.134
		1	34111.17	0.850			2	37736.977	
		5	34182.708	1.09			4	37950.044	1.13
		2	34324.08	1.131			3	37954.97	1.1
		4	34344.650	1.114			2	37970.270	
		2	34371.840	1.282			3	38053.028	1.08
		3	34430.22	1.213			2	38088.99	0.9
		4	34492.022	0.898			3	38216.95	1.13
		3	34583.008	1.172			1	38278.878	0.866
		1	34591.01	1.496			4	38306.376	1.05
		3	34704.406	1.103			2	38355.312	
		3	34725.43	1.090			5	38385.213	0.98
		2	34851.666	0.866			3	38416.222	1.18
		1	34878.665	1.478			4	38580.297	1.06
		5	34886.676	1.07			5	38665.559	1.078
		1	34989.778	1.619			2	38669.77	1.027
		5	35081.021	1.100			3	38675.356	0.94
		4	35131.22	1.212			3	38788.85	0.98
		3	35240.821	1.077			2	38814.252	0.77
		5	35273.877	1.16			1	38840.559	1.2
		1	35328.63	1.272			3	38998.975	1.314
		4	35351.439	1.19			5	39062.033	
		3	35462.05	1.250			3	39264.69	1.06
		2	35533.292	1.219			4	39311.261	1.10
		1	35678.85	1.02			1	39411.899	
		4	35733.465	1.1			3	39468.675	
		3	35812.518	1.10			4	39562.09	1.12
		2	35885.887	1.567			3	39611.52	1.26
		4	36062.875	1.100			5	39873.585	1.08
		3	36074.06	1.140			4	39906.930	1.10
		5	36132.494	1.167			3	39985.716	
		4	36178.040	1.04			2	40096.226	1.21
		2	36188.95	1.41			3	40254.944	
		5	36275.186	1.12			4	40270.098	1.10
		1	36361.456	1.109			4	40425.183	1.11
		4	36382.61	1.064			5	40724.599	
		3	36427.40	1.08			4	40776.519	1.16
		2	36488.828	1.0			3	40980.714	
		1	36556.77	1.054			4	41134.911	1.04
		5	36625.920	1.15			2	41200.38	1.35
		2	36668.670	0.92			2	41720.570	1.13
		3	36762.803	1.13			1	42624.127	1.29
		4	36800.658	0.97					
		1	36837.21	0.798					
		5	36837.988	1.168					
		2	36871.91	1.250					
		5	37008.760	1.136					
		4	37041.15	1.009					
		2	37149.10	1.060					
		1	37159.282	0.9					

TABLE 3. *Zeeman effect of* Th I

Wavelength (Å)	Intensity		Wavenumber (cm^{-1})	Type	J_1	g_1	J_2	g_2	Δg	p	n
	Lamp	Spark									
9094.821	400	100	10992.25	2	1	0.498	2	1.007			
9063.948	200	10	11029.69	3	2	0.766	2	1.186			
9048.248	800b	75	11048.83	2	2	1.006	3	1.136			
9045.341	200	20	11052.38	1	2	1.710	3	1.140			
9016.581	300	20	11087.63	7							0.918
9012.517	150	8	11092.63	7							1.090
8997.862	100	10	11110.70	1	1	0.727	2	0.627			
8967.635	500	100	11148.15	3						0.111	
8949.114	100	20	11171.22	7							0.984
8910.844	75	4	11219.20	1							0.118
8892.973	150	15	11241.75	2	2	0.734	3	1.014			
8889.187	100	10	11246.54	2	1	1.387	2	1.717			
8875.223	100	8	11264.23	1	3	1.165	4	0.975			
8868.822	200	50	11272.36	3	5	1.243	5	1.358			
8854.899	10	3	11290.08	3						0.288	
8852.784	10	3	11292.78	1							0.628
8841.170	150	20	11307.62	1							0.864
8829.686	15	5	11322.32	3	3	0.895	3	1.170			
8810.240	15		11347.31	3						0.359	
8781.093	25	1	11384.98	7							0.892
8775.575	200	40	11392.14	7							1.031
8772.803	150	8	11395.74	3	3	1.001	3	1.125			
8766.743	100	15	11403.61	2	4	0.994	5	1.150			
8760.449	100	8	11411.81	1	3	1.392	4	1.044			
8758.247	400	75	11414.67	2	3	1.182	4	1.310			
8749.169	100	20	11426.52	3						0.288	
8748.038	400	100	11428.00	3	3	0.976	3	1.249			
8739.779	75	10	11438.80	3						0.262	
8734.023	75	8	11446.33	3						0.136	
8732.426	150	50	11448.43	3	1	1.358	1	2.398			
8730.818	15	2	11450.54	2							1.274
8724.375	40	2	11458.99	3	2	0.928	2	1.166			
8717.754	10	2	11467.70	1							0.965
8709.233	200	50	11478.91	1	2	1.254	3	1.064			
8701.117	50	3	11489.62	2					0.190		1.682
8691.333	20l	1	11502.56	1							0.125
8687.841	50	4	11507.18	1							0.698
8682.216	10	1	11514.63	7							0.869
8668.118	100	20	11533.36	2	2		3		0.135		
8665.491	400	100	11536.86	2	2	1.088	3	1.248			
8655.873	50	8	11549.68	3						0.075	
8649.144	50	5	11558.66	2	4	0.715	5	1.115			
8645.310	150	25	11563.79	3	1	0.759	1	1.068			
8639.444	150	50	11571.64	1	3	0.870	4	0.746			
8638.360	100	5	11573.09	3						0.661	
8631.350	50	2	11582.49	7							1.567
8630.770	20h	2h	11583.27	7							1.180
8621.315	75	2	11595.97	2	2	0.813	3	1.089			
8607.724	8	2	11614.28	7							0.968
8593.103	100	10	11634.04	1					0.150		
8577.279	100	15	11655.51	2	1	0.462	2	0.968			
8575.327	75	5	11658.16	3						0.376	
8573.122	500	100	11661.16	2	1	0.055	2	1.036			
8560.425	100	4	11678.46	2	1	0.864	2	1.706			
8558.448	75l	4	11681.15	3						0.250	

TABLE 3. *Zeeman effect of* Th I—continued

Wavelength (Å)	Intensity		Wavenumber (cm^{-1})	Type	J_1	g_1	J_2	g_2	Δg	p	n
	Lamp	Spark									
8556.324	100	20	11684.05	3	4	0.736	4	0.982			
8554.945	200	50	11685.94	7							1.209
8544.593	150	50	11700.09	2							1.455
8543.721	150	40	11701.29	3						0.390	
8539.795	150	25	11706.67	2	2	1.004	3	1.136			
8516.555	150	50	11738.61	7							1.144
8510.622	150	25	11746.80	2	2	0.626	3	1.006			
8501.438	100	5	11759.48	3						0.065	
8496.449	100b		11766.39	3						0.271	
8496.340	75b		11766.54	7							1.136
8491.159	8	1	11773.72	7							1.409
8483.298	50	2	11784.63	7							1.266
8478.505	200		11791.29	7							1.294
8478.353	500		11791.50	2	1	0.074	2	0.503			
8471.823	200	50	11800.59	3	2	1.379	2	1.721			
8465.668	100	25	11809.17	7							2.420
8464.236	150	50	11811.17	3	2	0.778	2	0.878			
8446.516	500	150	11835.95	7							0.860
8445.495	200	150	11837.38	3	4	1.064	4	1.281			
8430.586	15	1	11858.31	7							1.110
8426.379	75		11864.23	7							0.375
8424.031	100		11867.54	3	1	0.375	1	1.201			
8421.227	500	100	11871.49	3	1	0.388	1	1.483			
8418.004	200	75	11876.04	3	2	0.886	2	0.978			
8416.742	500w	150	11877.82	7							0.745
8411.913	100	5	11884.64	7							1.116
8410.532	25	25	11886.59	2							1.980
8407.010	75	3	11891.57	3						0.364	
8406.674	40	2	11892.04	3						0.269	
8399.253	100	8	11902.55	2					0.320		
8398.171	75	8	11904.08	7							0.621
8388.528	100	10	11917.77	1	3	1.096	4	0.856			
8385.726	100	10	11921.75	3	3		3			0.737	
8384.927	8	2	11922.89	7							1.101
8383.073	8	2	11925.52	7							1.239
8379.219	100	8	11931.01	1	2	1.264	3	0.598			
8369.332	200	50	11945.10	7							1.084
8367.390	150	20	11947.87	1	2	0.811	3	0.591			
8366.073	150	15	11949.76	3	2	1.121	2	1.717			
8358.728	300	200	11960.26	3						0.170	
8346.537	100	3	11977.73	7					0.130		
8345.867	100	5	11978.69	1	1	1.369	2	1.038			
8340.933	20	3	11985.77	7							1.341
8339.403	5	2	11987.97	7							1.170
8335.700	100	8	11993.30	3						0.969	
8330.455	500	300	12000.85	3	3	1.088	3	1.240			
8320.859	500	150	12014.69	1	2	1.353	3	1.241			
8316.595	8	2	12020.85	1							0.226
8311.621	100	8	12028.04	1							0.731
8304.412	75	3	12038.48	3						0.142	
8297.172	100b	5	12048.99	2	1	0.390	2	1.255			
8295.542	100	8	12051.36	2					0.170		
8292.521	100	8	12055.75	3	2	0.836	2	1.078			
8288.404	100	5	12061.73	3						1.102	
8275.628	400	150	12080.35	3						0.130	

TABLE 3. *Zeeman effect of* Th I—continued

Wavelength (Å)	Intensity		Wavenumber (cm^{-1})	Type	J_1	g_1	J_2	g_2	Δg	p	n
	Lamp	Spark									
8263.926	150	20	12097.46	2	4	0.983	5	1.359			
8261.010	100	25	12101.73	3						0.534	
8254.741	100	15	12110.92	3	3	0.870	3	1.130			
8252.398	400	50	12114.36	2	2	0.734	2	0.966			
8246.011	25	4	12123.74	7							1.009
8237.739	20	2	12135.92	1							0.739
8234.937	100	4	12140.05	3	1	0.777	1	2.399			
8227.672	75	4	12150.77	2							1.232
8227.482	100	8	12151.05	1					0.340		
8224.956	8	2	12154.78	7							1.151
8214.147	100	10	12170.77	7							1.249
8209.444	100	8	12177.75	1	3	1.200	4	0.900			
8207.475	100	10	12180.67	2							1.440
8203.199	100		12187.02	2							1.246
8202.148	100	10	12188.58	7							0.969
8198.438	10	2	12194.09	7							1.046
8195.942	8	1	12197.81	7							1.006
8194.398	150	25	12200.11	2							1.863
8186.915	500	100	12211.26	7							1.061
8169.793	400	50	12236.85	3	2	1.194	2	1.362			
8162.064	50	3	12248.44	2							1.277
8159.737	400	100	12251.93	1	1	1.402	2	1.007			
8157.540	100	8	12255.23	1							0.673
8154.176	10		12260.28	7							0.830
8143.143	500	300	12276.89	1							1.063
8137.940	100	4	12284.74	1					0.150		
8129.681	100	5	12297.22	7							1.087
8122.725	200	50	12307.75	7							1.255
8122.350	100	5	12308.32	2							1.460
8114.539	75	4	12320.17	3	4	0.715	4	1.001			
8096.253	20	3	12348.00	7							0.963
8093.631	200	75	12352.00	1	1	1.476	2	1.066			
8086.568	15	4	12362.79	7							1.301
8075.651	150	20	12379.50	3	2	1.705	2	1.253			
8070.094	25	1	12388.02	7							1.390
8066.826	75	8	12393.04	2	4	0.999	5	1.209			
8057.973	50	2	12406.66	7							1.141
8032.433	200	50	12446.11	7							1.329
8026.192	100	8	12455.78	2							1.328
8025.708	100	8	12456.53	2							1.675
8024.235	100	500	12458.82	2					0.220		
8022.310	100b	20	12461.81	3						0.211	
8022.191	150b	25	12462.00	2					0.222		
8014.499	50	3	12473.96	7							1.393
8013.499	15	2	12475.51	2					0.170		
8010.708	100	4	12479.86	2					0.148		
8006.443	15		12486.51	7							1.055
8003.446	100	5	12491.18	2							1.038
8002.179	50	5	12493.16	3						0.208	
8000.033	100	10	12496.51	2							1.370
7996.963	40	3	12501.31	7							1.287
7993.676	150	8	12506.45	2	3	0.860	4	1.084			
7991.366	50	5	12510.06	1							0.490
7978.977	500	300	12529.49	3	2	1.066	2	1.253			
7976.175	8	2	12533.89	7							0.978

TABLE 3. *Zeeman effect of* Th I—continued

Wavelength (Å)	Intensity		Wavenumber (cm^{-1})	Type	J_1	g_1	J_2	g_2	Δg	p	n
	Lamp	Spark									
7972.598	200	20	12539.51	1	4	1.215	5	1.018			
7961.994	100	8	12556.21	2							1.598
7961.158	75	4	12557.53	3						0.250	
7954.592	150	15	12567.90	7							0.935
7941.721	200	75	12588.27	1	3	1.031	4	0.886			
7937.727	100	20	12594.60	3	5	0.935	5	1.371			
7929.938	5		12606.97	3						0.236	
7929.809	25c	2	12607.18	3	1	0.487	1	1.328			
7927.546	50l	3	12610.78	7							0.899
7925.734	75	3	12613.66	3						0.485	
7922.235	15		12619.23	3						0.096	
7916.790	40	5	12627.91	2					0.111		1.460
7914.493	8	2	12631.57	7							1.306
7908.148	100	5	12641.71	3	2	1.081	2	1.373			
7904.411	75	5	12647.69	3	4	0.907	4	1.231			
7903.319	8	1	12649.43	7							1.075
7900.309	200	75	12654.25	1	2	0.864	3	0.614			
7899.614	100	50	12655.36	7							1.276
7897.230	15	3	12659.18	7							1.241
7893.614	75	5	12664.98	3						0.452	
7869.771	15	2	12703.35	7							1.338
7868.924	40	10	12704.72	3						0.147	
7868.396	75	10h	12705.57	3						0.159	
7865.954	400	75	12709.52	7							1.362
7862.336	15	3	12715.37	7							1.040
7853.284	20		12730.02	7							1.384
7849.892	5	1	12735.52	7							1.146
7848.441	100	40	12737.88	2							1.455
7847.536	500b	150	12739.35	3	4	1.154	4	1.307			
7842.254	100	10	12747.93	3					0.130		
7841.781	200	50	12748.70	2	2	0.862	3	1.002			
7836.456	100	5	12757.36	3						0.475	
7823.475	50	2	12778.53	7							0.911
7822.392	100	4	12780.30	2	1	2.380	2	1.245			
7817.771	500	200	12787.85	2							1.070
7809.452	100	15	12801.47	2							1.282
7807.879	40		12804.05	3						0.327	
7804.533	100	5	12809.54	3						0.131	
7804.146	75	4	12810.18	2							1.362
7802.824	10	2	12812.35	7							1.101
7798.360	600	25	12819.68	7							0.059
7793.128	10	2	12828.29	7							1.255
7788.932	500	75	12835.20	7							0.808
7782.318	150	50	12846.11	7							1.272
7778.488	75	5	12852.43	3						0.481	
7776.671	40	2	12855.43	2	2	1.170	3	1.394			
7773.744	50	5	12860.28	7							1.100
7761.704	40	4	12880.22	2							1.357
7749.325	8	2	12900.80	7							1.099
7742.552	100	2	12912.09	1					0.320		
7734.617	8	2	12925.33	7							1.096
7728.939	100	15	12934.83	7							1.178
7721.188	100	8	12947.81	3						0.290	
7710.258	100	15	12966.17	2	4	1.072	5	1.262			
7703.679	100	10	12977.24	7							1.195

TABLE 3. *Zeeman effect of* Th I—continued

Wavelength (Å)	Intensity		Wavenumber (cm^{-1})	Type	J_1	g_1	J_2	g_2	Δg	p	n
	Lamp	Spark									
7699.765	100	5	12983.84	3						0.191	
7697.922	75	5	12986.94	3						0.472	
7693.797	100	5	12993.91	7							1.117
7691.765	75	3	12997.34	2	2	1.286	3	1.414			
7683.010	50	1	13012.15	7							1.239
7676.212	100	15	13023.67	3	2	0.892	2	1.192			
7668.955	50	1	13036.00	2	1	0.784	2	1.710			
7666.566	100	2	13040.06	7							1.279
7660.889	150	4	13049.72	1	4	1.207	5	1.017			
7654.695	100	5	13060.28	1					0.370		
7653.827	200	10	13061.76	7							1.137
7652.317	100	3	13064.34	7							1.188
7647.380	500	50	13072.78	3	5	1.198	5	1.370			
7642.873	15		13080.48	3						0.231	
7637.385	75	2	13089.88	2					0.381		2.444
7636.173	100	4	13091.96	3						0.095	
7633.767	150	2	13096.09	1					0.270		
7630.310	100	5	13102.02	3	4	0.986	4	1.306			
7627.175	150	5	13107.41	2							1.401
7620.080	100	5	13119.61	7							1.166
7616.686	50	1	13125.46	2	1	0.748	2	1.164			
7607.519	40	1	13141.27	2							1.368
7605.083	5		13145.48	2					0.485		
7602.795	40	1	13149.44	7							1.264
7598.203	200	3	13157.38	3						0.580	
7591.999	10		13168.14	7							1.109
7591.531	20		13168.95	3						0.157	
7586.988	8		13176.83	1					0.208		
7585.783	200	10	13178.93	7							0.386
7585.688	200	15	13179.09	7							1.106
7583.422	25		13183.03	1	3	1.092	4	0.920			
7580.686	40	1	13187.79	7							1.212
7577.266	20		13193.74	3						0.182	
7573.342	50	1	13200.58	1	3	1.377	4	1.111			
7571.029	8		13204.61	7							1.046
7569.509	100	2	13207.26	3	2	0.728	2	0.876			
7567.739	300	15	13210.35	3	5	1.080	5	1.372			
7557.751	50	1	13227.81	1					0.166		
7555.326	50	1	13232.05	1	2	0.986	3	0.902			
7549.316	200	8	13242.59	3	2	0.815	2	1.187			
7537.429	100	2	13263.47	1					0.270		
7531.818	50	2	13273.35	3						0.089	
7531.142	75	2	13274.54	7							1.067
7523.133	100	3	13288.67	3	4	0.998	4	1.169			
7520.694	15		13292.99	3						0.190	
7520.127	8		13293.99	2	2	1.034	3	1.174			
7517.963	100	2	13297.81	1	1	1.400	2	1.146			
7516.737	50	1	13299.98	3						0.420	
7511.788	100	4	13308.74	1	4	1.040	5	1.384			
7508.477	100	4	13314.61	3	4	0.938	4	1.176			
7505.292	75		13320.26	3						0.135	
7501.180	8		13327.57	7							1.250
7499.643	10	1	13330.30	3						0.124	
7499.000	100	2	13331.44	3	2	0.778	2	1.186			
7495.564	75	2	13337.55	2	4	0.887	5	1.176			

TABLE 3. *Zeeman effect of* Th I—continued

Wavelength (Å)	Intensity		Wavenumber (cm^{-1})	Type	J_1	g_1	J_2	g_2	Δg	p	n
	Lamp	Spark									
7493.427	100	2	13341.36	2	3	1.092	4	1.304			
7487.972	100	3	13351.07	2	2	0.780	3	1.040			
7483.624	200	10	13358.83	1	1	1.471	2	1.040			
7481.352	200	15	13362.89	3	4	0.996	4	1.306			
7474.559	10	1	13375.03	3						0.267	
7469.054	40	1	13384.89	7							0.770
7465.443	100	3	13391.36	1	2	1.439	3	1.189			
7462.990	75	1	13395.77	7							0.961
7461.290	8	1	13398.82	3	2	1.170	2	1.336			
7458.753	50	2	13403.38	2	1	0.506	2	0.984			
7457.648	25	1	13405.36	2	3	0.925	4	1.170			
7456.818	20	1	13406.85	2							1.283
7455.204	100	4	13409.76	3	4	0.878	4	1.090			
7452.516	20	1	13414.59	2	2	0.944	3	1.194			
7450.213	50w	5	13418.74	7							1.201
7447.848	150	5	13423.00	3	3	0.890	3	1.002			
7443.873	50	1	13430.17	1							0.840
7442.040	15		13433.48	3						0.463	
7430.255	500	15	13454.78	1	1	1.574	2	1.012			
7428.943	800	50	13457.16	1	1	1.363	2	1.179			
7422.013	100	2	13469.72	3						0.601	
7418.548	200		13476.02	2	1	0.066	2	1.088			
7417.789	100		13477.39	1	3	1.075	4	0.871			
7411.739	100	4	13488.39	2	3	1.050	4	0.872			
7410.968	50	1	13489.80	3						0.275	
7409.221	40		13492.98	3						0.525	
7404.719	40l		13501.18	7							1.174
7403.993	100	1	13502.51	3						0.603	
7402.248	400	8	13505.69	2	3	0.864	4	1.094			
7396.895	20	1	13515.46	2							1.499
7392.637	15	1	13523.25	7							1.296
7383.712	150	8	13539.59	7							1.203
7376.879	200	8	13552.14	2	5	1.082	6	1.172			
7376.178	25		13553.42	7							1.143
7370.827	100	2	13563.26	7							0.969
7362.195	50	1	13579.16	3						0.525	
7355.179	10		13592.12	3						0.270	
7353.644	15		13594.96	7							1.084
7353.007	15		13596.13	7							0.962
7350.454	75		13600.85	2	3	1.041	4	1.233			
7341.150	500	15	13618.09	3	4	0.986	4	1.088			
7339.599	150	3	13620.97	1					0.280		
7335.568	100	15	13628.45	7							0.834
7329.488	100	5	13639.76	1	2	1.713	3	1.093			
7324.808	300	10	13648.47	3						0.590	
7323.207	100	3	13651.46	3						0.571	
7315.609	150	3	13665.64	2	1	0.734	2	1.058			
7315.064	200	3	13666.65	2	1	0.522	2	1.262			
7311.510	100	3	13673.30	3	3	0.994	3	1.174			
7309.255	100	2	13677.52	1							0.938
7302.172	50	2	13690.78	2							1.622
7298.138	200b	3	13698.35	1	3	1.162	4	0.990			
7296.265	100	3	13701.87	2					0.094		
7294.316	15	1	13705.53	3						0.239	
7284.905	500	20	13723.23	1	2	1.248	3	1.133			

TABLE 3. *Zeeman effect of* Th I—continued

Wavelength (Å)	Intensity		Wavenumber (cm^{-1})	Type	J_1	g_1	J_2	g_2	Δg	p	n
	Lamp	Spark									
7282.732	100	2	13727.33	2							1.436
7279.142	8		13734.10	3						0.579	
7277.013	75	1	13738.12	3						0.099	
7274.294	15	1	13743.25	3						0.224	
7272.550	100	2	13746.55	3						0.294	
7270.558	100	2	13750.31	2	2	0.673	3	1.255			
7268.834	100	2	13753.58	7							1.182
7267.096	50	1	13756.86	7							1.362
7264.118	50		13762.50	2							1.546
7262.190	10		13766.16	3						0.187	
7258.177	200	5	13773.77	2	3	1.034	4	1.164			
7256.981	150	4	13776.04	3	2	0.974	2	1.110			
7255.351	200	5	13779.13	2	3	0.942	4	1.074			
7247.988	25	2	13793.13	7							1.144
7247.599	40		13793.87	7							1.018
7244.689	200	8	13799.41	1	3	1.030	4	0.856			
7242.086	200	10	13804.37	3	5	0.990	5	1.370			
7235.890	50	1	13816.19	1					0.160		
7233.390	100		13820.97	7							1.184
7230.888	500	5	13825.75	1							0.472
7220.989	100	2	13844.70	2	1	0.500	2	0.720			
7219.156	300	10	13848.22	3						0.230	
7208.000	500	150	13869.65	2	3	1.233	4	1.323			
7206.476	400	8	13872.58	3	3	0.836	3	0.881			
7201.803	100	2	13881.59	2	2	0.740	3	0.900			
7201.042	50	1	13883.05	2					0.284		
7200.041	400	10	13884.98	2	2	1.188	3	1.304			
7179.725	150	4	13924.27	3						0.332	
7177.284	75	2	13929.01	2					0.154		
7173.372	500	20	13936.60	1							0.879
7170.357	100	2	13942.46	1					0.260		
7168.896	800	75	13945.31	2	2	0.747	3	1.116			
7167.202	150	4	13948.60	1					0.088		
7159.943	300b	8	13962.74	1	3	1.105	4	0.984			
7159.877	100b	2	13962.87	7							1.132
7156.936	300	15	13968.61	3	4	0.989	4	1.155			
7154.952	200	8	13972.48	3	2	0.665	2	1.186			
7153.587	200	10	13975.15	3						0.829	
7150.285	400	25	13981.60	1	1	1.475	2	1.167			
7148.557	400	15	13984.98	2	3	0.826	4	0.988			
7142.328	300	8	13997.18	2	1	0.370	2	0.970			
7138.142	20		14005.39	7							1.171
7132.603	200	4	14016.26	2							1.192
7131.353	150	40	14018.72	3						0.076	1.140
7130.718	200	5	14019.97	1					.080		
7130.179	100	4	14021.03	3						0.174	
7126.814	100	3	14027.65	3						0.051	
7125.515	150	2	14030.21	3	3	3			0.480		
7124.562	500	50	14032.08	3	2	0.737	2	1.125			
7112.917	100	4	14055.06	2					0.180		
7111.045	75	2	14058.76	7					0.190		
7102.589	100	2	14075.49	1							0.968
7088.822	150	2	14102.83	7							1.199
7084.165	500	75	14112.10	2	4	1.248	5	1.363			
7072.394	300	8	14135.59	1	4	1.172	5	1.104			

TABLE 3. *Zeeman effect of* Th I—continued

Wavelength (Å)	Intensity		Wavenumber (cm^{-1})	Type	J_1	g_1	J_2	g_2	Δg	p	n
	Lamp	Spark									
7067.513	75		14145.35	7					0.250		
7066.287	100	2	14147.80	3	3	1.164	3	1.385			
7064.451	300	10	14151.48	7							1.143
7062.418	40	1	14155.55	3						0.125	
7061.392	100	2	14157.61	1	1	1.180	2	0.770			
7060.039	300	8	14160.32	3	2	0.820	2	1.008			
7059.526	150	3	14161.35	2					0.230		
7058.488	150	5	14163.43	1	3	0.998	4	0.913			
7054.416	150	2	14171.61	3						0.189	
7038.717	75	1	14203.22	7							1.194
7036.277	400	8	14208.14	2							1.479
7033.352	100	2	14214.05	3						0.313	
7028.017	100	2	14224.84	3	1	0.401	1	1.340			
7023.523	100	3	14233.94	2							1.057
7023.145	100	3	14234.71	1	1	1.380	2	1.090			
7021.279	150	8	14238.49	2							1.389
7009.047	50	1	14263.34	7							1.274
7007.092	100	4	14267.32	3						0.202	
7002.881	200	8	14275.90	2							1.609
7000.806	500	75	14280.13	1	5	1.349	6	1.211			
6998.247	100	2	14285.35	3						0.346	
6995.141	75	2	14291.70	7							1.106
6989.657	1000	150	14302.91	3	4	0.744	4	0.874			
6986.031	150	4	14310.33	3	2	0.962	2	1.702			
6981.082	100	3	14320.48	3						0.336	
6969.301	100	3	14344.68	3						0.079	
6965.946	500l	4	14351.59	2	1	0.699	2	1.097			
6962.862	75	2	14357.95	7					0.397		
6954.655	200	5	14374.89	1	1	1.364	2	1.008			
6948.205	300	20	14388.24	3	4	0.925	4	1.169			
6945.488	200	8	14393.87	2					0.350		
6942.535	150	8	14399.99	1					0.266		
6936.651	150	4	14412.20	3	3	1.383	3	1.119			
6920.037	150	5	14446.80	1							0.596
6916.129	200	10	14454.97	2	4	1.043	5	1.376			
6911.222	800r	200	14465.22	3						0.147	
6904.578	100		14479.15	3						0.105	
6900.762	100	5	14487.16	2					0.370		
6886.404	200	10	14517.36	7							1.478
6883.311	200	10	14523.89	1	3	1.132	4	0.912			
6880.769	15	1	14529.25	7							1.173
6874.752	200	10	14541.97	3						0.143	
6870.988	150	3	14549.93	3	1	0.392	1	0.619			
6868.455	100	3	14555.30	2	4	0.989	5	1.259			
6866.756	100s	2	14558.90	7					0.140		
6866.368	150	3	14559.72	3						0.312	
6862.873	100	2	14567.14	3	2	1.099	2	1.410			
6855.315	150	4	14583.20	2					0.157		
6853.511	100	4	14587.04	2					0.220		
6852.344	100	2	14589.52	7							1.150
6850.704	100h	2	14593.01	7							1.197
6846.469	100	2	14602.04	7							0.718
6841.690	10		14612.24	7							1.043
6839.287	100	2	14617.37	7							0.864
6834.925	400	50	14626.70	1							0.928

TABLE 3. *Zeeman effect of* Th I—continued

Wavelength (Å)	Intensity		Wavenumber (cm^{-1})	Type	J_1	g_1	J_2	g_2	Δg	p	n
	Lamp	Spark									
6829.037	500	25	14639.31	3	3	1.095	3	1.249			
6824.678	400	20	14648.66	1	2	1.101	3	1.000			
6823.500	150	4	14651.19	3						1.010	
6815.604	100	2	14668.17	7							1.054
6809.311	150	4	14681.72	1					0.160		
6805.746	100	2	14689.41	2							1.050
6802.783	100	3	14695.81	2	2	0.864	3	1.049			
6798.483	150	3	14705.10	1					0.630		
6795.797	100	2	14710.92	2					0.360		
6795.046	75	2	14712.54	7							0.952
6791.232	400	25	14720.81	2	3	1.087	4	1.318			
6788.837	300	25	14726.00	2	4	0.970	5	1.042			
6787.734	300	25	14728.39	2							1.232
6780.126	400	75	14744.91	3	2	0.622	2	0.772			
6776.230	100	3	14753.40	1					0.200		
6772.176	400b	15	14762.23	1					0.165		
6765.683	200	100	14776.40	3						0.720	
6763.340	50	2	14781.51	7							1.126
6762.500	40	1	14783.35	7							1.224
6760.667	100	3	14787.36	7							1.212
6758.202	200	8	14792.75	3						0.837	
6757.105	100	5	14795.75	1	3	1.099	4	0.891			
6751.426	100	3	14807.60	2	1	0.378	2	0.970			
6749.315	50	1	14812.23	3						0.370	
6742.881	200	8	14826.36	2	2	1.090	3	1.386			
6738.179	200	5	14836.71	3	3	1.020	3	1.241			
6735.128	100	2	14843.43	3						0.899	
6733.748	150	5	14846.47	3						0.100	
6732.650	100	3	14848.89	3						1.191	
6728.757	150	5	14857.48	3						0.203	
6727.459	500	75	14860.35	3	1	0.069	1	1.434			
6719.198	200	5	14878.62	2					0.044		
6717.384	100	3	14882.64	7							0.982
6715.515	100	2	14886.78	3						0.199	
6713.967	300	8	14890.21	3	2	0.665	2	1.015			
6711.249	100	4	14896.24	3						1.252	
6697.708	200	5	14926.36	1	1	1.380	2	1.240			
6696.140	200	5	14929.86	2							1.595
6694.492	100	2	14933.53	2					0.630		
6687.521	150	3	14949.10	3						0.258	
6684.049	100	2	14956.86	1					0.294		
6683.368	200	3	14958.39	2	2	0.782	3	0.946			
6680.087	100	1	14965.73	2	2	0.750	3	1.080			
6678.707	200	8	14968.83	3						0.083	
6673.590	200	5	14980.30	3	4	0.887	4	1.157			
6668.826	100	2	14991.00	3	4	0.922	4	0.982			
6663.702	100	3	15002.53	3						0.152	
6662.270	800	200	15005.75	1	2	1.379	3	1.250			
6658.678	400	15	15013.85	7							1.054
6654.371	100	3	15023.57	2							1.536
6638.912	150	20	15058.55	7							1.051
6626.125	75	1	15087.61	3	1	1.018	1	1.378			
6613.376	200	8	15116.70	1	1	1.518	2	1.182			
6593.940	500	150	15161.25	7							0.069
6593.464	100	15	15162.35	2							1.362

TABLE 3. *Zeeman effect of* Th I—continued

Wavelength (Å)	Intensity		Wavenumber (cm^{-1})	Type	J_1	g_1	J_2	g_2	Δg	p	n
	Lamp	Spark									
6591.485	400	75	15166.90	2	2	0.736	3	1.064			
6588.540	500r	200	15173.68	1	1	1.482	2	1.092			
6583.906	400r	200	15184.36	2							1.482
6580.231	75	3	15192.84	1					0.530		
6579.482	20	2	15194.57	3						0.122	
6577.216	100	75	15199.80	3						0.163	
6564.443	150	8	15229.38	1	2	0.966	3	0.686			
6562.105	50		15234.80	3	1	0.761	1	1.141			
6558.871	100	8	15242.32	1	2	1.246	3	0.964			
6551.703	100	5	15258.99	1	2	1.524	3	1.038			
6538.301	50	4	15290.27	2	1	0.762	2	0.998			
6531.342	800r	200	15306.56	1	1	1.582	2	1.014			
6522.044	100	15	15328.38	2	1	0.376	2	0.723			
6512.366	400	15	15351.16	3	2	1.093	2	1.249			
6506.989	100	15	15363.85	2	2	1.135	3	0.866			
6501.992	100	5	15375.65	2	2	0.532	2	1.004			
6497.490	50	3	15386.31	3						0.187	
6488.882	100	4	15406.72	7							0.638
6462.606	200b	100	15469.36	7							1.184
6457.280	800r	300	15482.12	2	4	0.866	5	1.006			
6450.007	200	15	15499.58	1	2	1.542	3	1.386			
6446.771	100	8	15507.35	3						0.216	
6438.918	100	8	15526.27	2	1	0.464	2	0.794			
6437.769	200	20	15529.04	3						0.164	
6427.507	50	4	15553.83	3						0.328	
6422.106	100	8	15566.91	2							1.410
6417.908	15	2	15577.09	3						0.141	
6415.536	75	5	15582.86	2					0.264		
6413.615	400	100	15587.52	1	3	1.200	4	1.002			
6411.899	500	75	15591.69	1							1.095
6406.446	100	5	15604.96	3						0.098	
6400.696	100	8	15618.98	1							0.310
6396.951	100	8	15628.13	2							1.510
6394.045	100	8	15635.23	3						0.440	
6392.371	75	8	15639.32	7							0.995
6387.393	200	10	15651.51	1	1	1.466	2	1.356			
6376.930	500	200	15677.19	7							1.138
6369.141	200	25	15696.37	7							1.062
6362.256	100	20	15713.35	7							1.008
6359.677	75	5	15719.72	7							0.824
6355.911	800	200	15729.04	2	3	0.862	4	1.032			
6355.633	75	8	15729.72	7							1.025
6348.737	200	15	15746.81	3						0.171	
6342.860	500	150	15761.40	2					0.120		1.668
6339.663	100	15	15769.35	1	1	1.366	2	1.179			
6331.415	200	15	15789.89	1					0.220		
6327.279	500	100	15800.21	2							1.496
6326.365	200	20	15802.50	3						0.527	
6322.866	20	2	15811.24	7							1.051
6317.183	150	8	15825.47	2	2	1.135	3	1.395			
6315.774	100	8	15829.00	3						0.232	
6307.868	25	3	15848.83	7							0.953
6303.251	200	20	15860.44	1	3	1.218	4	0.995			
6301.421	200	20	15865.05	7							0.832
6300.917	150	10	15866.32	7							1.119

TABLE 3. *Zeeman effect of* Th I—continued

Wavelength (Å)	Intensity		Wavenumber (cm^{-1})	Type	J_1	g_1	J_2	g_2	Δg	p	n
	Lamp	Spark									
6298.903	100	5	15871.39	3	2	1.099	2	1.705			
6293.241	150	15	15885.67	3						0.693	
6292.891	100	8	15886.55	3						0.296	
6291.192	300	15	15890.84	3						0.100	
6271.544	75	5	15940.63	7							1.332
6261.418	400	150	15966.41	7							1.148
6246.173	150	8	16005.38	7							0.929
6240.949	150	8	16018.77	3						0.525	
6234.856	400	75	16034.42	2	1	1.527	2	1.014			
6224.527	400	40	16061.03	3						0.239	
6220.011	100	5	16072.69	7					0.325		
6208.686	100	5	16102.01	7					0.320		
6207.220	500	200	16105.82	3	1	0.071	1	1.589			
6205.861	100	8	16109.34	7					0.340		
6203.493	500	100	16115.49	7							1.359
6198.223	400	75	16129.19	1	1	1.582	2	1.262			
6191.906	400	50	16145.65	3	2	1.009	2	1.381			
6189.145	75	2	16152.85	7					0.090		
6180.703	200	8	16174.91	2	1	0.058	2	0.518			
6178.432	200	20	16180.86	2	3	1.072	4	1.304			
6169.822	500	200	16203.44	1	3	1.305	4	1.213			
6164.480	200	20	16217.48	2	2	0.739	2	1.077			
6162.968	40	3	16221.46	7							1.018
6161.353	150	8	16225.71	7							1.317
6157.093	100	8	16236.94	3						0.916	
6155.587	200	15	16240.91	1	2	1.189	3	1.077			
6154.068	100	15	16244.92	7							1.435
6151.993	150r		16250.40	2	2	1.112	3	1.250			
6124.485	200	15	16323.39	3	2	1.189	2	1.379			
6123.838	75	8	16325.11	1					0.200		
6121.413	150	50	16331.58	3					0.110	0.665	
6119.704	75	8	16336.14	1	1	1.210	2	0.976			
6116.172	100	8	16345.57	3						0.130	
6114.546	150	10	16349.92	7							1.399
6107.539	400	15	16368.68	7							1.167
6106.847	10	2	16370.53	3						0.257	
6104.572	300	200	16376.63	2					0.335		
6102.595	300	50	16381.93	2	3	0.814	4	0.982			
6101.726	100	10	16384.27	2	1	0.507	2	0.782			
6088.031	400	50	16421.13	2	2	0.786	3	0.894			
6085.375	100	75	16428.29	3	2	0.782	2	1.118			
6079.220	200	25	16444.93	2							1.546
6077.870	150	25	16448.58	3						0.185	
6055.592	100	10	16509.09	7					0.080		
6053.381	300	15	16515.12	2	1	0.616	2	1.009			
6035.194	100	5	16564.89	7							0.967
6032.876	75	8	16571.25	1					0.300		
6030.448	75s	5	16577.93	3						0.205	
6021.036	200s	75	16603.84	2	3	0.834	4	0.870			
6014.062	75	5	16623.09	7							1.194
6007.073	300s	75	16642.43	2	3	1.095	4	1.313			
6005.174	200	15	16647.70	1	2	1.367	3	1.087			
6000.766	100	8	16659.92	7							1.137
5996.630	100	4	16671.42	2					0.404		
5995.221	100	4	16675.33	3						0.996	

201-606 O - 76 - 7

TABLE 3. *Zeeman effect of* Th I—continued

Wavelength (Å)	Intensity		Wavenumber (cm^{-1})	Type	J_1	g_1	J_2	g_2	Δg	p	n
	Lamp	Spark									
5994.126	500r	100	16678.38	7							1.483
5991.004	400s	50	16687.07	1	1	1.354	2	1.006			
5989.742	50	5	16690.59	3						0.391	
5982.095	100	5	16711.92	3						0.729	
5975.066	500	150	16731.58	3	2	1.010	2	1.323			
5973.665	500r	150	16735.50	1	1	1.433	2	1.257			
5969.742	150	10	16746.50	1	1	2.403	2	1.543			
5959.681	50	3	16774.77	3						1.043	
5956.263	100	8	16784.40	3						0.233	
5955.566	100	5	16786.37	1	2	1.709	3	1.179			
5953.587	100	4	16791.94	7					0.218		
5950.148	15	2	16801.65	7					0.234		
5949.373	50	5	16803.84	3						0.016	
5944.648	150	40	16817.19	3	3	0.696	3	0.875			
5942.359	40	3	16823.67	7							1.105
5940.567	50	3	16828.75	1					0.120		
5938.459	150	20	16834.72	3						0.869	
5937.665	100	10	16836.97	3						0.178	
5929.934	100	20	16858.92	7							1.481
5926.232	150	40	16869.45	7							0.798
5916.730	100	20	16896.55	3						0.735	
5914.648	100b	10	16902.49	1							0.068
5905.571	150	20	16928.48	2	3	0.932	4	1.214			
5902.602	100	2	16936.98	3						0.989	
5899.846	150	5	16944.90	2	1	0.071	2	1.387			
5899.521	75	4	16945.83	3						0.936	
5894.699	100	25	16959.70	3						0.796	
5892.434	75	5	16966.21	3						0.225	
5891.451	200	25	16969.04	2	3	0.859	4	0.997			
5886.531	100	8	16983.23	7							0.972
5885.702	200	50	16985.62	2	4	1.146	5	1.379			
5874.993	100	8	17016.58	3						0.084	
5874.040	50	3	17019.34	3						0.134	
5869.854	100	5	17031.48	2	2	0.833	3	1.011			
5868.382	150	25	17035.75	7							1.162
5866.814	75	5	17040.30	7							0.932
5863.720	100	8	17049.29	2	1	1.364	2	1.252			
5854.120	150	8	17077.26	3	4	1.041	4	1.313			
5853.474	100	5	17079.14	2					0.192		
5852.682	200	25	17081.45	3						0.050	
5843.805	100	5	17107.40	3						0.232	
5842.050	50	4	17112.54	3						0.236	
5840.639	100	5	17116.67	3	3					0.524	
5832.371	100	15	17140.94	7							1.144
5830.827	75	5	17145.47	3						0.264	
5829.876	50	5	17148.27	3						0.480	
5829.110	50	3	17150.52	3	2	1.117	2	1.339			
5822.796	100	8	17169.12	3						0.772	
5819.607	50	3	17178.53	7							1.132
5818.453	75	5	17181.93	7							1.296
5812.976	100	8	17198.13	2							1.154
5807.685	100	4	17213.79	3						0.433	
5806.201	40	2	17218.19	7					0.213		
5805.702	100	3	17219.67	7					0.186		
5804.141	500r	50	17224.30	3	2	0.734	2	1.045			

TABLE 3. *Zeeman effect of* Th I—continued

Wavelength (Å)	Intensity		Wavenumber (cm^{-1})	Type	J_1	g_1	J_2	g_2	Δg	p	n
	Lamp	Spark									
5800.830	300	20	17234.14	3	2	1.172	2	1.254			
5797.319	75	3	17244.57	3						0.282	
5796.070	200	15	17248.29	3	4	1.120	4	1.307			
5792.431	150	8	17259.12	7							1.573
5791.704	50	2	17261.29	7					0.200		
5789.644	200	15	17267.43	3	3	1.139	3	1.246			
5782.307	40b	4	17289.34	2	2	0.927	3	1.019			
5779.833	50	2	17296.74	7					0.298		
5777.398	100	8	17304.03	3						0.118	
5776.164	25	2	17307.73	7					0.128		
5773.946	150	10	17314.38	3	1	0.070	1	0.615			
5763.529	200	10	17345.67	3	3	1.085	3	1.180			
5762.796	100	10	17347.88	3						0.462	
5760.550	600r	150	17354.64	2	1	0.504	2	0.734			
5753.026	200	25	17377.34	2	3	1.016	4	1.208			
5736.031	150	8	17428.82	2	3	1.062	4	1.464			
5729.992	200d	10	17447.19	3						0.378	
5727.711	40	3	17454.14	3						0.511	
5727.021	50	3	17456.24	7							1.181
5725.390	400r	75	17461.21	2	4	1.150	5	1.368			
5724.463	75	4	17464.04	3						0.051	
5721.425	50	4	17473.32	3						0.053	
5719.625	200	50	17478.81	3	3	1.082	3	1.251			
5711.998	75	5	17502.15	7					0.080		
5708.679	50	3	17512.33	7							1.142
5705.637	50	4	17521.67	3						0.286	
5698.550	40	4	17543.46	3						0.346	
5698.292	100	5	17544.25	3	1	0.724	1	1.104			
5696.391	100	8	17550.10	1	3	1.168	4	0.921			
5685.192	100	8	17584.68	3	4	1.060	4	1.308			
5679.004	75	5	17603.84	7							0.903
5677.051	200b	8	17609.89	3						0.203	
5673.835	50	5	17619.87	2							1.436
5667.129	150	15	17640.72	2	2	0.871	3	1.016			
5665.181	200	50	17646.79	3	2	0.775	2	1.118			
5664.621	100	15	17648.53	7					0.057		
5660.662	25	3	17660.88	7					0.590		
5657.926	200	25	17669.41	2							1.632
5648.990	150	10	17697.37	2	3	1.083	4	1.233			
5646.455	100	10	17705.31	2	2	1.041	3	1.385			
5645.529	50	8	17708.22	7							1.235
5641.735	75	8	17720.13	2					0.125		
5641.562	50	5	17720.67	2					0.102		
5635.889	100	15	17738.50	7							1.233
5633.297	100	8	17746.67	7							0.907
5630.297	100	10	17756.12	3						0.754	
5629.312	50	3	17759.23	7							0.855
5624.911	50	3	17773.12	2					0.110		
5620.013	15b	5	17788.62	7					0.080		
5619.976	50b	8	17788.73	3						0.962	
5615.320	400r	15	17803.48	3	1	1.493	1	1.559			
5612.619	75	3	17812.05	7							1.126
5612.068	150	20	17813.80	3	4	0.986	4	1.128			
5610.685	200	20	17818.19	1	1	2.396	2	1.680			
5609.585	200	10	17821.68	2					0.660		

TABLE 3. *Zeeman effect of* Th I—continued

Wavelength (Å)	Intensity		Wavenumber (cm^{-1})	Type	J_1	g_1	J_2	g_2	Δg	p	n
	Lamp	Spark									
5606.390	150	10	17831.84	3	3	0.878	3	1.192			
5605.297	100b	8	17835.32	3						0.512	
5602.866	50	5	17843.05	2	2	0.789	3	0.844			
5601.604	200	8	17847.07	3	2	0.734	2	1.158			
5595.064	300	25	17867.94	2	1	0.374	2	0.775			
5587.027	500r	50	17893.64	2							
5582.367	75	4	17908.58	2							1.425
5580.756	100	10	17913.75	3					0.546		
5580.395	50	10	17914.90	3						0.587	
5579.359	300	40	17918.23	3	1	0.065	1	0.842		0.054	
5576.205	100	10	17928.36	2	4	0.992	5	1.098			
5573.355	400	20	17937.54	3							
5572.466	200	8	17940.40	3	3	1.094	3	1.248		0.198	
5570.928	50	2	17945.35	3	2	1.006	2	1.516			
5568.000	300b	150	17954.79	3							
5559.894	150	8	17980.96	1	1	1.570	2	1.252		0.081	
5558.342	400b	50	17985.98	2							
5557.045	300	15	17990.18	3	4	1.132	4	1.306			1.227
5555.534	75	4	17995.07	7					0.128		
5554.502	20	4	17998.42	7							1.276
5552.624	75	4	18004.50	1							0.791
5551.193	40	2	18009.14	3						0.092	
5548.176	400r	40b	18018.94	3	2	1.012	2	1.255			
5546.122	75	25	18025.61	3						0.131	
5542.890	300	10	18036.12	2	3	0.875	4	1.040			
5528.226	50b	5	18083.96	3	1	0.721	1	1.343			
5527.295	200	8	18087.01	7							1.217
5519.232	100	2	18113.43	7							1.270
5518.988	200b	50	18114.23	2	4	0.883	5	1.175			
5514.930	75b	3	18127.56	7							1.274
5514.873	200b	10	18127.74	3						0.354	
5509.993	400	20	18143.80	2	4	1.263	5	1.373			
5508.557	100	5	18148.53	3						0.177	
5507.542	100l	2	18151.88	3						0.752	
5501.281	100	10	18172.53	2	1	0.627	2	0.977			
5496.138	200	10	18189.54	2	1	0.068	2	1.106			
5494.330	75	10	18195.53	2	3	1.170	4	1.314			
5492.642	100	10	18201.12	2	2	1.177	3	1.263			
5492.416	50	10	18201.87	7					0.270		
5489.086	100	5	18212.91	7					0.544		
5482.498	100	8	18234.79	7							1.157
5479.072	75	75	18246.20	1					0.100		0.983
5478.742	50	3	18247.29	7					0.222		
5477.550	40	2	18251.26	3						0.084	
5474.733	50	3	18260.66	3						0.467	
5470.759	150	10	18273.94	7							1.064
5470.145	50	8	18275.97	3						0.192	
5464.205	200w	8	18295.84	3	3	1.082	3	1.310			
5463.771	50	4	18297.29	7					0.109		
5457.289	75	3	18319.02	7					0.110		
5455.149	100	8	18326.21	3						0.620	
5452.219	300	40	18336.06	2	4	1.222	5	1.364			
5441.213	100	8	18373.15	7							1.136
5440.600	75	2	18375.22	7					0.212		
5439.850	75	8	18377.75	3						0.522	

TABLE 3. *Zeeman effect of* Th I—continued

Wavelength (Å)	Intensity		Wavenumber (cm^{-1})	Type	J_1	g_1	J_2	g_2	Δg	p	n
	Lamp	Spark									
5431.112	200	40	18407.32	2	2	1.014	3	1.140			
5429.105	100	5	18414.12	3						0.305	
5424.008	300	40	18431.43	7							0.981
5419.136	100	8	18448.00	3						0.371	
5417.486	400r	40	18453.62	1	2	1.257	3	1.101			
5415.528	200b	2	18460.29	3	4	0.860	4	1.030			
5410.769	400	15	18476.52	2	1	0.770	2	1.012			
5407.652	400b	40b	18487.17	3	5	1.035	5	1.174			
5403.200	200	15	18502.41	2	4	0.884	5	1.109			
5400.145	150	5	18512.87	2					0.035		
5399.175	200	10	18516.20	3						1.208	
5398.920	400	40	18517.08	2					0.184		1.622
5398.704	150	4	18517.82	2					0.215		
5398.205	150	4	18519.53	7					0.110		
5393.972	150	8	18534.06	3						0.881	
5388.057	300	20	18554.41	1							0.907
5387.812	100	4	18555.25	7							1.195
5387.152	25	2	18557.52	7					0.213		
5386.611	500	20	18559.39	2	3	1.082	4	1.216			
5384.031	75	15	18568.28	1							0.452
5379.112	300	20	18585.26	2	4	0.877	5	1.049			
5378.837	400	40	18586.21	3						0.505	
5376.778	200	50	18593.33	3						0.134	
5374.823	150	15	18600.09	7							1.479
5372.703	200	25	18607.43	2							1.085
5369.284	200	8	18619.28	2	1	0.072	2	1.245			
5361.156	100	3	18647.51	7					0.238		
5360.150	300	5	18651.01	1	2	1.249	3	1.016			
5359.827	100	4	18652.13	7							1.032
5355.638	100	3	18666.72	2					0.260		
5351.839	150	8	18679.97	3						0.928	
5351.126	200	25	18682.46	2	3	0.590	4	0.905			
5349.003	100	3	18689.87	3						0.049	
5347.973	150	5	18693.48	3						0.160	
5343.581	500r	40	18708.84	1	1	1.526	2	1.252			
5340.501	200	10	18719.63	7							1.181
5337.018	200b	10	18731.85	3						0.580	
5330.082	200b	5	18756.22	1	2	1.186	3	0.954			
5326.976	500r	40	18767.15	2	3	0.903	4	1.068			
5326.278	200b	8	18769.61	3						0.171	
5320.767	75	20	18789.06	3						0.161	
5320.099	50	2	18791.42	7							1.111
5318.110	100	3	18798.44	7					0.430		
5317.494	200	4	18800.62	2					0.400		
5315.230	150	3	18808.63	7					0.576		
5312.904	300	15	18816.86	1	2	1.193	3	1.006			
5312.643	150b	15	18817.79	7					0.086		
5312.532	400	40	18818.18	2	1	0.077	2	1.257			
5312.001	400r	25	18820.06	3	2	1.259	2	1.386			
5311.870	75b	2	18820.53	3						0.670	
5309.616	300	5	18828.52	7					0.687		
5306.987	100	4	18837.84	3						0.453	
5303.483	100	3	18850.29	7					0.180		
5303.334	50	2	18850.82	3						0.140	
5300.524	300	5	18860.81	2					0.215	0.429	

TABLE 3. *Zeeman effect of* Th I—continued

Wavelength (Å)	Intensity		Wavenumber (cm^{-1})	Type	J_1	g_1	J_2	g_2	Δg	p	n
	Lamp	Spark									
5298.284	200	4	18868.79	2	2	0.537	3	1.089			
5297.746	300b	15	18870.70								1.587
5296.279	300	5	18875.93	2	4	1.192	5	1.372			
5295.674	50b	4b	18878.08	7							1.172
5295.089	75	1	18880.17	7					0.270		
5294.397	200	3	18882.64	1	3	1.253	4	1.073			
5291.818	200	5	18891.84	1	2	1.026	3	0.860			
5281.070	300	2	18930.29	2	2	0.728	3	0.969			
5280.346	75	2	18932.89	3						0.634	
5277.147	100	1	18944.36	3						0.324	
5274.391	100	3	18954.26	7							0.830
5274.121	300	5	18955.23	3						0.130	
5273.134	100b	10	18958.78	7					0.520		
5269.794	100	4	18970.80	3						0.067	
5262.621	100b	4	18996.65	3						0.620	
5261.474	75b	3	19000.79	7						0.106	
5258.361	400r	25	19012.41	3	1	0.615	1	1.481			
5258.212	150b	3	19012.58	7							2.402
5254.262	300l	8	19026.87	7					0.044		0.922
5238.812	75h	10	19082.98	3	2	1.047	2	1.193			
5234.107	150	1	19100.14	7					0.074		
5228.996	100	1	19118.81	2							1.460
5228.227	200	3	19121.62	3						0.198	
5220.928	100	1	19148.35	3						0.214	
5213.350	400	5	19176.18	3	4	0.863	4	1.036			
5209.724	500	3	19189.53	2	1	0.614	2	1.250			
5207.803	200	2	19196.61	7							1.078
5206.800	75	3	19200.31	3						0.158	
5205.154	200	2	19206.38	7							1.029
5203.850	500	25	19211.19	7					0.190		
5202.007	75	3	19218.00	2	1	0.724	2	1.327			
5199.323	300b	3	19227.92	1					0.100		
5198.802	500	100d	19229.85	2	3	0.869	4	1.101			
5197.236	200	5	19235.64	7					0.270		
5195.815	500	8	19240.90	3	4	1.212	4	1.380			
5194.456	400	12	19245.93	3						1.223	
5184.452	100	3	19283.07	3						0.183	
5177.621	200	3	19308.51	3						0.578	
5176.961	500	50	19310.94	3						0.354	
5175.323	200	2	19317.08	3						0.701	
5174.367	200	3	19320.65	3						0.067	
5174.242	200	75	19321.12	2							1.003
5173.671	400	2	19323.25	3						0.044	
5172.479	75	3	19327.71	3						1.439	
5161.540	400	8	19368.67	2	2	0.797	3	0.931			
5160.718	500b	150	19371.75	3						0.176	
5154.243	500r	40	19396.09	2	4	0.859	5	1.116			
5149.210	300	3	19415.05	7					0.170		
5146.059	300	10	19426.93	7					0.310		
5143.916	300b	15	19435.02	3						0.185	
5140.771	200b	5	19446.92	1					0.550		
5130.235	150	2	19486.86	7					0.324		
5125.950	300	3	19503.14	2	2	0.734	3	1.085			
5115.045	1000r	40	19544.72	7							1.481
5098.933	150	2	19606.48	7							1.093

TABLE 3. *Zeeman effect of* Th I—continued

Wavelength (Å)	Intensity		Wavenumber (cm^{-1})	Type	J_1	g_1	J_2	g_2	Δg	p	n
	Lamp	Spark									
5096.484	800	5	19615.90	3	1	0.842	1	1.480			
5090.052	400	5	19640.69	3						0.125	
5082.625	100	8	19669.39	3						0.338	
5067.974	1000r	75	19726.25	3						0.208	
5066.134	300	10	19733.42	7					0.166		
5065.190	300	5	19737.10	2	2	0.767	3	1.027			
5063.514	200l	50l	19743.63	2					1.090		
5062.932	300	5	19745.90	1	3	1.136	4	0.985			
5059.861	400b	75h	19757.88	3						0.374	
5057.982	300	2	19765.22	7							1.479
5051.885	500	5	19789.08	2	3	1.182	4	1.315			
5050.780	300	5	19793.40	2	1	0.844	2	1.256			
5044.715	100	8	19817.20	1	1	1.561	2	0.731			
5043.520	75	15l	19821.89	3						1.432	
5041.126	200	5	19831.31	1							0.967
5039.231	300r	8l	19838.77	2							1.536
5038.306	75	3	19842.41	3						0.336	
5034.297	100	2	19858.21	3						1.178	
5029.893	200	3	19875.60	3	1	0.768	1	1.480			
5029.013	75	2	19879.07	3						0.247	
5028.656	300r	15	19880.48	3	4	1.190	4	1.310			
5023.709	50	1	19900.06	3						0.233	
5023.486	50	1	19900.95	3						0.324	
5022.174	40	2	19906.14	3						0.798	
5018.059	150	5	19922.47	3						0.376	
5017.510	100	15	19924.65	2	1	0.708	2	1.012			
5011.478	75	4	19948.63	7							1.126
5010.417	50	4	19952.85	7					0.160		
5009.938	50b		19954.76	3						0.291	
5004.001	50	3	19978.44	3						0.233	
5002.097	500r	4	19986.05	3						0.116	
4992.638	20	5	20023.91	3						0.178	
4989.309	150	10	20037.26	1							0.890
4985.948	50	3	20050.77	7							0.926
4985.373	300	10	20053.09	2	1	0.770	2	1.254			
4982.488	150	25h	20064.70	3						0.292	
4980.186	150	10	20073.97	3						0.240	
4972.754	20	2	20103.97	3						0.179	
4972.057	40	1	20106.79	7							0.771
4965.731	200	10	20132.40	3						0.808	
4961.724	100	10	20148.66	3						0.095	
4961.379	10	2	20150.06	3						0.162	
4960.421	40b	10	20153.95	7							1.083
4958.093	50	2	20163.42	2					0.360		
4957.293	75	5	20166.67	3						0.890	
4946.663	100	100	20210.02	7							1.297
4945.458	200r	10	20214.93	2	2	0.741	3	1.182			
4943.064	200b	10	20224.72	1	2	1.321	3	1.084			
4939.642	300r	15	20238.73	2	4	0.865	5	1.074			
4939.270	75	2	20240.26	3						0.252	
4938.597	15	1	20243.02	3						0.129	
4937.829	300	8	20246.16	3	1	0.072	1	1.570			
4936.775	150	100	20250.49	1					0.188		
4933.003	20	1	20265.97	7					0.186		
4928.683	50	2	20283.73	7							1.150

TABLE 3. *Zeeman effect of* Th I—continued

Wavelength (Å)	Intensity		Wavenumber (cm^{-1})	Type	J_1	g_1	J_2	g_2	Δg	p	n
	Lamp	Spark									
4927.781	200	5	20287.45	3	2	0.779	2	0.910			
4927.299	50	1	20289.43	3						0.172	
4925.951	100	8	20294.98	7							1.017
4924.246	75b	2	20302.01	3						2.026	
4920.053	75b	25s	20319.31	2					0.180		
4911.380	200	10	20355.19	2					0.254		
4909.844	50	3	20361.56	2	1	0.751	2	1.131			
4907.209	100	4	20372.49	7							1.271
4907.044	50	2	20373.18	7							1.330
4901.987	50	2	20394.20	3						0.185	
4899.336	50	3	20405.23	3						0.341	
4899.240	50	3	20405.63	7							0.936
4892.758	50	2	20432.67	3						1.122	
4891.036	10	1	20439.86	7							1.089
4887.096	50	2	20456.33	7							1.210
4886.869	50	2	20457.29	3						0.354	
4886.133	25	2	20460.37	7							1.007
4881.204	75	2	20481.03	7					0.130		
4877.809	15	5	20495.28	3						0.092	
4877.265	20	1	20497.57	7							1.051
4876.495	100	5	20500.81	7							1.178
4876.244	50	2	20501.86	7							1.088
4874.365	150	10	20509.76	3					0.270	1.085	
4872.922	300r	25b	20515.84	1	1	1.467	2	1.246			
4872.030	100	4	20519.59	3						1.298	
4868.882	150	10	20532.86	3						0.114	
4865.974	50l	8l	20545.13	3						0.173	
4865.477	300r	150b	20547.23	2	4	0.862	5	1.088			
4861.720	75b	20h	20563.11	7					0.312		
4861.223	300r	50	20565.21	7							1.045
4852.868	200	50	20600.62	3						0.286	
4849.861	50	15	20613.39	3						0.648	
4849.139	50	25b	20616.46	2	4	0.684	5	0.848			
4848.363	400r	150	20619.76	3	2	1.253	2	1.512			
4847.330	150	15	20624.15	2					0.386		
4843.938	100b	50b	20638.59	7							1.171
4842.166	50	40	20646.14	7					0.256		
4840.928	100b	50	20651.43	3						0.812	
4833.674	20s	4s	20682.42	3						0.289	
4833.179	200b	50	20684.54	3						0.525	
4831.597	300r	150	20691.31	2	2	0.791	3	1.035			
4826.700	200b	50b	20712.30	3						0.931	
4823.997	200r	100h	20723.91	3						0.639	
4823.604	300r	75	20725.59	1							0.860
4822.855	300r	75	20728.81	7							1.187
4821.587	150	25	20734.26	1	2	1.386	3	1.082			
4820.463	150b	40h	20739.10	3						0.630	
4819.191	150	15	20744.57	1					0.123		
4817.017	75	8	20753.94	7							0.716
4814.919	15	3	20762.98	7							1.612
4813.893	200	100	20767.41	3						0.670	
4813.719	150	20	20768.15	7					0.220		
4813.004	75	15	20771.24	7					0.200		
4809.615	200	50	20785.88	2							1.352
4808.134	500r	150	20792.28	1	4	1.220	5	1.155			

TABLE 3. *Zeeman effect of* Th I—continued

Wavelength (Å)	Intensity		Wavenumber (cm^{-1})	Type	J_1	g_1	J_2	g_2	Δg	p	n
	Lamp	Spark									
4784.038	150	20	20897.00	3						0.671	
4778.294	400r	50	20922.12	3	2	0.736	2	1.169			
4775.313	100l	5b	20935.18	7					0.370		
4766.600	300-	100	20973.45	3	1	0.760	1	1.481			
4764.344	200	300	20983.38	3						0.830	
4758.145	100	75	21010.72	7							0.878
4749.968	300b	50	21046.89	1	3	1.216	4	1.064			
4749.200	400r	150	21050.30	3	4	0.858	4	0.972			
4743.693	150w	300	21074.73	7					0.250		
4741.301	150	40	21085.36	3						0.112	
4739.674	300	40	21092.60	1	1	1.802	2	1.188			
4737.915	150	15-	21100.43	7							1.212
4734.046	200	10	21117.67	3						0.100	
4729.128	400b	100b	21139.64	1	3	1.028	4	0.865			
4723.438	800r	200	21165.10	2	2	0.728	3	1.298			
4722.089	300	50	21171.15	2	2	1.135	3	1.251			
4721.276	200	15	21174.79	3	2	0.779	2	1.049			
4712.481	300b	100	21214.31	2					0.175		2.053
4706.575	100	5	21240.93	3						0.298	
4695.456	200	50	21291.23	3						0.315	
4695.039	300r	100	21293.12	1	2	1.244	3	1.073			
4691.883	100	8	21307.44	3						0.171	
4691.631	300b	50b	21308.59	2	2	1.015	3	1.219			
4691.500	100	15	21309.18	7							1.174
4689.252	200l	50b	21319.40	1							0.033
4686.195	500r	50	21333.30	2	3	1.079	4	1.373			
4683.349	200	20	21346.27	2					0.210		
4682.229	150	15	21351.37	3						0.292	
4678.233	150	20b	21369.61	7							1.120
4676.971	150	25b	21375.38	7							1.116
4676.056	500r	150	21379.56	3						0.425	
4673.661	800r	150	21390.52	1							0.975
4673.042	200	25	21393.35	3						0.102	
4669.984	500r	100	21407.36	3						0.120	
4668.172	800r	150	21415.67	2	2	0.941	3	1.241			
4666.797	500r	150	21421.97	2	2	0.867	2	1.004			
4663.202	300r	10	21438.49	1	2	1.510	3	1.080			
4658.522	100	8	21460.03	7							1.102
4658.376	100	5b	21460.70	7							1.002
4655.210	200	20	21475.30	2							1.338
4650.233	200	5	21498.28	2	1	0.064	2	0.988			
4649.975	100	8	21499.47	3						0.153	
4647.249	200	20	21512.08	1	2	1.261	3	1.091			
4643.557	150	10	21529.19	2							1.273
4641.244	400b	150b	21539.92	2							1.284
4639.896	100	25	21546.18	3						0.118	
4639.520	300	50	21547.92	3						0.420	
4638.686	150	10	21551.79	3						0.236	
4633.765	300b	75b	21574.68	7							0.981
4631.644	200	50	21584.56	7							0.880
4624.314	100	4	21618.78	3						0.162	
4621.165	150	40	21633.51	7							0.886
4620.448	200	10	21636.86	3						0.110	
4615.334	200	15	21660.84	3	1	1.063	1	1.483			
4615.025	200	40	21662.29	7							1.004

TABLE 3. *Zeeman effect of* Th I – continued

Wavelength (Å)	Intensity		Wavenumber (cm^{-1})	Type	J_1	g_1	J_2	g_2	Δg	p	n
	Lamp	Spark									
4613.605	200	15	21668.96	1	1	1.584	2	0.744			
4610.628	300b	50	21682.95	3						0.113	
4608.620	150	8	21692.39	3						0.319	
4603.143	300b	100b	21718.20	1	1	1.335	2	0.774			
4599.704	100	10	21734.44	3						0.515	
4595.420	800r	200	21754.70	1	2	1.240	3	1.084			
4593.645	300	150	21763.11	2	2	0.863	3	1.055			
4592.668	500r	150	21767.74	2	2	0.782	3	1.077			
4570.972	500r	200	21871.05	7							1.199
4567.240	300	100	21888.92	2					0.310		
4561.348	500r	200	21917.20	7							1.208
4558.346	300	40	21931.63	2					0.280		1.966
4551.473	200	75	21964.75	2					0.148		
4548.326	100b	10	21979.95	7							0.938
4545.915	200	300	21991.61	1					0.090		0.755
4544.512	150	200	21998.40	7							0.814
4540.999	300r	75	22015.41	3						0.207	
4535.255	300r	150	22043.30	2	1	0.621	2	0.772			
4530.319	200	100	22067.31	7							1.002
4519.259	300	75	22121.32	1	1	1.560	2	1.250			
4515.118	300r	50	22141.60	2	2	0.729	3	1.093			
4513.681	400r	150	22148.65	2	4	1.073	5	1.364			
4505.216	500	100	22190.27	2	3	1.092	4	1.306			
4499.984	500	200	22216.07	1	3	1.063	4	0.858			
4498.947	800r	200	22221.19	2	1	0.052	2	0.852			
4493.334	1000r	300	22248.95	3	2	0.738	2	1.141			
4489.664	200	100	22267.13	3						0.235	
4488.312	200	100	22273.84	2							1.621
4486.898	300r	100	22280.86	7							0.767
4485.713	150	40	22286.75	7							0.962
4482.169	400r	100	22304.37	3						0.227	
4480.823	200	200	22311.07	3						0.222	
4479.637	200	75	22316.98	2	2	0.989	3	1.051			
4478.594	150	40	22322.17	7							0.793
4475.221	200	40	22338.99	2	2	0.735	3	1.020			
4470.990	200	25	22360.14	2	1	0.956	2	1.191			
4469.526	400r	150	22367.46	3						0.395	
4468.320	200	50	22373.49	3						0.608	
4463.834	200	100	22395.98	7							1.070
4461.789	200b	100	22406.24	7							1.405
4461.528	200	150	22407.56	2	2	0.777	3	1.057			
4461.241	200	100	22409.00	1	2	1.244	3	0.994			
4459.004	100	75	22420.24	3	1	0.729	1	0.931			
4458.736	150	75	22421.59	3	1	0.723	1	1.482			
4458.002	600r	200	22425.28	3	2	0.980	2	1.250			
4457.236	200	100	22429.14	7							0.942
4452.565	200	100	22452.66	3	3	1.082	3	1.388			
4445.032	200	75	22490.71	1					0.650		
4443.665	150	100	22497.63	1	1	1.463	2	1.018			
4443.086	20	200	22500.56	3						0.272	
4438.746	400	200	22522.56	2	2	1.000	3	1.180			
4432.252	400	150	22555.56	3						0.112	
4424.836	200b	50	22593.36	2	2	0.984	3	1.187			
4423.719	400	150	22599.07	2	1	0.712	2	1.252			
4422.048	600	200	22607.61	7							0.772

TABLE 3. *Zeeman effect of* Th I—continued

Wavelength (Å)	Intensity		Wavenumber (cm^{-1})	Type	J_1	g_1	J_2	g_2	Δg	p	n
	Lamp	Spark									
4420.256	200	20	22616.77	7							1.209
4416.844	500	100	22634.24	2	4	1.141	5	1.362			
4414.486	500d	150	22646.34	7							0.804
4408.883	800r	200	22675.12	3	2	1.036	2	1.256			
4402.927	500	150	22705.79	7							0.976
4401.581	500	200	22712.73	2	4	0.885	5	1.126			
4393.759	400	150	22753.16	3	3	1.084	3	1.244			
4392.974	400	100	22757.23	3	4	0.854	4	1.194			
4391.390	150	50	22765.44	3						0.395	
4388.967	50	25	22778.00	7							1.032
4387.734	150	40	22784.40	2	1	0.071	2	1.541			
4384.656	150b	50b	22800.40	7							1.106
4380.289	200	25	22823.13	3	2		2			1.396	
4376.532	100	20	22842.73	7							1.287
4374.124	600r	150	22855.30	2	2	0.738	3	1.133			
4373.041	200	50	22860.96	1							0.771
4369.288	50b	25	22880.59	3						0.134	
4365.930	600	150	22898.19	2	2	0.778	3	1.093			
4359.372	600r	100	22932.64	2							1.151
4358.321	500	150	22938.17	3	2	0.732	2	1.159			
4354.483	400	100	22958.39	7							0.953
4353.449	300b	100b	22963.84	3	2	1.102	2	1.253			
4351.466	100	50	22974.30	7							1.177
4349.072	400	40	22986.95	3						0.142	
4348.599	400	75	22989.45	1	1	0.798	2	0.934			
4346.432	500r	200	23000.91	1	1	1.468	2	1.187			
4345.851	150	50	23003.99	3						0.582	
4343.381	100	25	23017.07	7							1.430
4342.445	500r	100	23022.03	1	2	0.777	3	1.074			
4340.896	200	40	23030.24	1	4	1.057	5	0.945			
4338.108	400	100	23045.04	3						0.130	
4337.277	800r	100	23049.45	1	1	1.356	2	0.726			
4332.339	150	40	23075.73	2	1	1.480	2	1.710			
4330.844	300	25	23083.70	3	4		4			1.307	
4328.915	300r	25	23093.98	3	2	0.733	2	1.320			
4327.715	150	25	23100.39	1	2	1.414	3	1.048			
4327.036	100	25	23104.01	7							1.135
4325.274	200	50	23113.42	3						0.639	
4320.738	75	8	23137.69	7					0.374		
4315.254	500r	150	23167.09	3	3	0.954	3	1.077			
4314.319	300	50	23172.11	1	3	1.122	4	1.072			
4312.992	800r	200	23179.24	7							1.208
4311.798	300	100	23185.66	1	1	1.294	2	0.774			
4311.625	150b	25	23186.59	7							1.396
4311.062	150	15	23189.62	3						0.139	
4308.121	300	100	23205.45	2							1.348
4307.176	600r	200	23210.54	2	5	1.041	6	1.192			
4306.365	200b	200b	23214.91	1					0.285		
4304.955	150	10	23222.51	3	1	1.164	1	1.467			
4304.417	100	25	23225.42	7							1.013
4303.096	50	8	23232.55	7							0.487
4299.839	500r	100	23250.15	1							0.796
4299.633	200	50	23251.26	7							1.570
4297.307	300b	75	23263.85	3	5	1.042	5	1.180			
4293.770	10	3	23283.01	7							1.376

TABLE 3. *Zeeman effect of* Th I—continued

Wavelength (Å)	Intensity		Wavenumber (cm^{-1})	Type	J_1	g_1	J_2	g_2	Δg	p	n
	Lamp	Spark									
4291.810	400	100	23293.64	2	2	0.790	3	0.899			
4289.655	100	40	23305.34	2	3	0.884	4	1.152			
4288.669	200	75	23310.70	2	2	0.927	3	1.248			
4288.471	200b	50b	23311.78	2							1.106
4287.082	200	40	23319.33	2							1.499
4286.229	200b	75b	23323.97	2	2	1.020	3	1.251			
4283.103	200b	50b	23340.99	7							1.340
4280.568	300r	100	23354.81	2	1	0.062	2	0.943			
4278.324	500r	200	23367.07	3	5	1.044	5	1.144			
4272.875	400r	50	23396.86	2	3	1.138	4	1.309			
4269.943	300	75	23412.92	1							1.000
4262.611	200	2	23453.20	2					0.170		
4260.984	100	2	23462.15	2	2		3		0.220		
4260.332	600r	5	23465.74	2	4	1.170	5	1.364			
4259.494	200	1	23470.36	7					0.216		
4258.521	400	2	23475.73	2	4	0.862	5	1.087			
4257.496	600r	4	23481.37	1	1	0.839	2	0.728			
4256.254	500r	8	23488.23	3	3	1.102	3	1.248			
4253.539	600r	20	23503.22	3						0.129	
4250.315	800r	75	23521.04	2	2	0.724	3	1.066			
4248.391	200	3	23531.70	3	4	0.880	4	1.160			
4235.463	600r	5	23603.52	3	2	0.732	2	1.375			
4230.427	500	5	23631.62	2					0.098		
4229.148	300r	4	23638.77	7							1.072
4228.761	150b	3	23640.93	3						0.522	
4227.387	400	8	23648.61	2	1	0.982	2	1.190			
4226.298	200	3	23654.71	2					0.107		
4221.691	75	2	23680.52	2	2	0.819	3	1.076			
4220.064	200	15	23689.65	2	1	0.064	2	0.979			
4216.068	300s	5	23712.10	1					0.080		
4214.828	200	4	23719.08	3						0.088	
4210.923	500r	10	23741.08	7							0.713
4210.765	400	10	23741.96	7							0.807
4210.455	75	2	23743.72	7							0.990
4208.412	150	4	23755.24	2					0.180		
4194.936	200	5	23831.55	2	4	0.861	5	1.111			
4187.142	50	3	23875.91	2	1	1.047	2	1.727			
4185.143	50	2	23887.31	3						0.304	
4184.603	50	3	23890.40	7							0.847
4179.314	100	8	23920.63	7					0.230		
4177.165	100	4	23932.94	3						0.256	
4170.533	500b	25	23970.99	3	4	1.111	4	1.205			
4165.766	800r	15	23998.42	3	4	0.869	4	1.090			
4162.509	400	15	24017.20	1	3	1.068	4	0.998			
4158.535	800	20	24040.15	3	5	1.119	5	1.362			
4157.280	150	5	24047.41	7							1.064
4154.719	200	5	24062.23	3						0.656	
4138.040	200	3	24159.22	3	1	1.030	1	1.478			
4136.432	200b	5b	24168.61	2	1	0.707	2	0.795			
4136.286	300	8	24169.46	2					0.104		
4134.062	200b	10b	24182.46	3	2	0.737	2	1.250			
4134.039	100b	8b	24182.60	7							2.397
4133.958	200	10	24183.07	3						0.420	
4131.207	50	2	24199.17	3						0.145	
4127.411	600b	40b	24221.43	7							0.876

TABLE 3. *Zeeman effect of* Th I—continued

Wavelength (Å)	Intensity		Wavenumber (cm^{-1})	Type	J_1	g_1	J_2	g_2	Δg	p	n
	Lamp	Spark									
4118.490	200	4	24273.90	2							1.156
4115.759	500r	50	24290.00	2	1	0.059	2	0.900			
4112.753	600b	15	24307.76	3	2	0.738	2	1.525			
4109.323	400r	5	24328.04	3						0.302	
4107.861	100	3	24336.70	2	1	1.024	2	1.250			
4107.050	40	2	24341.51	7							1.482
4102.617	400	3	24367.81	2	2	0.948	3	1.250			
4100.341	1000r	20	24381.33	3	2	0.734	2	1.252			
4099.553	100	4	24386.02	3	2	1.433	2	1.713			
4097.321	200	8	24399.30	2	2	1.014	3	1.192			
4096.077	150	4	24406.71	2	4	0.872	5	1.052			
4093.672	40	2	24421.06	2	2	0.741	3	1.172			
4091.737	40	2	24432.60	7							1.191
4087.285	200	5	24459.21	3						0.479	
4085.434	300r	10	24470.30	3						0.542	
4085.257	200	8	24471.36	2							1.472
4082.082	75	4	24490.39	2					0.085		1.413
4081.592	50	2	24493.33	3						0.197	
4081.368	800	8	24494.67	2					0.210		
4080.707	400	20	24498.64	2	4	0.866	5	1.186			
4080.359	100	4	24500.73	7							1.057
4078.875	75	4	24509.64	7							1.153
4073.856	200	3	24539.84	2	4	1.114	5	1.376			
4072.628	200s	5	24547.24	1							0.919
4071.750	200b	15	24552.53	2	2	0.758	3	1.145			
4070.756	100	2	24558.53	2	1	1.109	2	1.707			
4070.238	100	3	24561.65	2	2	0.735	3	1.189			
4067.451	400r	5	24578.48	7							1.098
4066.822	100	2	24582.28	7							1.110
4065.618	100	4	24589.56	3						0.550	
4064.332	400	10	24597.34	1	4	1.144	5	1.034			
4063.407	1500r	75	24602.94	2							1.279
4061.625	200	3	24613.73	7							1.210
4057.940	200	2	24636.08	1	2	1.405	3	0.985			
4057.327	50		24639.81	3	2	1.050	2	1.150			
4056.636	200	2	24644.01	3						0.183	
4054.302	200	8	24658.19	2	2	1.088	3	1.253			
4053.527	100	75	24662.91	3	4	0.862	4	1.133			
4050.888	800	25	24678.98	3						0.246	
4049.944	500	40	24684.72	1	1	1.802	2	1.252			
4048.432	800	50	24693.94	2	2	0.979	3	1.089			
4048.288	800	40	24694.83	3						0.322	
4047.058	50	1	24702.33	7							1.090
4046.824	200	15	24703.75	3						0.067	
4046.252	200	8	24707.25	2	1	0.760	2	1.036			
4045.226	200	2	24713.52	3						0.634	
4040.915	200	15	24739.88	2							1.067
4039.865	500	20	24746.31	1					0.060		
4038.960	100	2	24751.86	3						0.604	
4038.228	300	10	24756.34	1					0.390		
4037.562	500	15	24760.43	3	1	1.104	1	2.400			
4036.047	2000r	50	24769.72	2	2	0.744	3	1.143			
4035.352	150	5	24773.99	7	2			3	0.310		
4034.878	200	8	24776.90	3						0.789	
4033.907	600r	8	24782.86	2							1.381

TABLE 3. *Zeeman effect of* Th I—continued

Wavelength (Å)	Intensity		Wavenumber (cm^{-1})	Type	J_1	g_1	J_2	g_2	Δg	p	n
	Lamp	Spark									
4033.776	500	8	24783.67	3	1	1.082	1	1.477			
4032.595	600r	200	24790.92	2	3	1.013	4	1.312			
4029.827	400r	15	24807.95	1	1	1.481	2	1.128			
4029.658	400	15	24808.99	3	3	1.134	3	1.385			
4028.334	200	10	24817.15	3						0.258	
4027.546	150l	20	24822.00	3						0.163	
4027.007	500b	10	24825.32	3	2	1.104	2	1.248			
4026.159	150b		24830.55	7							1.042
4022.067	500b		24855.81	2	2	0.780	3	1.337			
4021.149	300	10	24861.49	7							1.297
4020.354	500	20	24866.41	3						0.172	
4019.862	200	10	24869.45	1	2	1.229	3	0.864			
4017.062	400	5	24886.78	1							0.485
4012.495	2000r	20	24915.11	2	2	0.856	3	1.074			
4011.739	500r	5b	24919.80	3						0.206	
4008.210	1500r	100	24941.74	2	4	0.860	5	1.136			
4005.960	300	8	24955.75	3	1	1.056	1	2.391			
4005.091	500	10	24961.16	2	1	1.096	2	1.255			
4003.574	400	25	24970.62	7							1.116
4001.894	300	2	24981.10	2	2	0.726	3	1.073			
4001.058	800r	40	24986.33	3	4	0.863	4	1.083			
4000.280	500	20	24991.18	1							0.767
4000.041	200b		24992.69	2					0.410		
3998.953	600	20	24999.48	3	4	1.157	4	1.322			
3998.657	300s	2	25001.33	2							1.273
3996.670	500	15	25013.76	3						0.129	
3991.731	800	40	25044.71	1	4	1.308	5	1.118			
3990.892	300	15	25049.97	3						0.991	
3990.809	300	25	25050.50	7							0.062
3990.492	800r	10	25052.48	1	1	1.476	2	0.947			
3987.219	100b	25	25073.05								0.862
3987.206	200b		25073.13	2	2	0.709	3	1.240			
3984.879	300		25087.77	7							0.941
3982.607	100	2	25102.08	1					0.268		
3975.831	150	5	25144.86	1							0.764
3975.468	200	20	25147.16	7							0.850
3974.829	200	4	25151.20	2					0.360		
3972.640	500	75	25165.06	2							1.772
3972.153	1500r	300	25168.14	2					0.350		
3971.136	100	4	25174.59	2							1.336
3969.665	300	15	25183.92	7							1.025
3967.797	100	3	25195.78	1	5	1.380	6	1.150			
3967.392	2000r	300	25198.35	3						0.393	
3966.334	200	4	25205.07	3						0.918	
3965.483	75	3	25210.48	3						0.219	
3964.329	200	3	25217.81	7							1.066
3964.030	300	15	25219.72	3						0.550	
3962.420	400r	15	25229.97	3	2	0.950	2	1.253			
3960.879	300	10	25239.78	7							1.110
3960.270	500	50	25243.66	1	2	1.275	3	1.005			
3959.300	1000r	100	25249.84	2	1	0.067	2	0.927			
3958.928	200	3	25252.22	3						0.349	
3957.798	100	2	25259.42	3						0.381	
3957.595	20h	5	25260.72	7							2.414
3957.059	100	20	25264.15	3						0.185	

TABLE 3. *Zeeman effect of* Th I—continued

Wavelength (Å)	Intensity		Wavenumber (cm^{-1})	Type	J_1	g_1	J_2	g_2	Δg	p	n
	Lamp	Spark									
3956.481	150	20	25267.83	7					0.284		
3956.005	400	10	25270.87	1							0.094
3955.891	400	50b	25271.60	3						0.570	
3955.170	800r	40	25276.21	3	5	1.095	5	1.361			
3954.727	150	2	25279.04	3						0.321	
3954.130	100	20	25282.86	3						0.228	
3953.338	400	20	25287.92	7							0.407
3952.761	500r	10	25291.62	3	1	0.876	1	1.486			
3950.804	300	8	25304.14	1					0.480		
3950.393	1000r	200	25306.77	3	2	0.742	2	1.166			
3949.975	50	2	25309.45	1							0.850
3948.133	500	40	25321.26	7					0.330		
3948.029	600r	15	25321.92	2	2	0.727	3	1.383			
3947.329	1000r	100	25326.42	2	4	1.213	5	1.359			
3946.481	400	10	25331.86	3	1	1.147	1	1.485			
3946.391	300	25	25332.44	7							1.281
3945.206	200	8	25340.04	1	3	1.118	4	0.882			
3944.253	500	20	25346.17	3	2	1.067	2	1.701			
3943.605	150	25	25350.33	7					0.170		
3942.072	500b	50	25360.19	7							0.838
3941.137	100	3	25366.21	2							1.953
3940.837	200	5	25368.14	2							1.309
3940.705	200	4	25368.99	3						0.794	
3939.538	75	2	25376.50	3						0.283	
3939.318	150	8	25377.92	2							1.150
3938.614	400b	150	25382.46	7					0.220		
3934.274	400b	50	25410.46	3						0.510	
3934.060	150	3	25411.84	1	2	1.198	3	1.008			
3933.970	150	5	25412.42	3	1	0.812	1	1.324			
3933.238	400	40	25417.15	1					0.202		
3932.911	1500r	200	25419.26	2	4	0.876	5	1.028			
3931.085	150	3	25431.07	3						1.241	
3930.658	100	3	25433.83	7							1.061
3930.331	150	20	25435.95	7							1.087
3928.865	300	50	25445.44	3						0.432	
3928.308	100	10	25449.05	3						0.476	
3927.806	400	10	25452.30	2	2	1.124	3	1.268			
3926.864	200	8	25458.40	1					0.350		
3926.056	20	1	25463.65	3						0.243	
3925.738	100	5	25465.70	3						0.247	
3925.219	600	50	25469.08	3						1.010	
3924.404	500l	10	25474.36	7							1.043
3923.799	500r	20	25478.29	1	2	1.543	3	1.083			
3922.747	50	2	25485.12	7							1.320
3922.394	100	8	25487.42	1	4	1.169	5	1.006			
3922.218	50	50	25488.56	2					0.160		1.504
3921.453	300	15	25493.53	1	1	1.248	2	0.966			
3920.442	300	15	25500.11	7							1.024
3920.058	300	10	25502.61	1					0.240		
3919.980	300	10	25503.11	7							1.145
3918.934	300	8	25509.92	3						0.243	
3918.498	300	300	25512.76	2	1	0.060	2	1.322			
3918.070	300	40	25515.54	3						0.307	
3916.417	800r	25	25526.31	1	1	1.066	2	0.738			
3915.848	200	15	25530.02	1	1	1.410	2	0.777			

TABLE 3. *Zeeman effect of* Th I—continued

Wavelength (Å)	Intensity		Wavenumber (cm^{-1})	Type	J_1	g_1	J_2	g_2	Δg	p	n
	Lamp	Spark									
3915.295	300	8	25533.63	3						0.106	
3914.291	50	3	25540.18	7							1.537
3913.865	100	10	25542.96	7							1.109
3913.823	75	20	25543.23	3						0.611	
3913.645	200l	5	25544.39	3						0.823	
3913.082	300	25	25548.07	1	1	2.398	2	1.067			
3911.950	300b	25	25555.46	7							1.101
3911.910	500r	40	25555.72	3	4	1.223	4	1.446			
3910.978	400b	10	25561.81	1					0.080		
3910.773	300	8	25563.15	2					0.210		
3910.251	50	2	25566.56	3						0.268	
3909.991	100	8	25568.26	3						0.623	
3909.139	300	20	25573.84	2	2	0.968	3	1.238			
3908.979	300	25	25574.88	1							0.626
3908.749	500	15	25576.39	7							1.118
3908.031	100	2	25581.09	7							1.002
3907.543	50	5	25584.28	3						0.420	
3907.160	200	10	25586.79	3						0.362	
3906.387	50	5	25591.85	7							1.055
3906.308	50	3	25592.37	3						0.686	
3905.298	100	2	25598.99	7							1.146
3903.916	200	5	25608.05	3						0.344	
3903.103	1000r	150	25613.39	1	3	1.113	4	0.856			
3902.788	200	10	25615.45	7							1.274
3902.171	500	50	25619.50	7							0.958
3901.662	500	15	25622.85	3	4	0.862	4	1.121			
3900.577	1000r	50	25629.97	2							1.595
3899.019	300	75	25640.21	3						0.948	
3898.795	300	100	25641.69	3						0.559	
3898.509	300b	100	25643.57	2							1.139
3897.778	200	5	25648.37	3						0.256	
3897.612	100	3	25649.47	7							1.169
3897.316	100	2	25651.41	7							0.907
3896.168	100	2	25658.98	7							1.029
3895.418	2000r	200	25663.91	3						0.305	
3894.022	40	2	25673.11	3						0.242	
3893.817	200	8	25674.47	3						0.163	
3893.651	300	40	25675.56	3						0.355	
3893.344	300	25	25677.59	2					0.268		
3892.708	200	8	25681.78	3						0.448	
3891.725	400	10	25688.27	7							0.993
3889.906	300	4	25700.28	3						0.188	
3889.542	200	8	25702.68	2							1.344
3888.242	20	1	25711.28	3						0.257	
3888.070	15	5	25712.41	7							1.041
3887.509	300	4	25716.12	7							1.208
3887.019	800r	100	25719.37	2							1.277
3886.917	800r	500	25720.04	3						0.238	
3886.256	300	8	25724.42	7							0.600
3886.064	75	25	25725.69	7					0.280		
3885.412	25	4	25730.00	3						0.548	
3885.224	200	5	25731.25	7					0.433		
3883.767	200	15	25740.90	2							1.696
3883.536	200	5	25742.44	3						0.933	
3882.853	25	1	25746.96	7							1.019

TABLE 3. *Zeeman effect of* Th I—continued

Wavelength (Å)	Intensity		Wavenumber (cm^{-1})	Type	J_1	g_1	J_2	g_2	Δg	p	n
	Lamp	Spark									
3882.324	200	8	25750.47	2							1.310
3881.792	100	2	25754.00	7					0.243		
3881.043	100	2	25758.97	1						0.485	0.662
3880.545	8	1	25762.27	3						0.126	
3880.323	100	3	25763.75	2					0.320		
3880.194	300	15	25764.61	7							1.116
3879.644	1000r	200	25768.26	1							0.987
3879.269	400	25	25770.75	2					0.266		
3878.662	400	150	25774.78	3	1	0.946	1	1.484			
3878.160	100	3	25778.12	7							1.121
3877.610	300b	15	25781.77	3						0.160	
3877.462	500	20	25782.75	2							1.720
3874.977	400	50	25799.29	7							1.208
3873.821	2000r	500	25806.99	7							1.085
3873.473	500r	50	25809.31	1	1	1.574	2	0.744			
3872.288	20	1	25817.21	7							1.040
3870.891	75		25826.53	7							1.062
3870.682	40	2	25827.92	7							1.230
3870.178	50	1	25831.28	7							0.707
3869.663	800r	50	25834.72	7							1.378
3868.389	200	2	25843.23	3						0.264	
3868.254	400	10	25844.13	2					0.191		
3866.907	500b	50	25853.13	1	2	1.151	3	1.004			
3866.771	200	2	25854.04	1					0.570		
3866.375	100	2	25856.69	3						0.136	
3864.837	200	25	25866.98	1							0.539
3862.654	200b	200	25881.28	7					0.150		
3862.419	500b	250b	25883.17	3						0.559	
3861.574	300b	40	25888.84	1							0.392
3861.502	300b	40	25889.32	3						0.371	
3861.051	200	2	25892.34	3						0.432	
3860.657	200	10	25894.98	3						0.240	
3859.466	40	5	25902.98	7							0.934
3858.358	200	150	25910.42	3	3	1.057	3	1.312			
3857.450	75	8	25916.51	7							1.161
3856.753	40	2	25921.20	3						0.350	
3856.622	200	15	25922.07	7							0.630
3856.354	200	40	25923.88	2	2	0.781	3	1.050			
3855.064	25	4	25932.55	3						0.640	
3854.289	100	5	25937.77	3						0.208	
3853.825	150b	15	25940.89	3						1.226	
3852.719	75	2	25948.34	7							1.254
3852.135	800r	50	25952.27	2	1	0.954	2	1.258			
3851.155	300	15	25958.87	1					0.410		
3850.690	50	2	25962.01	1	3	1.280	4	0.960			
3848.627	75	3	25975.92	3						0.300	
3847.617	500	10	25982.74	7							0.985
3846.886	1000r	100	25987.68	1	1	1.480	2	0.908			
3846.625	400	50	25989.44	3						0.116	
3845.092	400	10	25999.81	2							1.244
3844.933	400	15	26000.88	2							1.401
3844.571	50	1	26003.33	7							1.140
3843.507	200	8	26010.52	1					0.340		
3842.898	400r	75b	26014.65	3						0.074	
3840.613	200	75	26030.12	7					0.304		

201-606 O - 76 - 8

TABLE 3. *Zeeman effect of* Th I—continued

Wavelength (Å)	Intensity		Wavenumber (cm^{-1})	Type	J_1	g_1	J_2	g_2	Δg	p	n
	Lamp	Spark									
3840.430	300	250	26031.37	7							1.284
3838.801	50b	4b	26042.42	3						0.115	
3837.343	200b	5	26052.31	7							0.979
3837.024	200	3	26054.47	7							0.604
3836.584	800r	100	26057.46	7							1.211
3836.542	1000r	150b	26057.75	7							1.009
3836.213	100	4	26059.98	3						0.189	
3835.414	200	10	26065.41	7							1.000
3834.890	100	5	26068.97	7							0.707
3834.488	100	75	26071.51	7							1.168
3833.087	400	75	26081.24	3						0.213	
3832.583	200	3	26084.67	2					0.430		
3832.323	75	3b	26086.43	7					0.240		
3831.640	300	50	26091.08	7							1.111
3830.774	800r	150	26096.98	2	2	0.738	3	1.004			
3829.040	200	4	26108.80	3						0.250	
3828.385	3000r	300	26113.27	3	2	0.734	2	0.978			
3827.502	100	2	26119.29	2	1	0.733	2	1.083			
3826.368	400r	75	26127.03	1	2	1.205	3	0.866			
3825.515	200	25	26132.85	3						0.127	
3824.553	100b	10b	26139.43	7							1.201
3824.534	400b	15b	26139.56	7							1.188
3823.989	75	3	26143.29	3	1	0.696	1	1.096			
3823.067	500r	100	26149.59	3	1	0.062	1	1.157			
3822.709	300	25	26152.04	7					0.620		
3820.792	600r	75	26165.16	3	2	0.915	2	1.248			
3820.327	200	2	26168.34	7							0.836
3819.904	500	100b	26171.24	7							0.927
3819.189	200	10	26176.14	7							1.060
3818.685	400r	15	26179.60	1	4	1.204	5	0.939			
3817.478	400	40	26187.87	7							0.990
3817.117	300	8	26190.35	1	2	1.579	3	1.139			
3816.166	300	10	26196.87	1							0.696
3815.566	500	50	26201.00	3	2	0.772	2	1.099			
3813.815	500r	50	26213.02	3	2	0.718	2	1.008			
3812.667	75	5	26220.92	7							1.272
3812.398	400	40	26222.76	3						0.404	
3812.044	40	2	26225.20	3							1.612
3811.761	75	2	26227.15	3						0.255	
3810.995	600r	150	26232.42	7							1.202
3810.295	15	5	26237.24	3						0.372	
3808.614	500	20	26248.82	3						0.267	
3807.273	400	50	26258.07	2	4	1.100	5	1.369			
3806.317	100	1	26264.66	3						0.459	
3805.010	75		26273.68	2	2	1.052	3	1.262			
3804.699	500	50	26275.83	1							0.821
3804.127	400	20	26279.78	3						0.378	
3803.985	600r	150	26280.76	1	4	1.316	5	1.106			
3803.839	400	25	26281.77	3						0.694	
3801.571	400r	100	26297.45	7							0.902
3799.386	300	8	26312.57	7							1.029
3798.432	200	75	26319.22	1							0.582
3797.205	200	10	26327.68	3	5	1.072	5	1.372			
3796.687	400b	20	26331.27	7							1.111
3796.052	200	3	26335.68	3						0.717	

TABLE 3. *Zeeman effect of* Th I—continued

Wavelength (Å)	Intensity		Wavenumber (cm^{-1})	Type	J_1	g_1	J_2	g_2	Δg	p	n
	Lamp	Spark									
3795.386	600	100	26340.30	7							1.087
3794.981	200	3	26343.11	1					0.387		
3794.697	1500r	100	26345.09	3						0.341	
3793.815	300	25	26351.21	7							1.078
3793.504	200		26353.55	7							1.424
3793.097	300	10	26356.20	3						0.181	
3792.730	400l	75	26358.74	2	3	0.873	4	1.048			
3792.371	1000r	100	26361.24	7							0.986
3791.517	300	10	26367.18	2							1.649
3790.794	1500r	200	26372.21	1	3	1.032	4	0.860			
3790.356	300	40	26375.26	7							0.668
3787.638	300	40	26394.18	1							0.689
3787.218	75	2	26397.11	7					0.400		
3784.793	300	15	26414.02	1					0.570		
3784.574	400	20	26415.55	2							1.456
3784.138	50	2	26418.60	3						0.736	
3782.338	15	1	26431.17	7							1.134
3781.318	300	75	26438.30	3						0.216	
3780.966	300r	20b	26440.76	7							0.960
3780.147	200	8	26446.48	3						0.708	
3779.561	200	15	26450.59	2	4	1.023	5	1.208			
3778.498	300	2	26458.03	1							0.270
3778.045	300	15	26461.20	7							0.978
3777.745	200	40	26463.30	1					0.282		
3777.415	300	40	26465.61	3	3	0.794	3	1.254			
3777.184	400	8	26467.23	3						0.928	
3776.622	300	40b	26471.17	3						0.242	
3776.502	300	8	26472.01	7							0.722
3776.271	600r	150	26473.63	1					0.141		
3775.423	300	15	26479.58	2							1.278
3774.732	300	10	26484.42	7							1.070
3773.306	200	8	26494.43	3						0.376	
3772.649	400	10	26499.04	1	3	1.250	4	1.078			
3771.370	1500r	100	26508.03	2	2	0.734	3	1.074			
3770.722	100	2	26512.59	3						0.590	
3770.056	1500r	200	26517.27	3	1	0.053	1	0.783			
3768.047	200	8	26531.41	1	1	1.295	2	0.769			
3767.471	100	2	26535.46	3						0.312	
3766.447	300	10	26542.68	7							1.048
3765.412	400r	50	26549.98	1	2	1.686	3	1.084			
3764.193	200	8	26558.57	2	1	0.727	2	1.101			
3763.668	300	10	26562.28	7					0.104		
3762.257	200	8	26572.24	7							1.101
3761.704	200	20	26576.14	7							1.421
3761.470	200	25	26577.80	2	4	1.062	5	1.362			
3760.271	50b	25b	26586.27	3					0.130		
3758.706	400	20	26597.34	2	1	0.062	2	1.078			
3758.467	400r	25	26599.03	7							0.879
3757.694	1000r	200	26604.51	7							0.871
3756.451	200	8	26613.30	1					0.530		
3756.293	400	25	26614.43	7							1.019
3755.986	400	50	26616.60	3						0.296	
3755.211	800r	250	26622.09	7							1.017
3754.030	500r	50	26630.47	2	2	0.780	3	1.091			
3753.241	300	40	26636.07	1	3	1.041	4	0.853			

TABLE 3. *Zeeman effect of* Th I—continued

Wavelength (Å)	Intensity		Wavenumber (cm^{-1})	Type	J_1	g_1	J_2	g_2	Δg	p	n
	Lamp	Spark									
3752.789	300	8	26639.28	7							1.149
3751.121	300	25	26651.12	7					0.150		
3750.493	400	25	26655.58	1	5	1.353	6	1.020			
3749.617	300	20	26661.81	7							1.432
3749.514	300	10	26662.55	2						0.446	
3749.083	200	25	26665.61	2	4	0.860	5	1.170			
3748.820	100	8	26667.48	3						1.030	
3745.658	500r	100	26689.99	2							1.489
3745.176	400l	20	26693.43	3						0.279	
3744.910	300	10	26695.33	2	3	1.001	4	1.172			
3742.923	1000r	100	26709.49	7							1.198
3742.275	200	5	26714.12	1					0.255		0.364
3742.019	75b	5	26715.95	3						0.268	
3741.884	200	8	26716.91	2							1.282
3739.683	150	5	26732.63	3						0.374	
3738.436	150	2	26741.55	3						0.283	
3737.935	100	10	26745.14	1					0.400		0.516
3737.514	600r	75	26748.15	7							1.486
3736.502	200	40b	26755.39	7							0.922
3735.363	100	3	26763.55	3						0.351	
3734.664	75	3	26768.56	7							1.024
3733.672	300r	25	26775.67	7							1.066
3732.985	400r	40	26780.60	3	3	0.872	3	0.995			
3732.535	150	3	26783.82	3						0.443	
3729.945	400	40	26802.43	2	1	0.409	2	0.786			
3729.836	400	25	26803.21	7							1.172
3727.903	1000r	150	26817.10	3						0.518	
3725.966	75	2	26831.05	2	1	0.858	2	1.188			
3724.672	100	10	26840.36	3						0.181	
3724.397	100	2	26842.35	7					0.140		
3723.921	300s	8	26845.78	2	2	0.772	3	1.186			
3722.655	75	2	26854.91	3						0.094	
3722.179	300b	25b	26858.34	3						0.420	
3721.219	500r	50	26865.27	3						0.416	
3719.837	400r	40	26875.26	3						0.150	
3717.895	50	2	26889.29	3						0.143	
3717.384	100	3	26892.99	7							0.960
3716.583	300	40	26898.78	1							0.912
3715.862	300	20	26904.00	3						0.171	
3715.561	400	50	26906.18	3						0.590	
3715.060	100	2	26909.81	3						0.606	
3714.696	100	3	26912.45	1	3	1.165	4	0.857			
3712.373	100	3	26929.28	7							1.062
3710.292	300	8	26944.39	1							0.819
3709.861	300	25	26947.52	1	1	1.480	2	0.928			
3709.404	75	3	26950.84	3						0.542	
3708.396	200	5	26958.17	3						0.696	
3706.402	200	75	26972.67	3						0.429	
3705.979	150b		26975.74	1							0.706
3705.665	100	40	26978.04	7							1.248
3704.862	500r	50	26983.88	2	2	0.917	3	1.086			
3704.147	200	50	26989.09	2					0.075		1.294
3703.775	500r	50	26991.80	3						0.482	
3703.230	400r	25	26995.77	2					0.436		
3702.479	100	2	27001.25	3						0.544	

TABLE 3. *Zeeman effect of* Th I—continued

Wavelength (Å)	Intensity		Wavenumber (cm^{-1})	Type	J_1	g_1	J_2	g_2	$\Delta\sigma$	p	n
	Lamp	Spark									
3700.978	500		27012.20	7							1.327
3699.881	500r	50	27020.21	3	4	1.066	4	1.210			
3699.355	300	5	27024.05	3						0.440	
3699.182	500	75	27025.31	2						0.151	
3699.048	300	5	27026.29	2							1.518
3698.106	1000r	150	27033.17	3	5	1.168	5	1.362			
3695.288	500r	75	27053.79	2	4	0.872	5	1.113			
3694.177	400r	75	27061.93	7							1.034
3693.993	400r	200	27063.27	3	1	0.971	1	1.471			
3693.804	200b	25	27064.66	3						0.424	
3693.523	300l	25b	27066.72	3						0.824	
3693.247	200	10	27068.74	1	1	2.399	2	1.027			
3691.876	400r	100	27078.79	1	3	1.099	4	0.869			
3691.613	500r	200	27080.72	3						0.266	
3691.411	500r	50	27082.21	7							0.947
3690.624	600r	4	27087.98	1	1	1.164	2	0.734			
3690.115	200	300	27091.71	3						0.209	
3689.726	200	3	27094.57	7							1.106
3689.582	100	2	27095.63	1							0.916
3687.983	400r	75	27107.37	1	3	1.124	4	0.976			
3687.492	150b	5	27110.99	3						0.720	
3687.193	400l	20	27113.18	3						0.133	
3685.586	300b	10l	27125.00	3	2	0.931	2	1.252			
3685.214	200	4	27127.75	3						0.467	
3684.932	300	20	27129.82	7							1.052
3683.493	500	25	27140.42	7							0.999
3682.179	300	50	27150.10	7							1.324
3680.605	400r	40	27161.71	2	2	0.772	3	1.072			
3680.448	500r	50	27162.87	2							1.539
3679.544	400r	150	27169.54	7							1.036
3679.134	400	50	27172.57	7							0.967
3678.478	400r	50b	27177.42	1	1	1.158	2	0.773			
3677.304	150	4	27186.10	2					0.256		
3675.960	400	50	27196.04	1	2	1.715	3	1.315			
3675.790	400r	50	27197.29	2					0.310		
3675.137	500r	50	27202.12	3						0.445	
3674.891	300r	50	27203.95	3	5	1.137	5	1.361			
3674.089	300	40	27209.88	7							0.952
3674.013	300r	50b	27210.44	1	1		2		0.149		
3672.522	500	25	27221.50	1					0.130		
3672.300	500r	50	27223.14	3	3	1.090	3	1.249			
3670.654	15b		27235.35	2							1.422
3670.520	200	4	27236.34	7					0.365		
3669.640	400	50	27242.87	7							1.022
3668.390	300b	8	27252.16	3						1.176	
3667.882	20	4	27255.93	3						0.301	
3667.621	500	40	27257.87	1							0.603
3666.981	800r	75	27262.63	3	4	1.100	4	1.308			
3665.476	100b	10b	27273.82	2					0.170		1.821
3665.443	150b	500	27274.06	1	3	1.252	4	0.992			
3664.590	200	10	27280.41	7							1.103
3664.108	300	10	27284.00	1							0.875
3663.201	800r	100	27290.75	7							1.170
3662.955	150	15	27292.59	2					0.180		
3662.750	300r	20	27294.12	1	3	1.181	4	0.849			

TABLE 3. *Zeeman effect of* Th I—continued

Wavelength (Å)	Intensity		Wavenumber (cm^{-1})	Type	J_1	g_1	J_2	g_2	Δg	p	n
	Lamp	Spark									
3662.283	100	3	27297.59	2					0.116		
3660.500	400	25	27310.89	1	1	1.496	2	1.186			
3660.091	200b	4	27313.95	3						0.523	
3659.629	600r	150	27317.39	2	2	0.737	3	1.087			
3658.808	400r	25	27323.52	2							1.468
3657.641	200s	10	27332.24	1	4	1.306	5	1.062			
3657.054	300	20	27336.63	2							1.206
3655.125	300	50	27351.05	1	3	1.250	4	1.066			
3654.461	500r	50	27356.02	3						0.084	
3653.916	20	1	27360.10	7							0.974
3653.586	40		27362.57	1					0.340		
3653.366	150	3	27364.22	7					0.050		
3651.570	100		27377.68	7							1.256
3650.204	300l	2	27387.93	3						0.136	
3649.735	1000r	100	27391.45	1	1		2		1.040		
3648.856	150	8	27398.04	3						0.165	
3647.932	300	50	27404.98	3						0.210	
3647.575	300	15	27407.67	7							1.025
3646.268	300	8b	27417.49	1	2	1.194	3	1.000			
3645.706	300	15	27421.72	2	4	0.877	5	1.177			
3645.566	200	8	27422.77	7							1.177
3644.018	100	2	27434.42	1					0.273		
3643.512	600r	50	27438.23	7							1.276
3642.573	500r	50	27445.30	1							0.870
3641.363	100b	4	27454.42	7							0.855
3640.924	200	15h	27457.73	3	1	0.823	1	1.178			
3640.390	100	3	27461.76	7					0.660		
3639.867	400l	40	27465.70	2	3	0.901	4	1.043			
3638.644	500r	50	27474.93	1					0.186		
3638.319	400r	25	27477.39	3						0.244	
3638.146	200	4	27478.69	3						0.531	
3637.772	50b		27481.52	7					0.080		
3636.834	500r	25	27488.60	7							1.481
3636.295	150	3	27492.68	3						0.277	
3635.943	2000r	150	27495.34	7							0.614
3634.902	200	4	27503.22	1					0.194		
3634.582	600r	100b	27505.64	7							0.914
3633.910	100	3	27510.73	7					0.180		
3632.830	1000r	100	27518.90	2							1.207
3632.124	100	5	27524.26	7					0.080		0.836
3631.863	150	8	27526.23	3						0.055	
3631.708	100b	2	27527.41	3						0.372	
3630.986	25	2	27532.88	7							1.003
3630.851	25		27533.90	7							0.963
3629.851	400	20	27541.49	3	1	0.716	1	1.486			
3629.017	100	4	27547.82	3						0.668	
3628.867	100	4	27548.95	3						0.276	
3628.129	75	4	27554.56	7							1.254
3628.032	100	10	27555.30	7							1.035
3627.342	50	1	27560.54	3						0.227	
3626.939	300	50	27563.60	7							0.942
3626.471	200	10	27567.16	2							1.326
3625.895	500r	400b	27571.53	5	2	0.833	2	1.177			
3625.150	300	75	27577.20	1					0.270		
3625.026	300r	100	27578.15	3						0.091	

TABLE 3. *Zeeman effect of* Th I—continued

Wavelength (Å)	Intensity		Wavenumber (cm^{-1})	Type	J_1	g_1	J_2	g_2	Δg	p	n
	Lamp	Spark									
3624.472	300	50	27582.36	3	4	1.066	4	1.305			
3624.143	100	3	27584.87	3						0.485	
3623.773	300	25	27587.68	2	2	0.778	3	1.190			
3623.297	15	1	27591.31	3						0.174	
3622.795	600r	50	27595.13	1	2		3				0.803
3622.338	500r	20b	27598.61	3		0.06		1.33			
3622.338	500r	20b	27598.61	1		1.48		1.19			
3622.290	500r	50	27598.98	2	2		3				1.550
3621.435	50		27605.49	1							0.422
3620.839	300r	50	27610.04	1	3	1.062	4	0.858			
3619.211	200	40	27622.45	3						0.090	
3617.671	300	8	27634.21	3	2	0.775	2	1.412			
3616.177	200	8	27645.63	1					0.206		
3615.849	200	4	27648.14	2					0.372		
3614.352	500r	75	27659.59	7							1.215
3614.212	500r	75	27660.66	7							0.978
3612.864	600r	5	27670.98	7					0.476		
3610.650	300	20	27687.95	2							1.485
3608.377	800r	50	27705.39	1	5	1.360	6	1.123			
3607.819	75		27709.67	1							0.749
3606.793	200	4	27717.55	7							1.295
3606.090	200	3	27722.96	7							1.471
3605.820	150	4	27725.03	1					0.300		0.274
3605.194	500	40	27729.85	1							0.770
3604.680	600r	40	27733.80	1	1	1.468	2	1.216			
3604.064	200b		27738.54	3	3	1.077	3	1.243			
3602.909	100	40	27747.43	1							0.802
3602.328	20		27751.91	7							1.040
3601.770	200	10	27756.21	3						0.313	
3601.295	300	10	27759.87	7							0.954
3600.431	300	50	27766.53	3	5	1.361	5	1.037			
3599.723	300	20	27771.99	3						0.095	
3598.691	100	5	27779.96	3						0.182	
3598.523	150	10	27781.25	1	3	1.192	4	0.861			
3597.704	20	2	27787.57	3						0.281	
3597.021	75	2	27792.86	7							1.395
3596.536	100	5	27796.60	7							1.443
3595.975	150	5	27800.94	7					0.244		
3595.756	100	10	27802.63	2					0.265		
3595.617	500r	100	27803.70	3						0.109	
3594.985	300	20	27808.59	1	2	1.723	3	1.267			
3594.721	300	10	27810.63	1	1	0.972	2	0.740			
3592.777	800r	100	27825.67	1	4				0.160		
3592.122	75		27830.76	2					0.160		1.402
3591.253	200	50	27837.49	3						0.200	
3590.924	300		27840.04	2	3	0.878	4	1.042			
3589.992	200	20	27847.27	3	1	1.175	1	1.483			
3587.831	100	5	27864.04	7							1.266
3587.102	150	40	27869.70	7							1.071
3586.703	100		27872.80	3						0.406	
3586.478	150	4	27874.55	1	1	0.986	2	0.666			
3585.244	150	5	27884.15	3						1.220	
3585.050	20		27885.65	1					0.080		0.775
3583.298	150	10	27899.29	2							1.130
3583.100	600r	25	27900.83	3						0.229	

TABLE 3. *Zeeman effect of* Th I—continued

Wavelength (Å)	Intensity		Wavenumber (cm^{-1})	Type	J_1	g_1	J_2	g_2	Δg	p	n
	Lamp	Spark									
3581.353	150	25b	27914.44	2					0.110		1.562
3581.289	100	3	27914.93	7							1.141
3579.454	200		27929.25	7					0.300		
3577.746	200	8	27942.58	1	2	1.296	3	1.064			
3574.192	50		27970.36	7							0.872
3572.067	300	20	27987.00	3						0.515	
3571.008	300	10	27995.30	3						0.201	
3570.827	100		27996.72	7							1.054
3570.523	300	10	27999.11	3						1.141	
3570.357	500	10	28000.41	3						1.404	
3569.820	1000r	25	28004.62	1	1	1.470	2	0.937			
3569.207	75		28009.43	3	2	1.014	2	1.282			
3566.099	15		28033.84	2					0.088		1.226
3565.822	300	15	28036.02	7					0.332		
3564.508	100	10	28046.35	7							1.102
3564.235	200	8	28048.50	7							1.125
3563.911	200		28051.05	7							1.130
3563.375	600	75b	28055.27	3						0.162	
3563.299	200b	25	28055.87	3						0.117	
3562.599	75	5	28061.38	7							1.155
3562.253	100	8	28064.11	7							0.994
3561.780	500r	75	28067.83	2	2	1.020	3	1.213			
3561.408	200	8	28070.77	3						0.207	
3560.896	300	40	28074.80	7							0.958
3560.688	200	5	28076.44	1					0.267		
3558.638	100		28092.61	2					0.320		
3556.973	75	10	28105.76	7							1.205
3555.013	1000r	50	28121.26	7							1.091
3554.336	75s	2	28126.61	7							1.078
3553.960	20	2	28129.59	3						0.784	
3553.110	100	200	28136.32	3						0.163	
3551.744	75	2	28147.14	7							0.948
3551.401	1000r	150	28149.86	2							1.489
3550.783	200	40	28154.76	3						0.163	
3550.718	100s		28155.28	1	1	0.064	2	1.064			
3548.664	200	8	28171.57	1	1	0.062	2	1.298			
3547.918	300	15	28177.49	3						0.136	
3547.338	200b		28182.10	3	2	0.951	2	1.251			
3546.255	20		28190.71	3						0.306	
3545.958	500b		28193.07	1							0.831
3544.250	150	3	28206.65	1					0.244		
3544.018	800r	50	28208.50	1	4	1.314	5	1.136			
3543.208	150	3	28214.95	3					0.667	0.667	
3543.023	200	4	28216.42	3						0.699	
3542.498	500r	50	28220.60	2	2	1.013	3	1.171			
3539.843	300	25	28241.77	3						1.015	
3536.976	150	4	28264.66	3						0.149	
3535.250	150b		28278.46	7							0.967
3534.675	150b		28283.06	1							0.706
3534.210	100b	10	28286.78	1	1	2.390	2	1.195			
3533.600	40	3	28291.66	7							1.089
3533.181	200b	10	28295.02	1	1	1.483	2	1.080			
3531.450	1000r	50	28308.89	3						0.186	
3531.282	200	8	28310.24	3	3	1.111	3	1.240			
3530.514	800r	50	28316.39	7							1.051

TABLE 3. *Zeeman effect of* Th I—continued

Wavelength (Å)	Intensity		Wavenumber (cm^{-1})	Type	J_1	g_1	J_2	g_2	Δg	p	n
	Lamp	Spark									
3529.385	300l	40	28325.45	1	3	1.082	4	0.732			
3528.411	300	50	28333.27	2							1.547
3527.793	200	10	28338.23	2	4	0.857	5	1.041			
3526.764	300		28346.50	3						0.222	
3526.634	500r	10	28347.54	3	2	0.736	2	1.544			
3524.708	300	8	28363.03	2							1.217
3524.178	300	25	28367.30	3						0.660	
3523.758	300	8	28370.69	7							0.996
3523.505	300	50l	28372.72	1	1	1.812	2	0.738			
3523.022	75		28376.61	7							0.787
3521.059	500r	25	28 92.43	2	1	0.803	2	1.263			
3520.710	300	40	28395.24	3						1.151	
3518.885	400l	50	28409.97	3	2	0.788	2	1.206			
3517.961	200l	10	28417.43	3						0.194	
3517.257	40	3	28423.12	3						0.174	
3515.327	100	40	28438.72	7							1.025
3514.285	200	10	28447.16	7							0.974
3511.789	100	10h	28467.37	7							1.344
3511.157	800r	25	28472.50	3	2	1.075	2	1.249			
3510.729	75b		28475.96	7							1.125
3509.319	50		28487.41	7					0.060		
3509.089	500	25	28489.28	3	2	0.873	2	1.003			
3508.360	300	3	28495.20	1					1.183		
3508.100	300b		28497.30	3						0.133	
3507.520	100		28502.02	3						1.059	
3507.178	200	8	28504.80	3						0.133	
3506.345	300	10	28511.57	7							1.080
3506.132	300	3	28513.30	3	2	0.729	2	1.097			
3505.767	150	5	28516.27	1	1	1.475	2	1.025			
3504.992	300	8	28522.57	2	1	0.721	2	1.261			
3504.852	150	8	28523.71	1							0.745
3504.569	15		28526.02	3						1.254	
3503.786	500r	40	28532.40	1							0.948
3503.130	200	15	28537.74	7							1.136
3502.963	200	10	28539.10	7					0.104		
3499.821	200	5	28564.72	2	2	0.780	3	1.100			
3498.956	200b	20b	28571.78	3						0.322	
3498.621	800r	75	28574.51	3						0.358	
3496.811	500r	15	28589.31	2	2	0.746	3	1.179			
3496.060	200	10	28595.45	7					0.190		
3495.700	800r	25	28598.39	7							1.197
3494.801	100		28605.75	3	2	1.192	2	1.567			
3494.175	15	2	28610.87	3						0.334	
3492.158	25		28627.39	1					0.615		
3491.900	500	2	28629.51	2	3	1.017	4	1.210			
3490.848	50	1	28638.14	7					0.266		
3489.509	400	2	28649.13	1	1	1.076	2	0.730			
3488.834	500	3	28654.67	7							1.087
3487.991	150l	4	28661.60	3						0.539	
3486.551	1000r	10b	28673.44	3	2	0.738	2	1.123			
3486.269	50	1	28675.75	1							0.482
3486.210	50	1	28676.24	2	2	0.744	3	1.094			
3485.175	200b	2	28684.76	1							0.620
3484.732	200		28688.40	7					0.560		
3483.433	200b	1	28699.10	7							1.256

TABLE 3. *Zeeman effect of* Th I—continued

Wavelength (Å)	Intensity		Wavenumber (cm^{-1})	Type	J_1	g_1	J_2	g_2	Δg	p	n
	Lamp	Spark									
3481.620	100h		28714.04	7							1.108
3480.810	100		28720.72	7							0.940
3480.052	500	3	28726.98	7							1.581
3479.684	300	2	28730.02	1	2	1.195	3	1.072			
3478.612	150	1	28738.87	3						0.652	
3476.385	200	3	28757.28	2	3	0.860	4	1.010			
3474.530	200	3	28772.63	3						0.510	
3473.545	400	8	28780.79	3						1.515	
3472.691	150	4	28787.87	7							1.021
3471.959	500r	50l	28793.94	7							1.090
3471.001	300	15	28801.89	2							1.442
3470.568	300	20	28805.48	3	4	1.120	4	1.308			
3469.345	1000r	150	28815.63	7							1.237
3465.061	200b	25	28851.25	3	2	0.776	2	1.159			
3464.882	75		28852.74	3						0.184	
3462.981	100	2	28868.58	7							1.118
3461.574	200	3	28880.32	1	3	1.240	4	1.065			
3459.907	20	2	28894.24	3						0.237	
3458.752	15		28903.88	3						1.247	
3458.142	200	8	28908.98	7							1.194
3457.829	75		28911.60	3						0.248	
3457.434	150	5	28914.90	3						0.158	
3457.069	400r	25	28917.95	3	2	0.734	2	0.949			
3456.695	200b	8	28921.08	7							1.133
3455.612	200b	10	28930.14	3						0.269	
3455.273	20	5	28932.98	3						0.193	
3454.206	200	15	28941.92	3						0.448	
3452.335	25		28957.61	7							0.970
3452.207	75	1	28958.68	7							1.014
3451.308	100		28966.22	1	1	1.276	2	1.016			
3450.948	100	15	28969.25	3						0.158	
3450.268	150	8	28974.95	3	2	1.267	2	1.707			
3448.949	300	10	28986.03	2	4	0.864	5	1.118			
3446.546	300	8	29006.24	2	3	0.793	4	1.213			
3444.795	100	3	29020.98	3	2	0.720	2	0.984			
3443.980	100	8	29027.86	3						1.435	
3443.497	150l	2	29031.93	7							0.784
3443.409	200s	3	29032.67	7						0.474	
3442.305	25	1	29041.98	3						0.167	
3441.036	100	20	29052.69	3						0.488	
3440.070	25	3	29060.84	7							0.916
3435.487	25l		29099.61	7					0.231		
3434.727	200b	2	29106.05	7							0.997
3433.238	50		29118.68	7							0.822
3432.860	20	1	29121.88	7							0.590
3431.265	200	5	29135.42	7							0.816
3429.871	100b		29147.26	7							0.876
3429.574	200	10	29149.78	3						0.726	
3427.089	200s		29170.92	3	2	1.020	2	1.216			
3425.613	100	2	29183.49	3						0.966	
3425.435	150	15	29185.01	7							0.978
3425.140	200b	2	29187.52	3						0.302	
3421.678	200	4	29217.04	7							0.833
3420.372	200		29228.20	3						0.821	
3420.196	100	3	29229.70	7							1.080

TABLE 3. *Zeeman effect of* Th I—continued

Wavelength (Å)	Intensity		Wavenumber (cm^{-1})	Type	J_1	g_1	J_2	g_2	Δg	p	n
	Lamp	Spark									
3418.032	15		29248.21	3						0.462	
3417.498	400r	10	29252.78	3	2	0.733	2	0.978			
3416.595	150	3	29260.51	3						0.350	
3416.386	100b		29262.31	7							1.140
3415.885	500r	75	29266.60	3						0.282	
3414.299	75		29280.19	7							1.074
3412.181	200		29298.36	1					0.280		
3410.699	25		29311.09	3						0.236	
3410.184	150	3	29315.52	3	1	0.076	1	1.476			
3407.832	400b	10	29335.75	7							0.853
3406.978	10		29343.10	3						0.268	
3406.841	50		29344.29	7							1.066
3404.313	50		29366.08	3						0.263	
3403.903	200	8	29369.61	7							1.252
3400.680	25		29397.44	3						0.724	
3400.630	75	3	29397.88	3	1	1.109	1	2.408			
3399.041	100	4	29411.62	7							1.538
3398.545	1500r	50	29415.92	7							1.102
3395.986	200b	1	29438.08	7							0.959
3394.583	15	3	29450.24	3						0.332	
3393.993	200	2	29455.37	3						0.079	
3393.421	150	10	29460.33	7							1.036
3392.473	100	2	29468.57	7							1.168
3390.849	200	8	29482.67	7							1.043
3390.368	600r	75	29486.85	7							1.468
3389.038	300	8	29498.43	7							0.859
3388.348	50		29504.44	3						0.414	
3388.154	100b	5	29506.13	3						1.052	
3387.119	15		29515.14	7							0.949
3384.177	15		29540.80	3						0.495	
3383.586	200	8	29545.96	7							0.938
3382.829	15		29552.57	7							1.108
3381.907	25		29560.63	3						0.522	
3377.483	50	40	29599.35	1	1	2.407	2	1.351			
3375.587	200b		29615.97	2							1.623
3374.975	1500r	75	29621.34	7							1.283
3372.822	400r	100	29640.25	1							0.547
3370.887	100	5	29657.26	3						0.744	
3370.738	100	4	29658.58	7							0.482
3369.358	20		29670.73	7							1.192
3369.000	150	4	29673.87	3						0.427	
3368.318	10	3	29679.88	3						0.404	
3367.582	200r	10	29686.37	2	2	0.742	3	1.270			
3365.979	150	5b	29700.50	7							0.977
3365.337	400r	50	29706.17	2	2	0.724	3	1.084			
3365.137	300	15	29707.93	7							0.993
3364.154	20b	2	29716.62	2							1.294
3360.997	400r	150	29744.53	2	2	0.748	3	1.148			
3350.352	200	5	29839.04	3						0.193	
3348.288	40	1	29857.43	3	1	1.427	1	2.444			
3347.991	200	5	29860.08	7							1.018
3347.403	150		29865.32	1	4	1.303	5	1.078			
3345.170	150	3	29885.25	3						0.099	
3343.813	75s	3	29897.38	7							0.978
3343.499	150	5	29900.19	2							1.408

TABLE 3. *Zeeman effect of* Th I—continued

Wavelength (Å)	Intensity		Wavenumber (cm^{-1})	Type	J_1	g_1	J_2	g_2	Δg	p	n
	Lamp	Spark									
3343.344	200	10	29901.57	3						0.383	
3343.164	300	5	29903.19	2	2	1.244	3	1.004			
3342.898	20		29905.56	3						0.483	
3341.550	10	2	29917.63	3						1.118	
3341.205	50	2	29920.72	3						0.505	
3340.337	100b	1	29928.49	7							1.464
3340.021	15		29931.33	7							1.123
3339.257	15		29938.18	7							1.454
3337.275	200	5	29955.95	3						0.259	
3336.074	150		29966.74	3						0.607	
3335.694	150	4	29970.15	2	1	0.050	2	1.220			
3335.238	300	5	29974.24	2					0.210		
3332.479	100b	1	29999.06	7							0.952
3331.727	50	2	30005.83	7							1.074
3330.976	150	4	30012.60	7							0.998
3330.477	1500r	40	30017.10	2	2	0.733	3	1.129			
3329.728	300r	75	30023.85	3						0.705	
3327.527	50	2	30043.70	3						0.482	
3327.193	800r	25	30046.73	7							1.275
3322.093	400r	10	30092.85	7							1.139
3321.574	300r	40	30097.55	7							0.862
3320.879	20		30103.85	3						1.020	
3320.476	400r	25	30107.50	1							0.817
3320.301	600	500	30109.09	7							0.995
3319.572	50		30115.70	3						0.941	
3318.390	200	5	30126.43	7							0.993
3317.576	25		30133.82	7							1.051
3315.848	200	2	30149.52	2	1	0.733	2	1.027			
3314.793	400r		30159.12	7							1.044
3313.647	300r		30169.55	3						0.075	1.215
3313.437	50	4	30171.46	3						0.512	
3313.387	75b		30171.91	7							0.992
3313.073	200l	40	30174.77	2							1.575
3310.637	150d	15b	30196.98	3						0.587	
3310.446	100	10b	30198.72	7							1.298
3309.365	1000r	40	30208.58	3	2	0.744	2	1.095			
3305.303	400r	40	30245.71	3	1	0.846	1	1.481			
3304.238	3000r	200	30255.45	2	2	0.732	3	1.082			
3303.281	100	5	30264.22	7							1.048
3302.192	400r	5	30274.19	1							0.710
3301.651	1500r	150	30279.16	2							1.556
3300.775	75	4	30287.20	3						0.277	
3298.811	200	8	30305.22	1							0.809
3298.697	75	4	30306.27	3						0.178	
3296.372	150	8	30327.64	1					0.570		
3292.926	200	4	30359.39	3						0.635	
3291.410	50		30373.37	7					0.150		0.566
3291.037	40l	1	30376.81	7							1.087
3289.517	100	10	30390.85	3						0.332	
3283.671	100	4	30444.95	3						0.314	
3282.837	40	2	30452.68	3						0.398	
3281.049	400r	25	30469.28	7							1.060
3280.764	150b	20	30471.92	7							0.719
3279.025	75	4	30488.09	7							0.974
3278.733	100	25	30490.80	2							1.753

TABLE 3. *Zeeman effect of* Th I—continued

Wavelength (Å)	Intensity		Wavenumber (cm^{-1})	Type	J_1	g_1	J_2	g_2	Δg	p	n
	Lamp	Spark									
3277.702	50	3	30500.39	7							1.145
3276.721	300	5	30509.52	3						0.480	
3276.225	150	8	30514.14	7							1.328
3276.045	50	5	30515.82	3						0.287	
3272.027	800r	75	30553.29	3	2	0.730	2	1.044			
3271.892	300r	100	30554.55	7							1.080
3271.546	50	3	30557.78	2					0.280		
3270.874	150	10	30564.06	3						0.496	
3270.100	100	5	30571.20	3						0.665	
3265.604	20		30613.38	3						0.401	
3263.183	400r	20	30636.09	3						0.262	
3262.316	75	4	30644.24	7							1.256
3261.497	20		30651.93	3						0.301	
3259.061	600r	50	30674.84	7							0.961
3258.103	200r		30683.84	7							1.275
3256.503	20	3	30698.93	7							0.942
3255.920	150	8	30704.43	2					0.176		
3251.916	2000r	200	30742.23	7							1.156
3249.855	800r	25	30761.73	2	2	0.741	3	1.193			
3248.697	75b		30772.69	3						0.283	
3247.331	15		30785.64	7							0.964
3247.218	75	4	30786.71	3						0.072	
3245.994	200	8	30798.32	3						1.043	
3244.043	150	10	30816.84	3						0.255	
3243.916	50	5	30818.05	3						0.290	
3242.145	50	15b	30834.88	7							0.896
3240.644	400r	40b	30849.17	7							1.121
3238.934	400r	20	30865.45	1	2	1.307	3	1.095			
3236.573	100	8b	30887.96	1					0.240		
3234.996	400r	20	30903.02	1							1.030
3231.461	75		30936.83	7							1.049
3225.007	100	5	30998.74	2	1	0.866	2	1.194			
3222.807	200	15	31019.89	7							1.215
3221.291	400b		31034.49	7							1.128
3220.986	75b		31037.43	2							0.796
3219.490	20h	4	31051.85	7							0.859
3216.998	75	3	31075.91	3						1.185	
3215.778	100	100	31087.69	7							0.915
3214.648	150	5	31098.62	3						0.871	
3214.381	400r	25	31101.20	3						0.400	
3214.076	400r	50	31104.15	7							1.010
3211.997	100r	5	31124.29	3						0.131	
3210.779	200	5	31136.09	7							1.172
3207.938	50r	5	31163.67	3	2	0.878	2	1.262			
3202.521	200r	8	31216.38	3						0.653	
3198.969	75s		31251.04	3						0.214	
3198.694	50b		31253.73	7							0.806
3195.688	400r	50	31283.12	2	2	0.750	3	1.120			
3193.781	200r	5	31301.80	1	1	1.619	2	1.259			
3192.586	400r	20	31313.52	7							0.920
3189.711	200	8	31341.74	3						0.416	
3189.562	200	3	31343.20	7							1.109
3185.628	200	3	31381.91	3						3.269	
3184.843	300	8	31389.64	3						0.320	
3184.277	300	15b	31395.22	1					0.243		

TABLE 3. *Zeeman effect of* Th I—continued

Wavelength (Å)	Intensity		Wavenumber (cm^{-1})	Type	J_1	g_1	J_2	g_2	Δg	p	n
	Lamp	Spark									
3183.384	100	2	31404.03	7							1.056
3181.670	500r	20	31420.95	3						0.546	
3180.194	1000r	1500	31435.53	7							1.077
3178.622	200	4	31451.07	3						0.241	
3178.244	600r	100	31454.82	7							1.028
3177.402	100	2	31463.15	3	1	1.268	1	1.462			
3176.167	200r	5	31475.38	7							1.130
3174.840	200	4	31488.54	3						0.660	
3174.020	300	8	31496.68	3						0.142	
3173.427	500r	50	31502.56	7					0.220		
3171.276	500r	75	31523.93	2	2	0.743	3	1.108			
3168.342	100	2	31553.11	7							0.852
3165.048	150	3	31585.95	2	1	0.076	2	1.073			
3161.364	200d	5	31622.76	1	3	1.078	4	0.898			
3161.148	100	2	31624.93	3						0.795	
3158.394	100		31652.50	3					0.456		
3157.221	300r	8	31664.25	7							0.952
3156.866	300		31667.81	1	1	1.466	2	1.221			
3152.395	100	3	31712.73	1	1	1.175	2	0.745			
3152.295	100	3	31713.74	3						0.235	
3151.184	300	5	31724.92	3						0.459	
3151.017	200		31726.60	3						0.203	
3150.536	100	8	31731.44	7							1.157
3147.449	200	25	31762.56	7							1.149
3146.310	200r	8	31774.07	7							1.256
3145.637	400r	25	31780.86	2	2	0.738	3	1.175			
3144.145	100	3	31795.94	3						0.102	
3142.422	100	5	31813.37	3						0.482	
3139.892	150	100	31839.00	3	4	0.968	4	1.220			
3138.200	100	10	31856.17	7							1.088
3136.829	500r	8	31870.09	3	2	0.730	2	0.941			
3136.216	1000r	100	31876.32	7							1.088
3134.203	400	5	31896.79	2							1.160
3132.102	300	5	31918.19	7							1.477
3126.414	200	2	31976.26	3						0.485	
3124.986	75	2	31990.87	7					0.180		
3120.881	400r	25	32032.94	7							1.498
3116.352	300r	10	32079.50	3	4	1.008	4	1.213			
3116.263	500r		32080.42	7							0.674
3111.280	300	8	32131.79	7							1.202
3108.636	200	3	32159.12	3						0.139	
3108.504	300r	10	32160.48	3					0.340		
3104.966	100r	3	32197.13	2	2	0.761	3	1.155			
3102.125	200	20	32226.61	7						0.383	
3099.184	100	2	32257.20	3						0.322	
3098.726	300r	5	32261.96	2	3	1.070	4	1.200			
3098.119	100		32268.28	3						0.600	
3093.719	200	3	32314.17	3						0.159	
3092.828	300r	8	32323.48	2							1.382
3082.507	100b		32431.71	7							1.624
3079.574	150	2	32462.60	3						0.825	
3078.625	150b	2	32472.61	7							1.017
3077.718	300r	5	32482.17	2							1.483
3076.410	150	30	32495.98	3	1	1.116	1	1.493			
3075.687	100	3	32503.61	3						0.956	

TABLE 3. *Zeeman effect of* Th I—continued

Wavelength (Å)	Intensity		Wavenumber (cm^{-1})	Type	J_1	g_1	J_2	g_2	Δg	p	n
	Lamp	Spark									
3071.632	50		32546.53	7							1.225
3065.683	200r	2	32609.68	1					0.168		
3065.038	50	10	32616.54	7							1.164
3062.454	200r	2	32644.07	3						0.325	
3061.812	400r	3	32650.91	1					0.400		
3058.029	200r	2	32691.29	3						0.427	
3047.816	500r	2	32800.84	3						0.485	
3043.248	100	5	32850.07	7							1.928
3041.941	100		32864.19	7							1.121
3034.639	400r	2	32943.26	7							1.097
3032.016	100r	2	32971.76	3	1		1			0.700	
3031.195	100r	2	32980.68	3						0.654	
3030.487	400r	8	32988.39	3						0.218	
3029.477	100		32999.39	7							0.956
3027.896	150	3	33016.62	1					0.480		
3025.448	200r	2	33043.33	2	2	0.742	3	1.132			
3021.056	300	1	33091.37	7							1.401
3019.889	300		33104.15	7							1.028
3016.096	50		33145.79	7							1.297
3014.641	150r	1	33161.79	1					0.572		
3011.745	100s	1	33193.67	7							1.274
3008.924	200	2	33224.79	7							1.224
3006.634	200	2	33250.10	7							1.101
3006.164	300r	2	33255.29	7							1.455
3004.248	150r	1	33276.50	7							1.488
3003.210	200	1	33288.00	3						0.434	
3002.687	200r	2	33293.80	3						0.587	
3002.390	100r		33297.13	3						0.897	
2999.272	75	10	33331.71	3						0.329	
2998.147	200b	1	33344.21	3						0.507	
2997.196	100	8	33354.79	3						0.261	
2995.962	100	1	33368.53	7							0.803
2995.166	100	1	33377.40	7							0.862
2993.079	100		33400.67	7							0.966
2987.672	300r	2	33461.12	3						0.464	
2981.843	100	15	33526.52	7							0.788
2980.335	150	25	33543.48	7							1.399
2980.112	200r	2	33546.04	3						0.261	
2979.043	100b		33558.04	7							1.064
2973.675	100	1	33618.61	3						0.488	
2970.566	100	2	33653.79	7							1.150
2969.378	100	8	33667.26	3						0.618	
2963.608	75	8	33732.80	7							1.178
2963.442	75		33734.69	3						0.844	
2959.854	300	25b	33775.58	7							0.881
2959.137	200	2	33783.77	3						0.466	
2958.367	100b	2	33792.57	7							1.374
2957.332	150	10	33804.39	7							1.194
2943.729	400	3	33960.59	3						0.837	
2931.783	400	4	34098.96	7							0.685
2925.526	500r	5	34171.89	7							0.843
2918.922	200	20b	34249.20	7							1.167
2916.369	500r	10	34279.18	7							0.766
2909.103	300d	8d	34364.79	7							0.990
2907.451	100		34384.32	7							1.194

TABLE 3. *Zeeman effect of* Th I—continued

Wavelength (Å)	Intensity		Wavenumber (cm^{-1})	Type	J_1	g_1	J_2	g_2	Δg	p	n
	Lamp	Spark									
2905.097	100b	2	34412.18	7							1.238
2890.078	150r	5	34591.00	1					0.703		
2889.488	50	2	34598.07	7							1.506
2888.785	200	2	34606.48	7							1.396
2888.552	200	3	34609.28	7							1.307
2886.983	150b		34628.09	3						0.318	
2883.266	400	3	34672.72	7							1.329
2881.577	200	10	34693.04	7							0.912
2876.768	300	3	34751.04	7							1.073
2862.610	300r	20	34922.90	7							1.143
2860.776	100	2	34945.29	3						0.356	
2860.491	150	3	34948.77	7					0.697		
2850.597	300b	2	35070.06	3						0.820	
2848.084	300r	2	35101.01	7							1.426
2846.036	150	2	35126.26	3						0.980	
2843.906	300r	2	35152.58	7							1.234
2841.383	150h	2	35183.79	7							1.087
2832.314	1000r	400	35296.44	7							0.962
2829.346	150	10	35333.46	7							1.196
2828.502	200l	4	35344.00	7							1.079
2825.909	100b		35376.44	7							1.011
2808.323	200	2	35597.96	7							1.191
2804.912	200	2	35641.24	3						0.684	
2799.432	100	1	35711.01	7							0.990
2762.458	50r		36188.96	3						1.301	
2747.139	150b		36390.74	7							0.665

TABLE 4. *Classified lines of* Th I

Wavelength (Å)	Intensity		Wavenumber (cm^{-1})	Classification
	Lamp	Spark		
29662.822	0		3370.304	$9804_5 - 13175\frac{3}{4}$
28574.421	0		3498.679	$12847_3 - 16346\frac{3}{4}$
26734.663	0		3739.442	$7502_3 - 11241\frac{5}{8}$
26377.115	2		3790.131	$10414\frac{3}{4} - 14204_5$
25984.374	1		3847.417	$18549_2 - 22396\frac{1}{2}$
25971.332	0		3849.349	$14204_5 - 18053\frac{3}{4}$
25913.673	0		3857.914	$23113\frac{3}{4} - 26971_4$
25790.101	1		3876.399	$20522\frac{5}{8} - 24399_3$
25735.979	1		3884.551	$13962_1 - 17847\frac{1}{2}$
25561.646	1		3911.044	$17166_5 - 21077\frac{5}{8}$
25269.196	1		3956.308	$23015\frac{5}{8} - 26971_4$
25111.575	1		3981.141	$22399\frac{5}{8} - 26380_5$
25080.636	2		3986.052	$11877\frac{1}{2} - 15863_2$
25049.573	2		3990.995	$13175\frac{3}{4} - 17166_5$
25032.462	0		3993.723	$25690\frac{5}{8} - 29684_5$
24997.523	1		3999.305	$13847_2 - 17847\frac{1}{2}$
24973.732	1		4003.115	$26723\frac{5}{8} - 30726_7$
24931.344	1		4009.921	$15493_4 - 19503\frac{5}{8}$
24902.355	1		4014.589	$13945\frac{3}{4} - 17959_4$
24789.343	1		4032.891	$21890\frac{3}{4} - 25923_4$
24684.317	0		4050.050	$19227\frac{7}{8} - 23277_5$
24516.271	1		4077.811	$23113\frac{3}{4} - 27191_5$
24486.763	0		4082.725	$24259\frac{3}{4} - 28342_5$
24470.262	0		4085.478	$23481\frac{1}{2} - 27566_2$
24428.586	1		4092.448	$22163\frac{3}{4} - 26255_4$
24420.077	1		4093.874	$22877\frac{5}{8} - 26971_4$
24329.294	0		4109.150	$25575\frac{3}{4} - 29684_5$
24301.853	1		4113.790	$13297_4 - 17411\frac{5}{8}$
24262.390	1		4120.481	$18549_2 - 22669\frac{5}{8}$
24216.068	0		4128.363	$21575_2 - 25703\frac{3}{4}$
24172.879	2		4135.739	$13088_3 - 17224\frac{3}{4}$
24171.733	0		4135.935	$11601_1 - 15736\frac{1}{2}$
24138.665	0		4141.601	$24421\frac{5}{8} - 28562_4$
24136.264	3		4142.013	$20522\frac{5}{8} - 24664_3$
24120.715	1		4144.683	$17501\frac{5}{8} - 21645_4$
24007.982	4		4164.145	$6362_2 - 10526\frac{3}{4}$
23940.033	0		4175.964	$24182\frac{3}{4} - 28358_3$
23907.149	1		4181.708	$17959_4 - 22141\frac{5}{8}$
23865.994	0		4188.919	$22855\frac{3}{4} - 27044_3$
23781.839	4		4203.742	$13297_4 - 17501\frac{5}{8}$
23712.604	0		4216.016	$25336\frac{3}{4} - 29552_6$
23704.794	1		4217.405	$22163\frac{3}{4} - 26380_5$
23672.844	1		4223.097	$18809\frac{3}{4} - 23032_4$
23671.785	1		4223.286	$13175\frac{3}{4} - 17398_3$
23663.487	1		4224.767	$14206\frac{3}{4} - 18431_3$
23608.338	0		4234.636	$17411\frac{5}{8} - 21645_4$
23588.463	1		4238.204	$18431_3 - 22669\frac{5}{8}$
23551.636	1		4244.831	$15970_3 - 20214\frac{3}{4}$
23514.732	5		4251.493	$11241\frac{5}{8} - 15493_4$
23477.705	0		4258.198	$24421\frac{5}{8} - 28679_2$
23403.546	0		4271.691	$18930\frac{3}{4} - 23201_3$
23330.692	2		4285.030	$26645\frac{3}{4} - 30930_6$
23314.380	1		4288.028	$22508\frac{3}{4} - 26796_3$
23297.038	0		4291.220	$24850\frac{5}{8} - 29141_5$
23270.076	2		4296.192	$11197\frac{5}{8} - 15493_4$
23217.661	1		4305.891	$18549_2 - 22855\frac{3}{4}$
23175.469	3		4313.730	$16554_6 - 20867\frac{7}{8}$
23153.597	4		4317.805	$15736\frac{1}{2} - 20054_2$
23127.608	1		4322.657	$13088_3 - 17411\frac{5}{8}$
23121.211	0		4323.853	$25690\frac{5}{8} - 30014_4$
23085.081	0		4330.620	$14243\frac{1}{2} - 18574_1$
23007.044	1		4345.309	$27948\frac{3}{4} - 32293_5$
22978.346	0		4350.736	$17224\frac{3}{8} - 21575_2$
22964.759	1		4353.310	$21902\frac{3}{4} - 26255_4$
22900.906	2		4365.448	$21890\frac{3}{4} - 26255_4$
22900.565	0		4365.513	$15166\frac{3}{4} - 19532_4$
22875.089	0		4370.375	$17224\frac{3}{8} - 21594_3$
22864.133	2		4372.469	$25180\frac{7}{8} - 29552_6$
22860.040	0		4373.252	$24561\frac{5}{8} - 28934_3$
22855.180	2		4374.182	$18614\frac{1}{2} - 22988_2$
22851.632	3		4374.861	$8800_4 - 13175\frac{3}{4}$
22843.962	1		4376.330	$12847_3 - 17224\frac{3}{8}$
22834.596	2		4378.125	$3865_1 - 8243\frac{3}{8}$
22829.522	2		4379.098	$17959_4 - 22338\frac{3}{4}$
22806.940	0		4383.434	$21539\frac{3}{4} - 25923_4$
22785.721	1		4387.516	$14226_0 - 18614\frac{1}{2}$
22760.862	0		4392.308	$20522\frac{5}{8} - 24915_3$
22750.249	1		4394.357	$18699_2 - 23093\frac{3}{8}$
22723.153	0		4399.597	$14032\frac{3}{8} - 18431_3$
22710.196	3		4402.107	$9804_5 - 14206\frac{3}{4}$
22646.195	3		4414.548	$11802_2 - 16217\frac{3}{8}$
22616.700	1		4420.305	$13962_1 - 18382\frac{5}{8}$
22614.383	4		4420.758	$6362_2 - 10783\frac{3}{8}$
22544.420	1		4434.477	$25321\frac{5}{8} - 29756_4$
22537.763	3		4435.787	$15618\frac{5}{8} - 20054_2$
22518.913	0		4439.500	$17959_4 - 22399\frac{5}{8}$
22513.933	1		4440.482	$24701\frac{5}{8} - 29141_5$
22496.819	2		4443.860	$19588\frac{5}{8} - 24032_4$
22446.273	0		4453.867	$21594_3 - 26048\frac{3}{4}$
22439.688	0		4455.174	$15493_4 - 19948\frac{3}{4}$
22437.386	1		4455.631	$14243\frac{1}{2} - 18699_2$
22377.781	1		4467.499	$18809\frac{3}{4} - 23277_5$
22350.905	0		4472.871	$23093\frac{3}{8} - 27566_2$
22344.755	2		4474.102	$11877\frac{1}{2} - 16351_0$
22323.993	0		4478.263	$21902\frac{3}{4} - 26380_5$
22318.327	1		4479.400	$19273_2 - 23752\frac{3}{8}$
22283.623	0		4486.376	$13945\frac{3}{4} - 18431_3$
22215.926	1		4500.047	$18549_2 - 23049\frac{1}{2}$
22115.259	0		4520.531	$23752\frac{3}{8} - 28273_2$
22103.641	4		4522.907	$16554_6 - 21077\frac{5}{8}$
22082.481	1		4527.241	$25321\frac{5}{8} - 29849_4$
22073.514	1		4529.080	$19503\frac{5}{8} - 24032_4$
22029.034	0		4538.225	$21575_2 - 26113\frac{3}{8}$
21990.719	2		4546.132	$15166\frac{3}{4} - 19713_3$
21987.769	0		4546.742	$19713_3 - 24259\frac{3}{4}$
21987.769	0		4546.742	$26882\frac{5}{8} - 31429_1$
21986.275	0		4547.051	$21143_5 - 25690\frac{5}{8}$
21959.399	1		4552.616	$15970_3 - 20522\frac{3}{8}$
21952.080	1		4554.134	$17847\frac{1}{2} - 22401_1$
21944.958	4		4555.612	$3687_2 - 8243\frac{3}{8}$

201-606 O - 76 - 9

TABLE 4. *Classified lines of* Th I—continued

Wavelength (Å)	Intensity		Wavenumber (cm^{-1})	Classification
	Lamp	Spark		
21925.759	2		4559.601	$15863_2 - 20423^{\circ}_{1}$
21883.548	0		4568.396	$18069^{\circ}_{3} - 22637_3$
21862.515	1		4572.791	$23655^{\circ}_{4} - 28227_4$
21809.793	0		4583.845	$18053^{\circ}_{4} - 22637_3$
21756.165	1		4595.144	$17073_1 - 21668^{\circ}_{1}$
21749.619	1		4596.527	$15970_3 - 20566^{\circ}_{4}$
21747.329	1		4597.011	$17501^{\circ}_{5} - 22098_4$
21743.999	5		4597.715	$7280_2 - 11877^{\circ}_{1}$
21712.571	4		4604.370	$8243^{\circ}_{2} - 12847_3$
21706.674	1		4605.621	$14204_5 - 18809^{\circ}_{4}$
21706.264	1		4605.708	$23752^{\circ}_{2} - 28358_3$
21683.632	0		4610.515	$21143_5 - 25753^{\circ}_{6}$
21676.298	0		4612.075	$7502_3 - 12114^{\circ}_{2}$
21655.755	2		4616.450	$11601_1 - 16217^{\circ}_{2}$
21628.998	4		4622.161	$11241^{\circ}_{3} - 15863_2$
21605.654	1		4627.155	$24307^{\circ}_{2} - 28934_3$
21599.082	1		4628.563	$22637_3 - 27266^{\circ}_{4}$
21580.898	0		4632.463	$22338^{\circ}_{3} - 26971_4$
21556.115	0		4637.789	$21252^{\circ}_{2} - 25890_2$
21527.563	0		4643.940	$22877^{\circ}_{6} - 27521_4$
21519.111	0		4645.764	$23916^{\circ}_{4} - 28562_4$
21472.877	1		4655.767	$25355^{\circ}_{4} - 30011_3$
21442.806	1		4662.296	$18431_3 - 23093^{\circ}_{2}$
21424.751	0		4666.225	$22855^{\circ}_{3} - 27521_4$
21418.725	0		4667.538	$14032^{\circ}_{2} - 18699_2$
21415.242	2		4668.297	$19713_3 - 24381^{\circ}_{2}$
21406.777	1		4670.143	$19532_4 - 24202^{\circ}_{4}$
21375.118	3		4677.060	$9804_5 - 14481^{\circ}_{6}$
21353.185	3		4681.864	$18431_3 - 23113^{\circ}_{4}$
21328.149	0		4687.360	$23655^{\circ}_{4} - 28342_5$
21319.166	1		4689.335	$22877^{\circ}_{1} - 27566_2$
21260.824	0		4702.203	$24850^{\circ}_{6} - 29552_6$
21256.077	0		4703.253	$23655^{\circ}_{4} - 28358_3$
21250.077	0		4704.581	$25306^{\circ}_{2} - 30011_3$
21247.182	0		4705.222	$22338^{\circ}_{3} - 27044_3$
21239.694	1		4706.881	$23521^{\circ}_{3} - 28227_4$
21203.367	0		4714.945	$20054_2 - 24769^{\circ}_{3}$
21198.664	0		4715.991	$21539^{\circ}_{4} - 26255_4$
21173.002	1		4721.707	$15493_4 - 20214^{\circ}_{3}$
21148.510	3		4727.175	$23306^{\circ}_{8} - 28034_5$
21143.170	4		4728.369	$11241^{\circ}_{3} - 15970_3$
21132.654	2		4730.722	$19039^{\circ}_{2} - 23769_1$
21117.677	0		4734.077	$21143_5 - 25877^{\circ}_{4}$
21108.367	1		4736.165	$17166_5 - 21902^{\circ}_{4}$
21095.446	0		4739.066	$15493_4 - 20232^{\circ}_{2}$
21095.446	0		4739.066	$21645_4 - 26384^{\circ}_{4}$
21019.525	2		4756.183	$13297_4 - 18053^{\circ}_{4}$
21011.808	2		4757.930	$21165^{\circ}_{3} - 25923_4$
21009.229	1		4758.514	$13088_3 - 17847^{\circ}_{2}$
20981.790	0		4764.737	$17398_3 - 22163^{\circ}_{4}$
20973.743	1		4766.565	$13847_2 - 18614^{\circ}_{1}$
20965.562	1		4768.425	$21594_3 - 26363^{\circ}_{2}$
20951.480	1		4771.630	$13297_4 - 18069^{\circ}_{3}$
20920.513	1		4778.693	$26363^{\circ}_{2} - 31141_3$
20893.881	0		4784.784	$13175^{\circ}_{4} - 17959_4$
20879.577	1		4788.062	$21575_2 - 26363^{\circ}_{2}$
20869.452	4		4790.385	$17847^{\circ}_{2} - 22637_3$
20863.115	0		4791.840	$23481^{\circ}_{1} - 28273_2$
20862.579	2		4791.963	$22399^{\circ}_{6} - 27191_5$
20833.885	1		4798.563	$25753^{\circ}_{6} - 30552_4$
20792.737	1		4808.059	$14465^{\circ}_{2} - 19273_2$
20735.100	0		4821.424	$18699_2 - 23521^{\circ}_{3}$
20717.817	0		4825.446	$20054_2 - 24880^{\circ}_{1}$
20716.744	2		4825.696	$22669^{\circ}_{3} - 27495_4$
20715.963	0		4825.878	$25306^{\circ}_{2} - 30132_2$
20702.372	0		4829.046	$15493_4 - 20322^{\circ}_{6}$
20681.631	0		4833.889	$24850^{\circ}_{6} - 29684_5$
20680.125	4		4834.241	$7280_2 - 12114^{\circ}_{2}$
20661.764	1		4838.537	$20566^{\circ}_{4} - 25405_4$
20651.478	0		4840.947	$21539^{\circ}_{4} - 26380_5$
20634.364	6		4844.962	$8243^{\circ}_{2} - 13088_3$
20618.818	0		4848.615	$19713_3 - 24561^{\circ}_{3}$
20610.588	1		4850.551	$17398_3 - 22248^{\circ}_{2}$
20605.987	2		4851.634	$22669^{\circ}_{3} - 27521_4$
20584.349	0		4856.734	$24561^{\circ}_{3} - 29418_2$
20575.042	0		4858.931	$21252^{\circ}_{2} - 26111_1$
20562.003	0		4862.012	$16783^{\circ}_{4} - 21645_4$
20561.348	2		4862.167	$21645_4 - 26508^{\circ}_{3}$
20541.715	1		4866.814	$24274^{\circ}_{6} - 29141_5$
20513.976	0		4873.395	$15863_2 - 20737^{\circ}_{1}$
20489.032	1		4879.328	$6362_2 - 11241^{\circ}_{3}$
20478.858	1		4881.752	$24259^{\circ}_{4} - 29141_5$
20453.217	0		4887.872	$15166^{\circ}_{3} - 20054_2$
20450.008	1		4888.639	$19532_4 - 24421^{\circ}_{3}$
20428.437	1		4893.801	$21902^{\circ}_{4} - 26796_3$
20421.761	3		4895.401	$17959_4 - 22855^{\circ}_{3}$
20419.379	0		4895.972	$19503^{\circ}_{3} - 24399_3$
20392.064	0		4902.530	$26363^{\circ}_{2} - 31265_3$
20391.719	0		4902.613	$22141^{\circ}_{3} - 27044_3$
20381.309	3		4905.117	$21143_5 - 26048^{\circ}_{4}$
20377.894	1		4905.939	$21890^{\circ}_{3} - 26796_3$
20374.476	1		4906.762	$18574_1 - 23481^{\circ}_{1}$
20321.907	0		4919.455	$18069^{\circ}_{3} - 22988_2$
20317.777	4		4920.455	$23113^{\circ}_{4} - 28034_5$
20263.141	0		4933.722	$26995^{\circ}_{3} - 31929_3$
20234.945	0		4940.597	$17398_3 - 22338^{\circ}_{3}$
20205.662	0		4947.757	$25703^{\circ}_{2} - 30651_3$
20191.383	3		4951.256	$19039^{\circ}_{2} - 23990_2$
20183.242	0		4953.253	$27087^{\circ}_{1} - 32041_2$
20158.039	2		4959.446	$12114^{\circ}_{2} - 17073_1$
20139.866	1		4963.921	$18069^{\circ}_{3} - 23032_4$
20128.687	3		4966.678	$10526^{\circ}_{3} - 15493_4$
20122.241	0		4968.269	$20922^{\circ}_{2} - 25890_2$
20108.593	2		4971.641	$18549_2 - 23521^{\circ}_{3}$
20077.401	2		4979.365	$18053^{\circ}_{4} - 23032_4$
20047.945	2		4986.681	$24769^{\circ}_{3} - 29756_4$
19998.121	1		4999.105	$12847_3 - 17847^{\circ}_{2}$
19935.599	0		5014.783	$27948^{\circ}_{4} - 32963_5$
19922.803	1		5018.004	$23916^{\circ}_{4} - 28934_3$
19919.437	0		5018.852	$23015^{\circ}_{6} - 28034_5$

TABLE 4. *Classified lines of* Th I—continued

Wavelength (Å)	Intensity		Wavenumber (cm^{-1})	Classification
	Lamp	Spark		
19908.520	0		5021.604	$18011_{6} - 23032_{4}$
19902.706	4		5023.071	$14204_{5} - 19227_{6}$
19882.301	2		5028.226	$22163_{4} - 27191_{5}$
19862.586	0		5033.217	$24981_{5} - 30014_{4}$
19857.666	2		5034.464	$19273_{2} - 24307_{2}$
19852.906	2		5035.671	$23306_{6} - 28342_{5}$
19850.778	1		5036.211	$25336_{6} - 30372_{6}$
19847.455	0		5037.054	$24381_{2} - 29418_{2}$
19829.520	1		5041.610	$23521_{3} - 28562_{4}$
19797.857	0		5049.673	$23481_{1} - 28531_{2}$
19786.004	5		5052.698	$7795_{4} - 12847_{3}$
19784.595	1		5053.058	$18699_{2} - 23752_{2}$
19770.799	1		5056.584	$24084_{6} - 29141_{5}$
19765.178	3		5058.022	$21738_{2} - 26796_{3}$
19764.361	0		5058.231	$15863_{2} - 20922_{2}$
19762.115	0		5058.806	$22508_{2} - 27566_{2}$
19757.006	0		5060.114	$18930_{3} - 23990_{2}$
19741.428	5		5064.107	$8111_{4} - 13175_{4}$
19736.666	0		5065.329	$24769_{3} - 29835_{3}$
19733.467	1		5066.150	$26363_{2} - 31429_{1}$
19721.637	0		5069.189	$21902_{4} - 26971_{4}$
19705.256	0		5073.403	$15493_{4} - 20566_{4}$
19696.195	1		5075.737	$23603_{2} - 28679_{2}$
19692.738	1		5076.628	$13962_{1} - 19039_{2}$
19683.215	4		5079.084	$10414_{4} - 15493_{4}$
19676.823	1		5080.734	$10783_{2} - 15863_{2}$
19674.535	3		5081.325	$21890_{3} - 26971_{4}$
19669.905	2		5082.521	$13847_{2} - 18930_{3}$
19668.461	4		5082.894	$20322_{6} - 25405_{4}$
19643.457	1		5089.364	$18431_{3} - 23521_{3}$
19639.120	1		5090.488	$21165_{3} - 26255_{4}$
19622.548	0		5094.787	$22248_{2} - 27343_{3}$
19617.154	2		5096.188	$22399_{6} - 27495_{4}$
19595.083	3		5101.928	$18930_{3} - 24032_{4}$
19586.250	0		5104.229	$22508_{2} - 27612_{3}$
19571.602	2		5108.049	$19273_{2} - 24381_{2}$
19561.688	2		5110.638	$24307_{2} - 29418_{2}$
19535.499	0		5117.489	$26878_{3} - 31995_{4}$
19519.076	0		5121.795	$27674_{2} - 32796_{3}$
19505.411	0		5125.383	$22855_{3} - 27980_{3}$
19476.782	1		5132.917	$18069_{3} - 23201_{3}$
19444.483	1		5141.443	$17847_{2} - 22988_{2}$
19430.829	2		5145.056	$8800_{4} - 13945_{3}$
19420.664	1		5147.749	$19516_{2} - 24664_{3}$
19418.336	1		5148.366	$18053_{4} - 23201_{3}$
19400.479	3		5153.105	$20737_{1} - 25890_{2}$
19396.794	2		5154.084	$21890_{3} - 27044_{3}$
19391.319	1		5155.539	$18614_{1} - 23769_{1}$
19388.002	1		5156.421	$22877_{6} - 28034_{5}$
19345.173	0		5167.837	$22098_{4} - 27266_{4}$
19342.209	2		5168.629	$19532_{4} - 24701_{6}$
19336.983	0		5170.026	$22396_{1} - 27566_{2}$
19321.626	0		5174.135	$26363_{2} - 31537_{3}$
19317.885	3		5175.137	$17073_{1} - 22248_{2}$
19291.493	1		5182.217	$23752_{2} - 28934_{3}$
19290.328	0		5182.530	$22338_{3} - 27521_{4}$
19273.916	2		5186.943	$10783_{2} - 15970_{3}$
19264.749	1		5189.411	$20922_{2} - 26111_{1}$
19261.710	0		5190.230	$20214_{3} - 25405_{4}$
19261.001	0		5190.421	$23655_{4} - 28845_{4}$
19257.450	0		5191.378	$13847_{2} - 19039_{2}$
19256.382	1		5191.666	$18549_{2} - 23741_{1}$
19244.968	0		5194.745	$24561_{3} - 29756_{4}$
19244.035	1		5194.997	$15970_{3} - 21165_{3}$
19241.246	0		5195.750	$21594_{3} - 26790_{4}$
19240.420	0		5195.973	$11877_{1} - 17073_{1}$
19204.660	1		5205.648	$12847_{3} - 18053_{4}$
19190.670	2		5209.443	$27084_{6} - 32293_{5}$
19178.389	2		5212.779	$23015_{6} - 28227_{4}$
19162.549	1		5217.088	$26048_{4} - 31265_{3}$
19151.815	4		5220.012	$5563_{1} - 10783_{2}$
19147.846	3		5221.094	$12847_{3} - 18069_{3}$
19143.281	1		5222.339	$18809_{4} - 24032_{4}$
19138.077	1		5223.759	$18053_{4} - 23277_{5}$
19138.077	1		5223.759	$23049_{1} - 28273_{2}$
19113.116	2		5230.581	$25321_{3} - 30552_{4}$
19091.898	0		5236.394	$23609_{6} - 28845_{4}$
19088.610	3		5237.296	$19532_{4} - 24769_{3}$
19080.012	1		5239.656	$24182_{2} - 29422_{1}$
19078.887	1		5239.965	$25690_{6} - 30930_{6}$
19074.406	3		5241.196	$14032_{2} - 19273_{2}$
19073.289	2		5241.503	$21143_{5} - 26384_{4}$
19050.366	0		5247.810	$14465_{2} - 19713_{3}$
19035.208	0		5251.989	$20054_{2} - 25306_{2}$
19033.646	1		5252.420	$24880_{1} - 30132_{2}$
19018.615	2		5256.571	$13175_{4} - 18431_{3}$
18984.562	0		5266.000	$18011_{6} - 23277_{5}$
18964.790	1		5271.490	$17398_{3} - 22669_{3}$
18958.367	1		5273.276	$22338_{3} - 27612_{3}$
18957.939	0		5273.395	$24561_{3} - 29835_{3}$
18942.594	0		5277.667	$26651_{2} - 31929_{3}$
18942.109	1		5277.802	$24274_{6} - 29552_{6}$
18938.047	1		5278.934	$23603_{2} - 28882_{2}$
18925.238	0		5282.507	$15970_{3} - 21252_{2}$
18919.776	2		5284.032	$12114_{2} - 17398_{3}$
18907.334	2		5287.509	$24561_{3} - 29849_{4}$
18904.263	0		5288.368	$19273_{2} - 24561_{3}$
18893.288	0		5291.440	$27260_{3} - 32551_{3}$
18886.685	6		5293.290	$7795_{4} - 13088_{3}$
18885.154	1		5293.719	$24838_{1} - 30132_{2}$
18865.586	3		5299.210	$16346_{3} - 21645_{4}$
18858.490	1		5301.204	$15863_{2} - 21165_{3}$
18850.731	2		5303.386	$21077_{6} - 26380_{5}$
18840.854	0		5306.166	$21738_{2} - 27044_{3}$
18824.439	0		5310.793	$22669_{3} - 27980_{3}$
18811.879	7		5314.339	$16783_{4} - 22098_{4}$
18802.414	3		5317.014	$16351_{0} - 21668_{1}$
18799.282	0		5317.900	$22248_{2} - 27566_{2}$
18788.340	0		5320.997	$18431_{3} - 23752_{2}$
18781.224	1		5323.013	$17073_{1} - 22396_{1}$

TABLE 4. *Classified lines of* Th I—continued

Wavelength (Å)	Intensity		Wavenumber (cm^{-1})	Classification	Wavelength (Å)	Intensity		Wavenumber (cm^{-1})	Classification
	Lamp	Spark				Lamp	Spark		
18772.446	3		5325.502	$14206\frac{8}{4} - 19532_4$	17987.035	1		5558.042	$22669\frac{8}{3} - 28227_4$
18763.740	0		5327.973	$13945\frac{8}{3} - 19273_2$	17976.979	4		5561.151	$17959_4 - 23521\frac{8}{3}$
18737.838	0		5335.338	$24421\frac{8}{3} - 29756_4$	17969.554	0		5563.449	$24981\frac{8}{3} - 30544_2$
18730.785	2		5337.347	$10526\frac{8}{3} - 15863_2$	17964.920	6		5564.884	$4961_4 - 10526\frac{8}{3}$
18689.399	0		5349.166	$16554_6 - 21903\frac{8}{7}$	17962.477	0		5565.641	$19273_2 - 24838\frac{8}{1}$
18685.648	0		5350.240	$26645\frac{8}{6} - 31995_4$	17960.037	0		5566.397	$26363\frac{8}{2} - 31929_3$
18685.274	1		5350.347	$22877\frac{8}{6} - 28227_4$	17955.860	2		5567.692	$20543\frac{8}{6} - 26111_1$
18664.162	2		5356.399	$20566\frac{8}{4} - 25923_4$	17893.451	0		5587.111	$13945\frac{8}{3} - 19532_4$
18657.231	2		5358.389	$22163\frac{8}{4} - 27521_4$	17887.982	3		5588.819	$20522\frac{8}{2} - 26111_1$
18651.748	0		5359.964	$19039\frac{8}{2} - 24399_3$	17886.677	2		5589.227	$18809\frac{8}{4} - 24399_3$
18625.408	0		5367.544	$26645\frac{8}{6} - 32012_4$	17886.181	0		5589.382	$24259\frac{8}{4} - 29849_4$
18595.874	3		5376.069	$18614\frac{8}{1} - 23990_2$	17883.051	2		5590.360	$14226_0 - 19817\frac{8}{1}$
18557.981	3		5387.046	$18382\frac{8}{6} - 23769_1$	17873.738	2		5593.273	$24421\frac{8}{3} - 30014_4$
18546.830	1		5390.285	$25336\frac{8}{6} - 30726_7$	17873.620	1		5593.310	$21902\frac{8}{4} - 27495_4$
18520.188	0		5398.039	$19516\frac{8}{2} - 24915_3$	17872.284	1		5593.728	$19713_3 - 25306\frac{8}{2}$
18509.757	1		5401.081	$23481\frac{8}{1} - 28882_2$	17854.649	2		5599.253	$24084\frac{8}{8} - 29684_5$
18490.644	4		5406.664	$8800_4 - 14206\frac{8}{4}$	17849.848	1		5600.759	$20322\frac{8}{6} - 25923_4$
18468.454	3		5413.160	$17224\frac{8}{2} - 22637_3$	17838.977	1		5604.172	$8243\frac{8}{2} - 13847_2$
18452.242	0		5417.916	$22855\frac{8}{3} - 28273_2$	17834.907	1		5605.451	$21890\frac{8}{3} - 27495_4$
18440.493	4		5421.368	$11802_2 - 17224\frac{8}{2}$	17827.385	1		5607.816	$18574_1 - 24182\frac{8}{2}$
18427.858	0		5425.085	$27674\frac{8}{2} - 33099_3$	17826.416	0		5608.121	$18699_2 - 24307\frac{8}{2}$
18396.840	0		5434.232	$17073_1 - 22508\frac{8}{2}$	17825.875	5		5608.291	$11802_2 - 17411\frac{8}{3}$
18348.035	1		5448.687	$19532_4 - 24981\frac{8}{3}$	17823.987	1		5608.885	$19713_3 - 25321\frac{8}{3}$
18339.435	0		5451.242	$25306\frac{8}{2} - 30758_2$	17788.214	2		5620.165	$21645_4 - 27266\frac{8}{4}$
18335.284	2		5452.476	$4961_4 - 10414\frac{8}{2}$	17783.170	4		5621.759	$17411\frac{8}{3} - 23032_4$
18334.595	0		5452.681	$24561\frac{8}{3} - 30014_4$	17778.391	1		5623.270	$11601_1 - 17224\frac{8}{2}$
18331.495	1		5453.603	$21890\frac{8}{3} - 27343_3$	17763.368	0		5628.026	$26384\frac{8}{4} - 32012_4$
18331.136	0		5453.710	$24381\frac{8}{2} - 29835_3$	17757.108	2		5630.010	$24381\frac{8}{2} - 30011_3$
18320.410	0		5456.903	$17398_3 - 22855\frac{8}{3}$	17752.753	1		5631.391	$21890\frac{8}{3} - 27521_4$
18301.976	1		5462.399	$26995\frac{8}{3} - 32458_4$	17744.898	5		5633.884	$17354\frac{8}{1} - 22988_2$
18293.550	1		5464.915	$22877\frac{8}{6} - 28342_5$	17742.618	0		5634.608	$22399\frac{8}{6} - 28034_5$
18286.901	1		5466.902	$20423\frac{8}{1} - 25890_2$	17720.358	2		5641.686	$22338\frac{8}{3} - 27980_3$
18281.471	1		5468.526	$24182\frac{8}{2} - 29650_2$	17717.673	0		5642.541	$19713_3 - 25355\frac{8}{4}$
18280.488	0		5468.820	$18930\frac{8}{3} - 24399_3$	17703.673	3		5647.003	$21143_5 - 26790\frac{8}{4}$
18274.319	0		5470.666	$22141\frac{8}{3} - 27612_3$	17688.744	2		5651.769	$21539\frac{8}{4} - 27191_5$
18225.855	1		5485.213	$18431_3 - 23916\frac{8}{4}$	17683.810	3		5653.346	$15490\frac{8}{6} - 21143_5$
18221.955	1		5486.387	$23655\frac{8}{4} - 29141_5$	17683.237	0		5653.529	$22877\frac{8}{1} - 28531_2$
18209.323	0		5490.193	$27061\frac{8}{2} - 32551_3$	17677.481	3		5655.370	$13847_2 - 19503\frac{8}{3}$
18173.926	1		5500.886	$26036\frac{8}{3} - 31537_3$	17670.229	1		5657.691	$24850\frac{8}{6} - 30508_5$
18170.303	1		5501.983	$21143_5 - 26645\frac{8}{6}$	17669.614	3		5657.888	$25306\frac{8}{2} - 30964_3$
18169.715	1		5502.161	$7795\frac{8}{4} - 13297_4$	17663.853	0		5659.733	$25877\frac{8}{4} - 31537_3$
18166.638	1		5503.093	$22855\frac{8}{3} - 28358_3$	17658.896	0		5661.322	$26113\frac{8}{2} - 31774_3$
18161.579	2		5504.626	$21539\frac{8}{4} - 27044_3$	17649.490	2		5664.339	$24880\frac{8}{1} - 30544_2$
18156.664	0		5506.116	$14206\frac{8}{4} - 19713_3$	17634.332	4		5669.208	$13847_2 - 19516\frac{8}{2}$
18135.791	1		5512.453	$13297_4 - 18809\frac{8}{4}$	17633.725	0		5669.403	$23752\frac{8}{2} - 29422_1$
18125.969	5		5515.440	$6362_2 - 11877\frac{8}{1}$	17627.118	0		5671.528	$21645_4 - 27317\frac{8}{3}$
18103.118	2		5522.402	$24850\frac{8}{6} - 30372_6$	17626.046	3		5671.873	$15493_4 - 21165\frac{8}{3}$
18087.083	2		5527.298	$24307\frac{8}{2} - 29835_3$	17623.094	6		5672.823	$7502_3 - 13175\frac{8}{4}$
18072.340	4		5531.807	$17501\frac{8}{5} - 23032_4$	17614.900	1		5675.462	$20214\frac{8}{3} - 25890_2$
18070.540	1		5532.358	$23609\frac{8}{6} - 29141_5$	17614.015	1		5675.747	$22855\frac{8}{3} - 28531_2$
18023.692	1		5546.738	$25180\frac{8}{7} - 30726_7$	17597.889	1		5680.948	$14032\frac{8}{2} - 19713_3$
18007.579	2		5551.701	$11802_2 - 17354\frac{8}{1}$	17595.542	1		5681.706	$18699_2 - 24381\frac{8}{2}$
18000.660	1		5553.835	$24202\frac{8}{4} - 29756_4$	17584.517	7		5685.268	$9804_5 - 15490\frac{8}{6}$
17993.769	3		5555.962	$10414\frac{8}{2} - 15970_3$	17575.945	1		5688.041	$20423\frac{8}{1} - 26111_1$
17991.742	0		5556.588	$26645\frac{8}{6} - 32202_5$	17573.115	3		5688.957	$20566\frac{8}{4} - 26255_4$

TABLE 4. *Classified lines of* Th I—continued

Wavelength (Å)	Intensity		Wavenumber (cm^{-1})	Classification
	Lamp	Spark		
17553.728	1		5695.240	$17959_4 - 23655\frac{5}{4}$
17552.671	4		5695.583	$17398_3 - 23093\frac{2}{2}$
17551.531	1		5695.953	$25575\frac{2}{4} - 31271_5$
17549.205	0		5696.708	$26096\frac{3}{3} - 31793_4$
17547.178	0		5697.366	$27266\frac{2}{4} - 32963_5$
17521.738	2		5705.638	$24838\frac{1}{1} - 30544_2$
17516.448	0		5707.361	$22855\frac{3}{3} - 28562_4$
17508.350	2		5710.001	$21902\frac{4}{4} - 27612_3$
17503.828	1		5711.476	$17166_5 - 22877\frac{6}{6}$
17492.573	2		5715.151	$17398_3 - 23113\frac{4}{4}$
17481.041	7		5718.921	$8243\frac{2}{2} - 13962_1$
17473.699	2		5721.324	$13088_3 - 18809\frac{2}{4}$
17441.114	0		5732.013	$23113\frac{4}{4} - 28845_4$
17437.704	1		5733.134	$18574_1 - 24307\frac{2}{2}$
17404.332	4		5744.127	$14204_5 - 19948\frac{2}{4}$
17401.230	1		5745.151	$26048\frac{4}{4} - 31793_4$
17388.612	0		5749.320	$25877\frac{3}{4} - 31626_5$
17385.370	4		5750.392	$25180\frac{0}{7} - 30930_6$
17381.909	7		5751.537	$16346\frac{4}{4} - 22098_4$
17380.610	5		5751.967	$6362_2 - 12114\frac{2}{2}$
17375.665	1		5753.604	$11601_1 - 17354\frac{1}{1}$
17372.868	1		5754.530	$20054_2 - 25809\frac{1}{1}$
17334.404	1		5767.299	$23916\frac{4}{4} - 29684_5$
17333.121	1		5767.726	$13945\frac{3}{3} - 19713_3$
17323.648	0		5770.880	$18431_3 - 24202\frac{3}{3}$
17311.753	1		5774.845	$24769\frac{3}{3} - 30544_2$
17307.662	7		5776.210	$17501\frac{0}{0} - 23277_5$
17290.627	1		5781.901	$14204_5 - 19986\frac{6}{6}$
17277.735	0		5786.215	$25355\frac{4}{4} - 31141_3$
17271.005	0		5788.470	$23093\frac{2}{2} - 28882_2$
17267.932	3		5789.500	$19532_4 - 25321\frac{5}{5}$
17264.172	3		5790.761	$17411\frac{3}{3} - 23201_3$
17261.632	0		5791.613	$21252\frac{2}{2} - 27044_3$
17227.152	0		5803.205	$25442\frac{3}{3} - 31245_2$
17225.670	3		5803.704	$17073_1 - 22877\frac{1}{1}$
17221.632	1		5805.065	$15863_2 - 21668\frac{1}{1}$
17217.782	2		5806.363	$21165\frac{3}{3} - 26971_4$
17216.726	0		5806.719	$18574_1 - 24381\frac{2}{2}$
17198.807	0		5812.769	$26645\frac{6}{6} - 32458_4$
17195.420	0		5813.914	$20566\frac{4}{4} - 26380_5$
17192.605	1		5814.866	$23603\frac{2}{2} - 29418_2$
17186.894	2		5816.798	$19588\frac{6}{6} - 25405_4$
17173.440	0		5821.355	$23113\frac{4}{4} - 28934_3$
17168.126	0		5823.157	$19532_4 - 25355\frac{4}{4}$
17165.765	2		5823.958	$22855\frac{3}{3} - 28679_2$
17163.009	1		5824.893	$24307\frac{2}{2} - 30132_2$
17153.591	2		5828.091	$18431_3 - 24259\frac{3}{4}$
17152.288	1		5828.534	$22399\frac{6}{6} - 28227_4$
17151.508	1		5828.799	$21738\frac{2}{2} - 27566_2$
17151.178	0		5828.911	$24182\frac{2}{2} - 30011_3$
17146.766	0		5830.411	$23015\frac{5}{6} - 28845_4$
17135.330	4		5834.302	$8111_4 - 13945\frac{3}{3}$
17134.167	4		5834.698	$23306\frac{6}{6} - 29141_5$
17133.189	1		5835.031	$25306\frac{2}{2} - 31141_3$
17124.268	1		5838.071	$15736\frac{1}{1} - 21575_2$
17121.318	3		5839.077	$22141\frac{5}{5} - 27980_3$
17120.840	0		5839.240	$27260\frac{3}{3} - 33099_3$
17120.083	1		5839.498	$23916\frac{4}{4} - 29756_4$
17113.542	2		5841.730	$13088_3 - 18930\frac{3}{3}$
17103.520	1		5845.153	$16554_6 - 22399\frac{6}{6}$
17088.335	2		5850.347	$22508\frac{2}{2} - 28358_3$
17085.097	0		5851.456	$24701\frac{0}{0} - 30552_4$
17078.798	3		5853.614	$16783\frac{4}{4} - 22637_3$
17075.750	3		5854.659	$13962_1 - 19817\frac{1}{1}$
17054.299	0		5862.023	$18699_2 - 24561\frac{3}{3}$
17028.599	1		5870.870	$22163\frac{4}{4} - 28034_5$
17026.334	1		5871.651	$18549_2 - 24421\frac{3}{3}$
17019.670	0		5873.950	$20922\frac{2}{2} - 26796_3$
17018.885	2		5874.221	$21738\frac{2}{2} - 27612_3$
17014.114	1		5875.868	$19039\frac{2}{2} - 24915_3$
17013.556	0		5876.061	$18431_3 - 24307\frac{2}{2}$
17012.360	0		5876.474	$24850\frac{8}{8} - 30726_7$
17008.562	2		5877.786	$24880\frac{1}{1} - 30758_2$
17005.290	2		5878.917	$27084\frac{8}{8} - 32963_5$
17004.697	3		5879.122	$21165\frac{3}{3} - 27044_3$
16997.972	0		5881.448	$24769\frac{3}{3} - 30651_3$
16989.777	1		5884.285	$25442\frac{3}{3} - 31326_4$
16976.362	0		5888.935	$22338\frac{3}{3} - 28227_4$
16964.222	0		5893.149	$26036\frac{3}{3} - 31929_3$
16960.892	1		5894.306	$21077\frac{6}{6} - 26971_4$
16952.178	0		5897.336	$23521\frac{5}{5} - 29418_2$
16949.485	0		5898.273	$23752\frac{2}{2} - 29650_2$
16945.150	0		5899.782	$26651\frac{2}{2} - 32551_3$
16938.730	3		5902.018	$19503\frac{3}{3} - 25405_4$
16918.744	0		5908.990	$26384\frac{3}{3} - 32293_5$
16915.692	0		5910.056	$25355\frac{4}{4} - 31265_3$
16915.097	1		5910.264	$19532_4 - 25442\frac{3}{3}$
16900.345	1		5915.423	$25355\frac{4}{4} - 31271_5$
16887.173	1		5920.037	$15970_3 - 21890\frac{3}{3}$
16883.454	0		5921.341	$18069\frac{3}{3} - 23990_2$
16879.312	2		5922.794	$17847\frac{2}{2} - 23769_1$
16875.970	0		5923.967	$25321\frac{3}{3} - 31245_2$
16852.625	2		5932.173	$15970_3 - 21902\frac{4}{4}$
16849.382	0		5933.315	$20322\frac{8}{8} - 26255_4$
16846.815	0		5934.219	$22338\frac{3}{3} - 28273_2$
16846.017	0		5934.500	$25336\frac{2}{2} - 31271_5$
16840.767	0		5936.350	$25690\frac{0}{0} - 31626_5$
16832.896	0		5939.126	$25306\frac{2}{2} - 31245_2$
16820.947	1		5943.345	$23609\frac{6}{6} - 29552_6$
16811.787	0		5946.583	$26790\frac{3}{3} - 32737_5$
16801.531	0		5950.213	$24182\frac{2}{2} - 30132_2$
16800.478	1		5950.586	$13088_3 - 19039\frac{2}{2}$
16785.229	2		5955.992	$21539\frac{4}{4} - 27495_4$
16785.046	2		5956.057	$15618\frac{3}{3} - 21575_2$
16782.389	1		5957.000	$17959_4 - 23916\frac{4}{4}$
16768.550	6		5961.916	$12847_3 - 18809\frac{3}{4}$
16761.533	0		5964.412	$26048\frac{4}{4} - 32012_4$
16748.433	5		5969.077	$11197\frac{6}{6} - 17166_5$
16747.499	2		5969.410	$13847_2 - 19817\frac{1}{1}$
16741.938	0		5971.393	$25355\frac{4}{4} - 31326_4$

TABLE 4. *Classified lines of* Th I—continued

Wavelength (Å)	Intensity		Wavenumber (cm^{-1})	Classification	Wavelength (Å)	Intensity		Wavenumber (cm^{-1})	Classification
	Lamp	Spark				Lamp	Spark		
16730.028	3		5975.644	$17073_1 - 23049^{\circ}_{1}$	16211.744	0		6166.683	$26384^{a}_{4} - 32551_3$
16724.318	1		5977.684	$17224^{a}_{2} - 23201_3$	16204.604	1		6169.400	$19273_2 - 25442^{a}_{3}$
16720.218	0		5979.150	$24307^{a}_{2} - 30286_1$	16195.248	1		6172.964	$26790^{a}_{4} - 32963_5$
16712.444	3		5981.931	$21539^{a}_{4} - 27521_4$	16188.147	0		6175.672	$22669^{a}_{3} - 28845_4$
16707.945	0		5983.542	$24981^{a}_{3} - 30964_3$	16180.368	0		6178.641	$21165^{a}_{3} - 27343_3$
16704.639	3		5984.726	$18930^{a}_{3} - 24915_3$	16178.472	2		6179.365	$22163^{a}_{4} - 28342_5$
16694.697	0		5988.290	$24769^{a}_{3} - 30758_2$	16172.466	1		6181.660	$25355^{a}_{4} - 31537_3$
16691.676	1		5989.374	$18431_3 - 24421^{a}_{3}$	16147.600	3		6191.179	$12847_3 - 19039^{a}_{2}$
16688.906	1		5990.368	$19713_3 - 25703^{a}_{2}$	16145.326	1		6192.051	$22338^{a}_{3} - 28531_2$
16687.560	0		5990.851	$24561^{a}_{3} - 30552_4$	16142.758	2		6193.036	$15970_3 - 22163^{a}_{4}$
16686.678	1		5991.168	$26790^{a}_{4} - 32781_4$	16140.194	0		6194.020	$23655^{a}_{4} - 29849_4$
16624.607	2		6013.537	$18614^{\circ}_{1} - 24627_1$	16137.810	0		6194.935	$24769^{a}_{3} - 30964_3$
16606.290	1		6020.170	$17073_1 - 23093^{a}_{2}$	16125.805	0		6199.547	$25575^{a}_{4} - 31774_3$
16604.436	1		6020.842	$18011^{a}_{0} - 24032_4$	16109.798	5		6205.707	$13297_4 - 19503^{a}_{3}$
16599.350	3		6022.687	$14032^{a}_{2} - 20054_2$	16100.958	0		6209.114	$23752^{a}_{2} - 29961_1$
16594.999	0		6024.266	$22248^{a}_{2} - 28273_2$	16084.899	0		6215.313	$25321^{a}_{3} - 31537_3$
16589.555	1		6026.243	$15863_2 - 21890^{a}_{3}$	16081.086	1		6216.787	$22141^{a}_{3} - 28358_3$
16587.815	3		6026.875	$15618^{a}_{3} - 21645_4$	16071.988	1		6220.306	$18549_2 - 24769^{a}_{3}$
16587.044	0		6027.155	$22855^{a}_{3} - 28882_2$	16070.913	0		6220.722	$23741^{\circ}_{1} - 29961_1$
16569.667	0		6033.476	$19273_2 - 25306^{a}_{2}$	16068.852	1		6221.520	$19532_4 - 25753^{a}_{0}$
16540.424	5		6044.143	$11802_2 - 17847^{a}_{2}$	16056.201	0		6226.422	$22877^{a}_{0} - 29104_4$
16538.399	3		6044.883	$16351_0 - 22396^{\circ}_{1}$	16048.543	1		6229.393	$24701^{a}_{0} - 30930_6$
16534.332	2		6046.370	$15493_4 - 21539^{a}_{4}$	16045.762	0		6230.473	$25306^{a}_{2} - 31537_3$
16531.417	1		6047.436	$23603^{a}_{2} - 29650_2$	16038.518	3		6233.287	$24274^{a}_{0} - 30508_5$
16521.658	1		6051.008	$24838^{\circ}_{1} - 30889_1$	16033.162	2		6235.369	$4961_4 - 11197^{a}_{0}$
16503.791	4		6057.559	$18614^{\circ}_{1} - 24671_2$	16014.426	2		6242.664	$17959_4 - 24202^{a}_{4}$
16501.244	0		6058.494	$20054_2 - 26113^{a}_{2}$	16008.311	3		6245.049	$18382^{a}_{0} - 24627_1$
16461.254	1		6073.212	$19817^{\circ}_{1} - 25890_2$	16006.680	0		6245.685	$23306^{a}_{0} - 29552_6$
16452.932	0		6076.284	$21594_3 - 27670^{a}_{3}$	16005.763	4		6246.043	$11601_1 - 17847^{a}_{2}$
16447.180	0		6078.409	$21902^{a}_{4} - 27980_3$	15997.841	2		6249.136	$16783^{a}_{4} - 23032_4$
16414.399	1		6090.548	$21890^{a}_{3} - 27980_3$	15978.393	2		6256.742	$17398_3 - 23655^{a}_{4}$
16412.823	3		6091.133	$21252^{a}_{2} - 27343_3$	15973.502	1		6258.658	$23752^{a}_{2} - 30011_3$
16403.906	0		6094.444	$23916^{a}_{4} - 30011_3$	15972.593	0		6259.014	$25753^{a}_{0} - 32012_4$
16394.343	1		6097.999	$24274^{a}_{0} - 30372_6$	15960.024	2		6263.943	$22877^{a}_{0} - 29141_5$
16390.870	0		6099.291	$21575_2 - 27674^{a}_{2}$	15954.449	4		6266.132	$11802_2 - 18069^{a}_{3}$
16375.188	1		6105.132	$18809^{a}_{4} - 24915_3$	15941.439	0		6271.246	$25355^{a}_{4} - 31626_5$
16363.631	2		6109.444	$22248^{a}_{2} - 28358_3$	15936.069	3		6273.359	$20522^{a}_{2} - 26796_3$
16340.749	2		6117.999	$14204_5 - 20322^{a}_{0}$	15925.011	1		6277.715	$15863_2 - 22141^{a}_{3}$
16329.816	2		6122.095	$20922^{a}_{2} - 27044_3$	15924.829	0		6277.787	$24274^{a}_{0} - 30552_4$
16326.067	2		6123.501	$24421^{a}_{3} - 30544_2$	15922.130	4		6278.851	$15970_3 - 22248^{a}_{2}$
16310.703	3		6129.269	$20867^{\circ}_{7} - 26997_6$	15919.042	1		6280.069	$4961_4 - 11241^{a}_{3}$
16308.851	2		6129.965	$18431_3 - 24561^{a}_{3}$	15915.448	1		6281.487	$18699_2 - 24981^{a}_{3}$
16304.920	0		6131.443	$24421^{a}_{3} - 30552_4$	15913.906	0		6282.096	$22248^{a}_{2} - 28531_2$
16304.149	3		6131.733	$21902^{a}_{4} - 28034_5$	15899.553	3		6287.767	$24084^{a}_{0} - 30372_6$
16297.533	0		6134.222	$22396^{\circ}_{1} - 28531_2$	15895.139	1		6289.513	$18549_2 - 24838^{\circ}_{1}$
16284.058	1		6139.298	$18699_2 - 24838^{\circ}_{1}$	15893.090	1		6290.324	$25336^{a}_{0} - 31626_5$
16280.282	3		6140.722	$17166_5 - 23306^{a}_{0}$	15891.854	3		6290.813	$16346^{a}_{4} - 22637_3$
16273.373	0		6143.329	$17847^{a}_{2} - 23990_2$	15891.564	4		6290.928	$13297_4 - 19588^{a}_{0}$
16270.823	0		6144.292	$26651^{a}_{2} - 32796_3$	15887.023	1		6292.726	$24259^{a}_{4} - 30552_4$
16263.051	1		6147.228	$23609^{a}_{6} - 29756_4$	15868.987	2		6299.878	$17959_4 - 24259^{a}_{4}$
16240.450	2		6155.783	$15490^{a}_{0} - 21645_4$	15861.758	1		6302.749	$21645_4 - 27948^{a}_{4}$
16238.115	3		6156.668	$11241^{a}_{3} - 17398_3$	15854.989	1		6305.440	$24202^{a}_{4} - 30508_5$
16234.453	0		6158.057	$19532_4 - 25690^{a}_{0}$	15847.733	3		6308.327	$20054_2 - 26363^{a}_{2}$
16220.740	3		6163.263	$22399^{a}_{6} - 28562_4$	15833.507	0		6313.995	$23521^{a}_{3} - 29835_3$
16217.564	0		6164.470	$19713_3 - 25877^{a}_{3}$	15832.882	0		6314.244	$21252^{a}_{2} - 27566_2$

TABLE 4. *Classified lines of* Th I—continued

Wavelength (Å)	Intensity		Wavenumber (cm^{-1})	Classification
	Lamp	Spark		
15831.752	7		6314.695	$5563_1 - 11877^{\frac{1}{2}}$
15825.176	2		6317.319	$12114^{\frac{3}{2}} - 18431_3$
15810.170	1		6323.315	$19713_3 - 26036^{\frac{3}{2}}$
15807.445	0		6324.405	$23093^{\frac{1}{2}} - 29418_2$
15804.308	1		6325.660	$21902^{\frac{3}{2}} - 28227_4$
15793.353	0		6330.048	$18069^{\frac{5}{2}} - 24399_3$
15792.250	0		6330.490	$21165^{\frac{3}{2}} - 27495_4$
15791.447	1		6330.812	$18549_2 - 24880^{\frac{1}{2}}$
15788.721	0		6331.905	$25442^{\frac{5}{2}} - 31774_3$
15781.849	1		6334.662	$19588^{\frac{5}{2}} - 25923_4$
15754.904	1		6345.496	$18053^{\frac{3}{2}} - 24399_3$
15743.881	2		6349.939	$24202^{\frac{3}{2}} - 30552_4$
15733.987	0		6353.932	$21594_3 - 27948^{\frac{3}{2}}$
15732.702	0		6354.451	$25575^{\frac{3}{2}} - 31929_3$
15728.365	0		6356.203	$23655^{\frac{3}{2}} - 30011_3$
15727.808	0		6356.428	$21165^{\frac{3}{2}} - 27521_4$
15720.977	1		6359.190	$23655^{\frac{3}{2}} - 30014_4$
15719.798	1		6359.667	$21252^{\frac{5}{2}} - 27612_3$
15713.149	4		6362.358	$14204_5 - 20566^{\frac{3}{2}}$
15702.559	1		6366.649	$8800_4 - 15166^{\frac{3}{2}}$
15701.306	3		6367.157	$13847_2 - 20214^{\frac{3}{2}}$
15697.019	1		6368.896	$15970_3 - 22338^{\frac{3}{2}}$
15696.943	1		6368.927	$23049^{\frac{1}{2}} - 29418_2$
15676.166	3		6377.368	$23306^{\frac{5}{2}} - 29684_5$
15662.128	0		6383.084	$21890^{\frac{5}{2}} - 28273_2$
15641.777	0		6391.389	$24259^{\frac{3}{2}} - 30651_3$
15641.344	3		6391.566	$23741^{\frac{1}{2}} - 30132_2$
15634.482	2		6394.371	$19986^{\frac{5}{2}} - 26380_5$
15628.272	3		6396.912	$15493_4 - 21890^{\frac{5}{2}}$
15621.888	0		6399.526	$22163^{\frac{3}{2}} - 28562_4$
15620.165	2		6400.232	$19713_3 - 26113^{\frac{3}{2}}$
15616.447	1		6401.756	$21165^{\frac{3}{2}} - 27566_2$
15608.939	2		6404.835	$20566^{\frac{3}{2}} - 26971_4$
15608.145	1		6405.161	$23609^{\frac{5}{2}} - 30014_4$
15602.299	0		6407.561	$17073_1 - 23481^{\frac{1}{2}}$
15598.808	4		6408.995	$7795^{\frac{3}{2}} - 14204_5$
15598.676	4		6409.049	$15493_4 - 21902^{\frac{3}{2}}$
15585.229	3		6414.579	$13088_3 - 19503^{\frac{3}{2}}$
15583.635	2		6415.235	$17354^{\frac{1}{2}} - 23769_1$
15576.584	6		6418.139	$16783^{\frac{3}{2}} - 23201_3$
15575.870	1		6418.433	$21077^{\frac{5}{2}} - 27495_4$
15574.463	1		6419.013	$25355^{\frac{3}{2}} - 31774_3$
15572.352	2		6419.883	$19503^{\frac{3}{2}} - 25923_4$
15572.117	4		6419.980	$16217^{\frac{5}{2}} - 22637_3$
15569.510	3		6421.055	$22141^{\frac{3}{2}} - 28562_4$
15568.155	0		6421.614	$20922^{\frac{3}{2}} - 27343_3$
15565.585	0		6422.674	$26645^{\frac{5}{2}} - 33068_6$
15553.233	2		6427.775	$15166^{\frac{3}{2}} - 21594_3$
15551.679	4		6428.417	$13088_3 - 19516^{\frac{5}{2}}$
15547.561	1		6430.120	$19273_2 - 25703^{\frac{3}{2}}$
15542.668	2		6432.144	$19948^{\frac{1}{2}} - 26380_5$
15537.904	0		6434.116	$22669^{\frac{3}{2}} - 29104_4$
15523.156	1		6440.229	$21902^{\frac{3}{2}} - 28342_5$
15516.436	6		6443.018	$7502_3 - 13945^{\frac{3}{2}}$
15513.174	1		6444.373	$21077^{\frac{5}{2}} - 27521_4$
15508.866	1		6446.163	$22399^{\frac{5}{2}} - 28845_4$
15505.455	0		6447.581	$26651^{\frac{3}{2}} - 33099_3$
15503.005	0		6448.600	$24202^{\frac{3}{2}} - 30651_3$
15499.015	1		6450.260	$24307^{\frac{5}{2}} - 30758_2$
15475.060	1		6460.245	$12114^{\frac{3}{2}} - 18574_1$
15473.472	1		6460.908	$16554_6 - 23015^{\frac{5}{2}}$
15473.326	1		6460.969	$13962_1 - 20423^{\frac{1}{2}}$
15472.864	3		6461.162	$17959_4 - 24421^{\frac{5}{2}}$
15456.917	1		6467.828	$25306^{\frac{3}{2}} - 31774_3$
15455.882	0		6468.261	$21890^{\frac{5}{2}} - 28358_3$
15454.759	0		6468.731	$24182^{\frac{5}{2}} - 30651_3$
15440.113	4		6474.867	$18930^{\frac{5}{2}} - 25405_4$
15439.546	2		6475.105	$15863_2 - 22338^{\frac{5}{2}}$
15429.783	7		6479.202	$15618^{\frac{5}{2}} - 22098_4$
15395.715	2		6493.539	$16783^{\frac{3}{2}} - 23277_5$
15390.079	0		6495.917	$24769^{\frac{5}{2}} - 31265_3$
15373.158	0		6503.067	$26048^{\frac{3}{2}} - 32551_3$
15364.893	1		6506.565	$22338^{\frac{5}{2}} - 28845_4$
15355.694	5		6510.463	$14226_0 - 20737^{\frac{1}{2}}$
15342.358	1		6516.122	$19532_4 - 26048^{\frac{3}{2}}$
15336.766	0		6518.498	$17398_3 - 23916^{\frac{3}{2}}$
15320.133	0		6525.575	$16351_0 - 22877^{\frac{1}{2}}$
15307.300	6		6531.046	$17501^{\frac{5}{2}} - 24032_4$
15297.656	0		6535.163	$21738^{\frac{5}{2}} - 28273_2$
15295.651	0		6536.020	$19273_2 - 25809^{\frac{1}{2}}$
15292.511	1		6537.362	$23015^{\frac{5}{2}} - 29552_6$
15291.203	2		6537.921	$13175^{\frac{3}{2}} - 19713_3$
15284.311	0		6540.869	$22877^{\frac{1}{2}} - 29418_2$
15282.038	2		6541.842	$9804_5 - 16346^{\frac{3}{2}}$
15278.264	1		6543.458	$22338^{\frac{3}{2}} - 28882_2$
15273.332	2		6545.571	$17224^{\frac{5}{2}} - 23769_1$
15265.258	0		6549.033	$24880^{\frac{1}{2}} - 31429_1$
15264.344	2		6549.425	$18431_3 - 24981^{\frac{5}{2}}$
15260.157	2		6551.222	$5563_1 - 12114^{\frac{3}{2}}$
15246.115	1		6557.256	$24769^{\frac{5}{2}} - 31326_4$
15239.289	4		6560.193	$13962_1 - 20522^{\frac{5}{2}}$
15215.038	0		6570.649	$23113^{\frac{3}{2}} - 29684_5$
15203.638	0		6575.576	$24182^{\frac{5}{2}} - 30758_2$
15195.303	0		6579.183	$17411^{\frac{5}{2}} - 23990_2$
15190.777	3		6581.143	$20214^{\frac{3}{2}} - 26796_3$
15190.369	2		6581.320	$13962_1 - 20543^{\frac{5}{2}}$
15167.182	0		6591.381	$26508^{\frac{3}{2}} - 33099_3$
15158.232	1		6595.273	$18809^{\frac{3}{2}} - 25405_4$
15157.340	0		6595.661	$18069^{\frac{5}{2}} - 24664_3$
15156.775	1		6595.907	$22338^{\frac{3}{2}} - 28934_3$
15143.355	2		6601.752	$17959_4 - 24561^{\frac{5}{2}}$
15137.607	0		6604.259	$21668^{\frac{1}{2}} - 28273_2$
15112.474	2		6615.242	$10783^{\frac{5}{2}} - 17398_2$
15100.835	2		6620.341	$21738^{\frac{5}{2}} - 28358_3$
15099.336	4		6620.998	$17411^{\frac{5}{2}} - 24032_4$
15095.376	1		6622.735	$25306^{\frac{3}{2}} - 31929_3$
15090.817	2		6624.736	$20566^{\frac{3}{2}} - 27191_1$
15065.723	1		6635.770	$17354^{\frac{1}{2}} - 23990_2$
15051.950	2		6641.842	$24084^{\frac{3}{2}} - 30726_4$
15049.671	2		6642.848	$23113^{\frac{3}{2}} - 29756_4$

TABLE 4. *Classified lines of* Th I—continued

Wavelength (Å)	Intensity		Wavenumber (cm^{-1})	Classification
	Lamp	Spark		
15045.413	3		6644.728	$20922\frac{5}{2}^{\circ} - 27566_{2}$
15037.137	0		6648.385	$15493_{4} - 22141\frac{3}{3}^{\circ}$
15035.312	0		6649.192	$20322\frac{5}{5}^{\circ} - 26971_{4}$
15031.317	1		6650.959	$13297_{4} - 19948\frac{3}{4}^{\circ}$
15021.804	3		6655.171	$12847_{3} - 19503\frac{3}{3}^{\circ}$
15017.893	0		6656.904	$24307\frac{5}{2}^{\circ} - 30964_{3}$
15010.031	3		6660.391	$21902\frac{3}{4}^{\circ} - 28562_{4}$
15007.406	0		6661.556	$14481\frac{3}{3}^{\circ} - 21143_{5}$
14994.654	3		6667.221	$19588\frac{5}{5}^{\circ} - 26255_{4}$
14994.569	2		6667.259	$17073_{1} - 23741\frac{1}{1}^{\circ}$
14990.632	1		6669.010	$12847_{3} - 19516\frac{2}{2}^{\circ}$
14988.603	4		6669.913	$15493_{4} - 22163\frac{3}{4}^{\circ}$
14984.882	4		6671.569	$11877\frac{1}{1}^{\circ} - 18549_{2}$
14982.726	1		6672.529	$21890\frac{3}{3}^{\circ} - 28562_{4}$
14980.034	0		6673.728	$25321\frac{3}{3}^{\circ} - 31995_{4}$
14977.332	3		6674.932	$22877\frac{5}{5}^{\circ} - 29552_{6}$
14968.497	2		6678.872	$17073_{1} - 23752\frac{2}{2}^{\circ}$
14960.529	0		6682.429	$22163\frac{4}{4}^{\circ} - 28845_{4}$
14956.476	2		6684.240	$24561\frac{3}{3}^{\circ} - 31245_{2}$
14955.641	1		6684.613	$26096\frac{3}{3}^{\circ} - 32781_{4}$
14951.792	1		6686.334	$16346\frac{4}{4}^{\circ} - 23032_{4}$
14947.310	2		6688.339	$21539\frac{2}{2}^{\circ} - 28227_{4}$
14947.021	1		6688.468	$26048\frac{4}{4}^{\circ} - 32737_{5}$
14943.987	6		6689.826	$8800_{4} - 15490\frac{6}{6}^{\circ}$
14928.485	4		6696.773	$11877\frac{1}{1}^{\circ} - 18574_{1}$
14921.758	0		6699.792	$15970_{3} - 22669\frac{5}{5}^{\circ}$
14911.028	2		6704.613	$22399\frac{6}{6}^{\circ} - 29104_{4}$
14880.943	0		6718.168	$11241\frac{3}{3}^{\circ} - 17959_{4}$
14875.259	1		6720.735	$24421\frac{5}{5}^{\circ} - 31141_{3}$
14873.575	1		6721.496	$23113\frac{4}{4}^{\circ} - 29835_{3}$
14850.034	0		6732.151	$18574_{1} - 25306\frac{2}{2}^{\circ}$
14842.404	0		6735.612	$23113\frac{4}{4}^{\circ} - 29849_{4}$
14830.215	3		6741.148	$17959_{4} - 24701\frac{6}{6}^{\circ}$
14830.001	1		6741.245	$23015\frac{6}{6}^{\circ} - 29756_{4}$
14809.031	2		6750.791	$17166_{5} - 23916\frac{4}{4}^{\circ}$
14806.456	5		6751.965	$7280_{2} - 14032\frac{2}{2}^{\circ}$
14805.415	3		6752.440	$19503\frac{3}{3}^{\circ} - 26255_{4}$
14805.099	1		6752.584	$16554_{6} - 23306\frac{6}{6}^{\circ}$
14796.452	0		6756.530	$20214\frac{3}{3}^{\circ} - 26971_{4}$
14789.356	1		6759.772	$26036\frac{3}{3}^{\circ} - 32796_{3}$
14784.758	1		6761.874	$13962_{1} - 20724\frac{6}{6}^{\circ}$
14781.114	0		6763.541	$23609\frac{6}{6}^{\circ} - 30372_{6}$
14777.907	1		6765.009	$22338\frac{3}{3}^{\circ} - 29104_{4}$
14777.230	1		6765.319	$24561\frac{3}{3}^{\circ} - 31326_{4}$
14772.419	0		6767.522	$24769\frac{5}{5}^{\circ} - 31537_{3}$
14772.031	3		6767.700	$25690\frac{6}{6}^{\circ} - 32458_{4}$
14764.746	2		6771.039	$16217\frac{2}{2}^{\circ} - 22988_{2}$
14756.630	3		6774.763	$13962_{1} - 20737\frac{1}{1}^{\circ}$
14751.515	0		6777.112	$20566\frac{4}{4}^{\circ} - 27343_{3}$
14741.329	5		6781.795	$11601_{1} - 18382\frac{6}{6}^{\circ}$
14740.403	0		6782.221	$24182\frac{2}{2}^{\circ} - 30964_{3}$
14736.470	0		6784.031	$17398_{3} - 24182\frac{2}{2}^{\circ}$
14719.449	1		6791.876	$23752\frac{2}{2}^{\circ} - 30544_{2}$
14718.799	5		6792.176	$19588\frac{6}{6}^{\circ} - 26380_{5}$
14716.370	2		6793.297	$22141\frac{3}{3}^{\circ} - 28934_{3}$
14695.579	3		6802.908	$21539\frac{4}{4}^{\circ} - 28342_{5}$
14690.666	0		6805.183	$21143_{5} - 27948\frac{4}{4}^{\circ}$
14689.932	0		6805.523	$23481\frac{1}{1}^{\circ} - 30286_{1}$
14688.909	0		6805.997	$15863_{2} - 22669\frac{5}{5}^{\circ}$
14687.576	0		6806.615	$22877\frac{5}{5}^{\circ} - 29684_{5}$
14680.667	0		6809.818	$17959_{4} - 24769\frac{5}{5}^{\circ}$
14677.249	5		6811.404	$11802_{2} - 18614\frac{1}{1}^{\circ}$
14661.334	0		6818.798	$21539\frac{4}{4}^{\circ} - 28358_{3}$
14654.914	7		6821.785	$11877\frac{1}{1}^{\circ} - 18699_{2}$
14651.482	3		6823.383	$20054_{2} - 26878\frac{3}{3}^{\circ}$
14644.393	1		6826.686	$18699_{2} - 25526\frac{1}{1}^{\circ}$
14638.811	0		6829.289	$20214\frac{3}{3}^{\circ} - 27044_{3}$
14638.217	1		6829.566	$20737\frac{1}{1}^{\circ} - 27566_{2}$
14628.703	2		6834.008	$23015\frac{6}{6}^{\circ} - 29849_{4}$
14618.976	7		6838.555	$3687_{2} - 10526\frac{3}{3}^{\circ}$
14615.924	1		6839.983	$19273_{2} - 26113\frac{2}{2}^{\circ}$
14604.155	2		6845.495	$24084\frac{6}{6}^{\circ} - 30930_{6}$
14603.558	3		6845.775	$15493_{4} - 22338\frac{3}{3}^{\circ}$
14603.174	0		6845.955	$18069\frac{3}{3}^{\circ} - 24915_{3}$
14599.499	1		6847.678	$19948\frac{4}{4}^{\circ} - 26796_{3}$
14591.907	1		6851.241	$19039\frac{2}{2}^{\circ} - 25890_{2}$
14573.635	2		6859.831	$13088_{3} - 19948\frac{4}{4}^{\circ}$
14570.349	3		6861.378	$17398_{3} - 24259\frac{4}{4}^{\circ}$
14563.603	0		6864.556	$24381\frac{2}{2}^{\circ} - 31245_{2}$
14553.980	1		6869.095	$20322\frac{5}{5}^{\circ} - 27191_{5}$
14548.134	2		6871.855	$10526\frac{3}{3}^{\circ} - 17398_{3}$
14545.954	2		6872.885	$14204_{5} - 21077\frac{6}{6}^{\circ}$
14541.314	1		6875.078	$18431_{3} - 25306\frac{2}{2}^{\circ}$
14533.419	4		6878.813	$22877\frac{5}{5}^{\circ} - 29756_{4}$
14519.935	2		6885.201	$15970_{3} - 22855\frac{3}{3}^{\circ}$
14510.851	0		6889.511	$13847_{2} - 20737\frac{1}{1}^{\circ}$
14502.932	1		6893.273	$18549_{2} - 25442\frac{3}{3}^{\circ}$
14493.424	2		6897.795	$23113\frac{4}{4}^{\circ} - 30011_{3}$
14491.248	1		6898.831	$23609\frac{6}{6}^{\circ} - 30508_{5}$
14476.391	0		6905.911	$24421\frac{5}{5}^{\circ} - 31326_{4}$
14475.836	4		6906.176	$15493_{4} - 22399\frac{6}{6}^{\circ}$
14469.188	2		6909.349	$17398_{3} - 24307\frac{2}{2}^{\circ}$
14467.109	0		6910.342	$22508\frac{2}{2}^{\circ} - 29418_{2}$
14452.427	0		6917.362	$23093\frac{2}{2}^{\circ} - 30011_{3}$
14452.147	2		6917.496	$13297_{4} - 20214\frac{3}{3}^{\circ}$
14451.758	4		6917.682	$3865_{1} - 10783\frac{2}{2}^{\circ}$
14449.799	1		6918.620	$25877\frac{4}{4}^{\circ} - 32796_{3}$
14449.350	2		6918.835	$17166_{5} - 24084\frac{6}{6}^{\circ}$
14438.799	3		6923.891	$18431_{3} - 25355\frac{4}{4}^{\circ}$
14424.537	7		6930.737	$16346\frac{4}{4}^{\circ} - 23277_{5}$
14423.392	2		6931.287	$15166\frac{3}{3}^{\circ} - 22098_{4}$
14412.536	4		6936.508	$14206\frac{4}{4}^{\circ} - 21143_{5}$
14407.785	1		6938.795	$19713_{3} - 26651\frac{2}{2}^{\circ}$
14403.474	1		6940.872	$22163\frac{4}{4}^{\circ} - 29104_{4}$
14403.132	0		6941.037	$23603\frac{2}{2}^{\circ} - 30544_{2}$
14398.454	2		6943.292	$21902\frac{4}{4}^{\circ} - 28845_{4}$
14374.424	2		6954.899	$20566\frac{4}{4}^{\circ} - 27521_{4}$
14373.329	1		6955.429	$21890\frac{3}{3}^{\circ} - 28845_{4}$
14370.393	0		6956.850	$21077\frac{6}{6}^{\circ} - 28034_{5}$
14364.711	2		6959.602	$13962_{1} - 20922\frac{2}{2}^{\circ}$

TABLE 4. *Classified lines of* Th I—continued

Wavelength (Å)	Intensity		Wavenumber (cm^{-1})	Classification
	Lamp	Spark		
14363.687	2		6960.098	$18930\frac{5}{2} - 25890_2$
14358.938	2		6962.400	$22141\frac{3}{2} - 29104_4$
14357.839	3		6962.933	$7502_3 - 14465\frac{5}{2}$
14355.909	0		6963.869	$7280_2 - 14243\frac{1}{2}$
14340.036	0		6971.577	$22877\frac{5}{6} - 29849_4$
14326.032	1		6978.392	$22163\frac{3}{4} - 29141_5$
14324.702	0		6979.040	$9804_5 - 16783\frac{3}{4}$
14323.255	1		6979.745	$22855\frac{3}{2} - 29835_3$
14313.992	4		6984.262	$10414\frac{3}{4} - 17398_3$
14306.560	2		6987.890	$17411\frac{3}{2} - 24399_3$
14297.496	0		6992.320	$21890\frac{3}{2} - 28882_2$
14296.656	2		6992.731	$18930\frac{5}{2} - 25923_4$
14294.346	0		6993.861	$22855\frac{3}{2} - 29849_4$
14283.487	1		6999.178	$23015\frac{5}{6} - 30014_4$
14271.876	1		7004.872	$24769\frac{3}{2} - 31774_3$
14270.962	1		7005.321	$23752\frac{1}{2} - 30758_2$
14259.243	5		7011.078	$19986\frac{5}{2} - 26997_6$
14254.713	5		7013.306	$11601_1 - 18614\frac{1}{2}$
14254.065	0		7013.625	$15863_2 - 22877\frac{1}{2}$
14253.783	1		7013.764	$19273_2 - 26287\frac{1}{2}$
14244.211	2		7018.477	$15618\frac{3}{2} - 22637_3$
14239.881	1		7020.611	$21252\frac{1}{2} - 28273_2$
14238.660	2		7021.213	$17959_4 - 24981\frac{3}{2}$
14237.955	1		7021.561	$22396\frac{1}{2} - 29418_2$
14235.729	2		7022.659	$17398_3 - 24421\frac{3}{2}$
14234.902	2		7023.067	$19948\frac{3}{2} - 26971_4$
14234.902	2		7023.067	$21539\frac{3}{4} - 28562_4$
14233.051	0		7023.980	$24769\frac{3}{2} - 31793_4$
14231.327	4		7024.831	$13297_4 - 20322\frac{5}{6}$
14230.620	0		7025.180	$20566\frac{3}{4} - 27591_5$
14230.460	0		7025.259	$22396\frac{1}{2} - 29422_1$
14217.138	1		7031.842	$24981\frac{3}{2} - 32012_4$
14214.389	0		7033.202	$20054_2 - 27087\frac{1}{2}$
14192.323	4		7044.137	$20522\frac{3}{2} - 27566_2$
14191.050	2		7044.769	$21890\frac{3}{2} - 28934_3$
14189.283	0		7045.646	$20566\frac{3}{4} - 27612_3$
14187.489	2		7046.537	$25690\frac{5}{6} - 32737_5$
14170.625	0		7054.923	$16554_6 - 23609\frac{5}{6}$
14168.671	7		7055.896	$8111_4 - 15166\frac{3}{2}$
14160.194	1		7060.120	$24981\frac{3}{2} - 32041_2$
14154.750	0		7062.835	$21165\frac{3}{2} - 28227_4$
14148.646	2		7065.882	$23306\frac{3}{2} - 30372_6$
14107.467	1		7086.507	$22669\frac{3}{2} - 29756_4$
14101.396	3		7089.558	$20522\frac{3}{2} - 27612_3$
14100.879	2		7089.818	$19273_2 - 26363\frac{3}{2}$
14095.249	1		7092.650	$24701\frac{5}{6} - 31793_4$
14090.246	7		7095.168	$3687_2 - 10783\frac{3}{2}$
14079.818	5		7100.423	$12847_3 - 19948\frac{3}{2}$
14063.614	2		7108.604	$17166_5 - 24274\frac{5}{6}$
14063.614	2		7108.604	$17073_1 - 24182\frac{3}{2}$
14061.486	0		7109.680	$18699_2 - 25809\frac{1}{2}$
14061.215	1		7109.817	$14465\frac{1}{2} - 21575_2$
14054.652	1		7113.137	$18809\frac{3}{4} - 25923_4$
14038.143	0		7121.502	$24307\frac{3}{2} - 31429_1$
14032.419	1		7124.407	$24202\frac{3}{4} - 31326_4$
14028.560	4		7126.367	$13088_3 - 20214\frac{3}{2}$
14026.605	5		7127.360	$11802_2 - 18930\frac{5}{2}$
14008.158	0		7136.746	$22877\frac{5}{6} - 30014_4$
14007.173	0		7137.248	$23752\frac{1}{2} - 30889_1$
13995.011	0		7143.450	$15970_3 - 23113\frac{3}{4}$
13993.145	1		7144.403	$21738\frac{1}{2} - 28882_2$
13976.090	2		7153.121	$22399\frac{5}{6} - 29552_6$
13975.932	4		7153.202	$19227\frac{5}{6} - 26380_5$
13974.383	1		7153.995	$18549_2 - 25703\frac{1}{2}$
13970.381	2		7156.044	$22855\frac{3}{2} - 30011_3$
13964.777	2		7158.916	$12114\frac{1}{2} - 19273_2$
13936.736	5		7173.320	$20322\frac{5}{6} - 27495_4$
13930.234	3		7176.668	$15493_4 - 22669\frac{3}{2}$
13904.491	6		7189.955	$11241\frac{3}{2} - 18431_3$
13898.031	1		7193.297	$21165\frac{3}{2} - 28358_3$
13886.527	4		7199.256	$20322\frac{5}{6} - 27521_4$
13882.834	1		7201.171	$23306\frac{3}{2} - 30508_5$
13872.468	0		7206.552	$25575\frac{3}{4} - 32781_4$
13862.050	0		7211.968	$23752\frac{1}{2} - 30964_3$
13859.106	1		7213.500	$21668\frac{1}{2} - 28882_2$
13844.566	0		7221.076	$25575\frac{3}{4} - 32796_3$
13818.508	1		7234.693	$18574_1 - 25809\frac{1}{2}$
13815.598	1		7236.217	$11802_2 - 19039\frac{3}{2}$
13828.453	1		7229.490	$24307\frac{3}{2} - 31537_3$
13814.181	0		7236.959	$23521\frac{3}{2} - 30758_2$
13813.265	0		7237.439	$23049\frac{1}{2} - 30286_1$
13809.796	1		7239.257	$21902\frac{3}{2} - 29141_5$
13799.139	0		7244.848	$25306\frac{3}{2} - 32551_3$
13795.378	1		7246.823	$24182\frac{3}{2} - 31429_1$
13792.422	5		7248.376	$16783\frac{3}{4} - 24032_4$
13786.380	1		7251.553	$15736\frac{1}{2} - 22988_2$
13779.592	1		7255.125	$22877\frac{1}{2} - 30132_2$
13774.118	1		7258.008	$19532_4 - 26790\frac{3}{4}$
13760.203	2		7265.348	$21077\frac{5}{6} - 28342_5$
13752.928	2		7269.191	$13297_4 - 20566\frac{3}{4}$
13752.277	0		7269.535	$20322\frac{5}{6} - 27591_5$
13748.535	0		7271.514	$24769\frac{3}{2} - 32041_2$
13748.149	2		7271.718	$18431_3 - 25703\frac{1}{2}$
13745.894	0		7272.911	$25690\frac{5}{6} - 32963_5$
13739.956	5		7276.054	$18614\frac{1}{2} - 25890_2$
13738.583	3		7276.781	$22141\frac{3}{2} - 29418_2$
13735.446	2		7278.443	$21252\frac{1}{2} - 28531_2$
13734.218	2		7279.094	$19516\frac{3}{2} - 26796_3$
13731.271	2		7280.656	$20214\frac{5}{2} - 27495_4$
13727.340	1		7282.741	$19713_3 - 26995\frac{5}{2}$
13723.460	0		7284.800	$22399\frac{5}{6} - 29684_5$
13680.790	0		7307.521	$17073_1 - 24381\frac{1}{2}$
13680.494	1		7307.679	$11241\frac{3}{2} - 18549_2$
13677.064	2		7309.512	$23655\frac{3}{4} - 30964_3$
13672.580	0		7311.909	$24701\frac{5}{6} - 32012_4$
13672.490	0		7311.957	$22338\frac{5}{2} - 29650_2$
13668.402	0		7314.144	$25753\frac{5}{6} - 33068_6$
13662.574	2		7317.264	$17354\frac{1}{2} - 24671_2$
13662.466	1		7317.322	$13847_2 - 21165\frac{3}{2}$
13647.606	5		7325.289	$18930\frac{5}{2} - 26255_4$

TABLE 4. *Classified lines of* Th I—continued

Wavelength (Å)	Intensity		Wavenumber (cm^{-1})	Classification
	Lamp	Spark		
13628.932	1		7335.326	$14204_5 - 21539^{\frac{3}{2}}_{\frac{3}{2}}$
13612.012	0		7344.444	$22669^{\frac{5}{2}}_{\frac{5}{2}} - 30014_4$
13609.614	2		7345.738	$19532_4 - 26878^{\frac{3}{2}}_{\frac{3}{2}}$
13599.702	3		7351.092	$20922^{\frac{3}{2}}_{\frac{3}{2}} - 28273_2$
13598.599	3		7351.688	$24850^{\frac{5}{2}}_{\frac{5}{2}} - 32202_5$
13598.167	2		7351.922	$20214^{\frac{3}{2}}_{\frac{3}{2}} - 27566_2$
13597.830	1		7352.104	$24274^{\frac{5}{2}}_{\frac{5}{2}} - 31626_5$
13595.363	0		7353.438	$25442^{\frac{3}{2}}_{\frac{3}{2}} - 32796_3$
13592.829	0		7354.809	$24182^{\frac{3}{2}}_{\frac{3}{2}} - 31537_3$
13588.783	4		7356.999	$22399^{\frac{5}{2}}_{\frac{5}{2}} - 29756_4$
13587.748	0		7357.559	$23015^{\frac{5}{2}}_{\frac{5}{2}} - 30372_6$
13579.410	4		7362.077	$15493_4 - 22855^{\frac{3}{2}}_{\frac{3}{2}}$
13572.266	0		7365.952	$21165^{\frac{3}{2}}_{\frac{3}{2}} - 28531_2$
13570.411	3		7366.959	$12847_3 - 20214^{\frac{3}{2}}_{\frac{3}{2}}$
13565.665	7		7369.536	$15618^{\frac{3}{2}}_{\frac{3}{2}} - 22988_2$
13562.388	2		7371.317	$17398_3 - 24769^{\frac{3}{2}}_{\frac{3}{2}}$
13549.102	2		7378.545	$19273_2 - 26651^{\frac{1}{2}}_{\frac{1}{2}}$
13540.748	3		7383.097	$19588^{\frac{5}{2}}_{\frac{5}{2}} - 26971_4$
13538.429	2		7384.362	$15493_4 - 22877^{\frac{7}{2}}_{\frac{7}{2}}$
13532.204	2		7387.759	$14206^{\frac{3}{2}}_{\frac{3}{2}} - 21594_3$
13529.689	1		7389.132	$16351_0 - 23741^{\frac{1}{2}}_{\frac{1}{2}}$
13518.143	6		7395.443	$11877^{\frac{1}{2}}_{\frac{1}{2}} - 19273_2$
13517.712	2		7395.679	$17959_4 - 25355^{\frac{3}{2}}_{\frac{3}{2}}$
13514.671	1		7397.343	$20214^{\frac{3}{2}}_{\frac{3}{2}} - 27612_3$
13508.886	0		7400.511	$25336^{\frac{5}{2}}_{\frac{5}{2}} - 32737_5$
13501.001	4		7404.833	$13847_2 - 21252^{\frac{3}{2}}_{\frac{3}{2}}$
13491.454	1		7410.073	$23916^{\frac{3}{2}}_{\frac{3}{2}} - 31326_4$
13484.963	1		7413.640	$18699_2 - 26113^{\frac{3}{2}}_{\frac{3}{2}}$
13484.304	3		7414.002	$15618^{\frac{3}{2}}_{\frac{3}{2}} - 23032_4$
13478.127	0		7417.400	$22338^{\frac{5}{2}}_{\frac{5}{2}} - 29756_4$
13465.671	0		7424.261	$24202^{\frac{3}{2}}_{\frac{3}{2}} - 31626_5$
13449.197	4		7433.355	$10526^{\frac{5}{2}}_{\frac{5}{2}} - 17959_4$
13448.036	1		7433.997	$24561^{\frac{5}{2}}_{\frac{5}{2}} - 31995_4$
13447.755	4		7434.152	$13088_3 - 20522^{\frac{3}{2}}_{\frac{3}{2}}$
13443.925	4		7436.270	$20922^{\frac{3}{2}}_{\frac{3}{2}} - 28358_3$
13440.583	4		7438.119	$11601_1 - 19039^{\frac{3}{2}}_{\frac{3}{2}}$
13439.085	1		7438.948	$14206^{\frac{3}{2}}_{\frac{3}{2}} - 21645_4$
13436.414	0		7440.427	$17224^{\frac{1}{2}}_{\frac{1}{2}} - 24664_3$
13433.332	3		7442.134	$14226_0 - 21668^{\frac{1}{2}}_{\frac{1}{2}}$
13426.907	3		7445.695	$18809^{\frac{3}{2}}_{\frac{3}{2}} - 26255_4$
13426.686	2		7445.818	$18431_3 - 25877^{\frac{3}{2}}_{\frac{3}{2}}$
13423.480	2		7447.596	$17224^{\frac{1}{2}}_{\frac{1}{2}} - 24671_2$
13419.576	4		7449.763	$22399^{\frac{5}{2}}_{\frac{5}{2}} - 29849_4$
13418.102	0		7450.581	$23093^{\frac{1}{2}}_{\frac{1}{2}} - 30544_2$
13404.943	4		7457.895	$11241^{\frac{5}{2}}_{\frac{5}{2}} - 18699_2$
13395.136	1		7463.355	$19532_4 - 26995^{\frac{5}{2}}_{\frac{5}{2}}$
13387.914	0		7467.381	$20566^{\frac{3}{2}}_{\frac{3}{2}} - 28034_5$
13386.236	2		7468.317	$19503^{\frac{3}{2}}_{\frac{3}{2}} - 26971_4$
13382.214	4		7470.562	$15166^{\frac{3}{2}}_{\frac{3}{2}} - 22637_3$
13370.573	1		7477.066	$24981^{\frac{5}{2}}_{\frac{5}{2}} - 32458_4$
13368.792	6		7478.062	$13088_3 - 20566^{\frac{3}{2}}_{\frac{3}{2}}$
13360.349	0		7482.788	$17959_4 - 25442^{\frac{5}{2}}_{\frac{5}{2}}$
13355.490	0		7485.510	$21077^{\frac{5}{2}}_{\frac{5}{2}} - 28562_4$
13353.446	0		7486.656	$23655^{\frac{3}{2}}_{\frac{3}{2}} - 31141_3$
13352.939	0		7486.940	$18549_2 - 26036^{\frac{5}{2}}_{\frac{5}{2}}$
13348.625	1		7489.360	$25306^{\frac{1}{2}}_{\frac{1}{2}} - 32796_3$
13342.411	1		7492.848	$23015^{\frac{5}{2}}_{\frac{5}{2}} - 30508_5$
13336.712	3		7496.050	$22338^{\frac{5}{2}}_{\frac{5}{2}} - 29835_3$
13334.671	1		7497.197	$18614^{\frac{1}{2}}_{\frac{1}{2}} - 26111_1$
13322.946	0		7503.795	$17411^{\frac{3}{2}}_{\frac{3}{2}} - 24915_3$
13315.518	1		7507.981	$8111_4 - 15618^{\frac{3}{2}}_{\frac{3}{2}}$
13314.704	1		7508.440	$24421^{\frac{3}{2}}_{\frac{3}{2}} - 31929_3$
13303.409	1		7514.815	$24259^{\frac{3}{2}}_{\frac{3}{2}} - 31774_3$
13296.036	1		7518.982	$24274^{\frac{5}{2}}_{\frac{5}{2}} - 31793_4$
13292.355	0		7521.064	$22163^{\frac{3}{2}}_{\frac{3}{2}} - 29684_5$
13290.823	1		7521.931	$15493_4 - 23015^{\frac{5}{2}}_{\frac{5}{2}}$
13286.526	0		7524.364	$25575^{\frac{3}{2}}_{\frac{3}{2}} - 33099_3$
13281.453	4		7527.238	$19516^{\frac{1}{2}}_{\frac{1}{2}} - 27044_3$
13279.662	0		7528.253	$21890^{\frac{3}{2}}_{\frac{3}{2}} - 29418_2$
13275.351	5		7530.698	$16554_6 - 24084^{\frac{5}{2}}_{\frac{5}{2}}$
13269.677	1		7533.918	$24259^{\frac{3}{2}}_{\frac{3}{2}} - 31793_4$
13267.880	2		7534.938	$17166_5 - 24701^{\frac{5}{2}}_{\frac{5}{2}}$
13263.633	2		7537.351	$23015^{\frac{5}{2}}_{\frac{5}{2}} - 30552_4$
13261.338	0		7538.655	$18574_1 - 26113^{\frac{1}{2}}_{\frac{1}{2}}$
13257.081	3		7541.076	$19503^{\frac{3}{2}}_{\frac{3}{2}} - 27044_3$
13253.863	5		7542.907	$15490^{\frac{5}{2}}_{\frac{5}{2}} - 23032_4$
13250.406	1		7544.875	$2869_3 - 10414^{\frac{3}{2}}_{\frac{3}{2}}$
13248.848	2		7545.762	$10414^{\frac{3}{2}}_{\frac{3}{2}} - 17959_4$
13247.730	4		7546.399	$8800_4 - 16346^{\frac{3}{2}}_{\frac{3}{2}}$
13246.336	0		7547.193	$19948^{\frac{3}{2}}_{\frac{3}{2}} - 27495_4$
13245.664	2		7547.576	$18549_2 - 26096^{\frac{5}{2}}_{\frac{5}{2}}$
13239.744	4		7550.951	$15970_3 - 23521^{\frac{3}{2}}_{\frac{3}{2}}$
13236.164	3		7552.993	$19713_3 - 27266^{\frac{3}{2}}_{\frac{3}{2}}$
13234.852	2		7553.742	$3687_2 - 11241^{\frac{5}{2}}_{\frac{5}{2}}$
13219.366	0		7562.591	$14032^{\frac{5}{2}}_{\frac{5}{2}} - 21594_3$
13217.149	0		7563.859	$18549_2 - 26113^{\frac{3}{2}}_{\frac{3}{2}}$
13216.178	1		7564.415	$21539^{\frac{3}{2}}_{\frac{3}{2}} - 29104_4$
13215.207	0		7564.971	$22396^{\frac{1}{2}}_{\frac{1}{2}} - 29961_1$
13205.290	6		7570.652	$18809^{\frac{3}{2}}_{\frac{3}{2}} - 26380_5$
13202.889	1		7572.029	$24202^{\frac{3}{2}}_{\frac{3}{2}} - 31774_3$
13200.969	1		7573.130	$19948^{\frac{3}{2}}_{\frac{3}{2}} - 27521_4$
13184.286	2		7582.713	$17398_3 - 24981^{\frac{5}{2}}_{\frac{5}{2}}$
13183.941	3		7582.911	$6362_2 - 13945^{\frac{5}{2}}_{\frac{5}{2}}$
13183.783	3		7583.002	$15618^{\frac{3}{2}}_{\frac{3}{2}} - 23201_3$
13176.103	2		7587.422	$18699_2 - 26287^{\frac{1}{2}}_{\frac{1}{2}}$
13169.665	0		7591.131	$24202^{\frac{3}{2}}_{\frac{3}{2}} - 31793_4$
13168.345	0		7591.892	$24421^{\frac{3}{2}}_{\frac{3}{2}} - 32012_4$
13167.879	0		7592.161	$24182^{\frac{3}{2}}_{\frac{3}{2}} - 31774_3$
13156.601	1		7598.669	$12114^{\frac{3}{2}}_{\frac{3}{2}} - 19713_3$
13150.947	1		7601.936	$21539^{\frac{3}{2}}_{\frac{3}{2}} - 29141_5$
13146.765	1		7604.354	$19713_3 - 27317^{\frac{5}{2}}_{\frac{5}{2}}$
13146.229	1		7604.664	$18431_3 - 26036^{\frac{5}{2}}_{\frac{5}{2}}$
13144.547	1		7605.637	$19986^{\frac{5}{2}}_{\frac{5}{2}} - 27591_5$
13136.162	0		7610.492	$23655^{\frac{3}{2}}_{\frac{3}{2}} - 31265_3$
13128.501	2		7614.933	$22399^{\frac{5}{2}}_{\frac{5}{2}} - 30014_4$
13127.923	5		7615.268	$16783^{\frac{3}{2}}_{\frac{3}{2}} - 24399_3$
13126.337	0		7616.188	$20054_2 - 27670^{\frac{5}{2}}_{\frac{5}{2}}$
13124.108	1		7617.482	$15863_2 - 23481^{\frac{1}{2}}_{\frac{1}{2}}$
13120.544	1		7619.551	$20054_2 - 27674^{\frac{3}{2}}_{\frac{3}{2}}$
13119.476	1		7620.171	$24421^{\frac{3}{2}}_{\frac{3}{2}} - 32041_2$

TABLE 4. *Classified lines of* Th I—continued

Wavelength (Å)	Intensity		Wavenumber (cm^{-1})	Classification
	Lamp	Spark		
13116.755	1		7621.752	$24307\frac{2}{2}$ – 31929_3
13111.862	0		7624.596	$22508\frac{2}{2}$ – 30132_2
13107.912	1		7626.894	$25336\frac{6}{8}$ – 32963_5
13103.036	0		7629.732	$13945\frac{3}{3}$ – 21575_2
13102.832	1		7629.851	$21252\frac{2}{1}$ – 28882_2
13101.858	1		7630.418	$22877\frac{7}{6}$ – 30508_5
13079.586	1		7643.411	$19948\frac{4}{4}$ – 27591_5
13070.834	6		7648.529	$10783\frac{2}{2}$ – 18431_3
13069.399	3		7649.369	$13945\frac{3}{3}$ – 21594_3
13056.097	2		7657.162	15863_2 – $23521\frac{3}{3}$
13055.889	6		7657.284	2869_3 – $10526\frac{3}{3}$
13049.034	2		7661.307	$20566\frac{4}{4}$ – 28227_4
13048.139	1		7661.832	$23609\frac{6}{6}$ – 31271_5
13045.340	1		7663.476	18699_2 – $26363\frac{2}{2}$
13043.407	4		7664.612	7502_3 – $15166\frac{3}{3}$
13034.773	2		7669.689	6362_2 – $14032\frac{2}{2}$
13031.133	3		7671.831	$23655\frac{4}{4}$ – 31326_4
13030.257	0		7672.347	$22338\frac{8}{8}$ – 30011_3
13026.187	6		7674.744	12847_3 – $20522\frac{2}{2}$
13023.092	1		7676.568	$23752\frac{2}{2}$ – 31429_1
13010.439	1		7684.034	$21738\frac{2}{2}$ – 29422_1
13010.154	3		7684.202	17166_5 – $24850\frac{8}{8}$
13008.742	0		7685.036	15970_3 – $23655\frac{4}{4}$
13007.832	5		7685.574	$16346\frac{4}{4}$ – 24032_4
12994.532	3		7693.440	$22141\frac{3}{3}$ – 29835_3
12989.585	1		7696.370	9804_5 – $17501\frac{6}{6}$
12988.177	1		7697.204	$22855\frac{3}{3}$ – 30552_4
12986.920	4		7697.949	$7795\frac{4}{4}$ – 15493_4
12983.105	0		7700.211	11802_2 – $19503\frac{3}{3}$
12982.529	1		7700.553	$13945\frac{3}{3}$ – 21645_4
12970.735	2		7707.555	$22141\frac{3}{3}$ – 29849_4
12966.746	0		7709.926	$23916\frac{4}{4}$ – 31626_5
12963.697	2		7711.739	$20322\frac{6}{6}$ – 28034_5
12959.819	7		7714.047	11802_2 – $19516\frac{2}{2}$
12952.082	5		7718.655	12847_3 – $20566\frac{4}{4}$
12949.037	1		7720.470	16554_6 – $24274\frac{6}{6}$
12948.255	0		7720.936	$24274\frac{6}{6}$ – 31995_4
12938.933	2		7726.499	$8243\frac{2}{2}$ – 15970_3
12936.840	1		7727.749	19532_4 – $27260\frac{3}{3}$
12935.233	3		7728.709	$18382\frac{6}{6}$ – 26111_1
12933.760	1		7729.589	20054_2 – $27784\frac{2}{2}$
12932.107	2		7730.577	17959_4 – $25690\frac{8}{8}$
12930.425	1		7731.583	$25336\frac{6}{8}$ – 33068_6
12925.197	1		7734.710	19713_3 – $27447\frac{2}{2}$
12923.256	0		7735.872	$24259\frac{4}{4}$ – 31995_4
12920.304	0		7737.639	18549_2 – $26287\frac{1}{1}$
12919.299	3		7738.241	$24274\frac{6}{6}$ – 32012_4
12916.981	4		7739.630	15863_2 – $23603\frac{2}{2}$
12900.246	2		7749.670	$19817\frac{1}{1}$ – 27566_2
12898.865	4		7750.500	$20522\frac{2}{2}$ – 28273_2
12888.182	2		7756.924	$19039\frac{2}{2}$ – 26796_3
12881.709	0		7760.822	$21890\frac{3}{3}$ – 29650_2
12874.595	1		7765.110	17073_1 – $24838\frac{1}{1}$
12873.533	1		7765.751	$20214\frac{3}{3}$ – 27980_3
12872.702	3		7766.252	$10783\frac{2}{2}$ – 18549_2
12866.644	7		7769.909	$19227\frac{8}{8}$ – 26997_6
12861.651	4		7772.925	$16217\frac{2}{2}$ – 23990_2
12854.102	1		7777.490	$25321\frac{3}{3}$ – 33099_3
12846.823	1		7781.897	$24769\frac{3}{3}$ – 32551_3
12845.690	1		7782.583	15970_3 – $23752\frac{2}{2}$
12841.750	2		7784.971	19532_4 – $27317\frac{3}{3}$
12837.894	2		7787.309	$15490\frac{8}{8}$ – 23277_5
12836.536	1		7788.133	19273_2 – $27061\frac{2}{2}$
12831.063	0		7791.455	$10783\frac{2}{2}$ – 18574_1
12830.547	3		7791.768	$20566\frac{4}{4}$ – 28358_3
12828.379	1		7793.085	$24202\frac{4}{4}$ – 31995_4
12827.456	0		7793.646	$22338\frac{8}{8}$ – 30132_2
12826.806	3		7794.041	17959_4 – $25753\frac{6}{6}$
12799.956	2		7810.390	$24202\frac{4}{4}$ – 32012_4
12782.294	1		7821.182	13847_2 – $21668\frac{1}{1}$
12782.059	2		7821.326	$18069\frac{3}{3}$ – 25890_2
12781.578	4		7821.620	$15166\frac{3}{3}$ – 22988_2
12773.189	1		7826.757	$19516\frac{2}{2}$ – 27343_3
12762.096	6		7833.560	13088_3 – $20922\frac{2}{2}$
12750.649	0		7840.593	$19503\frac{3}{3}$ – 27343_3
12738.275	0		7848.209	$22163\frac{4}{4}$ – 30011_3
12733.582	3		7851.102	$23113\frac{4}{4}$ – 30964_3
12709.820	4		7865.780	$18930\frac{3}{3}$ – 26796_3
12709.330	5		7866.083	$15166\frac{3}{3}$ – 23032_4
12703.962	0		7869.407	$18053\frac{4}{4}$ – 25923_4
12703.428	1		7869.738	$22141\frac{3}{3}$ – 30011_3
12691.421	4		7877.183	15863_2 – $23741\frac{1}{1}$
12685.466	1		7880.881	$16783\frac{4}{4}$ – 24664_3
12684.317	0		7881.595	6362_2 – $14243\frac{1}{1}$
12683.507	1		7882.098	$23655\frac{4}{4}$ – 31537_3
12682.679	0		7882.613	$22669\frac{8}{8}$ – 30552_4
12680.944	1		7883.691	$22248\frac{2}{2}$ – 30132_2
12673.959	2		7888.036	$25180\frac{2}{2}$ – 33068_6
12670.355	1		7890.280	13847_2 – $21738\frac{2}{2}$
12668.767	2		7891.269	$14206\frac{4}{4}$ – 22098_4
12648.388	1		7903.983	$17501\frac{6}{6}$ – 25405_4
12646.536	8		7905.141	$10526\frac{3}{3}$ – 18431_3
12645.697	4		7905.665	$20322\frac{6}{6}$ – 28227_4
12641.383	3		7908.363	17398_3 – $25306\frac{2}{2}$
12636.142	5		7911.643	$18011\frac{6}{6}$ – 25923_4
12632.545	3		7913.896	2869_3 – $10783\frac{2}{2}$
12629.269	0		7915.949	11601_1 – $19516\frac{2}{2}$
12617.200	1		7923.521	17398_3 – $25321\frac{3}{3}$
12611.214	0		7927.282	$24274\frac{6}{6}$ – 32202_5
12604.640	2		7931.416	18431_3 – $26363\frac{2}{2}$
12587.889	4		7941.971	$20737\frac{1}{1}$ – 28679_2
12583.229	1		7944.912	$21890\frac{3}{3}$ – 29835_3
12580.239	1		7946.800	15970_3 – $23916\frac{4}{4}$
12580.100	1		7946.888	$21902\frac{4}{4}$ – 29849_4
12571.690	2		7952.204	18699_2 – $26651\frac{2}{2}$
12563.833	0		7957.177	17398_3 – $25355\frac{4}{4}$
12562.651	2		7957.926	19713_3 – $27670\frac{3}{3}$
12561.555	3		7958.620	18549_2 – $26508\frac{3}{3}$
12561.165	1		7958.867	14204_5 – $22163\frac{4}{4}$
12558.855	1		7960.331	$20922\frac{2}{2}$ – 28882_2

TABLE 4. *Classified lines of* Th I—continued

Wavelength (Å)	Intensity		Wavenumber (cm^{-1})	Classification
	Lamp	Spark		
12553.032	5		7964.024	$19227\frac{6}{8}$ – 27191_5
12552.801	4		7964.170	$23306\frac{8}{8}$ – 31271_5
12540.971	2		7971.683	$23655\frac{3}{4}$ – 31626_5
12522.256	1		7983.597	8800_4 – $16783\frac{3}{4}$
12518.195	3		7986.187	$18809\frac{3}{4}$ – 26796_3
12508.396	2		7992.443	$19503\frac{3}{3}$ – 27495_4
12502.774	2		7996.037	$20566\frac{3}{4}$ – 28562_4
12488.669	1		8005.068	$19039\frac{2}{2}$ – 27044_3
12477.297	7		8012.364	3865_1 – $11877\frac{1}{1}$
12476.305	3		8013.001	$20214\frac{3}{3}$ – 28227_4
12474.364	2		8014.248	11802_2 – $19817\frac{1}{1}$
12471.346	1		8016.187	$23521\frac{5}{5}$ – 31537_3
12469.228	4		8017.549	$10414\frac{4}{4}$ – 18431_3
12466.651	0		8019.206	$24274\frac{6}{6}$ – 32293_5
12465.053	3		8020.234	$20322\frac{6}{6}$ – 28342_5
12460.967	4		8022.864	$10526\frac{3}{3}$ – 18549_2
12455.465	0		8026.408	$24769\frac{8}{8}$ – 32796_3
12453.262	3		8027.828	15493_4 – $23521\frac{5}{5}$
12447.488	5		8031.552	$11241\frac{5}{5}$ – 19273_2
12446.347	1		8032.288	$19948\frac{4}{4}$ – 27980_3
12445.393	3		8032.904	$15736\frac{1}{1}$ – 23769_1
12442.013	5		8035.086	$15166\frac{3}{3}$ – 23201_3
12440.650	2		8035.966	$24701\frac{6}{6}$ – 32737_5
12437.583	0		8037.948	$22248\frac{2}{2}$ – 30286_1
12430.756	1		8042.362	13847_2 – $21890\frac{8}{8}$
12429.285	1		8043.314	$17847\frac{2}{2}$ – 25890_2
12422.300	4		8047.837	$19986\frac{6}{6}$ – 28034_5
12419.161	2		8049.871	$19516\frac{2}{2}$ – 27566_2
12415.160	5		8052.465	$16346\frac{4}{4}$ – 24399_3
12406.195	1		8058.284	$20214\frac{3}{3}$ – 28273_2
12397.849	4		8063.709	$19503\frac{3}{3}$ – 27566_2
12396.828	0		8064.373	$21077\frac{6}{6}$ – 29141_5
12381.813	3		8074.152	12847_3 – $20922\frac{2}{2}$
12378.451	1		8076.345	18431_3 – $26508\frac{3}{3}$
12378.290	2		8076.450	17959_4 – $26036\frac{5}{5}$
12377.115	0		8077.217	18574_1 – $26651\frac{1}{2}$
12372.007	2		8080.552	$24701\frac{6}{6}$ – 32781_4
12364.267	1		8085.610	$19948\frac{4}{4}$ – 28034_5
12359.625	2		8088.647	17959_4 – $26048\frac{3}{4}$
12355.491	0		8091.353	$24202\frac{4}{4}$ – 32293_5
12349.478	2		8095.293	$19516\frac{2}{2}$ – 27612_3
12348.314	0		8096.056	$23916\frac{4}{4}$ – 32012_4
12346.884	0		8096.994	$21738\frac{2}{2}$ – 29835_3
12338.612	0		8102.422	18549_2 – $26651\frac{1}{2}$
12337.998	7		8102.825	6362_2 – $14465\frac{2}{2}$
12330.800	1		8107.555	$20423\frac{1}{1}$ – 28531_2
12329.207	2		8108.603	$22399\frac{6}{6}$ – 30508_5
12328.492	1		8109.073	$21902\frac{2}{4}$ – 30011_3
12328.408	0		8109.128	$19503\frac{3}{3}$ – 27612_3
12323.962	0		8112.054	$21902\frac{2}{4}$ – 30014_4
12322.400	1		8113.082	$24850\frac{6}{6}$ – 32963_5
12321.120	3		8113.925	$18930\frac{3}{3}$ – 27044_3
12318.050	3		8115.947	15493_4 – $23609\frac{6}{6}$
12316.913	2		8116.696	7502_3 – $15618\frac{3}{3}$
12316.372	1		8117.053	$24084\frac{8}{8}$ – 32202_5
12312.736	2		8119.450	$23655\frac{3}{4}$ – 31774_3
12310.069	3		8121.209	$21890\frac{5}{5}$ – 30011_3
12295.924	0		8130.551	$24421\frac{3}{3}$ – 32551_3
12294.985	1		8131.172	$16783\frac{3}{4}$ – 24915_3
12283.851	1		8138.542	19532_4 – $27670\frac{8}{8}$
12283.851	1		8138.542	$23655\frac{3}{4}$ – 31793_4
12276.430	0		8143.462	$20214\frac{3}{3}$ – 28358_3
12273.859	2		8145.168	$20737\frac{1}{1}$ – 28882_2
12271.398	2		8146.801	16554_6 – $24701\frac{6}{6}$
12263.449	1		8152.082	$23113\frac{2}{4}$ – 31265_3
12262.250	1		8152.879	$13945\frac{3}{3}$ – 22098_4
12261.910	2		8153.105	$22399\frac{6}{6}$ – 30552_4
12256.743	2		8156.542	$20522\frac{2}{2}$ – 28679_2
12249.188	4		8161.573	$18809\frac{3}{4}$ – 26971_4
12245.483	3		8164.042	13088_3 – $21252\frac{2}{2}$
12242.874	0		8165.782	$21252\frac{2}{2}$ – 29418_2
12237.332	1		8169.480	$21252\frac{2}{2}$ – 29422_1
12236.549	2		8170.003	14226_0 – $22396\frac{1}{1}$
12234.949	1		8171.071	$23603\frac{2}{2}$ – 31774_3
12233.199	5		8172.240	$14465\frac{2}{2}$ – 22637_3
12231.942	8		8173.080	$10526\frac{3}{3}$ – 18699_2
12229.332	1		8174.824	$7795\frac{4}{4}$ – 15970_3
12226.604	1		8176.648	17398_3 – $25575\frac{4}{4}$
12226.177	4		8176.934	$11877\frac{1}{1}$ – 20054_2
12223.788	2		8178.532	18699_2 – $26878\frac{8}{8}$
12219.156	0		8181.632	$16217\frac{2}{2}$ – 24399_3
12216.424	1		8183.462	$24274\frac{6}{6}$ – 32458_4
12211.865	2		8186.517	$18069\frac{3}{3}$ – 26255_4
12206.894	7		8189.851	3687_2 – $11877\frac{1}{1}$
12188.866	1		8201.964	$18053\frac{3}{4}$ – 26255_4
12182.019	3		8206.574	9804_5 – $18011\frac{6}{6}$
12178.456	2		8208.975	$24084\frac{8}{8}$ – 32293_5
12171.815	4		8213.454	4961_4 – $13175\frac{4}{4}$
12167.821	3		8216.150	11601_1 – $19817\frac{1}{1}$
12166.851	0		8216.805	$21539\frac{4}{4}$ – 29756_4
12161.908	0		8220.144	18431_3 – $26651\frac{1}{2}$
12143.705	0		8232.466	15970_3 – $24202\frac{4}{4}$
12140.955	3		8234.331	$18809\frac{3}{4}$ – 27044_3
12140.751	1		8234.469	$24561\frac{3}{3}$ – 32796_3
12139.017	1		8235.645	8111_4 – $16346\frac{4}{4}$
12132.020	3		8240.395	$20322\frac{6}{6}$ – 28562_4
12129.427	5		8242.157	13297_4 – $21539\frac{4}{4}$
12128.913	1		8242.506	$21890\frac{5}{5}$ – 30132_2
12127.302	8		8243.601	0_2 – $8243\frac{2}{2}$
12126.918	1		8243.862	$24307\frac{2}{2}$ – 32551_3
12126.419	5		8244.201	$18011\frac{6}{6}$ – 26255_4
12119.644	3		8248.810	9804_5 – $18053\frac{3}{4}$
12117.950	0		8249.963	$22508\frac{2}{2}$ – 30758_2
12113.062	0		8253.292	$21165\frac{5}{5}$ – 29418_2
12109.655	0		8255.614	$24202\frac{4}{4}$ – 32458_4
12109.434	3		8255.765	$20423\frac{1}{1}$ – 28679_2
12109.313	1		8255.847	$23015\frac{6}{6}$ – 31271_5
12099.785	2		8262.348	$24701\frac{6}{6}$ – 32963_5
12083.777	0		8273.294	$21738\frac{2}{2}$ – 30011_3
12082.221	2		8274.359	$23655\frac{3}{4}$ – 31929_3

TABLE 4. *Classified lines of* Th I—continued

Wavelength (Å)	Intensity		Wavenumber (cm^{-1})	Classification	Wavelength (Å)	Intensity		Wavenumber (cm^{-1})	Classification
	Lamp	Spark				Lamp	Spark		
12075.537	1		8278.939	$20566\frac{3}{2} - 28845_4$	11829.730	4		8450.965	$15970_3 - 24421\frac{5}{2}$
12074.667	2		8279.536	$19948\frac{3}{2} - 28227_4$	11829.640	5		8451.029	$13088_3 - 21539\frac{3}{2}$
12066.559	0		8285.099	$23916\frac{3}{2} - 32202_5$	11827.583	4		8452.499	$17073_1 - 25526\frac{1}{2}$
12059.895	0		8289.677	$15970_3 - 24259\frac{3}{4}$	11824.901	1		8454.416	$16217\frac{7}{2} - 24671_2$
12058.422	0		8290.690	$11241\frac{5}{2} - 19532_4$	11822.640	4		8456.033	$19817\frac{1}{2} - 28273_2$
12055.291	0		8292.843	$21668\frac{1}{2} - 29961_1$	11821.839	1		8456.606	$22508\frac{5}{2} - 30964_3$
12051.267	1		8295.612	$22248\frac{5}{2} - 30544_2$	11821.500	0		8456.848	$7280_2 - 15736\frac{1}{2}$
12050.486	0		8296.150	$18699_2 - 26995\frac{3}{2}$	11818.546	1		8458.962	$20423\frac{1}{2} - 28882_2$
12038.242	1		8304.588	$19039\frac{3}{2} - 27343_3$	11811.926	2		8463.703	$19516\frac{3}{2} - 27980_3$
12037.639	4		8305.004	$17398_3 - 25703\frac{3}{2}$	11811.055	0		8464.327	$20214\frac{5}{2} - 28679_2$
12020.095	1		8317.125	$12847_3 - 21165\frac{3}{2}$	11804.617	6		8468.943	$5563_1 - 14032\frac{3}{2}$
12018.718	7		8318.078	$16346\frac{3}{2} - 24664_3$	11804.116	3		8469.303	$21903\frac{7}{2} - 30372_6$
12018.054	4		8318.538	$15863_2 - 24182\frac{3}{2}$	11802.102	1		8470.748	$13175\frac{3}{4} - 21645_4$
12015.950	4		8319.994	$23306\frac{3}{2} - 31626_5$	11801.327	0		8471.304	$11241\frac{5}{2} - 19713_3$
12015.478	1		8320.321	$19532_4 - 27852\frac{5}{2}$	11793.069	1		8477.236	$24259\frac{3}{4} - 32737_5$
12007.313	0		8325.979	$23603\frac{3}{2} - 31929_3$	11792.645	1		8477.541	$19503\frac{5}{2} - 27980_3$
12005.953	1		8326.922	$18053\frac{3}{4} - 26380_5$	11790.382	1		8479.168	$17411\frac{5}{2} - 25890_2$
11986.392	0		8340.511	$23655\frac{3}{4} - 31995_4$	11779.528	2		8486.981	$16351_0 - 24838\frac{1}{2}$
11980.135	1		8344.867	$22163\frac{3}{4} - 30508_5$	11775.163	4		8490.127	$10783\frac{3}{2} - 19273_2$
11976.025	1		8347.731	$20214\frac{5}{2} - 28562_4$	11772.698	1		8491.905	$23521\frac{5}{2} - 32012_4$
11974.134	1		8349.049	$24202\frac{3}{4} - 32551_3$	11761.537	1		8499.963	$20922\frac{3}{2} - 29422_1$
11961.578	1		8357.813	$23655\frac{3}{4} - 32012_4$	11746.174	1		8511.080	$19273_2 - 27784\frac{3}{2}$
11956.759	0		8361.182	$22396\frac{1}{2} - 30758_2$	11729.339	1		8523.296	$14465\frac{3}{2} - 22988_2$
11955.885	0		8361.793	$18699_2 - 27061\frac{3}{2}$	11729.339	1		8523.296	$20322\frac{5}{2} - 28845_4$
11952.063	4		8364.467	$19227\frac{7}{2} - 27591_5$	11723.279	2		8527.702	$19039\frac{3}{2} - 27566_2$
11946.618	1		8368.279	$20566\frac{3}{2} - 28934_3$	11722.487	1		8528.278	$16351_0 - 24880\frac{1}{2}$
11945.362	6		8369.159	$18011\frac{5}{2} - 26380_5$	11712.220	3		8535.754	$17354\frac{1}{2} - 25890_2$
11942.130	5		8371.424	$15618\frac{3}{2} - 23990_2$	11709.471	0		8537.758	$24561\frac{3}{2} - 33099_3$
11940.638	7		8372.470	$2869_3 - 11241\frac{3}{2}$	11704.645	1		8541.278	$23916\frac{3}{2} - 32458_4$
11927.809	0		8381.475	$18809\frac{3}{4} - 27191_5$	11703.457	7		8542.145	$15490\frac{5}{2} - 24032_4$
11916.586	3		8389.369	$22163\frac{3}{4} - 30552_4$	11698.831	3		8545.523	$13962_1 - 22508\frac{5}{2}$
11910.840	0		8393.416	$22877\frac{5}{2} - 31271_5$	11695.263	2		8548.130	$17959_4 - 26508\frac{3}{2}$
11909.862	1		8394.105	$19948\frac{3}{4} - 28342_5$	11694.285	3		8548.845	$21738\frac{5}{2} - 30286_1$
11904.795	2		8397.678	$19273_2 - 27670\frac{3}{2}$	11694.000	2		8549.053	$13847_2 - 22396\frac{1}{2}$
11899.837	4		8401.177	$13847_2 - 22248\frac{5}{2}$	11690.334	0		8551.734	$22877\frac{1}{2} - 31429_1$
11894.942	3		8404.634	$12847_3 - 21252\frac{3}{2}$	11682.909	1		8557.169	$15863_2 - 24421\frac{5}{2}$
11887.357	1		8409.997	$19948\frac{3}{4} - 28358_3$	11678.305	1		8560.543	$18699_2 - 27260\frac{3}{2}$
11886.085	2		8410.897	$22141\frac{5}{2} - 30552_4$	11673.465	1		8564.092	$18431_3 - 26995\frac{3}{2}$
11884.530	5		8411.997	$11802_2 - 20214\frac{5}{2}$	11667.638	5		8568.369	$16346\frac{3}{4} - 24915_3$
11882.776	2		8413.239	$15618\frac{3}{2} - 24032_4$	11661.167	3		8573.124	$19039\frac{3}{2} - 27612_3$
11878.611	2		8416.189	$19532_4 - 27948\frac{3}{4}$	11657.259	1		8575.998	$22669\frac{3}{2} - 31245_2$
11874.629	2		8419.011	$22338\frac{3}{2} - 30758_2$	11653.134	1		8579.034	$24202\frac{3}{4} - 32781_4$
11873.851	2		8419.563	$13175\frac{3}{4} - 21594_3$	11648.509	1		8582.440	$21252\frac{3}{2} - 29835_3$
11870.629	1		8421.848	$17501\frac{5}{2} - 25923_4$	11641.195	1		8587.832	$17166_5 - 25753\frac{5}{2}$
11868.045	0		8423.682	$15493_4 - 23916\frac{3}{4}$	11636.590	2		8591.231	$18930\frac{5}{2} - 27521_4$
11864.247	7		8426.378	$3687_2 - 12114\frac{3}{2}$	11636.496	1		8591.300	$21165\frac{3}{2} - 29756_4$
11858.382	4		8430.546	$14206\frac{3}{4} - 22637_3$	11636.155	3		8591.552	$15970_3 - 24561\frac{5}{2}$
11853.098	1		8434.304	$13962_1 - 22396\frac{1}{2}$	11634.601	4		8592.699	$13297_4 - 21890\frac{5}{2}$
11848.313	1		8437.710	$23603\frac{3}{2} - 32041_2$	11630.479	0		8595.745	$22669\frac{3}{2} - 31265_3$
11840.529	0		8443.257	$23093\frac{3}{2} - 31537_3$	11618.190	3		8604.837	$13297_4 - 21902\frac{3}{4}$
11839.689	1		8443.856	$15863_2 - 24307\frac{7}{2}$	11617.462	5		8605.376	$14032\frac{3}{2} - 22637_3$
11837.186	2		8445.642	$19588\frac{5}{2} - 28034_5$	11615.211	1		8607.044	$21077\frac{5}{2} - 29684_5$
11836.168	0		8446.368	$18549_2 - 26995\frac{3}{2}$	11609.914	2		8610.971	$8800_4 - 17411\frac{5}{2}$
11834.938	1		8447.246	$16217\frac{7}{2} - 24664_3$	11606.246	1		8613.692	$24182\frac{3}{2} - 32796_3$
11831.941	0		8449.386	$22877\frac{5}{2} - 31326_4$	11605.473	3		8614.266	$19948\frac{3}{4} - 28562_4$

TABLE 4. *Classified lines of* Th I—continued

Wavelength (Å)	Intensity		Wavenumber (cm^{-1})	Classification
	Lamp	Spark		
11602.596	0		8616.402	$22141^{5}_{3} - 30758_{2}$
11600.761	0		8617.765	$18699_{2} - 27317^{3}_{3}$
11600.523	0		8617.942	$21668^{1}_{1} - 30286_{1}$
11597.002	1		8620.558	$11802_{2} - 20423^{1}_{1}$
11595.985	6		8621.314	$16783^{4}_{4} - 25405_{4}$
11589.953	4		8625.801	$16554_{6} - 25180^{2}_{2}$
11584.866	0		8629.589	$17073_{1} - 25703^{2}_{2}$
11584.675	1		8629.731	$18431_{3} - 27061^{2}_{2}$
11583.465	0		8630.633	$20214^{3}_{3} - 28845_{4}$
11577.991	1		8634.713	$23916^{4}_{4} - 32551_{3}$
11575.518	4		8636.558	$18930^{5}_{5} - 27566_{2}$
11573.652	1		8637.950	$17398_{3} - 26036^{3}_{3}$
11571.485	5		8639.568	$19588^{6}_{6} - 28227_{4}$
11558.214	3		8649.488	$13088_{3} - 21738^{2}_{2}$
11557.337	3		8650.144	$17398_{3} - 26048^{4}_{4}$
11557.225	0		8650.228	$21902^{4}_{4} - 30552_{4}$
11554.767	0		8652.068	$24084^{6}_{6} - 32737_{5}$
11551.616	0		8654.428	$21890^{5}_{5} - 30544_{2}$
11543.824	2		8660.270	$13847_{2} - 22508^{2}_{2}$
11541.028	0		8662.368	$21890^{5}_{5} - 30552_{4}$
11536.071	2		8666.090	$17224^{2}_{2} - 25890_{2}$
11530.938	3		8669.948	$21165^{3}_{3} - 29835_{3}$
11526.460	4		8673.316	$14204_{5} - 22877^{6}_{6}$
11517.393	1		8680.144	$23113^{4}_{4} - 31793_{4}$
11516.456	5		8680.850	$5563_{1} - 14243^{1}_{1}$
11514.959	4		8681.979	$18930^{5}_{5} - 27612_{3}$
11512.063	3		8684.163	$5563_{1} - 14247^{6}_{6}$
11511.566	6		8684.538	$20867^{7}_{7} - 29552_{6}$
11511.286	1		8684.749	$23609^{6}_{6} - 32293_{5}$
11510.028	3		8685.698	$18809^{4}_{4} - 27495_{4}$
11506.079	1		8688.679	$24274^{8}_{8} - 32963_{5}$
11502.185	3		8691.621	$12847_{3} - 21539^{4}_{4}$
11501.478	4		8692.155	$13945^{5}_{5} - 22637_{3}$
11494.068	2		8697.759	$15863_{2} - 24561^{5}_{5}$
11489.885	5		8700.925	$8800_{4} - 17501^{6}_{6}$
11478.781	1		8709.342	$15493_{4} - 24202^{2}_{2}$
11476.910	0		8710.762	$18549_{2} - 27260^{5}_{5}$
11476.074	1		8711.396	$17166_{5} - 25877^{4}_{4}$
11475.757	3		8711.637	$18809^{4}_{4} - 27521_{4}$
11472.823	2		8713.865	$19817^{1}_{1} - 28531_{2}$
11471.073	0		8715.194	$7502_{3} - 16217^{2}_{2}$
11465.039	5		8719.781	$11802_{2} - 20522^{2}_{2}$
11464.786	2		8719.973	$20214^{3}_{3} - 28934_{3}$
11458.461	1		8724.787	$19503^{3}_{3} - 28227_{4}$
11455.545	1d		8727.008	$18069^{3}_{3} - 26796_{3}$
11444.419	2		8735.492	$17073_{1} - 25809^{1}_{1}$
11442.751	1		8736.765	$14465^{2}_{2} - 23201_{3}$
11432.593	4		8744.528	$14243^{1}_{1} - 22988_{2}$
11429.704	6		8746.738	$10526^{3}_{3} - 19273_{2}$
11427.901	1		8748.118	$18699_{2} - 27447^{2}_{2}$
11426.433	0		8749.242	$22877^{6}_{6} - 31626_{5}$
11420.044	1		8754.137	$19588^{6}_{6} - 28342_{5}$
11419.693	1		8754.406	$17501^{6}_{6} - 26255_{4}$
11417.309	3		8756.234	$19516^{2}_{2} - 28273_{2}$
11415.542	1		8757.589	$22508^{2}_{2} - 31265_{3}$
11411.321	1		8760.829	$24202^{4}_{4} - 32963_{5}$
11402.009	0		8767.984	$18549_{2} - 27317^{3}_{3}$
11386.235	5		8780.130	$15618^{3}_{3} - 24399_{3}$
11384.471	3		8781.491	$15493_{4} - 24274^{6}_{6}$
11383.920	3		8781.916	$18809^{4}_{4} - 27591_{5}$
11371.299	1		8791.663	$24307^{2}_{2} - 33099_{3}$
11369.091	2		8793.370	$24274^{8}_{8} - 33068_{6}$
11366.315	2		8795.518	$14481^{8}_{6} - 23277_{5}$
11358.564	1		8801.520	$22163^{3}_{4} - 30964_{3}$
11358.499	3		8801.570	$13088_{3} - 21890^{8}_{8}$
11357.450	0		8802.383	$18809^{4}_{4} - 27612_{3}$
11356.910	0		8802.802	$22338^{3}_{3} - 31141_{3}$
11356.608	1		8803.036	$23655^{8}_{4} - 32458_{4}$
11354.715	8		8804.503	$6362_{2} - 15166^{3}_{3}$
11352.128	2		8806.510	$21738^{2}_{2} - 30544_{2}$
11351.924	6		8806.668	$19227^{8}_{6} - 28034_{5}$
11346.494	1		8810.883	$14204_{5} - 23015^{5}_{5}$
11343.709	4		8813.046	$11241^{5}_{5} - 20054_{2}$
11342.857	3		8813.708	$13088_{3} - 21902^{4}_{4}$
11335.713	0		8819.262	$20322^{6}_{6} - 29141_{5}$
11332.045	4		8822.117	$13847_{2} - 22669^{5}_{5}$
11331.384	1		8822.632	$14226_{0} - 23049^{1}_{1}$
11326.973	3		8826.067	$14206^{4}_{4} - 23032_{4}$
11323.876	0		8828.481	$18431_{3} - 27260^{5}_{5}$
11321.659	2		8830.210	$8243^{2}_{2} - 17073_{1}$
11321.249	2		8830.530	$17959_{4} - 26790^{4}_{4}$
11307.314	3		8841.412	$19516^{2}_{2} - 28358_{3}$
11303.787	5		8844.171	$13297_{4} - 22141^{5}_{5}$
11303.544	4		8844.361	$7502_{3} - 16346^{4}_{4}$
11303.544	4		8844.361	$17411^{3}_{3} - 26255_{4}$
11301.136	1		8846.246	$21165^{3}_{3} - 30011_{3}$
11297.608	1		8849.008	$23609^{6}_{6} - 32458_{4}$
11289.645	2		8855.250	$19503^{3}_{3} - 28358_{3}$
11277.612	0		8864.698	$23916^{4}_{4} - 32781_{4}$
11276.818	4		8865.322	$15166^{3}_{3} - 24032_{4}$
11276.338	2		8865.700	$13297_{4} - 22163^{4}_{4}$
11273.574	4		8867.873	$21890^{5}_{5} - 30758_{2}$
11260.143	1		8878.451	$24084^{6}_{6} - 32963_{5}$
11258.986	4		8879.363	$17501^{6}_{6} - 26380_{5}$
11258.130	3		8880.038	$21252^{2}_{2} - 30132_{2}$
11255.513	0		8882.103	$23113^{4}_{4} - 31995_{4}$
11255.092	3		8882.435	$17166_{5} - 26048^{4}_{4}$
11249.018	0		8887.231	$17224^{2}_{2} - 26111_{1}$
11246.685	1		8889.075	$20214^{3}_{3} - 29104_{4}$
11245.412	2		8890.081	$12847_{3} - 21738^{2}_{2}$
11238.982	2		8895.167	$23306^{8}_{6} - 32202_{5}$
11238.344	0		8895.672	$20522^{2}_{2} - 29418_{2}$
11236.858	1		8896.849	$24202^{4}_{4} - 33099_{3}$
11233.671	2		8899.373	$20522^{2}_{2} - 29422_{1}$
11230.255	9		8902.080	$5563_{1} - 14465^{2}_{2}$
11225.532	3		8905.825	$15863_{2} - 24769^{5}_{5}$
11221.176	1		8909.282	$14204_{5} - 23113^{4}_{4}$
11215.651	2		8913.671	$20737^{1}_{1} - 29650_{2}$
11212.583	1		8916.110	$22877^{6}_{6} - 31793_{4}$
11211.484	0		8916.984	$24182^{2}_{2} - 33099_{3}$

TABLE 4. *Classified lines of* Th I—continued

Wavelength (Å)	Intensity		Wavenumber (cm^{-1})	Classification	Wavelength (Å)	Intensity		Wavenumber (cm^{-1})	Classification
	Lamp	Spark				Lamp	Spark		
11205.579	4		8921.683	$11601_1 - 20522^{\frac{3}{2}}$	10956.004	1		9124.916	$18549_2 - 27674^{\frac{3}{2}}$
11203.831	1		8923.075	$13175^{\frac{3}{4}} - 22098_4$	10948.154	4		9131.459	$13962_1 - 23093^{\frac{1}{2}}$
11195.293	1		8929.880	$10783^{\frac{1}{2}} - 19713_3$	10942.432	3		9136.234	$16554_6 - 25690^{\frac{6}{2}}$
11189.689	2		8934.352	$11802_2 - 20737^{\frac{1}{2}}$	10942.432	3		9136.234	$11601_1 - 20737^{\frac{1}{2}}$
11185.925	5		8937.359	$7280_2 - 16217^{\frac{3}{2}}$	10938.909	1		9139.176	$16783^{\frac{3}{4}} - 25923_4$
11184.628	0		8938.395	$22855^{\frac{5}{2}} - 31793_4$	10923.725	2		9151.880	$21738^{\frac{3}{2}} - 30889_1$
11179.105	3		8942.811	$11601_1 - 20543^{\frac{6}{2}}$	10913.581	3		9160.386	$13088_3 - 22248^{\frac{3}{2}}$
11171.377	1		8948.997	$17847^{\frac{3}{2}} - 26796_3$	10911.329	2		9162.277	$19516^{\frac{5}{2}} - 28679_2$
11162.099	3		8956.436	$14032^{\frac{3}{2}} - 22988_2$	10901.193	4		9170.796	$18809^{\frac{3}{4}} - 27980_3$
11157.560	1		8960.079	$18011^{\frac{6}{2}} - 26971_4$	10894.875	1		9176.114	$19503^{\frac{5}{2}} - 28679_2$
11151.802	0		8964.706	$17398_3 - 26363^{\frac{3}{2}}$	10890.287	4		9179.980	$18011^{\frac{6}{2}} - 27191_5$
11148.272	0		8967.544	$21165^{\frac{5}{2}} - 30132_2$	10887.285	0		9182.511	$23916^{\frac{3}{4}} - 33099_3$
11147.197	0		8968.409	$21539^{\frac{9}{4}} - 30508_5$	10883.902	1		9185.365	$22141^{\frac{5}{2}} - 31326_4$
11139.881	3		8974.299	$19588^{\frac{6}{2}} - 28562_4$	10883.233	0		9185.930	$22855^{\frac{5}{2}} - 32041_2$
11138.971	1		8975.032	$15863_2 - 24838^{\frac{1}{2}}$	10882.569	1		9186.490	$10526^{\frac{5}{2}} - 19713_3$
11138.821	4		8975.153	$18069^{\frac{5}{2}} - 27044_3$	10882.153	0		9186.842	$23015^{\frac{6}{2}} - 32202_5$
11134.469	1		8978.661	$22163^{\frac{9}{4}} - 31141_3$	10869.967	4		9197.141	$17847^{\frac{3}{2}} - 27044_3$
11128.287	5		8983.649	$4961_4 - 13945^{\frac{5}{2}}$	10866.949	1		9199.695	$16554_6 - 25753^{\frac{6}{2}}$
11125.541	4		8985.866	$18011^{\frac{6}{2}} - 26997_6$	10864.601	2		9201.683	$13847_2 - 23049^{\frac{1}{2}}$
11124.745	2		8986.509	$19948^{\frac{9}{4}} - 28934_3$	10862.508	4		9203.456	$20214^{\frac{5}{2}} - 29418_2$
11124.026	3		8987.090	$23306^{\frac{8}{2}} - 32293_5$	10857.355	1		9207.824	$15493_4 - 24701^{\frac{6}{2}}$
11114.372	0		8994.896	$20423^{\frac{1}{2}} - 29418_2$	10853.458	3		9211.130	$8800_4 - 18011^{\frac{6}{2}}$
11114.157	3		8995.070	$14206^{\frac{3}{4}} - 23201_3$	10844.405	4		9218.820	$17166_5 - 26384^{\frac{3}{2}}$
11101.804	5		9005.079	$9804_5 - 18809^{\frac{3}{4}}$	10837.713	0		9224.512	$20737^{\frac{1}{2}} - 29961_1$
11098.788	2		9007.526	$13847_2 - 22855^{\frac{5}{2}}$	10826.499	0		9234.067	$19039^{\frac{9}{2}} - 28273_2$
11094.494	2		9011.012	$15970_3 - 24981^{\frac{5}{2}}$	10813.573	4		9245.105	$2869_3 - 12114^{\frac{3}{2}}$
11092.159	1		9012.909	$21539^{\frac{9}{4}} - 30552_4$	10813.395	6		9245.257	$4961_4 - 14206^{\frac{3}{4}}$
11090.735	3		9014.066	$19516^{\frac{5}{2}} - 28531_2$	10812.281	5		9246.209	$13847_2 - 23093^{\frac{1}{2}}$
11073.735	3		9027.904	$19503^{\frac{5}{2}} - 28531_2$	10807.344	3		9250.433	$13088_3 - 22338^{\frac{5}{2}}$
11071.478	1		9029.745	$13847_2 - 22877^{\frac{1}{2}}$	10803.918	4		9253.367	$8800_4 - 18053^{\frac{3}{4}}$
11057.009	4		9041.561	$13297_4 - 22338^{\frac{5}{2}}$	10802.535	1		9254.551	$14226_6 - 23481^{\frac{1}{2}}$
11054.989	4		9043.213	$13945^{\frac{5}{2}} - 22988_2$	10800.157	4		9256.589	$6362_2 - 15618^{\frac{5}{2}}$
11051.898	7		9045.742	$15618^{\frac{5}{2}} - 24664_3$	10800.053	5		9256.678	$13945^{\frac{5}{2}} - 23201_3$
11050.978	1		9046.495	$23916^{\frac{3}{4}} - 32963_5$	10788.554	1		9266.544	$22508^{\frac{3}{2}} - 31774_3$
11046.224	4		9050.389	$18930^{\frac{5}{2}} - 27980_3$	10786.371	3		9268.420	$20566^{\frac{3}{4}} - 29835_3$
11043.146	3		9052.911	$15618^{\frac{5}{2}} - 24671_2$	10785.912	4		9268.814	$8800_4 - 18069^{\frac{5}{2}}$
11042.986	2		9053.042	$13088_3 - 22141^{\frac{5}{2}}$	10779.100	2		9274.672	$18069^{\frac{5}{2}} - 27343_3$
11036.319	4		9058.511	$16346^{\frac{3}{4}} - 25405_4$	10778.635	1		9275.072	$23521^{\frac{5}{2}} - 32796_3$
11035.091	0		9059.519	$19503^{\frac{5}{2}} - 28562_4$	10776.984	4		9276.493	$15493_4 - 24769^{\frac{5}{2}}$
11031.608	1		9062.380	$21902^{\frac{3}{4}} - 30964_3$	10774.344	1		9278.766	$23015^{\frac{6}{2}} - 32293_5$
11028.089	1		9065.271	$19817^{\frac{1}{2}} - 28882_2$	10759.049	1		9291.956	$21252^{\frac{3}{2}} - 30544_2$
11021.768	3		9070.470	$14206^{\frac{3}{4}} - 23277_5$	10754.878	0		9295.560	$21077^{\frac{6}{2}} - 30372_6$
11016.787	4		9074.571	$13088_3 - 22163^{\frac{9}{4}}$	10754.328	4		9296.035	$15618^{\frac{5}{2}} - 24915_3$
11001.800	3		9086.933	$13962_1 - 23049^{\frac{1}{2}}$	10752.475	2		9297.637	$18930^{\frac{5}{2}} - 28227_4$
11000.900	1		9087.676	$13945^{\frac{5}{2}} - 23032_4$	10749.434	3d		9300.268	$17959_4 - 27260^{\frac{5}{2}}$
10999.236	0		9089.051	$21668^{\frac{1}{2}} - 30758_2$	10744.370	2		9304.651	$14465^{\frac{3}{2}} - 23769_1$
10983.633	5		9101.963	$13297_4 - 22399^{\frac{6}{2}}$	10732.245	5		9315.163	$12847_3 - 22163^{\frac{9}{4}}$
10982.982	3		9102.502	$22163^{\frac{9}{4}} - 31265_3$	10726.926	8		9319.782	$2558_0 - 11877^{\frac{1}{2}}$
10982.910	4		9102.562	$14204_5 - 23306^{\frac{8}{2}}$	10725.418	6		9321.092	$11601_1 - 20922^{\frac{3}{2}}$
10976.518	0		9107.863	$22163^{\frac{9}{4}} - 31271_5$	10720.051	0		9325.759	$22669^{\frac{5}{2}} - 31995_4$
10974.389	1		9109.630	$17398_3 - 26508^{\frac{5}{2}}$	10707.531	1		9336.663	$15970_3 - 25306^{\frac{3}{2}}$
10965.252	1		9117.220	$15863_2 - 24981^{\frac{5}{2}}$	10700.359	1		9342.921	$18930^{\frac{5}{2}} - 28273_2$
10964.829	1		9117.572	$20566^{\frac{3}{4}} - 29684_5$	10700.194	0		9343.065	$22669^{\frac{5}{2}} - 32012_4$
10963.975	1		9118.282	$10414^{\frac{3}{4}} - 19532_4$	10690.175	1		9351.822	$15970_3 - 25321^{\frac{5}{2}}$
10962.885	5		9119.189	$11802_2 - 20922^{\frac{3}{2}}$	10678.631	1		9361.931	$20322^{\frac{6}{2}} - 29684_5$

TABLE 4. *Classified lines of* Th I—continued

Wavelength (Å)	Intensity		Wavenumber (cm^{-1})	Classification
	Lamp	Spark		
10678.369	3		9362.161	$11802_2 - 21165\frac{5}{3}$
10668.486	2		9370.834	$7795\frac{3}{4} - 17166_5$
10666.640	0		9372.456	$13297_4 - 22669\frac{9}{2}$
10664.767	0		9374.102	$22163\frac{4}{4} - 31537_3$
10664.234	5		9374.570	$6362_2 - 15736\frac{7}{1}$
10663.178	1		9375.499	$21890\frac{5}{3} - 31265_3$
10651.842	0		9385.476	$15970_3 - 25355\frac{4}{4}$
10649.651	1		9387.407	$21165\frac{3}{3} - 30552_4$
10646.516	2		9390.171	$8111_4 - 17501\frac{6}{6}$
10640.329	1		9395.631	$22141\frac{3}{3} - 31537_3$
10629.842	2		9404.901	$14204_5 - 23609\frac{8}{6}$
10615.008	4		9418.044	$18809\frac{4}{4} - 28227_4$
10613.388	4		9419.481	$13088_3 - 22508\frac{8}{2}$
10609.955	1		9422.529	$9804_5 - 19227\frac{8}{8}$
10607.108	1		9425.058	$21539\frac{4}{4} - 30964_3$
10605.464	4		9426.519	$18069\frac{5}{5} - 27495_4$
10601.345	2		9430.182	$23306\frac{8}{8} - 32737_5$
10600.597	1		9430.847	$21077\frac{6}{6} - 30508_5$
10596.909	1		9434.129	$20322\frac{6}{6} - 29756_4$
10595.264	1		9435.594	$22338\frac{8}{3} - 31774_3$
10594.780	1		9436.025	$20214\frac{3}{3} - 29650_2$
10592.495	0		9438.061	$23113\frac{4}{4} - 32551_3$
10591.350	2		9439.081	$20522\frac{2}{2} - 29961_1$
10587.100	3		9442.870	$15863_2 - 25306\frac{2}{2}$
10586.930	1		9443.022	$23015\frac{6}{6} - 32458_4$
10585.524	0		9444.276	$23655\frac{4}{4} - 33099_3$
10585.028	2		9444.718	$20566\frac{3}{4} - 30011_3$
10581.711	1		9447.679	$13962_1 - 23410\frac{8}{8}$
10579.481	1		9449.670	$11802_2 - 21252\frac{2}{2}$
10578.136	1		9450.872	$14204_5 - 23655\frac{3}{4}$
10576.362	2		9452.457	$18069\frac{5}{5} - 27521_4$
10570.129	0		9458.031	$15863_2 - 25321\frac{3}{3}$
10569.146	0		9458.911	$23609\frac{8}{6} - 33068_6$
10567.177	1		9460.673	$12114\frac{2}{2} - 21575_2$
10565.306	6		9462.349	$13175\frac{3}{4} - 22637_3$
10559.107	0		9467.904	$18053\frac{4}{4} - 27521_4$
10556.454	7		9470.283	$17501\frac{6}{6} - 26971_4$
10554.837	4		9471.734	$16783\frac{4}{4} - 26255_4$
10553.890	1		9472.584	$15970_3 - 25442\frac{5}{3}$
10545.902	1		9479.759	$17398_3 - 26878\frac{5}{5}$
10545.290	2		9480.309	$12114\frac{2}{2} - 21594_3$
10540.958	5		9484.205	$18011\frac{6}{6} - 27495_4$
10536.866	2		9487.888	$15493_4 - 24981\frac{3}{3}$
10533.385	3		9491.024	$12847_3 - 22338\frac{8}{8}$
10527.789	5		9496.069	$17501\frac{6}{6} - 26997_6$
10527.134	1		9496.660	$17847\frac{2}{2} - 27343_3$
10518.190	2		9504.735	$20867\frac{7}{7} - 30372_6$
10512.209	5		9510.143	$18011\frac{6}{6} - 27521_4$
10502.592	4		9518.851	$13962_1 - 23481\frac{7}{1}$
10498.496	5		9522.565	$14247\frac{6}{6} - 23769_1$
10495.610	1		9525.183	$14465\frac{2}{2} - 23990_2$
10494.843	6		9525.879	$14243\frac{7}{1} - 23769_1$
10492.255	6		9528.229	$10526\frac{3}{3} - 20054_2$
10487.427	1		9532.615	$18809\frac{4}{4} - 28342_5$
10459.723	4		9557.864	$13297_4 - 22855\frac{5}{3}$
10469.974	1		9548.506	$18809\frac{4}{4} - 28358_3$
10477.700	1		9541.465	$20214\frac{3}{3} - 29756_4$
10481.173	0		9538.303	$20423\frac{7}{1} - 29961_1$
10450.448	3		9566.346	$19986\frac{8}{6} - 29552_6$
10439.505	3		9576.374	$16346\frac{4}{4} - 25923_4$
10436.870	2		9578.792	$15863_2 - 25442\frac{5}{3}$
10435.094	3		9580.422	$18011\frac{6}{6} - 27591_5$
10434.109	1		9581.326	$13088_3 - 22669\frac{9}{2}$
10424.126	1		9590.502	$22338\frac{8}{3} - 31929_3$
10421.511	0		9592.909	$21165\frac{3}{3} - 30758_2$
10417.881	1		9596.251	$22399\frac{9}{6} - 31995_4$
10412.996	4		9600.753	$18930\frac{8}{3} - 28531_2$
10412.507	0		9601.204	$19817\frac{7}{1} - 29418_2$
10410.424	2		9603.125	$7795\frac{3}{4} - 17398_3$
10408.497	1		9604.903	$19817\frac{7}{1} - 29422_1$
10403.056	1		9609.927	$20522\frac{2}{2} - 30132_2$
10401.401	1		9611.456	$22163\frac{4}{4} - 31774_3$
10392.041	0		9620.113	$20214\frac{3}{3} - 29835_3$
10387.498	1		9624.320	$17166_5 - 26790\frac{4}{4}$
10378.821	1		9632.366	$18930\frac{8}{3} - 28562_4$
10378.146	1		9632.993	$17411\frac{3}{3} - 27044_3$
10377.490	2		9633.601	$13847_2 - 23481\frac{7}{1}$
10376.812	0		9634.231	$20214\frac{3}{3} - 29849_4$
10376.020	1		9634.966	$21902\frac{4}{4} - 31537_3$
10369.528	4		9640.998	$13962_1 - 23603\frac{2}{2}$
10362.966	1		9647.103	$21890\frac{5}{3} - 31537_3$
10358.167	3		9651.573	$11601_1 - 21252\frac{2}{2}$
10357.615	0		9652.087	$22141\frac{3}{3} - 31793_4$
10350.334	1		9658.877	$18614\frac{6}{1} - 28273_2$
10349.051	5		9660.074	$12847_3 - 22508\frac{8}{2}$
10346.540	3		9662.419	$15863_2 - 25526\frac{7}{1}$
10345.899	0		9663.017	$17398_3 - 27061\frac{8}{2}$
10334.926	3		9673.277	$13847_2 - 23521\frac{3}{3}$
10316.894	4		9690.184	$17501\frac{6}{6} - 27191_5$
10314.894	2		9692.063	$20322\frac{6}{6} - 30014_4$
10308.549	5		9698.028	$19986\frac{8}{6} - 29684_5$
10304.082	2		9702.233	$22338\frac{8}{3} - 32041_2$
10294.714	0		9711.062	$17959_4 - 27670\frac{8}{3}$
10293.052	4		9712.630	$14204_5 - 23916\frac{3}{3}$
10285.485	0		9719.775	$17847\frac{2}{2} - 27566_2$
10283.118	4		9722.012	$7502_3 - 17224\frac{8}{2}$
10278.860	1		9726.040	$21539\frac{4}{4} - 31265_3$
10275.694	0		9729.036	$20922\frac{2}{2} - 30651_3$
10271.191	2		9733.302	$15970_3 - 25703\frac{5}{3}$
10268.554	1		9735.801	$19948\frac{8}{4} - 29684_5$
10257.374	5		9746.413	$14243\frac{7}{1} - 23990_2$
10255.580	2		9748.118	$15166\frac{3}{3} - 24915_3$
10250.684	4		9752.773	$18809\frac{4}{4} - 28562_4$
10247.561	4		9755.746	$13847_2 - 23603\frac{2}{2}$
10241.779	2		9761.253	$23306\frac{8}{8} - 33068_6$
10236.031	4		9766.735	$13088_3 - 22855\frac{5}{3}$
10223.662	3		9778.551	$13962_1 - 23741\frac{7}{1}$
10218.434	5		9783.554	$9804_5 - 19588\frac{8}{6}$
10214.442	1		9787.377	$21539\frac{4}{4} - 31326_4$
10211.538	2		9790.161	$13962_1 - 23752\frac{8}{2}$

TABLE 4. *Classified lines of* Th I—continued

Wavelength (Å)	Intensity		Wavenumber (cm^{-1})	Classification
	Lamp	Spark		
10205.020	1		9796.414	$20214\frac{3}{3} - 30011_3$
10202.133	1		9799.186	$21738\frac{2}{2} - 31537_3$
10193.720	0		9807.273	$20737\frac{1}{1} - 30544_2$
10192.965	0		9808.000	$19948\frac{4}{4} - 29756_4$
10184.539	2		9816.114	$13297_4 - 23113\frac{4}{4}$
10180.596	2		9819.916	$17224\frac{2}{2} - 27044_3$
10178.522	5		9821.917	$12847_3 - 22669\frac{3}{3}$
10175.012	4		9825.305	$14206\frac{4}{4} - 24032_4$
10160.324	0		9839.509	$15863_2 - 25703\frac{2}{2}$
10156.406	0		9843.305	$19039\frac{2}{2} - 28882_2$
10144.266	4		9855.084	$6362_2 - 16217\frac{2}{2}$
10141.399	6		9857.870	$13175\frac{3}{3} - 23032_4$
10140.434	4		9858.808	$20867\frac{7}{7} - 30726_7$
10137.390	2		9861.769	$17398_3 - 27260\frac{3}{3}$
10136.787	0		9862.355	$15493_4 - 25355\frac{4}{4}$
10131.371	2		9867.628	$17398_3 - 27266\frac{4}{4}$
10127.552	0		9871.349	$22141\frac{5}{5} - 32012_4$
10126.557	1		9872.318	$21902\frac{4}{4} - 31774_3$
10117.993	2		9880.675	$14204_5 - 24084\frac{6}{6}$
10111.877	1		9886.651	$19948\frac{3}{3} - 29835_3$
10107.000	0		9891.421	$21902\frac{4}{4} - 31793_4$
10105.549	0		9892.842	$17959_4 - 27852\frac{6}{6}$
10105.080	2		9893.301	$13847_2 - 23741\frac{1}{1}$
10104.307	1		9894.058	$16217\frac{2}{2} - 26111_1$
10102.579	2		9895.750	$19039\frac{2}{2} - 28934_3$
10098.624	1		9899.625	$22141\frac{5}{5} - 32041_2$
10097.463	1		9900.764	$19948\frac{4}{4} - 29849_4$
10089.136	7		9908.935	$7502_3 - 17411\frac{3}{3}$
10089.136	7		9908.935	$16346\frac{3}{3} - 26255_4$
10086.406	2		9911.617	$18069\frac{3}{3} - 27980_3$
10083.788	5		9914.190	$19227\frac{8}{8} - 29141_5$
10082.880	4		9915.083	$15490\frac{8}{8} - 25405_4$
10082.719	1		9915.242	$19503\frac{3}{3} - 29418_2$
10082.719	1		9915.242	$18930\frac{3}{3} - 28845_4$
10081.227	1		9916.709	$18614\frac{1}{1} - 28531_2$
10078.906	1		9918.993	$17398_3 - 27317\frac{3}{3}$
10065.187	1		9932.512	$17411\frac{3}{3} - 27343_3$
10056.214	2		9941.375	$20566\frac{3}{3} - 30508_5$
10054.960	1		9942.615	$8111_4 - 18053\frac{3}{4}$
10053.375	0		9944.182	$7280_2 - 17224\frac{2}{2}$
10048.041	3		9949.461	$15493_4 - 25442\frac{5}{5}$
10045.316	2		9952.160	$18930\frac{3}{3} - 28882_2$
10039.364	7		9958.060	$8111_4 - 18069\frac{3}{3}$
10039.101	2		9958.321	$14032\frac{2}{2} - 23990_2$
10033.226	2		9964.152	$19588\frac{6}{6} - 29552_6$
10029.545	1		9967.809	$20922\frac{2}{2} - 30889_1$
10011.398	3		9985.877	$20566\frac{3}{3} - 30552_4$
9999.614	0		9997.645	$21539\frac{4}{4} - 31537_3$
9998.963	2		9998.296	$14204_5 - 24202\frac{4}{4}$
9992.656	3		10004.607	$18930\frac{3}{3} - 28934_3$
9991.846	0		10005.418	$13088_3 - 23093\frac{2}{2}$
9989.939	2		10007.327	$12847_3 - 22855\frac{3}{3}$
9987.636	6		10009.635	$8800_4 - 18809\frac{4}{4}$
9985.052	5		10012.225	$16783\frac{3}{4} - 26796_3$
9974.693	3		10022.623	$18011\frac{6}{6} - 28034_5$
9970.467	4		10026.872	$13175\frac{3}{3} - 23201_3$
9963.495	3		10033.888	$16346\frac{4}{4} - 26380_5$
9958.059	1		10039.365	$21890\frac{3}{3} - 31929_3$
9952.375	3		10045.099	$13945\frac{5}{5} - 23990_2$
9948.171	1		10049.344	$17398_3 - 27447\frac{2}{2}$
9947.082	1		10050.444	$20322\frac{6}{6} - 30372_6$
9938.839	1		10058.779	$22399\frac{6}{6} - 32458_4$
9935.203	2		10062.461	$20867\frac{7}{7} - 30930_6$
9934.723	1		10062.947	$19948\frac{3}{3} - 30011_3$
9932.777	0		10064.918	$18614\frac{1}{1} - 28679_2$
9929.814	3		10067.922	$11601_1 - 21668\frac{1}{1}$
9927.326	2		10070.445	$14204_5 - 24274\frac{6}{6}$
9923.310	1		10074.520	$18574_1 - 28649\frac{1}{1}$
9919.448	0		10078.443	$15970_3 - 26048\frac{3}{3}$
9916.122	1		10081.823	$15493_4 - 25575\frac{4}{4}$
9913.628	1		10084.360	$17411\frac{3}{3} - 27495_4$
9912.205	2		10085.807	$22877\frac{6}{6} - 32963_5$
9911.116	4		10086.915	$13945\frac{5}{5} - 24032_4$
9910.837	2		10087.199	$11802_2 - 21890\frac{3}{3}$
9907.464	1q		10090.634	$17501\frac{6}{6} - 27591_5$
9906.948	1		10091.159	$16554_6 - 26645\frac{6}{6}$
9904.771	1		10093.377	$21902\frac{4}{4} - 31995_4$
9902.362	4		10095.833	$19588\frac{6}{6} - 29684_5$
9898.356	2		10099.918	$17166_5 - 27266\frac{4}{4}$
9896.050	3		10102.272	$13175\frac{3}{4} - 23277_5$
9873.821	3		10125.015	$18809\frac{4}{4} - 28934_3$
9872.635	1		10126.231	$22669\frac{3}{3} - 32796_3$
9871.998	2		10126.885	$15970_3 - 26096\frac{3}{3}$
9868.922	2		10130.041	$8800_4 - 18930\frac{3}{3}$
9867.890	2		10131.101	$7280_2 - 17411\frac{3}{3}$
9865.451	1		10133.605	$17847\frac{7}{2} - 27980_3$
9862.127	0		10137.021	$11601_1 - 21738\frac{2}{2}$
9855.745	3		10143.585	$9804_5 - 19948\frac{4}{4}$
9840.923	1		10158.863	$18069\frac{3}{3} - 28227_4$
9838.008	1		10161.873	$21165\frac{3}{3} - 31326_4$
9837.258	0		10162.648	$14465\frac{2}{2} - 24627_1$
9833.424	8		10166.610	$3865_1 - 14032\frac{2}{2}$
9826.452	7		10173.823	$5563_1 - 15736\frac{1}{1}$
9819.178	1		10181.360	$9804_5 - 19986\frac{6}{6}$
9814.962	1		10185.733	$20322\frac{6}{6} - 30508_5$
9813.153	0		10187.611	$16783\frac{3}{4} - 26971_4$
9812.698	7		10188.083	$8243\frac{2}{2} - 18431_3$
9801.710	0		10199.505	$14465\frac{2}{2} - 24664_3$
9797.252	1		10204.145	$18069\frac{3}{3} - 28273_2$
9796.200	5		10205.241	$4961_4 - 15166\frac{3}{3}$
9789.508	2		10212.218	$17354\frac{1}{1} - 27566_2$
9785.356	0		10216.551	$18011\frac{6}{6} - 28227_4$
9782.141	0		10219.908	$13962_1 - 24182\frac{2}{2}$
9769.538	2		10233.092	$15863_2 - 26096\frac{3}{3}$
9764.606	0		10238.261	$15166\frac{3}{3} - 25405_4$
9757.222	1		10246.009	$12847_3 - 23093\frac{2}{2}$
9754.019	1		10249.374	$15863_2 - 26113\frac{2}{2}$
9753.597	2		10249.817	$21077\frac{8}{8} - 31326_4$
9746.464	7		10257.318	$3687_2 - 13945\frac{5}{5}$
9743.565	4		10260.370	$16783\frac{3}{4} - 27044_3$

201-606 O - 76 - 10

TABLE 4. *Classified lines of* Th I—continued

Wavelength (Å)	Intensity		Wavenumber (cm^{-1})	Classification
	Lamp	Spark		
9738.624	1		10265.576	$12847_3 - 23113\frac{3}{4}$
9736.216	1		10268.115	$18614\frac{0}{1} - 28882_2$
9716.146	2		10289.325	$18069\frac{3}{2} - 28358_3$
9702.272	3		10304.038	$15618\frac{3}{3} - 25923_4$
9701.580	1		10304.773	$18053\frac{3}{4} - 28358_3$
9700.564	7		10305.852	$2869_3 - 13175\frac{3}{4}$
9695.033	2		10311.732	$13297_4 - 23609\frac{5}{6}$
9678.235	0		10329.629	$20214\frac{3}{3} - 30544_2$
9676.940	0		10331.012	$8243\frac{2}{2} - 18574_1$
9676.840	3		10331.118	$18011\frac{5}{5} - 28342_5$
9676.107	2		10331.901	$19503\frac{3}{3} - 29835_3$
9674.790	2		10333.308	$11241\frac{3}{3} - 21575_2$
9664.700	6		10344.096	$3687_2 - 14032\frac{2}{2}$
9663.647	1		10345.223	$13962_1 - 24307\frac{2}{2}$
9656.439	1		10352.945	$11241\frac{3}{3} - 21594_3$
9652.004	0		10357.702	$13297_4 - 23655\frac{3}{4}$
9643.322	1		10367.027	$14032\frac{2}{2} - 24399_3$
9643.147	0		10367.215	$20522\frac{2}{2} - 30889_1$
9636.906	1		10373.929	$17073_1 - 27447\frac{2}{2}$
9632.647	6		10378.516	$3865_1 - 14243\frac{1}{1}$
9630.745	1		10380.565	$14247\frac{6}{6} - 24627_1$
9629.572	6		10381.830	$3865_1 - 14247\frac{6}{6}$
9629.231	0		10382.198	$22399\frac{6}{6} - 32781_4$
9627.672	1		10383.879	$14243\frac{1}{1} - 24627_1$
9625.204	3		10386.541	$19986\frac{6}{6} - 30372_6$
9623.414	0		10388.473	$22163\frac{3}{4} - 32551_3$
9619.222	1		10393.001	$15970_3 - 26363\frac{2}{2}$
9608.933	1		10404.129	$11241\frac{3}{3} - 21645_4$
9605.809	0		10407.513	$16783\frac{4}{4} - 27191_5$
9595.395	4		10418.808	$13962_1 - 24381\frac{2}{2}$
9588.809	0		10425.964	$19588\frac{6}{6} - 30014_4$
9587.027	1		10427.902	$14243\frac{1}{1} - 24671_2$
9582.816	4		10432.484	$13088_3 - 23521\frac{3}{3}$
9571.505	1		10444.813	$19516\frac{2}{2} - 29961_1$
9570.405	1		10446.013	$11802_2 - 22248\frac{2}{2}$
9567.826	2		10448.829	$11197\frac{6}{6} - 21645_4$
9567.283	1		10449.422	$16346\frac{4}{4} - 26796_3$
9561.245	5		10456.021	$8243\frac{2}{2} - 18699_2$
9510.950	0		10511.313	$17847\frac{2}{2} - 28358_3$
9507.656	2		10514.955	$13088_3 - 23603\frac{2}{2}$
9505.395	5		10517.456	$9804_5 - 20322\frac{6}{6}$
9501.443	0		10521.831	$19986\frac{6}{6} - 30508_5$
9500.302	2		10523.095	$12114\frac{2}{2} - 22637_3$
9497.191	7		10526.541	$0_2 - 10526\frac{3}{3}$
9495.500	7		10528.416	$4961_4 - 15490\frac{6}{6}$
9486.929	3		10537.928	$15970_3 - 26508\frac{3}{3}$
9474.882	7		10551.327	$7502_3 - 18053\frac{3}{4}$
9470.684	6		10556.003	$3687_2 - 14243\frac{1}{1}$
9467.200	5		10559.888	$16783\frac{4}{4} - 27343_3$
9461.208	3		10566.576	$13088_3 - 23655\frac{4}{4}$
9461.031	6		10566.774	$7502_3 - 18069\frac{3}{2}$
9460.871	2		10566.952	$7280_2 - 17847\frac{2}{2}$
9458.629	0		10569.457	$17411\frac{3}{3} - 27980_3$
9455.205	2q		10573.284	$13847_2 - 24421\frac{3}{3}$
9450.464	1		10578.589	$16217\frac{2}{2} - 26796_3$
9436.815	2		10593.889	$11802_2 - 22396\frac{1}{1}$
9431.600	5		10599.747	$3865_1 - 14465\frac{2}{2}$
9430.921	0		10600.510	$17073_1 - 27674\frac{2}{2}$
9422.317	0		10610.190	$18069\frac{3}{3} - 28679_2$
9420.621	2u		10612.100	$14226_0 - 24838\frac{1}{1}$
9417.463	0		10615.659	$19516\frac{2}{2} - 30132_2$
9414.090	2		10619.462	$13297_4 - 23916\frac{4}{4}$
9409.353	4		10624.808	$16346\frac{4}{4} - 26971_4$
9399.091	7		10636.408	$7795\frac{4}{4} - 18431_3$
9392.268	0		10644.135	$15863_2 - 26508\frac{3}{3}$
9390.588	2		10646.040	$14204_5 - 24850\frac{6}{6}$
9388.933	4		10647.916	$11601_1 - 22248\frac{2}{2}$
9388.933	4		10647.916	$18549_2 - 29197\frac{1}{1}$
9384.103	0		10653.397	$14226_0 - 24880\frac{1}{1}$
9383.275	5		10654.337	$5563_1 - 16217\frac{2}{2}$
9380.642	0		10657.327	$4961_4 - 15618\frac{3}{3}$
9366.797	0u		10673.079	$12847_3 - 23521\frac{3}{3}$
9357.253	0		10683.966	$17847\frac{2}{2} - 28531_2$
9344.207	1u		10698.882	$8111_4 - 18809\frac{2}{2}$
9344.096	1d		10699.009	$20566\frac{4}{4} - 31265_3$
9340.708	4		10702.890	$8800_4 - 19503\frac{3}{3}$
9336.161	1q		10708.102	$14206\frac{4}{4} - 24915_3$
9320.071	0		10726.589	$13945\frac{3}{3} - 24671_2$
9317.727	3		10729.287	$10414\frac{3}{3} - 21143_5$
9310.448	2		10737.675	$16783\frac{4}{4} - 27521_4$
9307.899	4		10740.616	$19986\frac{6}{6} - 30726_7$
9300.018	1		10749.718	$20214\frac{3}{3} - 30964_3$
9294.976	1		10755.549	$12847_3 - 23603\frac{2}{2}$
9289.564	5		10761.815	$9804_5 - 20566\frac{4}{4}$
9276.273	5		10777.234	$3687_2 - 14465\frac{2}{2}$
9271.181	1		10783.153	$0_2 - 10783\frac{2}{2}$
9270.155	2		10784.347	$19588\frac{6}{6} - 30372_6$
9266.920	4		10788.111	$8800_4 - 19588\frac{6}{6}$
9266.208	6		10788.941	$7280_2 - 18069\frac{3}{3}$
9263.682	0		10791.882	$10783\frac{2}{2} - 21575_2$
9260.327	2		10795.792	$11601_1 - 22396\frac{1}{1}$
9250.579	0		10807.168	$12847_3 - 23655\frac{3}{4}$
9245.257	1		10813.389	$18069\frac{3}{3} - 28882_2$
9239.328	1		10820.329	$15970_3 - 26790\frac{4}{4}$
9237.550	2		10822.411	$20423\frac{1}{1} - 31245_2$
9234.396	3		10826.108	$18930\frac{3}{3} - 29756_4$
9233.858	50	5	10826.738	$16217\frac{2}{2} - 27044_3$
9232.493	50	4	10828.339	$13088_3 - 23916\frac{4}{4}$
9230.616	1		10830.541	$21165\frac{3}{3} - 31995_4$
9229.218	1		10832.181	$17847\frac{2}{2} - 28679_2$
9227.870	1		10833.764	$22855\frac{5}{5} - 33689_2$
9227.517	300	50	10834.178	$18011\frac{5}{5} - 28845_4$
9227.057	2		10834.718	$21902\frac{4}{4} - 32737_5$
9222.345	20	5	10840.254	$19713_3 - 30553\frac{3}{3}$
9221.439	40	5	10841.319	$17501\frac{5}{5} - 28342_5$
9218.851	2		10844.363	$21594_3 - 32439\frac{4}{4}$
9218.670	1		10844.576	$18574_1 - 29419\frac{2}{2}$
9218.612	1		10844.644	$18574_1 - 29419\frac{2}{2}$
9218.612	1		10844.644	$18574_1 - 29419\frac{2}{2}$
9208.593	50		10856.443	$11241\frac{3}{3} - 22098_4$

TABLE 4. *Classified lines of* Th I—continued

Wavelength (Å)	Intensity		Wavenumber (cm^{-1})	Classification
	Lamp	Spark		
9208.035	8	2	10857.101	$13175\frac{3}{4} - 24032_4$
9203.988	500	75	10861.874	$6362_2 - 17224\frac{2}{2}$
9200.638	1h		10865.829	$18069\frac{3}{3} - 28934_3$
9199.676	8		10866.966	$11802_2 - 22669\frac{3}{3}$
9197.246	3		10869.837	$18549_2 - 29419\frac{2}{2}$
9191.681	2		10876.418	$13962_1 - 24838\frac{1}{1}$
9188.503	2		10880.179	$21143_5 - 32023\frac{6}{6}$
9186.364	1		10882.713	$22508\frac{2}{2} - 33390_1$
9179.820	2		10890.471	$15490\frac{6}{6} - 26380_5$
9178.777	200	15	10891.708	$15493_4 - 26384\frac{4}{4}$
9176.967	2		10893.856	$21902\frac{4}{4} - 32796_3$
9175.085	2		10896.091	$22877\frac{1}{1} - 33773_1$
9171.262	2		10900.633	$22508\frac{2}{2} - 33408_3$
9170.810	100	4	10901.170	$11197\frac{6}{6} - 22098_4$
9167.793	20	2	10904.758	$18930\frac{3}{3} - 29835_3$
9167.469	1		10905.143	$13297_4 - 24202\frac{4}{4}$
9166.738	1		10906.013	$21890\frac{3}{3} - 32796_3$
9165.890	400	25	10907.022	$11601_1 - 22508\frac{2}{2}$
9165.008	5	1	10908.071	$15970_3 - 26878\frac{5}{5}$
9164.261	4		10908.961	$21594_3 - 32503\frac{2}{2}$
9156.909	4		10917.719	$13962_1 - 24880\frac{1}{1}$
9155.929	4	1	10918.888	$18930\frac{3}{3} - 29849_4$
9153.352	8	2	10921.962	$13847_2 - 24769\frac{3}{3}$
9152.771	3		10922.655	$19039\frac{2}{2} - 29961_1$
9147.790	3	1	10928.602	$21575_2 - 32503\frac{2}{2}$
9141.782	8	2	10935.785	$21077\frac{6}{6} - 32012_4$
9141.337	2h		10936.317	$22163\frac{3}{4} - 33099_3$
9141.245	1		10936.427	$22669\frac{3}{3} - 33606_2$
9137.725	8	2	10940.640	$18699_2 - 29640\frac{1}{1}$
9134.679	150	10	10944.288	$19986\frac{6}{6} - 30930_6$
9132.261	40	8	10947.186	$17411\frac{3}{3} - 28358_3$
9129.173	20	5	10950.889	$17073_1 - 28024\frac{1}{1}$
9126.321	20	4	10954.311	$22877\frac{1}{1} - 33831_4$
9123.393	1		10957.827	$22141\frac{3}{3} - 33099_3$
9118.125	50	3	10964.158	$19588\frac{6}{6} - 30552_4$
9113.239	1		10970.036	$22338\frac{3}{3} - 33309_2$
9110.964	2		10972.775	$17959_4 - 28932\frac{2}{2}$
9107.788	2		10976.601	$22855\frac{3}{3} - 33831_4$
9107.216	100		10977.291	$13297_4 - 24274\frac{0}{0}$
9103.165	2		10982.176	$19273_2 - 30255\frac{3}{3}$
9101.064	20	3	10984.711	$19532_4 - 30517\frac{0}{0}$
9099.364	2		10986.763	$18699_2 - 29686\frac{3}{3}$
9095.713	4		10991.173	$13847_2 - 24838\frac{1}{1}$
9094.821	400	100	10992.251	$6362_2 - 17354\frac{1}{1}$
9090.809	200	10	10997.103	$16346\frac{4}{4} - 27343_3$
9084.511	3		11004.726	$20322\frac{0}{0} - 31326_4$
9082.305	3	1	11007.399	$20922\frac{2}{2} - 31929_3$
9076.185	8	1	11014.821	$15493_4 - 26508\frac{3}{3}$
9074.980	1		11016.284	$19948\frac{3}{4} - 30964_3$
9072.954	1		11018.744	$22399\frac{6}{6} - 33418_4$
9067.890	1		11024.897	$22248\frac{2}{2} - 33273_1$
9067.657	2		11025.181	$18809\frac{4}{4} - 29835_3$
9067.234	5	1	11025.695	$15970_3 - 26995\frac{5}{5}$
9063.948	200	10	11029.692	$8243\frac{2}{2} - 19273_2$
9062.879	2		11030.993	$20214\frac{3}{3} - 31245_2$
9061.672	2		11032.463	$13847_2 - 24880\frac{1}{1}$
9059.264	3		11035.395	$17847\frac{2}{2} - 28882_2$
9056.071	15	2	11039.286	$18382\frac{0}{0} - 29422_1$
9054.306	2		11041.438	$19503\frac{3}{3} - 30544_2$
9048.503	50		11048.519	$10526\frac{3}{3} - 21575_2$
9048.248	800b	75	11048.830	$6362_2 - 17411\frac{3}{3}$
9046.960	3		11050.403	$18053\frac{4}{4} - 29104_4$
9046.137	4		11051.409	$22163\frac{4}{4} - 33214_5$
9046.137	4		11051.409	$22669\frac{3}{3} - 33721_2$
9045.341	200	20	11052.381	$11802_2 - 22855\frac{3}{3}$
9041.717	2		11056.811	$22508\frac{2}{2} - 33564_3$
9039.277	2		11059.796	$22399\frac{6}{6} - 33459_4$
9038.935	2		11060.214	$20566\frac{4}{4} - 31626_5$
9037.880	200	10	11061.505	$17501\frac{6}{6} - 28562_4$
9034.490	2		11065.656	$18574_1 - 29640\frac{1}{1}$
9032.457	3		11068.146	$10526\frac{3}{3} - 21594_3$
9031.811	150	10	11068.938	$12847_3 - 23916\frac{4}{4}$
9026.157	2		11075.872	$21575_2 - 32650\frac{1}{1}$
9026.004	2		11076.059	$2869_3 - 13945\frac{3}{3}$
9016.581	300	20	11087.634	$12114\frac{2}{2} - 23201_3$
9016.382	3		11087.879	$18053\frac{4}{4} - 29141_5$
9013.959	5	1	11090.860	$17959_4 - 29050\frac{6}{6}$
9013.959	5	1	11090.860	$18549_2 - 29640\frac{1}{1}$
9013.581	1		11091.325	$15970_3 - 27061\frac{2}{2}$
9012.517	150	8	11092.634	$18011\frac{6}{6} - 29104_4$
9011.500	4	1	11093.886	$13088_3 - 24182\frac{2}{2}$
8997.862	100	10	11110.701	$11877\frac{1}{1} - 22988_2$
8995.178	100	10	11114.016	$13088_3 - 24202\frac{4}{4}$
8994.447	2		11114.919	$17398_3 - 28513\frac{2}{2}$
8991.072	1		11119.092	$20922\frac{3}{3} - 32041_2$
8990.879	10	2	11119.330	$10526\frac{3}{3} - 21645_4$
8987.396	75	10	11123.640	$13297_4 - 24421\frac{3}{3}$
8985.270	15	4	11126.271	$16217\frac{2}{2} - 27343_3$
8983.722	2		11128.189	$22399\frac{6}{6} - 33527_4$
8982.127	2		11130.165	$18011\frac{6}{6} - 29141_5$
8980.723	10	3	11131.905	$15863_2 - 26995\frac{5}{5}$
8978.886	3		11134.182	$19516\frac{2}{2} - 30651_3$
8976.639	3	1	11136.969	$18549_2 - 29686\frac{3}{3}$
8969.853	100	15	11145.395	$19227\frac{8}{8} - 30372_6$
8967.635	500	100	11148.151	$8800_4 - 19948\frac{4}{4}$
8965.074	2		11151.336	$14204_5 - 25355\frac{4}{4}$
8956.495	2		11162.017	$22669\frac{3}{3} - 33831_4$
8955.834	200	15	11162.841	$2869_3 - 14032\frac{2}{2}$
8952.133	2		11167.456	$22141\frac{3}{3} - 33309_2$
8949.114	100	20	11171.223	$13088_3 - 24259\frac{4}{4}$
8944.447	1		11177.052	$15618\frac{3}{3} - 26796_3$
8942.502	2		11179.483	$21575_2 - 32754\frac{3}{3}$
8941.641	8	2	11180.560	$10414\frac{3}{3} - 21594_3$
8935.225	1		11188.588	$22338\frac{3}{3} - 33527_4$
8933.357	1		11190.928	$17398_3 - 28589\frac{3}{3}$
8930.006	2		11195.127	$18549_2 - 29744\frac{3}{3}$
8928.384	2		11197.161	$21902\frac{4}{4} - 33099_3$
8928.078	25	5	11197.545	$15863_2 - 27061\frac{2}{2}$
8927.723	15	5	11197.990	$17959_4 - 29157\frac{5}{5}$
8924.217	3w		11202.389	$18930\frac{3}{3} - 30132_2$

TABLE 4. *Classified lines of* Th I—continued

Wavelength (Å)	Intensity		Wavenumber (cm^{-1})	Classification
	Lamp	Spark		
8922.566	2		11204.462	$18809\frac{3}{4} - 30014_4$
8918.698	1		11209.321	$21890\frac{5}{8} - 33099_3$
8918.584	1		11209.465	$22396\frac{1}{1} - 33606_2$
8912.867	2		11216.655	$21645_4 - 32862\frac{3}{4}$
8910.844	75	4	11219.201	$13088_3 - 24307\frac{1}{2}$
8907.016	40	2	11224.023	$13175\frac{3}{4} - 24399_3$
8905.566	2		11225.850	$22338\frac{3}{8} - 33564_3$
8902.815	2		11229.319	$19532_4 - 30761\frac{3}{5}$
8900.891	2		11231.746	$10414\frac{3}{4} - 21645_4$
8893.533	15	5	11241.039	$19516\frac{2}{2} - 30758_2$
8892.973	150	15	11241.747	$0_2 - 11241\frac{3}{5}$
8892.778	2		11241.993	$21539\frac{3}{4} - 32781_4$
8889.970	2		11245.544	$22163\frac{3}{4} - 33408_3$
8889.187	100	10	11246.535	$11802_2 - 23049\frac{1}{1}$
8882.601	1		11254.873	$19503\frac{3}{3} - 30758_2$
8877.739	1		11261.037	$22401_1 - 33662\frac{1}{1}$
8875.223	100	8	11264.229	$13297_4 - 24561\frac{3}{3}$
8874.156	2		11265.584	$22508\frac{2}{2} - 33773_1$
8872.787	1		11267.322	$22338\frac{3}{8} - 33606_2$
8872.409	1		11267.802	$21594_3 - 32862\frac{3}{4}$
8868.822	200	50	11272.359	$9804_5 - 21077\frac{5}{6}$
8867.740	1		11273.735	$17073_1 - 28347\frac{2}{2}$
8865.566	100	8	11276.499	$11601_1 - 22877\frac{1}{1}$
8862.284	2		11280.675	$19227\frac{5}{6} - 30508_5$
8860.973	4	1	11282.344	$17398_3 - 28680\frac{3}{4}$
8857.869	4	1	11286.298	$23015\frac{5}{6} - 34301_4$
8854.899	10	3	11290.083	$15970_3 - 27260\frac{3}{5}$
8854.136	1		11291.056	$11802_2 - 23093\frac{2}{2}$
8852.784	10	3	11292.781	$13088_3 - 24381\frac{2}{2}$
8852.552	1		11293.077	$21165\frac{3}{3} - 32458_4$
8850.543	2		11295.640	$21143_5 - 32439\frac{3}{4}$
8848.294	8	3	11298.511	$16554_6 - 27852\frac{0}{6}$
8847.513	2		11299.508	$14226_0 - 25526\frac{1}{1}$
8843.549	2		11304.573	$20322\frac{0}{6} - 31626_5$
8842.359	1		11306.095	$19713_3 - 31019\frac{3}{4}$
8841.841	4		11306.757	$17224\frac{2}{2} - 28531_2$
8841.170	150	20	11307.615	$7502_3 - 18809\frac{3}{4}$
8836.139	3		11314.053	$17166_5 - 28480\frac{3}{4}$
8833.471	2		11317.471	$18699_2 - 30017\frac{3}{3}$
8829.686	15	5	11322.322	$20214\frac{5}{5} - 31537_3$
8829.470	2		11322.599	$19948\frac{3}{4} - 31271_5$
8827.897	2		11324.616	$17354\frac{1}{1} - 28679_2$
8821.739	4	1	11332.521	$13088_3 - 24421\frac{3}{3}$
8820.409	50b	10	11334.230	$7280_2 - 18614\frac{1}{1}$
8820.214	20	3	11334.481	$12847_3 - 24182\frac{2}{2}$
8812.507	4		11344.393	$17501\frac{0}{6} - 28845_4$
8810.240	15		11347.312	$15970_3 - 27317\frac{3}{3}$
8808.667	2		11349.339	$18069\frac{3}{5} - 29418_2$
8806.220	2		11352.492	$15618\frac{3}{5} - 26971_4$
8804.580	75	3	11354.607	$12847_3 - 24202\frac{4}{4}$
8800.465	3		11359.916	$21594_3 - 32954\frac{2}{2}$
8799.353	1		11361.352	$21738\frac{2}{2} - 33099_3$
8798.171	10	3	11362.878	$19713_3 - 31075\frac{2}{2}$
8792.058	100	5	11370.779	$14204_5 - 25575\frac{4}{4}$
8790.372	10	2	11372.960	$19516\frac{2}{2} - 30889_1$
8786.029	2		11378.581	$19948\frac{3}{4} - 31326_4$
8784.139	3	1	11381.029	$21077\frac{0}{6} - 32458_4$
8781.093	25	1	11384.977	$4961_4 - 16346\frac{2}{4}$
8780.337	1		11385.958	$22141\frac{3}{3} - 33527_4$
8779.898	1		11386.527	$21165\frac{3}{3} - 32551_3$
8775.575	200	40	11392.136	$8111_4 - 19503\frac{3}{3}$
8773.524	5	1	11394.799	$16217\frac{2}{2} - 27612_3$
8772.803	150	8	11395.736	$11241\frac{3}{3} - 22637_3$
8772.384	8	1	11396.280	$15863_2 - 27260\frac{3}{5}$
8771.465	1		11397.474	$21645_4 - 33043\frac{5}{5}$
8768.195	5	1	11401.725	$22163\frac{3}{4} - 33564_3$
8766.743	100	15	11403.613	$13297_4 - 24701\frac{0}{6}$
8760.449	100	8	11411.806	$12847_3 - 24259\frac{3}{4}$
8758.247	400	75	11414.675	$8800_4 - 20214\frac{3}{3}$
8755.001	3	1	11418.907	$21890\frac{5}{5} - 33309_2$
8753.738	2h		11420.555	$22877\frac{1}{1} - 34298_1$
8751.202	10	2	11423.864	$22877\frac{0}{6} - 34301_4$
8750.176	1		11425.204	$14465\frac{2}{2} - 25890_2$
8748.038	400	100	11427.996	$7502_3 - 18930\frac{3}{5}$
8747.498	2		11428.701	$19817\frac{1}{1} - 31245_2$
8747.258	2		11429.015	$20566\frac{3}{4} - 31995_4$
8744.965	2	1	11432.012	$23015\frac{0}{6} - 34447_4$
8744.598	5	1	11432.492	$22399\frac{0}{6} - 33831_4$
8743.269	15	2	11434.229	$23655\frac{4}{4} - 35089_3$
8739.251	1		11439.486	$17073_1 - 28513\frac{2}{2}$
8735.735	2		11444.091	$16783\frac{3}{4} - 28227_4$
8734.482	5	1	11445.732	$23015\frac{0}{6} - 34460_5$
8734.023	75	8	11446.334	$20566\frac{3}{4} - 32012_4$
8732.992	2		11447.685	$19516\frac{2}{2} - 30964_3$
8732.426	150	50	11448.427	$11601_1 - 23049\frac{1}{1}$
8730.818	15	2	11450.536	$19273_2 - 30723\frac{1}{1}$
8728.550	2		11453.511	$15863_2 - 27317\frac{5}{5}$
8727.446	4		11454.960	$17224\frac{2}{2} - 28679_2$
8724.375	40	2	11458.992	$13847_2 - 25306\frac{2}{2}$
8723.718	15	2	11459.855	$13945\frac{3}{3} - 25405_4$
8722.459	15	2	11461.509	$19503\frac{3}{3} - 30964_3$
8717.754	10	2	11467.695	$18549_2 - 30017\frac{3}{3}$
8716.427	2		11469.441	$8243\frac{2}{2} - 19713_3$
8715.065	1		11471.233	$17411\frac{3}{3} - 28882_2$
8714.917	1		11471.428	$20322\frac{0}{6} - 31793_4$
8714.257	8	1	11472.297	$13297_4 - 24769\frac{3}{3}$
8713.654	20	2	11473.090	$13088_3 - 24561\frac{3}{3}$
8712.838	10	2	11474.165	$13847_2 - 25321\frac{3}{3}$
8710.410	50	2	11477.363	$8111_4 - 19588\frac{0}{6}$
8709.233	200	50	11478.914	$3687_2 - 15166\frac{3}{3}$
8707.356	75	3	11481.389	$15490\frac{0}{6} - 26971_4$
8704.855	25	3	11484.688	$6362_2 - 17847\frac{2}{2}$
8703.697	25	2	11486.216	$14204_5 - 25690\frac{0}{6}$
8703.340	3		11486.687	$19532_4 - 31019\frac{3}{4}$
8702.021	8	1	11488.428	$19273_2 - 30761\frac{3}{5}$
8701.117	50	3	11489.622	$13175\frac{3}{4} - 24664_3$
8693.669	2		11499.465	$19227\frac{5}{6} - 30726_7$
8691.333	20l	1	11502.556	$15493_4 - 26995\frac{3}{3}$
8689.176	8	3	11505.411	$19039\frac{2}{2} - 30544_2$
8688.429	2		11506.400	$21902\frac{3}{4} - 33408_3$

TABLE 4. *Classified lines of* Th I—continued

Wavelength (Å)	Intensity		Wavenumber (cm^{-1})	Classification
	Lamp	Spark		
8687.841	50	4	11507.179	$15490^{6}_{6} - 26997_{6}$
8682.216	10	1	11514.634	$17166_{5} - 28680^{4}_{4}$
8681.305	2		11515.842	$21902^{3}_{3} - 33418_{4}$
8679.439	15	1	11518.318	$18614^{1}_{1} - 30132_{2}$
8679.303	1		11518.499	$20522^{2}_{2} - 32041_{2}$
8679.303	1		11518.499	$21890^{5}_{5} - 33408_{3}$
8678.490	10	1	11519.578	$17398_{3} - 28917^{2}_{2}$
8676.629	2s		11522.048	$8800_{4} - 20322^{6}_{6}$
8675.392	15	2	11523.691	$17411^{3}_{3} - 28934_{3}$
8674.634	1		11524.698	$22248^{2}_{2} - 33773_{1}$
8672.281	1		11527.825	$17354^{1}_{1} - 28882_{2}$
8672.159	3		11527.987	$21890^{3}_{3} - 33418_{4}$
8668.118	100	20	11533.362	$12847_{3} - 24381^{2}_{2}$
8667.444	15	2	11534.258	$17398_{3} - 28932^{4}_{4}$
8665.491	400	100	11536.858	$7502_{3} - 19039^{2}_{2}$
8663.348	4		11539.712	$19273_{2} - 30812^{2}_{2}$
8662.270	2		11541.148	$18011^{6}_{6} - 29552_{6}$
8660.494	1		11543.515	$21252^{2}_{2} - 32796_{3}$
8659.754	2		11544.501	$20054_{2} - 31599^{2}_{2}$
8657.541	3		11547.452	$22141^{3}_{3} - 33689_{2}$
8655.873	50	8	11549.677	$14204_{5} - 25753^{6}_{6}$
8651.256	3		11555.841	$18699_{2} - 30255^{3}_{3}$
8650.455	2		11556.911	$21902^{3}_{3} - 33459_{4}$
8649.144	50	5	11558.663	$16783^{3}_{4} - 28342_{5}$
8648.386	40	4	11559.676	$20214^{3}_{3} - 31774_{3}$
8648.282	5		11559.815	$21539^{2}_{4} - 33099_{3}$
8645.310	150	25	11563.789	$13962_{1} - 25526^{1}_{1}$
8642.849	1		11567.081	$22877^{1}_{1} - 34444_{2}$
8641.383	3	1	11569.044	$21890^{3}_{3} - 33459_{4}$
8640.972	4		11569.594	$22877^{1}_{1} - 34447_{4}$
8639.655	8		11571.358	$17847^{2}_{2} - 29418_{2}$
8639.444	150	5	11571.640	$10526^{3}_{3} - 22098_{4}$
8638.360	100	5	11573.092	$12847_{3} - 24421^{3}_{3}$
8637.271	5	1	11574.551	$16783^{3}_{4} - 28358_{3}$
8636.928	2		11575.011	$17847^{2}_{2} - 29422_{1}$
8636.680	2		11575.343	$17073_{1} - 28649^{1}_{1}$
8634.114	3		11578.784	$20214^{3}_{3} - 31793_{4}$
8634.022	5h	1	11578.907	$19516^{2}_{2} - 31095_{1}$
8633.966	3		11578.982	$18382^{6}_{6} - 29961_{1}$
8633.455	3	1	11579.667	$22141^{3}_{3} - 33721_{2}$
8632.169	3	1	11581.393	$18699_{2} - 30281^{1}_{1}$
8631.788	2		11581.904	$18069^{3}_{3} - 29650_{2}$
8631.350	50	2	11582.491	$14226_{0} - 25809^{1}_{1}$
8630.770	20h	2h	11583.270	$22877^{6}_{6} - 34460_{5}$
8630.330	5	1	11583.860	$15863_{2} - 27447^{2}_{2}$
8626.611	1		11588.854	$19948^{4}_{4} - 31537_{3}$
8626.254	1		11589.334	$22855^{3}_{3} - 34444_{2}$
8622.093	5	1	11594.927	$13847_{2} - 25442^{3}_{3}$
8621.315	75	2	11595.973	$2869_{3} - 14465^{2}_{2}$
8618.598	5	1	11599.629	$17073_{1} - 28673^{2}_{2}$
8616.218	100	10	11602.833	$17501^{6}_{6} - 29104_{4}$
8614.687	5	1	11604.895	$21668^{1}_{1} - 33273_{1}$
8611.754	3		11608.847	$19532_{4} - 31141^{6}_{6}$
8609.370	4	1	11612.062	$19817^{1}_{1} - 31429_{1}$
8607.724	8	2	11614.282	$18930^{3}_{3} - 30544_{2}$
8605.146	2		11617.762	$20423^{1}_{1} - 32041_{2}$
8604.922	4		11618.064	$10783^{2}_{2} - 22401_{1}$
8601.844	1		11622.221	$18930^{3}_{3} - 30552_{4}$
8600.016	3		11624.692	$21645_{4} - 33270^{3}_{4}$
8596.686	5		11629.195	$15166^{3}_{3} - 26796_{3}$
8596.466	8	1	11629.492	$20922^{2}_{2} - 32551_{3}$
8595.655	1		11630.590	$18053^{3}_{4} - 29684_{5}$
8595.359	1		11630.990	$21165^{3}_{3} - 32796_{3}$
8595.307	1		11631.060	$21165^{3}_{3} - 32796_{3}$
8594.965	1		11631.523	$22669^{3}_{3} - 34301_{4}$
8593.103	100	10	11634.044	$16346^{4}_{4} - 27980_{3}$
8589.687	3		11638.670	$19503^{3}_{3} - 31141_{3}$
8588.435	50	2	11640.367	$17501^{6}_{6} - 29141_{5}$
8588.221	8		11640.657	$19986^{8}_{8} - 31626_{5}$
8583.974	2		11646.416	$14243^{1}_{1} - 25890_{2}$
8582.016	4		11649.074	$21645_{4} - 33294^{3}_{3}$
8579.355	3		11652.687	$21738^{2}_{2} - 33390_{1}$
8577.279	100	15	11655.507	$12114^{2}_{2} - 23769_{1}$
8575.327	75	5	11658.160	$17224^{2}_{2} - 28882_{2}$
8574.577	2		11659.180	$18549_{2} - 30208^{2}_{2}$
8574.081	50	10	11659.854	$21077^{6}_{6} - 32737_{5}$
8573.122	500	100	11661.159	$5563_{1} - 17224^{2}_{2}$
8572.075	4	1	11662.583	$21902^{3}_{4} - 33564_{3}$
8564.748	50	4	11672.560	$18614^{1}_{1} - 30286_{1}$
8564.570	5		11672.803	$18011^{6}_{6} - 29684_{5}$
8564.141	25	3	11673.387	$20322^{6}_{6} - 31995_{4}$
8563.151	15	2	11674.737	$21890^{3}_{3} - 33564_{3}$
8563.003	3		11674.939	$21539^{2}_{4} - 33214_{5}$
8562.314	5	1	11675.878	$21594_{3} - 33270^{3}_{4}$
8560.425	100	4	11678.454	$11802_{2} - 23481^{1}_{1}$
8558.448	75l	4	11681.152	$13088_{3} - 24769^{3}_{3}$
8556.589	10b		11683.690	$13297_{4} - 24981^{3}_{3}$
8556.324	100	20	11684.052	$10414^{3}_{3} - 22098_{4}$
8554.945	200	50	11685.935	$2558_{0} - 14243^{1}_{1}$
8553.895	1		11687.370	$16346^{4}_{4} - 28034_{5}$
8551.763	8	1	11690.284	$22141^{3}_{3} - 33831_{4}$
8551.460	2		11690.698	$20322^{6}_{6} - 32012_{4}$
8549.932	1		11692.787	$17411^{3}_{3} - 29104_{4}$
8543.721	150	40	11701.287	$15490^{6}_{6} - 27191_{5}$
8542.618	3h		11702.798	$18053^{3}_{4} - 29756_{4}$
8540.232	4	1	11706.068	$18549_{2} - 30255^{3}_{3}$
8539.795	150	25	11706.667	$6362_{2} - 18069^{3}_{3}$
8537.379	3		11709.979	$22401_{1} - 34111^{1}_{1}$
8534.674	50	2	11713.691	$12847_{3} - 24561^{3}_{3}$
8532.907	10	1	11716.117	$14206^{3}_{4} - 25923_{4}$
8532.096	8	1	11717.230	$19273_{2} - 30990^{3}_{3}$
8531.445	50	2	11718.124	$11802_{2} - 23521^{3}_{3}$
8530.911	40	3	11718.858	$19039^{2}_{2} - 30758_{2}$
8530.159	2		11719.891	$21575_{2} - 33294^{3}_{3}$
8528.762	3		11721.811	$21668^{1}_{1} - 33390_{1}$
8528.548	2		11722.105	$21575_{2} - 33297^{2}_{2}$
8526.603	3		11724.779	$15618^{3}_{3} - 27343_{3}$
8525.651	4		11726.088	$20054_{2} - 31780^{3}_{3}$
8525.386	3		11726.452	$17959_{4} - 29686^{3}_{3}$
8524.785	2		11727.279	$20566^{3}_{4} - 32293_{5}$

TABLE 4. *Classified lines of* Th I—continued

Wavelength (Å)	Intensity		Wavenumber (cm^{-1})	Classification
	Lamp	Spark		
8521.620	4		11731.635	$18549_2 - 30281\frac{1}{1}$
8519.327	50	3	11734.792	$9804_5 - 21539\frac{3}{4}$
8516.555	150	50	11738.612	$19588\frac{5}{6} - 31326_4$
8515.615	2		11739.907	$13175\frac{3}{4} - 24915_3$
8514.901	8	1	11740.892	$13962_1 - 25703\frac{2}{2}$
8513.624	2		11742.653	$18809\frac{3}{4} - 30552_4$
8511.906	50	3	11745.023	$18011\frac{5}{6} - 29756_4$
8510.622	150	25	11746.795	$11241\frac{5}{5} - 22988_2$
8509.273	2		11748.657	$19516\frac{2}{2} - 31265_3$
8508.186	5	1	11750.158	$23655\frac{3}{4} - 35405_3$
8501.756	8		11759.045	$7280_2 - 19039\frac{2}{2}$
8501.438	50	5	11759.485	$17398_3 - 29157\frac{3}{3}$
8500.011	10	2	11761.459	$22669\frac{3}{3} - 34431_3$
8498.731	2		11763.230	$16217\frac{2}{2} - 27980_3$
8496.449	50b		11766.390	$8800_4 - 20566\frac{4}{4}$
8496.340	25b		11766.541	$17166_5 - 28932\frac{4}{4}$
8496.044	4		11766.951	$15493_4 - 27260\frac{5}{5}$
8491.811	10		11772.816	$15493_4 - 27266\frac{3}{3}$
8491.368	2		11773.430	$17959_4 - 29733\frac{6}{6}$
8488.564	1		11777.320	$22669\frac{3}{3} - 34447_4$
8487.478	15	1	11778.826	$16783\frac{4}{4} - 28562_4$
8486.561	50	2	11780.099	$18069\frac{3}{3} - 29849_4$
8486.108	2		11780.728	$20214\frac{5}{5} - 31995_4$
8485.600	3		11781.433	$18053\frac{4}{4} - 29835_3$
8483.298	50	2	11784.630	$17959_4 - 29744\frac{3}{3}$
8482.478	1		11785.769	$23655\frac{4}{4} - 35440_3$
8478.505	200		11791.292	$11241\frac{3}{3} - 23032_4$
8478.353	500		11791.504	$5563_1 - 17354\frac{1}{1}$
8473.657	1		11798.038	$20214\frac{3}{3} - 32012_4$
8472.593	40	3	11799.520	$17398_3 - 29197\frac{2}{2}$
8471.823	200	50	11800.592	$11802_2 - 23603\frac{2}{2}$
8470.358	5		11802.633	$19273_2 - 31075\frac{2}{2}$
8469.451	3		11803.897	$17847\frac{2}{2} - 29650_2$
8468.973	8	2	11804.563	$15166\frac{3}{3} - 26971_4$
8467.164	5	1	11807.086	$15863_2 - 27670\frac{3}{3}$
8465.668	100	25	11809.172	$11601_1 - 23410\frac{6}{6}$
8464.753	50	3	11810.448	$15863_2 - 27674\frac{2}{2}$
8464.236	150	50	11811.170	$8243\frac{2}{2} - 20054_2$
8462.015	4		11814.270	$15970_3 - 27784\frac{2}{2}$
8456.341	50	2	11822.197	$4961_4 - 16783\frac{4}{4}$
8455.209	2		11823.780	$19503\frac{3}{3} - 31326_4$
8454.924	50	4	11824.178	$15493_4 - 27317\frac{5}{5}$
8453.419	5	1	11826.283	$20214\frac{3}{3} - 32041_2$
8451.839	2		11828.494	$22338\frac{3}{3} - 34167_3$
8450.836	15b		11829.898	$15736\frac{1}{1} - 27566_2$
8449.925	2		11831.173	$21890\frac{3}{3} - 33721_2$
8447.968	4	1	11833.914	$23015\frac{6}{6} - 34849_5$
8446.516	500	150	11835.948	$11197\frac{6}{6} - 23032_4$
8445.495	200	150	11837.379	$8111_4 - 19948\frac{3}{3}$
8445.214	100b	8	11837.773	$18011\frac{6}{6} - 29849_4$
8440.671	25		11844.145	$17073_1 - 28917\frac{2}{2}$
8440.660	50w	4	11844.160	$17073_1 - 28917\frac{2}{2}$
8440.578	25		11844.275	$14204_5 - 26048\frac{3}{3}$
8439.849	1		11845.298	$19948\frac{3}{4} - 31793_4$
8438.789	8		11846.786	$13962_1 - 25809\frac{1}{1}$
8434.780	2		11852.417	$22855\frac{3}{3} - 34707_3$
8433.885	8	1	11853.674	$18699_2 - 30553\frac{2}{2}$
8432.485	10	2	11855.643	$13847_2 - 25703\frac{2}{2}$
8430.586	15	1	11858.313	$14032\frac{2}{2} - 25890_2$
8426.379	75		11864.233	$14247\frac{6}{6} - 26111_1$
8424.031	100		11867.540	$14243\frac{1}{1} - 26111_1$
8423.529	3		11868.247	$21738\frac{2}{2} - 33606_2$
8422.942	2h		11869.075	$21539\frac{3}{4} - 33408_3$
8422.464	1		11869.748	$22098_4 - 33967\frac{3}{3}$
8421.227	500	100	11871.492	$3865_1 - 15736\frac{1}{1}$
8419.431	2		11874.024	$20922\frac{2}{2} - 32796_3$
8418.004	200	75	11876.037	$12114\frac{2}{2} - 23990_2$
8417.605	8	2	11876.600	$15618\frac{3}{3} - 27495_4$
8417.071	75	3	11877.353	$15166\frac{3}{3} - 27044_3$
8416.742	500w	150	11877.818	$0_2 - 11877\frac{1}{1}$
8415.375	75	4	11879.747	$20322\frac{6}{6} - 32202_5$
8414.938	50	1	11880.364	$11601_1 - 23481\frac{1}{1}$
8414.273	4		11881.303	$16346\frac{3}{4} - 28227_4$
8414.005	2		11881.681	$21645\frac{3}{4} - 33527_4$
8411.913	100	5	11884.636	$17166_5 - 29050\frac{6}{6}$
8410.763	5		11886.261	$19713_3 - 31599\frac{2}{2}$
8407.010	75	3	11891.567	$20566\frac{3}{4} - 32458_4$
8406.674	40	2	11892.043	$11877\frac{1}{1} - 23769_1$
8406.314	20	1	11892.552	$13088_3 - 24981\frac{3}{3}$
8401.986	100	8	11898.678	$14481\frac{6}{6} - 26380_5$
8400.154	2		11901.273	$22396\frac{1}{1} - 34298_1$
8399.253	100	8	11902.550	$15618\frac{3}{3} - 27521_4$
8398.171	100	8	11904.083	$18382\frac{6}{6} - 30286_1$
8392.847	50	3	11911.634	$17398_3 - 29310\frac{4}{4}$
8392.397	40		11912.273	$19516\frac{2}{2} - 31429_1$
8388.528	100	10	11917.767	$7795\frac{3}{4} - 19713_3$
8385.726	100	10	11921.750	$12847_3 - 24769\frac{3}{3}$
8384.927	8	2	11922.886	$22401_1 - 34324\frac{2}{2}$
8384.639	1		11923.295	$22508\frac{2}{2} - 34431_3$
8383.073	8	2	11925.522	$19039\frac{2}{2} - 30964_3$
8379.754	75	4	11930.246	$18614\frac{1}{1} - 30544_2$
8379.219	100	8	11931.008	$3687_2 - 15618\frac{3}{3}$
8376.896	3		11934.316	$21165\frac{3}{3} - 33099_3$
8375.333	1		11936.543	$22508\frac{2}{2} - 34444_2$
8374.766	50	2	11937.351	$21668\frac{1}{1} - 33606_2$
8374.202	50	3	11938.155	$11802_2 - 23741\frac{1}{1}$
8371.658	2		11941.783	$21890\frac{3}{3} - 33831_4$
8371.303	1		11942.290	$18069\frac{3}{3} - 30011_3$
8369.332	200	50	11945.102	$13945\frac{3}{3} - 25890_2$
8367.390	150	20	11947.874	$15618\frac{3}{3} - 27566_2$
8366.073	150	15	11949.755	$11802_2 - 23752\frac{2}{2}$
8365.198	2		11951.005	$21738\frac{2}{2} - 33689_2$
8360.487	75	5	11957.739	$18053\frac{4}{4} - 30011_3$
8358.728	150	200	11960.256	$11241\frac{3}{3} - 23201_3$
8357.829	50	3	11961.542	$13847_2 - 25809\frac{1}{1}$
8357.192	1		11962.454	$22338\frac{3}{3} - 34301_4$
8355.142	50	4	11965.389	$21594_3 - 33560\frac{4}{4}$
8350.865	2		11971.517	$22877\frac{1}{1} - 34849_5$
8346.537	50	3	11977.725	$13945\frac{3}{3} - 25923_4$
8345.867	50	5	11978.686	$18574_1 - 30553\frac{2}{2}$

TABLE 4. *Classified lines of* Th I – continued

Wavelength (Å)	Intensity		Wavenumber (cm^{-1})	Classification
	Lamp	Spark		
8344.174	8	2	11981.117	$19948\frac{3}{4} - 31929_3$
8341.475	50	8	11984.993	$20566\frac{3}{4} - 32551_3$
8339.403	5	2	11987.971	$17847\frac{1}{2} - 29835_3$
8337.330	2h	1	11990.952	$21077\frac{5}{6} - 33068_6$
8336.934	20	2	11991.521	$19532_4 - 31523\frac{3}{5}$
8335.700	50	8	11993.297	$15618\frac{3}{5} - 27612_3$
8333.441	50	5	11996.548	$21594_3 - 33591\frac{3}{5}$
8330.455	500	300	12000.848	$7502_3 - 19503\frac{3}{5}$
8329.299	2		12002.513	$11601_1 - 23603\frac{1}{2}$
8328.990	15	2	12002.959	$18011\frac{5}{6} - 30014_4$
8328.338	15	2	12003.898	$18549_2 - 30553\frac{1}{2}$
8327.213	15	2	12005.520	$15490\frac{5}{6} - 27495_4$
8326.068	5	1	12007.171	$17411\frac{3}{5} - 29418_2$
8322.891	5	1	12011.754	$16346\frac{3}{4} - 28358_3$
8320.859	500	150	12014.688	$7502_3 - 19516\frac{1}{2}$
8317.106	2		12020.109	$21668\frac{1}{2} - 33689_2$
8316.595	8	2	12020.848	$17398_3 - 29419\frac{1}{2}$
8314.281	4	1	12024.193	$18699_2 - 30723\frac{1}{2}$
8314.067	5	1	12024.503	$13297_4 - 25321\frac{3}{5}$
8313.281	2		12025.640	$20054_2 - 32080\frac{1}{2}$
8311.019	2		12028.913	$20522\frac{1}{2} - 32551_3$
8309.257	15		12031.463	$15490\frac{5}{6} - 27521_4$
8307.245	1		12034.377	$18930\frac{3}{5} - 30964_3$
8306.411	1		12035.586	$21738\frac{1}{2} - 33773_1$
8304.844	5	1	12037.857	$22669\frac{3}{5} - 34707_3$
8304.412	50	3	12038.483	$19588\frac{5}{6} - 31626_5$
8304.030	8	1	12039.037	$18574_1 - 30613\frac{5}{6}$
8298.353	10	2	12047.273	$19948\frac{3}{4} - 31995_4$
8297.984	3		12047.808	$22399\frac{5}{6} - 34447_4$
8297.377	25	2	12048.690	$14206\frac{3}{4} - 26255_4$
8297.172	50b	5	12048.987	$3687_2 - 15736\frac{1}{2}$
8295.542	100	8	12051.355	$17501\frac{5}{6} - 29552_6$
8294.880	8c		12052.317	$21668\frac{1}{2} - 33721_2$
8292.521	100	8	12055.745	$16217\frac{1}{2} - 28273_2$
8292.039	4		12056.446	$21252\frac{1}{2} - 33309_2$
8291.869	1		12056.693	$19039\frac{1}{2} - 31095_1$
8291.523	2		12057.196	$17959_4 - 30017\frac{3}{5}$
8290.864	2		12058.155	$13297_4 - 25355\frac{3}{4}$
8289.447	2		12060.216	$14226_0 - 26287\frac{1}{2}$
8288.404	50	5	12061.733	$16783\frac{3}{4} - 28845_4$
8287.110	25	3	12063.617	$18069\frac{3}{5} - 30132_2$
8287.023	8		12063.744	$17354\frac{1}{2} - 29418_2$
8284.481	3		12067.445	$17354\frac{1}{2} - 29422_1$
8276.232	20	2	12079.473	$14032\frac{1}{2} - 26111_1$
8275.628	400	150	12080.354	$11197\frac{5}{6} - 23277_5$
8273.609	8	1	12083.302	$17073_1 - 29157\frac{1}{2}$
8270.940	3	1	12087.202	$21575_2 - 33662\frac{1}{2}$
8267.412	2		12092.360	$22338\frac{3}{5} - 34431_3$
8263.926	150	20	12097.460	$9804_5 - 21902\frac{3}{4}$
8261.010	100	25	12101.731	$15490\frac{5}{6} - 27591_5$
8260.391	1		12102.638	$19039\frac{1}{2} - 31141_3$
8259.505	100	8	12103.936	$8111_4 - 20214\frac{3}{5}$
8258.339	8	2	12105.645	$22338\frac{3}{5} - 34444_2$
8254.741	100	15	12110.921	$10526\frac{3}{5} - 22637_3$
8253.613	75	8	12112.576	$11877\frac{1}{2} - 23990_2$
8252.398	400	50	12114.360	$0_2 - 12114\frac{1}{2}$
8246.170	2h		12123.509	$17073_1 - 29197\frac{1}{2}$
8246.011	25	4	12123.743	$21594_3 - 33718\frac{1}{2}$
8245.781	2		12124.081	$17073_1 - 29197\frac{1}{2}$
8243.712	2		12127.124	$21143_5 - 33270\frac{3}{4}$
8239.619	5	1	12133.148	$12847_3 - 24981\frac{3}{5}$
8237.739	20	2	12135.917	$20322\frac{5}{6} - 32458_4$
8236.739	4		12137.390	$21077\frac{5}{6} - 33214_5$
8235.819	4	1	12138.746	$19532_4 - 31671\frac{3}{4}$
8235.484	1		12139.240	$23655\frac{3}{4} - 35794_4$
8234.937	50	4	12140.046	$11601_1 - 23741\frac{1}{2}$
8234.937	50	4	12140.046	$21594_3 - 33734\frac{1}{2}$
8234.346	25	3	12140.918	$16217\frac{1}{2} - 28358_3$
8233.377	2		12142.347	$20054_2 - 32197\frac{3}{5}$
8232.673	1		12143.385	$21575_2 - 33718\frac{1}{2}$
8232.451	3		12143.712	$18614\frac{1}{2} - 30758_2$
8232.310	2		12143.920	$21165\frac{3}{5} - 33309_2$
8231.410	100	15	12145.248	$13297_4 - 25442\frac{3}{5}$
8228.725	1		12149.211	$18574_1 - 30723\frac{1}{2}$
8227.672	50	4	12150.766	$13962_1 - 26113\frac{1}{2}$
8227.482	50	8	12151.046	$16783\frac{3}{4} - 28934_3$
8227.096	3		12151.617	$11601_1 - 23752\frac{1}{2}$
8224.956	8	2	12154.778	$21645_4 - 33800\frac{3}{5}$
8223.407	8		12157.068	$19713_3 - 31870\frac{1}{2}$
8221.666	1		12159.642	$21575_2 - 33734\frac{1}{2}$
8220.872	3		12160.817	$15863_2 - 28024\frac{1}{2}$
8214.147	100	10	12170.773	$15970_3 - 28140\frac{3}{4}$
8212.219	5	1	12173.630	$14206\frac{3}{4} - 26380_5$
8210.525	2		12176.142	$23655\frac{3}{4} - 35831_3$
8210.047	4		12176.851	$15166\frac{3}{5} - 27343_3$
8209.444	100	8	12177.745	$15493_4 - 27670\frac{3}{5}$
8208.596	2		12179.003	$17073_1 - 29252\frac{1}{2}$
8208.596	2		12179.003	$17073_1 - 29252\frac{1}{2}$
8207.475	100	10	12180.666	$14204_5 - 26384\frac{3}{4}$
8205.892	8		12183.016	$17501\frac{5}{6} - 29684_5$
8205.103	20	2	12184.188	$19532_4 - 31716\frac{5}{6}$
8202.148	100	10	12188.577	$13847_2 - 26036\frac{3}{5}$
8201.354	1		12189.757	$22401_1 - 34591\frac{1}{2}$
8198.438	10	2	12194.093	$17224\frac{1}{2} - 29418_2$
8195.942	8	1	12197.806	$17224\frac{1}{2} - 29422_1$
8194.698	3		12199.658	$22508\frac{1}{2} - 34707_3$
8194.398	100	25	12200.105	$17959_4 - 30160\frac{3}{4}$
8194.398	100	25	12200.105	$20867\frac{1}{2} - 33068_6$
8193.239	5	1	12201.831	$23015\frac{5}{6} - 35216_5$
8192.136	3		12203.473	$22669\frac{3}{5} - 34873_4$
8191.069	10	1	12205.063	$21594_3 - 33799\frac{3}{4}$
8190.889	50	8	12205.331	$19588\frac{5}{6} - 31793_4$
8190.479	2		12205.942	$21594_3 - 33800\frac{3}{5}$
8189.938	4		12206.749	$19039\frac{1}{2} - 31245_2$
8186.915	500	100	12211.256	$8111_4 - 20322\frac{5}{6}$
8186.217	8		12212.297	$18549_2 - 30761\frac{3}{5}$
8183.838	10	2	12215.847	$19986\frac{3}{5} - 32202_5$
8183.723	2		12216.019	$16346\frac{3}{4} - 28562_4$
8179.030	8	1	12223.028	$7280_2 - 19503\frac{3}{5}$
8178.829	2		12223.329	$10414\frac{3}{4} - 22637_3$

TABLE 4. *Classified lines of* Th I—continued

Wavelength (Å)	Intensity		Wavenumber (cm^{-1})	Classification
	Lamp	Spark		
8178.318	2		12224.092	$19817_{\frac{1}{2}} - 32041_2$
8174.704	2		12229.496	$20566_{\frac{3}{4}} - 32796_3$
8174.328	2		12230.059	$13175_{\frac{3}{4}} - 25405_4$
8174.086	4		12230.421	$20054_2 - 32285_{\frac{5}{2}}$
8172.122	50	3	12233.360	$13088_3 - 25321_{\frac{5}{2}}$
8171.652	2		12234.064	$22855_{\frac{5}{2}} - 35089_3$
8169.793	400	50	12236.848	$7280_2 - 19516_{\frac{5}{2}}$
8168.775	5		12238.373	$18574_1 - 30812_{\frac{5}{2}}$
8167.865	3		12239.736	$17411_{\frac{3}{2}} - 29650_2$
8163.355	1		12246.498	$22098_4 - 34344_{\frac{3}{4}}$
8162.064	50	3	12248.435	$19532_4 - 31780_{\frac{5}{2}}$
8161.552	2		12249.204	$13847_2 - 26096_{\frac{5}{2}}$
8159.737	400	100	12251.928	$6362_2 - 18614_{\frac{1}{2}}$
8159.016	2		12253.011	$21165_{\frac{5}{2}} - 33418_4$
8157.540	50	8	12255.228	$17501_{\frac{5}{2}} - 29756_4$
8155.949	5	1	12257.619	$19516_{\frac{5}{2}} - 31774_3$
8151.973	2		12263.597	$18549_2 - 30812_{\frac{5}{2}}$
8150.878	1		12265.245	$21902_{\frac{3}{4}} - 34167_3$
8150.703	25		12265.508	$13847_2 - 26113_{\frac{5}{2}}$
8149.704	50	4	12267.011	$13088_3 - 25355_{\frac{3}{4}}$
8148.901	3		12268.220	$22163_{\frac{3}{4}} - 34431_3$
8146.748	5		12271.462	$19503_{\frac{5}{2}} - 31774_3$
8146.237	5		12272.232	$22877_{\frac{1}{2}} - 35149_2$
8144.017	4		12275.577	$18614_{\frac{1}{2}} - 30889_1$
8143.143	500	300	12276.895	$8800_4 - 21077_{\frac{5}{2}}$
8142.679	20	3	12277.595	$13297_4 - 25575_{\frac{3}{4}}$
8138.474	200	100	12283.938	$5563_1 - 17847_{\frac{5}{2}}$
8137.940	50	4	12284.744	$12114_{\frac{5}{2}} - 24399_3$
8137.367	4		12285.609	$17847_{\frac{5}{2}} - 30132_2$
8137.256	2		12285.777	$23015_{\frac{5}{2}} - 35300_5$
8135.798	2		12287.979	$17398_3 - 29686_{\frac{5}{2}}$
8134.633	5		12289.738	$22141_{\frac{5}{2}} - 34431_3$
8134.085	2		12290.566	$19503_{\frac{5}{2}} - 31793_4$
8133.855	1		12290.914	$18699_2 - 30990_{\frac{5}{2}}$
8132.964	50	1	12292.260	$21539_{\frac{3}{4}} - 33831_4$
8131.517	5	1	12294.448	$22855_{\frac{5}{2}} - 35149_2$
8129.681	50	5	12297.224	$16351_0 - 28649_{\frac{1}{2}}$
8129.405	150	25	12297.642	$2869_3 - 15166_{\frac{5}{2}}$
8125.877	4		12302.981	$22141_{\frac{5}{2}} - 34444_2$
8122.725	200	50	12307.755	$19986_{\frac{5}{2}} - 32293_5$
8121.058	15	1	12310.282	$13945_{\frac{5}{2}} - 26255_4$
8117.557	5		12315.591	$18930_{\frac{5}{2}} - 31245_2$
8114.539	50	4	12320.171	$16783_{\frac{3}{4}} - 29104_4$
8108.929	4	1	12328.695	$15166_{\frac{5}{2}} - 27495_4$
8107.508	3		12330.855	$14465_{\frac{5}{2}} - 26796_3$
8106.805	2		12331.925	$18809_{\frac{3}{4}} - 31141_3$
8104.536	2		12335.377	$18930_{\frac{5}{2}} - 31265_3$
8103.669	3	1	12336.697	$20214_{\frac{5}{2}} - 32551_3$
8101.873	2		12339.432	$22877_{\frac{1}{2}} - 35216_5$
8100.839	1		12341.007	$21077_{\frac{5}{2}} - 33418_4$
8097.857	4		12345.551	$19948_{\frac{3}{4}} - 32293_5$
8097.483	4		12346.122	$17398_3 - 29744_{\frac{5}{2}}$
8096.253	20	3	12347.997	$17501_{\frac{5}{2}} - 29849_4$
8093.631	200	75	12351.997	$3865_1 - 16217_{\frac{5}{2}}$
8092.238	75	5	12354.124	$13088_3 - 25442_{\frac{5}{2}}$
8092.238	75	5	12354.124	$18574_1 - 30928_{\frac{1}{2}}$
8091.356	2		12355.470	$21645_4 - 34001_{\frac{3}{4}}$
8089.896	4		12357.700	$16783_{\frac{3}{4}} - 29141_5$
8089.481	75	8	12358.334	$9804_5 - 22163_{\frac{3}{4}}$
8088.701	4		12359.526	$15493_4 - 27852_{\frac{5}{2}}$
8087.495	5	2	12361.369	$18011_{\frac{5}{2}} - 30372_6$
8087.263	2		12361.723	$15618_{\frac{5}{2}} - 27980_3$
8085.228	200	50	12364.835	$8800_4 - 21165_{\frac{5}{2}}$
8084.451	1		12366.023	$22508_{\frac{5}{2}} - 34874_3$
8076.980	5	1	12377.461	$15970_3 - 28347_{\frac{5}{2}}$
8075.651	150	20	12379.498	$11802_2 - 24182_{\frac{5}{2}}$
8074.472	3		12381.306	$18431_3 - 30812_{\frac{5}{2}}$
8070.785	2		12386.962	$20922_{\frac{5}{2}} - 33309_2$
8068.729	5	1	12390.118	$19039_{\frac{5}{2}} - 31429_1$
8066.826	75	8	12393.041	$13297_4 - 25690_{\frac{5}{2}}$
8064.380	2		12396.800	$20566_{\frac{3}{4}} - 32963_5$
8062.640	200	50	12399.475	$19227_{\frac{5}{2}} - 31626_5$
8062.345	4		12399.929	$15166_{\frac{5}{2}} - 27566_2$
8061.918	3		12400.586	$13962_1 - 26363_{\frac{5}{2}}$
8057.973	50	2	12406.657	$21594_3 - 34001_{\frac{3}{4}}$
8054.929	2		12411.345	$21890_{\frac{5}{2}} - 34301_4$
8052.715	5		12414.758	$20322_{\frac{5}{2}} - 32737_5$
8051.486	1		12416.653	$21143_5 - 33560_{\frac{3}{4}}$
8050.067	5	1	12418.841	$10783_{\frac{5}{2}} - 23201_3$
8048.611	2		12421.088	$19532_4 - 31953_{\frac{3}{4}}$
8046.838	5		12423.825	$17411_{\frac{5}{2}} - 29835_3$
8046.331	8	3	12424.608	$19588_{\frac{5}{2}} - 32012_4$
8045.182	5	1	12426.382	$19503_{\frac{5}{2}} - 31929_3$
8044.989	4b		12426.680	$17224_{\frac{5}{2}} - 29650_2$
8043.239	1		12429.384	$21738_{\frac{5}{2}} - 34167_3$
8038.691	2		12436.416	$21252_{\frac{5}{2}} - 33689_2$
8037.699	3		12437.951	$17411_{\frac{5}{2}} - 29849_4$
8035.618	50		12441.172	$21165_{\frac{5}{2}} - 33606_2$
8032.883	10		12445.408	$15166_{\frac{5}{2}} - 27612_3$
8032.433	200	50	12446.105	$7502_3 - 19948_{\frac{3}{4}}$
8031.574	1		12447.436	$19713_3 - 32160_{\frac{5}{2}}$
8030.188	50	4	12449.585	$4961_4 - 17411_{\frac{5}{2}}$
8027.103	3		12454.369	$18053_{\frac{3}{4}} - 30508_5$
8026.438	10	1	12455.401	$15493_4 - 27948_{\frac{3}{4}}$
8026.192	50	8	12455.783	$18809_{\frac{3}{4}} - 31265_3$
8025.708	50	8	12456.534	$13297_4 - 25753_{\frac{5}{2}}$
8024.235	100	100	12458.821	$12847_3 - 25306_{\frac{5}{2}}$
8023.886	2		12459.363	$20322_{\frac{5}{2}} - 32781_4$
8022.733	3		12461.153	$18809_{\frac{3}{4}} - 31271_5$
8022.191	75b	25	12461.995	$10526_{\frac{5}{2}} - 22988_2$
8014.499	50	3	12473.955	$12847_3 - 25321_{\frac{5}{2}}$
8013.499	15	2	12475.512	$18069_{\frac{5}{2}} - 30544_2$
8010.708	50	4	12479.859	$22669_{\frac{5}{2}} - 35149_2$
8008.645	2		12483.073	$17398_3 - 29881_{\frac{3}{4}}$
8008.397	5		12483.460	$18069_{\frac{5}{2}} - 30552_4$
8008.272	2		12483.655	$15863_2 - 28347_{\frac{5}{2}}$
8007.988	1		12484.098	$19713_3 - 32197_{\frac{5}{2}}$
8006.477	25		12486.454	$13088_3 - 25575_{\frac{3}{4}}$
8006.443	15		12486.507	$20922_{\frac{5}{2}} - 33408_3$
8003.446	50	5	12491.182	$19532_4 - 32023_{\frac{5}{2}}$

TABLE 4. *Classified lines of* Th I—continued

Wavelength (Å)	Intensity		Wavenumber (cm^{-1})	Classification	Wavelength (Å)	Intensity		Wavenumber (cm^{-1})	Classification
	Lamp	Spark				Lamp	Spark		
8002.589	4		12492.520	$19503_{\frac{3}{2}} - 31995_4$	7941.164	2		12589.149	$14206_{\frac{3}{2}} - 26796_3$
8000.033	100	10	12496.511	$16554_6 - 29050_6^0$	7937.727	100	20	12594.600	$9804_5 - 22399_6^0$
7999.045	2		12498.055	$19039_{\frac{3}{2}} - 31537_3$	7936.762	4		12596.132	$20054_2 - 32650_1^1$
7999.009	4		12498.111	$19039_{\frac{3}{2}} - 31537_3$	7932.280	3	1	12603.249	$19948_{\frac{3}{2}} - 32551_3$
7998.488	2		12498.925	$16346_{\frac{3}{2}} - 28845_4$	7929.938	5		12606.971	$18930_{\frac{3}{2}} - 31537_3$
7996.963	40	3	12501.309	$18574_1 - 31075_{\frac{3}{2}}$	7929.809	25c	2	12607.176	$17354_1^1 - 29961_1$
7994.709	3		12504.833	$11802_2 - 24307_{\frac{3}{2}}$	7928.680	3		12608.971	$15618_{\frac{3}{2}} - 28227_4$
7993.676	150	8	12506.449	$10526_{\frac{3}{2}} - 23032_4$	7927.546	25	3	12610.775	$20054_2 - 32665_1^1$
7993.253	15	1	12507.111	$18382_6^0 - 30889_1$	7925.734	50	3	12613.658	$19588_6^0 - 32202_5$
7992.936	10	2	12507.607	$12847_3 - 25355_{\frac{3}{2}}$	7924.977	50	4	12614.863	$13088_3 - 25703_{\frac{3}{2}}$
7992.936	10	2	12507.607	$19273_2 - 31780_{\frac{3}{2}}$	7922.912	8	2	12618.151	$11802_2 - 24421_{\frac{3}{2}}$
7992.156	50	3	12508.828	$15863_2 - 28372_1^1$	7922.549	50	5	12618.729	$17398_3 - 30017_{\frac{3}{2}}$
7991.515	4h		12509.831	$19503_{\frac{3}{2}} - 32012_4$	7922.235	15		12619.229	$15970_3 - 28589_{\frac{3}{2}}$
7991.515	4h		12509.831	$19948_{\frac{3}{2}} - 32458_4$	7917.236	15	1	12627.197	$22098_4 - 34725_{\frac{3}{2}}$
7991.366	50	5	12510.064	$15970_3 - 28480_{\frac{3}{2}}$	7916.790	40	5	12627.908	$21539_{\frac{3}{2}} - 34167_3$
7989.163	8	1	12513.514	$12114_{\frac{3}{2}} - 24627_1$	7914.493	8	2	12631.573	$18614_1^1 - 31245_2$
7987.974	200	50	12515.377	$14481_{\frac{3}{2}} - 26997_6$	7908.484	8	2	12641.171	$20322_6^0 - 32963_5$
7986.904	1		12517.053	$18809_{\frac{3}{2}} - 31326_4$	7908.148	50	5	12641.708	$22508_{\frac{3}{2}} - 35149_2$
7984.603	1		12520.660	$20054_2 - 32575_{\frac{3}{2}}$	7907.856	4		12642.175	$23655_{\frac{3}{2}} - 36297_4$
7984.032	1		12521.556	$21645_{\frac{3}{2}} - 34167_3$	7904.411	50	5	12647.685	$15493_4 - 28140_{\frac{3}{2}}$
7982.495	10	2	12523.967	$21165_{\frac{3}{2}} - 33689_2$	7904.294	4		12647.872	$20566_{\frac{3}{2}} - 33214_5$
7982.289	8	2	12524.290	$19516_{\frac{3}{2}} - 32041_2$	7903.319	8	1	12649.432	$15863_2 - 28513_{\frac{3}{2}}$
7980.878	2		12526.504	$18549_2 - 31075_{\frac{3}{2}}$	7900.778	5		12653.500	$20737_1^1 - 33390_1$
7978.977	500	300	12529.489	$3687_2 - 16217_{\frac{3}{2}}$	7900.309	200	75	12654.251	$15618_{\frac{3}{2}} - 28273_2$
7976.870	3		12532.798	$20566_{\frac{3}{2}} - 33099_3$	7899.018	8	1	12656.320	$21143_5 - 33799_{\frac{3}{2}}$
7975.874	2		12534.363	$22338_{\frac{3}{2}} - 34873_4$	7896.541	5		12660.290	$13847_2 - 26508_{\frac{3}{2}}$
7974.743	3		12536.141	$21575_2 - 34111_1^1$	7893.614	50	5	12664.984	$16217_{\frac{3}{2}} - 28882_2$
7974.459	4		12536.587	$20737_1^1 - 33273_1$	7892.770	8		12666.338	$20724_6^0 - 33390_1$
7974.164	100	8	12537.051	$7280_2 - 19817_1^1$	7886.273	400l	50	12676.773	$6362_2 - 19039_{\frac{3}{2}}$
7972.598	200	20	12539.514	$4961_4 - 17501_6^0$	7883.595	4		12681.080	$23655_{\frac{3}{2}} - 36336_3$
7970.254	50	5	12543.201	$15970_3 - 28513_{\frac{3}{2}}$	7881.667	2		12684.182	$20922_{\frac{3}{2}} - 33606_2$
7969.785	10	1	12543.940	$15490_6^0 - 28034_5$	7880.577	5		12685.936	$22163_{\frac{3}{2}} - 34849_5$
7969.359	4		12544.610	$22163_{\frac{3}{2}} - 34707_3$	7878.483	5		12689.308	$13962_1 - 26651_{\frac{3}{2}}$
7968.784	2		12545.515	$17166_5 - 29711_6^0$	7869.771	15	2	12703.355	$15970_3 - 28673_{\frac{3}{2}}$
7966.264	2		12549.484	$20724_6^0 - 33273_1$	7868.924	40	10	12704.722	$22877_1^1 - 35582_5$
7965.711	8	1	12550.355	$12114_{\frac{3}{2}} - 24664_3$	7868.396	75	10h	12705.575	$19588_6^0 - 32293_5$
7961.994	100	8	12556.214	$21165_{\frac{3}{2}} - 33721_2$	7867.683	40l	3	12706.726	$11601_1 - 24307_{\frac{3}{2}}$
7961.343	50	8	12557.241	$17959_4 - 30517_6^0$	7865.954	400	75	12709.519	$14481_{\frac{3}{2}} - 27191_5$
7961.158	50	4	12557.533	$12114_{\frac{3}{2}} - 24671_2$	7865.248	10	2	12710.660	$15970_3 - 28680_{\frac{3}{2}}$
7960.474	1		12558.612	$21902_{\frac{3}{2}} - 34460_5$	7865.077	8		12710.936	$22163_{\frac{3}{2}} - 34874_3$
7955.709	4	1	12566.133	$22141_{\frac{3}{2}} - 34707_3$	7864.009	100	8	12712.663	$7502_3 - 20214_{\frac{3}{2}}$
7955.491	2		12566.478	$17073_1 - 29640_1^1$	7862.336	15	3	12715.368	$17166_5 - 29881_{\frac{3}{2}}$
7955.066	75	4	12567.149	$23015_6^0 - 35582_5$	7858.703	2		12721.246	$22855_{\frac{3}{2}} - 35576_3$
7954.592	150	15	12567.898	$6362_2 - 18930_{\frac{3}{2}}$	7858.583	2		12721.440	$17411_{\frac{3}{2}} - 30132_2$
7952.148	3		12571.760	$20737_1^1 - 33309_2$	7855.074	3		12727.123	$12847_3 - 25575_{\frac{3}{2}}$
7951.885	8	1	12572.176	$19713_3 - 32285_{\frac{3}{2}}$	7854.919	8		12727.374	$18809_{\frac{3}{2}} - 31537_3$
7949.019	3	1	12576.709	$20522_{\frac{3}{2}} - 33099_3$	7853.645	2		12729.439	$21594_3 - 34324_{\frac{3}{2}}$
7947.930	4		12578.432	$11802_2 - 24381_{\frac{3}{2}}$	7853.284	20		12730.024	$20543_6^0 - 33273_1$
7946.113	100	8	12581.309	$22508_{\frac{3}{2}} - 35089_3$	7852.227	1		12731.738	$22141_{\frac{3}{2}} - 34873_4$
7946.074	2		12581.370	$11601_1 - 24182_{\frac{3}{2}}$	7851.006	3		12733.718	$18549_2 - 31283_{\frac{3}{2}}$
7945.611	3		12582.103	$18069_{\frac{3}{2}} - 30651_3$	7848.645	5h		12737.548	$17224_{\frac{3}{2}} - 29961_1$
7944.708	2		12583.534	$18699_2 - 31283_{\frac{3}{2}}$	7848.441	100	40	12737.879	$15490_6^0 - 28227_4$
7943.393	2		12585.617	$22855_{\frac{3}{2}} - 35440_3$	7847.784	100b	40	12738.946	$13297_4 - 26036_{\frac{3}{2}}$
7943.050	20	2	12586.160	$14204_5 - 26790_{\frac{3}{2}}$	7847.536	500b	150	12739.348	$8800_4 - 21539_{\frac{3}{2}}$
7941.721	200	75	12588.266	$16346_{\frac{3}{2}} - 28934_3$	7843.545	4	1	12745.830	$20322_6^0 - 33068_6$

TABLE 4. *Classified lines of* Th I—continued

Wavelength (Å)	Intensity		Wavenumber (cm^{-1})	Classification
	Lamp	Spark		
7842.254	100	10	12747.928	$13175^{\frac{3}{4}} - 25923_{4}$
7841.781	200	50	12748.697	$11241^{\frac{5}{3}} - 23990_{2}$
7841.596	5		12748.998	$21575_{2} - 34324^{\frac{2}{2}}$
7841.134	8		12749.749	$2869_{3} - 15618^{\frac{5}{5}}$
7840.992	8		12749.980	$21594_{3} - 34344^{\frac{2}{4}}$
7840.445	100	75	12750.870	$19986^{\frac{6}{6}} - 32737_{5}$
7840.290	100	50	12751.122	$13297_{4} - 26048^{\frac{3}{4}}$
7839.276	10	2	12752.771	$19532_{4} - 32285^{\frac{5}{3}}$
7838.062	2		12754.746	$21077^{\frac{6}{6}} - 33831_{4}$
7836.456	100	5	12757.360	$16346^{\frac{4}{4}} - 29104_{4}$
7835.620	100		12758.721	$11802_{2} - 24561^{\frac{3}{3}}$
7828.073	3		12771.022	$22669^{\frac{5}{5}} - 35440_{3}$
7825.245	2		12775.637	$21668^{\frac{7}{7}} - 34444_{2}$
7824.291	1		12777.195	$21594_{3} - 34371^{\frac{2}{2}}$
7823.787	2		12778.018	$17354^{\frac{6}{7}} - 30132_{2}$
7823.475	50	2	12778.528	$22855^{\frac{5}{5}} - 35633_{4}$
7822.392	100	4	12780.297	$11601_{1} - 24381^{\frac{2}{2}}$
7819.888	2		12784.389	$21645_{4} - 34430^{\frac{5}{5}}$
7819.350	3		12785.269	$15863_{2} - 28649^{\frac{6}{7}}$
7818.694	2		12786.342	$20522^{\frac{2}{2}} - 33309_{2}$
7817.771	500	200	12787.851	$10414^{\frac{4}{4}} - 23201_{3}$
7817.130	4		12788.900	$13088_{3} - 25877^{\frac{4}{4}}$
7816.135	50	4	12790.528	$11241^{\frac{5}{3}} - 24032_{4}$
7813.970	50	5	12794.072	$11877^{\frac{7}{7}} - 24671_{2}$
7813.970	50	5	12794.072	$15736^{\frac{6}{7}} - 28531_{2}$
7813.481	50	8	12794.872	$16346^{\frac{4}{4}} - 29141_{5}$
7810.627	100	10	12799.547	$13297_{4} - 26096^{\frac{5}{5}}$
7809.950	2		12800.657	$12114^{\frac{2}{2}} - 24915_{3}$
7809.245	25b	2	12801.813	$17959_{4} - 30761^{\frac{5}{3}}$
7807.879	40		12804.052	$13847_{2} - 26651^{\frac{2}{2}}$
7804.533	50	5	12809.542	$15863_{2} - 28673^{\frac{2}{2}}$
7804.146	50	4	12810.177	$17398_{3} - 30208^{\frac{2}{2}}$
7803.811	3	1	12810.727	$22338^{\frac{5}{5}} - 35149_{2}$
7802.824	10	2	12812.347	$15863_{2} - 28676^{\frac{5}{5}}$
7801.945	2		12813.791	$15166^{\frac{5}{5}} - 27980_{3}$
7800.029	3		12816.938	$18809^{\frac{4}{4}} - 31626_{5}$
7799.629	8	1	12817.596	$21890^{\frac{5}{5}} - 34707_{3}$
7799.629	8	1	12817.596	$22399^{\frac{6}{6}} - 35216_{5}$
7798.360	300	25	12819.681	$5563_{1} - 18382^{\frac{6}{6}}$
7795.533	1		12824.330	$18699_{2} - 31523^{\frac{5}{5}}$
7793.128	10	2	12828.288	$17959_{4} - 30788^{\frac{6}{6}}$
7790.132	10		12833.221	$19948^{\frac{2}{4}} - 32781_{4}$
7788.932	500	75	12835.199	$11197^{\frac{6}{6}} - 24032_{4}$
7787.659	25		12837.297	$14206^{\frac{4}{4}} - 27044_{3}$
7785.771	2h		12840.410	$22248^{\frac{2}{2}} - 35089_{3}$
7784.779	3		12842.046	$20566^{\frac{4}{4}} - 33408_{3}$
7783.417	5	1	12844.293	$18930^{\frac{5}{5}} - 31774_{3}$
7782.742	4	1	12845.407	$16351_{0} - 29197^{\frac{7}{7}}$
7782.318	150	50	12846.107	$21645_{4} - 34492^{\frac{4}{4}}$
7781.843	100	4	12846.891	$20543^{\frac{6}{6}} - 33390_{1}$
7781.329	2		12847.740	$19948^{\frac{2}{4}} - 32796_{3}$
7779.741	8	2	12850.362	$20423^{\frac{7}{7}} - 33273_{1}$
7779.472	2		12850.806	$13945^{\frac{5}{5}} - 26796_{3}$
7778.488	50	5	12852.432	$15490^{\frac{6}{6}} - 28342_{5}$
7776.804	4		12855.215	$21575_{2} - 34430^{\frac{5}{5}}$
7776.671	40	2	12855.435	$12847_{3} - 25703^{\frac{5}{2}}$
7775.688	2		12857.060	$17398_{3} - 30255^{\frac{5}{3}}$
7773.389	3		12860.863	$23655^{\frac{4}{4}} - 36515_{3}$
7772.457	2		12862.405	$19713_{3} - 32575^{\frac{2}{2}}$
7771.942	100	50	12863.257	$10414^{\frac{4}{4}} - 23277_{5}$
7769.052	2		12868.042	$20522^{\frac{2}{2}} - 33390_{1}$
7768.470	2		12869.006	$20737^{\frac{7}{7}} - 33606_{2}$
7767.963	3		12869.846	$19588^{\frac{6}{6}} - 32458_{4}$
7766.941	4		12871.540	$17501^{\frac{6}{6}} - 30372_{6}$
7762.722	50	3	12878.535	$14465^{\frac{2}{2}} - 27343_{3}$
7759.127	2		12884.502	$20214^{\frac{3}{3}} - 33099_{3}$
7758.486	3		12885.566	$20423^{\frac{7}{7}} - 33309_{2}$
7758.251	3h		12885.957	$20522^{\frac{2}{2}} - 33408_{3}$
7755.600	4		12890.362	$19039^{\frac{2}{2}} - 31929_{3}$
7754.748	1		12891.778	$21539^{\frac{2}{4}} - 34431_{3}$
7754.433	1		12892.301	$20322^{\frac{6}{6}} - 33214_{5}$
7754.271	2		12892.571	$20566^{\frac{4}{4}} - 33459_{4}$
7752.440	3		12895.616	$18069^{\frac{5}{5}} - 30964_{3}$
7751.435	5		12897.288	$22508^{\frac{2}{2}} - 35405_{3}$
7749.578	5		12900.378	$16783^{\frac{4}{4}} - 29684_{5}$
7749.325	8	2	12900.799	$22248^{\frac{2}{2}} - 35149_{2}$
7748.880	3		12901.540	$22399^{\frac{6}{6}} - 35300_{5}$
7745.813	15	3	12906.649	$19532_{4} - 32439^{\frac{4}{4}}$
7745.235	3		12907.612	$21539^{\frac{2}{4}} - 34447_{4}$
7744.786	4		12908.360	$17224^{\frac{2}{2}} - 30132_{2}$
7742.552	100	2	12912.085	$15618^{\frac{3}{3}} - 28531_{2}$
7742.019	2		12912.974	$22508^{\frac{2}{2}} - 35421_{1}$
7740.867	15	1	12914.895	$21252^{\frac{2}{2}} - 34167_{3}$
7739.704	2		12916.836	$22877^{\frac{7}{7}} - 35794_{4}$
7738.356	5	1	12919.086	$18011^{\frac{6}{6}} - 30930_{6}$
7737.779	4		12920.049	$13962_{1} - 26882^{\frac{6}{6}}$
7736.364	2		12922.412	$22877^{\frac{7}{7}} - 35799_{6}$
7735.479	2		12923.891	$19273_{2} - 32197^{\frac{3}{3}}$
7733.362	2		12927.429	$22401_{1} - 35328^{\frac{7}{7}}$
7730.107	5	1	12932.872	$22508^{\frac{2}{2}} - 35440_{3}$
7728.939	100	15	12934.827	$7280_{2} - 20214^{\frac{3}{3}}$
7727.552	2		12937.148	$21645_{4} - 34583^{\frac{3}{3}}$
7726.384	2		12939.104	$22855^{\frac{5}{5}} - 35794_{4}$
7723.641	3		12943.699	$15618^{\frac{3}{3}} - 28562_{4}$
7721.780	2		12946.819	$21902^{\frac{3}{3}} - 34849_{5}$
7721.188	100	8	12947.811	$22141^{\frac{3}{3}} - 35089_{3}$
7718.812	3		12951.797	$20737^{\frac{7}{7}} - 33689_{2}$
7713.337	4		12960.990	$20566^{\frac{4}{4}} - 33527_{4}$
7712.394	50	4	12962.575	$15970_{3} - 28932^{\frac{4}{4}}$
7711.113	40	3	12964.728	$18809^{\frac{4}{4}} - 31774_{3}$
7710.258	100	15	12966.166	$8111_{4} - 21077^{\frac{6}{6}}$
7709.882	50		12966.798	$11802_{2} - 24769^{\frac{5}{5}}$
7708.149	2		12969.714	$21738^{\frac{2}{2}} - 34707_{3}$
7706.909	1		12971.800	$21902^{\frac{3}{3}} - 34874_{3}$
7706.448	3		12972.576	$16783^{\frac{4}{4}} - 29756_{4}$
7705.268	2		12974.563	$18549_{2} - 31523^{\frac{5}{5}}$
7703.679	100	10	12977.239	$19986^{\frac{6}{6}} - 32963_{5}$
7699.765	100	5	12983.836	$18809^{\frac{4}{4}} - 31793_{4}$
7699.660	10	1	12984.013	$20737^{\frac{7}{7}} - 33721_{2}$
7699.399	75	1	12984.453	$14206^{\frac{4}{4}} - 27191_{5}$

TABLE 4. *Classified lines of* Th I—continued

Wavelength (Å)	Intensity		Wavenumber (cm^{-1})	Classification
	Lamp	Spark		
7698.035	20b		12986.754	$10783\frac{3}{2} - 23769_1$
7697.922	75		12986.944	$15493_4 - 28480\frac{4}{4}$
7697.077	2		12988.370	$21594_3 - 34583\frac{3}{3}$
7693.797	100	5	12993.907	$17166_5 - 30160\frac{4}{4}$
7690.658	5		12999.211	$18930\frac{3}{3} - 31929_3$
7689.993	1		13000.335	$22877\frac{1}{1} - 35877_2$
7688.949	3		13002.100	$19039\frac{2}{2} - 32041_2$
7686.149	50	1	13006.836	$17501\frac{0}{0} - 30508_5$
7683.150	3b		13011.913	$19273_2 - 32285\frac{3}{3}$
7683.010	50	1	13012.150	$14032\frac{2}{2} - 27044_3$
7682.438	3		13013.119	$18699_2 - 31712\frac{1}{1}$
7681.318	3		13015.017	$19948\frac{4}{4} - 32963_5$
7678.123	150	5	13020.432	$7502_3 - 20522\frac{2}{2}$
7676.888	2		13022.527	$22855\frac{3}{3} - 35877_2$
7675.925	2		13024.161	$22396\frac{1}{1} - 35421_1$
7675.621	3		13024.677	$13088_3 - 26113\frac{2}{2}$
7675.621	3		13024.677	$18574_1 - 31599\frac{2}{2}$
7672.749	2		13029.552	$12847_3 - 25877\frac{4}{4}$
7672.252	50	2	13030.396	$13847_2 - 26878\frac{3}{3}$
7672.123	1		13030.615	$17959_4 - 30990\frac{3}{3}$
7669.750	8		13034.647	$19516\frac{2}{2} - 32551_3$
7668.955	50	1	13035.998	$11802_2 - 24838\frac{1}{1}$
7667.018	2		13039.291	$21143_5 - 34182\frac{0}{0}$
7665.734	8		13041.475	$19713_3 - 32754\frac{3}{3}$
7665.344	2		13042.139	$20522\frac{2}{2} - 33564_3$
7661.621	8	1	13048.476	$19503\frac{3}{3} - 32551_3$
7661.162	2		13049.258	$20724\frac{0}{0} - 33773_1$
7660.889	150	4	13049.723	$4961_4 - 18011\frac{0}{0}$
7660.029	75	1	13051.188	$5563_1 - 18614\frac{1}{1}$
7660.029	75	1	13051.188	$16783\frac{4}{4} - 29835_3$
7658.323	150	5	13054.096	$8111_4 - 21165\frac{3}{3}$
7655.702	8		13058.565	$21645_4 - 34704\frac{3}{3}$
7655.307	2		13059.239	$17959_4 - 31019\frac{4}{4}$
7654.695	100	5	13060.283	$15618\frac{3}{3} - 28679_2$
7653.827	200	10	13061.764	$14204_5 - 27266\frac{4}{4}$
7653.327	1		13062.617	$17224\frac{2}{2} - 30286_1$
7652.317	100	3	13064.341	$7502_3 - 20566\frac{4}{4}$
7651.739	100	2	13065.328	$16783\frac{4}{4} - 29849_4$
7651.143	1		13066.346	$22338\frac{3}{3} - 35405_3$
7650.996	75	1	13066.597	$19227\frac{6}{6} - 32293_5$
7649.891	2		13068.484	$22508\frac{2}{2} - 35576_3$
7648.545	4		13070.784	$14226_0 - 27297\frac{1}{1}$
7647.380	500	50	13072.775	$9804_5 - 22877\frac{6}{6}$
7647.380	500	50	13072.775	$18069\frac{3}{3} - 31141_3$
7646.337	2		13074.558	$23015\frac{0}{0} - 36089_4$
7644.737	25	1	13077.295	$11802_2 - 24880\frac{1}{1}$
7643.413	1		13079.560	$21645_4 - 34725\frac{3}{3}$
7642.873	15		13080.484	$13175\frac{4}{4} - 26255_4$
7642.425	2		13081.251	$18699_2 - 31780\frac{3}{3}$
7642.028	10	1	13081.931	$19986\frac{6}{6} - 33068_6$
7641.605	2		13082.655	$18930\frac{3}{3} - 32012_4$
7641.066	1		13083.578	$20522\frac{2}{2} - 33606_2$
7638.777	100	3	13087.498	$13297_4 - 26384\frac{4}{4}$
7637.385	75	2	13089.883	$8800_4 - 21890\frac{3}{3}$
7636.173	100	4	13091.961	$4961_4 - 18053\frac{4}{4}$
7634.919	3		13094.111	$20214\frac{3}{3} - 33309_2$
7633.767	75	2	13096.087	$15493_4 - 28589\frac{3}{3}$
7632.129	50	2	13098.898	$13962_1 - 27061\frac{2}{2}$
7632.129	50	2	13098.898	$13945\frac{3}{3} - 27044_3$
7630.536	50	2	13101.633	$14465\frac{2}{2} - 27566_2$
7630.310	100	5	13102.021	$8800_4 - 21902\frac{4}{4}$
7627.428	3		13106.971	$20054_2 - 33161\frac{1}{1}$
7627.428	3		13106.971	$20054_2 - 33161\frac{1}{1}$
7627.175	150	5	13107.406	$4961_4 - 18069\frac{3}{3}$
7625.705	150	5	13109.933	$14481\frac{3}{3} - 27591_5$
7625.120	50	2	13110.938	$18930\frac{3}{3} - 32041_2$
7620.815	5		13118.345	$23015\frac{0}{0} - 36133_5$
7620.443	3		13118.985	$17398_3 - 30517\frac{4}{4}$
7620.080	100	5	13119.610	$18809\frac{2}{4} - 31929_3$
7617.255	2		13124.476	$22669\frac{3}{3} - 35794_4$
7616.686	50	1	13125.456	$13962_1 - 27087\frac{1}{1}$
7614.421	1		13129.360	$21575_2 - 34704\frac{3}{3}$
7612.122	4	1	13133.326	$17411\frac{3}{3} - 30544_2$
7611.293	8		13134.756	$17073_1 - 30208\frac{2}{2}$
7610.378	2		13136.335	$21165\frac{3}{3} - 34301_4$
7610.101	5		13136.813	$14206\frac{4}{4} - 27343_3$
7609.546	2		13137.772	$22163\frac{4}{4} - 35300_5$
7609.359	3		13138.094	$18574_1 - 31712\frac{1}{1}$
7607.824	100	4	13140.745	$6362_2 - 19503\frac{3}{3}$
7607.519	40	1	13141.272	$17411\frac{3}{3} - 30552_4$
7606.314	5		13143.354	$7280_2 - 20423\frac{1}{1}$
7605.083	5		13145.481	$15736\frac{1}{1} - 28882_2$
7604.177	3		13147.048	$14465\frac{2}{2} - 27612_3$
7603.623	40	1	13148.005	$13847_2 - 26995\frac{3}{3}$
7603.249	40	1	13148.652	$19588\frac{8}{8} - 32737_5$
7602.795	40	1	13149.437	$19713_3 - 32862\frac{4}{4}$
7602.247	2		13150.385	$21575_2 - 34725\frac{3}{3}$
7601.880	5		13151.020	$19948\frac{4}{4} - 33099_3$
7600.637	2		13153.171	$23655\frac{4}{4} - 36808_3$
7599.815	2		13154.593	$6362_2 - 19516\frac{2}{2}$
7599.638	5		13154.900	$17398_3 - 30553\frac{2}{2}$
7598.203	200	3	13157.384	$16554_6 - 29711\frac{0}{0}$
7598.203	200	3	13157.384	$11241\frac{3}{3} - 24399_3$
7591.999	10		13168.136	$21539\frac{4}{4} - 34707_3$
7586.988	8		13176.833	$18069\frac{3}{3} - 31245_2$
7586.207	20		13178.190	$11802_2 - 24981\frac{3}{3}$
7585.783	200	10	13178.926	$2558_0 - 15736\frac{1}{1}$
7585.688	200	15	13179.091	$16554_6 - 29733\frac{6}{6}$
7583.574	2		13182.765	$20423\frac{1}{1} - 33606_2$
7583.534	2		13182.835	$20423\frac{1}{1} - 33606_2$
7583.422	25		13183.029	$15493_4 - 28676\frac{3}{3}$
7581.856	4		13185.752	$18809\frac{2}{4} - 31995_4$
7581.088	2		13187.088	$21902\frac{4}{4} - 35089_3$
7580.866	4		13187.474	$15493_4 - 28680\frac{4}{4}$
7580.829	5		13187.539	$15493_4 - 28680\frac{4}{4}$
7580.686	40	1	13187.787	$15970_3 - 29157\frac{3}{3}$
7580.340	50	1	13188.389	$12847_3 - 26036\frac{3}{3}$
7579.456	3		13189.928	$17354\frac{1}{1} - 30544_2$
7578.274	2		13191.985	$21252\frac{2}{2} - 34444_2$
7578.274	2		13191.985	$22248\frac{2}{2} - 35440_3$

TABLE 4. *Classified lines of* Th I—continued

Wavelength (Å)	Intensity		Wavenumber (cm^{-1})	Classification	Wavelength (Å)	Intensity		Wavenumber (cm^{-1})	Classification
	Lamp	Spark				Lamp	Spark		
7578.274	2		13191.985	$22855_{3}^{3} - 36047_{2}$	7517.963	50	2	13297.814	$20423_{1}^{1} - 33721_{2}$
7577.550	25		13193.245	$19588_{0}^{0} - 32781_{4}$	7515.504	1		13302.164	$19273_{2} - 32575_{2}^{2}$
7577.266	20		13193.740	$20214_{3}^{3} - 33408_{3}$	7514.681	2		13303.621	$21575_{2} - 34878_{1}^{1}$
7574.484	5		13198.585	$20522_{2}^{2} - 33721_{2}$	7512.237	3		13307.949	$21738_{2}^{2} - 35046_{1}$
7574.116	3		13199.227	$21890_{3}^{3} - 35089_{3}$	7511.788	100	4	13308.745	$9804_{8} - 23113_{4}^{4}$
7573.342	50	1	13200.576	$12847_{3} - 26048_{4}^{4}$	7510.144	1		13311.658	$14032_{2}^{2} - 27343_{3}$
7573.155	3		13200.902	$16217_{2}^{2} - 29418_{2}$	7509.595	2		13312.631	$20214_{3}^{3} - 33527_{4}$
7572.973	4		13201.219	$21143_{5} - 34344_{4}^{4}$	7508.477	100	4	13314.614	$14206_{4}^{4} - 27521_{4}$
7571.931	3		13203.036	$18809_{4}^{4} - 32012_{4}$	7507.923	75		13315.596	$18011_{0}^{0} - 31326_{4}$
7571.029	8		13204.609	$16217_{2}^{2} - 29422_{1}$	7507.737	50		13315.926	$15618_{3}^{3} - 28934_{3}$
7570.636	2		13205.294	$20322_{0}^{0} - 33527_{4}$	7505.292	50		13320.264	$17224_{2}^{2} - 30544_{2}$
7569.509	50	2	13207.260	$10783_{2}^{2} - 23990_{2}$	7505.052	1		13320.690	$18549_{2} - 31870_{2}^{2}$
7567.739	300	15	13210.349	$9804_{8} - 23015_{6}$	7503.829	50	8	13322.861	$14243_{1}^{1} - 27566_{2}$
7567.596	50	3	13210.599	$13297_{4} - 26508_{3}^{3}$	7503.626	2		13323.221	$17959_{4} - 31283_{2}^{3}$
7566.732	3		13212.107	$22877_{6} - 36089_{4}$	7501.180	8		13327.566	$22248_{2}^{2} - 35576_{3}$
7565.850	50	2	13213.647	$13847_{2} - 27061_{2}^{2}$	7499.786	1		13330.043	$19532_{4} - 32862_{4}^{4}$
7563.711	5		13217.384	$18053_{4}^{4} - 31271_{5}$	7499.579	8	1	13330.411	$21077_{6}^{6} - 34407_{6}$
7557.751	50	1	13227.807	$15970_{3} - 29197_{2}^{2}$	7499.000	75	2	13331.440	$8243_{2}^{2} - 21575_{2}$
7557.438	2		13228.355	$19986_{6}^{6} - 33214_{5}$	7497.552	10	1	13334.015	$15863_{2} - 29197_{2}^{2}$
7556.646	1		13229.742	$20543_{6}^{6} - 33773_{1}$	7497.305	3		13334.454	$21539_{4}^{4} - 34874_{3}$
7556.309	2		13230.332	$19273_{2} - 32503_{2}^{2}$	7496.988	15	1	13335.018	$13962_{1} - 27297_{1}^{1}$
7556.225	5		13230.479	$16783_{4}^{4} - 30014_{4}$	7495.564	50	2	13337.551	$16346_{4}^{4} - 29684_{5}$
7553.974	10w	2	13234.421	$22399_{6}^{6} - 35633_{4}$	7494.237	2		13339.913	$15970_{3} - 29310_{4}^{4}$
7553.974	10w	2	13234.421	$22855_{3}^{3} - 36089_{4}$	7493.427	75	2	13341.355	$8800_{4} - 22141_{3}^{3}$
7553.753	2		13234.808	$17959_{4} - 31194_{4}^{4}$	7490.379	5		13346.784	$17411_{3}^{3} - 30758_{2}$
7551.997	4		13237.886	$11601_{1} - 24838_{1}^{1}$	7489.709	50	2	13347.978	$13297_{4} - 26645_{6}^{6}$
7550.831	1		13239.930	$17411_{3}^{3} - 30651_{3}$	7489.612	50	2	13348.151	$7795_{4}^{4} - 21143_{5}$
7550.677	5		13240.200	$13847_{2} - 27087_{1}^{1}$	7489.361	1		13348.598	$21143_{5} - 34492_{4}^{4}$
7549.923	2		13241.522	$19713_{3} - 32954_{2}^{2}$	7487.972	100	3	13351.074	$8243_{2}^{2} - 21594_{3}$
7549.532	4		13242.208	$22163_{4}^{4} - 35405_{3}$	7487.869	3		13351.258	$17166_{8} - 30517_{4}^{4}$
7549.439	1		13242.371	$20054_{2} - 33297_{2}^{2}$	7485.500	5		13355.483	$15490_{6}^{6} - 28845_{4}$
7549.316	200	8	13242.587	$7280_{2} - 20522_{2}^{2}$	7483.624	200	10	13358.831	$3865_{1} - 17224_{2}^{2}$
7547.742	3		13245.348	$20922_{3}^{3} - 34167_{3}$	7481.352	200	15	13362.888	$8800_{4} - 22163_{4}^{4}$
7545.657	5		13249.008	$12847_{3} - 26096_{3}^{3}$	7481.110	50	1	13363.320	$17398_{3} - 30761_{3}^{3}$
7544.592	2		13250.879	$20522_{2}^{2} - 33773_{1}$	7480.802	2		13363.870	$22098_{4} - 35462_{3}^{3}$
7540.596	15		13257.901	$18069_{3}^{3} - 31326_{4}$	7477.364	8		13370.015	$21077_{6}^{6} - 34447_{4}$
7539.622	4		13259.613	$18011_{0}^{0} - 31271_{5}$	7474.559	10	1	13375.032	$19588_{0}^{0} - 32963_{5}$
7537.429	50	2	13263.471	$15618_{3}^{3} - 28882_{2}$	7474.043	2		13375.956	$20922_{3}^{3} - 34298_{1}$
7536.407	50	10	13265.270	$20566_{4}^{4} - 33831_{4}$	7473.440	20	1	13377.035	$21668_{1}^{1} - 35046_{1}$
7536.244	1		13265.557	$20423_{1}^{1} - 33689_{2}$	7471.346	5		13380.784	$18699_{2} - 32080_{1}^{1}$
7535.850	5		13266.250	$21165_{3}^{3} - 34431_{3}$	7469.705	4		13383.724	$21077_{6}^{6} - 34460_{5}$
7531.818	50	2	13273.352	$18053_{4}^{4} - 31326_{4}$	7469.054	40	1	13384.890	$14206_{4}^{4} - 27591_{5}$
7531.142	75	2	13274.543	$13088_{3} - 26363_{2}^{2}$	7466.819	5		13388.897	$15863_{2} - 29252_{2}^{2}$
7529.408	2		13277.600	$22401_{1} - 35678_{1}^{1}$	7465.443	100	3	13391.364	$20214_{3}^{3} - 33606_{2}$
7529.318	3		13277.759	$22163_{4}^{4} - 35440_{3}$	7465.236	50	1	13391.736	$15493_{4} - 28884_{3}^{3}$
7528.919	5		13278.463	$19503_{5}^{5} - 32781_{4}$	7465.025	15	1	13392.114	$18809_{4}^{4} - 32202_{5}$
7528.490	40	8	13279.220	$11601_{1} - 24880_{1}^{1}$	7463.427	1		13394.981	$22399_{6}^{6} - 35794_{4}$
7526.832	2		13282.145	$23015_{6}^{6} - 36297_{4}$	7462.990	75	1	13395.766	$15166_{3}^{3} - 28562_{4}$
7523.335	8		13288.318	$16351_{0} - 29640_{1}^{1}$	7461.502	5		13398.437	$13945_{3}^{3} - 27343_{3}$
7523.133	100	3	13288.675	$14206_{4}^{4} - 27495_{4}$	7461.385	3		13398.647	$21902_{4}^{4} - 35300_{5}$
7520.694	15		13292.985	$19503_{5}^{5} - 32796_{3}$	7461.290	8	1	13398.818	$17847_{2}^{2} - 31245_{2}$
7520.567	2		13293.209	$15863_{2} - 29157_{1}^{1}$	7460.310	10	1	13400.578	$22399_{6}^{6} - 35799_{6}$
7520.127	8		13293.987	$15863_{2} - 29157_{3}^{3}$	7458.753	50	2	13403.375	$17354_{1}^{1} - 30758_{2}$
7519.279	1		13295.486	$18574_{1} - 31870_{2}^{2}$	7457.648	25	1	13405.361	$14206_{4}^{4} - 27612_{3}$
7518.780	50	1	13296.369	$13088_{3} - 26384_{4}^{4}$	7455.204	100	4	13409.756	$16346_{4}^{4} - 29756_{4}$

TABLE 4. *Classified lines of* Th I—continued

Wavelength (Å)	Intensity		Wavenumber (cm^{-1})	Classification
	Lamp	Spark		
7453.730	20	1	13412.408	$13847_2 - 27260^{\frac{5}{2}}$
7453.188	5		13413.383	$22163^{\frac{3}{4}} - 35576_3$
7452.516	20	1	13414.593	$17398_3 - 30812^{\frac{2}{2}}$
7452.432	2		13414.744	$21575_2 - 34989^{\frac{0}{1}}$
7450.306	8		13418.572	$17847^{\frac{2}{2}} - 31265_3$
7449.979	3		13419.161	$22163^{\frac{3}{4}} - 35582_5$
7449.808	75	2	13419.469	$13088_3 - 26508^{\frac{5}{3}}$
7449.605	75	3	13419.834	$7502_3 - 20922^{\frac{2}{2}}$
7447.848	150	5	13423.000	$11241^{\frac{5}{4}} - 24664_3$
7445.697	3		13426.878	$17224^{\frac{2}{2}} - 30651_3$
7445.697	3		13426.878	$18614^{\frac{0}{1}} - 32041_2$
7444.751	200	8	13428.584	$8111_4 - 21539^{\frac{3}{4}}$
7444.373	8	1	13429.266	$17501^{\frac{5}{5}} - 30930_6$
7443.873	50	1	13430.168	$11241^{\frac{5}{3}} - 24671_2$
7443.573	1		13430.709	$23655^{\frac{3}{4}} - 37085_4$
7442.040	15		13433.476	$16217^{\frac{2}{2}} - 29650_2$
7441.125	25	1	13435.128	$21645_4 - 35081^{\frac{5}{5}}$
7439.314	3		13438.398	$18431_3 - 31870^{\frac{5}{2}}$
7437.331	1		13441.981	$22855^{\frac{5}{3}} - 36297_4$
7433.375	8		13449.135	$15970_3 - 29419^{\frac{2}{2}}$
7433.005	5		13449.804	$13847_2 - 27297^{\frac{0}{1}}$
7430.255	500	15	13454.782	$6362_2 - 19817^{\frac{0}{1}}$
7429.212	3		13456.671	$19817^{\frac{0}{1}} - 33273_1$
7428.943	800	50	13457.159	$7280_2 - 20737^{\frac{0}{1}}$
7427.224	2		13460.273	$19948^{\frac{3}{4}} - 33408_3$
7426.906	4		13460.849	$18699_2 - 32160^{\frac{2}{2}}$
7422.013	75	2	13469.724	$19948^{\frac{3}{4}} - 33418_4$
7421.465	5		13470.718	$22163^{\frac{3}{4}} - 35633_4$
7419.593	10		13474.117	$20214^{\frac{3}{3}} - 33689_2$
7418.548	200		13476.015	$5563_1 - 19039^{\frac{2}{2}}$
7417.789	100		13477.394	$2869_3 - 16346^{\frac{2}{4}}$
7416.503	3		13479.731	$19588^{\frac{5}{5}} - 33068_6$
7415.923	10		13480.785	$21668^{\frac{0}{1}} - 35149_2$
7415.817	5		13480.978	$22396^{\frac{0}{1}} - 35877_2$
7415.679	3		13481.228	$19273_2 - 32754^{\frac{3}{3}}$
7414.361	10		13483.625	$18053^{\frac{3}{4}} - 31537_3$
7414.139	3		13484.029	$18809^{\frac{3}{4}} - 32293_5$
7413.592	25		13485.024	$15618^{\frac{3}{3}} - 29104_4$
7413.484	3		13485.220	$13962_1 - 27447^{\frac{2}{2}}$
7413.410	2		13485.355	$21645_4 - 35131^{\frac{3}{4}}$
7411.739	100	4	13488.395	$16346^{\frac{2}{4}} - 29835_3$
7411.322	10		13489.154	$3865_1 - 17354^{\frac{0}{1}}$
7409.836	3		13491.859	$19817^{\frac{0}{1}} - 33309_2$
7409.618	1		13492.256	$22141^{\frac{5}{3}} - 35633_4$
7409.618	1		13492.256	$22338^{\frac{3}{3}} - 35831_3$
7409.221	40		13492.979	$13297_4 - 26790^{\frac{3}{4}}$
7404.262	50		13502.016	$9804_5 - 23306^{\frac{5}{6}}$
7403.993	50	1	13502.506	$16346^{\frac{2}{4}} - 29849_4$
7403.698	2		13503.044	$21902^{\frac{3}{4}} - 35405_3$
7403.273	3		13503.819	$11802_2 - 25306^{\frac{2}{2}}$
7402.248	400	8	13505.689	$10526^{\frac{5}{3}} - 24032_4$
7401.872	50		13506.375	$20214^{\frac{3}{3}} - 33721_2$
7400.309	2		13509.228	$20922^{\frac{2}{2}} - 34431_3$
7400.071	40	2	13509.663	$19227^{\frac{5}{6}} - 32737_5$
7399.391	8		13510.904	$19532_4 - 33043^{\frac{3}{3}}$
7398.583	50	1	13512.380	$15166^{\frac{5}{3}} - 28679_2$
7398.540	8		13512.458	$19039^{\frac{2}{2}} - 32551_3$
7397.074	4		13515.136	$12847_3 - 26363^{\frac{2}{2}}$
7396.895	20	1	13515.463	$14465^{\frac{2}{2}} - 27980_3$
7394.970	1		13518.981	$11802_2 - 25321^{\frac{3}{3}}$
7390.097	50		13527.896	$18930^{\frac{3}{3}} - 32458_4$
7388.403	5		13530.997	$18549_2 - 32080^{\frac{1}{1}}$
7386.924	50	2	13533.706	$17224^{\frac{2}{2}} - 30758_2$
7386.347	50	10	13534.764	$14032^{\frac{2}{2}} - 27566_2$
7386.055	8		13535.299	$17354^{\frac{0}{1}} - 30889_1$
7385.498	500	15	13536.320	$3687_2 - 17224^{\frac{2}{2}}$
7385.391	8b		13536.516	$21594_3 - 35131^{\frac{3}{4}}$
7385.154	20		13536.950	$12847_3 - 26384^{\frac{2}{2}}$
7384.174	200	5	13538.747	$8800_4 - 22338^{\frac{3}{3}}$
7383.712	150	8	13539.594	$20867^{\frac{2}{1}} - 34407_6$
7383.596	50	2	13539.806	$17073_1 - 30613^{\frac{5}{6}}$
7378.165	2		13549.773	$21539^{\frac{3}{4}} - 35089_3$
7377.891	40	1	13550.276	$13945^{\frac{3}{3}} - 27495_4$
7377.626	2		13550.763	$21890^{\frac{3}{3}} - 35440_3$
7376.879	200	8	13552.135	$14481^{\frac{6}{6}} - 28034_5$
7376.178	25		13553.423	$17411^{\frac{3}{3}} - 30964_3$
7375.142	1		13555.327	$15863_2 - 29419^{\frac{2}{2}}$
7374.483	5		13556.538	$23655^{\frac{4}{4}} - 37211_5$
7373.960	1		13557.500	$15493_4 - 29050^{\frac{6}{6}}$
7373.960	1		13557.500	$19713_3 - 33270^{\frac{4}{4}}$
7370.827	50	2	13563.262	$13088_3 - 26651^{\frac{2}{2}}$
7370.409	4		13564.031	$17959_4 - 31523^{\frac{3}{3}}$
7365.427	50	20	13573.206	$18053^{\frac{3}{4}} - 31626_5$
7365.233	50	20	13573.564	$19817^{\frac{0}{1}} - 33390_1$
7365.166	3h		13573.687	$20724^{\frac{5}{6}} - 34298_1$
7363.794	10	1	13576.216	$13945^{\frac{3}{3}} - 27521_4$
7362.195	50	1	13579.165	$19948^{\frac{3}{4}} - 33527_4$
7361.348	150	5	13580.727	$13297_4 - 26878^{\frac{3}{3}}$
7360.715	2		13581.895	$19713_3 - 33294^{\frac{3}{3}}$
7360.553	2		13582.194	$17847^{\frac{2}{2}} - 31429_1$
7360.428	3		13582.425	$19516^{\frac{2}{2}} - 33099_3$
7359.530	2		13584.082	$19713_3 - 33297^{\frac{2}{2}}$
7358.738	2		13585.544	$18699_2 - 32285^{\frac{3}{3}}$
7358.568	8		13585.858	$18574_1 - 32160^{\frac{2}{2}}$
7355.179	10		13592.118	$17398_3 - 30990^{\frac{3}{3}}$
7353.644	15		13594.955	$21645_4 - 35240^{\frac{3}{3}}$
7352.937	8		13596.262	$19503^{\frac{3}{3}} - 33099_3$
7351.371	1		13599.158	$8800_4 - 22399^{\frac{6}{6}}$
7350.934	5		13599.967	$13847_2 - 27447^{\frac{2}{2}}$
7350.454	50		13600.855	$20566^{\frac{3}{4}} - 34167_3$
7346.898	2		13607.438	$20054_2 - 33662^{\frac{1}{1}}$
7346.671	2		13607.858	$22877^{\frac{1}{1}} - 36485_2$
7344.939	10		13611.067	$18549_2 - 32160^{\frac{2}{2}}$
7343.396	5h		13613.927	$15490^{\frac{5}{6}} - 29104_4$
7342.573	150	5	13615.453	$18011^{\frac{6}{6}} - 31626_5$
7342.300	75	2	13615.959	$10783^{\frac{2}{2}} - 24399_3$
7342.035	75	2	13616.451	$19948^{\frac{3}{4}} - 33564_3$
7341.769	5		13616.944	$20214^{\frac{3}{3}} - 33831_4$
7341.433	8		13617.567	$16217^{\frac{2}{2}} - 29835_3$
7341.150	500	15	13618.092	$10414^{\frac{4}{4}} - 24032_4$

TABLE 4. *Classified lines of* Th I—continued

Wavelength (Å)	Intensity		Wavenumber (cm^{-1})	Classification
	Lamp	Spark		
7339.729	3		13620.729	$17398_3 - 31019^{\frac{3}{4}}$
7339.599	150	3	13620.970	$13175^{\frac{1}{4}} - 26796_3$
7339.409	50	1	13621.322	$18930^{\frac{5}{8}} - 32551_3$
7339.330	2		13621.469	$21252^{\frac{3}{8}} - 34874_3$
7339.005	8		13622.072	$17166_5 - 30788^{\frac{6}{8}}$
7336.798	4		13626.170	$19588^{\frac{6}{8}} - 33214_5$
7336.134	2		13627.403	$22669^{\frac{5}{8}} - 36297_4$
7335.802	5		13628.020	$21645_4 - 35273^{\frac{6}{8}}$
7335.357	1		13628.847	$22248^{\frac{3}{4}} - 35877_2$
7334.067	4		13631.244	$22163^{\frac{1}{4}} - 35794_4$
7331.906	2		13635.262	$22098_4 - 35733^{\frac{3}{4}}$
7329.488	100	5	13639.760	$11802_2 - 25442^{\frac{5}{8}}$
7328.283	300s	50d	13642.003	$7280_2 - 20922^{\frac{2}{8}}$
7326.801	5		13644.762	$20522^{\frac{2}{8}} - 34167_3$
7326.058	3		13646.146	$21594_3 - 35240^{\frac{5}{8}}$
7325.219	8		13647.709	$18549_2 - 32197^{\frac{5}{8}}$
7324.894	20b		13648.314	$23655^{\frac{1}{4}} - 37303_4$
7324.808	300	10	13648.475	$14204_5 - 27852^{\frac{6}{8}}$
7323.988	10		13650.003	$17073_1 - 30723^{\frac{7}{8}}$
7323.740	2		13650.465	$22396^{\frac{7}{8}} - 36047_2$
7323.207	100	3	13651.458	$15490^{\frac{6}{8}} - 29141_5$
7318.595	8		13660.061	$12847_3 - 26508^{\frac{3}{8}}$
7318.272	2h		13660.664	$22855^{\frac{3}{8}} - 36515_3$
7317.122	3		13662.811	$7502_3 - 21165^{\frac{5}{8}}$
7316.676	2		13663.644	$20054_2 - 33718^{\frac{2}{8}}$
7316.124	100	1	13664.675	$15493_4 - 29157^{\frac{5}{8}}$
7315.609	150		13665.637	$17224^{\frac{2}{8}} - 30889_1$
7315.064	200	3	13666.655	$3687_2 - 17354^{\frac{7}{8}}$
7314.743	2		13667.255	$21738^{\frac{2}{8}} - 35405_3$
7311.510	100	3	13673.298	$11241^{\frac{3}{8}} - 24915_3$
7311.003	10	2	13674.246	$21902^{\frac{4}{8}} - 35576_3$
7309.311	2b		13677.412	$21539^{\frac{4}{8}} - 35216_5$
7309.255	100	2	13677.516	$17398_3 - 31075^{\frac{2}{8}}$
7308.640	150	3	13678.667	$15166^{\frac{3}{8}} - 28845_4$
7307.933	4		13679.991	$21902^{\frac{4}{8}} - 35582_5$
7307.233	4		13681.301	$19273_2 - 32954^{\frac{2}{8}}$
7307.176	5		13681.408	$15736^{\frac{7}{8}} - 29418_2$
7305.193	50	1	13685.122	$15736^{\frac{7}{8}} - 29422_1$
7304.521	4		13686.381	$21890^{\frac{3}{8}} - 35576_3$
7302.496	3b		13690.176	$17847^{\frac{2}{8}} - 31537_3$
7302.428	75	2	13690.303	$22399^{\frac{6}{8}} - 36089_4$
7298.138	200b	3	13698.351	$13297_4 - 26995^{\frac{3}{8}}$
7296.265	100	3	13701.867	$13088_3 - 26790^{\frac{4}{8}}$
7294.316	15	1	13705.528	$18069^{\frac{5}{8}} - 31774_3$
7294.217	5		13705.714	$11601_1 - 25306^{\frac{2}{8}}$
7293.374	15	1	13707.298	$20737^{\frac{7}{8}} - 34444_2$
7292.864	2		13708.257	$21165^{\frac{3}{8}} - 34873_4$
7292.864	2		13708.257	$22338^{\frac{3}{8}} - 36047_2$
7292.494	3		13708.952	$21165^{\frac{3}{8}} - 34874_3$
7291.276	8	2	13711.242	$17959_4 - 31671^{\frac{3}{4}}$
7289.812	4		13713.996	$19713_3 - 33427^{\frac{2}{8}}$
7289.659	2		13714.284	$22098_4 - 35812^{\frac{5}{8}}$
7288.990	10	1	13715.543	$15166^{\frac{3}{8}} - 28882_2$
7288.610	50	1	13716.258	$15970_3 - 29686^{\frac{5}{8}}$
7286.110	3		13720.964	$18053^{\frac{3}{4}} - 31774_3$
7284.905	500	20	13723.233	$3687_2 - 17411^{\frac{5}{8}}$
7284.419	40	1	13724.149	$16783^{\frac{3}{4}} - 30508_5$
7284.166	8	1	13724.626	$18069^{\frac{5}{8}} - 31793_4$
7281.962	2		13728.780	$18431_3 - 32160^{\frac{2}{8}}$
7280.478	20	1	13731.578	$21902^{\frac{4}{8}} - 35633_4$
7279.142	8		13734.098	$22399^{\frac{6}{8}} - 36133_5$
7278.767	1		13734.806	$20566^{\frac{4}{8}} - 34301_4$
7278.272	1		13735.740	$18549_2 - 32285^{\frac{5}{8}}$
7278.101	3		13736.063	$19227^{\frac{6}{8}} - 32963_5$
7278.032	4		13736.193	$22141^{\frac{5}{8}} - 35877_2$
7277.013	75	1	13738.116	$19532_4 - 33270^{\frac{3}{8}}$
7276.453	10	1	13739.174	$17073_1 - 30812^{\frac{2}{8}}$
7275.972	2		13740.082	$18053^{\frac{3}{4}} - 31793_4$
7275.833	15	1	13740.344	$17224^{\frac{2}{8}} - 30964_3$
7274.294	15	1	13743.251	$21143_5 - 34886^{\frac{6}{8}}$
7274.048	3		13743.716	$21890^{\frac{3}{8}} - 35633_4$
7273.732	40	1	13744.313	$16217^{\frac{2}{8}} - 29961_1$
7270.993	8		13749.491	$23655^{\frac{1}{4}} - 37404_3$
7270.558	100	2	13750.313	$7502_3 - 21252^{\frac{2}{8}}$
7268.834	100	2	13753.575	$21575_2 - 35328^{\frac{7}{8}}$
7268.490	5	1	13754.226	$20543^{\frac{6}{8}} - 34298_1$
7267.096	50	1	13756.864	$19516^{\frac{2}{8}} - 33273_1$
7264.747	2		13761.312	$21539^{\frac{4}{8}} - 35300_5$
7264.118	50		13762.504	$19532_4 - 33294^{\frac{3}{8}}$
7262.578	2		13765.422	$18431_3 - 32197^{\frac{5}{8}}$
7262.190	10		13766.157	$23015^{\frac{6}{8}} - 36781_5$
7261.217	5		13768.002	$15166^{\frac{3}{8}} - 28934_3$
7260.874	5		13768.652	$16783^{\frac{3}{4}} - 30552_4$
7260.258	8		13769.821	$17501^{\frac{6}{8}} - 31271_5$
7258.177	200	5	13773.769	$14206^{\frac{3}{8}} - 27980_3$
7257.334	2		13775.369	$20522^{\frac{2}{8}} - 34298_1$
7256.981	150	2	13776.039	$12114^{\frac{2}{8}} - 25890_2$
7256.807	75	2	13776.369	$15863_2 - 29640^{\frac{7}{8}}$
7255.351	200	5	13779.133	$8111_4 - 21890^{\frac{3}{8}}$
7253.672	100	3	13782.323	$18011^{\frac{6}{8}} - 31793_4$
7251.943	2		13785.609	$20922^{\frac{2}{8}} - 34707_3$
7250.100	15		13789.113	$19817^{\frac{7}{8}} - 33606_2$
7249.842	75	1	13789.604	$13088_3 - 26878^{\frac{5}{8}}$
7248.964	75	1	13791.274	$8111_4 - 21902^{\frac{4}{8}}$
7248.547	2		13792.067	$19516^{\frac{2}{8}} - 33309_2$
7247.843	2		13793.407	$21252^{\frac{2}{8}} - 35046_1$
7247.599	40		13793.872	$16217^{\frac{2}{8}} - 30011_3$
7246.370	3		13796.211	$21077^{\frac{6}{8}} - 34873_4$
7246.318	5h		13796.310	$17398_3 - 31194^{\frac{3}{4}}$
7245.500	8		13797.868	$14226_0 - 28024^{\frac{7}{8}}$
7245.292	2		13798.264	$22855^{\frac{3}{8}} - 36653_2$
7244.689	200	8	13799.412	$7795^{\frac{3}{4}} - 21594_3$
7244.689	200	8	13799.412	$15618^{\frac{3}{8}} - 29418_2$
7242.345	150	2	13803.878	$12847_3 - 26651^{\frac{2}{8}}$
7242.282	20b		13803.998	$18699_2 - 32503^{\frac{2}{8}}$
7242.086	200	10	13804.372	$9804_5 - 23609^{\frac{6}{8}}$
7241.280	2		13805.908	$19503^{\frac{3}{8}} - 33309_2$
7240.181	100	2	13808.004	$14465^{\frac{2}{8}} - 28273_2$
7238.404	8		13811.394	$22399^{\frac{6}{8}} - 36210_5$
7236.257	20		13815.492	$22669^{\frac{5}{8}} - 36485_2$
7235.899	50	1	13816.175	$21645_4 - 35462^{\frac{3}{8}}$
7235.551	20		13816.840	$15493_4 - 29310^{\frac{4}{8}}$

TABLE 4. *Classified lines of* Th I—continued

Wavelength (Å)	Intensity		Wavenumber (cm^{-1})	Classification	Wavelength (Å)	Intensity		Wavenumber (cm^{-1})	Classification
	Lamp	Spark				Lamp	Spark		
7233.390	100		13820.967	$17959_4 - 31780\frac{3}{3}$	7180.959	8		13921.879	$20522\frac{2}{2} - 34444_2$
7232.946	10		13821.816	$13962_1 - 27784\frac{2}{2}$	7179.725	150	4	13924.272	$21165\frac{3}{3} - 35089_3$
7226.246	15		13834.631	$17411\frac{3}{3} - 31245_2$	7179.189	1		13925.312	$11601_1 - 25526\frac{1}{1}$
7225.125	20	5	13836.778	$21252\frac{2}{2} - 35089_3$	7178.539	10	1	13926.572	$18069\frac{3}{3} - 31995_4$
7220.989	100	2	13844.703	$10783\frac{2}{2} - 24627_1$	7178.252	8		13927.129	$18809\frac{4}{4} - 32737_5$
7219.782	25	1	13847.017	$19713_3 - 33560\frac{3}{3}$	7177.284	50	2	13929.008	$18574_1 - 32503\frac{2}{2}$
7219.156	300	10	13848.218	$4961_4 - 18809\frac{4}{4}$	7173.372	500	20	13936.604	$13847_2 - 27784\frac{2}{2}$
7218.056	500	75	13850.328	$9804_5 - 23655\frac{4}{4}$	7173.372	500	20	13936.604	$14204_5 - 28140\frac{3}{3}$
7216.911	8		13852.526	$6362_2 - 20214\frac{3}{3}$	7173.117	8		13937.099	$15166\frac{3}{3} - 29104_4$
7216.666	40	2	13852.996	$17166_5 - 31019\frac{4}{4}$	7172.867	8		13937.585	$21143_5 - 35081\frac{5}{5}$
7215.933	8		13854.403	$17411\frac{3}{3} - 31265_3$	7170.575	2		13942.040	$18053\frac{3}{4} - 31995_4$
7215.667	10		13854.914	$17073_1 - 30928\frac{1}{1}$	7170.357	100	2	13942.464	$12847_3 - 26790\frac{3}{3}$
7212.687	500	50	13860.638	$14481\frac{0}{0} - 28342_5$	7169.621	4		13943.895	$18069\frac{3}{3} - 32012_4$
7211.769	2		13862.403	$18431_3 - 32294\frac{3}{4}$	7168.896	800	75	13945.305	$0_2 - 13945\frac{3}{3}$
7210.562	2		13864.723	$20566\frac{4}{4} - 34431_3$	7167.202	150	4	13948.601	$14032\frac{2}{2} - 27980_3$
7210.036	5		13865.735	$21539\frac{4}{4} - 35405_3$	7165.492	8	1	13951.930	$20922\frac{2}{2} - 34874_3$
7209.981	5		13865.840	$18930\frac{3}{3} - 32796_3$	7165.176	25	1	13952.545	$20214\frac{3}{3} - 34167_3$
7209.177	5		13867.387	$21594_3 - 35462\frac{3}{3}$	7164.508	2		13953.846	$5563_1 - 19516\frac{2}{2}$
7208.275	100b		13869.122	$13175\frac{4}{4} - 27044_3$	7164.323	8		13954.206	$18549_2 - 32503\frac{2}{2}$
7208.000	500	150	13869.651	$8800_4 - 22669\frac{3}{3}$	7163.374	2		13956.055	$19503\frac{3}{3} - 33459_4$
7207.756	50b	2	13870.121	$23015\frac{5}{5} - 36885_4$	7163.180	5		13956.433	$19817\frac{1}{1} - 33773_1$
7207.392	5		13870.821	$19588\frac{6}{6} - 33459_4$	7162.250	8	1	13958.245	$21575_2 - 35533\frac{3}{3}$
7207.016	50	2	13871.545	$17224\frac{2}{2} - 31095_1$	7161.689	2		13959.339	$18053\frac{4}{4} - 32012_4$
7206.476	400	8	13872.584	$10526\frac{3}{3} - 24399_3$	7159.943	300b	8	13962.743	$13297_4 - 27260\frac{3}{3}$
7205.435	2		13874.589	$20423\frac{1}{1} - 34298_1$	7159.877	100b	2	13962.871	$16554_6 - 30517\frac{6}{6}$
7204.761	3h		13875.887	$18053\frac{4}{4} - 31929_3$	7156.936	300	15	13968.609	$4961_4 - 18930\frac{3}{3}$
7203.593	4		13878.136	$19713_3 - 33591\frac{3}{3}$	7156.936	300	15	13968.609	$13297_4 - 27266\frac{4}{4}$
7202.335	5		13880.560	$20566\frac{4}{4} - 34447_4$	7155.349	8		13971.707	$18809\frac{4}{4} - 32781_4$
7201.803	100	2	13881.586	$10783\frac{2}{2} - 24664_3$	7154.952	200	8	13972.482	$7280_2 - 21252\frac{2}{2}$
7201.042	50	1	13883.053	$15970_3 - 29853\frac{2}{2}$	7154.762	200	20	13972.853	$13088_3 - 27061\frac{2}{2}$
7200.815	2		13883.490	$19948\frac{2}{2} - 33831_4$	7153.587	200	10	13975.149	$17166_5 - 31141\frac{6}{6}$
7200.171	50		13884.732	$17398_3 - 31283\frac{3}{3}$	7151.525	20	1	13979.178	$20322\frac{6}{6} - 34301_4$
7200.041	400	10	13884.983	$7280_2 - 21165\frac{3}{3}$	7150.285	400	25	13981.602	$3865_1 - 17847\frac{2}{2}$
7198.986	5		13887.018	$21575_2 - 35462\frac{3}{3}$	7149.224	5		13983.677	$22669\frac{3}{3} - 36653_2$
7198.214	4		13888.507	$19273_2 - 33161\frac{1}{1}$	7148.923	8	1	13984.266	$18011\frac{6}{6} - 31995_4$
7198.092	20		13888.742	$10783\frac{2}{2} - 24671_2$	7148.728	50	1	13984.647	$21165\frac{3}{3} - 35149_2$
7196.791	2		13891.253	$17354\frac{1}{1} - 31245_2$	7148.557	400	15	13984.982	$10414\frac{4}{4} - 24399_3$
7196.569	8		13891.682	$19516\frac{2}{2} - 33408_3$	7147.913	3		13986.242	$18809\frac{4}{4} - 32796_3$
7195.797	4		13893.172	$14465\frac{2}{2} - 28358_3$	7147.423	15	1	13987.201	$19227\frac{8}{8} - 33214_5$
7195.236	3		13894.255	$20566\frac{4}{4} - 34460_5$	7147.167	2		13987.702	$21890\frac{3}{3} - 35877_2$
7193.357	1		13897.885	$22399\frac{6}{6} - 36297_4$	7146.373	8	1	13989.256	$15863_2 - 29853\frac{2}{2}$
7192.019	40	2	13900.470	$11802_2 - 25703\frac{2}{2}$	7144.169	8		13993.572	$17959_4 - 31953\frac{4}{4}$
7191.585	3		13901.309	$21539\frac{4}{4} - 35440_3$	7142.328	300	8	13997.179	$12114\frac{2}{2} - 26111_1$
7190.332	2		13903.731	$22877\frac{1}{1} - 36781_5$	7140.080	4		14001.585	$18011\frac{6}{6} - 32012_4$
7190.124	5		13904.134	$19817\frac{1}{1} - 33721_2$	7138.142	20		14005.387	$19713_3 - 33718\frac{2}{2}$
7190.050	5		13904.277	$21890\frac{3}{3} - 35794_4$	7137.635	$\frac{3}{2}$		14006.382	$11802_2 - 25809\frac{1}{1}$
7189.407	10	1	13905.520	$19503\frac{3}{3} - 33408_3$	7137.133	5		14007.367	$18431_3 - 32439\frac{4}{4}$
7189.323	1		13905.683	$22141\frac{3}{3} - 36047_2$	7136.956	8		14007.714	$22877\frac{1}{1} - 36885_4$
7188.530	100	3	13907.217	$13088_3 - 26995\frac{3}{3}$	7136.841	4		14007.940	$22508\frac{2}{2} - 36515_3$
7185.031	3		13913.989	$15736\frac{1}{1} - 29650_2$	7134.484	8		14012.568	$11877\frac{1}{1} - 25890_2$
7184.721	4		13914.590	$2869_3 - 16783\frac{4}{4}$	7132.603	200	4	14016.263	$13175\frac{4}{4} - 27191_5$
7184.542	3		13914.936	$19503\frac{3}{3} - 33418_4$	7130.718	200	5	14019.968	$13297_4 - 27317\frac{3}{3}$
7184.426	4		13915.161	$16217\frac{2}{2} - 30132_2$	7130.179	100	4	14021.028	$14206\frac{4}{4} - 28227_4$
7184.111	8		13915.771	$17411\frac{3}{3} - 31326_4$	7129.871	20		14021.634	$19273_2 - 33294\frac{3}{3}$
7183.225	2		13917.488	$17224\frac{2}{2} - 31141_3$	7128.450	8	1	14024.429	$19503\frac{3}{3} - 33527_4$

TABLE 4. *Classified lines of* Th I—continued

Wavelength (Å)	Intensity		Wavenumber (cm^{-1})	Classification
	Lamp	Spark		
7127.640	10		14026.022	$18549_2 - 32575^{\circ}_{2}$
7126.814	100	3	14027.648	$19532_4 - 33560^{\circ}_{4}$
7126.324	8		14028.613	$17166_5 - 31194^{2}_{4}$
7126.009	5		14029.233	$14243^{1}_{1} - 28273_2$
7125.515	150	2	14030.205	$12847_3 - 26878^{3}_{3}$
7125.313	10	1	14030.603	$8111_4 - 22141^{3}_{3}$
7124.556	1000	50	14032.094	$0_2 - 14032^{2}_{2}$
7122.887	3		14035.382	$13945^{3}_{3} - 27980_3$
7122.098	3		14036.937	$21539^{4}_{4} - 35576_3$
7121.908	8		14037.311	$7502_3 - 21539^{2}_{4}$
7119.870	3		14041.329	$17224^{2}_{2} - 31265_3$
7119.174	2		14042.702	$21539^{4}_{4} - 35582_5$
7116.992	20	1	14047.007	$15970_3 - 30017^{3}_{3}$
7116.551	8		14047.878	$19516^{2}_{2} - 33564_3$
7114.394	150	3	14052.137	$8111_4 - 22163^{4}_{4}$
7113.007	5h		14054.877	$18699_2 - 32754^{3}_{3}$
7112.917	100	4	14055.055	$8800_4 - 22855^{3}_{3}$
7111.045	75	2	14058.755	$19532_4 - 33591^{3}_{3}$
7110.278	2		14060.271	$19039^{2}_{2} - 33099_3$
7109.857	150	4	14061.104	$6362_2 - 20423^{1}_{1}$
7109.550	40	2	14061.711	$19503^{3}_{3} - 33564_3$
7109.320	10		14062.166	$13962_1 - 28024^{1}_{1}$
7109.175	50		14062.453	$15490^{0}_{0} - 29552_6$
7108.550	2		14063.689	$17959_4 - 32023^{0}_{0}$
7107.469	10	1	14065.828	$14465^{2}_{2} - 28531_2$
7105.654	10		14069.421	$16217^{2}_{2} - 30286_1$
7104.404	4l		14071.896	$18431_3 - 32503^{2}_{2}$
7103.029	8		14074.620	$17354^{1}_{1} - 31429_1$
7102.185	10		14076.293	$18574_1 - 32650^{1}_{1}$
7101.660	4		14077.334	$8800_4 - 22877^{6}_{6}$
7100.391	2		14079.850	$22098_4 - 36178^{4}_{4}$
7099.094	4		14082.422	$17847^{2}_{2} - 31929_3$
7097.645	5		14085.297	$20322^{6}_{6} - 34407_6$
7097.032	10		14086.513	$20214^{3}_{3} - 34301_4$
7096.665	5		14087.242	$22248^{2}_{2} - 36336_3$
7096.478	4		14087.613	$19713_3 - 33800^{3}_{3}$
7096.000	3		14088.562	$22396^{1}_{1} - 36485_2$
7095.623	4		14089.311	$19516^{2}_{2} - 33606_2$
7094.803	3		14090.939	$18574_1 - 32665^{1}_{1}$
7093.128	3		14094.266	$21539^{4}_{4} - 35633_4$
7089.489	8		14101.501	$18549_2 - 32650^{1}_{1}$
7089.052	8		14102.370	$11601_1 - 25703^{2}_{2}$
7088.663	1		14103.144	$19503^{3}_{3} - 33606_2$
7088.330	8		14103.807	$21575_2 - 35678^{0}_{1}$
7087.506	3		14105.446	$22669^{3}_{3} - 36775_3$
7084.165	500	75	14112.099	$9804_5 - 23916^{2}_{4}$
7082.137	20		14116.140	$18549_2 - 32665^{1}_{1}$
7077.740	4		14124.909	$20322^{6}_{6} - 34447_4$
7077.422	50b	3	14125.544	$17398_3 - 31523^{3}_{3}$
7077.380	50b	4	14125.628	$17501^{6}_{6} - 31626_5$
7077.194	4		14125.999	$17411^{3}_{3} - 31537_3$
7074.257	50	1	14131.863	$10783^{2}_{2} - 24915_3$
7073.110	8		14134.155	$22163^{4}_{4} - 36297_4$
7072.394	300	8	14135.586	$14206^{2}_{4} - 28342_5$
7071.482	100		14137.409	$15618^{3}_{3} - 29756_4$
7071.096	150	3	14138.181	$10526^{3}_{3} - 24664_3$
7070.984	10		14138.405	$22669^{3}_{3} - 36808_3$
7070.891	2		14138.591	$20322^{6}_{6} - 34460_5$
7070.793	1		14138.787	$21594_3 - 35733^{4}_{4}$
7070.279	2		14139.815	$21077^{6}_{6} - 35216_5$
7068.330	2		14143.713	$18431_3 - 32575^{2}_{2}$
7067.513	75		14145.348	$10526^{3}_{3} - 24671_2$
7067.247	10		14145.881	$14226_0 - 28372^{1}_{1}$
7066.996	3		14146.383	$22338^{3}_{3} - 36485_2$
7066.287	100	2	14147.803	$12847_3 - 26995^{3}_{3}$
7064.451	300	10	14151.480	$14206^{2}_{4} - 28358_3$
7063.844	8		14152.696	$21252^{2}_{2} - 35405_3$
7063.585	10		14153.214	$15863_2 - 30017^{3}_{3}$
7063.314	8		14153.757	$19273_2 - 33427^{2}_{2}$
7062.418	40	1	14155.553	$22401_1 - 36556^{1}_{1}$
7061.607	1		14157.179	$21890^{3}_{3} - 36047_2$
7061.392	100	2	14157.610	$8243^{2}_{2} - 22401_1$
7060.651	400	10	14159.096	$3687_2 - 17847^{2}_{2}$
7060.039	300	8	14160.323	$6362_2 - 20522^{2}_{2}$
7059.526	150	3	14161.352	$16346^{3}_{4} - 30508_5$
7058.488	150	5	14163.435	$11241^{3}_{3} - 25405_4$
7058.221	2		14163.970	$23655^{3}_{4} - 37819_4$
7056.885	4		14166.652	$21645_4 - 35812^{3}_{3}$
7056.595	10		14167.234	$20922^{2}_{2} - 35089_3$
7055.900	50		14168.629	$13175^{0}_{4} - 27343_3$
7055.660	1		14169.111	$18930^{3}_{3} - 33099_3$
7054.416	150	2	14171.610	$13088_3 - 27260^{3}_{3}$
7051.787	50		14176.893	$13847_2 - 28024^{1}_{1}$
7051.503	8		14177.464	$13088_3 - 27266^{4}_{4}$
7049.844	20		14180.801	$16783^{3}_{4} - 30964_3$
7047.762	2		14184.990	$20522^{2}_{2} - 34707_3$
7047.319	2		14185.882	$19503^{3}_{3} - 33689_2$
7046.560	40		14187.409	$21902^{4}_{4} - 36089_4$
7046.124	10		14188.287	$21252^{2}_{2} - 35440_3$
7045.332	1		14189.882	$15970_3 - 30160^{4}_{4}$
7044.969	50	1	14190.613	$18011^{6}_{6} - 32202_5$
7043.714	15		14193.142	$15493_4 - 29686^{3}_{3}$
7043.228	8		14194.121	$15490^{6}_{6} - 29684_5$
7042.997	8		14194.587	$22141^{3}_{3} - 36336_3$
7042.031	3		14196.534	$23015^{6}_{6} - 37211_5$
7040.530	2		14199.560	$21890^{3}_{3} - 36089_4$
7039.877	5		14200.878	$17398_3 - 31599^{2}_{2}$
7038.165	40		14204.332	$19516^{2}_{2} - 33721_2$
7037.852	10		14204.964	$17224^{2}_{2} - 31429_1$
7037.781	8		14205.107	$18549_2 - 32754^{3}_{3}$
7037.410	4		14205.856	$16346^{3}_{4} - 30552_4$
7036.277	400	8	14208.143	$11197^{6}_{6} - 25405_4$
7036.206	50b		14208.287	$11601_1 - 25809^{1}_{1}$
7033.646	50	1	14213.458	$12847_3 - 27061^{2}_{2}$
7033.352	100	2	14214.052	$14465^{2}_{2} - 28679_2$
7032.924	100	1	14214.917	$8800_4 - 23015^{6}_{6}$
7032.677	3		14215.416	$22669^{3}_{3} - 36885_4$
7032.350	3		14216.077	$15618^{3}_{3} - 29835_3$
7032.178	15	1	14216.425	$20214^{3}_{3} - 34431_3$
7031.469	15	1	14217.858	$21594_3 - 35812^{3}_{3}$
7031.310	50	1	14218.180	$19503^{3}_{3} - 33721_2$
7031.194	10		14218.415	$15493_4 - 29711^{6}_{6}$

TABLE 4. *Classified lines of* Th I—continued

Wavelength (Å)	Intensity		Wavenumber (cm^{-1})	Classification
	Lamp	Spark		
7030.858	50	1	14219.094	$19948\frac{3}{4} - 34167_3$
7028.017	100	2	14224.842	$15736\frac{1}{2} - 29961_1$
7026.454	100	1	14228.006	$8111_4 - 22338\frac{3}{3}$
7026.041	8		14228.842	$13088_3 - 27317\frac{3}{3}$
7025.379	1		14230.183	$15618\frac{3}{3} - 29849_4$
7025.188	4		14230.570	$22855\frac{3}{3} - 37085_4$
7023.776	8		14233.431	$11802_2 - 26036\frac{3}{3}$
7023.636	25	1	14233.715	$11877\frac{1}{2} - 26111_1$
7023.523	100	3	14233.944	$16554_6 - 30788\frac{0}{0}$
7023.145	100	3	14234.710	$19039\frac{2}{2} - 33273_1$
7022.847	2		14235.314	$23655\frac{3}{4} - 37890_5$
7022.619	8		14235.776	$7502_3 - 21738\frac{2}{2}$
7021.899	40		14237.236	$17959_4 - 32197\frac{3}{3}$
7021.784	2		14237.469	$21575_2 - 35812\frac{3}{3}$
7021.668	3		14237.704	$23655\frac{3}{4} - 37892_4$
7021.279	150	8	14238.493	$15970_3 - 30208\frac{2}{2}$
7020.476	100	1	14240.121	$15493_4 - 29733\frac{0}{0}$
7019.970	4		14241.148	$14032\frac{2}{2} - 28273_2$
7018.784	3		14243.554	$19588\frac{0}{0} - 33831_4$
7018.563	500	75	14244.003	$0_2 - 14243\frac{1}{1}$
7015.311	100	3	14250.605	$10414\frac{3}{4} - 24664_3$
7014.965	100	4	14251.308	$15493_4 - 29744\frac{3}{3}$
7014.873	50	1	14251.495	$15166\frac{3}{3} - 29418_2$
7013.617	8		14254.047	$5563_1 - 19817\frac{1}{1}$
7013.171	1		14254.954	$18699_2 - 32954\frac{2}{2}$
7007.092	100	4	14267.321	$19532_4 - 33799\frac{4}{4}$
7006.655	4		14268.210	$19532_4 - 33800\frac{3}{3}$
7006.113	50	2	14269.314	$20054_2 - 34324\frac{2}{2}$
7005.825	8		14269.901	$19039\frac{2}{2} - 33309_2$
7002.881	200	8	14275.900	$14204_5 - 28480\frac{4}{4}$
7000.806	500	75	14280.131	$9804_5 - 24084\frac{6}{6}$
6999.624	100	3	14282.543	$18011\frac{0}{0} - 32293_5$
6998.247	100	2	14285.353	$15970_3 - 30255\frac{3}{3}$
6997.412	50	1	14287.058	$14243\frac{1}{1} - 28531_2$
6996.812	1		14288.283	$19713_3 - 34001\frac{3}{3}$
6996.757	50l		14288.395	$8111_4 - 22399\frac{6}{6}$
6996.202	8		14289.528	$18809\frac{4}{4} - 33099_3$
6995.141	75	2	14291.696	$21539\frac{4}{4} - 35831_3$
6994.736	100	3	14292.523	$17501\frac{0}{0} - 31793_4$
6993.988	100	2	14294.052	$11802_2 - 26096\frac{3}{3}$
6989.657	1000	150	14302.909	$7795\frac{4}{4} - 22098_4$
6988.871	20	1	14304.517	$16346\frac{4}{4} - 30651_3$
6987.790	20	2	14306.730	$20566\frac{4}{4} - 34873_4$
6987.444	3		14307.439	$20566\frac{4}{4} - 34874_3$
6986.565	3		14309.239	$21738\frac{2}{2} - 36047_2$
6986.159	2		14310.070	$22508\frac{2}{2} - 36818_2$
6986.031	150	4	14310.332	$11802_2 - 26113\frac{2}{2}$
6985.783	10	1	14310.840	$21575_2 - 35885\frac{2}{2}$
6984.952	3		14312.543	$19532_4 - 33844\frac{0}{0}$
6984.759	5		14312.939	$17224\frac{2}{2} - 31537_3$
6984.585	4		14313.295	$8800_4 - 23113\frac{3}{3}$
6983.965	5		14314.566	$22338\frac{3}{3} - 36653_2$
6982.752	3		14317.052	$20054_2 - 34371\frac{2}{2}$
6982.608	50	2	14317.348	$23015\frac{6}{6} - 37332_6$
6981.082	100	3	14320.477	$13175\frac{4}{4} - 27495_4$
6980.543	4	1	14321.583	$20724\frac{0}{0} - 35046_1$
6979.944	1		14322.812	$18431_3 - 32754\frac{3}{3}$
6978.753	2		14325.256	$17959_4 - 32285\frac{3}{3}$
6978.241	50	2	14326.307	$14032\frac{2}{2} - 28358_3$
6977.875	3		14327.059	$16217\frac{2}{2} - 30544_2$
6977.462	25	1	14327.907	$13945\frac{3}{3} - 28273_2$
6977.061	3	1	14328.730	$19503\frac{3}{3} - 33831_4$
6976.839	2		14329.186	$22098_4 - 36427\frac{3}{3}$
6974.446	10		14334.103	$22877\frac{1}{1} - 37211_5$
6974.381	1		14334.236	$17959_4 - 32294\frac{3}{3}$
6970.054	5	1	14343.135	$18069\frac{3}{3} - 32412_4$
6969.779	2		14343.701	$18699_2 - 33043\frac{3}{3}$
6969.301	100	3	14344.685	$15863_2 - 30208\frac{2}{2}$
6966.905	3		14349.618	$22399\frac{6}{6} - 36749_6$
6966.064	3h		14351.350	$20522\frac{2}{2} - 34874_3$
6965.946	500l	4	14351.593	$19039\frac{2}{2} - 33390_1$
6965.240	5		14353.048	$19948\frac{3}{4} - 34301_4$
6964.271	50	1	14355.045	$2869_3 - 17224\frac{2}{2}$
6963.930	50	1	14355.748	$14206\frac{3}{4} - 28562_4$
6962.862	75	2	14357.950	$16783\frac{3}{4} - 31141_3$
6962.310	100	4	14359.088	$15490\frac{3}{3} - 29849_4$
6960.232	4		14363.375	$17411\frac{3}{3} - 31774_3$
6957.265	1		14369.501	$19039\frac{2}{2} - 33408_3$
6956.113	1		14371.880	$16351_0 - 30723\frac{1}{1}$
6955.315	100	3	14373.529	$13297_4 - 27670\frac{3}{3}$
6954.655	200	5	14374.893	$6362_2 - 20737\frac{1}{1}$
6954.387	2		14375.447	$20054_2 - 34430\frac{3}{3}$
6952.796	1		14378.737	$18930\frac{3}{3} - 33309_2$
6952.189	2		14379.992	$18574_1 - 32954\frac{2}{2}$
6951.654	20	1	14381.099	$3687_2 - 18069\frac{3}{3}$
6951.259	5	1	14381.916	$22399\frac{6}{6} - 36781_5$
6950.990	5		14382.473	$17398_3 - 31780\frac{3}{3}$
6950.990	5		14382.473	$17411\frac{3}{3} - 31793_4$
6949.754	10		14385.030	$13962_1 - 28347\frac{2}{2}$
6948.391	100	3	14387.852	$7502_3 - 21890\frac{3}{3}$
6948.205	300	20	14388.237	$15493_4 - 29881\frac{4}{4}$
6948.090	75	1	14388.475	$10526\frac{3}{3} - 24915_3$
6947.914	100	3	14388.840	$7280_2 - 21668\frac{1}{1}$
6947.783	2		14389.111	$18069\frac{3}{3} - 32458_4$
6946.599	50	3	14391.564	$15863_2 - 30255\frac{3}{3}$
6946.210	100	3	14392.370	$15618\frac{3}{3} - 30011_3$
6945.488	200	8	14393.866	$8243\frac{2}{2} - 22637_3$
6944.926	2		14395.031	$21902\frac{4}{4} - 36297_4$
6944.773	8		14395.348	$15618\frac{3}{3} - 30014_4$
6944.611	8		14395.684	$15736\frac{1}{1} - 30132_2$
6943.612	800	200	14397.755	$9804_5 - 24202\frac{4}{4}$
6942.535	150	8	14399.988	$7502_3 - 21902\frac{4}{4}$
6940.327	50	3	14404.569	$18053\frac{4}{4} - 32458_4$
6940.037	3		14405.171	$18549_2 - 32954\frac{2}{2}$
6937.618	10		14410.194	$13962_1 - 28372\frac{1}{1}$
6937.033	8		14411.409	$21165\frac{3}{3} - 35576_3$
6936.651	150	4	14412.203	$12847_3 - 27260\frac{3}{3}$
6936.223	10		14413.092	$13945\frac{3}{3} - 28358_3$
6934.839	4	1	14415.969	$22669\frac{3}{3} - 37085_4$
6934.488	15	1	14416.698	$13175\frac{4}{4} - 27591_5$

201-606 O - 76 - 11

TABLE 4. *Classified lines of* Th I—continued

Wavelength (Å)	Intensity		Wavenumber (cm^{-1})	Classification	Wavelength (Å)	Intensity		Wavenumber (cm^{-1})	Classification
	Lamp	Spark				Lamp	Spark		
6934.274	100b	5	14417.143	$15863_2 - 30281\frac{1}{1}$	6882.807	200	8	14524.948	$13847_2 - 28372\frac{2}{1}$
6934.232	100b	3	14417.231	$14465\frac{2}{2} - 28882_2$	6881.932	2		14526.795	$20322\frac{0}{0} - 34849_5$
6933.836	2		14418.054	$12847_3 - 27266\frac{4}{4}$	6881.674	5		14527.340	$19273_2 - 33800\frac{3}{3}$
6932.227	15	1	14421.400	$19986\frac{6}{6} - 34407_6$	6881.250	5		14528.235	$20054_2 - 34583\frac{3}{3}$
6931.784	3h		14422.322	$14226_0 - 28649\frac{1}{1}$	6880.945	1		14528.879	$18930\frac{3}{3} - 33459_4$
6930.094	5		14425.839	$22877\frac{6}{6} - 37303_4$	6879.376	1		14532.193	$21645_4 - 36178\frac{4}{4}$
6928.959	3		14428.202	$21645_4 - 36074\frac{3}{3}$	6877.469	2		14536.222	$20054_2 - 34591\frac{1}{1}$
6927.721	2		14430.780	$18431_3 - 32862\frac{4}{4}$	6875.440	2		14540.512	$16217\frac{2}{2} - 30758_2$
6926.311	2		14433.718	$16217\frac{2}{2} - 30651_3$	6874.984	10		14541.476	$4961_4 - 19503\frac{3}{3}$
6925.566	8		14435.271	$14243\frac{1}{1} - 28679_2$	6874.752	200	10	14541.967	$2869_3 - 17411\frac{3}{3}$
6925.471	10	1	14435.469	$19532_4 - 33967\frac{3}{3}$	6874.192	50b		14543.151	$16783\frac{4}{4} - 31326_4$
6925.040	4		14436.367	$22338\frac{8}{8} - 36775_3$	6872.234	8		14547.295	$15970_3 - 30517\frac{4}{4}$
6924.657	50	1	14437.166	$13175\frac{4}{4} - 27612_3$	6871.271	50		14549.334	$22855\frac{3}{3} - 37404_3$
6920.834	1		14445.141	$19273_2 - 33718\frac{2}{2}$	6870.988	150	3	14549.933	$15736\frac{1}{1} - 30286_1$
6920.391	5		14446.065	$21890\frac{3}{3} - 36336_3$	6870.911	2		14550.096	$21539\frac{3}{4} - 36089_4$
6920.037	150	5	14446.804	$18011\frac{0}{0} - 32458_4$	6870.807	2		14550.316	$17224\frac{2}{2} - 31774_3$
6919.415	1		14448.103	$22855\frac{3}{3} - 37303_4$	6870.727	150	3	14550.486	$17166_5 - 31716\frac{0}{0}$
6916.129	200	10	14454.967	$9804_5 - 24259\frac{4}{4}$	6868.455	100	3	14555.299	$13297_4 - 27852\frac{6}{6}$
6914.713	100	2	14457.928	$7280_2 - 21738\frac{2}{2}$	6866.756	100s	2	14558.900	$8111_4 - 22669\frac{3}{3}$
6913.173	2		14461.148	$22669\frac{3}{3} - 37131_3$	6866.368	150	3	14559.723	$6362_2 - 20922\frac{2}{2}$
6913.051	4		14461.403	$19273_2 - 33734\frac{3}{3}$	6866.157	100	2	14560.170	$11802_2 - 26363\frac{2}{2}$
6912.694	2		14462.150	$18699_2 - 33161\frac{1}{1}$	6863.104	8		14566.647	$20522\frac{3}{3} - 35089_3$
6911.222	800r	200	14465.231	$0_2 - 14465\frac{2}{2}$	6862.873	100	2	14567.138	$19039\frac{2}{2} - 33606_2$
6909.222	100l	1	14469.418	$12847_3 - 27317\frac{3}{3}$	6858.317	1		14576.814	$16351_0 - 30928\frac{1}{1}$
6908.989	100	2	14469.906	$9804_5 - 24274\frac{6}{6}$	6857.436	2		14578.687	$21252\frac{2}{2} - 35831_3$
6908.630	2		14470.658	$22401_1 - 36871\frac{2}{2}$	6855.689	100	3	14582.402	$13088_3 - 27670\frac{3}{3}$
6908.599	2h		14470.723	$22401_1 - 36871\frac{2}{2}$	6855.315	150	4	14583.198	$15970_3 - 30553\frac{2}{2}$
6906.698	20	1	14474.705	$19986\frac{6}{6} - 34460_5$	6854.107	400	10	14585.768	$13088_3 - 27674\frac{2}{2}$
6905.856	40	1	14476.470	$14204_5 - 28680\frac{3}{3}$	6853.511	100	4	14587.036	$16554_6 - 31141\frac{0}{0}$
6904.578	50		14479.150	$17959_4 - 32439\frac{4}{4}$	6852.344	50	2	14589.521	$15166\frac{3}{3} - 29756_4$
6904.468	8		14479.380	$21594_3 - 36074\frac{3}{3}$	6852.099	1		14590.042	$21143_5 - 35733\frac{4}{4}$
6903.317	8		14481.795	$16783\frac{4}{4} - 31265_3$	6850.111	8		14594.276	$21594_3 - 36188\frac{2}{2}$
6902.957	10		14482.550	$18069\frac{3}{3} - 32551_3$	6849.623	25		14595.316	$18699_2 - 33294\frac{3}{3}$
6902.767	2		14482.948	$19948\frac{4}{4} - 34431_3$	6848.697	3		14597.290	$18930\frac{3}{3} - 33527_4$
6902.210	150	3	14484.117	$11802_2 - 26287\frac{1}{1}$	6848.279	2		14598.181	$21738\frac{2}{2} - 36336_3$
6901.357	10		14485.907	$22399\frac{8}{8} - 36885_4$	6847.989	3		14598.799	$18809\frac{4}{4} - 33408_3$
6901.019	3		14486.617	$21645_4 - 36132\frac{6}{6}$	6847.517	4		14599.805	$12847_3 - 27447\frac{2}{2}$
6900.762	100	5	14487.156	$16783\frac{4}{4} - 31271_5$	6846.603	15	1	14601.754	$17411\frac{3}{3} - 32012_4$
6900.442	10		14487.828	$18930\frac{3}{3} - 33418_4$	6843.556	3		14608.255	$18809\frac{4}{4} - 33418_4$
6898.073	25		14492.804	$20214\frac{3}{3} - 34707_3$	6842.724	50		14610.031	$7280_2 - 21890\frac{3}{3}$
6897.277	20		14494.476	$17501\frac{3}{3} - 31995_4$	6841.962	8		14611.659	$18431_3 - 33043\frac{3}{3}$
6895.227	10		14498.786	$19948\frac{4}{4} - 34447_4$	6841.690	10		14612.239	$22163\frac{3}{4} - 36775_3$
6895.116	8		14499.019	$21575_2 - 36074\frac{3}{3}$	6840.993	2		14613.728	$21902\frac{3}{4} - 36515_3$
6894.229	50	4	14500.884	$10414\frac{3}{3} - 24915_3$	6840.899	2		14613.929	$21575_2 - 36188\frac{2}{2}$
6893.626	10	1	14502.153	$20543\frac{6}{6} - 35046_1$	6839.287	100	2	14617.373	$13945\frac{3}{3} - 28562_4$
6892.247	200	5	14505.054	$17166_5 - 31671\frac{4}{4}$	6838.979	2		14618.032	$16346\frac{4}{4} - 30964_3$
6889.052	8	1	14511.781	$17501\frac{6}{6} - 32012_4$	6838.902	8		14618.196	$22163\frac{3}{4} - 36781_5$
6888.832	100	3	14512.245	$11601_1 - 26113\frac{2}{2}$	6836.881	50		14622.518	$20423\frac{1}{1} - 35046_1$
6888.158	50	2	14513.665	$15618\frac{3}{3} - 30132_2$	6836.651	3		14623.009	$22508\frac{2}{2} - 37131_3$
6886.404	200	10	14517.362	$3865_1 - 18382\frac{6}{6}$	6835.613	8		14625.230	$21252\frac{2}{2} - 35877_2$
6885.964	2		14518.289	$17411\frac{3}{3} - 31929_3$	6834.925	400	50	14626.702	$4961_4 - 19588\frac{6}{6}$
6885.721	1		14518.802	$20922\frac{2}{2} - 35440_3$	6834.780	5b		14627.012	$20522\frac{2}{2} - 35149_2$
6883.849	75		14522.750	$20566\frac{4}{4} - 35089_3$	6834.585	1		14627.430	$19817\frac{1}{1} - 34444_2$
6883.311	200	10	14523.885	$15493_4 - 30017\frac{3}{3}$	6833.697	3		14629.330	$21645_4 - 36275\frac{6}{6}$
6883.135	50	4	14524.256	$15490\frac{6}{6} - 30014_4$	6833.373	10		14630.024	$17411\frac{3}{3} - 32041_2$

TABLE 4. *Classified lines of* Th I—continued

Wavelength (Å)	Intensity		Wavenumber (cm^{-1})	Classification
	Lamp	Spark		
6831.719	3		14633.566	$22669\frac{3}{3} - 37303_4$
6831.621	2		14633.776	$22141\frac{1}{3} - 36775_3$
6831.249	8		14634.573	$18930\frac{3}{3} - 33564_3$
6829.339	100	3	14638.666	$14206\frac{3}{4} - 28845_4$
6829.212	8		14638.938	$17073_1 - 31712\frac{2}{1}$
6829.037	500	25	14639.313	$7502_3 - 22141\frac{1}{3}$
6826.296	50l	2	14645.191	$22163\frac{3}{4} - 36808_3$
6824.678	400	20	14648.663	$11241\frac{1}{3} - 25890_2$
6824.380	1		14649.303	$18809\frac{2}{4} - 33459_4$
6824.097	8		14649.911	$19039\frac{2}{2} - 33689_2$
6823.911	10	1	14650.310	$19532_4 - 34182\frac{2}{3}$
6823.500	150	4	14651.192	$13297_4 - 27948\frac{3}{4}$
6819.796	10		14659.150	$20214\frac{3}{3} - 34874_3$
6819.549	5		14659.681	$14481\frac{2}{6} - 29141_5$
6818.996	5		14660.870	$7502_3 - 22163\frac{3}{4}$
6817.248	2		14664.629	$22098_4 - 36762\frac{3}{3}$
6816.821	25		14665.547	$13847_2 - 28513\frac{2}{2}$
6816.510	50	2	14666.216	$21165\frac{3}{3} - 35831_3$
6816.510	50	2	14666.216	$22855\frac{3}{3} - 37521_3$
6816.246	50w		14666.784	$15493_4 - 30160\frac{3}{4}$
6815.604	100	2	14668.166	$15166\frac{3}{3} - 29835_3$
6814.184	2		14671.222	$21539\frac{2}{4} - 36210_5$
6813.602	10		14672.476	$16217\frac{2}{2} - 30889_1$
6811.958	50	1	14676.017	$18930\frac{3}{3} - 33606_2$
6811.725	4		14676.519	$22141\frac{1}{3} - 36818_2$
6809.504	100	3	14681.306	$11241\frac{1}{3} - 25923_4$
6809.311	150	4	14681.722	$12114\frac{2}{2} - 26796_3$
6809.103	400	10	14682.170	$19039\frac{2}{2} - 33721_2$
6808.530	75	2	14683.406	$18053\frac{3}{4} - 32737_5$
6808.373	2		14683.744	$20737\frac{2}{1} - 35421_1$
6807.314	100	3	14686.029	$11601_1 - 26287\frac{2}{1}$
6807.108	8	1	14686.473	$22399\frac{6}{6} - 37085_4$
6807.035	15	1	14686.631	$13962_1 - 28649\frac{2}{1}$
6805.746	100	2	14689.412	$15863_2 - 30553\frac{2}{2}$
6803.292	10		14694.711	$18614\frac{2}{1} - 33309_2$
6802.783	100	3	14695.810	$13088_3 - 27784\frac{2}{2}$
6802.410	3		14696.616	$20724\frac{6}{6} - 35421_1$
6801.772	2		14697.995	$22396\frac{2}{1} - 37094_2$
6800.461	100	4	14700.828	$17501\frac{6}{6} - 32202_5$
6799.707	2		14702.458	$22098_4 - 36800\frac{4}{4}$
6798.743	100	3	14704.543	$17847\frac{2}{2} - 32551_3$
6798.483	150	3	14705.105	$11802_2 - 26508\frac{3}{3}$
6795.797	100	2	14710.917	$13962_1 - 28673\frac{2}{2}$
6795.046	75	2	14712.543	$18069\frac{3}{3} - 32781_4$
6794.965	25	1	14712.719	$21165\frac{3}{3} - 35877_2$
6794.795	8	1	14713.087	$19588\frac{6}{6} - 34301_4$
6792.900	15	1	14717.191	$19713_3 - 34430\frac{3}{3}$
6792.674	4		14717.681	$18809\frac{2}{4} - 33527_4$
6791.232	400	25	14720.806	$8800_4 - 23521\frac{3}{3}$
6789.000	100		14725.645	$18011\frac{6}{6} - 32737_5$
6788.837	300	25	14725.999	$11197\frac{6}{6} - 25923_4$
6788.730	50h	1	14726.231	$20423\frac{2}{1} - 35149_2$
6788.343	20		14727.071	$18069\frac{3}{3} - 32796_3$
6788.180	50		14727.424	$18699_2 - 33427\frac{3}{2}$
6787.913	25		14728.004	$14206\frac{3}{4} - 28934_3$
6787.913	25		14728.004	$18053\frac{3}{4} - 32781_4$
6787.734	300	25	14728.392	$14204_5 - 28932\frac{2}{4}$
6784.927	10		14734.485	$19039\frac{2}{2} - 33773_1$
6784.807	50	2	14734.746	$22669\frac{3}{3} - 37404_3$
6782.498	1		14739.762	$22098_4 - 36837\frac{6}{6}$
6781.676	3		14741.549	$13847_2 - 28589\frac{3}{3}$
6781.234	3		14742.509	$18053\frac{3}{4} - 32796_3$
6780.415	400	100	14744.290	$8111_4 - 22855\frac{3}{3}$
6780.126	400	1	14744.919	$8243\frac{3}{2} - 22988_2$
6779.323	100	1	14746.665	$7502_3 - 22248\frac{2}{2}$
6779.085	4		14747.183	$16217\frac{2}{2} - 30964_3$
6778.312	400	40	14748.865	$3865_1 - 18614\frac{2}{1}$
6776.230	100	3	14753.396	$16783\frac{4}{4} - 31537_3$
6775.501	2		14754.984	$18809\frac{2}{4} - 33564_3$
6775.101	15	2	14755.855	$22338\frac{3}{3} - 37094_2$
6774.254	1		14757.700	$21539\frac{2}{4} - 36297_4$
6774.086	8		14758.066	$22401_1 - 37159\frac{2}{1}$
6773.770	40	1	14758.754	$18930\frac{3}{3} - 33689_2$
6772.237	50b		14762.095	$17398_3 - 32160\frac{2}{2}$
6772.176	400	15	14762.228	$15493_4 - 30255\frac{3}{3}$
6771.623	5		14763.433	$21890\frac{3}{3} - 36653_2$
6770.175	5		14766.591	$8111_4 - 22877\frac{6}{6}$
6768.511	3		14770.221	$18011\frac{6}{6} - 32781_4$
6765.683	200	100	14776.395	$18614\frac{2}{1} - 33390_1$
6764.987	1		14777.915	$21738\frac{2}{2} - 36515_3$
6763.532	8	1	14781.094	$19516\frac{2}{2} - 34298_1$
6763.340	50	2	14781.514	$21645_4 - 36427\frac{3}{3}$
6760.667	100	3	14787.358	$17166_5 - 31953\frac{4}{4}$
6760.400	2		14787.942	$21594_3 - 36382\frac{4}{4}$
6758.716	2		14791.627	$15970_3 - 30761\frac{3}{3}$
6758.521	5		14792.053	$22338\frac{3}{3} - 37131_3$
6758.202	200	8	14792.752	$17501\frac{6}{6} - 32293_5$
6757.349	15		14794.619	$17959_4 - 32754\frac{3}{3}$
6757.105	100	5	14795.153	$16346\frac{4}{4} - 31141_3$
6756.454	800b	75	14796.579	$2558_0 - 17354\frac{2}{1}$
6756.323	15		14796.866	$20054_2 - 34851\frac{2}{2}$
6756.323	15		14796.866	$20054_2 - 34851\frac{2}{2}$
6755.663	4		14798.311	$19503\frac{3}{3} - 34301_4$
6755.475	20	1	14798.723	$17398_3 - 32197\frac{3}{3}$
6755.305	2		14799.096	$22508\frac{2}{2} - 37307_3$
6754.265	150	4	14801.374	$13847_2 - 28649\frac{2}{1}$
6753.657	150	4	14802.707	$6362_2 - 21165\frac{3}{3}$
6751.426	100	3	14807.598	$15736\frac{1}{1} - 30544_2$
6749.315	50	1	14812.230	$19532_4 - 34344\frac{4}{4}$
6747.402	2		14816.429	$21668\frac{3}{1} - 36485_2$
6747.172	5		14816.934	$17224\frac{2}{2} - 32041_2$
6746.137	75	2	14819.207	$19588\frac{6}{6} - 34407_6$
6743.199	10		14825.664	$13847_2 - 28673\frac{2}{2}$
6742.881	200	8	14826.363	$12847_3 - 27674\frac{2}{2}$
6741.924	100	2	14828.468	$13847_2 - 28676\frac{3}{3}$
6739.963	50h		14832.782	$22401_1 - 37234\frac{2}{2}$
6738.179	200	5	14836.709	$7502_3 - 22338\frac{3}{3}$
6737.643	50	8	14837.889	$19273_2 - 34111\frac{2}{1}$
6737.281	50		14838.687	$20566\frac{4}{4} - 35405_3$
6735.686	2		14842.201	$7795\frac{4}{4} - 22637_3$

TABLE 4. *Classified lines of* Th I – continued

Wavelength (Å)	Intensity		Wavenumber (cm^{-1})	Classification
	Lamp	Spark		
6735.369	100	2	14842.899	$15970_3 - 30812^{\frac{5}{2}}_{\frac{5}{2}}$
6735.128	100	2	14843.430	$13297_4 - 28140^{\frac{3}{2}}_{\frac{3}{2}}$
6734.667	20		14844.446	$15166^{\frac{3}{2}}_{\frac{3}{2}} - 30011_3$
6734.003	4		14845.910	$22248^{\frac{5}{2}}_{\frac{5}{2}} - 37094_2$
6733.748	150	5	14846.472	$14204_5 - 29050^{\frac{7}{2}}_{\frac{7}{2}}$
6733.314	8		14847.429	$15166^{\frac{3}{2}}_{\frac{3}{2}} - 30014_4$
6732.650	50	3	14848.893	$11802_2 - 26651^{\frac{1}{2}}_{\frac{1}{2}}$
6731.047	25		14852.430	$18574_1 - 33427^{\frac{5}{2}}_{\frac{5}{2}}$
6729.932	50	1	14854.890	$8800_4 - 23655^{\frac{3}{2}}_{\frac{3}{2}}$
6728.757	300	5	14857.484	$17166_5 - 32023^{\frac{5}{2}}_{\frac{5}{2}}$
6728.117	150	5	14858.898	$13175^{\frac{3}{2}}_{\frac{3}{2}} - 28034_5$
6727.649	100s	2	14859.931	$15863_2 - 30723^{\frac{7}{2}}_{\frac{7}{2}}$
6727.459	500	75	14860.351	$5563_1 - 20423^{\frac{7}{2}}_{\frac{7}{2}}$
6726.946	10	2	14861.484	$7280_2 - 22141^{\frac{5}{2}}_{\frac{5}{2}}$
6726.310	100	2	14862.889	$19986^{\frac{9}{2}}_{\frac{9}{2}} - 34849_5$
6725.482	2		14864.719	$22877^{\frac{7}{2}}_{\frac{7}{2}} - 37742_6$
6725.128	1		14865.502	$18431_3 - 33297^{\frac{5}{2}}_{\frac{5}{2}}$
6723.120	2		14869.941	$19713_3 - 34583^{\frac{5}{2}}_{\frac{5}{2}}$
6722.852	1		14870.534	$22877^{\frac{7}{2}}_{\frac{7}{2}} - 37748_2$
6721.958	5		14872.512	$19588^{\frac{9}{2}}_{\frac{9}{2}} - 34460_5$
6721.703	1		14873.076	$21902^{\frac{3}{2}}_{\frac{3}{2}} - 36775_3$
6721.089	25		14874.435	$20214^{\frac{5}{2}}_{\frac{5}{2}} - 35089_3$
6720.699	1		14875.298	$23015^{\frac{9}{2}}_{\frac{9}{2}} - 37890_5$
6719.630	20		14877.664	$18549_2 - 33427^{\frac{5}{2}}_{\frac{5}{2}}$
6719.307	2		14878.380	$16217^{\frac{3}{2}}_{\frac{3}{2}} - 31095_1$
6719.198	200	5	14878.621	$10526^{\frac{3}{2}}_{\frac{3}{2}} - 25405_4$
6719.011	3		14879.035	$21902^{\frac{3}{2}}_{\frac{3}{2}} - 36781_5$
6717.582	1		14882.200	$21165^{\frac{3}{2}}_{\frac{3}{2}} - 36047_2$
6717.384	100	3	14882.639	$15490^{\frac{9}{2}}_{\frac{9}{2}} - 30372_6$
6716.215	3		14885.229	$21890^{\frac{3}{2}}_{\frac{3}{2}} - 36775_3$
6715.515	100	2	14886.781	$17398_3 - 32285^{\frac{5}{2}}_{\frac{5}{2}}$
6713.967	300	8	14890.213	$6362_2 - 21252^{\frac{5}{2}}_{\frac{5}{2}}$
6713.602	100		14891.023	$18382^{\frac{9}{2}}_{\frac{9}{2}} - 33273_1$
6712.838	2		14892.717	$22855^{\frac{5}{2}}_{\frac{5}{2}} - 37748_2$
6712.194	5		14894.146	$21594_3 - 36488^{\frac{3}{2}}_{\frac{3}{2}}$
6711.495	50		14895.698	$17398_3 - 32294^{\frac{1}{2}}_{\frac{1}{2}}$
6711.249	100	4	14896.243	$9804_5 - 24701^{\frac{9}{2}}_{\frac{9}{2}}$
6710.865	10		14897.096	$14206^{\frac{7}{2}}_{\frac{7}{2}} - 29104_4$
6710.545	100	2	14897.806	$15863_2 - 30761^{\frac{5}{2}}_{\frac{5}{2}}$
6710.545	100	2	14897.806	$19532_4 - 34430^{\frac{3}{2}}_{\frac{3}{2}}$
6710.325	3		14898.295	$20522^{\frac{5}{2}}_{\frac{5}{2}} - 35421_1$
6709.443	2		14900.253	$13945^{\frac{3}{2}}_{\frac{3}{2}} - 28845_4$
6709.248	2		14900.686	$19948^{\frac{1}{2}}_{\frac{1}{2}} - 34849_5$
6708.839	50	1	14901.595	$18930^{\frac{3}{2}}_{\frac{3}{2}} - 33831_4$
6708.391	5		14902.590	$17959_4 - 32862^{\frac{3}{2}}_{\frac{3}{2}}$
6708.283	5		14902.830	$14032^{\frac{5}{2}}_{\frac{5}{2}} - 28934_3$
6707.733	3h		14904.052	$22399^{\frac{9}{2}}_{\frac{9}{2}} - 37303_4$
6706.835	15	1	14906.047	$21902^{\frac{3}{2}}_{\frac{3}{2}} - 36808_3$
6706.451	2		14906.901	$22877^{\frac{7}{2}}_{\frac{7}{2}} - 37784_2$
6705.428	8		14909.175	$20922^{\frac{5}{2}}_{\frac{5}{2}} - 35831_3$
6705.151	10		14909.791	$18053^{\frac{1}{2}}_{\frac{1}{2}} - 32963_5$
6703.348	5		14913.801	$21575_2 - 36488^{\frac{5}{2}}_{\frac{5}{2}}$
6703.091	2		14914.373	$19516^{\frac{5}{2}}_{\frac{5}{2}} - 34431_3$
6702.576	1		14915.519	$21738^{\frac{5}{2}}_{\frac{5}{2}} - 36653_2$
6701.373	10	1	14918.196	$20522^{\frac{5}{2}}_{\frac{5}{2}} - 35440_3$
6701.373	10	1	14918.196	$21890^{\frac{3}{2}}_{\frac{3}{2}} - 36808_3$
6701.010	2		14919.004	$16346^{\frac{1}{2}}_{\frac{1}{2}} - 31265_3$
6700.798	8		14919.477	$21143_5 - 36062^{\frac{3}{2}}_{\frac{3}{2}}$
6699.335	2		14922.735	$22163^{\frac{3}{2}}_{\frac{3}{2}} - 37085_4$
6698.610	10		14924.350	$16346^{\frac{1}{2}}_{\frac{1}{2}} - 31271_5$
6698.516	2		14924.559	$21165^{\frac{3}{2}}_{\frac{3}{2}} - 36089_4$
6698.029	200	4	14925.644	$19948^{\frac{1}{2}}_{\frac{1}{2}} - 34874_3$
6697.708	200	5	14926.360	$3687_2 - 18614^{\frac{9}{2}}_{\frac{9}{2}}$
6697.139	5		14927.628	$19516^{\frac{5}{2}}_{\frac{5}{2}} - 34444_2$
6696.996	1		14927.947	$21890^{\frac{3}{2}}_{\frac{3}{2}} - 36818_2$
6696.886	1		14928.192	$19503^{\frac{3}{2}}_{\frac{3}{2}} - 34431_3$
6696.140	200	5	14929.855	$12114^{\frac{5}{2}}_{\frac{5}{2}} - 27044_3$
6695.175	8	1	14932.007	$20867^{\frac{7}{2}}_{\frac{7}{2}} - 35799_6$
6694.492	100	2	14933.530	$15618^{\frac{3}{2}}_{\frac{3}{2}} - 30552_4$
6694.002	100	1	14934.623	$14206^{\frac{7}{2}}_{\frac{7}{2}} - 29141_5$
6693.205	75		14936.401	$12847_3 - 27784^{\frac{5}{2}}_{\frac{5}{2}}$
6690.906	50		14941.534	$22877^{\frac{9}{2}}_{\frac{9}{2}} - 37819_4$
6690.271	4		14942.952	$22098_4 - 37041^{\frac{3}{2}}_{\frac{3}{2}}$
6689.783	5		14944.042	$19503^{\frac{3}{2}}_{\frac{3}{2}} - 34447_4$
6687.521	150	3	14949.096	$15863_2 - 30812^{\frac{5}{2}}_{\frac{5}{2}}$
6686.214	10		14952.019	$18011^{\frac{9}{2}}_{\frac{9}{2}} - 32963_5$
6685.701	4		14953.166	$14465^{\frac{5}{2}}_{\frac{5}{2}} - 29418_2$
6684.687	8		14955.434	$13962_1 - 28917^{\frac{5}{2}}_{\frac{5}{2}}$
6684.049	50	2	14956.862	$14465^{\frac{5}{2}}_{\frac{5}{2}} - 29422_1$
6683.991	8h		14956.991	$17501^{\frac{9}{2}}_{\frac{9}{2}} - 32458_4$
6683.368	200	3	14958.386	$8243^{\frac{5}{2}}_{\frac{5}{2}} - 23201_3$
6682.838	5		14959.572	$5563_1 - 20522^{\frac{5}{2}}_{\frac{5}{2}}$
6681.486	15		14962.599	$18699_2 - 33662^{\frac{7}{2}}_{\frac{7}{2}}$
6680.943	2		14963.815	$22855^{\frac{5}{2}}_{\frac{5}{2}} - 37819_4$
6680.664	2		14964.440	$22338^{\frac{5}{2}}_{\frac{5}{2}} - 37303_4$
6680.087	50	1	14965.733	$15166^{\frac{3}{2}}_{\frac{3}{2}} - 30132_2$
6678.994	1		14968.182	$22338^{\frac{5}{2}}_{\frac{5}{2}} - 37307_3$
6678.707	200	8	14968.825	$7280_2 - 22248^{\frac{5}{2}}_{\frac{5}{2}}$
6677.964	15		14970.490	$14226_0 - 29197^{\frac{7}{2}}_{\frac{7}{2}}$
6675.341	4		14976.373	$21539^{\frac{1}{2}}_{\frac{1}{2}} - 36515_3$
6675.023	8		14977.086	$23015^{\frac{9}{2}}_{\frac{9}{2}} - 37992_4$
6674.698	400	8	14977.816	$2869_3 - 17847^{\frac{5}{2}}_{\frac{5}{2}}$
6674.339	5		14978.621	$20322^{\frac{9}{2}}_{\frac{9}{2}} - 35300_5$
6673.590	200	5	14980.302	$16346^{\frac{7}{2}}_{\frac{7}{2}} - 31326_4$
6673.428	5		14980.666	$5563_1 - 20543^{\frac{9}{2}}_{\frac{9}{2}}$
6672.971	2		14981.692	$21575_2 - 36556^{\frac{7}{2}}_{\frac{7}{2}}$
6672.383	1		14983.012	$21902^{\frac{3}{2}}_{\frac{3}{2}} - 36885_4$
6671.684	3		14984.582	$21668^{\frac{7}{2}}_{\frac{7}{2}} - 36653_2$
6670.741	1		14986.700	$4961_4 - 19948^{\frac{3}{2}}_{\frac{3}{2}}$
6669.531	3		14989.419	$22141^{\frac{5}{2}}_{\frac{5}{2}} - 37131_3$
6669.463	8		14989.572	$13945^{\frac{3}{2}}_{\frac{3}{2}} - 28934_3$
6668.826	100		14991.004	$10414^{\frac{3}{2}}_{\frac{3}{2}} - 25405_4$
6668.673	8		14991.348	$19713_3 - 34704^{\frac{5}{2}}_{\frac{5}{2}}$
6668.673	8		14991.348	$19713_3 - 34704^{\frac{5}{2}}_{\frac{5}{2}}$
6668.414	8		14991.930	$18614^{\frac{7}{2}}_{\frac{7}{2}} - 33606_2$
6666.987	4		14995.139	$21890^{\frac{3}{2}}_{\frac{3}{2}} - 36885_4$
6663.702	50	3	15002.531	$8111_4 - 23113^{\frac{5}{2}}_{\frac{5}{2}}$
6662.270	800	200	15005.755	$7502_3 - 22508^{\frac{5}{2}}_{\frac{5}{2}}$
6661.320	3		15007.895	$18382^{\frac{9}{2}}_{\frac{9}{2}} - 33390_1$
6659.331	3		15012.378	$19713_3 - 34725^{\frac{5}{2}}_{\frac{5}{2}}$

TABLE 4. *Classified lines of* Th I—continued

Wavelength (Å)	Intensity		Wavenumber (cm^{-1})	Classification
	Lamp	Spark		
6659.266	2		15012.524	$21077_{6}^{6} - 36089_{4}$
6659.118	10	2	15012.858	$22877_{6}^{6} - 37890_{5}$
6658.869	2		15013.419	$22508_{2}^{2} - 37521_{3}$
6658.678	400	15	15013.850	$11241_{3}^{3} - 26255_{4}$
6658.071	2		15015.219	$22877_{6}^{6} - 37892_{4}$
6657.879	3		15015.652	$20566_{4}^{4} - 35582_{5}$
6656.876	50	1	15017.914	$15490_{6}^{6} - 30508_{5}$
6656.708	4		15018.293	$22669_{3}^{3} - 37688_{3}$
6656.503	1		15018.756	$18699_{2} - 33718_{2}^{2}$
6655.773	15		15020.403	$15970_{3} - 30990_{3}^{3}$
6655.494	50	2	15021.033	$15736_{1}^{1} - 30758_{2}$
6655.071	5		15021.988	$18809_{4}^{4} - 33831_{4}$
6654.236	10		15023.872	$15493_{4} - 30517_{6}^{6}$
6654.110	5		15024.157	$15493_{4} - 30517_{4}^{4}$
6652.225	2		15028.414	$16217_{2}^{2} - 31245_{2}$
6651.371	5		15030.344	$18069_{3}^{3} - 33099_{3}$
6650.561	50	1	15032.174	$15618_{3}^{3} - 30651_{3}$
6649.487	1		15034.602	$21143_{5} - 36178_{4}^{4}$
6649.278	8	1	15035.075	$18699_{2} - 33734_{2}^{2}$
6648.347	5		15037.180	$13847_{2} - 28884_{3}^{3}$
6646.814	8		15040.648	$17398_{3} - 32439_{3}^{3}$
6646.323	20	1	15041.760	$18549_{2} - 33591_{3}^{3}$
6644.839	2		15045.119	$23655_{4}^{4} - 38700_{4}$
6644.661	200	150	15045.522	$9804_{5} - 24850_{6}^{6}$
6644.550	4	1	15045.773	$18053_{4}^{4} - 33099_{3}$
6644.029	50	2	15046.953	$17411_{5}^{5} - 32458_{4}$
6643.501	3		15048.149	$16217_{2}^{2} - 31265_{3}$
6643.120	8		15049.012	$15970_{3} - 31019_{4}^{4}$
6642.426	40b	1	15050.584	$19532_{4} - 34583_{3}^{3}$
6642.333	50b	4	15050.795	$11601_{1} - 26651_{2}^{2}$
6642.333	50b	4	15050.795	$19273_{2} - 34324_{2}^{2}$
6641.668	4		15052.302	$13088_{3} - 28140_{4}^{4}$
6641.439	4		15052.821	$13175_{4}^{4} - 28227_{4}$
6641.006	4		15053.802	$20522_{2}^{2} - 35576_{3}$
6639.726	8		15056.704	$18011_{5}^{5} - 33068_{6}$
6638.912	150	20	15058.551	$11197_{6}^{6} - 26255_{4}$
6638.774	8		15058.864	$7280_{2} - 22338_{3}^{3}$
6637.204	15	1	15062.426	$15490_{6}^{6} - 30552_{4}$
6636.143	2		15064.834	$15863_{2} - 30928_{1}^{1}$
6633.784	50	2	15070.191	$13847_{2} - 28917_{2}^{2}$
6633.581	8		15070.652	$14481_{8}^{8} - 29552_{6}$
6632.110	5		15073.995	$21594_{3} - 36668_{2}^{2}$
6631.568	40	1	15075.227	$11802_{2} - 26878_{3}^{3}$
6629.447	1		15080.050	$21738_{2}^{2} - 36818_{2}$
6626.544	2		15086.656	$17073_{1} - 32160_{2}^{2}$
6626.125	50	1	15087.610	$18574_{1} - 33662_{1}^{1}$
6623.482	2		15093.630	$21575_{2} - 36668_{2}^{2}$
6621.329	1		15098.538	$19273_{2} - 34371_{2}^{2}$
6620.408	40	1	15100.639	$12847_{3} - 27948_{4}^{4}$
6620.248	2		15101.004	$18699_{2} - 33800_{5}^{5}$
6618.398	10	1	15105.225	$17398_{3} - 32503_{2}^{2}$
6618.163	200	8	15105.761	$15970_{3} - 31075_{2}^{2}$
6618.163	200	8	15105.761	$14204_{5} - 29310_{4}^{4}$
6617.626	5		15106.987	$18614_{1}^{1} - 33721_{2}$
6617.512	75	4	15107.247	$10783_{2}^{2} - 25890_{2}$
6615.071	50	2	15112.822	$18549_{2} - 33662_{1}^{1}$
6613.376	200	8	15116.695	$7280_{2} - 22396_{1}^{1}$
6613.280	4h		15116.914	$21645_{4} - 36762_{3}^{3}$
6609.668	5		15125.175	$20922_{2}^{2} - 36047_{2}$
6609.031	5	1	15126.633	$15863_{2} - 30990_{3}^{3}$
6608.438	50	2	15127.991	$17166_{5} - 32294_{4}^{4}$
6606.790	25	2	15131.764	$21143_{5} - 36275_{6}^{6}$
6606.597	20	2	15132.206	$21165_{3}^{3} - 36297_{4}$
6604.528	1		15136.947	$22855_{3}^{3} - 37992_{4}$
6603.788	5	1	15138.643	$19713_{3} - 34851_{2}^{2}$
6603.618	75	5	15139.033	$15618_{3}^{3} - 30758_{2}$
6603.026	20	2	15140.390	$17411_{5}^{5} - 32551_{3}$
6602.771	100	8	15140.975	$19948_{4}^{4} - 35089_{3}$
6601.452	3	1	15144.000	$22163_{4}^{4} - 37307_{3}$
6600.730	50	2	15145.656	$16783_{4}^{4} - 31929_{3}$
6599.183	3		15149.207	$21668_{1}^{1} - 36818_{2}$
6599.183	3		15149.207	$22669_{3}^{3} - 37819_{4}$
6597.542	2		15152.975	$15736_{1}^{1} - 30889_{1}$
6596.750	10	1	15154.794	$21645_{4} - 36800_{4}^{4}$
6594.798	2		15159.280	$18614_{1}^{1} - 33773_{1}$
6594.442	8	1	15160.098	$18574_{1} - 33734_{2}^{2}$
6593.940	500	150	15161.252	$5563_{1} - 20724_{6}^{6}$
6593.464	100	15	15162.347	$16554_{6} - 31716_{6}^{6}$
6591.485	400	75	15166.899	$0_{2} - 15166_{3}^{3}$
6591.278	8	1	15167.375	$13175_{4}^{4} - 28342_{5}$
6591.181	100	40	15167.598	$7502_{3} - 22669_{3}^{3}$
6588.540	500r	200	15173.678	$3865_{1} - 19039_{2}^{2}$
6588.340	50	5	15174.139	$5563_{1} - 20737_{1}^{1}$
6588.247	1		15174.353	$14243_{1}^{1} - 29418_{2}$
6588.063	2		15174.777	$14247_{6}^{6} - 29422_{1}$
6586.624	4		15178.092	$14243_{1}^{1} - 29422_{1}$
6585.696	100	5	15180.231	$19227_{8}^{8} - 34407_{6}$
6584.615	100	8	15182.723	$13297_{4} - 28480_{4}^{4}$
6584.374	50	5	15183.279	$13175_{4}^{4} - 28358_{3}$
6583.906	400r	200	15184.358	$2869_{3} - 18053_{4}^{4}$
6583.501	8	2	15185.292	$18549_{2} - 33734_{2}^{2}$
6583.177	10	2	15186.039	$20054_{2} - 35240_{3}^{3}$
6582.431	1		15187.760	$21575_{2} - 36762_{3}^{3}$
6581.297	4		15190.377	$20214_{3}^{3} - 35405_{3}$
6581.135	1		15190.751	$19516_{2}^{2} - 34707_{3}$
6580.544	3		15192.116	$21645_{4} - 36837_{6}^{6}$
6580.231	75	3	15192.838	$11802_{2} - 26995_{3}^{3}$
6579.482	20	2	15194.568	$13962_{1} - 29157_{1}^{1}$
6578.980	3		15195.727	$21890_{3}^{3} - 37085_{4}$
6577.216	100	75	15199.803	$2869_{3} - 18069_{3}^{3}$
6576.123	75	8	15202.329	$14481_{8}^{8} - 29684_{5}$
6575.770	2		15203.145	$18011_{5}^{5} - 33214_{5}$
6575.148	3		15204.583	$19503_{3}^{3} - 34707_{3}$
6574.542	4		15205.985	$21594_{3} - 36800_{4}^{4}$
6572.026	10	2	15211.806	$16783_{4}^{4} - 31995_{4}$
6571.937	5		15212.012	$15863_{2} - 31075_{2}^{2}$

TABLE 4. *Classified lines of* Th I—continued

Wavelength (Å)	Intensity		Wavenumber (cm^{-1})	Classification	Wavelength (Å)	Intensity		Wavenumber (cm^{-1})	Classification
	Lamp	Spark				Lamp	Spark		
6568.423	3	1	15220.150	$21077^{6}_{6} - 36297_{4}$	6515.875	5		15342.894	$22399^{6}_{6} - 37742_{6}$
6567.213	2		15222.954	$22669^{3}_{3} - 37892_{4}$	6514.699	3		15345.663	$15618^{3}_{3} - 30964_{3}$
6565.068	50	5	15227.928	$7280_{2} - 22508^{2}_{2}$	6513.200	2		15349.195	$22338^{3}_{3} - 37688_{3}$
6564.700	2		15228.782	$21902^{3}_{4} - 37131_{3}$	6513.052	20	1	15349.544	$13847_{2} - 29197^{1}_{1}$
6564.443	100	8	15229.378	$12114^{2}_{2} - 27343_{3}$	6512.802	4		15350.133	$13847_{2} - 29197^{2}_{2}$
6562.647	4		15233.546	$19227^{6}_{6} - 34460_{5}$	6512.366	400	15	15351.161	$3687_{2} - 19039^{2}_{2}$
6562.105	50		15234.804	$13962_{1} - 29197^{1}_{1}$	6511.583	4		15353.007	$7502_{3} - 22855^{3}_{3}$
6561.854	3		15235.387	$13962_{1} - 29197^{2}_{2}$	6511.050	3		15354.263	$19532_{4} - 34886^{6}_{6}$
6560.849	5		15237.720	$7795^{3}_{4} - 23032_{4}$	6510.269	5		15356.105	$17398_{3} - 32754^{3}_{3}$
6559.876	5	1	15239.981	$18069^{3}_{3} - 33309_{2}$	6509.975	1		15356.799	$21738^{2}_{2} - 37094_{2}$
6559.462	1		15240.942	$21890^{3}_{3} - 37131_{3}$	6509.857	3		15357.077	$19516^{2}_{2} - 34874_{3}$
6559.217	50	8	15241.512	$22163^{3}_{4} - 37404_{3}$	6509.653	2		15357.559	$18809^{3}_{4} - 34167_{3}$
6559.120	5h		15241.737	$21539^{3}_{4} - 36781_{5}$	6509.311	3		15358.365	$22163^{3}_{4} - 37521_{3}$
6558.871	100	8	15242.316	$3687_{2} - 18930^{3}_{3}$	6509.053	150	8	15358.974	$5563_{1} - 20922^{2}_{2}$
6554.563	1		15252.334	$17847^{2}_{2} - 33099_{3}$	6508.362	50	1	15360.605	$4961_{4} - 20322^{6}_{6}$
6554.160	150	40	15253.272	$4961_{4} - 20214^{3}_{3}$	6508.292	2		15360.770	$16351_{0} - 31712^{1}_{1}$
6551.917	4		15258.493	$11802_{2} - 27061^{2}_{2}$	6507.948	4	1	15361.582	$20214^{3}_{3} - 35576_{3}$
6551.703	100	5	15258.992	$13088_{3} - 28347^{2}_{2}$	6507.409	1		15362.854	$21645_{4} - 37008^{6}_{6}$
6551.265	4		15260.012	$20322^{6}_{6} - 35582_{5}$	6506.989	100	15	15363.846	$10526^{3}_{3} - 25890_{2}$
6550.335	5		15262.178	$21575_{2} - 36837^{1}_{1}$	6505.221	1		15368.022	$18431_{3} - 33799^{3}_{4}$
6549.820	4		15263.378	$21252^{2}_{2} - 36515_{3}$	6504.835	2		15368.933	$18431_{3} - 33800^{3}_{3}$
6547.720	2		15268.274	$18699_{2} - 33967^{3}_{3}$	6504.458	5		15369.824	$14465^{2}_{2} - 29835_{3}$
6547.618	1		15268.512	$15493_{4} - 30761^{1}_{1}$	6504.226	15	2	15370.372	$17411^{3}_{3} - 32781_{4}$
6547.531	3		15268.714	$21539^{3}_{4} - 36808_{3}$	6501.992	100	5	15375.653	$6362_{2} - 21738^{2}_{2}$
6545.880	2		15272.566	$22248^{2}_{2} - 37521_{3}$	6500.659	75	3	15378.806	$13297_{4} - 28676^{3}_{3}$
6545.719	100	8	15272.941	$17166_{5} - 32439^{3}_{4}$	6498.769	8	1	15383.279	$13297_{4} - 28680^{3}_{4}$
6545.345	1		15273.814	$20054_{2} - 35328^{1}_{1}$	6497.788	2		15385.601	$15166^{3}_{3} - 30552_{4}$
6543.893	1		15277.203	$21594_{3} - 36871^{2}_{2}$	6497.490	50	3	15386.307	$14032^{2}_{2} - 29418_{2}$
6542.511	50	3	15280.430	$17501^{6}_{6} - 32781_{4}$	6496.965	8	1	15387.550	$13175^{3}_{4} - 28562_{4}$
6542.049	50	3	15281.509	$11601_{1} - 26882^{6}_{6}$	6496.028	10	1	15389.770	$7280_{2} - 22669^{3}_{3}$
6540.542	15	1	15285.030	$11802_{2} - 27087^{1}_{1}$	6495.930	5		15390.002	$14032^{2}_{2} - 29422_{1}$
6538.301	50	4	15290.269	$13962_{1} - 29252^{2}_{2}$	6495.595	3		15390.796	$18382^{6}_{6} - 33773_{1}$
6537.615	75	5	15291.873	$13297_{4} - 28589^{3}_{3}$	6495.255	20	2	15391.601	$13088_{3} - 28480^{3}_{4}$
6537.178	50	2	15292.896	$12847_{3} - 28140^{3}_{4}$	6495.004	1		15392.196	$19039^{2}_{2} - 34431_{3}$
6536.295	2		15294.961	$15493_{4} - 30788^{6}_{6}$	6493.702	4		15395.282	$21645_{4} - 37041^{3}_{3}$
6535.486	4		15296.855	$21575_{2} - 36871^{2}_{2}$	6493.198	150	8	15396.477	$10526^{3}_{3} - 25923_{4}$
6531.342	800r	200	15306.560	$6362_{2} - 21668^{1}_{1}$	6491.222	2		15401.164	$21902^{3}_{4} - 37303_{4}$
6530.500	4	1	15308.534	$20522^{2}_{2} - 35831_{3}$	6490.736	500	50	15402.317	$8800_{4} - 24202^{3}_{4}$
6530.500	4	1	15308.534	$22877^{6}_{6} - 38186_{4}$	6489.598	10	1	15405.018	$13847_{2} - 29252^{2}_{2}$
6530.157	20	2	15309.338	$13847_{2} - 29157^{1}_{1}$	6489.362	2		15405.578	$18053^{3}_{4} - 33459_{4}$
6530.125	25	3	15309.413	$21902^{3}_{4} - 37211_{5}$	6488.882	50	4	15406.718	$7795^{3}_{4} - 23201_{3}$
6529.994	25	2	15309.720	$19273_{2} - 34583^{3}_{3}$	6488.882	50	4	15406.716	$18011^{6}_{6} - 33418_{4}$
6529.877	3h		15309.994	$20737^{1}_{1} - 36047_{2}$	6488.785	2		15406.948	$14243^{1}_{1} - 29650_{2}$
6529.597	20	2	15310.651	$17959_{4} - 33270^{3}_{4}$	6487.920	3		15409.002	$22338^{3}_{3} - 37748_{2}$
6529.193	1		15311.598	$20322^{6}_{6} - 35633_{4}$	6487.479	50	4	15410.050	$8111_{4} - 23521^{3}_{3}$
6528.592	4		15313.008	$15970_{3} - 31283^{3}_{3}$	6486.848	4		15411.549	$18699_{2} - 34111^{1}_{1}$
6527.858	1		15314.730	$19986^{6}_{6} - 35300_{5}$	6484.067	15	3	15418.159	$16783^{3}_{4} - 32202_{5}$
6526.584	20	2	15317.719	$19273_{2} - 34591^{1}_{1}$	6484.067	15	3	15418.159	$19713_{3} - 35131^{3}_{4}$
6525.714	2		15319.761	$16217^{2}_{2} - 31537_{3}$	6483.931	2		15418.482	$18549_{2} - 33967^{3}_{3}$
6525.490	3		15320.287	$21165^{3}_{3} - 36485_{2}$	6483.741	3	1	15418.934	$20214^{3}_{3} - 35633_{4}$
6522.499	20	5	15327.312	$17224^{2}_{2} - 32551_{3}$	6483.618	20	1	15419.226	$15863_{2} - 31283^{3}_{3}$
6522.044	100	15	15328.381	$10783^{2}_{2} - 26111_{1}$	6481.299	50	5	15424.743	$13088_{3} - 28513^{2}_{2}$
6520.998	4		15330.840	$22855^{3}_{3} - 38186_{4}$	6480.444	5	1	15426.778	$17847^{2}_{2} - 33273_{1}$
6519.224	1		15335.012	$17959_{4} - 33294^{3}_{3}$	6479.952	4		15427.950	$16346^{2}_{4} - 31774_{3}$
6517.277	3		15339.593	$18069^{3}_{3} - 33408_{3}$	6478.616	8	1	15431.131	$19273_{2} - 34704^{3}_{3}$

TABLE 4. *Classified lines of* Th I—continued

Wavelength (Å)	Intensity		Wavenumber (cm^{-1})	Classification	Wavelength (Å)	Intensity		Wavenumber (cm^{-1})	Classification
	Lamp	Spark				Lamp	Spark		
6474.742	50	5	15440.364	$15490_8^8 - 30930_6$	6430.684	2		15546.148	$14465_2^2 - 30011_3$
6472.193	1		15446.445	$21594_3 - 37041_4^4$	6430.499	5	1	15546.596	$22141_3^3 - 37688_3$
6471.936	10	1	15447.058	$16346_4^2 - 31793_4$	6429.673	2		15548.593	$19532_4 - 35081_6^6$
6467.807	3		15456.919	$19948_4^4 - 35405_3$	6428.773	40	2	15550.770	$9804_5 - 25355_4^4$
6467.671	50	4	15457.244	$11802_2 - 27260_5^5$	6427.507	50	4	15553.832	$15970_3 - 31523_3^3$
6467.145	8	1	15458.502	$18069_5^5 - 33527_4$	6427.507	50	4	15553.832	$22338_5^5 - 37892_4$
6466.712	75	4	15459.537	$8800_4 - 24259_4^4$	6427.264	3		15554.421	$21594_3 - 37149_2^2$
6466.352	50	100	15460.397	$11601_1 - 27061_2^2$	6426.723	1		15555.730	$21252_2^2 - 36808_3$
6465.692	5	1	15461.976	$17847_2^2 - 33309_2$	6426.534	2		15556.187	$17398_3 - 32954_2^2$
6465.585	10	2	15462.231	$17501_6^6 - 32963_5$	6426.151	5		15557.115	$16217_2^2 - 31774_3$
6462.606	200b	100	15469.359	$16554_6 - 32023_6^6$	6422.948	4		15564.873	$21594_3 - 37159_3^3$
6461.454	2		15472.117	$20322_8^8 - 35794_4$	6422.683	2		15565.515	$21252_2^2 - 36818_2$
6460.689	2		15473.949	$18053_3^3 - 33527_4$	6422.106	100	8	15566.913	$17501_6^6 - 33068_6$
6460.470	50	3	15474.473	$8800_4 - 24274_6^6$	6421.194	2		15569.124	$21738_2^2 - 37307_3$
6459.295	5	1	15477.288	$14206_3^3 - 29684_5$	6420.980	3		15569.643	$18431_3 - 34001_4^4$
6459.116	5	1	15477.717	$20322_8^8 - 35799_6$	6420.225	2		15571.474	$13847_2 - 29419_2^2$
6458.118	2		15480.109	$22338_3^3 - 37819_4$	6420.080	3		15571.826	$17224_2^2 - 32796_3$
6457.280	800r	300	15482.118	$7795_4^4 - 23277_5$	6419.849	5	1	15572.386	$19516_2^2 - 35089_3$
6455.987	1		15485.219	$21645_3^3 - 37131_3$	6419.160	2		15574.057	$21575_2 - 37149_2^2$
6455.265	50	4	15486.951	$11601_1 - 27087_1^1$	6418.697	4		15575.181	$7280_2 - 22855_3^3$
6454.629	4		15488.477	$21165_3^3 - 36653_2$	6417.908	15	2	15577.096	$17073_1 - 32650_1^1$
6453.551	3		15491.064	$22399_8^8 - 37890_5$	6416.930	3		15579.470	$20214_3^3 - 35794_4$
6453.344	5	1	15491.561	$18809_4^4 - 34301_4$	6415.536	50	5	15582.855	$16346_4^4 - 31929_3$
6452.951	40	2	15492.504	$19948_4^4 - 35440_3$	6414.703	15	2	15584.878	$13088_3 - 28673_2^2$
6452.057	25	2	15494.651	$11802_2 - 27297_1^1$	6414.148	75	10	15586.227	$19503_3^3 - 35089_3$
6451.582	2		15495.792	$18069_5^5 - 33564_3$	6413.615	400	100	15587.522	$13297_4 - 28884_3^3$
6451.258	4		15496.570	$14465_2^2 - 29961_1$	6412.977	1		15589.073	$22508_2^2 - 38097_2$
6450.956	150	8	15497.295	$15493_4 - 30990_3^3$	6412.129	2		15591.134	$15166_3^3 - 30758_2$
6450.697	5		15497.917	$12114_2^2 - 27612_3$	6411.899	500	75	15591.694	$7502_3 - 23093_2^2$
6450.593	5		15498.167	$8111_4 - 23609_8^8$	6411.412	2		15592.878	$22399_8^8 - 37992_4$
6450.007	200	15	15499.575	$12847_3 - 28347_2^2$	6410.091	1		15596.091	$19986_8^8 - 35582_5$
6449.518	5		15500.751	$13088_3 - 28589_3^3$	6410.069	2		15596.145	$19986_8^8 - 35582_5$
6449.164	2		15501.601	$17073_1 - 32575_2^2$	6409.553	3		15597.401	$7280_2 - 22877_1^1$
6448.850	3		15502.356	$21902_4^4 - 37404_3$	6408.425	2		15600.146	$17959_4 - 33560_3^3$
6446.771	100	8	15507.355	$14204_5 - 29711_6^6$	6406.446	100	5	15604.965	$4961_4 - 20566_4^4$
6446.133	25	1	15508.890	$10414_3^3 - 25923_4$	6403.860	4		15611.266	$7502_3 - 23113_4^4$
6445.639	75	2	15510.079	$16783_4^4 - 32293_5$	6400.696	100	8	15618.983	$0_2 - 15618_3^3$
6444.150	1		15513.663	$21645_4 - 37159_3^3$	6399.944	40		15620.819	$8800_4 - 24421_3^3$
6444.150	1		15513.663	$21645_4 - 37159_3^3$	6399.571	20		15621.729	$19227_8^8 - 34849_5$
6443.878	10	1	15514.318	$18930_3^3 - 34444_2$	6398.602	1		15624.095	$20054_2 - 35678_1^1$
6443.819	25	1	15514.460	$11802_2 - 27317_3^3$	6398.451	15	2	15624.463	$18699_2 - 34324_2^2$
6443.090	4		15516.215	$18011_6^6 - 33527_4$	6397.447	20	2	15626.915	$15618_3^3 - 31245_2$
6443.090	4		15516.215	$22669_3^3 - 38186_4$	6396.951	200	8	15628.127	$14206_4^4 - 29835_3$
6440.353	5	1	15522.809	$15618_3^3 - 31141_3$	6396.518	3	1	15629.185	$15970_3 - 31599_2^2$
6440.245	1		15523.069	$20566_4^4 - 36089_4$	6395.617	3	1	15631.387	$21890_3^3 - 37521_3$
6439.418	4		15525.063	$22163_4^4 - 37688_3$	6395.279	3		15632.213	$12847_3 - 28480_4^4$
6438.918	50	8	15526.268	$8243_2^2 - 23769_1$	6395.057	75	4	15632.756	$19516_2^2 - 35149_2$
6438.303	20	2	15527.751	$6362_2 - 21890_3^3$	6394.589	3	1	15633.900	$19948_4^4 - 35582_5$
6437.769	200	20	15529.039	$14204_5 - 29733_6^6$	6394.045	200	8	15635.230	$13297_4 - 28932_4^4$
6437.769	200	20	15529.039	$19516_2^2 - 35046_1$	6393.201	5	1	15637.294	$18809_4^4 - 34447_4$
6435.108	1		15535.461	$22248_2^2 - 37784_2$	6392.371	75	8	15639.324	$21594_3 - 37234_2^2$
6434.800	2		15536.204	$18431_3 - 33967_3^3$	6391.173	50	2	15642.256	$14206_4^4 - 29849_4$
6434.654	3		15536.557	$18574_1 - 34111_1^1$	6390.388	5	1	15644.177	$20566_4^4 - 36210_5$
6431.715	5		15543.656	$17847_2^2 - 33390_1$	6390.126	75	4	15644.819	$11802_2 - 27447_2^2$
6431.518	2		15544.132	$8111_4 - 23655_4^4$	6389.391	200b	15	15646.618	$15618_3^3 - 31265_3$

TABLE 4. *Classified lines of* Th I—continued

Wavelength (Å)	Intensity		Wavenumber (cm^{-1})	Classification	Wavelength (Å)	Intensity		Wavenumber (cm^{-1})	Classification
	Lamp	Spark				Lamp	Spark		
6389.391	200b	15	15646.618	$19503\frac{3}{3} - 35149_2$	6342.292	4	1	15762.812	$18069\frac{3}{3} - 33831_4$
6388.813	100	8	15648.034	$15493_4 - 31141\frac{0}{0}$	6341.873	5h	1	15763.854	$21539\frac{2}{4} - 37303_4$
6388.416	100	5	15649.006	$16346\frac{4}{4} - 31995_4$	6340.383	5	1	15767.558	$21539\frac{2}{4} - 37307_3$
6387.595	2		15651.018	$18809\frac{2}{4} - 34460_5$	6339.663	100	15	15769.349	$7280_2 - 23049\frac{0}{1}$
6387.393	200	10	15651.513	$3865_1 - 19516\frac{2}{2}$	6339.297	10	1	15770.259	$9804_5 - 25575\frac{2}{4}$
6387.096	8	1	15652.240	$18069\frac{3}{3} - 33721_2$	6337.620	100	4	15774.432	$11197\frac{0}{0} - 26971_4$
6386.780	4	1	15653.015	$21165\frac{3}{3} - 36818_2$	6337.528	2		15774.661	$18549_2 - 34324\frac{2}{2}$
6385.059	20	3	15657.234	$21143_5 - 36800\frac{4}{4}$	6336.416	10	2	15777.429	$18930\frac{3}{3} - 34707_3$
6383.911	2		15660.049	$15863_2 - 31523\frac{3}{3}$	6336.081	10	2	15778.264	$18053\frac{3}{4} - 33831_4$
6381.759	25	2	15665.330	$12847_3 - 28513\frac{2}{2}$	6335.701	10	1	15779.210	$6362_2 - 22141\frac{3}{3}$
6381.361	50	5	15666.307	$16346\frac{4}{4} - 32012_4$	6335.012	8	2	15780.926	$15490\frac{6}{6} - 31271_5$
6380.445	3		15668.556	$19039\frac{2}{2} - 34707_3$	6333.017	1		15785.897	$21902\frac{4}{4} - 37688_3$
6379.673	50	8	15670.452	$13175\frac{5}{4} - 28845_4$	6332.684	8	1	15786.727	$22399\frac{6}{6} - 38186_4$
6379.105	3		15671.848	$21077\frac{6}{6} - 36749_6$	6331.415	200	15	15789.891	$15493_4 - 31283\frac{3}{3}$
6379.005	4		15672.093	$21539\frac{4}{4} - 37211_5$	6330.374	10	2	15792.488	$13847_2 - 29640\frac{1}{1}$
6378.958	1		15672.209	$18699_2 - 34371\frac{2}{2}$	6328.807	50	2	15796.398	$13088_3 - 28884\frac{3}{3}$
6378.092	1		15674.337	$16783\frac{4}{4} - 32458_4$	6328.263	2		15797.756	$15166\frac{3}{3} - 30964_3$
6376.930	500	200	15677.193	$14204_5 - 29881\frac{4}{4}$	6328.115	1		15798.126	$21890\frac{3}{3} - 37688_3$
6376.712	50	5	15677.729	$13962_1 - 29640\frac{1}{1}$	6327.279	500	100	15800.213	$11197\frac{0}{0} - 26997_6$
6374.269	5	1	15683.737	$18614\frac{1}{1} - 34298_1$	6326.365	200	20	15802.496	$11241\frac{3}{3} - 27044_3$
6372.460	50	2	15688.190	$17411\frac{3}{3} - 33099_3$	6326.178	8	2	15802.963	$14032\frac{2}{2} - 29835_3$
6372.125	50	8	15689.014	$11877\frac{1}{1} - 27566_2$	6325.590	8l	1	15804.432	$14206\frac{4}{4} - 30011_3$
6371.944	150	15	15689.460	$5563_1 - 21252\frac{2}{2}$	6325.003	5		15805.898	$8111_4 - 23916\frac{6}{4}$
6370.796	25	2	15692.287	$15736\frac{1}{1} - 31429_1$	6324.662	2		15806.751	$22338\frac{3}{3} - 38145_3$
6369.876	2		15694.554	$21143_5 - 36837\frac{6}{6}$	6324.395	40	2	15807.418	$14206\frac{4}{4} - 30014_4$
6369.141	200	25	15696.365	$17166_5 - 32862\frac{4}{4}$	6324.104	3		15808.145	$21077\frac{6}{6} - 36885_4$
6369.071	50b	2	15696.537	$11601_1 - 27297\frac{1}{1}$	6323.055	2		15810.768	$15970_3 - 31780\frac{3}{3}$
6367.242	15		15701.046	$15970_3 - 31671\frac{4}{4}$	6322.866	20	2	15811.240	$20322\frac{6}{6} - 36133_5$
6367.066	3		15701.480	$15493_4 - 31194\frac{2}{2}$	6321.965	2		15813.494	$20522\frac{2}{2} - 36336_3$
6365.984	2		15704.149	$21077\frac{6}{6} - 36781_5$	6321.820	75	5	15813.856	$7280_2 - 23093\frac{2}{2}$
6364.651	20	3	15707.438	$22399\frac{6}{6} - 38106_5$	6321.298	50	2	15815.162	$3687_2 - 19503\frac{3}{3}$
6364.431	10	2	15707.981	$15618\frac{3}{3} - 31326_4$	6319.753	2		15819.029	$19532_4 - 35351\frac{4}{4}$
6364.265	5	1	15708.390	$19532_4 - 35240\frac{3}{3}$	6319.261	20	3	15820.260	$19713_3 - 35533\frac{2}{2}$
6362.797	2		15712.015	$16217\frac{2}{2} - 31929_3$	6319.163	40	5	15820.506	$18011\frac{6}{6} - 33831_4$
6362.583	2		15712.543	$19588\frac{6}{6} - 35300_5$	6318.693	8	1	15821.682	$14465\frac{2}{2} - 30286_1$
6362.256	100	20	15713.351	$17501\frac{6}{6} - 33214_5$	6318.399	1		15822.419	$18549_2 - 34371\frac{2}{2}$
6361.796	3		15714.487	$14247\frac{6}{6} - 29961_1$	6318.299	8	1	15822.669	$22877\frac{6}{6} - 38700_4$
6360.981	2		15716.500	$19273_2 - 34989\frac{1}{1}$	6317.183	150	8	15825.464	$12847_3 - 28673\frac{2}{2}$
6360.466	5		15717.773	$17847\frac{2}{2} - 33564_3$	6316.061	5	1	15828.276	$12847_3 - 28676\frac{3}{3}$
6359.488	5		15720.190	$21165\frac{3}{3} - 36885_4$	6315.774	100	8	15828.995	$3687_2 - 19516\frac{2}{2}$
6357.363	2		15725.445	$22877\frac{1}{1} - 38602_2$	6315.271	2		15830.256	$18614\frac{1}{1} - 34444_2$
6356.603	2		15727.325	$22163\frac{4}{4} - 37890_5$	6314.440	2		15832.339	$20214\frac{5}{5} - 36047_2$
6356.139	2		15728.473	$16351_0 - 32080\frac{1}{1}$	6314.269	8	2	15832.768	$12847_3 - 28680\frac{4}{4}$
6355.911	800	200	15729.037	$10526\frac{3}{3} - 26255_4$	6312.622	50	4	15836.898	$15490\frac{6}{6} - 31326_4$
6355.633	75	8	15729.725	$11241\frac{3}{3} - 26971_4$	6311.945	8	2	15838.597	$13847_2 - 29686\frac{3}{3}$
6355.283	10	1	15730.591	$18699_2 - 34430\frac{3}{3}$	6311.453	10	1	15839.832	$17959_4 - 33799\frac{4}{4}$
6352.709	4		15736.965	$0_2 - 15736\frac{1}{1}$	6311.097	5	1	15840.725	$17959_4 - 33800\frac{3}{3}$
6350.893	8	1	15741.465	$19532_4 - 35273\frac{6}{6}$	6310.808	150	8	15841.451	$10414\frac{3}{4} - 26255_4$
6348.737	200	15	15746.810	$8243\frac{2}{2} - 23990_2$	6309.756	4		15844.092	$13088_3 - 28932\frac{2}{4}$
6348.213	2		15748.110	$20737\frac{1}{1} - 36485_2$	6308.710	20	2	15846.719	$11601_1 - 27447\frac{2}{2}$
6346.963	1		15751.212	$22141\frac{3}{3} - 37892_4$	6307.868	25	3	15848.834	$15863_2 - 31712\frac{1}{1}$
6346.119	100	8	15753.306	$13297_4 - 29050\frac{6}{6}$	6305.276	50	4	15855.349	$16346\frac{4}{4} - 32202_5$
6344.331	4		15757.746	$20054_2 - 35812\frac{3}{3}$	6303.251	200	20	15860.443	$13297_4 - 29157\frac{3}{3}$
6343.728	1		15759.244	$17847\frac{3}{3} - 33606_2$	6301.421	200	20	15865.049	$23655\frac{4}{4} - 39520_4$
6342.860	500	150	15761.401	$8800_4 - 24561\frac{3}{3}$	6300.917	150	10	15866.318	$12114\frac{2}{2} - 27980_3$

TABLE 4. *Classified lines of* Th I—continued

Wavelength (Å)	Intensity		Wavenumber (cm^{-1})	Classification	Wavelength (Å)	Intensity		Wavenumber (cm^{-1})	Classification
	Lamp	Spark				Lamp	Spark		
6298.903	50	5	15871.391	$11802_2 - 27674^{\frac{5}{2}}$	6261.418	400	150	15966.407	$10414^{\frac{3}{4}} - 26380_5$
6297.777	10	1	15874.229	$17847^{\frac{7}{2}} - 33721_2$	6260.218	8	1	15969.467	$8800_4 - 24769^{\frac{3}{2}}$
6297.581	1		15874.723	$20214^{\frac{3}{2}} - 36089_4$	6258.097	2		15974.880	$15166^{\frac{3}{2}} - 31141_3$
6297.426	3		15875.113	$17224^{\frac{5}{2}} - 33099_3$	6257.424	200	8	15976.598	$6362_2 - 22338^{\frac{5}{2}}$
6296.426	1		15877.634	$22401_1 - 38278^{\frac{9}{2}}$	6255.531	5	1	15981.432	$11802_2 - 27784^{\frac{5}{2}}$
6295.170	10	1	15880.802	$17073_1 - 32954^{\frac{5}{2}}$	6255.344	4	1	15981.910	$21539^{\frac{9}{4}} - 37521_3$
6295.170	10	1	15880.802	$18549_2 - 34430^{\frac{5}{2}}$	6254.774	20	2	15983.367	$15970_3 - 31953^{\frac{3}{4}}$
6294.340	2		15882.896	$19948^{\frac{3}{4}} - 35831_3$	6252.887	4	1	15988.190	$21902^{\frac{9}{4}} - 37890_5$
6294.283	2		15883.040	$22877^{\frac{9}{2}} - 38760_4$	6252.314	8	1	15989.655	$19227^{\frac{9}{2}} - 35216_5$
6293.480	5		15885.067	$17959_4 - 33844^{\frac{9}{2}}$	6251.964	8	2	15990.550	$21902^{\frac{9}{4}} - 37892_4$
6293.241	150	15	15885.670	$9804_5 - 25690^{\frac{9}{2}}$	6250.484	50	4	15994.337	$11197^{\frac{9}{2}} - 27191_5$
6293.036	3		15886.188	$20922^{\frac{5}{2}} - 36808_3$	6249.270	3		15997.444	$17411^{\frac{3}{2}} - 33408_3$
6292.891	100	8	15886.554	$6362_2 - 22248^{\frac{5}{2}}$	6249.146	5	1	15997.761	$16783^{\frac{9}{4}} - 32781_4$
6292.187	4		15888.331	$19516^{\frac{5}{2}} - 35405_3$	6247.222	3		16002.688	$21890^{\frac{5}{2}} - 37892_4$
6292.061	50	3	15888.649	$14243^{\frac{7}{2}} - 30132_2$	6246.664	1		16004.117	$22141^{\frac{3}{2}} - 38145_3$
6291.629	50	15	15889.740	$13945^{\frac{3}{2}} - 29835_3$	6246.400	4		16004.794	$18699_2 - 34704^{\frac{3}{2}}$
6291.192	150	15	15890.844	$14481^{\frac{5}{2}} - 30372_6$	6246.173	75	8	16005.376	$13847_2 - 29853^{\frac{5}{2}}$
6290.576	2		15892.400	$18431_3 - 34324^{\frac{5}{2}}$	6245.848	5	1	16006.208	$15863_2 - 31870^{\frac{9}{2}}$
6289.159	2		15895.981	$20922^{\frac{5}{2}} - 36818_2$	6245.601	50	15	16006.841	$19039^{\frac{5}{2}} - 35046_1$
6288.852	3	1	15896.757	$13847_2 - 29744^{\frac{3}{2}}$	6245.149	3		16008.000	$17959_4 - 33967^{\frac{3}{2}}$
6288.424	8	1	15897.839	$17411^{\frac{3}{2}} - 33309_2$	6244.875	2		16008.702	$21077^{\frac{9}{2}} - 37085_4$
6288.074	2		15898.724	$17398_3 - 33297^{\frac{5}{2}}$	6244.381	8h	2	16009.969	$21738^{\frac{5}{2}} - 37748_2$
6287.570	50	3	15899.998	$15970_3 - 31870^{\frac{9}{2}}$	6243.953	2		16011.066	$21594_3 - 37605^{\frac{3}{2}}$
6287.254	75	4	15900.797	$8800_4 - 24701^{\frac{9}{2}}$	6243.358	50	4	16012.592	$13297_4 - 29310^{\frac{3}{4}}$
6286.712	3		15902.168	$19503^{\frac{3}{2}} - 35405_3$	6241.873	10	3	16016.402	$18574_1 - 34591^{\frac{7}{2}}$
6286.043	50	4	15903.860	$13945^{\frac{3}{2}} - 29849_4$	6240.949	150	8	16018.773	$7502_3 - 23521^{\frac{3}{2}}$
6285.453	1		15905.353	$22855^{\frac{5}{2}} - 38760_4$	6240.305	15	2	16020.426	$19713_3 - 35733^{\frac{3}{4}}$
6282.449	2		15912.958	$18431_3 - 34344^{\frac{3}{4}}$	6239.742	2		16021.871	$22508^{\frac{5}{2}} - 38529_3$
6281.543	5		15915.253	$18382^{\frac{9}{2}} - 34298_1$	6239.306	5	1	16022.991	$22163^{\frac{3}{4}} - 38186_4$
6280.875	2b		15916.946	$17501^{\frac{9}{2}} - 33418_4$	6238.208	5		16025.811	$18699_2 - 34725^{\frac{3}{2}}$
6280.359	2		15918.254	$15618^{\frac{3}{2}} - 31537_3$	6238.080	20	2	16026.140	$14481^{\frac{5}{2}} - 30508_5$
6279.982	75	4	15919.209	$17354^{\frac{7}{2}} - 33273_1$	6237.982	5	1	16026.392	$17501^{\frac{9}{2}} - 33527_4$
6279.369	2		15920.763	$21165^{\frac{3}{2}} - 37085_4$	6237.101	5	1	16028.655	$17398_3 - 33427^{\frac{5}{2}}$
6278.125	4		15923.918	$19516^{\frac{5}{2}} - 35440_3$	6235.176	1		16033.604	$18549_2 - 34583^{\frac{3}{2}}$
6277.512	2		15925.473	$21645_4 - 37571^{\frac{9}{2}}$	6234.856	400	75	16034.427	$6362_2 - 22396^{\frac{7}{2}}$
6276.162	100	8	15928.899	$13175^{\frac{3}{4}} - 29104_4$	6234.200	150	10	16036.114	$17354^{\frac{7}{2}} - 33390_1$
6275.849	3		15929.693	$14032^{\frac{5}{2}} - 29961_1$	6233.858	3		16036.994	$12847_3 - 28884^{\frac{3}{2}}$
6275.679	2		15930.125	$22877^{\frac{7}{2}} - 38807_2$	6233.004	8		16039.191	$23655^{\frac{3}{4}} - 39694_5$
6274.523	2		15933.059	$22669^{\frac{5}{2}} - 38602_2$	6232.845	2		16039.600	$14247^{\frac{9}{2}} - 30286_1$
6272.676	3		15937.751	$19503^{\frac{3}{2}} - 35440_3$	6232.186	8	1	16041.296	$21575_2 - 37616^{\frac{7}{2}}$
6271.733	1		15940.147	$18431_3 - 34371^{\frac{5}{2}}$	6232.129	25	1	16041.443	$17959_4 - 34001^{\frac{3}{4}}$
6271.544	75	5	15940.628	$2869_3 - 18809^{\frac{3}{4}}$	6232.068	50	4	16041.600	$18549_2 - 34591^{\frac{7}{2}}$
6271.131	2		15941.678	$23015^{\frac{9}{2}} - 38956_4$	6230.933	3		16044.522	$22141^{\frac{3}{2}} - 38186_4$
6270.331	8	2	15943.711	$22163^{\frac{3}{4}} - 38106_5$	6230.548	1		16045.514	$19588^{\frac{9}{2}} - 35633_4$
6268.923	2		15947.292	$16346^{\frac{3}{4}} - 32293_5$	6230.221	1		16046.356	$21738^{\frac{5}{2}} - 37784_2$
6268.200	20	2	15949.132	$9804_5 - 25753^{\frac{9}{2}}$	6227.179	8		16054.194	$14226_0 - 30281^{\frac{7}{2}}$
6267.800	2		15950.150	$21738^{\frac{5}{2}} - 37688_3$	6226.370	100	8	16056.280	$2558_0 - 18614^{\frac{7}{2}}$
6267.188	2		15951.707	$3865_1 - 19817^{\frac{7}{2}}$	6225.105	5	1	16059.543	$19516^{\frac{5}{2}} - 35576_3$
6266.614	75	5	15953.168	$16783^{\frac{3}{4}} - 32737_5$	6224.678	8	1	16060.645	$19817^{\frac{7}{2}} - 35877_2$
6265.962	3		15954.828	$22098_4 - 38053^{\frac{3}{2}}$	6224.527	400	40	16061.034	$2869_3 - 18930^{\frac{3}{2}}$
6265.604	75	10	15955.740	$14204_5 - 30160^{\frac{9}{4}}$	6224.043	5		16062.283	$21594_3 - 37656^{\frac{3}{2}}$
6264.715	100	8	15958.004	$17501^{\frac{9}{2}} - 33459_4$	6223.308	5		16064.180	$18809^{\frac{3}{4}} - 34874_3$
6262.884	3		15962.669	$20522^{\frac{5}{2}} - 36485_2$	6222.769	4h	1	16065.572	$16346^{\frac{3}{4}} - 32412_4$
6261.584	2h		15965.983	$21165^{\frac{3}{2}} - 37131_3$	6222.588	3		16066.039	$13945^{\frac{3}{2}} - 30011_3$
6261.418	400	150	15966.407	$13175^{\frac{3}{4}} - 29141_5$	6221.426	5		16069.040	$13945^{\frac{3}{2}} - 30014_4$

TABLE 4. *Classified lines of* Th I – continued

Wavelength (Å)	Intensity		Wavenumber (cm^{-1})	Classification	Wavelength (Å)	Intensity		Wavenumber (cm^{-1})	Classification
	Lamp	Spark				Lamp	Spark		
6221.320	100	15	16069.313	$13088_3 - 29157^{8}_{3}$	6180.285	1		16176.007	$18549_2 - 34725^{3}_{3}$
6221.059	75	3	16069.988	$12847_3 - 28917^{2}_{2}$	6179.548	4		16177.937	$15493_4 - 31671^{4}_{4}$
6220.011	100	5	16072.695	$9804_5 - 25877^{4}_{4}$	6178.930	15	2	16179.555	$16783^{2}_{4} - 32963_5$
6219.775	50	3	16073.305	$11601_1 - 27674^{2}_{2}$	6178.432	200	20	16180.859	$8800_4 - 24981^{3}_{3}$
6219.672	1		16073.571	$19227^{8}_{8} - 35300_5$	6177.489	1		16183.329	$11601_1 - 27784^{2}_{2}$
6218.862	2		16075.665	$22877^{1}_{1} - 38953_5$	6177.081	1		16184.398	$17224^{2}_{2} - 33408_3$
6217.572	10	1	16079.000	$15166^{3}_{3} - 31245_2$	6176.490	4		16185.946	$14465^{2}_{2} - 30651_3$
6217.437	1		16079.349	$14465^{2}_{2} - 30544_2$	6175.956	10	1	16187.346	$13945^{3}_{3} - 30132_2$
6217.437	1		16079.349	$22877^{1}_{1} - 38956_4$	6174.797	4		16190.384	$15970_3 - 32160^{2}_{2}$
6216.865	15	2	16080.829	$20737^{1}_{1} - 36818_2$	6173.881	4		16192.786	$17398_3 - 33591^{3}_{3}$
6216.441	4	1	16081.925	$21575_2 - 37656^{8}_{8}$	6173.004	2		16195.087	$17411^{3}_{3} - 33606_2$
6216.270	3		16082.368	$20214^{3}_{3} - 36297_4$	6170.733	15	2	16201.047	$19532_4 - 35733^{4}_{4}$
6215.360	1		16084.722	$17224^{2}_{2} - 33309_2$	6170.652	15	2	16201.260	$7280_2 - 23481^{1}_{1}$
6214.106	5	1	16087.968	$17073_1 - 33161^{1}_{1}$	6169.822	500	200	16203.439	$4961_4 - 21165^{3}_{3}$
6213.328	3		16089.983	$21902^{4}_{4} - 37992_4$	6169.394	1		16204.563	$21902^{4}_{4} - 38106_5$
6212.721	100	5	16091.555	$8111_4 - 24202^{4}_{4}$	6168.837	4	1	16206.026	$19588^{6}_{6} - 35794_4$
6209.949	8	1	16098.738	$15166^{3}_{3} - 31265_3$	6168.482	2		16206.959	$21890^{3}_{3} - 38097_2$
6209.659	2		16099.489	$19713_3 - 35812^{5}_{5}$	6166.709	4	1	16211.619	$19588^{6}_{6} - 35799_6$
6208.986	8	1	16101.234	$7502_3 - 23603^{2}_{2}$	6165.538	4	1	16214.697	$20566^{4}_{4} - 36781_5$
6208.861	2		16101.559	$22855^{3}_{3} - 38956_4$	6164.842	8	1	16216.528	$15863_2 - 32080^{1}_{1}$
6208.686	100	5	16102.013	$11241^{3}_{3} - 27343_3$	6164.480	200	20	16217.480	$0_2 - 16217^{2}_{2}$
6207.751	150	8	16104.438	$17166_5 - 33270^{4}_{4}$	6163.732	100	5	16219.448	$18930^{3}_{3} - 35149_2$
6207.220	500	200	16105.815	$5563_1 - 21668^{1}_{1}$	6162.968	40	3	16221.459	$13088_3 - 29310^{4}_{4}$
6205.861	100	8	16109.342	$13088_3 - 29197^{2}_{2}$	6162.854	8	1	16221.759	$11802_2 - 28024^{1}_{1}$
6205.018	50	2	16111.531	$16346^{2}_{4} - 32458_4$	6162.456	4		16222.807	$17959_4 - 34182^{6}_{6}$
6203.493	500	100	16115.492	$4961_4 - 21077^{6}_{6}$	6162.261	2		16223.320	$17073_1 - 33297^{2}_{2}$
6203.169	3	1	16116.333	$17411^{3}_{3} - 33527_4$	6161.765	50	4	16224.626	$19986^{8}_{8} - 36210_5$
6198.223	400	75	16129.193	$3687_2 - 19817^{1}_{1}$	6161.646	1		16224.939	$22141^{3}_{3} - 38366_4$
6197.591	1		16130.838	$20522^{2}_{2} - 36653_2$	6158.829	1		16232.361	$18069^{3}_{3} - 34301_4$
6196.311	5		16134.171	$20054_2 - 36188^{2}_{2}$	6157.093	100	8	16236.937	$7795^{3}_{3} - 24032_4$
6196.172	4		16134.532	$21077^{6}_{6} - 37211_5$	6156.114	8	1	16239.519	$21165^{3}_{3} - 37404_3$
6195.322	25	3	16136.746	$15490^{6}_{6} - 31626_5$	6155.587	200	15	16240.910	$7280_2 - 23521^{3}_{3}$
6194.928	1		16137.772	$22669^{5}_{5} - 38807_2$	6155.299	8	1	16241.670	$20566^{4}_{4} - 36808_3$
6193.576	2		16141.295	$19948^{4}_{4} - 36089_4$	6154.627	4	1	16243.443	$21902^{4}_{4} - 38145_3$
6193.290	2		16142.040	$21165^{3}_{3} - 37307_3$	6154.515	40	8	16243.738	$9804_5 - 26048^{3}_{3}$
6193.194	5		16142.291	$21594_3 - 37736^{2}_{2}$	6154.419	3		16243.992	$12114^{2}_{2} - 28358_3$
6191.906	400	50	16145.648	$6362_2 - 22508^{2}_{2}$	6154.068	100	15	16244.918	$14481^{6}_{6} - 30726_7$
6191.261	2		16147.330	$19986^{6}_{6} - 36133_5$	6152.950	2		16247.870	$18053^{4}_{4} - 34301_4$
6190.771	10	2	16148.609	$21539^{4}_{4} - 37688_3$	6151.993	150r		16250.398	$7502_3 - 23752^{2}_{2}$
6190.710	10		16148.768	$8111_4 - 24259^{4}_{4}$	6151.517	8	2	16251.655	$17354^{1}_{1} - 33606_2$
6189.145	50	2	16152.851	$7502_3 - 23655^{3}_{3}$	6151.142	1		16252.646	$20522^{2}_{2} - 36775_3$
6188.863	1		16153.587	$17411^{3}_{3} - 33564_3$	6150.683	20	4	16253.859	$11241^{3}_{3} - 27495_4$
6188.126	200	75	16155.511	$8243^{2}_{2} - 24399_3$	6150.323	4	1	16254.810	$14032^{2}_{2} - 30286_1$
6186.763	2		16159.070	$18930^{3}_{3} - 35089_3$	6150.120	2		16255.347	$21077^{6}_{6} - 37332_6$
6186.380	8	1	16160.070	$15166^{3}_{3} - 31326_4$	6150.031	1		16255.582	$21890^{3}_{3} - 38145_3$
6185.774	25	2	16161.654	$17398_3 - 33560^{4}_{4}$	6148.361	3	1	16259.997	$19273_2 - 35533^{2}_{2}$
6185.683	1		16161.891	$21575_2 - 37736^{2}_{2}$	6147.959	2		16261.060	$10783^{2}_{2} - 27044_3$
6184.985	4		16163.715	$8111_4 - 24274^{8}_{8}$	6145.128	2		16268.551	$22401_1 - 38669^{2}_{2}$
6184.985	4		16163.715	$8111_4 - 24274^{8}_{8}$	6145.000	2		16268.890	$21252^{2}_{2} - 37521_3$
6184.788	150	15	16164.230	$13088_3 - 29252^{2}_{2}$	6144.760	20	3	16269.526	$10526^{3}_{3} - 26796_3$
6183.942	5		16166.441	$17224^{2}_{2} - 33390_1$	6144.414	1		16270.442	$20214^{3}_{3} - 36485_2$
6182.830	50b		16169.349	$13847_2 - 30017^{3}_{3}$	6141.928	1		16277.027	$18574_1 - 34851^{2}_{2}$
6182.623	500	1	16169.890	$2869_3 - 19039^{2}_{2}$	6141.629	2		16277.820	$17411^{3}_{3} - 33689_2$
6181.537	10	1	16172.731	$20922^{2}_{2} - 37094_2$	6140.994	1		16279.503	$18809^{4}_{4} - 35089_3$
6180.703	200	8	16174.913	$5563_1 - 21738^{2}_{2}$	6140.994	1		16279.503	$21539^{4}_{4} - 37819_4$

TABLE 4. *Classified lines of* Th I—continued

Wavelength (Å)	Intensity		Wavenumber (cm^{-1})	Classification
	Lamp	Spark		
6140.884	4		16279.795	$11241\frac{5}{2}$ – 27521_4
6140.772	25	4	16280.092	19532_4 – $35812\frac{3}{2}$
6140.449	1		16280.948	$22248\frac{3}{2}$ – 38529_3
6139.364	2		16283.825	$21902\frac{3}{4}$ – 38186_4
6137.025	5	1	16290.031	$18011\frac{5}{2}$ – 34301_4
6135.996	5	1	16292.763	$14465\frac{3}{2}$ – 30758_2
6135.628	5	1	16293.740	18431_3 – $34725\frac{5}{2}$
6135.014	2		16295.371	$20522\frac{5}{2}$ – 36818_2
6134.563	8	1	16296.569	15863_2 – $32160\frac{3}{2}$
6133.821	50	2	16298.540	$11197\frac{5}{2}$ – 27495_4
6133.671	2		16298.939	16351_0 – $32650\frac{1}{2}$
6133.064	75	4	16300.552	$14243\frac{1}{2}$ – 30544_2
6132.874	50	4	16301.057	$14206\frac{3}{4}$ – 30508_5
6132.874	50	4	16301.057	$20214\frac{5}{2}$ – 36515_3
6132.426	4	1	16302.248	18549_2 – $34851\frac{3}{2}$
6131.753	3		16304.037	18574_1 – $34878\frac{1}{2}$
6131.673	5	1	16304.250	$15736\frac{1}{2}$ – 32041_2
6130.765	25	2	16306.665	20054_2 – $36361\frac{1}{2}$
6130.459	20	1	16307.479	6362_2 – $22669\frac{3}{2}$
6129.551	75	8	16309.894	12847_3 – $29157\frac{5}{2}$
6129.492	15	2	16310.051	8111_4 – $24421\frac{5}{2}$
6129.322	2		16310.504	$15618\frac{5}{2}$ – 31929_3
6128.448	25	2	16312.830	14204_5 – $30517\frac{7}{2}$
6128.344	40	3	16313.107	14204_5 – $30517\frac{7}{2}$
6128.160	10	2	16313.596	16351_0 – $32665\frac{1}{2}$
6127.899	3		16314.291	$19516\frac{3}{2}$ – 35831_3
6127.609	50	2	16315.063	15970_3 – $32285\frac{5}{2}$
6127.425	50	2	16315.553	$16783\frac{3}{4}$ – 33099_3
6126.509	1		16317.993	22098_4 – $38416\frac{5}{2}$
6126.328	2		16318.475	13962_1 – $30281\frac{1}{2}$
6126.328	2		16318.475	13962_1 – $30281\frac{1}{2}$
6125.610	4		16320.387	$17847\frac{3}{2}$ – 34167_3
6124.485	200	15	16323.385	7280_2 – $23603\frac{3}{2}$
6124.073	50	3	16324.483	$11197\frac{5}{2}$ – 27521_4
6123.838	75	8	16325.110	$11241\frac{5}{2}$ – 27566_2
6122.709	3		16328.120	$19503\frac{5}{2}$ – 35831_3
6121.757	2		16330.659	13088_3 – $29419\frac{3}{2}$
6120.801	50	4	16333.210	15863_2 – $32197\frac{5}{2}$
6120.359	8	2	16334.389	$17354\frac{1}{2}$ – 33689_2
6119.649	25	2	16336.285	17398_3 – $33734\frac{3}{2}$
6118.056	4	1	16340.538	$17224\frac{3}{2}$ – 33564_3
6116.172	100	8	16345.572	$14206\frac{3}{4}$ – 30552_4
6114.931	8	1	16348.889	$19948\frac{3}{4}$ – 36297_4
6114.546	150	10	16349.918	12847_3 – $29197\frac{3}{2}$
6113.314	3		16353.213	17073_1 – $33427\frac{3}{2}$
6111.700	2		16357.532	$20737\frac{1}{2}$ – 37094_2
6110.677	3		16360.270	21594_3 – $37954\frac{5}{2}$
6110.476	2		16360.808	13847_2 – $30208\frac{3}{2}$
6110.476	2		16360.808	$19516\frac{3}{2}$ – 35877_2
6110.331	51	1	16361.197	$22399\frac{5}{2}$ – 38760_4
6108.293	100	5	16366.655	$17354\frac{1}{2}$ – 33721_2
6106.919	5	1	16370.338	$15166\frac{5}{2}$ – 31537_3
6106.847	10	2	16370.531	$11241\frac{5}{2}$ – 27612_3
6105.304	4	1	16374.668	$19503\frac{5}{2}$ – 35877_2
6104.970	2		16375.564	$18069\frac{5}{2}$ – 34444_2
6104.572	300	200	16376.631	$15618\frac{5}{2}$ – 31995_4
6104.170	4	1	16377.710	$18053\frac{3}{4}$ – 34431_3
6104.027	5	1	16378.094	$18069\frac{5}{2}$ – 34447_4
6103.354	2		16379.899	21575_2 – $37954\frac{5}{2}$
6102.595	300	50	16381.937	$10414\frac{3}{4}$ – 26796_3
6101.726	100	10	16384.270	$8243\frac{3}{2}$ – 24627_1
6101.554	3	1	16384.732	17959_4 – $34344\frac{3}{2}$
6100.414	3	1	16387.793	$19948\frac{3}{4}$ – 36336_3
6099.994	50	3	16388.922	13297_4 – $29686\frac{5}{2}$
6099.458	2		16390.362	$16346\frac{3}{4}$ – 32737_5
6098.126	200	25	16393.942	17166_5 – $33560\frac{3}{4}$
6097.821	4	1	16394.762	$11197\frac{5}{2}$ – 27591_5
6097.592	5		16395.378	$11877\frac{1}{2}$ – 28273_2
6097.292	4		16396.184	$18011\frac{5}{2}$ – 34407_6
6095.389	1		16401.303	17398_3 – $33799\frac{3}{2}$
6095.050	20	4	16402.216	17398_3 – $33800\frac{5}{2}$
6094.089	10	1	16404.802	12847_3 – $29252\frac{3}{2}$
6093.813	5	1	16405.545	19273_2 – $35678\frac{1}{2}$
6093.558	1		16406.232	$22877\frac{7}{2}$ – 39283_4
6093.240	8	1	16407.088	$18809\frac{3}{4}$ – 35216_5
6093.027	10	1	16407.661	$21738\frac{3}{2}$ – 38145_3
6090.607	2		16414.181	13297_4 – $29711\frac{5}{2}$
6090.451	15	2	16414.601	7502_3 – $23916\frac{3}{2}$
6090.241	1		16415.167	18574_1 – $34989\frac{1}{2}$
6088.828	10	2	16418.976	$17354\frac{1}{2}$ – 33773_1
6088.459	4	1	16419.972	18431_3 – $34851\frac{3}{2}$
6088.203	10	2	16420.662	$17411\frac{5}{2}$ – 33831_4
6088.031	400	50	16421.126	$8243\frac{3}{2}$ – 24664_3
6086.702	8	1	16424.711	$14465\frac{3}{2}$ – 30889_1
6085.375	100	75	16428.293	$8243\frac{3}{2}$ – 24671_2
6084.486	2		16430.693	$16783\frac{3}{4}$ – 33214_5
6084.127	5	1	16431.663	$18614\frac{1}{2}$ – 35046_1
6083.533	2		16433.267	13847_2 – $30281\frac{1}{2}$
6083.242	10	2	16434.053	20054_2 – $36488\frac{3}{2}$
6082.910	2h		16434.950	$16346\frac{3}{4}$ – 32781_4
6082.669	4		16435.601	$21252\frac{3}{2}$ – 37688_3
6082.561	10	1	16435.893	13297_4 – $29733\frac{5}{2}$
6081.299	1		16439.304	22401_1 – $38840\frac{1}{2}$
6080.900	5	1	16440.382	18549_2 – $34989\frac{1}{2}$
6079.469	50	4	16444.252	$14206\frac{3}{4}$ – 30651_3
6079.220	200	25	16444.926	$10526\frac{5}{2}$ – 26971_4
6078.419	200	40	16447.093	13297_4 – $29744\frac{5}{2}$
6077.870	150	25	16448.578	$14481\frac{5}{2}$ – 30930_6
6077.533	4	1	16449.490	$16346\frac{3}{4}$ – 32796_3
6077.533	4	1	16449.490	$18011\frac{5}{2}$ – 34460_5
6077.103	100	15	16450.654	8111_4 – $24561\frac{5}{2}$
6076.984	4	1	16450.977	$17847\frac{3}{2}$ – 34298_1
6074.001	5		16459.056	$20322\frac{5}{2}$ – 36781_5
6073.561	3		16460.248	15493_4 – $31953\frac{3}{4}$
6072.894	5	1	16462.056	12847_3 – $29310\frac{3}{4}$
6072.799	20	2	16462.313	21143_5 – $37605\frac{3}{4}$
6072.061	3	1	16464.314	$21902\frac{3}{4}$ – 38366_4
6071.981	15	2	16464.531	$20867\frac{7}{2}$ – 37332_6
6071.904	3		16464.740	$17224\frac{3}{2}$ – 33689_2
6071.802	1		16465.017	19713_3 – $36178\frac{3}{4}$

TABLE 4. *Classified lines of* Th I—continued

Wavelength (Å)	Intensity		Wavenumber (cm^{-1})	Classification
	Lamp	Spark		
6070.458	1		16468.662	$22338^{\circ}_{3} - 38807_{2}$
6070.339	25	2	16468.985	$15970_{3} - 32439^{\circ}_{4}$
6069.844	20	2	16470.328	$17959_{4} - 34430^{\circ}_{5}$
6069.019	100	5	16472.567	$7280_{2} - 23752^{\circ}_{2}$
6068.136	1		16474.964	$18930^{\circ}_{5} - 35405_{3}$
6064.289	1		16485.415	$22248^{\circ}_{2} - 38734_{3}$
6062.846	8		16489.338	$14481^{\circ}_{6} - 30971_{5}$
6062.225	1		16491.028	$18809^{\circ}_{4} - 35300_{5}$
6061.535	75	3	16492.905	$6362_{2} - 22855^{\circ}_{3}$
6059.136	10	1	16499.435	$14465^{\circ}_{2} - 30964_{3}$
6058.438	4	1	16501.336	$19588^{\circ}_{6} - 36089_{4}$
6056.881	5		16505.578	$15490^{\circ}_{6} - 31995_{4}$
6055.592	50	10	16509.091	$13175^{\circ}_{4} - 29684_{5}$
6055.036	8	1	16510.607	$18930^{\circ}_{5} - 35440_{3}$
6054.350	1		16512.478	$14032^{\circ}_{2} - 30544_{2}$
6053.790	3		16514.005	$14243^{\circ}_{1} - 30758_{2}$
6053.381	300	15	16515.121	$6362_{2} - 22877^{\circ}_{1}$
6052.444	8	1	16517.678	$10526^{\circ}_{3} - 27044_{3}$
6050.981	100	4	16521.671	$8800_{4} - 25321^{\circ}_{3}$
6050.545	1		16522.862	$15490^{\circ}_{6} - 32012_{4}$
6050.457	3		16523.102	$21165^{\circ}_{3} - 37688_{3}$
6049.051	800	100	16526.942	$3687_{2} - 20214^{\circ}_{3}$
6047.794	10s	1	16530.377	$15493_{4} - 32023^{\circ}_{6}$
6047.273	3		16531.802	$21252^{\circ}_{2} - 37784_{2}$
6047.159	1		16532.113	$17959_{4} - 34492^{\circ}_{2}$
6046.643	10	2	16533.524	$15970_{3} - 32503^{\circ}_{2}$
6045.246	1		16537.345	$19039^{\circ}_{2} - 35576_{3}$
6044.554	8		16539.238	$19273_{2} - 35812^{\circ}_{3}$
6043.676	2h		16541.641	$19532_{4} - 36074^{\circ}_{5}$
6042.750	2		16544.175	$19503^{\circ}_{3} - 36047_{2}$
6042.593	75	5	16544.605	$11802_{2} - 28347^{\circ}_{2}$
6042.401	5	1	16545.131	$19588^{\circ}_{6} - 36133_{5}$
6040.873	5		16549.316	$17224^{\circ}_{2} - 33773_{1}$
6039.228	15	2	16553.824	$22399^{\circ}_{6} - 38953_{5}$
6038.681	75	5	16555.323	$8800_{4} - 25355^{\circ}_{4}$
6037.942	3g		16557.349	$10414^{\circ}_{4} - 26971_{4}$
6037.697	400	150	16558.021	$3865_{1} - 20423^{\circ}_{1}$
6036.765	50	2	16560.578	$10783^{\circ}_{2} - 27343_{3}$
6035.365	1		16564.419	$20566^{\circ}_{4} - 37131_{3}$
6035.194	75	5	16564.889	$12114^{\circ}_{2} - 28679_{2}$
6034.334	3		16567.249	$21539^{\circ}_{4} - 38106_{5}$
6034.215	5		16567.576	$19948^{\circ}_{4} - 36515_{3}$
6033.515	15	2	16569.498	$17398_{3} - 33967^{\circ}_{5}$
6033.416	50	5	16569.770	$11802_{2} - 28372^{\circ}_{1}$
6032.876	75	8	16571.253	$12847_{3} - 29419^{\circ}_{2}$
6032.555	2		16572.135	$20522^{\circ}_{2} - 37094_{2}$
6032.370	50b	8	16572.643	$19227^{\circ}_{6} - 35799_{6}$
6030.448	75s	5	16577.925	$4961_{4} - 21539^{\circ}_{4}$
6030.189	5	1	16578.637	$16217^{\circ}_{2} - 32796_{3}$
6029.651	50	2	16580.116	$9804_{5} - 26384^{\circ}_{3}$
6029.228	50	4	16581.279	$13175^{\circ}_{4} - 29756_{4}$
6028.631	3	1	16582.922	$21165^{\circ}_{3} - 37748_{2}$
6026.047	50	2	16590.032	$8111_{4} - 24701^{\circ}_{5}$
6025.784	75b	5	16590.756	$13962_{1} - 30553^{\circ}_{2}$
6025.049	1		16592.780	$22141^{\circ}_{3} - 38734_{3}$
6024.835	2		16593.370	$20214^{\circ}_{3} - 36808_{3}$
6024.082	1		16595.444	$18809^{\circ}_{4} - 35405_{3}$
6023.332	3b		16597.510	$17847^{\circ}_{2} - 34444_{2}$
6023.229	100	8	16597.794	$13088_{3} - 29686^{\circ}_{3}$
6022.702	5	1	16599.246	$13945^{\circ}_{3} - 30544_{2}$
6022.387	5	1	16600.114	$19532_{4} - 36132^{\circ}_{6}$
6021.036	200s	75	16603.839	$7795^{\circ}_{4} - 24399_{3}$
6020.502	25	2	16605.312	$15970_{3} - 32575^{\circ}_{2}$
6019.821	5	1	16607.190	$13945^{\circ}_{3} - 30552_{4}$
6019.642	25	3	16607.684	$15166^{\circ}_{3} - 31774_{3}$
6019.411	1		16608.321	$20522^{\circ}_{2} - 37131_{3}$
6016.362	50	4	16616.738	$16346^{\circ}_{4} - 32963_{5}$
6014.307	50	2	16622.416	$19588^{\circ}_{6} - 36210_{5}$
6014.062	75	5	16623.093	$17959_{4} - 34583^{\circ}_{5}$
6013.442	8	2	16624.807	$16783^{\circ}_{4} - 33408_{3}$
6012.410	3	1	16627.661	$21902^{\circ}_{4} - 38529_{3}$
6011.537	50	5	16630.075	$10414^{\circ}_{4} - 27044_{3}$
6011.203	15	3	16630.999	$18809^{\circ}_{4} - 35440_{3}$
6010.253	50b	8	16633.628	$17166_{5} - 33799^{\circ}_{4}$
6010.163	100	10	16633.877	$2869_{3} - 19503^{\circ}_{5}$
6010.028	40	3	16634.251	$16783^{\circ}_{4} - 33418_{4}$
6008.052	5	1	16639.721	$15863_{2} - 32503^{\circ}_{2}$
6007.261	10	1	16641.912	$21575_{2} - 38216^{\circ}_{3}$
6007.073	300s	75	16642.433	$8800_{4} - 25442^{\circ}_{5}$
6006.294	4		16644.592	$17073_{1} - 33718^{\circ}_{2}$
6005.921	1		16645.625	$19532_{4} - 36178^{\circ}_{4}$
6005.600	10	1	16646.515	$21539^{\circ}_{4} - 38186_{4}$
6005.174	200	15	16647.696	$2869_{3} - 19516^{\circ}_{2}$
6003.946	5		16651.101	$13962_{1} - 30613^{\circ}_{6}$
6002.198	10	1	16655.950	$13088_{3} - 29744^{\circ}_{3}$
6001.734	10	2	16657.238	$3865_{1} - 20522^{\circ}_{2}$
6001.207	300	15	16658.701	$8111_{4} - 24769^{\circ}_{3}$
6000.766	50	8	16659.925	$13175^{\circ}_{4} - 29835_{3}$
6000.554	5	1	16660.513	$21645_{4} - 38306^{\circ}_{4}$
6000.418	8	1	16660.891	$17073_{1} - 33734^{\circ}_{2}$
5999.594	5	1	16663.179	$18382^{\circ}_{6} - 35046_{1}$
5997.788	5		16668.197	$19817^{\circ}_{1} - 36485_{2}$
5997.010	8	1	16670.359	$20214^{\circ}_{3} - 36885_{4}$
5996.630	50	4	16671.415	$8243^{\circ}_{2} - 24915_{3}$
5995.682	10		16674.051	$13175^{\circ}_{4} - 29849_{4}$
5995.221	50	4	16675.333	$16783^{\circ}_{4} - 33459_{4}$
5994.126	500r	100	16678.380	$3865_{1} - 20543^{\circ}_{6}$
5993.960	50	8	16678.842	$17166_{5} - 33844^{\circ}_{6}$
5993.494	40	1	16680.138	$7502_{3} - 24182^{\circ}_{2}$
5991.457	15		16685.809	$5563_{1} - 22248^{\circ}_{2}$
5991.004	400s	50	16687.071	$6362_{2} - 23049^{\circ}_{1}$
5989.445	20	2	16691.414	$18549_{2} - 35240^{\circ}_{3}$
5986.268	50	3	16700.273	$7502_{3} - 24202^{\circ}_{4}$
5985.679	20	1	16701.916	$14226_{0} - 30928^{\circ}_{1}$
5984.998	15	3	16703.816	$21575_{2} - 38278^{\circ}_{1}$
5984.390	3l		16705.513	$13847_{2} - 30553^{\circ}_{2}$
5984.278	2		16705.826	$13945^{\circ}_{3} - 30651_{3}$
5983.163	5		16708.939	$19588^{\circ}_{6} - 36297_{4}$
5982.651	10		16710.369	$11802_{2} - 28513^{\circ}_{2}$
5982.229	5		16711.548	$15863_{2} - 32575^{\circ}_{2}$

TABLE 4. *Classified lines of* Th I—continued

Wavelength (Å)	Intensity		Wavenumber (cm^{-1})	Classification
	Lamp	Spark		
5982.171	5		16711.710	$21594_3 - 38306\frac{2}{4}$
5982.095	50	5	16711.922	$15490\frac{8}{8} - 32202_5$
5981.782	1		16712.797	$21890\frac{3}{8} - 38602_2$
5981.233	2		16714.331	$19713_3 - 36427\frac{3}{8}$
5979.325	4		16719.664	$13297_4 - 30017\frac{3}{8}$
5977.087	10	2	16725.925	$14032\frac{2}{8} - 30758_2$
5975.066	500	150	16731.582	$6362_2 - 23093\frac{2}{2}$
5973.665	500r	150	16735.506	$3687_2 - 20423\frac{1}{1}$
5973.203	10	1	16736.800	$20566\frac{4}{4} - 37303_4$
5972.300	3		16739.331	$21645_4 - 38385\frac{6}{8}$
5971.881	3		16740.505	$20566\frac{4}{4} - 37307_3$
5971.369	3		16741.941	$21077\frac{6}{8} - 37819_4$
5971.073	4		16742.771	$19532_4 - 36275\frac{6}{8}$
5970.456	50	2	16744.501	$17959_4 - 34704\frac{8}{8}$
5969.742	150	10	16746.504	$11601_1 - 28347\frac{2}{2}$
5967.515	50	2	16752.753	$16346\frac{4}{4} - 33099_3$
5966.273	5		16756.240	$17411\frac{5}{8} - 34167_3$
5965.832	40	1	16757.479	$7502_3 - 24259\frac{8}{8}$
5965.745	15	1	16757.723	$14206\frac{4}{4} - 30964_3$
5964.714	4h		16760.620	$21594_3 - 38355\frac{2}{2}$
5964.481	40	2	16761.275	$13962_1 - 30723\frac{1}{1}$
5964.012	15	1	16762.593	$15166\frac{3}{8} - 31929_3$
5963.930	15	1	16762.823	$19986\frac{8}{8} - 36749_6$
5963.661	10	1	16763.579	$20322\frac{6}{8} - 37085_4$
5963.308	10	1	16764.572	$13088_3 - 29853\frac{2}{2}$
5962.975	3		16765.508	$17959_4 - 34725\frac{3}{8}$
5962.773	4		16766.076	$20922\frac{2}{8} - 37688_3$
5962.579	5		16766.621	$18809\frac{4}{4} - 35576_3$
5962.060	40	3	16768.081	$12114\frac{8}{8} - 28882_2$
5961.249	4		16770.362	$21645_4 - 38416\frac{3}{8}$
5960.785	50		16771.668	$11601_1 - 28372\frac{1}{1}$
5960.529	5		16772.388	$18809\frac{4}{4} - 35582_5$
5959.681	50	3	16774.774	$8800_4 - 25575\frac{4}{4}$
5958.811	15	1	16777.223	$10414\frac{3}{8} - 27191_5$
5957.592	50	2	16780.656	$14465\frac{2}{8} - 31245_2$
5957.472	50	2	16780.994	$16783\frac{4}{4} - 33564_3$
5956.514	5		16783.693	$10783\frac{2}{8} - 27566_2$
5956.263	100	8	16784.400	$15970_3 - 32754\frac{3}{8}$
5955.566	100	5	16786.365	$11802_2 - 28589\frac{3}{8}$
5954.588	40	2	16789.122	$14481\frac{8}{8} - 31271_5$
5953.587	100	4	16791.945	$15493_4 - 32285\frac{3}{8}$
5953.255	50	2	16792.881	$13088_3 - 29881\frac{4}{4}$
5952.807	2		16794.145	$19503\frac{3}{8} - 36297_4$
5952.456	2		16795.135	$19986\frac{8}{8} - 36781_5$
5950.641	25	2	16800.258	$17501\frac{8}{8} - 34301_4$
5950.429	50	2	16800.856	$15493_4 - 32294\frac{4}{4}$
5950.148	15	2	16801.650	$15863_2 - 32665\frac{1}{1}$
5949.373	50	5	16803.838	$15490\frac{8}{8} - 32293_5$
5949.218	15	1	16804.276	$18069\frac{8}{8} - 34873_4$
5948.965	5		16804.991	$18069\frac{8}{8} - 34874_3$
5948.803	100	8	16805.448	$7502_3 - 24307\frac{2}{2}$
5948.393	15	1	16806.607	$21143_5 - 37950\frac{4}{4}$
5947.502	4		16809.124	$18431_3 - 35240\frac{8}{8}$
5947.243	1		16809.857	$16351_0 - 33161\frac{1}{1}$
5946.239	40	2	16812.695	$13945\frac{3}{8} - 30758_2$
5946.027	8		16813.294	$21077\frac{6}{8} - 37890_5$
5945.480	10	1	16814.841	$14204_5 - 31019\frac{3}{4}$
5945.334	4		16815.254	$22141\frac{3}{8} - 38956_4$
5945.191	8	1	16815.658	$21077\frac{6}{8} - 37892_4$
5944.806	15	1	16816.747	$22877\frac{6}{8} - 39694_5$
5944.648	150	40	16817.194	$10526\frac{3}{8} - 27343_3$
5943.934	1		16819.214	$19516\frac{2}{2} - 36336_3$
5943.496	25	3	16820.454	$18053\frac{4}{4} - 34874_3$
5943.470	50	4	16820.528	$12114\frac{2}{2} - 28934_3$
5942.259	8	1	16823.956	$18809\frac{4}{4} - 35633_4$
5941.568	2		16825.912	$20922\frac{2}{2} - 37748_2$
5941.188	3		16826.988	$19948\frac{4}{4} - 36775_3$
5941.188	3		16826.988	$21539\frac{4}{4} - 38366_4$
5941.126	5	1	16827.164	$21165\frac{3}{8} - 37992_4$
5940.567	50	3	16828.747	$15166\frac{3}{8} - 31995_4$
5939.374	5b		16832.127	$21902\frac{4}{4} - 38734_3$
5939.044	15		16833.063	$19503\frac{3}{8} - 36336_3$
5938.825	400	75	16833.683	$5563_1 - 22396\frac{1}{1}$
5938.459	150	20	16834.721	$3687_2 - 20522\frac{2}{2}$
5938.285	15	1	16835.214	$17166_5 - 34001\frac{2}{2}$
5938.041	1	3	16835.906	$22338\frac{3}{8} - 39174_3$
5937.925	50	3	16836.235	$13175\frac{2}{4} - 30011_3$
5937.665	100	2	16836.972	$11197\frac{6}{8} - 28034_5$
5937.297	25	2	16838.016	$20566\frac{4}{4} - 37404_3$
5937.166	100	10	16838.387	$12847_3 - 29686\frac{3}{8}$
5936.876	20	2	16839.210	$13175\frac{2}{4} - 30014_4$
5936.876	20	2	16839.210	$15618\frac{3}{8} - 32458_4$
5936.387	50	5	16840.597	$9804_5 - 26645\frac{6}{8}$
5934.458	50b	3	16846.071	$15166\frac{3}{8} - 32012_4$
5934.412	75b	15	16846.201	$11802_2 - 28649\frac{1}{1}$
5934.103	1		16847.078	$22163\frac{2}{4} - 39010_3$
5932.911	15	1	16850.463	$13962_1 - 30812\frac{2}{2}$
5932.426	50	2	16851.841	$14243\frac{1}{1} - 31095_1$
5932.056	4		16852.892	$22399\frac{6}{8} - 39252_5$
5930.311	10	1	16857.851	$14032\frac{2}{8} - 30889_1$
5929.934	100	20	16858.923	$3865_1 - 20724\frac{6}{8}$
5929.586	10	2	16859.912	$19948\frac{4}{4} - 36808_3$
5929.328	20	2	16860.646	$17847\frac{2}{2} - 34707_3$
5928.861	20	2	16861.974	$18011\frac{6}{8} - 34873_4$
5928.755	3		16862.275	$20922\frac{2}{2} - 37784_2$
5928.654	15	2	16862.563	$13297_4 - 30160\frac{4}{4}$
5928.123	4	1	16864.073	$18930\frac{3}{8} - 35794_4$
5926.545	4		16868.563	$22141\frac{3}{8} - 39010_3$
5926.232	150	40	16869.454	$7795\frac{4}{4} - 24664_3$
5926.001	50	4	16870.112	$8111_4 - 24981\frac{3}{8}$
5925.719	15	1	16870.914	$20214\frac{3}{8} - 37085_4$
5925.404	100	8	16871.811	$3865_1 - 20737\frac{1}{1}$
5924.519	15	2	16874.332	$15166\frac{3}{8} - 32041_2$
5924.519	15	2	16874.332	$20867\frac{2}{2} - 37742_6$
5923.919	20	1	16876.041	$13847_2 - 30723\frac{1}{1}$
5922.860	50	2	16879.058	$7502_3 - 24381\frac{2}{2}$
5921.102	4		16884.069	$21645\frac{4}{4} - 38529_3$
5920.977	15	2	16884.426	$22399\frac{6}{8} - 39283_4$
5919.224	15	2	16889.426	$20322\frac{6}{8} - 37211_5$
5918.946	100	8	16890.220	$8800_4 - 25690\frac{6}{8}$

TABLE 4. *Classified lines of* Th I—continued

Wavelength (Å)	Intensity		Wavenumber (cm^{-1})	Classification	Wavelength (Å)	Intensity		Wavenumber (cm^{-1})	Classification
	Lamp	Spark				Lamp	Spark		
5918.946	100	8	16890.220	$17411\frac{8}{3} - 34301_4$	5874.993	150	8	17016.580	$17166_5 - 34182\frac{6}{6}$
5918.189	15	1	16892.380	$15970_3 - 32862\frac{2}{4}$	5874.040	50	3	17019.341	$13945\frac{8}{3} - 30964_3$
5917.285	10	1	16894.961	$19532_4 - 36427\frac{8}{3}$	5873.920	4	1	17019.689	$21645_4 - 38665\frac{6}{6}$
5916.730	100	20	16896.545	$12847_3 - 29744\frac{8}{3}$	5873.774	8	1	17020.112	$17411\frac{8}{3} - 34431_3$
5915.168	3		16901.007	$18930\frac{8}{3} - 35831_3$	5873.462	8		17021.016	$21165\frac{8}{3} - 38186_4$
5914.716	50b	7	16902.299	$7280_2 - 24182\frac{8}{2}$	5873.332	10		17021.393	$18809\frac{2}{4} - 35831_3$
5913.362	50	5	16906.169	$19227\frac{8}{6} - 36133_5$	5871.405	15		17026.979	$17847\frac{2}{2} - 34874_3$
5913.286	8	2	16906.386	$17501\frac{6}{6} - 34407_6$	5871.186	100	20	17027.614	$7280_2 - 24307\frac{2}{2}$
5911.229	50	8	16912.269	$11601_1 - 28513\frac{2}{2}$	5870.054	20	1	17030.898	$11197\frac{6}{6} - 28227_4$
5911.097	8	1	16912.647	$18549_2 - 35462\frac{8}{3}$	5869.854	100	5	17031.478	$11241\frac{8}{3} - 28273_2$
5910.640	4	1	16913.954	$13847_2 - 30761\frac{8}{3}$	5869.200	2b		17033.376	$17411\frac{8}{3} - 34444_2$
5910.237	15	2	16915.108	$21077\frac{6}{6} - 37992_4$	5869.164	8		17033.480	$12847_3 - 29881\frac{2}{4}$
5909.887	1		16916.109	$20214\frac{8}{3} - 37131_3$	5868.382	150	25	17035.750	$18053\frac{2}{4} - 35089_3$
5908.957	200		16918.772	$7502_3 - 24421\frac{8}{6}$	5867.841	20	1	17037.321	$17073_1 - 34111\frac{2}{1}$
5906.550	3		16925.666	$17398_3 - 34324\frac{2}{2}$	5867.542	1		17038.189	$18382\frac{6}{6} - 35421_1$
5906.164	3		16926.773	$17959_4 - 34886\frac{6}{6}$	5866.814	50	5	17040.303	$10526\frac{8}{3} - 27566_2$
5905.571	150	20	16928.472	$4961_4 - 21890\frac{8}{3}$	5864.128	4		17048.108	$11601_1 - 28649\frac{2}{1}$
5905.176	50	2	16929.605	$10414\frac{4}{4} - 27343_3$	5863.720	100	8	17049.294	$3687_2 - 20737\frac{2}{1}$
5903.646	2		16933.992	$21668\frac{2}{1} - 38602_2$	5863.562	10		17049.754	$19713_3 - 36762\frac{8}{3}$
5903.496	20	2	16934.422	$21645_4 - 38580\frac{4}{4}$	5863.146	3	1	17050.963	$21902\frac{4}{4} - 38953_5$
5903.337	15	1	16934.879	$14206\frac{6}{4} - 31141_3$	5861.894	2		17054.605	$21902\frac{4}{4} - 38956_4$
5902.602	50	2	16936.987	$14204_5 - 31141\frac{6}{6}$	5861.289	8		17056.366	$16217\frac{8}{2} - 33273_1$
5900.448	2		16943.170	$17224\frac{2}{2} - 34167_3$	5861.192	15		17056.648	$3865_1 - 20922\frac{2}{2}$
5900.355	5		16943.437	$17354\frac{2}{1} - 34298_1$	5860.480	15	1	17058.720	$14206\frac{4}{4} - 31265_3$
5899.846	150	5	16944.899	$5563_1 - 22508\frac{2}{2}$	5860.259	15	1	17059.363	$7502_3 - 24561\frac{8}{3}$
5899.521	50	4	16945.832	$15493_4 - 32439\frac{4}{4}$	5859.348	15	1	17062.016	$16346\frac{4}{4} - 33408_3$
5899.466	8b	1	16945.990	$17501\frac{6}{6} - 34447_4$	5858.752	50	3	17063.751	$14032\frac{2}{2} - 31095_1$
5897.246	1		16952.370	$22399\frac{6}{6} - 39351_5$	5858.641	50	2	17064.075	$14206\frac{4}{4} - 31271_5$
5896.786	20l	1	16953.692	$8800_4 - 25753\frac{6}{6}$	5857.725	2		17066.743	$21890\frac{8}{3} - 38956_4$
5896.114	2		16955.624	$19713_3 - 36668\frac{2}{2}$	5856.112	15	1	17071.444	$13088_3 - 30160\frac{4}{4}$
5895.283	150	25	16958.014	$13297_4 - 30255\frac{8}{3}$	5855.914	5		17072.021	$14465\frac{2}{2} - 31537_3$
5895.053	10	1	16958.676	$18574_1 - 35533\frac{2}{2}$	5855.789	1		17072.385	$11601_1 - 28673\frac{2}{2}$
5894.699	50	25	16959.694	$17501\frac{6}{6} - 34460_5$	5854.858	3		17075.100	$21594_3 - 38669\frac{2}{2}$
5893.191	20	2	16964.034	$14465\frac{2}{2} - 31429_1$	5854.120	150	8	17077.253	$8800_4 - 25877\frac{4}{4}$
5892.780	8		16965.217	$13847_2 - 30812\frac{2}{2}$	5853.474	100	5	17079.137	$2869_3 - 19948\frac{4}{4}$
5892.434	50	5	16966.213	$13962_1 - 30928\frac{2}{1}$	5852.945	10		17080.681	$18069\frac{8}{3} - 35149_2$
5891.774	5	1	16968.114	$15490\frac{6}{6} - 32458_4$	5852.844	15		17080.976	$13847_2 - 30928\frac{2}{1}$
5891.670	5		16968.414	$19516\frac{2}{2} - 36485_2$	5852.682	200	25	17081.449	$10414\frac{4}{4} - 27495_4$
5891.451	200	25	16969.044	$10526\frac{8}{3} - 27495_4$	5852.487	100	8	17082.018	$11802_2 - 28884\frac{8}{3}$
5887.919	8		16979.223	$18699_2 - 35678\frac{2}{1}$	5851.214	8	2	17085.734	$10526\frac{8}{3} - 27612_3$
5887.437	2		16980.613	$21165\frac{8}{3} - 38145_3$	5850.566	5		17087.627	$19713_3 - 36800\frac{4}{4}$
5886.851	5		16982.304	$22855\frac{8}{3} - 39837_3$	5850.378	10	1	17088.176	$19273_2 - 36361\frac{2}{1}$
5886.456	15		16983.443	$19227\frac{8}{6} - 36210_5$	5850.270	3		17088.491	$20214\frac{8}{3} - 37303_4$
5886.093	15	1	16984.491	$15970_3 - 32954\frac{2}{2}$	5849.765	8	1	17089.966	$17354\frac{2}{1} - 34444_2$
5885.702	200	50	16985.619	$9804_5 - 26790\frac{4}{4}$	5849.514	15	1	17090.700	$15863_2 - 32954\frac{2}{2}$
5885.502	75	2	16986.196	$11241\frac{8}{3} - 28227_4$	5849.217	10		17091.567	$16217\frac{8}{2} - 33309_2$
5884.033	50	2	16990.437	$14204_5 - 31194\frac{4}{4}$	5848.554	25	2	17093.505	$19532_4 - 36625\frac{6}{6}$
5882.460	10	1	16994.980	$10526\frac{8}{3} - 27521_4$	5848.277	1		17094.315	$20054_2 - 37149\frac{2}{2}$
5881.988	2		16996.344	$21738\frac{2}{2} - 38734_3$	5848.135	4		17094.729	$21575_2 - 38669\frac{2}{2}$
5881.065	4		16999.011	$19516\frac{2}{2} - 36515_3$	5845.919	100	5	17101.209	$7280_2 - 24381\frac{2}{2}$
5879.127	50	2	17004.615	$11877\frac{2}{1} - 28882_2$	5844.873	5		17104.270	$18574_1 - 35678\frac{2}{1}$
5878.933	100	3	17005.176	$12847_3 - 29853\frac{2}{2}$	5844.793	75	3	17104.504	$20054_2 - 37159\frac{2}{1}$
5877.186	2		17010.231	$20322\frac{8}{3} - 37332_6$	5844.704	3		17104.765	$20054_2 - 37159\frac{8}{3}$
5877.013	25	2	17010.732	$20737\frac{1}{1} - 37748_2$	5843.805	50	5	17107.396	$10414\frac{4}{4} - 27521_4$
5876.647	3		17011.791	$22163\frac{4}{4} - 39174_3$	5843.267	10	1	17108.971	$21077\frac{6}{6} - 38186_4$

TABLE 4. *Classified lines of* Th I – continued

Wavelength (Å)	Intensity		Wavenumber (cm^{-1})	Classification
	Lamp	Spark		
5843.012	5		17109.718	$14032\frac{2}{2} - 31141_3$
5842.050	50	4	17112.535	$16346\frac{4}{4} - 33459_4$
5841.915	15	2	17112.930	$18699_2 - 35812\frac{3}{3}$
5841.758	3		17113.390	$13962_1 - 31075\frac{2}{2}$
5841.281	4		17114.788	$21645\frac{3}{3} - 38760_4$
5841.199	10		17115.028	$11802_2 - 28917\frac{2}{2}$
5840.639	50	5	17116.669	$11241\frac{3}{3} - 28358_3$
5840.535	8		17116.974	$18930\frac{3}{3} - 36047_2$
5839.850	40	2	17118.982	$6362_2 - 23481\frac{1}{1}$
5839.584	40	2	17119.761	$7795\frac{4}{4} - 24915_3$
5839.492	50	8	17120.031	$13088_3 - 30208\frac{2}{2}$
5839.266	8		17120.694	$22163\frac{4}{4} - 39283_4$
5833.849	8		17136.591	$19516\frac{2}{2} - 36653_2$
5833.132	2		17138.697	$21668\frac{1}{1} - 38807_2$
5832.371	100	15	17140.934	$7280_2 - 24421\frac{3}{3}$
5831.923	5	1	17142.250	$22141\frac{3}{3} - 39283_4$
5831.754	8		17142.747	$13847_2 - 30990\frac{3}{3}$
5831.682	5		17142.959	$21645_4 - 38788\frac{3}{3}$
5831.002	3	1	17144.958	$14481\frac{6}{6} - 31626_5$
5830.827	50	5	17145.472	$11197\frac{5}{5} - 28342_5$
5827.900	2		17154.083	$19273_2 - 36427\frac{3}{3}$
5826.344	40b	1	17158.665	$6362_2 - 23521\frac{3}{3}$
5826.280	50b	5	17158.853	$19713_3 - 36871\frac{2}{2}$
5826.097	25	2	17159.392	$18930\frac{3}{3} - 36089_4$
5825.675	8		17160.635	$19588\frac{6}{6} - 36749_6$
5825.003	40	3	17162.615	$15618\frac{3}{3} - 32781_4$
5824.895	50	5	17162.933	$21143_5 - 38306\frac{2}{2}$
5823.555	3		17166.882	$13088_3 - 30255\frac{3}{3}$
5823.261	2		17167.749	$22669\frac{3}{3} - 39837_3$
5822.796	100	8	17169.120	$12847_3 - 30017\frac{3}{3}$
5822.054	40	1	17171.308	$17959_4 - 35131\frac{1}{1}$
5821.691	3		17172.379	$22508\frac{2}{2} - 39680_2$
5820.820	10		17174.948	$20922\frac{2}{2} - 38097_2$
5820.081	25	2	17177.129	$15618\frac{3}{3} - 32796_3$
5819.902	15	1	17177.657	$10414\frac{4}{4} - 27591_5$
5819.607	50	3	17178.528	$17166_5 - 34344\frac{3}{3}$
5819.367	4b		17179.236	$20054_2 - 37234\frac{2}{2}$
5819.302	15	1	17179.428	$15863_2 - 33043\frac{3}{3}$
5819.130	20	1	17179.936	$4961_4 - 22141\frac{3}{3}$
5818.453	50	5	17181.935	$14247\frac{6}{6} - 31429_1$
5818.218	2		17182.629	$19948\frac{4}{4} - 37131_3$
5817.545	10	1	17184.617	$17398_3 - 34583\frac{3}{3}$
5816.188	15	1	17188.626	$22163\frac{4}{4} - 39351_5$
5815.823	2		17189.705	$20214\frac{3}{3} - 37404_3$
5814.729	50	2	17192.939	$19588\frac{6}{6} - 36781_5$
5814.101	8	2	17194.796	$21539\frac{4}{4} - 38734_3$
5813.534	1		17196.473	$13945\frac{3}{3} - 31141_3$
5813.181	8		17197.517	$10783\frac{2}{2} - 27980_3$
5812.976	100	8	17198.124	$10414\frac{4}{4} - 27612_3$
5812.709	50	2	17198.914	$17847\frac{2}{2} - 35046_1$
5811.848	40	1	17201.462	$4961_4 - 22163\frac{4}{4}$
5810.453	5		17205.591	$18011\frac{6}{6} - 35216_5$
5808.659	50	25	17210.905	$8111_4 - 25321\frac{3}{3}$
5807.932	1		17213.060	$22098_4 - 39311\frac{4}{4}$
5807.685	50	4	17213.792	$14032\frac{2}{2} - 31245_2$
5807.685	50	4	17213.792	$21575_2 - 38788\frac{3}{3}$
5806.201	40	2	17218.191	$16346\frac{4}{4} - 33564_3$
5805.702	50	3	17219.671	$13297_4 - 30517\frac{6}{6}$
5805.612	1		17219.938	$13297_4 - 30517\frac{4}{4}$
5805.495	25	1	17220.285	$17224\frac{2}{2} - 34444_2$
5805.244	2		17221.030	$21539\frac{4}{4} - 38760_4$
5804.141	500r	50	17224.302	$0_2 - 17224\frac{2}{2}$
5803.805	5	1	17225.299	$20522\frac{2}{2} - 37748_2$
5803.735	8	1	17225.507	$19986\frac{6}{6} - 37211_5$
5802.851	50l	1	17228.131	$13847_2 - 31075\frac{2}{2}$
5802.097	3		17230.370	$19532_4 - 36762\frac{3}{3}$
5801.027	40	1	17233.548	$14032\frac{2}{2} - 31265_3$
5800.830	200	20	17234.133	$3687_2 - 20922\frac{2}{2}$
5800.159	1	1	17236.127	$8800_4 - 26036\frac{3}{3}$
5798.479	50	4	17241.121	$6362_2 - 23603\frac{2}{2}$
5798.260	4		17241.772	$21143_5 - 38385\frac{6}{6}$
5798.088	5		17242.284	$17847\frac{2}{2} - 35089_3$
5797.319	75	3	17244.571	$8111_4 - 25355\frac{4}{4}$
5796.521	50	1	17246.945	$15490\frac{6}{6} - 32737_5$
5796.070	200	15	17248.287	$8800_4 - 26048\frac{4}{4}$
5795.407	1		17250.260	$17073_1 - 34324\frac{2}{2}$
5792.685	4		17258.366	$19516\frac{2}{2} - 36775_3$
5792.431	150	8	17259.123	$2558_0 - 19817\frac{1}{1}$
5791.704	50	2	17261.289	$15493_4 - 32754\frac{3}{3}$
5791.558	5	1	17261.724	$20522\frac{2}{2} - 37784_2$
5791.032	5	1	17263.292	$19948\frac{4}{4} - 37211_5$
5789.644	200	15	17267.431	$7502_3 - 24769\frac{3}{3}$
5789.374	10	1	17268.236	$19532_4 - 36800\frac{4}{4}$
5788.027	4		17272.255	$19503\frac{3}{3} - 36775_3$
5787.896	3		17272.646	$21902\frac{4}{4} - 39174_3$
5786.209	3	2	17277.681	$19817\frac{1}{1} - 37094_2$
5785.122	8	1	17280.928	$17959_4 - 35240\frac{5}{5}$
5784.913	4		17281.552	$7280_2 - 24561\frac{3}{3}$
5782.307	40b	5	17289.341	$11241\frac{3}{3} - 28531_2$
5781.655	50	1	17291.290	$15166\frac{3}{3} - 32458_4$
5780.438	2		17294.931	$22399\frac{6}{6} - 39694_5$
5779.833	50	2	17296.741	$8800_4 - 26096\frac{3}{3}$
5779.735	8	3	17297.034	$19039\frac{2}{2} - 36336_3$
5779.407	20	2	17298.016	$17073_1 - 34371\frac{2}{2}$
5778.594	10	1	17300.450	$15970_3 - 33270\frac{4}{4}$
5778.364	1		17301.138	$19516\frac{2}{2} - 36818_2$
5777.856	10	1	17302.659	$17847\frac{2}{2} - 35149_2$
5777.398	75	8	17304.031	$12114\frac{2}{2} - 29418_2$
5777.023	2		17305.154	$19503\frac{3}{3} - 36808_3$
5776.550	2		17306.571	$20214\frac{3}{3} - 37521_3$
5776.164	25	2	17307.728	$12114\frac{2}{2} - 29422_1$
5775.615	8	1	17309.373	$14465\frac{2}{2} - 31774_3$
5775.312	3		17310.281	$16351_0 - 33662\frac{1}{1}$
5774.981	5	1	17311.273	$18574_1 - 35885\frac{2}{2}$
5774.726	10	1	17312.038	$12847_3 - 30160\frac{4}{4}$
5774.073	8	2	17313.995	$17959_4 - 35273\frac{6}{6}$
5773.946	150	10	17314.376	$5563_1 - 22877\frac{1}{1}$
5773.750	10	1	17314.964	$19503\frac{3}{3} - 36818_2$
5771.960	15	1	17320.334	$13945\frac{3}{3} - 31265_3$
5771.758	75	5	17320.940	$11241\frac{3}{3} - 28562_4$

TABLE 4. *Classified lines of* Th I—continued

Wavelength (Å)	Intensity		Wavenumber (cm^{-1})	Classification	Wavelength (Å)	Intensity		Wavenumber (cm^{-1})	Classification
	Lamp	Spark				Lamp	Spark		
5770.865	10	2	17323.620	18809$\frac{3}{4}$ – 36133$_5$	5734.579	8		17433.236	15863$_2$ – 33297$\frac{2}{2}$
5770.795	5	1	17323.830	20566$\frac{6}{4}$ – 37890$_5$	5733.887	20	2	17435.340	13847$_2$ – 31283$\frac{3}{3}$
5770.562	4	1	17324.530	20423$\frac{2}{1}$ – 37748$_2$	5733.651	4	1	17436.057	19713$_3$ – 37149$\frac{2}{2}$
5770.461	10	1	17324.833	15970$_3$ – 33294$\frac{3}{3}$	5733.388	5	1	17436.857	21738$\frac{2}{2}$ – 39174$_3$
5770.100	15b		17325.917	17166$_5$ – 34492$\frac{4}{4}$	5733.096	20	2	17437.745	4961$_4$ – 22399$\frac{6}{6}$
5769.730	8		17327.028	15970$_3$ – 33297$\frac{2}{2}$	5730.307	2		17446.232	19039$\frac{2}{2}$ – 36485$_2$
5769.730	8		17327.028	17398$_3$ – 34725$\frac{3}{3}$	5729.236	2		17449.493	21902$\frac{4}{4}$ – 39351$_5$
5768.633	10	1	17330.323	14206$\frac{6}{4}$ – 31537$_3$	5729.119	5		17449.850	11802$_2$ – 29252$\frac{2}{2}$
5768.181	200	15	17331.681	8111$_4$ – 25442$\frac{3}{3}$	5727.997	8		17453.268	17398$_3$ – 34851$\frac{2}{2}$
5767.779	150	10	17332.889	13175$\frac{4}{4}$ – 30508$_5$	5727.711	40	3	17454.139	10526$\frac{3}{3}$ – 27980$_3$
5766.662	5		17336.246	18069$\frac{3}{3}$ – 35405$_3$	5727.021	50	3	17456.242	19948$\frac{4}{4}$ – 37404$_3$
5766.589	1		17336.466	18549$_2$ – 35885$\frac{2}{2}$	5726.792	1		17456.940	15970$_3$ – 33427$\frac{2}{2}$
5763.529	200	10	17345.670	2869$_3$ – 20214$\frac{3}{3}$	5725.390	300	75	17461.215	9804$_5$ – 27266$\frac{4}{4}$
5763.312	5	1	17346.323	19986$\frac{6}{6}$ – 37332$_6$	5724.863	2		17462.822	17411$\frac{3}{3}$ – 34874$_3$
5762.959	15	1	17347.386	16217$\frac{2}{2}$ – 33564$_3$	5724.463	75	4	17464.043	8111$_4$ – 25575$\frac{4}{4}$
5762.796	100	10	17347.876	17501$\frac{8}{8}$ – 34849$_5$	5724.386	20	2	17464.277	13297$_4$ – 30761$\frac{3}{3}$
5762.078	3b		17350.038	21902$\frac{4}{4}$ – 39252$_5$	5724.386	20	2	17464.277	14465$\frac{2}{2}$ – 31929$_3$
5761.527	25	2	17351.697	18053$\frac{4}{4}$ – 35405$_3$	5724.240	100	10	17464.723	13088$_3$ – 30553$\frac{2}{2}$
5760.550	600r	150	17354.640	0$_2$ – 17354$\frac{1}{1}$	5723.532	10	1	17466.883	14204$_5$ – 31671$\frac{4}{4}$
5760.447	75b	15	17354.950	11802$_2$ – 29157$\frac{3}{3}$	5722.012	2		17471.523	16217$\frac{2}{2}$ – 33689$_2$
5759.190	5	1	17358.738	19948$\frac{4}{4}$ – 37307$_3$	5721.425	50	4	17473.316	15490$\frac{6}{6}$ – 32963$_5$
5758.471	5		17360.906	20423$\frac{1}{1}$ – 37784$_2$	5720.185	500r	150	17477.103	3687$_2$ – 21165$\frac{3}{3}$
5757.360	1		17364.256	21645$\frac{4}{4}$ – 39010$_3$	5719.625	200	50	17478.815	7502$_3$ – 24981$\frac{3}{3}$
5757.336	1		17364.328	21645$\frac{4}{4}$ – 39010$_3$	5719.098	20	2	17480.425	15618$\frac{3}{3}$ – 33099$_3$
5756.904	4	1	17365.631	11197$\frac{6}{6}$ – 28562$_4$	5718.657	2		17481.773	21252$\frac{2}{2}$ – 38734$_3$
5756.463	1		17366.961	18930$\frac{3}{3}$ – 36297$_4$	5718.118	8	1	17483.421	17224$\frac{2}{2}$ – 34707$_3$
5756.445	1		17367.016	18930$\frac{3}{3}$ – 36297$_4$	5717.526	20	2	17485.231	16346$\frac{4}{4}$ – 33831$_4$
5754.844	8	1	17371.847	18069$\frac{3}{3}$ – 35440$_3$	5717.172	50	15	17486.314	5563$_1$ – 23049$\frac{1}{1}$
5754.734	15	3	17372.179	17501$\frac{6}{6}$ – 34873$_4$	5716.815	10	1	17487.406	18809$\frac{4}{4}$ – 36297$_4$
5753.984	3		17374.444	18699$_2$ – 36074$\frac{3}{3}$	5716.106	1		17489.575	7280$_2$ – 24769$\frac{3}{3}$
5753.026	200	25	17377.337	4961$_4$ – 22338$\frac{3}{3}$	5715.948	8	1	17490.058	10783$\frac{2}{2}$ – 28273$_2$
5752.580	15	1	17378.684	6362$_2$ – 23741$\frac{1}{1}$	5715.725	20	2	17490.741	13297$_4$ – 30788$\frac{6}{6}$
5751.629	4b	1	17381.557	21902$\frac{4}{4}$ – 39283$_4$	5713.732	2		17496.842	20322$\frac{6}{6}$ – 37819$_4$
5751.594	5b	1	17381.663	13945$\frac{3}{3}$ – 31326$_4$	5711.998	50	5	17502.153	17959$_4$ – 35462$\frac{3}{3}$
5751.432	10	2	17382.153	19503$\frac{3}{3}$ – 36885$_4$	5711.454	1		17503.820	16217$\frac{2}{2}$ – 33721$_2$
5749.782	50b	8	17387.141	3865$_1$ – 21252$\frac{2}{2}$	5711.023	1		17505.141	14032$\frac{2}{2}$ – 31537$_3$
5749.733	20b	3	17387.289	18053$\frac{4}{4}$ – 35440$_3$	5710.270	4		17507.449	18069$\frac{3}{3}$ – 35576$_3$
5749.230	15	1	17388.810	16217$\frac{2}{2}$ – 33606$_2$	5709.858	1		17508.713	19532$_4$ – 37041$\frac{4}{4}$
5748.741	150	25	17390.289	6362$_2$ – 23752$\frac{2}{2}$	5708.679	50	3	17512.329	14204$_5$ – 31716$\frac{6}{6}$
5748.323	100	8	17391.554	17959$_4$ – 35351$\frac{4}{4}$	5705.866	8	1	17520.962	19713$_3$ – 37234$\frac{2}{2}$
5747.193	50	4	17394.973	11802$_2$ – 29197$\frac{2}{2}$	5705.637	50	4	17521.665	19227$\frac{6}{6}$ – 36749$_6$
5747.058	2		17395.382	19273$_2$ – 36668$\frac{2}{2}$	5705.483	10	1	17522.138	21143$_5$ – 38665$\frac{6}{6}$
5746.468	4		17397.168	14032$\frac{2}{2}$ – 31429$_1$	5705.232	4	1	17522.909	18053$\frac{4}{4}$ – 35576$_3$
5745.233	5	1	17400.908	18809$\frac{4}{4}$ – 36210$_5$	5704.124	8	1	17526.313	18809$\frac{4}{4}$ – 36336$_3$
5743.583	8	1	17405.906	18930$\frac{3}{3}$ – 36336$_3$	5702.650	50	25	17530.843	5563$_1$ – 23093$\frac{2}{2}$
5743.063	15	1	17407.483	12847$_3$ – 30255$\frac{3}{3}$	5702.543	1		17531.172	22163$\frac{4}{4}$ – 39694$_5$
5741.829	50	10	17411.224	0$_2$ – 17411$\frac{3}{3}$	5700.782	50	8	17536.587	12114$\frac{2}{2}$ – 29650$_2$
5741.715	5	1	17411.569	23015$\frac{6}{6}$ – 40426$_4$	5698.292	50	5	17544.250	11877$\frac{1}{1}$ – 29422$_1$
5740.196	2		17416.177	21645$_4$ – 39062$\frac{6}{6}$	5696.391	50	8	17550.105	15493$_4$ – 33043$\frac{3}{3}$
5739.837	3	1	17417.266	21539$\frac{4}{4}$ – 38956$_4$	5694.434	10	1	17556.136	16217$\frac{2}{2}$ – 33773$_1$
5738.965	20	2	17419.912	14206$\frac{6}{4}$ – 31626$_5$	5693.759	1		17558.218	17847$\frac{2}{2}$ – 35405$_3$
5737.645	2		17423.920	21575$_2$ – 38998$\frac{3}{3}$	5693.571	8		17558.798	7280$_2$ – 24838$\frac{1}{1}$
5736.031	100	8	17428.823	13088$_3$ – 30517$\frac{4}{4}$	5692.159	10	1	17563.153	15863$_2$ – 33427$\frac{2}{2}$
5735.304	8	1	17431.032	15863$_2$ – 33294$\frac{3}{3}$	5691.906	3		17563.934	19273$_2$ – 36837$\frac{1}{1}$
5735.146	1		17431.512	22248$\frac{2}{2}$ – 39680$_2$	5691.681	5		17564.628	3687$_2$ – 21252$\frac{2}{2}$

TABLE 4. *Classified lines of* Th I—continued

Wavelength (Å)	Intensity		Wavenumber (cm^{-1})	Classification
	Lamp	Spark		
5691.060	10b		17566.545	$10414\frac{5}{2} - 27980_3$
5690.693	40	3	17567.678	$14206\frac{5}{4} - 31774_3$
5690.118	10	3	17569.453	$20214\frac{5}{2} - 37784_2$
5689.647	10	1	17570.907	$18011\frac{5}{6} - 35582_5$
5689.477	1		17571.432	$22855\frac{5}{3} - 40426_4$
5688.527	1		17574.367	$20522\frac{3}{2} - 38097_2$
5687.997	2c		17576.004	$14465\frac{3}{2} - 32041_2$
5687.350	50l	3	17578.004	$15490\frac{5}{6} - 33068_6$
5686.876	10	1	17579.469	$8111_4 - 25690\frac{5}{6}$
5685.826	3		17582.715	$19503\frac{5}{3} - 37085_4$
5685.192	100	8	17584.676	$8800_4 - 26384\frac{3}{2}$
5684.866	4		17585.684	$18930\frac{5}{3} - 36515_3$
5683.486	20	2	17589.954	$15970_3 - 33560\frac{3}{4}$
5682.846	8	1	17591.935	$13945\frac{5}{3} - 31537_3$
5682.238	4		17593.818	$17847\frac{7}{2} - 35440_3$
5681.441	1		17596.286	$11601_1 - 29197\frac{7}{4}$
5679.535	3		17602.191	$20054_2 - 37656\frac{5}{3}$
5679.004	50	5	17603.836	$11241\frac{5}{3} - 28845_4$
5677.729	2h		17607.790	$20922\frac{5}{2} - 38529_3$
5677.051	200b	8	17609.892	$7795\frac{5}{4} - 25405_4$
5675.701	2		17614.081	$19516\frac{5}{2} - 37131_3$
5675.601	2		17614.391	$19039\frac{5}{2} - 36653_2$
5675.501	15	2	17614.702	$15166\frac{5}{3} - 32781_4$
5674.990	200b	25	17616.288	$11802_2 - 29419\frac{5}{2}$
5674.461	15	2	17617.930	$21902\frac{5}{4} - 39520_4$
5674.171	2		17618.830	$21645_4 - 39264\frac{5}{3}$
5673.955	5	1	17619.501	$20566\frac{3}{4} - 38186_4$
5673.835	50	5	17619.874	$10414\frac{5}{4} - 28034_5$
5673.009	5	1	17622.439	$18011\frac{5}{6} - 35633_4$
5672.724	5	1	17623.325	$19588\frac{5}{6} - 37211_5$
5671.498	15	2	17627.134	$19532_4 - 37159\frac{5}{3}$
5671.250	10	2	17627.905	$19503\frac{5}{3} - 37131_3$
5671.072	40	2	17628.458	$16554_6 - 34182\frac{5}{6}$
5670.827	3		17629.220	$15166\frac{5}{3} - 32796_3$
5670.199	1		17631.172	$18431_3 - 36062\frac{3}{4}$
5668.402	3		17636.762	$13962_1 - 31599\frac{5}{2}$
5668.016	1		17637.963	$21645\frac{5}{4} - 39283_4$
5667.509	2		17639.541	$18549_2 - 36188\frac{5}{2}$
5667.129	150	15	17640.723	$11241\frac{5}{3} - 28882_2$
5666.419	10	1	17642.934	$8111_4 - 25753\frac{5}{6}$
5665.181	200	50	17646.789	$8243\frac{5}{2} - 25890_2$
5664.621	75	15	17648.534	$11197\frac{5}{6} - 28845_4$
5664.228	40	2	17649.758	$17224\frac{5}{2} - 34874_3$
5663.041	50	3	17653.458	$2869_3 - 20522\frac{5}{2}$
5662.949	3		17653.745	$15736\frac{7}{4} - 33390_1$
5660.364	1		17661.807	$18699_2 - 36361\frac{7}{4}$
5659.878	2		17663.323	$16783\frac{3}{4} - 34447_4$
5659.216	5	1	17665.389	$21645_4 - 39311\frac{3}{4}$
5657.926	100	25	17669.417	$12847_3 - 30517\frac{3}{4}$
5656.729	40	2	17673.156	$13088_3 - 30761\frac{5}{3}$
5656.302	10	2	17674.490	$22163\frac{3}{4} - 39837_3$
5655.750	10	3	17676.215	$13847_2 - 31523\frac{5}{3}$
5655.490	20	2	17677.028	$16783\frac{3}{4} - 34460_5$
5655.213	2		17677.893	$20214\frac{5}{3} - 37892_4$
5655.135	2		17678.137	$17411\frac{5}{3} - 35089_3$
5653.838	2		17682.193	$20054_2 - 37736\frac{5}{2}$
5653.426	2		17683.481	$21077\frac{5}{6} - 38760_4$
5652.570	1		17686.159	$23015\frac{5}{6} - 40701_4$
5651.326	5		17690.052	$15618\frac{5}{3} - 33309_2$
5650.912	1		17691.348	$17354\frac{7}{4} - 35046_1$
5650.354	75	15	17693.095	$13297_4 - 30990\frac{5}{3}$
5649.737	1		17695.028	$22401_1 - 40096\frac{5}{2}$
5648.990	75	10	17697.368	$2869_3 - 20566\frac{3}{4}$
5647.708	20	2	17701.385	$10526\frac{5}{3} - 28227_4$
5646.455	50	10	17705.313	$12847_3 - 30553\frac{5}{3}$
5646.255	1		17705.940	$21645\frac{3}{4} - 39351_5$
5646.205	1		17706.097	$18809\frac{3}{4} - 36515_3$
5645.668	50	20	17707.781	$8800_4 - 26508\frac{3}{4}$
5645.529	50	8	17708.217	$4961_4 - 22669\frac{5}{3}$
5643.346	8	1	17715.067	$19588\frac{5}{6} - 37303_4$
5643.110	20	2	17715.808	$17501\frac{5}{6} - 35216_5$
5641.735	75	8	17720.125	$14481\frac{5}{4} - 32202_5$
5641.562	50	5	17720.669	$12114\frac{5}{2} - 29835_3$
5641.242	20	5	17721.674	$13297_4 - 31019\frac{5}{4}$
5640.363	50	2	17724.436	$13088_3 - 30812\frac{5}{2}$
5639.460	10	1	17727.274	$15863_2 - 33591\frac{5}{3}$
5638.767	1		17729.452	$17847\frac{5}{3} - 35576_3$
5636.625	1		17736.190	$19039\frac{5}{2} - 36775_3$
5635.889	75	15	17738.506	$17411\frac{5}{3} - 35149_2$
5635.482	2		17739.787	$19948\frac{3}{4} - 37688_3$
5635.175	5	1	17740.753	$18053\frac{3}{4} - 35794_4$
5634.619	10	2	17742.504	$14032\frac{5}{3} - 31774_3$
5634.097	8s	1	17744.148	$19588\frac{5}{6} - 37332_6$
5633.297	75	8	17746.668	$10526\frac{3}{4} - 28273_2$
5632.903	2b		17747.909	$10783\frac{5}{3} - 28531_2$
5632.776	50	3	17748.309	$15970_3 - 33718\frac{5}{2}$
5632.494	25	1	17749.198	$14204_5 - 31953\frac{3}{4}$
5632.164	5b		17750.238	$13962_1 - 31712\frac{7}{4}$
5630.297	75	10	17756.123	$19986\frac{5}{6} - 37742_6$
5629.312	50	3	17759.230	$16351_0 - 34111\frac{7}{4}$
5628.365	8	1	17762.218	$18069\frac{5}{3} - 35831_3$
5627.606	3		17764.614	$15970_3 - 33734\frac{5}{2}$
5627.012	3		17766.489	$8111_4 - 25877\frac{3}{4}$
5626.169	1		17769.151	$19039\frac{5}{2} - 36808_3$
5624.911	50	3	17773.125	$11877\frac{7}{4} - 29650_2$
5624.775	15	2	17773.555	$17959_4 - 35733\frac{3}{4}$
5623.581	25	2	17777.329	$15493_4 - 33270\frac{5}{3}$
5623.474	1		17777.667	$18053\frac{3}{4} - 35831_3$
5623.411	2		17777.866	$17073_1 - 34851\frac{5}{2}$
5621.788	20	3	17782.998	$18011\frac{5}{6} - 35794_4$
5621.287	8	2	17784.583	$20322\frac{5}{6} - 38106_5$
5620.013	15b	5	17788.615	$18011\frac{5}{6} - 35799_6$
5619.976	50b	8	17788.732	$14206\frac{3}{4} - 31995_4$
5619.719	5b	1	17789.546	$13175\frac{3}{4} - 30964_3$
5619.684	4b		17789.656	$15618\frac{5}{3} - 33408_3$
5619.526	1		17790.156	$19516\frac{5}{2} - 37307_3$
5619.478	1		17790.308	$21890\frac{5}{3} - 39680_2$
5619.017	50	4	17791.768	$21165\frac{5}{3} - 38956_4$
5618.927	15	1	17792.053	$21902\frac{5}{4} - 39694_5$
5617.964	2		17795.103	$17354\frac{7}{4} - 35149_2$

201-606 O - 76 - 12

TABLE 4. *Classified lines of* Th I—continued

Wavelength (Å)	Intensity		Wavenumber (cm^{-1})	Classification
	Lamp	Spark		
5617.291	15	2	17797.235	$14243^{\circ}_{1} - 32041_{2}$
5616.945	3	1	17798.331	$15863_{2} - 33662^{\circ}_{1}$
5616.691	20	2	17799.136	$15618^{5}_{3} - 33418_{4}$
5616.503	10	2	17799.732	$17501^{6}_{6} - 35300_{5}$
5616.438	2		17799.938	$20566^{4}_{4} - 38366_{4}$
5616.328	8	2	17800.286	$19503^{3}_{3} - 37303_{4}$
5615.879	10	3	17801.709	$15493_{4} - 33294^{3}_{3}$
5615.320	400r	15	17803.482	$3865_{1} - 21668^{1}_{1}$
5614.515	5	1	17806.034	$14206^{5}_{4} - 32012_{4}$
5613.659	5		17808.749	$18069^{8}_{8} - 35877_{2}$
5612.619	75	3	17812.049	$14481^{8}_{6} - 32293_{5}$
5612.619	75	3	17812.049	$18549_{2} - 36361^{1}_{1}$
5612.068	150	20	17813.798	$10414^{3}_{4} - 28227_{4}$
5610.685	200	20	17818.189	$11601_{1} - 29419^{2}_{2}$
5610.329	50	3	17819.320	$14204_{5} - 32023^{6}_{6}$
5610.235	75	5	17819.618	$7502_{3} - 25321^{5}_{5}$
5610.111	75	4	17820.012	$6362_{2} - 24182^{2}_{2}$
5609.857	15	1	17820.819	$16346^{2}_{4} - 34167_{3}$
5609.585	150	10	17821.683	$17224^{2}_{2} - 35046_{1}$
5607.197	15	1	17829.273	$13945^{5}_{3} - 31774_{3}$
5607.087	10	1	17829.623	$15970_{3} - 33799^{4}_{4}$
5606.390	100	10	17831.839	$10526^{3}_{3} - 28358_{3}$
5604.814	2		17836.853	$21575_{2} - 39411^{1}_{1}$
5603.764	20	1	17840.195	$15618^{5}_{3} - 33459_{4}$
5603.060	8s		17842.437	$17398_{3} - 35240^{5}_{5}$
5602.627	15	1	17843.816	$13297_{4} - 31141^{6}_{6}$
5602.216	2b		17845.125	$8800_{4} - 26645^{6}_{6}$
5601.934	2		17846.023	$22855^{5}_{5} - 40701_{4}$
5601.604	200	8	17847.074	$0_{2} - 17847^{2}_{2}$
5601.604	200	8	17847.074	$5563_{1} - 23410^{6}_{6}$
5601.506	8b		17847.387	$12114^{2}_{2} - 29961_{1}$
5601.191	4		17848.390	$13945^{5}_{3} - 31793_{4}$
5599.865	3		17852.617	$17959_{4} - 35812^{5}_{5}$
5599.655	50	2	17853.286	$7502_{3} - 25355^{4}_{4}$
5599.573	2		17853.548	$14226_{0} - 32080^{1}_{1}$
5599.274	10b		17854.501	$15863_{2} - 33718^{2}_{2}$
5598.445	4		17857.145	$18699_{2} - 36556^{1}_{1}$
5596.836	5		17862.278	$11241^{5}_{5} - 29104_{4}$
5595.962	75	8	17865.068	$17224^{2}_{2} - 35089_{3}$
5595.847	50	3	17865.435	$2558_{0} - 20423^{1}_{1}$
5595.778	5		17865.656	$20737^{1}_{1} - 38602_{2}$
5595.064	300	25	17867.935	$8243^{2}_{2} - 26111_{1}$
5594.161	15	1	17870.820	$15863_{2} - 33734^{2}_{2}$
5592.597	2		17875.817	$19273_{2} - 37149^{2}_{2}$
5591.907	15b	3	17878.023	$18549_{2} - 36427^{5}_{5}$
5591.907	15b	3	17878.023	$18930^{5}_{5} - 36808_{3}$
5590.215	20		17883.434	$11802_{2} - 29686^{3}_{3}$
5589.560	1		17885.530	$20922^{2}_{2} - 38807_{2}$
5589.412	2		17886.003	$19273_{2} - 37159^{1}_{1}$
5589.328	5	1	17886.272	$19273_{2} - 37159^{3}_{3}$
5587.027	500r	50	17893.638	$4961_{4} - 22855^{5}_{5}$
5586.255	2		17896.111	$10783^{2}_{2} - 28679_{2}$
5585.981	4		17896.989	$12114^{2}_{2} - 30011_{3}$
5585.884	5b		17897.300	$13297_{4} - 31194^{4}_{4}$
5585.848	15l	1	17897.415	$14032^{2}_{2} - 31929_{3}$
5584.983	2		17900.187	$20054_{2} - 37954^{3}_{3}$
5584.430	4		17901.960	$13088_{3} - 30990^{3}_{3}$
5582.865	50	2	17906.978	$11197^{6}_{6} - 29104_{4}$
5582.678	50	3	17907.578	$13962_{1} - 31870^{2}_{2}$
5582.367	75	4	17908.575	$15618^{5}_{3} - 33527_{4}$
5580.756	100	10	17913.745	$12847_{3} - 30761^{3}_{3}$
5580.395	50	10	17914.904	$17166_{5} - 35081^{6}_{6}$
5580.221	3		17915.462	$20054_{2} - 37970^{2}_{2}$
5580.076	50	2	17915.928	$4961_{4} - 22877^{6}_{6}$
5579.990	4		17916.204	$21645_{4} - 39562^{3}_{3}$
5579.359	300	40	17918.230	$5563_{1} - 23481^{1}_{1}$
5578.091	2		17922.303	$21252^{2}_{2} - 39174_{3}$
5577.602	10		17923.875	$16783^{4}_{4} - 34707_{3}$
5577.115	5	1	17925.440	$17224^{2}_{2} - 35149_{2}$
5576.300	40	3	17928.060	$15490^{6}_{6} - 33418_{4}$
5576.205	100	10	17928.365	$10414^{3}_{4} - 28342_{5}$
5575.524	3		17930.555	$13088_{3} - 31019^{2}_{2}$
5575.446	4		17930.806	$20214^{5}_{3} - 38145_{3}$
5574.028	2		17935.367	$21902^{4}_{4} - 39837_{3}$
5573.599	2		17936.748	$15863_{2} - 33800^{3}_{3}$
5573.355	400	20	17937.533	$8111_{4} - 26048^{4}_{4}$
5572.766	10s	1	17939.429	$18549_{2} - 36488^{2}_{2}$
5572.466	200	8	17940.394	$7502_{3} - 25442^{5}_{5}$
5572.095	20	1	17941.589	$11802_{2} - 29744^{3}_{3}$
5571.253	75b	10	17944.301	$10414^{4}_{4} - 28358_{3}$
5570.928	50	2	17945.347	$6362_{2} - 24307^{2}_{2}$
5570.762	8	1	17945.882	$15618^{5}_{3} - 33564_{3}$
5570.265	1		17947.483	$21890^{5}_{5} - 39837_{3}$
5569.486	2		17949.993	$16217^{2}_{2} - 34167_{3}$
5568.840	15		17952.076	$15736^{1}_{1} - 33689_{2}$
5568.542	50	3	17953.036	$17398_{3} - 35351^{4}_{4}$
5568.000	300b	150	17954.784	$16346^{4}_{4} - 34301_{4}$
5567.942	25b	10	17954.971	$18930^{5}_{5} - 36885_{4}$
5564.806	25	2	17965.089	$17166_{5} - 35131^{4}_{4}$
5564.691	2		17965.461	$18809^{4}_{4} - 36775_{3}$
5563.582	4		17969.042	$18699_{2} - 36668^{2}_{2}$
5562.847	5		17971.416	$18809^{4}_{4} - 36781_{5}$
5560.000	3h		17980.618	$21539^{4}_{4} - 39520_{4}$
5559.894	150	8	17980.961	$3687_{2} - 21668^{1}_{1}$
5559.526	3		17982.151	$18574_{1} - 36556^{1}_{1}$
5558.882	8b	3	17984.234	$17847^{2}_{2} - 35831_{3}$
5558.848	75b	3	17984.344	$15736^{1}_{1} - 33721_{2}$
5558.848	75b	3	17984.344	$19227^{6}_{6} - 37211_{5}$
5558.433	75b	25b	17985.687	$13297_{4} - 31283^{5}_{5}$
5558.342	400b	50	17985.981	$8111_{4} - 26096^{3}_{3}$
5557.924	25	5	17987.334	$13088_{3} - 31075^{2}_{2}$
5557.045	300	15	17990.179	$8800_{4} - 26790^{4}_{4}$
5555.839	10	1	17994.084	$17411^{5}_{3} - 35405_{3}$
5555.534	75	4	17995.072	$14206^{4}_{4} - 32202_{5}$
5554.695	5		17997.790	$15970_{3} - 33967^{5}_{5}$
5554.546	10b	2	17998.273	$20054_{2} - 38053^{5}_{5}$
5554.502	20	4	17998.415	$18809^{4}_{4} - 36808_{3}$
5552.624	75	4	18004.503	$10526^{3}_{3} - 28531_{2}$
5551.744	25	5	18007.357	$18549_{2} - 36556^{1}_{1}$
5551.193	40	2	18009.144	$14032^{2}_{2} - 32041_{2}$

TABLE 4. *Classified lines of* Th I—continued

Wavelength (Å)	Intensity		Wavenumber (cm^{-1})	Classification
	Lamp	Spark		
5550.988	2		18009.809	$21165\frac{3}{3} - 39174_3$
5550.476	2		18011.470	$21668\frac{1}{1} - 39680_2$
5550.456	1		18011.535	$21668\frac{1}{1} - 39680_2$
5548.377	15	5	18018.284	$12114\frac{2}{2} - 30132_2$
5548.176	400r	40b	18018.937	$6362_2 - 24381\frac{2}{2}$
5547.654	15	1	18020.632	$18069\frac{3}{3} - 36089_4$
5547.135	75	3	18022.318	$13847_2 - 31870\frac{2}{2}$
5546.638	4		18023.933	$19713_3 - 37736\frac{2}{2}$
5545.806	15		18026.637	$7280_2 - 25306\frac{2}{2}$
5545.586	2		18027.352	$22399\frac{3}{3} - 40426_4$
5544.879	1		18029.651	$17411\frac{3}{3} - 35440_3$
5544.543	2		18030.743	$17847\frac{2}{2} - 35877_2$
5544.385	3		18031.257	$15970_3 - 34001\frac{4}{4}$
5544.385	3		18031.257	$15970_3 - 34001\frac{4}{4}$
5544.252	4	1	18031.690	$22855\frac{3}{3} - 40886_2$
5543.480	10	1	18034.201	$20054_2 - 38088\frac{2}{2}$
5542.890	300	10	18036.121	$10526\frac{3}{3} - 28562_4$
5542.027	3		18038.929	$19532_4 - 37571\frac{0}{0}$
5541.936	50	2	18039.225	$11601_1 - 29640\frac{1}{1}$
5541.936	50	2	18039.225	$18614\frac{1}{1} - 36653_2$
5541.581	50	2	18040.381	$5563_1 - 23603\frac{2}{2}$
5541.146	50	2	18041.797	$7280_2 - 25321\frac{3}{3}$
5540.521	2		18043.832	$19948\frac{3}{3} - 37992_4$
5540.380	1		18044.292	$20322\frac{0}{0} - 38366_4$
5539.262	500r	50	18047.933	$9804_5 - 27852\frac{0}{0}$
5538.608	75	4	18050.065	$3687_2 - 21738\frac{2}{2}$
5537.749	1		18052.864	$2869_3 - 20922\frac{2}{2}$
5537.555	50	2	18053.497	$4961_4 - 23015\frac{0}{0}$
5536.436	4		18057.146	$18431_3 - 36488\frac{2}{2}$
5535.970	50	1	18058.666	$6362_2 - 24421\frac{3}{3}$
5534.586	5		18063.181	$18699_2 - 36762\frac{3}{3}$
5534.439	5		18063.661	$17398_3 - 35462\frac{3}{3}$
5533.963	4		18065.215	$16783\frac{3}{3} - 34849_5$
5533.608	5		18066.374	$17354\frac{1}{1} - 35421_1$
5533.467	5	1	18066.834	$15493_4 - 33560\frac{3}{3}$
5533.219	10b		18067.644	$13945\frac{3}{3} - 32012_4$
5532.780	5		18069.077	$0_2 - 18069\frac{3}{3}$
5532.481	1		18070.054	$15618\frac{3}{3} - 33689_2$
5531.483	1		18073.314	$19532_4 - 37605\frac{3}{3}$
5530.843	2		18075.405	$18809\frac{2}{2} - 36885_4$
5530.075	50	2	18077.916	$8800_4 - 26878\frac{3}{3}$
5529.472	8		18079.887	$18053\frac{3}{3} - 36133_5$
5529.096	75	10	18081.117	$17501\frac{0}{0} - 35582_5$
5528.226	50b	5	18083.962	$11877\frac{1}{1} - 29961_1$
5527.480	10	1	18086.403	$14465\frac{2}{2} - 32551_3$
5527.295	200	8	18087.008	$14206\frac{3}{3} - 32293_5$
5527.074	2		18087.731	$22338\frac{3}{3} - 40426_4$
5526.983	1		18088.029	$20922\frac{2}{2} - 39010_3$
5526.528	50	8	18089.518	$16783\frac{3}{3} - 34873_4$
5526.434	8	1	18089.826	$14204_5 - 32294\frac{4}{4}$
5526.313	8		18090.222	$16783\frac{3}{3} - 34874_3$
5525.799	2		18091.905	$19039\frac{2}{2} - 37131_3$
5525.155	20	2	18094.013	$18574_1 - 36668\frac{2}{2}$
5524.583	150b	10b	18095.887	$13175\frac{2}{2} - 31271_5$
5523.951	10		18097.957	$15493_4 - 33591\frac{3}{3}$
5523.539	8	2	18099.307	$10783\frac{2}{2} - 28882_2$
5523.451	5		18099.596	$21738\frac{2}{2} - 39837_3$
5523.164	25	1	18100.536	$16346\frac{3}{4} - 34447_4$
5522.616	8		18102.332	$15618\frac{3}{3} - 33721_2$
5522.416	3		18102.988	$17959_4 - 36062\frac{3}{4}$
5522.104	8		18104.010	$15863_2 - 33967\frac{3}{3}$
5521.751	200	8	18105.168	$19227\frac{8}{8} - 37332_6$
5520.954	5		18107.781	$17166_5 - 35273\frac{0}{0}$
5518.988	200b	50	18114.232	$16346\frac{3}{4} - 34460_5$
5517.874	3		18117.889	$13962_1 - 32080\frac{1}{1}$
5517.616	4		18118.736	$21165\frac{3}{3} - 39283_4$
5517.455	4		18119.265	$18549_2 - 36668\frac{2}{2}$
5515.845	4		18124.554	$19532_4 - 37656\frac{3}{3}$
5514.873	200b	10	18127.748	$7795\frac{4}{4} - 25923_4$
5513.370	2		18132.690	$17501\frac{0}{0} - 35633_4$
5513.084	2		18133.630	$20566\frac{4}{4} - 38700_4$
5510.495	20	1	18142.150	$15166\frac{3}{3} - 33309_2$
5510.372	15	1	18142.555	$12847_3 - 30990\frac{3}{3}$
5509.993	400	20	18143.803	$9804_5 - 27948\frac{3}{3}$
5508.557	75	5	18148.533	$10414\frac{4}{4} - 28562_4$
5508.050	8	1	18150.203	$21902\frac{4}{4} - 40052_4$
5507.542	100l	2	18151.877	$4961_4 - 23113\frac{3}{3}$
5507.542	100l	2	18151.877	$13175\frac{2}{2} - 31326_4$
5507.295	1		18152.691	$10526\frac{3}{3} - 28679_2$
5506.919	50	5	18153.931	$19588\frac{0}{0} - 37742_6$
5506.676	1		18154.732	$21539\frac{2}{4} - 39694_5$
5506.423	3		18155.566	$18930\frac{3}{3} - 37085_4$
5506.078	5		18156.703	$21165\frac{3}{3} - 39321_3$
5505.934	5		18157.178	$18053\frac{3}{3} - 36210_5$
5505.547	2		18158.455	$19948\frac{3}{3} - 38106_5$
5504.302	200	20	18162.562	$7280_2 - 25442\frac{3}{3}$
5503.698	2		18164.555	$18930\frac{3}{3} - 37094_2$
5503.473	3		18165.298	$17411\frac{3}{3} - 35576_3$
5502.718	5		18167.790	$20566\frac{4}{4} - 38734_3$
5501.701	8	2	18171.148	$12847_3 - 31019\frac{4}{4}$
5501.467	5		18171.921	$22098_4 - 40270\frac{3}{3}$
5501.281	100	10	18172.536	$12114\frac{2}{2} - 30286_1$
5500.032	8		18176.662	$11241\frac{3}{3} - 29418_2$
5499.647	75	5	18177.935	$5563_1 - 23741\frac{1}{1}$
5499.255	300	40	18179.230	$2558_0 - 20737\frac{1}{1}$
5498.716	8	1	18181.012	$17224\frac{2}{2} - 35405_3$
5497.401	2b		18185.361	$17166_5 - 35351\frac{4}{4}$
5496.138	200	10	18189.540	$5563_1 - 23752\frac{2}{2}$
5494.797	2		18193.979	$20566\frac{4}{4} - 38760_4$
5494.619	5		18194.569	$13088_3 - 31283\frac{3}{3}$
5494.330	75	10	18195.526	$8800_4 - 26995\frac{3}{3}$
5493.973	5		18196.708	$17224\frac{2}{2} - 35421_1$
5493.594	10	1	18197.963	$13962_1 - 32160\frac{2}{2}$
5493.196	100	8	18199.282	$6362_2 - 24561\frac{3}{3}$
5492.912	15	3	18200.223	$17847\frac{2}{2} - 36047_2$
5492.642	100	10	18201.117	$7502_3 - 25703\frac{2}{2}$
5492.332	40	20	18202.145	$3687_2 - 21890\frac{3}{3}$
5489.086	75	5	18212.909	$15618\frac{3}{3} - 33831_4$
5488.795	3		18213.874	$16217\frac{2}{2} - 34431_3$
5488.207	4		18215.826	$23015\frac{0}{0} - 41230_4$

TABLE 4. *Classified lines of* Th I – continued

Wavelength (Å)	Intensity		Wavenumber (cm^{-1})	Classification	Wavelength (Å)	Intensity		Wavenumber (cm^{-1})	Classification
	Lamp	Spark				Lamp	Spark		
5487.971	15	1	18216.609	$17224^{2}_{2} - 35440_{3}$	5449.058	1		18346.697	$12847_{3} - 31194^{4}_{4}$
5487.837	15	2	18217.054	$22669^{5}_{5} - 40886_{2}$	5448.272	50	3	18349.344	$13847_{2} - 32197^{5}_{5}$
5487.505	15	2	18218.156	$17959_{4} - 36178^{4}_{4}$	5447.574	2		18351.695	$15493_{4} - 33844^{6}_{6}$
5485.714	4		18224.104	$20054_{2} - 38278^{1}_{1}$	5447.417	2		18352.223	$17224^{2}_{2} - 35576_{3}$
5484.988	50	3	18226.516	$13297_{4} - 31523^{3}_{3}$	5447.071	1		18353.389	$22877^{6}_{6} - 41230_{4}$
5484.556	20	1	18227.951	$12847_{3} - 31075^{2}_{2}$	5446.894	10		18353.986	$15970_{3} - 34324^{2}_{2}$
5484.469	8	1	18228.241	$18069^{3}_{3} - 36297_{4}$	5446.321	8		18355.917	$10526^{3}_{3} - 28882_{2}$
5483.709	2		18230.767	$19588^{6}_{6} - 37819_{4}$	5444.668	2		18361.489	$20054_{2} - 38416^{5}_{5}$
5483.623	3		18231.053	$19516^{2}_{2} - 37748_{2}$	5444.477	5	1	18362.133	$13175^{4}_{4} - 31537_{3}$
5483.143	50	2	18232.649	$13847_{2} - 32080^{1}_{1}$	5444.421	1		18362.322	$22338^{3}_{3} - 40701_{4}$
5482.498	75	8	18234.794	$14204_{5} - 32439^{4}_{4}$	5443.481	1		18365.493	$19039^{2}_{2} - 37404_{3}$
5481.828	8	1	18237.023	$19713_{3} - 37950^{3}_{3}$	5441.213	75	8	18373.148	$18930^{3}_{3} - 37303_{4}$
5481.612	2		18237.741	$19948^{4}_{4} - 38186_{4}$	5441.042	25	1	18373.726	$13297_{4} - 31671^{4}_{4}$
5481.211	5		18239.075	$16351_{0} - 34591^{1}_{1}$	5440.796	3		18374.556	$15970_{3} - 34344^{4}_{4}$
5480.402	4	1	18241.768	$15166^{3}_{3} - 33408_{3}$	5440.600	50	2	18375.218	$7502_{3} - 25877^{3}_{3}$
5479.462	8		18244.897	$19503^{3}_{3} - 37748_{2}$	5440.385	4		18375.944	$19713_{3} - 38088^{2}_{2}$
5479.072	75	75	18246.196	$7280_{2} - 25526^{1}_{1}$	5440.116	4		18376.853	$18930^{3}_{3} - 37307_{3}$
5478.742	50	3	18247.295	$15863_{2} - 34111^{1}_{1}$	5439.495	2		18378.951	$22508^{2}_{2} - 40886_{2}$
5477.550	40	2	18251.266	$14206^{3}_{4} - 32458_{4}$	5438.250	10	1	18383.159	$17411^{3}_{3} - 35794_{4}$
5476.482	20	2	18254.825	$11877^{1}_{1} - 30132_{2}$	5437.958	3		18384.146	$20423^{1}_{1} - 38807_{2}$
5476.482	20	2	18254.825	$17073_{1} - 35328^{1}_{1}$	5437.232	10	1	18386.600	$20566^{2}_{4} - 38953_{5}$
5475.767	4h		18257.208	$19713_{3} - 37970^{2}_{2}$	5436.814	2		18388.014	$20214^{3}_{3} - 38602_{2}$
5474.145	2		18262.618	$18574_{1} - 36837^{1}_{1}$	5436.326	2		18389.665	$19503^{3}_{3} - 37892_{4}$
5473.849	10	1	18263.606	$22163^{4}_{4} - 40426_{4}$	5436.146	1		18390.273	$20566^{2}_{4} - 38956_{4}$
5472.701	8		18267.437	$19516^{2}_{2} - 37784_{2}$	5434.152	100	10	18397.022	$8111_{4} - 26508^{3}_{3}$
5472.535	25	1	18267.991	$19039^{2}_{2} - 37307_{3}$	5433.876	15	2	18397.956	$15166^{3}_{3} - 33564_{3}$
5470.759	150	10	18273.921	$8111_{4} - 26384^{4}_{4}$	5432.127	2		18403.879	$19588^{6}_{6} - 37992_{4}$
5470.145	50	8	18275.972	$18809^{4}_{4} - 37085_{4}$	5431.605	15	2	18405.648	$11802_{2} - 30208^{2}_{2}$
5468.569	1		18281.239	$19503^{3}_{3} - 37784_{2}$	5431.112	150	40	18407.319	$6362_{2} - 24769^{3}_{3}$
5468.166	2		18282.586	$18053^{4}_{4} - 36336_{3}$	5430.807	4		18408.353	$10526^{3}_{3} - 28934_{3}$
5467.403	5	1	18285.138	$22141^{3}_{3} - 40426_{4}$	5430.593	10		18409.078	$11877^{1}_{1} - 30286_{1}$
5467.167	75	4	18285.927	$18011^{6}_{6} - 36297_{4}$	5430.121	3		18410.678	$21575_{2} - 39985^{3}_{3}$
5466.602	5	1	18287.817	$18549_{2} - 36837^{1}_{1}$	5429.105	100	5	18414.124	$17398_{3} - 35812^{3}_{3}$
5465.268	5		18292.281	$15166^{3}_{3} - 33459_{4}$	5428.069	10		18417.638	$19532_{4} - 37950^{4}_{4}$
5464.205	200w	8	18295.839	$2869_{3} - 21165^{3}_{3}$	5427.767	15	1	18418.663	$21143_{5} - 39562^{4}_{4}$
5463.771	50	4	18297.293	$18574_{1} - 36871^{2}_{2}$	5427.618	20	2	18419.168	$13297_{4} - 31716^{6}_{6}$
5463.320	40	10h	18298.803	$17501^{6}_{6} - 35799_{6}$	5427.352	2h		18420.071	$17411^{3}_{3} - 35831_{3}$
5462.809	3b		18300.515	$20054_{2} - 38355^{2}_{2}$	5426.621	15b	1	18422.552	$19532_{4} - 37954^{3}_{3}$
5462.336	50	15	18302.099	$19588^{6}_{6} - 37890_{5}$	5426.574	10b		18422.712	$17959_{4} - 36382^{4}_{4}$
5461.636	5	2b	18304.445	$19588^{6}_{6} - 37892_{4}$	5426.407	50	3	18423.279	$7280_{2} - 25703^{2}_{2}$
5461.314	3		18305.524	$16783^{4}_{4} - 35089_{3}$	5426.170	50	2	18424.084	$14226_{0} - 32650^{1}_{1}$
5461.019	5		18306.513	$15493_{4} - 33799^{4}_{4}$	5424.368	5		18430.204	$12114^{2}_{2} - 30544_{2}$
5459.171	15	3	18312.710	$13847_{2} - 32160^{2}_{2}$	5424.008	300	40	18431.427	$10414^{3}_{3} - 28845_{4}$
5458.492	1		18314.988	$20214^{3}_{3} - 38529_{3}$	5423.501	20b	3	18433.150	$16783^{4}_{4} - 35216_{5}$
5457.289	50	3	18319.025	$10526^{3}_{3} - 28845_{4}$	5422.914	15	1	18435.146	$12847_{3} - 31283^{3}_{3}$
5456.654	8	1	18321.157	$18809^{4}_{4} - 37131_{3}$	5422.847	8b		18435.373	$13088_{3} - 31523^{3}_{3}$
5456.255	40	2	18322.497	$18549_{2} - 36871^{2}_{2}$	5422.250	2		18437.403	$13847_{2} - 32285^{3}_{3}$
5454.919	10	1	18326.984	$22098_{4} - 40425^{5}_{5}$	5421.966	5	1	18438.369	$20322^{6}_{6} - 38760_{4}$
5453.757	1		18330.889	$14465^{2}_{2} - 32796_{3}$	5421.664	100	5	18439.396	$15166^{3}_{3} - 33606_{2}$
5453.686	4	1	18331.128	$18431_{3} - 36762^{3}_{3}$	5420.451	4		18443.522	$20566^{2}_{4} - 39010_{3}$
5453.297	5		18332.435	$16554_{6} - 34886^{6}_{6}$	5419.463	1		18446.884	$18069^{3}_{3} - 36515_{3}$
5452.219	300	40	18336.060	$9804_{5} - 28140^{4}_{4}$	5418.702	3		18449.475	$18699_{2} - 37149^{2}_{2}$
5451.091	15	2	18339.854	$21645_{4} - 39985^{3}_{3}$	5417.808	75	1	18452.520	$11802_{2} - 30255^{3}_{3}$
5450.511	25		18341.806	$15490^{6}_{6} - 33831_{4}$	5417.486	400r	40	18453.616	$3687_{2} - 22141^{3}_{3}$
5450.146	5		18343.034	$19273_{2} - 37616^{1}_{1}$	5415.775	4		18459.446	$17073_{1} - 35533^{2}_{2}$

TABLE 4. *Classified lines of* Th I—continued

Wavelength (Å)	Intensity		Wavenumber (cm^{-1})	Classification
	Lamp	Spark		
5415.711	8		18459.664	$18699_2 - 37159^{\circ}_1$
5415.558	75b		18460.186	$15863_2 - 34324^{\circ}_2$
5415.528	200b	2	18460.288	$7795^{\circ}_4 - 26255_4$
5414.920	5	1	18462.361	$18053^{\circ}_4 - 36515_3$
5414.920	5	1	18462.361	$21738^{\circ}_2 - 40200_3$
5413.917	10	1	18465.781	$8800_4 - 27266^{\circ}_4$
5411.406	3		18474.350	$18930^{\circ}_3 - 37404_3$
5411.311	5		18474.674	$15493_4 - 33967^{\circ}_3$
5410.769	400	15	18476.525	$6362_2 - 24838^{\circ}_1$
5410.313	15b		18478.082	$11802_2 - 30281^{\circ}_1$
5409.603	2		18480.507	$18614^{\circ}_1 - 37094_2$
5409.304	4		18481.528	$14481^{\circ}_8 - 32963_5$
5408.749	20	2h	18483.425	$13297_4 - 31780^{\circ}_3$
5408.192	2		18485.328	$20214^{\circ}_3 - 38700_4$
5407.652	400b	40b	18487.175	$11197^{\circ}_6 - 29684_5$
5407.567	75b	10b	18487.465	$20522^{\circ}_2 - 39010_3$
5406.755	50	4	18490.241	$16217^{\circ}_2 - 34707_3$
5405.787	20	1	18493.552	$18809^{\circ}_4 - 37303_4$
5404.708	15		18497.244	$18809^{\circ}_4 - 37307_3$
5403.200	200	15	18502.407	$16346^{\circ}_4 - 34849_5$
5401.582	8b	1u	18507.949	$15863_2 - 34371^{\circ}_2$
5401.536	10b	1	18508.107	$15493_4 - 34001^{\circ}_3$
5400.775	8		18510.714	$13088_3 - 31599^{\circ}_2$
5400.145	150	5	18512.874	$13945^{\circ}_3 - 32458_4$
5399.620	50	100	18514.674	$11241^{\circ}_3 - 29756_4$
5399.427	8h		18515.336	$21165^{\circ}_3 - 39680_2$
5398.920	400	40	18517.075	$16783^{\circ}_4 - 35300_5$
5398.704	150	4	18517.815	$6362_2 - 24880^{\circ}_1$
5398.510	8	1	18518.481	$19588^{\circ}_6 - 38106_5$
5398.205	150	4	18519.527	$14032^{\circ}_2 - 32551_3$
5397.890	20	1	18520.608	$19532_4 - 38053^{\circ}_3$
5397.731	1		18521.153	$21575_2 - 40096^{\circ}_2$
5397.499	2		18521.949	$15970_3 - 34492^{\circ}_4$
5397.445	5		18522.135	$15166^{\circ}_3 - 33689_2$
5397.139	20l		18523.185	$17354^{\circ}_1 - 35877_2$
5396.109	50	4	18526.720	$16346^{\circ}_4 - 34873_4$
5396.109	50	4	18526.720	$16351_0 - 34878^{\circ}_1$
5394.761	300	20	18531.350	$3865_1 - 22396^{\circ}_1$
5393.972	150	8	18534.060	$7502_3 - 26036^{\circ}_3$
5393.873	50b	3	18534.401	$8111_4 - 26645^{\circ}_6$
5393.873	50b	3	18534.401	$18699_2 - 37234^{\circ}_2$
5392.768	5		18538.198	$22163^{\circ}_4 - 40701_4$
5390.575	2		18545.740	$20214^{\circ}_3 - 38760_4$
5390.429	300	75	18546.242	$7502_3 - 26048^{\circ}_4$
5388.057	300	20	18554.407	$15166^{\circ}_3 - 33721_2$
5386.611	500	20	18559.388	$4961_4 - 23521^{\circ}_3$
5386.611	500	20	18559.388	$11197^{\circ}_6 - 29756_4$
5386.149	2b		18560.980	$3687_2 - 22248^{\circ}_2$
5386.111	20l		18561.110	$15736^{\circ}_1 - 34298_1$
5384.301	100	15	18567.350	$17166_5 - 35733^{\circ}_4$
5382.175	15b	1u	18574.684	$14206^{\circ}_4 - 32781_4$
5381.368	25b	1	18577.470	$10526^{\circ}_3 - 29104_4$
5379.884	8	1	18582.594	$13088_3 - 31671^{\circ}_4$
5379.325	8b		18584.525	$18069^{\circ}_3 - 36653_2$
5379.285	10b	1	18584.663	$18574_1 - 37159^{\circ}_1$
5379.112	300	20	18585.261	$7795^{\circ}_4 - 26380_5$
5378.837	400	40	18586.211	$14481^{\circ}_8 - 33068_6$
5378.169	50	4	18588.520	$17501^{\circ}_8 - 36089_4$
5377.970	10	1	18589.207	$14206^{\circ}_4 - 32796_3$
5376.778	200	50	18593.328	$11241^{\circ}_3 - 29835_3$
5376.600	4		18593.944	$19503^{\circ}_5 - 38097_2$
5376.366	2b		18594.753	$18809^{\circ}_4 - 37404_3$
5375.497	20		18597.759	$19588^{\circ}_6 - 38186_4$
5374.998	50	8h	18599.486	$13175^{\circ}_4 - 31774_3$
5373.394	40	2	18605.038	$17073_1 - 35678^{\circ}_1$
5372.703	200	25	18607.431	$11241^{\circ}_3 - 29849_4$
5372.230	1		18609.069	$21645_4 - 40254^{\circ}_3$
5372.117	3		18609.460	$18431_3 - 37041^{\circ}_4$
5371.999	8		18609.869	$18549_2 - 37159^{\circ}_1$
5371.678	3		18610.981	$7502_3 - 26113^{\circ}_2$
5371.124	50	1	18612.901	$13962_1 - 32575^{\circ}_2$
5371.124	50	1	18612.901	$15970_3 - 34583^{\circ}_3$
5370.709	150	2	18614.339	$0_2 - 18614^{\circ}_1$
5370.522	5		18614.987	$20054_2 - 38669^{\circ}_2$
5369.890	10	1	18617.178	$21077^{\circ}_8 - 39694_5$
5369.447	200	5	18618.714	$6362_2 - 24981^{\circ}_3$
5369.284	200	8	18619.279	$5563_1 - 24182^{\circ}_2$
5368.902	5		18620.604	$20054_2 - 38675^{\circ}_3$
5368.654	10	1	18621.464	$16783^{\circ}_4 - 35405_3$
5367.849	3		18624.257	$21645_4 - 40270^{\circ}_4$
5367.234	5l		18626.391	$22098_4 - 40724^{\circ}_6$
5366.557	2		18628.740	$19516^{\circ}_2 - 38145_3$
5365.913	2		18630.976	$20322^{\circ}_6 - 38953_5$
5365.520	50b	3b	18632.341	$17501^{\circ}_8 - 36133_5$
5364.985	4	1	18634.199	$14465^{\circ}_2 - 33099_3$
5364.682	8b		18635.251	$10783^{\circ}_2 - 29418_2$
5364.447	15	5	18636.067	$17411^{\circ}_3 - 36047_2$
5363.931	5		18637.860	$16351_0 - 34989^{\circ}_1$
5363.880	5		18638.037	$22248^{\circ}_2 - 40886_2$
5362.576	200	5	18642.570	$3865_1 - 22508^{\circ}_2$
5361.156	75	3	18647.507	$4961_4 - 23609^{\circ}_6$
5360.697	8		18649.104	$19039^{\circ}_2 - 37688_3$
5360.150	300	5	18651.007	$3687_2 - 22338^{\circ}_3$
5359.827	100	4	18652.131	$11197^{\circ}_6 - 29849_4$
5359.432	5		18653.506	$17224^{\circ}_2 - 35877_2$
5358.713	300	15	18656.009	$13297_4 - 31953^{\circ}_4$
5358.558	2		18656.548	$16217^{\circ}_2 - 34874_3$
5358.415	3		18657.046	$16783^{\circ}_4 - 35440_3$
5358.081	5		18658.209	$14204_5 - 32862^{\circ}_4$
5357.743	8	1	18659.386	$18574_1 - 37234^{\circ}_2$
5357.338	2		18660.797	$21539^{\circ}_3 - 40200_3$
5356.672	10		18663.117	$19227^{\circ}_8 - 37890_5$
5356.278	1		18664.490	$17398_3 - 36062^{\circ}_4$
5356.137	10		18664.981	$15166^{\circ}_3 - 33831_4$
5355.638	100	3	18666.720	$11877^{\circ}_1 - 30544_2$
5354.602	40	1	18670.332	$2869_3 - 21539^{\circ}_4$
5353.977	5h		18672.511	$21165^{\circ}_3 - 39837_3$
5353.154	2		18675.382	$21594_3 - 40270^{\circ}_4$
5353.154	2		18675.382	$9804_5 - 28480^{\circ}_4$
5353.073	50	4	18675.664	$17398_3 - 36074^{\circ}_3$

TABLE 4. *Classified lines of* Th I—continued

Wavelength (Å)	Intensity		Wavenumber (cm^{-1})	Classification
	Lamp	Spark		
5352.992	50b	15	18675.947	$12847_3 - 31523^{\frac{3}{2}}$
5352.304	3b		18678.347	$22098_4 - 40776^{\frac{3}{2}}$
5352.272	5b		18678.459	$17411^{\frac{5}{2}} - 36089_4$
5351.996	10		18679.423	$8111_4 - 26790^{\frac{3}{2}}$
5351.839	150	8	18679.970	$11601_1 - 30281^{\frac{1}{2}}$
5351.126	200	25	18682.459	$15618^{\frac{5}{2}} - 34301_4$
5350.538	50	4	18684.512	$19532_4 - 38216^{\frac{3}{2}}$
5350.206	50	1	18685.672	$20566^{\frac{3}{2}}_4 - 39252_5$
5349.425	3		18688.400	$13962_1 - 32650^{\frac{1}{2}}$
5349.003	75	3	18689.874	$10414^{\frac{3}{2}}_4 - 29104_4$
5348.532	4	1	18691.520	$22669^{\frac{5}{2}}_3 - 41361_3$
5348.310	50	1	18692.296	$13088_3 - 31780^{\frac{5}{2}}$
5347.973	150	5	18693.474	$4961_4 - 23655^{\frac{3}{2}}$
5346.766	50	2	18697.694	$23015^{\frac{5}{2}} - 41712_5$
5345.241	5		18703.028	$13962_1 - 32665^{\frac{1}{2}}$
5344.308	3		18706.293	$18069^{\frac{5}{2}}_3 - 36775_3$
5343.581	500r	40	18708.838	$3687_2 - 22396^{\frac{1}{2}}$
5343.361	50b		18709.608	$17501^{\frac{5}{2}} - 36210_5$
5341.206	75	3	18717.157	$20566^{\frac{3}{2}}_4 - 39283_4$
5340.650	20l		18719.106	$15863_2 - 34583^{\frac{5}{2}}$
5340.501	200	10	18719.628	$16554_6 - 35273^{\frac{5}{2}}$
5339.896	50	5	18721.749	$18053^{\frac{3}{2}}_4 - 36775_3$
5338.641	40	1	18726.150	$13297_4 - 32023^{\frac{5}{2}}$
5338.366	40	15	18727.114	$15863_2 - 34591^{\frac{1}{2}}$
5338.285	25b	1	18727.399	$10414^{\frac{3}{2}}_4 - 29141_5$
5338.215	50b	1	18727.644	$13847_2 - 32575^{\frac{3}{2}}_2$
5337.502	2		18730.146	$21143_5 - 39873^{\frac{5}{2}}$
5336.785	50	1	18732.662	$14481^{\frac{5}{2}}_6 - 33214_5$
5336.315	40	1	18734.312	$15970_3 - 34704^{\frac{3}{2}}_3$
5335.373	10	3	18737.620	$18011^{\frac{5}{2}}_6 - 36749_6$
5334.145	75l	1	18741.933	$20214^{\frac{3}{2}}_3 - 38956_4$
5333.386	75b	1	18744.601	$5563_1 - 24307^{\frac{3}{2}}_2$
5333.200	8b		18745.254	$19039^{\frac{5}{2}}_2 - 37784_2$
5332.120	2		18749.051	$18069^{\frac{5}{2}}_3 - 36818_2$
5331.749	50	2	18750.356	$11802_2 - 30553^{\frac{3}{2}}_2$
5331.481	8		18751.298	$12847_3 - 31599^{\frac{3}{2}}_2$
5330.517	8		18754.689	$18053^{\frac{3}{2}}_4 - 36808_3$
5330.340	5l		18755.312	$15970_3 - 34725^{\frac{5}{2}}_3$
5330.082	200b	5	18756.220	$7280_2 - 26036^{\frac{5}{2}}$
5330.016	50b		18756.452	$14206^{\frac{3}{2}}_4 - 32963_5$
5329.605	2		18757.899	$18930^{\frac{5}{2}} - 37688_3$
5328.009	8		18763.517	$21143_5 - 39906^{\frac{3}{2}}$
5327.862	10		18764.035	$14032^{\frac{5}{2}}_2 - 32796_3$
5326.976	500r	40	18767.156	$8111_4 - 26878^{\frac{5}{2}}$
5326.278	100b	8	18769.615	$11241^{\frac{5}{2}}_3 - 30011_3$
5326.192	50	2	18769.918	$18011^{\frac{5}{2}}_6 - 36781_5$
5325.434	100	2	18772.590	$11241^{\frac{5}{2}}_3 - 30014_4$
5324.591	10		18775.562	$12114^{\frac{3}{2}}_2 - 30889_1$
5323.851	15l	3	18778.172	$19588^{\frac{5}{2}}_6 - 38366_4$
5323.527	8	1	18779.315	$21645_4 - 40425^{\frac{3}{2}}_4$
5323.406	150	3	18779.741	$19273_2 - 38053^{\frac{5}{2}}$
5322.901	200	5	18781.523	$13088_3 - 31870^{\frac{3}{2}}_2$
5321.873	2		18785.151	$20566^{\frac{3}{2}}_3 - 39351_5$
5321.691	3		18785.793	$19817^{\frac{1}{2}} - 38602_2$
5319.742	8		18792.676	$16783^{\frac{3}{2}}_4 - 35576_3$
5319.023	2		18795.216	$20214^{\frac{3}{2}}_3 - 39010_3$
5318.110	75	3	18798.443	$16783^{\frac{3}{2}}_4 - 35582_5$
5317.912	8		18799.143	$22401_1 - 41200^{\frac{3}{2}}_2$
5317.494	200	4	18800.620	$8243^{\frac{5}{2}}_2 - 27044_3$
5316.783	15		18803.135	$13847_2 - 32650^{\frac{1}{2}}$
5315.834	5		18806.491	$17847^{\frac{5}{2}}_2 - 36653_2$
5315.230	150		18808.629	$14465^{\frac{5}{2}}_2 - 33273_1$
5314.251	8b	1	18812.093	$17073_1 - 35885^{\frac{5}{2}}_2$
5314.205	10b	2	18812.256	$19948^{\frac{3}{2}}_4 - 38760_4$
5314.178	10b		18812.352	$15618^{\frac{5}{2}}_3 - 34431_3$
5313.233	5h		18815.698	$19273_2 - 38088^{\frac{5}{2}}_2$
5312.904	200	15	18816.863	$7280_2 - 26096^{\frac{5}{2}}_3$
5312.781	50	3	18817.298	$11197^{\frac{5}{2}}_6 - 30014_4$
5312.643	150	15	18817.787	$13847_2 - 32665^{\frac{1}{2}}$
5312.532	400	40	18818.180	$5563_1 - 24381^{\frac{3}{2}}_2$
5312.001	400r	25	18820.062	$3687_2 - 22508^{\frac{5}{2}}_2$
5311.870	75b	2	18820.526	$13175^{\frac{3}{2}}_4 - 31995_4$
5311.174	20	1	18822.992	$17224^{\frac{3}{2}}_2 - 36047_2$
5310.432	5		18825.622	$15618^{\frac{5}{2}}_3 - 34444_2$
5309.616	150	5	18828.515	$16217^{\frac{3}{2}}_2 - 35046_1$
5309.052	2h		18830.515	$21594_3 - 40425^{\frac{3}{2}}_4$
5308.808	10	1	18831.381	$22855^{\frac{5}{2}}_3 - 41686_3$
5308.726	10	1	18831.672	$18053^{\frac{3}{2}}_4 - 36885_4$
5308.310	100	10	18833.147	$7280_2 - 26113^{\frac{3}{2}}_2$
5306.987	75	4	18837.842	$13175^{\frac{3}{2}}_4 - 32012_4$
5306.166	5		18840.757	$17959_4 - 36800^{\frac{5}{2}}_3$
5305.304	5l		18843.818	$14465^{\frac{5}{2}}_2 - 33309_2$
5303.557	20	1	18850.025	$16783^{\frac{3}{2}}_4 - 35633_4$
5303.483	75	3	18850.288	$12114^{\frac{3}{2}}_2 - 30964_3$
5303.334	50	2	18850.818	$13945^{\frac{5}{2}}_3 - 32796_3$
5303.162	40	1	18851.429	$15493_4 - 34344^{\frac{3}{2}}_4$
5302.779	1		18852.791	$19532_4 - 38385^{\frac{5}{2}}_6$
5302.407	10		18854.114	$18930^{\frac{5}{2}}_3 - 37784_2$
5300.524	300	5	18860.811	$7502_3 - 26363^{\frac{5}{2}}_2$
5300.321	4		18861.534	$15863_2 - 34725^{\frac{5}{2}}_3$
5299.787	2		18863.434	$19503^{\frac{5}{2}}_3 - 38366_4$
5299.376	2		18864.897	$13088_3 - 31953^{\frac{3}{2}}_4$
5298.714	8	2	18867.254	$19713_3 - 38580^{\frac{3}{2}}_4$
5298.559	75	2	18867.806	$10783^{\frac{3}{2}}_2 - 29650_2$
5298.284	200	4	18868.785	$2869_3 - 21738^{\frac{5}{2}}_2$
5297.844	100b	5	18870.352	$16346^{\frac{3}{2}}_3 - 35216_5$
5297.746	300b	15	18870.701	$8800_4 - 27670^{\frac{5}{2}}_3$
5296.845	50	2	18873.911	$18011^{\frac{5}{2}}_6 - 36885_4$
5296.279	300	5	18875.928	$9804_5 - 28680^{\frac{3}{2}}_4$
5295.674	50b	4b	18878.085	$17959_4 - 36837^{\frac{5}{2}}_6$
5295.089	50	1	18880.170	$11877^{\frac{1}{2}} - 30758_2$
5294.697	25b	1	18881.568	$15970_3 - 34851^{\frac{3}{2}}_2$
5294.397	200	3	18882.638	$7502_3 - 26384^{\frac{3}{2}}_4$
5294.070	50	1	18883.804	$19532_4 - 38416^{\frac{5}{2}}_3$
5293.435	3	1	18886.070	$17411^{\frac{5}{2}}_3 - 36297_4$
5293.137	50	1	18887.133	$21539^{\frac{3}{2}}_4 - 40426_4$
5293.077	3		18887.347	$21165^{\frac{5}{2}}_3 - 40052_4$
5292.666	3		18888.814	$18930^{\frac{5}{2}}_3 - 37819_4$
5292.077	10		18890.916	$11241^{\frac{5}{2}}_3 - 30132_2$
5291.818	200	5	18891.840	$10526^{\frac{5}{2}}_3 - 29418_2$

TABLE 4. *Classified lines of* Th I—continued

Wavelength (Å)	Intensity		Wavenumber (cm^{-1})	Classification
	Lamp	Spark		
5291.638	3		18892.483	$14206\frac{0}{4} - 33099_3$
5289.624	75	2	18899.676	$13297_4 - 32197\frac{0}{3}$
5287.648	3		18906.739	$13847_2 - 32754\frac{0}{3}$
5285.183	3h		18915.557	$20922\frac{0}{2} - 39837_3$
5283.697	50	2	18920.877	$11802_2 - 30723\frac{0}{1}$
5282.552	15		18924.978	$17411\frac{0}{5} - 36336_3$
5282.402	200	4	18925.515	$14465\frac{0}{2} - 33390_1$
5281.070	300	2	18930.288	$0_2 - 18930\frac{0}{3}$
5280.520	50		18932.260	$16217\frac{0}{2} - 35149_2$
5280.346	50	2	18932.884	$12847_3 - 31780\frac{0}{3}$
5279.766	2		18934.964	$14226_0 - 33161\frac{0}{1}$
5279.200	50	1	18936.994	$15493_4 - 34430\frac{0}{3}$
5277.404	10		18943.438	$14465\frac{0}{2} - 33408_3$
5277.341	3		18943.665	$19273_2 - 38216\frac{0}{3}$
5277.147	75	1	18944.361	$6362_2 - 25306\frac{0}{2}$
5276.198	2		18947.768	$21252\frac{0}{2} - 40200_3$
5274.948	8	1	18952.258	$11601_1 - 30553\frac{0}{2}$
5274.581	5		18953.577	$20566\frac{0}{4} - 39520_4$
5274.391	75	3	18954.260	$16346\frac{0}{4} - 35300_5$
5274.121	200	5	18955.230	$4961_4 - 23916\frac{0}{3}$
5273.595	2		18957.121	$15490\frac{0}{6} - 34447_4$
5273.531	40		18957.351	$18699_2 - 37656\frac{0}{3}$
5273.134	100b	10	18958.778	$11802_2 - 30761\frac{0}{3}$
5272.929	100	20	18959.515	$6362_2 - 25321\frac{0}{3}$
5272.092	5		18962.525	$18930\frac{0}{3} - 37892_4$
5271.023	20	3	18966.371	$17166_5 - 36132\frac{0}{6}$
5270.832	50	2	18967.058	$19986\frac{0}{6} - 38953_5$
5269.794	75	4	18970.794	$15490\frac{0}{6} - 34460_5$
5268.539	2		18975.313	$21077\frac{0}{6} - 40052_4$
5268.158	2		18976.685	$16351_0 - 35328\frac{0}{1}$
5266.829	2		18981.474	$12114\frac{0}{2} - 31095_1$
5266.710	300	15	18981.902	$3687_2 - 22669\frac{0}{3}$
5266.073	1		18984.199	$17398_3 - 36382\frac{0}{4}$
5265.081	10		18987.775	$15863_2 - 34851\frac{0}{2}$
5264.335	20		18990.466	$19817\frac{0}{1} - 38807_2$
5263.892	15b	1	18992.064	$13962_1 - 32954\frac{0}{2}$
5262.621	50b	4	18996.651	$13297_4 - 32294\frac{0}{4}$
5262.024	5	1	18998.806	$15493_4 - 34492\frac{0}{4}$
5261.530	50b	1	19000.590	$15166\frac{0}{3} - 34167_3$
5261.474	50b	3	19000.792	$7795\frac{0}{4} - 26796_3$
5260.106	200	8	19005.734	$7502_3 - 26508\frac{0}{3}$
5259.779	75	2	19006.915	$7280_2 - 26287\frac{0}{1}$
5259.587	20	1	19007.609	$14206\frac{0}{4} - 33214_5$
5259.353	3		19008.455	$19948\frac{0}{4} - 38956_4$
5258.908	8		19010.063	$11802_2 - 30812\frac{0}{2}$
5258.779	5		19010.530	$16783\frac{0}{4} - 35794_4$
5258.361	400r	25	19012.041	$3865_1 - 22877\frac{0}{1}$
5258.212	150b	3	19012.580	$11601_1 - 30613\frac{0}{6}$
5257.607	4		19014.767	$15863_2 - 34878\frac{0}{1}$
5257.051	10	1	19016.778	$18069\frac{0}{3} - 37085_4$
5255.921	10b		19020.867	$2869_3 - 21890\frac{0}{3}$
5255.576	100	3	19022.115	$12847_3 - 31870\frac{0}{2}$
5254.262	150l	8	19026.872	$13175\frac{0}{4} - 32202_5$
5254.111	40	4	19027.419	$12114\frac{0}{2} - 31141_3$
5253.682	50	2	19028.973	$17398_3 - 36427\frac{0}{3}$

Wavelength (Å)	Intensity		Wavenumber (cm^{-1})	Classification
	Lamp	Spark		
5253.534	8		19029.509	$20322\frac{0}{6} - 39351_5$
5252.568	15		19033.009	$2869_3 - 21902\frac{0}{4}$
5251.373	50l	2	19037.340	$18699_2 - 37736\frac{0}{2}$
5250.874	50	1	19039.149	$0_2 - 19039\frac{0}{2}$
5250.171	10		19041.698	$18574_1 - 37616\frac{0}{1}$
5248.587	10		19047.445	$16783\frac{0}{4} - 35831_3$
5248.199	20		19048.853	$17959_4 - 37008\frac{0}{6}$
5247.361	40		19051.895	$10783\frac{0}{2} - 29835_3$
5247.200	50b	2	19052.480	$8800_4 - 27852\frac{0}{6}$
5245.698	10		19057.935	$19039\frac{0}{2} - 38097_2$
5244.647	8b	1	19061.754	$19948\frac{0}{4} - 39010_3$
5244.594	10b	1	19061.947	$18069\frac{0}{3} - 37131_3$
5244.594	10b	1	19061.947	$18930\frac{0}{3} - 37992_4$
5243.746	50	1	19065.029	$14243\frac{0}{1} - 33309_2$
5243.406	8		19066.265	$14204_5 - 33270\frac{0}{4}$
5243.237	3		19066.880	$18549_2 - 37616\frac{0}{1}$
5243.120	3		19067.305	$14032\frac{0}{2} - 33099_3$
5242.687	20		19068.880	$20214\frac{0}{3} - 39283_4$
5241.858	50	20	19071.896	$13088_3 - 32160\frac{0}{2}$
5241.223	8	1	19074.206	$17411\frac{0}{5} - 36485_2$
5241.153	8	1	19074.461	$18011\frac{0}{6} - 37085_4$
5240.789	3		19075.786	$19713_3 - 38788\frac{0}{3}$
5240.789	3		19075.786	$19713_3 - 38788\frac{0}{3}$
5240.341	2		19077.417	$18053\frac{0}{4} - 37131_3$
5239.984	2		19078.717	$21645_4 - 40724\frac{0}{6}$
5239.550	50	3	19080.297	$6362_2 - 25442\frac{0}{3}$
5239.079	2		19082.012	$19273_2 - 38355\frac{0}{2}$
5238.812	75h	10	19082.985	$7280_2 - 26363\frac{0}{2}$
5237.989	3		19085.983	$19516\frac{0}{2} - 38602_2$
5237.229	5	1	19088.753	$15618\frac{0}{3} - 34707_3$
5236.766	10	1	19090.440	$17398_3 - 36488\frac{0}{2}$
5235.720	4	1	19094.254	$16346\frac{0}{4} - 35440_3$
5234.243	75		19099.642	$14465\frac{0}{2} - 33564_3$
5234.107	100	1	19100.138	$8243\frac{0}{2} - 27343_3$
5232.841	8		19104.759	$17411\frac{0}{5} - 36515_3$
5232.341	40b	2	19106.585	$19039\frac{0}{2} - 38145_3$
5232.278	25b	1	19106.815	$13847_2 - 32954\frac{0}{2}$
5231.800	40	1	19108.561	$13088_3 - 32197\frac{0}{3}$
5231.659	3		19109.076	$17166_5 - 36275\frac{0}{6}$
5231.160	1000r	40	19110.899	$2558_0 - 21668\frac{0}{1}$
5230.012	15		19115.093	$17073_1 - 36188\frac{0}{2}$
5228.996	75	1	19118.807	$13175\frac{0}{4} - 32293_5$
5227.904	8		19122.801	$11601_1 - 30723\frac{0}{1}$
5227.461	8		19124.421	$10526\frac{0}{3} - 29650_2$
5227.078	40		19125.823	$11802_2 - 30928\frac{0}{1}$
5226.527	50		19127.839	$9804_5 - 28932\frac{0}{4}$
5225.755	5	1	19130.665	$21645_4 - 40776\frac{0}{4}$
5225.518	4		19131.532	$12114\frac{0}{2} - 31245_2$
5224.928	3		19133.693	$18614\frac{0}{1} - 37748_2$
5224.693	5		19134.553	$15166\frac{0}{3} - 34301_4$
5222.909	2		19141.089	$14465\frac{0}{2} - 33606_2$
5222.765	40	1	19141.617	$13297_4 - 32439\frac{0}{4}$
5222.268	50	1	19143.438	$14247\frac{0}{6} - 33390_1$
5220.928	100	1	19148.352	$8800_4 - 27948\frac{0}{4}$
5220.707	100	1	19149.162	$8111_4 - 27260\frac{0}{3}$

TABLE 4. *Classified lines of* Th I—continued

Wavelength (Å)	Intensity		Wavenumber (cm^{-1})	Classification
	Lamp	Spark		
5220.131	4		19151.275	$12114\frac{3}{2} - 31265_3$
5219.357	20	1	19154.115	$13945\frac{3}{2} - 33099_3$
5219.110	400r	15	19155.022	$8111_4 - 27266\frac{4}{2}$
5218.272	2		19158.098	$18053\frac{4}{2} - 37211_5$
5217.284	8h		19161.726	$21539\frac{4}{2} - 40701_4$
5217.109	2		19162.368	$18574_1 - 37736\frac{2}{2}$
5216.683	20		19163.933	$6362_2 - 25526\frac{1}{2}$
5215.762	5		19167.317	$3687_2 - 22855\frac{3}{2}$
5214.414	4	1	19172.272	$19588\frac{6}{2} - 38760_4$
5213.930	2		19174.052	$18431_3 - 37605\frac{4}{2}$
5213.485	75	2	19175.688	$11197\frac{6}{2} - 30372_6$
5213.350	400	5	19176.185	$7795\frac{4}{2} - 26971_4$
5212.681	15	1	19178.646	$10783\frac{2}{2} - 29961_1$
5211.668	4		19182.374	$18809\frac{4}{2} - 37992_4$
5211.231	600r	25	19183.982	$3865_1 - 23049\frac{1}{2}$
5210.253	10	1	19187.583	$11802_2 - 30990\frac{5}{2}$
5210.185	8	1	19187.834	$16217\frac{2}{2} - 35405_3$
5209.724	300	3	19189.531	$3687_2 - 22877\frac{1}{2}$
5208.087	8		19195.563	$13847_2 - 33043\frac{3}{2}$
5207.803	100	2	19196.610	$13088_3 - 32285\frac{5}{2}$
5207.670	20	1	19197.100	$19503\frac{3}{2} - 38700_4$
5207.084	50	1	19199.261	$13962_1 - 33161\frac{1}{2}$
5206.990	3		19199.607	$17959_4 - 37159\frac{5}{2}$
5206.800	50	3	19200.308	$18011\frac{6}{2} - 37211_5$
5206.410	5		19201.746	$14206\frac{4}{2} - 33408_3$
5205.928	15	2	19203.524	$16217\frac{2}{2} - 35421_1$
5205.154	200	2	19206.379	$8111_4 - 27317\frac{5}{2}$
5203.850	300	25	19211.192	$14206\frac{4}{2} - 33418_4$
5203.850	300	25	19211.192	$15493_4 - 34704\frac{3}{2}$
5203.641	5		19211.964	$11601_1 - 30812\frac{2}{2}$
5202.410	5		19216.510	$17166_5 - 36382\frac{4}{2}$
5202.007	75	3	19217.998	$11877\frac{1}{2} - 31095_1$
5199.323	300b	3	19227.919	$7280_2 - 26508\frac{3}{2}$
5199.164	1000r	25b	19228.507	$3865_1 - 23093\frac{2}{2}$
5198.802	500	100d	19229.846	$10526\frac{3}{2} - 29756_4$
5198.162	4		19232.213	$15493_4 - 34725\frac{3}{2}$
5197.577	8		19234.378	$18069\frac{5}{2} - 37303_4$
5197.236	200	5	19235.640	$16346\frac{4}{2} - 35582_5$
5196.574	5		19238.090	$18069\frac{5}{2} - 37307_3$
5195.815	500	8	19240.900	$4961_4 - 24202\frac{4}{2}$
5195.581	15	4	19241.767	$14032\frac{2}{2} - 33273_1$
5194.456	400	12	19245.934	$9804_5 - 29050\frac{6}{2}$
5193.946	75	2	19247.824	$17501\frac{6}{2} - 36749_6$
5193.636	8b		19248.973	$7795\frac{4}{2} - 27044_3$
5193.406	15	1	19249.825	$18053\frac{4}{2} - 37303_4$
5192.746	50	1	19252.272	$14206\frac{4}{2} - 33459_4$
5192.409	4	1	19253.522	$18053\frac{4}{2} - 37307_3$
5192.176	5		19254.385	$15618\frac{3}{2} - 34873_4$
5191.986	20	1	19255.090	$15618\frac{3}{2} - 34874_3$
5191.919	2		19255.339	$18699_2 - 37954\frac{3}{2}$
5191.715	4	1	19256.095	$14465\frac{2}{2} - 33721_2$
5191.487	3		19256.941	$20423\frac{1}{2} - 39680_2$
5191.337	15		19257.497	$19503\frac{3}{2} - 38760_4$
5190.368	8		19261.093	$17224\frac{2}{2} - 36485_2$
5190.219	5		19261.645	$21165\frac{3}{2} - 40426_4$
5189.464	3		19264.448	$15166\frac{3}{2} - 34431_3$
5189.008	50	1	19266.141	$19986\frac{6}{2} - 39252_5$
5187.948	40		19270.077	$10414\frac{4}{2} - 29684_5$
5187.773	40	1	19270.727	$15970_3 - 35240\frac{3}{2}$
5187.336	300	200	19272.350	$2869_3 - 22141\frac{3}{2}$
5187.166	100	75b	19272.982	$11802_2 - 31075\frac{2}{2}$
5186.412	100	75	19275.784	$5563_1 - 24838\frac{1}{2}$
5185.895	15	2	19277.706	$15166\frac{3}{2} - 34444_2$
5185.215	100		19280.234	$15166\frac{3}{2} - 34447_4$
5184.803	10		19281.766	$21143_5 - 40425\frac{4}{2}$
5184.452	100	3	19283.071	$13175\frac{4}{2} - 32458_4$
5183.336	50	3	19287.223	$16346\frac{4}{2} - 35633_4$
5183.086	50	15	19288.153	$7502_3 - 26790\frac{4}{2}$
5182.405	5		19290.688	$19516\frac{2}{2} - 38807_2$
5182.135	3	1	19291.693	$17224\frac{2}{2} - 36515_3$
5181.553	8	1	19293.860	$2869_3 - 22163\frac{4}{2}$
5180.718	100	3	19296.969	$18809\frac{4}{2} - 38106_5$
5180.406	3		19298.131	$4961_4 - 24259\frac{4}{2}$
5180.184	4b		19298.958	$17354\frac{1}{2} - 36653_2$
5179.140	20		19302.849	$11241\frac{3}{2} - 30544_2$
5178.852	3		19303.922	$19948\frac{4}{2} - 39252_5$
5178.691	5h		19304.522	$19503\frac{3}{2} - 38807_2$
5178.486	150	3	19305.286	$20214\frac{3}{2} - 39520_4$
5178.338	75	2	19305.838	$16783\frac{4}{2} - 36089_4$
5177.621	100	3	19308.512	$10526\frac{3}{2} - 29835_3$
5177.482	100	2	19309.030	$15736\frac{1}{2} - 35046_1$
5176.961	500	50	19310.973	$11197\frac{6}{2} - 30508_5$
5176.546	8	3	19312.521	$12847_3 - 32160\frac{2}{2}$
5176.402	75	1	19313.059	$4961_4 - 24274\frac{6}{2}$
5176.297	5		19313.450	$22399\frac{6}{2} - 41712_5$
5176.145	8		19314.017	$13847_2 - 33161\frac{1}{2}$
5175.911	100	3	19314.891	$12114\frac{3}{2} - 31429_1$
5175.323	100	2	19317.085	$5563_1 - 24880\frac{1}{2}$
5174.367	100	3	19320.654	$14206\frac{4}{2} - 33527_4$
5174.242	100	75	19321.121	$18011\frac{6}{2} - 37332_6$
5173.838	50		19322.629	$10526\frac{3}{2} - 29849_4$
5173.671	200	2	19323.253	$8243\frac{2}{2} - 27566_2$
5172.691	40		19326.914	$16351_0 - 35678\frac{1}{2}$
5172.479	75	3	19327.706	$11601_1 - 30928\frac{1}{2}$
5172.212	10		19328.704	$21902\frac{4}{2} - 41230_4$
5170.631	1		19334.614	$13962_1 - 33297\frac{2}{2}$
5170.569	1		19334.846	$21645_4 - 40980\frac{5}{2}$
5170.300	8		19335.852	$18809\frac{4}{2} - 38145_3$
5169.019	4		19340.643	$8800_4 - 28140\frac{4}{2}$
5168.920	100	1	19341.014	$6362_2 - 25703\frac{2}{2}$
5168.583	100	2	19342.275	$10414\frac{4}{2} - 29756_4$
5166.650	40b	1	19349.511	$10783\frac{2}{2} - 30132_2$
5166.618	10b		19349.631	$16783\frac{4}{2} - 36133_5$
5166.392	4		19350.477	$13088_3 - 32439\frac{4}{2}$
5166.245	50	1	19351.028	$18053\frac{4}{2} - 37404_3$
5165.610	100	5	19353.407	$18699_2 - 38053\frac{3}{2}$
5165.055	20	3	19355.486	$11197\frac{6}{2} - 30552_4$
5164.975	20	1	19355.786	$14204_5 - 33560\frac{4}{2}$
5164.789	3l	1	19356.483	$22399\frac{6}{2} - 41755_4$
5164.400	50	2	19357.941	$14206\frac{4}{2} - 33564_3$

TABLE 4. *Classified lines of* Th I – continued

Wavelength (Å)	Intensity		Wavenumber (cm^{-1})	Classification
	Lamp	Spark		
5164.206	40	1	19358.669	$14032\frac{2}{2} - 33390_1$
5164.108	40	1	19359.036	$16217\frac{2}{2} - 35576_3$
5163.459	400	250	19361.469	$3687_2 - 23049\frac{1}{1}$
5163.236	25	1	19362.305	$14243\frac{1}{1} - 33606_2$
5162.852	8		19363.745	$13945\frac{3}{3} - 33309_2$
5162.740	4		19364.166	$17411\frac{3}{3} - 36775_3$
5162.673	15	1	19364.417	$17398_3 - 36762\frac{3}{3}$
5162.553	50	8	19364.867	$19588\frac{0}{0} - 38953_5$
5162.356	75	5	19365.606	$19986\frac{0}{0} - 39351_5$
5161.540	400	8	19368.667	$8243\frac{2}{2} - 27612_3$
5160.718	300	50	19371.752	$7280_2 - 26651\frac{2}{2}$
5160.280	5		19373.396	$19948\frac{4}{4} - 39321_3$
5159.621	100	2	19375.871	$7502_3 - 26878\frac{3}{3}$
5159.451	20	2	19376.509	$13175\frac{4}{4} - 32551_3$
5159.339	15		19376.930	$15863_2 - 35240\frac{3}{3}$
5158.605	800r	50	19379.687	$2869_3 - 22248\frac{2}{2}$
5157.426	100	2	19384.117	$17501\frac{0}{0} - 36885_4$
5154.243	500	40	19396.088	$7795\frac{4}{4} - 27191_5$
5153.975	4b		19397.096	$17411\frac{3}{3} - 36808_3$
5152.305	4		19403.383	$19948\frac{4}{4} - 39351_5$
5151.612	500	15	19405.993	$3687_2 - 23093\frac{2}{2}$
5151.382	50	1	19406.860	$17411\frac{3}{3} - 36818_2$
5150.701	50	2	19409.426	$11241\frac{3}{3} - 30651_3$
5149.816	100	10	19412.761	$15736\frac{1}{1} - 35149_2$
5149.210	300	3	19415.046	$13088_3 - 32503\frac{2}{2}$
5147.135	40	1	19422.873	$12114\frac{2}{2} - 31537_3$
5146.059	200	10	19426.934	$16783\frac{4}{4} - 36210_5$
5143.916	300b	15	19435.027	$10414\frac{4}{4} - 29849_4$
5143.823	150b	4	19435.379	$14226_0 - 33662\frac{1}{1}$
5141.264	50	1	19445.052	$14243\frac{1}{1} - 33689_2$
5140.983	3	1	19446.115	$12847_3 - 32294\frac{4}{4}$
5140.771	200b	5	19446.917	$6362_2 - 25809\frac{1}{1}$
5140.716	100b	20b	19447.125	$13847_2 - 33294\frac{3}{3}$
5140.543	50	1	19447.779	$16346\frac{4}{4} - 35794_4$
5140.126	40	50	19449.357	$13847_2 - 33297\frac{2}{2}$
5139.314	3		19452.430	$18069\frac{3}{3} - 37521_3$
5138.961	15		19453.766	$19503\frac{3}{3} - 38956_4$
5138.934	15		19453.868	$21902\frac{4}{4} - 41356_5$
5138.086	8	1	19457.079	$13297_4 - 32754\frac{3}{3}$
5137.531	10b		19459.181	$21902\frac{4}{4} - 41361_3$
5137.475	150b	1	19459.393	$4961_4 - 24421\frac{3}{3}$
5137.375	2		19459.772	$17166_5 - 36625\frac{0}{0}$
5137.357	1		19459.840	$17166_5 - 36625\frac{0}{0}$
5137.300	3		19460.056	$17847\frac{2}{2} - 37307_3$
5136.396	15		19463.481	$17354\frac{1}{1} - 36818_2$
5136.121	100	1	19464.523	$13962_1 - 33427\frac{2}{2}$
5136.067	10b		19464.728	$15863_2 - 35328\frac{1}{1}$
5135.856	5	1	19465.527	$20214\frac{3}{3} - 39680_2$
5135.585	75	1	19466.554	$19532_4 - 38998\frac{3}{3}$
5134.746	300	3	19469.735	$2869_3 - 22338\frac{3}{3}$
5134.572	50	2	19470.395	$15618\frac{3}{3} - 35089_3$
5134.337	15	1	19471.286	$21890\frac{3}{3} - 41361_3$
5133.922	3		19472.860	$13945\frac{3}{3} - 33418_4$
5133.751	50	1	19473.509	$17398_3 - 36871\frac{2}{2}$
5133.602	5		19474.074	$17411\frac{3}{3} - 36885_4$
5133.389	10		19474.882	$11601_1 - 31075\frac{2}{2}$
5132.748	50	1	19477.314	$14243\frac{1}{1} - 33721_2$
5131.992	150	1	19480.183	$11802_2 - 31283\frac{3}{3}$
5131.257	5		19482.973	$17073_1 - 36556\frac{1}{1}$
5130.814	20b		19484.656	$16346\frac{4}{4} - 35831_3$
5130.777	20b		19484.796	$10526\frac{3}{3} - 30011_3$
5130.235	150	2	19486.855	$13088_3 - 32575\frac{2}{2}$
5129.988	8		19487.793	$10526\frac{3}{3} - 30014_4$
5129.656	20		19489.054	$21645_4 - 41134\frac{4}{4}$
5129.206	50	1	19490.764	$19039\frac{2}{2} - 38529_3$
5128.891	2		19491.961	$15970_3 - 35462\frac{3}{3}$
5128.574	20		19493.166	$19516\frac{2}{2} - 39010_3$
5128.489	300	5	19493.489	$7502_3 - 26995\frac{3}{3}$
5125.950	200	3	19503.144	$0_2 - 19503\frac{3}{3}$
5125.827	50b	1	19503.612	$18549_2 - 38053\frac{3}{3}$
5125.797	50b	2	19503.727	$10783\frac{2}{2} - 30286_1$
5125.307	5b		19505.591	$21077\frac{0}{0} - 40582_5$
5124.925	3		19507.045	$19503\frac{3}{3} - 39010_3$
5123.239	50	3	19513.464	$16783\frac{4}{4} - 36297_4$
5123.131	50		19513.876	$13945\frac{3}{3} - 33459_4$
5123.006	8		19514.352	$18574_1 - 38088\frac{2}{2}$
5122.226	10		19517.323	$18699_2 - 38216\frac{3}{3}$
5121.953	4		19518.364	$18431_3 - 37950\frac{2}{2}$
5121.699	2		19519.332	$22508\frac{2}{2} - 42027_2$
5120.593	4		19523.548	$22163\frac{4}{4} - 41686_3$
5119.867	20		19526.316	$14247\frac{0}{0} - 33773_1$
5119.000	1		19529.623	$14243\frac{1}{1} - 33773_1$
5118.176	15		19532.767	$14032\frac{2}{2} - 33564_3$
5116.661	2h		19538.551	$18431_3 - 37970\frac{2}{2}$
5115.045	500r	40	19544.724	$3865_1 - 23410\frac{0}{0}$
5114.065	8	1	19548.469	$7795\frac{4}{4} - 27343_3$
5113.733	2		19549.738	$22163\frac{4}{4} - 41712_5$
5113.050	10	3	19552.349	$16783\frac{4}{4} - 36336_3$
5111.911	4		19556.706	$18809\frac{4}{4} - 38366_4$
5111.685	25	2	19557.570	$17847\frac{2}{2} - 37404_3$
5111.280	150	4	19559.120	$7502_3 - 27061\frac{2}{2}$
5111.063	200	5	19559.951	$8111_4 - 27670\frac{3}{3}$
5110.555	150	2	19561.895	$13175\frac{4}{4} - 32737_5$
5110.216	25		19563.192	$15970_3 - 35533\frac{2}{2}$
5110.056	50	2	19563.805	$19039\frac{2}{2} - 38602_2$
5109.735	200	3	19565.034	$13297_4 - 32862\frac{4}{4}$
5107.970	3		19571.794	$19948\frac{4}{4} - 39520_4$
5107.338	5		19574.216	$14032\frac{2}{2} - 33606_2$
5106.023	5		19579.257	$13847_2 - 33427\frac{2}{2}$
5105.242	5		19582.252	$13945\frac{3}{3} - 33527_4$
5102.509	3		19592.741	$22163\frac{4}{4} - 41755_4$
5102.228	2		19593.820	$17224\frac{2}{2} - 36818_2$
5101.799	40	1	19595.468	$14204_5 - 33799\frac{3}{3}$
5101.344	40	1	19597.215	$10414\frac{4}{4} - 30011_3$
5101.130	300	4	19598.037	$7280_2 - 26878\frac{3}{3}$
5100.621	300b		19599.993	$4961_4 - 24561\frac{3}{3}$
5100.573	150b	2b	19600.178	$10414\frac{4}{4} - 30014_4$
5099.030	50	1	19606.109	$10526\frac{3}{3} - 30132_2$
5098.933	150	2	19606.482	$13175\frac{4}{4} - 32781_4$
5097.644	8	1	19611.439	$17959_4 - 37571\frac{0}{0}$

TABLE 4. *Classified lines of* Th I—continued

Wavelength (Å)	Intensity		Wavenumber (cm^{-1})	Classification
	Lamp	Spark		
5097.039	2		19613.767	$16217\frac{2}{2} - 35831_3$
5096.484	500	5	19615.903	$3865_1 - 23481\frac{0}{1}$
5095.644	5	1	19619.137	$18069\frac{3}{3} - 37688_3$
5095.539	3		19619.541	$13945\frac{3}{3} - 33564_3$
5095.149	20h		19621.043	$13175\frac{4}{4} - 32796_3$
5095.074	300	50	19621.331	$18431_3 - 38053\frac{3}{3}$
5094.546	20	3	19623.365	$21738\frac{2}{2} - 41361_3$
5094.334	2		19624.182	$21077\frac{0}{0} - 40701_4$
5094.127	200	50	19624.979	$14206\frac{4}{4} - 33831_4$
5092.023	1		19633.088	$21143_5 - 40776\frac{4}{4}$
5091.641	2h		19634.561	$17166_5 - 36800\frac{4}{4}$
5090.548	300	2	19638.777	$2869_3 - 22508\frac{2}{2}$
5090.052	400	5	19640.690	$14204_5 - 33844\frac{0}{0}$
5086.180	150	3	19655.642	$12847_3 - 32503\frac{2}{2}$
5085.839	15	1	19656.960	$14032\frac{2}{2} - 33689_2$
5085.761	4		19657.261	$18431_3 - 38088\frac{2}{2}$
5084.997	200	8	19660.215	$12114\frac{2}{2} - 31774_3$
5084.800	150		19660.976	$13945\frac{3}{3} - 33606_2$
5084.038	15	1	19663.923	$19588\frac{0}{0} - 39252_5$
5083.516	1		19665.942	$13088_3 - 32754\frac{3}{3}$
5082.625	100	8	19669.390	$15863_2 - 35533\frac{2}{2}$
5082.005	20	8	19671.789	$19503\frac{3}{3} - 39174_3$
5081.778	15	2	19672.668	$18930\frac{3}{3} - 38602_2$
5081.449	200	4	19673.942	$6362_2 - 26036\frac{3}{3}$
5081.326	2		19674.418	$17847\frac{2}{2} - 37521_3$
5080.157	1		19678.945	$18069\frac{3}{3} - 37748_2$
5079.911	15	2	19679.898	$8800_4 - 28480\frac{4}{4}$
5078.848	40	1	19684.017	$15736\frac{1}{1} - 35421_1$
5077.510	5	1	19689.204	$14032\frac{2}{2} - 33721_2$
5075.955	50	1	19695.236	$19039\frac{2}{2} - 38734_3$
5074.807	10		19699.691	$13962_1 - 33662\frac{1}{1}$
5074.649	25	1	19700.304	$7795\frac{4}{4} - 27495_4$
5072.885	150	1	19707.155	$15166\frac{3}{3} - 34874_3$
5070.781	75	2	19715.332	$18069\frac{3}{3} - 37784_2$
5070.456	50	1	19716.595	$18699_2 - 38416\frac{3}{3}$
5069.626	1		19719.823	$17411\frac{3}{3} - 37131_3$
5069.337	200	4	19720.948	$16554_6 - 36275\frac{0}{0}$
5069.093	20	2	19721.897	$21165\frac{3}{3} - 40886_2$
5068.829	25	2	19722.924	$11241\frac{3}{3} - 30964_3$
5067.974	1000r	75	19726.251	$7795\frac{4}{4} - 27521_4$
5067.807	20		19726.901	$15490\frac{0}{0} - 35216_5$
5067.667	5	5	19727.446	$12847_3 - 32575\frac{2}{2}$
5067.138	50	2	19729.506	$18549_2 - 38278\frac{1}{1}$
5066.959	80	20	19730.203	$20322\frac{0}{0} - 40052_4$
5066.777	200	40	19730.911	$18011\frac{0}{0} - 37742_6$
5066.461	4		19732.142	$16783\frac{4}{4} - 36515_3$
5066.134	300	10	19733.416	$11197\frac{0}{0} - 30930_6$
5065.190	300	5	19737.093	$8243\frac{2}{2} - 27980_3$
5064.945	300r	8	19738.048	$3865_1 - 23603\frac{2}{2}$
5064.601	300	40	19739.389	$4961_4 - 24701\frac{0}{0}$
5064.004	100b	2d	19741.716	$8111_4 - 27852\frac{0}{0}$
5063.658	8	1	19743.065	$16346\frac{4}{4} - 36089_4$
5063.565	20h		19743.427	$13847_2 - 33591\frac{3}{3}$
5063.514	200l	50l	19743.626	$5563_1 - 25306\frac{2}{2}$
5062.932	300	5	19745.896	$13297_4 - 33043\frac{3}{3}$
5062.494	50	2	19747.604	$15493_4 - 35240\frac{3}{3}$
5061.654	200	5	19750.881	$6362_2 - 26113\frac{2}{2}$
5060.366	3		19755.908	$13962_1 - 33718\frac{2}{2}$
5059.861	400b	75	19757.880	$7502_3 - 27260\frac{3}{3}$
5059.021	8	1	19761.161	$17398_3 - 37159\frac{3}{3}$
5058.446	100	3	19763.407	$17073_1 - 36837\frac{0}{1}$
5058.446	100	3	19763.407	$19588\frac{0}{0} - 39351_5$
5058.359	200	3	19763.747	$7502_3 - 27266\frac{4}{4}$
5057.137	5		19768.522	$19039\frac{2}{2} - 38807_2$
5056.766	10		19769.973	$18930\frac{3}{3} - 38700_4$
5056.194	50	2	19772.209	$13962_1 - 33734\frac{2}{2}$
5055.751	10b		19773.942	$13088_3 - 32862\frac{4}{4}$
5055.225	300	4	19775.999	$13945\frac{3}{3} - 33721_2$
5054.493	3		19778.863	$19532_4 - 39311\frac{4}{4}$
5053.067	3		19784.445	$21902\frac{3}{4} - 41686_3$
5052.854	8	1	19785.279	$18431_3 - 38216\frac{3}{3}$
5052.448	15		19786.869	$16346\frac{4}{4} - 36133_5$
5051.885	500	5	19789.074	$8800_4 - 28589\frac{3}{3}$
5050.780	300	5	19793.403	$3687_2 - 23481\frac{0}{1}$
5050.029	5b		19796.347	$11802_2 - 31599\frac{2}{2}$
5049.976	10b		19796.554	$7795\frac{4}{4} - 27591_5$
5049.976	10b		19796.554	$21890\frac{3}{3} - 41686_3$
5049.841	50b	1	19797.083	$14204_5 - 34001\frac{4}{4}$
5049.580	40	8	19798.107	$17073_1 - 36871\frac{2}{2}$
5048.937	20	1	19800.628	$2869_3 - 22669\frac{3}{3}$
5047.600	2		19805.873	$18549_2 - 38355\frac{2}{2}$
5047.122	5h	1	19807.748	$18011\frac{0}{0} - 37819_4$
5047.047	150b	5	19808.043	$4961_4 - 24769\frac{3}{3}$
5045.417	3		19814.442	$13847_2 - 33662\frac{1}{1}$
5045.252	100	5	19815.090	$7502_3 - 27317\frac{3}{3}$
5044.715	400r	8	19817.199	$0_2 - 19817\frac{1}{1}$
5044.349	5	1	19818.637	$19503\frac{3}{3} - 39321_3$
5043.520	75	15l	19821.895	$15618\frac{3}{3} - 35440_3$
5041.514	2		19829.782	$16217\frac{2}{2} - 36047_2$
5041.377	3		19830.320	$18930\frac{3}{3} - 38760_4$
5041.126	150	5	19831.308	$17501\frac{0}{0} - 37332_6$
5040.683	25l	1	19833.051	$3687_2 - 23521\frac{3}{3}$
5040.032	2		19835.612	$17398_3 - 37234\frac{2}{2}$
5039.717	1		19836.852	$18053\frac{4}{4} - 37890_5$
5039.529	50	1	19837.592	$8111_4 - 27948\frac{4}{4}$
5039.231	300r	8l	19838.765	$2558_0 - 22396\frac{1}{1}$
5038.618	1		19841.179	$17847\frac{2}{2} - 37688_3$
5038.306	75	3	19842.407	$15970_3 - 35812\frac{3}{3}$
5036.623	3		19849.038	$19713_3 - 39562\frac{4}{4}$
5035.466	5		19853.598	$21902\frac{3}{4} - 41755_4$
5034.297	100	2	19858.209	$15493_4 - 35351\frac{4}{4}$
5033.010	2		19863.286	$19817\frac{1}{1} - 39680_2$
5032.786	1		19864.171	$16346\frac{4}{4} - 36210_5$
5032.119	4		19866.803	$18549_2 - 38416\frac{3}{3}$
5031.815	10		19868.004	$10783\frac{2}{2} - 30651_3$
5031.148	20		19870.638	$13847_2 - 33718\frac{2}{2}$
5030.116	2		19874.714	$18431_3 - 38306\frac{4}{4}$
5030.031	3		19875.050	$17166_5 - 37041\frac{4}{4}$
5029.893	200	3	19875.595	$3865_1 - 23741\frac{1}{1}$
5029.013	75	2	19879.073	$18011\frac{0}{0} - 37890_5$

TABLE 4. *Classified lines of* Th I—continued

Wavelength (Å)	Intensity		Wavenumber (cm^{-1})	Classification
	Lamp	Spark		
5028.656	300b	15	19880.485	$8800_4 - 28680^{\frac{3}{4}}$
5027.679	5		19884.348	$14226_0 - 34111^{\frac{1}{2}}$
5027.318	2		19885.776	$22141^{\frac{3}{4}} - 42027_2$
5027.122	4		19886.551	$13945^{\frac{3}{4}} - 33831_4$
5027.024	5		19886.939	$13847_2 - 33734^{\frac{3}{4}}$
5026.956	5		19887.208	$3865_1 - 23752^{\frac{3}{4}}$
5026.159	5		19890.361	$18809^{\frac{3}{4}} - 38700_4$
5024.110	8		19898.473	$19713_3 - 39611^{\frac{3}{4}}$
5023.709	50	1	19900.061	$11241^{\frac{3}{4}} - 31141_3$
5023.486	50	1	19900.945	$17847^{\frac{1}{2}} - 37748_2$
5022.070	5		19906.556	$12847_3 - 32754^{\frac{3}{4}}$
5022.005	75	2	19906.813	$9804_5 - 29711^{\frac{1}{2}}$
5021.254	75	2	19909.791	$11802_2 - 31712^{\frac{1}{2}}$
5019.806	200	25	19915.534	$3687_2 - 23603^{\frac{1}{2}}$
5019.752	10b		19915.748	$15970_3 - 35885^{\frac{1}{2}}$
5018.059	150	5	19922.467	$15166^{\frac{3}{4}} - 35089_3$
5017.877	10	2	19923.190	$18069^{\frac{3}{4}} - 37992_4$
5017.769	10	2	19923.619	$18431_3 - 38355^{\frac{1}{2}}$
5017.589	5		19924.333	$13175^{\frac{1}{4}} - 33099_3$
5017.510	100	15	19924.647	$6362_2 - 26287^{\frac{1}{2}}$
5016.951	8		19926.867	$12114^{\frac{1}{2}} - 32041_2$
5016.535	40	2	19928.520	$9804_5 - 29733^{\frac{1}{2}}$
5012.274	5		19945.461	$7502_3 - 27447^{\frac{1}{2}}$
5011.478	75	4	19948.629	$15863_2 - 35812^{\frac{1}{2}}$
5011.478	75	4	19948.629	$21738^{\frac{1}{2}} - 41686_3$
5010.951	100	2	19950.727	$18809^{\frac{3}{4}} - 38760_4$
5010.417	50	4	19952.853	$13847_2 - 33800^{\frac{3}{4}}$
5009.938	50b		19954.761	$13088_3 - 33043^{\frac{3}{4}}$
5009.240	10	1	19957.541	$15618^{\frac{3}{4}} - 35576_3$
5008.481	2		19960.565	$14206^{\frac{3}{4}} - 34167_3$
5007.087	5		19966.123	$14465^{\frac{1}{2}} - 34431_3$
5006.405	5		19968.842	$15493_4 - 35462^{\frac{3}{4}}$
5006.073	1		19970.167	$18699_2 - 38669^{\frac{1}{2}}$
5005.970	20	5	19970.578	$20522^{\frac{1}{2}} - 40493_3$
5005.334	15	1	19973.115	$13297_4 - 33270^{\frac{1}{4}}$
5004.900	2		19974.847	$10783^{\frac{1}{2}} - 30758_2$
5004.685	1		19975.705	$18699_2 - 38675^{\frac{3}{4}}$
5004.128	150	10	19977.929	$11802_2 - 31780^{\frac{3}{4}}$
5004.001	50	3	19978.436	$14204_5 - 34182^{\frac{1}{2}}$
5003.857	20	2	19979.011	$14481^{\frac{1}{2}} - 34460_5$
5003.767	3		19979.370	$14465^{\frac{1}{2}} - 34444_2$
5003.597	75	4	19980.049	$7280_2 - 27260^{\frac{3}{4}}$
5003.385	10s	2	19980.895	$18011^{\frac{1}{2}} - 37992_4$
5002.898	15	3	19982.840	$15166^{\frac{3}{4}} - 35149_2$
5002.472	3		19984.542	$18431_3 - 38416^{\frac{3}{4}}$
5002.225	3		19985.529	$20214^{\frac{3}{4}} - 40200_3$
5002.097	500r	40	19986.040	$2869_3 - 22855^{\frac{3}{4}}$
5001.450	8	1	19988.626	$18614^{\frac{1}{2}} - 38602_2$
5001.068	2		19990.152	$17959_4 - 37950^{\frac{1}{4}}$
5001.068	2		19990.152	$17959_4 - 37950^{\frac{1}{4}}$
5000.730	15	1	19991.504	$16783^{\frac{1}{4}} - 36775_3$
5000.252	100	25d	19993.414	$17411^{\frac{3}{4}} - 37404_3$
4999.841	2		19995.058	$17959_4 - 37954^{\frac{3}{4}}$
4999.239	10	2	19997.466	$16783^{\frac{1}{4}} - 36781_5$
4998.419	1		20000.746	$6362_2 - 26363^{\frac{1}{2}}$
4997.566	3		20004.160	$11241^{\frac{3}{4}} - 31245_2$
4996.229	5	1	20009.513	$16351_0 - 36361^{\frac{1}{2}}$
4994.982	10		20014.509	$12847_3 - 32862^{\frac{1}{4}}$
4994.891	5		20014.873	$15618^{\frac{3}{4}} - 35633_4$
4994.576	10	3	20016.135	$20566^{\frac{1}{4}} - 40582_5$
4994.105	50	2	20018.023	$10526^{\frac{3}{4}} - 30544_2$
4993.749	50	4	20019.450	$4961_4 - 24981^{\frac{3}{4}}$
4993.111	1		20022.008	$15863_2 - 35885^{\frac{1}{2}}$
4992.638	20	5	20023.905	$11241^{\frac{3}{4}} - 31265_3$
4992.375	8	2	20024.960	$19227^{\frac{3}{4}} - 39252_5$
4992.125	15	2	20025.963	$10526^{\frac{3}{4}} - 30552_4$
4991.603	1		20028.057	$18069^{\frac{3}{4}} - 38097_2$
4989.309	150	10	20037.265	$7280_2 - 27317^{\frac{3}{4}}$
4988.772	4		20039.422	$13175^{\frac{1}{4}} - 33214_5$
4988.262	1		20041.471	$20054_2 - 40096^{\frac{1}{2}}$
4985.948	50	3	20050.772	$14247^{\frac{3}{4}} - 34298_1$
4985.373	300	10	20053.085	$3687_2 - 23741^{\frac{1}{2}}$
4985.125	8		20054.082	$14243^{\frac{1}{2}} - 34298_1$
4982.488	150	25h	20064.696	$3687_2 - 23752^{\frac{1}{2}}$
4981.877	4l		20067.157	$11802_2 - 31870^{\frac{1}{2}}$
4980.757	20	3	20071.669	$16554_6 - 36625^{\frac{3}{4}}$
4980.186	150	10	20073.970	$11197^{\frac{3}{4}} - 31271_5$
4979.521	4b		20076.651	$9804_5 - 29881^{\frac{1}{4}}$
4979.521	4b		20076.651	$18069^{\frac{3}{4}} - 38145_3$
4978.727	2		20079.853	$18930^{\frac{3}{4}} - 39010_3$
4977.522	5		20084.714	$8800_4 - 28884^{\frac{3}{4}}$
4977.389	8	1	20085.251	$11241^{\frac{3}{4}} - 31326_4$
4976.471	1		20088.956	$20522^{\frac{1}{2}} - 40611_2$
4976.406	1		20089.218	$18699_2 - 38788^{\frac{3}{4}}$
4975.524	5		20092.779	$15970_3 - 36062^{\frac{1}{4}}$
4975.442	3		20093.110	$17959_4 - 38053^{\frac{3}{4}}$
4975.254	2		20093.869	$10414^{\frac{3}{4}} - 30508_5$
4975.088	10	1	20094.540	$14206^{\frac{1}{4}} - 34301_4$
4972.754	20	2	20103.971	$15970_3 - 36074^{\frac{3}{4}}$
4972.258	15	1	20105.977	$19588^{\frac{1}{2}} - 39694_5$
4972.057	40	1	20106.789	$10783^{\frac{1}{2}} - 30889_1$
4971.553	2		20108.828	$21252^{\frac{1}{2}} - 41361_3$
4970.074	150b	2	20114.812	$8243^{\frac{3}{4}} - 28358_3$
4969.518	2		20117.062	$18069^{\frac{3}{4}} - 38186_4$
4968.753	200	20	20120.159	$13847_2 - 33967^{\frac{3}{4}}$
4967.649	5		20124.631	$10526^{\frac{3}{4}} - 30651_3$
4967.334	5	1	20125.907	$18549_2 - 38675^{\frac{3}{4}}$
4967.334	5	1	20125.907	$21594_3 - 41720^{\frac{1}{2}}$
4965.731	200	10	20132.404	$8800_4 - 28932^{\frac{1}{4}}$
4964.538	2		20137.242	$21890^{\frac{3}{4}} - 42027_2$
4964.255	10	2	20138.390	$10414^{\frac{3}{4}} - 30552_4$
4963.763	75	50	20140.386	$14204_5 - 34344^{\frac{3}{4}}$
4963.031	8		20143.356	$18809^{\frac{3}{4}} - 38953_5$
4962.466	5		20145.650	$6362_2 - 26508^{\frac{3}{4}}$
4961.724	200	10	20148.662	$13962_1 - 34111^{\frac{1}{2}}$
4958.878	2		20160.226	$17073_1 - 37234^{\frac{1}{2}}$
4958.093	50	2	20163.418	$11877^{\frac{1}{2}} - 32041_2$
4957.057	15		20167.632	$7280_2 - 27447^{\frac{1}{2}}$
4956.798	20b		20168.685	$7502_3 - 27670^{\frac{3}{4}}$

TABLE 4. *Classified lines of* Th I—continued

Wavelength (Å)	Intensity		Wavenumber (cm^{-1})	Classification
	Lamp	Spark		
4956.637	50	2	20169.340	$16346_{4}^{2} - 36515_{3}$
4955.303	3		20174.770	$18011_{6}^{6} - 38186_{4}$
4953.936	25	3	20180.337	$17224_{2}^{2} - 37404_{3}$
4953.646	2		20181.519	$10783_{2}^{2} - 30964_{3}$
4953.529	50	10	20181.995	$13088_{3} - 33270_{4}^{4}$
4952.688	40	3	20185.422	$7795_{4}^{4} - 27980_{3}$
4952.009	2		20188.190	$20423_{1}^{1} - 40611_{2}$
4950.755	8		20193.303	$18614_{1}^{1} - 38807_{2}$
4950.250	150	10	20195.363	$12847_{3} - 33043_{3}^{3}$
4949.065	2		20200.199	$20054_{2} - 40254_{3}^{3}$
4948.964	8		20200.611	$14243_{1}^{1} - 34444_{2}$
4948.565	1		20202.240	$23655_{4}^{4} - 43857_{5}$
4947.015	5		20208.570	$13088_{3} - 33297_{2}^{2}$
4946.220	2		20211.818	$20214_{3}^{3} - 40426_{4}$
4945.458	200r	10	20214.932	$0_{2} - 20214_{3}^{3}$
4943.130	50b	2	20224.452	$14206_{4}^{4} - 34431_{3}$
4943.064	200b	10	20224.722	$2869_{3} - 23093_{2}^{2}$
4941.415	15	1	20231.471	$10526_{3}^{3} - 30758_{2}$
4940.907	20	2	20233.551	$13175_{4}^{4} - 33408_{3}$
4940.057	5		20237.033	$10414_{4}^{4} - 30651_{3}$
4939.642	300r	15	20238.733	$7795_{4}^{4} - 28034_{5}$
4939.270	75	2	20240.257	$14206_{4}^{4} - 34447_{4}$
4939.059	10	1	20241.122	$17501_{6}^{6} - 37742_{6}$
4938.720	3		20242.511	$14465_{2}^{2} - 34707_{3}$
4938.597	15	1	20243.015	$13175_{4}^{4} - 33418_{4}$
4938.439	10	1	20243.663	$18431_{3} - 38675_{3}^{3}$
4938.283	15		20244.302	$2869_{3} - 23113_{4}^{4}$
4938.206	20	2	20244.618	$18930_{3}^{3} - 39174_{3}$
4937.829	300	8	20246.164	$5563_{1} - 25809_{1}^{1}$
4936.889	25	1	20250.019	$17847_{2}^{2} - 38097_{2}$
4936.775	150	100	20250.486	$8800_{4} - 29050_{6}^{6}$
4935.929	20	1	20253.957	$14206_{4}^{4} - 34460_{5}$
4935.177	5		20257.043	$17959_{4} - 38216_{3}^{3}$
4934.807	3		20258.562	$17398_{3} - 37656_{3}^{3}$
4934.748	1		20258.804	$15618_{3}^{3} - 35877_{2}$
4934.337	15	1	20260.492	$20322_{6}^{6} - 40582_{5}$
4933.825	15b		20262.594	$13297_{4} - 33560_{4}^{4}$
4933.283	3		20264.820	$18549_{2} - 38814_{2}^{2}$
4933.003	20	1	20265.970	$14032_{2}^{2} - 34298_{1}$
4932.250	5		20269.064	$11601_{1} - 31870_{2}^{2}$
4931.373	10b		20272.669	$19713_{3} - 39985_{3}^{3}$
4931.050	10		20273.997	$15166_{3}^{3} - 35440_{3}$
4930.322	3		20276.990	$17411_{3}^{3} - 37688_{3}$
4929.832	5		20279.006	$21077_{6}^{6} - 41356_{5}$
4929.086	100	3	20282.075	$7502_{3} - 27784_{2}^{2}$
4928.949	5		20282.639	$19039_{2}^{2} - 39321_{3}$
4928.683	50	2	20283.733	$16554_{6} - 36837_{6}^{6}$
4928.604	8		20284.058	$13175_{4}^{4} - 33459_{4}$
4927.781	200	5	20287.446	$8243_{2}^{2} - 28531_{2}$
4927.299	50	1	20289.431	$6362_{2} - 26651_{2}^{2}$
4926.254	40	2	20293.734	$13297_{4} - 33591_{3}^{3}$
4925.822	8b	1b	20295.514	$11241_{3}^{3} - 31537_{3}$
4925.339	5	2	20297.505	$18069_{3}^{3} - 38366_{4}$
4925.097	3b		20298.502	$16217_{2}^{2} - 36515_{3}$
4924.896	8	1	20299.330	$18699_{2} - 38998_{3}^{3}$
4924.246	75b	2	20302.010	$16783_{4}^{4} - 37085_{4}$
4923.690	5		20304.302	$15490_{6}^{6} - 35794_{4}$
4922.338	2		20309.879	$15490_{6}^{6} - 35799_{6}$
4922.231	5		20310.321	$15736_{1}^{1} - 36047_{2}$
4921.653	40b		20312.706	$10783_{2}^{2} - 31095_{1}$
4920.624	50	2	20316.954	$3865_{1} - 24182_{2}^{2}$
4920.053	75b	25s	20319.312	$15493_{4} - 35812_{3}^{3}$
4920.018	75b	2	20319.456	$2558_{0} - 22877_{1}^{1}$
4918.659	3		20325.070	$15863_{2} - 36188_{2}^{2}$
4916.383	2h		20334.479	$19503_{3}^{3} - 39837_{3}$
4915.823	10	1	20336.796	$17411_{3}^{3} - 37748_{2}$
4915.416	50	1	20338.480	$13088_{3} - 33427_{2}^{2}$
4913.480	5	1	20346.493	$17959_{4} - 38306_{4}^{4}$
4912.043	10	1	20352.445	$13175_{4}^{4} - 33527_{4}$
4911.784	2		20353.519	$18930_{3}^{3} - 39283_{4}$
4911.380	200	10	20355.193	$9804_{5} - 30160_{4}^{4}$
4911.380	200	10	20355.193	$18011_{6}^{6} - 38366_{4}$
4910.807	100b	2	20357.568	$11802_{2} - 32160_{2}^{2}$
4910.792	100b	2	20357.630	$8800_{4} - 29157_{3}^{3}$
4910.549	15	1	20358.637	$10783_{2}^{2} - 31141_{3}$
4910.158	100	4	20360.259	$4961_{4} - 25321_{3}^{3}$
4909.844	50	3	20361.561	$13962_{1} - 34324_{2}^{2}$
4909.213	15	1	20364.178	$14226_{0} - 34591_{1}^{1}$
4909.010	8	1	20365.020	$18809_{2}^{2} - 39174_{3}$
4908.478	100	1	20367.227	$14481_{6}^{6} - 34849_{5}$
4908.012	5		20369.161	$8111_{4} - 28480_{4}^{4}$
4907.044	50	2	20373.179	$17411_{3}^{3} - 37784_{2}$
4906.731	2		20374.479	$19532_{4} - 39906_{4}^{4}$
4905.631	2		20379.047	$20322_{6}^{6} - 40701_{4}$
4904.407	1		20384.133	$21902_{4}^{2} - 42286_{3}$
4903.057	8	1	20389.746	$13175_{4}^{4} - 33564_{3}$
4902.793	75	5	20390.843	$7280_{2} - 27670_{3}^{3}$
4902.600	50	5	20391.646	$17501_{6}^{6} - 37892_{4}$
4902.177	2		20393.406	$17354_{1}^{1} - 37748_{2}$
4902.051	75	5	20393.930	$4961_{4} - 25355_{4}^{4}$
4901.987	50	2	20394.196	$7280_{2} - 27674_{2}^{2}$
4901.987	50	2	20394.196	$11802_{2} - 32197_{3}^{3}$
4901.479	4		20396.310	$21890_{3}^{3} - 42286_{3}$
4901.371	3		20396.759	$20214_{3}^{3} - 40611_{2}$
4899.336	50	3	20405.231	$17166_{5} - 37571_{6}^{6}$
4898.697	10	1	20407.893	$17411_{3}^{3} - 37819_{4}$
4898.358	25b	1	20409.305	$13962_{1} - 34371_{2}^{2}$
4897.586	8	1	20412.522	$14032_{2}^{2} - 34444_{2}$
4897.586	8	1	20412.522	$15970_{3} - 36382_{4}^{4}$
4895.168	3		20422.605	$12847_{3} - 33270_{3}^{3}$
4894.955	400r	10	20423.494	$0_{2} - 20423_{1}^{1}$
4894.520	4		20425.309	$17959_{4} - 38385_{6}^{6}$
4893.910	4		20427.855	$16783_{4}^{4} - 37211_{5}$
4893.704	10	1	20428.715	$16346_{4}^{4} - 36775_{3}$
4893.444	50	2	20429.800	$11197_{6}^{6} - 31626_{5}$
4892.758	50	2	20432.664	$7795_{4}^{4} - 28227_{4}$
4892.415	1		20434.097	$21252_{2}^{2} - 41686_{3}$
4892.276	5	1	20434.677	$16346_{4}^{4} - 36781_{5}$
4892.038	5		20435.671	$8243_{2}^{2} - 28679_{2}$
4891.658	15	1	20437.259	$12114_{2}^{2} - 32551_{3}$

TABLE 4. *Classified lines of* Th I—continued

Wavelength (Å)	Intensity		Wavenumber (cm^{-1})	Classification
	Lamp	Spark		
4891.453	4		20438.115	$10526\frac{5}{3} - 30964_3$
4890.455	50	8	20442.286	$3865_1 - 24307\frac{2}{2}$
4889.489	50	2	20446.325	$7502_3 - 27948\frac{4}{4}$
4888.811	4		20449.161	$12847_3 - 33297\frac{2}{2}$
4888.714	4		20449.566	$18549_2 - 38998\frac{3}{3}$
4887.822	1		20453.298	$19532_4 - 39985\frac{3}{3}$
4887.538	1		20454.486	$16554_6 - 37008\frac{6}{6}$
4887.096	50	2	20456.336	$17959_4 - 38416\frac{3}{3}$
4886.869	50	2	20457.287	$15970_3 - 36427\frac{3}{3}$
4886.014	3b		20460.867	$18069\frac{3}{3} - 38529_3$
4885.825	4l		20461.658	$16346\frac{4}{4} - 36808_3$
4885.565	5b	1	20462.747	$10783\frac{2}{2} - 31245_2$
4885.290	2		20463.899	$17224\frac{2}{2} - 37688_3$
4885.241	3		20464.104	$19588\frac{5}{5} - 40052_4$
4884.549	50	2	20467.003	$19227\frac{8}{8} - 39694_5$
4883.663	2		20470.716	$15618\frac{3}{3} - 36089_4$
4883.490	3	1	20471.441	$13088_3 - 33560\frac{4}{4}$
4882.894	5		20473.940	$18809\frac{2}{4} - 39283_4$
4882.328	3		20476.313	$13847_2 - 34324\frac{2}{2}$
4882.328	3		20476.313	$18053\frac{4}{4} - 38529_3$
4881.853	75	2	20478.306	$8111_4 - 28589\frac{5}{5}$
4881.597	50	2	20479.380	$11601_1 - 32080\frac{1}{1}$
4881.204	75	2	20481.029	$4961_4 - 25442\frac{3}{3}$
4881.070	3		20481.591	$17411\frac{3}{3} - 37892_4$
4880.912	50b	2	20482.254	$11802_2 - 32285\frac{3}{3}$
4880.859	25b	2	20482.476	$10783\frac{2}{2} - 31265_3$
4880.190	15b	1	20485.284	$16351_0 - 36837\frac{1}{1}$
4880.010	5	1	20486.040	$13945\frac{3}{3} - 34431_3$
4878.733	300b	8	20491.402	$2558_0 - 23049\frac{1}{1}$
4878.009	100	3	20494.443	$3687_2 - 24182\frac{2}{2}$
4877.265	20	1	20497.569	$15863_2 - 36361\frac{1}{1}$
4876.856	4		20499.288	$13945\frac{5}{3} - 34444_2$
4876.495	100	5	20500.806	$14206\frac{4}{4} - 34707_3$
4876.244	50	2	20501.861	$13945\frac{3}{3} - 34447_4$
4876.142	3		20502.290	$13297_4 - 33799\frac{4}{4}$
4876.067	4		20502.605	$13088_3 - 33591\frac{3}{3}$
4875.677	4		20504.245	$7280_2 - 27784\frac{2}{2}$
4874.365	150	10	20509.764	$8800_4 - 29310\frac{4}{4}$
4873.855	2		20511.910	$18809\frac{2}{4} - 39321_3$
4872.922	300r	25b	20515.838	$3865_1 - 24381\frac{2}{2}$
4872.229	10b	1	20518.756	$15970_3 - 36488\frac{2}{2}$
4872.030	100	4	20519.594	$16783\frac{4}{4} - 37303_4$
4871.558	3		20521.582	$21165\frac{5}{3} - 41686_3$
4871.286	50	2	20522.728	$0_2 - 20522\frac{2}{2}$
4868.882	150	10	20532.860	$11241\frac{3}{3} - 31774_3$
4868.636	8h	1	20533.898	$18069\frac{3}{3} - 38602_2$
4867.502	5b	1b	20538.682	$16346\frac{4}{4} - 36885_4$
4866.740	2		20541.898	$18809\frac{2}{4} - 39351_5$
4865.477	300r	150b	20547.230	$7795\frac{3}{3} - 28342_5$
4865.415	75b	15b	20547.492	$13297_4 - 33844\frac{6}{6}$
4864.985	2		20549.308	$19503\frac{3}{3} - 40052_4$
4864.789	2		20550.136	$5563_1 - 26113\frac{2}{2}$
4864.433	8	2	20551.640	$17398_3 - 37950\frac{3}{3}$
4864.357	3	1	20551.961	$11241\frac{3}{3} - 31793_4$
4862.962	4		20557.856	$16217\frac{2}{2} - 36775_3$
4862.597	1		20559.399	$11601_1 - 32160\frac{2}{2}$
4861.720	75b	20h	20563.108	$7795\frac{3}{4} - 28358_3$
4861.635	50	2	20563.467	$15863_2 - 36427\frac{3}{3}$
4861.223	300r	50	20565.210	$8111_4 - 28676\frac{3}{3}$
4860.738	3	1	20567.262	$18431_3 - 38998\frac{3}{3}$
4860.173	5	2	20569.653	$15493_4 - 36062\frac{4}{4}$
4857.949	5	1	20579.070	$12847_3 - 33427\frac{2}{2}$
4857.536	100	15	20580.819	$14465\frac{2}{2} - 35046_1$
4857.536	100	15	20580.819	$15493_4 - 36074\frac{3}{3}$
4852.868	200	50	20600.616	$16217\frac{2}{2} - 36818_2$
4851.676	5	2	20605.677	$17501\frac{0}{0} - 38106_5$
4849.861	50	15	20613.389	$4961_4 - 25575\frac{4}{4}$
4849.417	2		20615.276	$10526\frac{3}{3} - 31141_3$
4848.363	400r	150	20619.758	$3687_2 - 24307\frac{2}{2}$
4848.216	20	8	20620.383	$17959_4 - 38580\frac{4}{4}$
4847.330	150	15	20624.152	$14465\frac{2}{2} - 35089_3$
4847.144	20	2	20624.943	$15863_2 - 36488\frac{2}{2}$
4845.990	1		20629.854	$13088_3 - 33718\frac{2}{2}$
4845.161	100	10	20633.384	$6362_2 - 26995\frac{3}{3}$
4844.929	75	5	20634.372	$19948\frac{3}{4} - 40582_5$
4844.612	5b		20635.722	$21077\frac{8}{8} - 41712_5$
4843.938	100b	50b	20638.594	$7502_3 - 28140\frac{3}{3}$
4843.876	75b	10b	20638.858	$8243\frac{3}{3} - 28882_2$
4843.103	3	1	20642.152	$14206\frac{4}{4} - 34849_5$
4840.843	400r	75	20651.789	$2869_3 - 23521\frac{3}{3}$
4839.780	2		20656.324	$20922\frac{2}{2} - 41578_2$
4839.674	5	2b	20656.777	$13175\frac{4}{4} - 33831_4$
4837.903	1		20664.339	$20566\frac{4}{4} - 41230_4$
4837.409	40	4	20666.449	$14206\frac{4}{4} - 34873_4$
4837.245	20	3	20667.150	$14206\frac{4}{4} - 34874_3$
4836.091	3		20672.081	$20214\frac{3}{3} - 40886_2$
4834.632	2		20678.319	$15618\frac{3}{3} - 36297_4$
4834.537	3	1	20678.726	$21077\frac{8}{8} - 41755_4$
4833.674	20s	4s	20682.418	$14204_5 - 34886\frac{6}{6}$
4833.179	200b	50	20684.536	$14465\frac{2}{2} - 35149_2$
4833.112	50b	8	20684.823	$15493_4 - 36178\frac{4}{4}$
4832.423	5l	2l	20687.772	$11241\frac{3}{3} - 31929_3$
4831.767	1		20690.580	$17398_3 - 38088\frac{2}{2}$
4831.597	300r	150	20691.309	$8243\frac{3}{3} - 28934_3$
4831.121	500r	200	20693.347	$3687_2 - 24381\frac{2}{2}$
4830.206	1		20697.267	$19503\frac{3}{3} - 40200_3$
4829.796	50	8	20699.024	$6362_2 - 27061\frac{2}{2}$
4829.407	5	2	20700.691	$11802_2 - 32503\frac{2}{2}$
4828.658	20	4	20703.902	$13297_4 - 34001\frac{4}{4}$
4828.246	1		20705.669	$17959_4 - 38665\frac{6}{6}$
4826.700	200b	50b	20712.301	$30517\frac{8}{8} - 9804_5$
4826.637	50b	15b	20712.571	$9804_5 - 30517\frac{4}{4}$
4826.008	50	4	20715.271	$18549_2 - 39264\frac{3}{3}$
4825.553	5	1	20717.224	$15618\frac{3}{3} - 36336_3$
4824.736	1		20720.732	$15490\frac{6}{6} - 36210_5$
4823.997	200r	100h	20723.906	$5563_1 - 26287\frac{1}{1}$
4823.604	300r	75	20725.595	$6362_2 - 27087\frac{1}{1}$
4823.122	5b	1	20727.666	$10414\frac{4}{4} - 31141_3$
4822.855	300r	75	20728.814	$4961_4 - 25690\frac{6}{6}$
4821.862	15	2	20733.082	$3687_2 - 24421\frac{3}{3}$

TABLE 4. *Classified lines of* Th I—continued

Wavelength (Å)	Intensity		Wavenumber (cm^{-1})	Classification
	Lamp	Spark		
4821.587	150	25	20734.265	$2869_3 - 23603^{\frac{3}{2}}_{\frac{3}{2}}$
4821.387	50	15	20735.125	$14481^{\frac{5}{2}}_{\frac{5}{2}} - 35216_5$
4820.884	100	200	20737.288	$0_2 - 20737^{\frac{7}{2}}_{\frac{7}{2}}$
4820.788	2h	1	20737.701	$16783^{\frac{3}{4}}_{\frac{3}{4}} - 37521_3$
4820.463	150b	40h	20739.099	$10526^{\frac{5}{2}}_{\frac{5}{2}} - 31265_3$
4819.508	10	3	20743.209	$12847_3 - 33591^{\frac{3}{2}}_{\frac{3}{2}}$
4819.191	150	15	20744.573	$7280_2 - 28024^{\frac{7}{2}}_{\frac{7}{2}}$
4818.294	5	2	20748.435	$15736^{\frac{7}{2}}_{\frac{7}{2}} - 36485_2$
4818.102	4	2	20749.262	$18011^{\frac{5}{2}}_{\frac{5}{2}} - 38760_4$
4817.017	75	8	20753.935	$11241^{\frac{3}{2}}_{\frac{3}{2}} - 31995_4$
4816.566	1		20755.879	$17847^{\frac{5}{2}}_{\frac{5}{2}} - 38602_2$
4815.046	5	2	20762.431	$13945^{\frac{3}{2}}_{\frac{3}{2}} - 34707_3$
4814.919	15	3	20762.978	$14226_0 - 34989^{\frac{7}{2}}_{\frac{7}{2}}$
4814.553	2		20764.557	$20922^{\frac{5}{2}}_{\frac{5}{2}} - 41686_3$
4813.893	200	100	20767.404	$7795^{\frac{5}{2}}_{\frac{5}{2}} - 28562_4$
4813.499	1		20769.103	$18699_2 - 39468^{\frac{3}{2}}_{\frac{3}{2}}$
4813.004	75	15	20771.239	$11241^{\frac{3}{2}}_{\frac{3}{2}} - 32012_4$
4812.712	1		20772.500	$11802_2 - 32575^{\frac{5}{2}}_{\frac{5}{2}}$
4812.373	150	25	20773.963	$8111_4 - 28884^{\frac{3}{2}}_{\frac{3}{2}}$
4810.519	8	4	20781.969	$15493_4 - 36275^{\frac{5}{2}}_{\frac{5}{2}}$
4809.615	200	50	20785.875	$2869_3 - 23655^{\frac{5}{2}}_{\frac{5}{2}}$
4808.764	5	2	20789.554	$20566^{\frac{3}{2}}_{\frac{3}{2}} - 41356_5$
4808.134	500r	150	20792.278	$4961_4 - 25753^{\frac{5}{2}}_{\frac{5}{2}}$
4807.550	4	2	20794.803	$20566^{\frac{3}{2}}_{\frac{3}{2}} - 41361_3$
4806.459	5	2	20799.524	$11241^{\frac{3}{2}}_{\frac{3}{2}} - 32041_2$
4806.355	5	1	20799.974	$5563_1 - 26363^{\frac{3}{2}}_{\frac{3}{2}}$
4806.248	3	1	20800.437	$10526^{\frac{5}{2}}_{\frac{5}{2}} - 31326_4$
4805.244	15	3	20804.782	$15863_2 - 36668^{\frac{5}{2}}_{\frac{5}{2}}$
4802.670	10	3	20815.933	$11197^{\frac{5}{2}}_{\frac{5}{2}} - 32012_4$
4801.951	2		20819.050	$14481^{\frac{5}{2}}_{\frac{5}{2}} - 35300_5$
4801.349	4	1	20821.660	$8111_4 - 28932^{\frac{5}{2}}_{\frac{5}{2}}$
4801.054	25	4	20822.939	$19273_2 - 40096^{\frac{5}{2}}_{\frac{5}{2}}$
4799.670	3	1	20828.943	$17959_4 - 38788^{\frac{3}{2}}_{\frac{3}{2}}$
4798.734	4	2	20833.006	$18431_3 - 39264^{\frac{3}{2}}_{\frac{3}{2}}$
4797.497	75	50	20838.378	$19588^{\frac{5}{2}}_{\frac{5}{2}} - 40426_4$
4796.667	3	1	20841.983	$14032^{\frac{5}{2}}_{\frac{5}{2}} - 34874_3$
4795.913	150	75	20845.260	$7502_3 - 28347^{\frac{5}{2}}_{\frac{5}{2}}$
4795.289	3	1	20847.973	$11802_2 - 32650^{\frac{7}{2}}_{\frac{7}{2}}$
4794.474	2		20851.516	$10414^{\frac{3}{2}}_{\frac{3}{2}} - 31265_3$
4793.285	8		20856.689	$13847_2 - 34704^{\frac{3}{2}}_{\frac{3}{2}}$
4793.246	100l	25	20856.858	$10414^{\frac{3}{2}}_{\frac{3}{2}} - 31271_5$
4792.007	3		20862.251	$21165^{\frac{3}{2}}_{\frac{3}{2}} - 42027_2$
4791.921	5	1	20862.625	$11802_2 - 32665^{\frac{7}{2}}_{\frac{7}{2}}$
4791.362	8	3	20865.059	$16346^{\frac{3}{2}}_{\frac{3}{2}} - 37211_5$
4789.387	400r	75	20873.663	$3687_2 - 24561^{\frac{5}{2}}_{\frac{5}{2}}$
4788.678	25	5	20876.754	$14204_5 - 35081^{\frac{7}{2}}_{\frac{7}{2}}$
4788.542	3	1	20877.347	$16217^{\frac{5}{2}}_{\frac{5}{2}} - 37094_2$
4788.472	2		20877.652	$13847_2 - 34725^{\frac{5}{2}}_{\frac{5}{2}}$
4788.079	1		20879.366	$13088_3 - 33967^{\frac{5}{2}}_{\frac{5}{2}}$
4787.148	150	25	20883.426	$2869_3 - 23752^{\frac{5}{2}}_{\frac{5}{2}}$
4786.914	5	1	20884.447	$18809^{\frac{3}{2}}_{\frac{3}{2}} - 39694_5$
4786.724	75	5	20885.276	$13297_4 - 34182^{\frac{5}{2}}_{\frac{5}{2}}$
4786.532	200	50	20886.114	$8800_4 - 29686^{\frac{5}{2}}_{\frac{5}{2}}$
4785.780	5	2	20889.395	$15493_4 - 36382^{\frac{3}{2}}_{\frac{3}{2}}$
4785.007	1		20892.770	$19532_4 - 40425^{\frac{3}{2}}_{\frac{3}{2}}$
4784.163	2h		20896.456	$17073_1 - 37970^{\frac{5}{2}}_{\frac{5}{2}}$
4784.038	150	20	20897.002	$15618^{\frac{3}{2}}_{\frac{3}{2}} - 36515_3$
4783.864	150l	10b	20897.762	$6362_2 - 27260^{\frac{5}{2}}_{\frac{5}{2}}$
4783.605	2b		20898.893	$15863_2 - 36762^{\frac{5}{2}}_{\frac{5}{2}}$
4782.936	5	2	20901.816	$15970_3 - 36871^{\frac{5}{2}}_{\frac{5}{2}}$
4781.671	8	2	20907.346	$18930^{\frac{3}{2}}_{\frac{3}{2}} - 39837_3$
4781.527	100	5	20907.976	$17398_3 - 38306^{\frac{3}{2}}_{\frac{3}{2}}$
4781.363	2		20908.693	$20322^{\frac{5}{2}}_{\frac{5}{2}} - 41230_4$
4780.751	75	8	20911.369	$8800_4 - 29711^{\frac{5}{2}}_{\frac{5}{2}}$
4780.633	3		20911.885	$18699_2 - 39611^{\frac{3}{2}}_{\frac{3}{2}}$
4780.427	150	25	20912.786	$13088_3 - 34001^{\frac{3}{2}}_{\frac{3}{2}}$
4779.728	50	5	20915.845	$4961_4 - 25877^{\frac{3}{2}}_{\frac{3}{2}}$
4779.661	4	1	20916.138	$13962_1 - 34878^{\frac{7}{2}}_{\frac{7}{2}}$
4779.566	2b		20916.554	$15736^{\frac{7}{2}}_{\frac{7}{2}} - 36653_2$
4778.453	5	2	20921.425	$17224^{\frac{3}{2}}_{\frac{3}{2}} - 38145_3$
4778.294	400r	50	20922.122	$0_2 - 20922^{\frac{5}{2}}_{\frac{5}{2}}$
4778.021	2		20923.317	$2558_0 - 23481^{\frac{7}{2}}_{\frac{7}{2}}$
4777.421	1		20925.945	$20054_2 - 40980^{\frac{5}{2}}_{\frac{5}{2}}$
4777.192	300	75	20926.948	$14204_5 - 35131^{\frac{3}{2}}_{\frac{3}{2}}$
4775.793	100	15	20933.078	$8800_4 - 29733^{\frac{5}{2}}_{\frac{5}{2}}$
4775.313	100l	5b	20935.182	$6362_2 - 27297^{\frac{7}{2}}_{\frac{7}{2}}$
4774.275	40b		20939.734	$8111_4 - 29050^{\frac{5}{2}}_{\frac{5}{2}}$
4773.241	100	8	20944.270	$8800_4 - 29744^{\frac{3}{2}}_{\frac{3}{2}}$
4772.962	3		20945.494	$18011^{\frac{5}{2}}_{\frac{5}{2}} - 38956_4$
4771.533	4	1	20951.767	$12847_3 - 33799^{\frac{3}{2}}_{\frac{3}{2}}$
4771.330	8	2	20952.658	$12847_3 - 33800^{\frac{5}{2}}_{\frac{5}{2}}$
4770.796	15	1	20955.003	$6362_2 - 27317^{\frac{5}{2}}_{\frac{5}{2}}$
4770.440	10b	3	20956.567	$18053^{\frac{5}{2}}_{\frac{5}{2}} - 39010_3$
4770.390	15b	3	20956.787	$16346^{\frac{3}{2}}_{\frac{3}{2}} - 37303_4$
4769.543	50	3	20960.508	$16346^{\frac{3}{2}}_{\frac{3}{2}} - 37307_3$
4766.600	300r	100	20973.450	$3865_1 - 24838^{\frac{7}{2}}_{\frac{7}{2}}$
4766.382	2		20974.409	$11601_1 - 32575^{\frac{5}{2}}_{\frac{5}{2}}$
4766.098	1		20975.659	$14465^{\frac{5}{2}}_{\frac{5}{2}} - 35440_3$
4765.593	100b	100	20977.881	$7502_3 - 28480^{\frac{3}{2}}_{\frac{3}{2}}$
4763.963	4	1	20985.059	$12114^{\frac{5}{2}}_{\frac{5}{2}} - 33099_3$
4762.805	2		20990.161	$19503^{\frac{3}{2}}_{\frac{3}{2}} - 40493_3$
4762.302	8	2	20992.378	$13175^{\frac{5}{2}}_{\frac{5}{2}} - 34167_3$
4759.687	75	10	21003.911	$13847_2 - 34851^{\frac{5}{2}}_{\frac{5}{2}}$
4759.441	2		21004.997	$11197^{\frac{5}{2}}_{\frac{5}{2}} - 32202_5$
4758.286	50	15	21010.095	$14206^{\frac{3}{2}}_{\frac{3}{2}} - 35216_5$
4758.150	100	75	21010.696	$10526^{\frac{5}{2}}_{\frac{5}{2}} - 31537_3$
4758.075	50	15	21011.027	$7502_3 - 28513^{\frac{5}{2}}_{\frac{5}{2}}$
4757.415	15	2	21013.942	$14032^{\frac{5}{2}}_{\frac{5}{2}} - 35046_1$
4757.133	50	5	21015.187	$17073_1 - 38088^{\frac{5}{2}}_{\frac{5}{2}}$
4756.699	100	25	21017.105	$16554_6 - 37571^{\frac{5}{2}}_{\frac{5}{2}}$
4756.532	75		21017.843	$17398_3 - 38416^{\frac{5}{2}}_{\frac{5}{2}}$
4753.581	2l		21030.890	$13847_2 - 34878^{\frac{7}{2}}_{\frac{7}{2}}$
4752.900	10	3	21033.904	$20322^{\frac{5}{2}}_{\frac{5}{2}} - 41356_5$
4752.588	50b	10b	21035.284	$16783^{\frac{3}{4}}_{\frac{3}{4}} - 37819_4$
4752.199	2		21037.006	$18431_3 - 39468^{\frac{3}{2}}_{\frac{3}{2}}$
4749.968	300b	50	21046.887	$8111_4 - 29157^{\frac{5}{2}}_{\frac{5}{2}}$
4749.892	20	4	21047.224	$13297_4 - 34344^{\frac{3}{2}}_{\frac{3}{2}}$
4749.795	25	3	21047.654	$2869_3 - 23916^{\frac{3}{2}}_{\frac{3}{2}}$
4749.466	3b	1	21049.111	$21575_2 - 42624^{\frac{7}{2}}_{\frac{7}{2}}$

TABLE 4. *Classified lines of* Th I—continued

Wavelength (Å)	Intensity		Wavenumber (cm^{-1})	Classification
	Lamp	Spark		
4749.287	5		21049.905	$11601_1 - 32650^{\frac{1}{2}}$
4749.200	400r	150	21050.290	$7795^{\frac{3}{4}} - 28845_4$
4747.617	100	4	21057.309	$14032^{\frac{3}{2}} - 35089_3$
4745.629	8	2	21066.130	$18614^{\frac{1}{2}} - 39680_2$
4745.331	200b	25b	21067.453	$7280_2 - 28347^{\frac{5}{2}}$
4744.838	5	1	21069.642	$14204_5 - 35273^{\frac{5}{2}}$
4744.797	5	2	21069.824	$19817^{\frac{1}{2}} - 40886_2$
4744.706	3		21070.228	$13945^{\frac{3}{2}} - 35015_2$
4744.516	2		21071.072	$15970_3 - 37041^{\frac{3}{4}}$
4742.114	200	8	21081.745	$3687_2 - 24769^{\frac{5}{2}}$
4741.301	150	40	21085.360	$6362_2 - 27447^{\frac{5}{2}}$
4740.951	200b	15	21086.916	$4961_4 - 26048^{\frac{3}{4}}$
4740.929	100b	8	21087.014	$7502_3 - 28589^{\frac{3}{2}}$
4740.332	15	3	21089.670	$16217^{\frac{5}{2}} - 37307_3$
4739.674	300	40	21092.598	$7280_2 - 28372^{\frac{1}{2}}$
4739.353	5	2	21094.026	$14206^{\frac{3}{4}} - 35300_5$
4738.839	8	2	21096.314	$21539^{\frac{3}{4}} - 42635_5$
4737.915	150	15	21100.428	$14481^{\frac{5}{2}} - 35582_5$
4737.604	10l	2	21101.813	$14226_0 - 35328^{\frac{1}{2}}$
4737.529	20	3	21102.148	$17959_4 - 39062^{\frac{5}{2}}$
4736.523	10	2	21106.629	$16783^{\frac{3}{4}} - 37890_5$
4735.995	200	20	21108.982	$16783^{\frac{3}{4}} - 37892_4$
4735.474	4	1	21111.305	$14465^{\frac{5}{2}} - 35576_3$
4734.046	200	10	21117.673	$14032^{\frac{3}{2}} - 35149_2$
4733.536	2		21119.948	$12847_3 - 33967^{\frac{5}{2}}$
4733.504	1		21120.091	$20566^{\frac{3}{4}} - 41686_3$
4733.224	1		21121.340	$18053^{\frac{3}{4}} - 39174_3$
4732.826	4	1	21123.116	$10414^{\frac{3}{4}} - 31537_3$
4732.103	40	4	21126.344	$13175^{\frac{3}{4}} - 34301_4$
4731.192	20	3	21130.411	$15166^{\frac{5}{2}} - 36297_4$
4730.657	150	8	21132.801	$13297_4 - 34430^{\frac{5}{2}}$
4730.089	40	5	21135.339	$4961_4 - 26096^{\frac{5}{2}}$
4729.128	400b	100b	21139.634	$7795^{\frac{3}{4}} - 28934_3$
4728.985	50	8	21140.273	$17166_5 - 38306^{\frac{3}{4}}$
4728.591	40	3	21142.034	$13847_2 - 34989^{\frac{1}{2}}$
4728.133	300	25d	21144.082	$13945^{\frac{3}{2}} - 35089_3$
4727.619	3h		21146.381	$10783^{\frac{5}{2}} - 31929_3$
4727.440	75	4	21147.182	$14204_5 - 35351^{\frac{3}{4}}$
4726.598	5	2	21150.949	$3687_2 - 24838^{\frac{1}{2}}$
4726.441	8		21151.651	$11802_2 - 32954^{\frac{3}{2}}$
4726.054	4		21153.383	$12847_3 - 34001^{\frac{3}{4}}$
4725.384	8	2	21156.383	$15618^{\frac{5}{2}} - 36775_3$
4724.691	2		21159.486	$12114^{\frac{3}{2}} - 33273_1$
4724.292	2		21161.273	$19039^{\frac{3}{2}} - 40200_3$
4723.438	800r	200	21165.099	$0_2 - 21165^{\frac{5}{2}}$
4722.499	75	5	21169.307	$15166^{\frac{5}{2}} - 36336_3$
4722.089	300	50	21171.145	$7502_3 - 28673^{\frac{3}{2}}$
4721.456	3		21173.983	$7502_3 - 28676^{\frac{5}{2}}$
4721.276	200	15	21174.791	$8243^{\frac{3}{2}} - 29418_2$
4720.780	150	15	21177.015	$14243^{\frac{1}{2}} - 35421_1$
4720.457	75	8	21178.465	$7502_3 - 28680^{\frac{3}{4}}$
4720.338	3	1	21178.998	$15970_3 - 37149^{\frac{3}{2}}$
4720.160	50	3	21179.797	$18431_3 - 39611^{\frac{3}{4}}$
4719.692	150	5	21181.897	$17398_3 - 38580^{\frac{3}{4}}$
4719.441	20	2	21183.024	$2558_0 - 23741^{\frac{1}{2}}$
4718.051	100	5	21189.264	$20566^{\frac{3}{4}} - 41755_4$
4717.487	3	1	21191.798	$17411^{\frac{5}{2}} - 38602_2$
4717.390	20	2	21192.233	$3687_2 - 24880^{\frac{1}{2}}$
4716.862	5b		21194.605	$13297_4 - 34492^{\frac{3}{2}}$
4716.849	8b	1	21194.664	$12114^{\frac{3}{2}} - 33309_2$
4715.955	5b	1	21198.682	$18053^{\frac{3}{4}} - 39252_5$
4715.856	8	1	21199.127	$15618^{\frac{5}{2}} - 36818_2$
4714.673	150	8	21204.446	$13945^{\frac{3}{2}} - 35149_2$
4713.789	25	4b	21208.422	$16783^{\frac{3}{4}} - 37992_4$
4712.839	100	8	21212.698	$10414^{\frac{3}{4}} - 31626_5$
4712.481	300b	100	21214.309	$9804_5 - 31019^{\frac{3}{2}}$
4712.004	50	4	21216.456	$11241^{\frac{5}{2}} - 32458_4$
4711.917	5	1	21216.848	$8800_4 - 30017^{\frac{5}{2}}$
4711.417	75	5	21219.100	$17166_5 - 38385^{\frac{5}{2}}$
4708.948	3	1	21230.225	$18053^{\frac{3}{4}} - 39283_4$
4708.294	200	25	21233.174	$7280_2 - 28513^{\frac{3}{2}}$
4707.772	25b	3	21235.529	$13088_3 - 34324^{\frac{3}{2}}$
4706.691	10	2	21240.406	$11802_2 - 33043^{\frac{5}{2}}$
4706.575	100	5	21240.929	$18011^{\frac{5}{2}} - 39252_5$
4705.873	8	1	21244.098	$19532_4 - 40776^{\frac{3}{4}}$
4704.997	5	1	21248.053	$10526^{\frac{3}{2}} - 31774_3$
4704.935	8	2	21248.333	$17354^{\frac{1}{2}} - 38602_2$
4703.990	500r	200	21252.602	$0_2 - 21252^{\frac{3}{2}}$
4703.213	50	2	21256.112	$13088_3 - 34344^{\frac{3}{4}}$
4703.190	50	5	21256.216	$13175^{\frac{3}{4}} - 34431_3$
4702.778	15	2	21258.079	$10783^{\frac{5}{2}} - 32041_2$
4702.591	25	3	21258.924	$15490^{\frac{5}{2}} - 36749_6$
4702.475	25	3	21259.449	$17501^{\frac{5}{2}} - 38760_4$
4701.388	20	4	21264.364	$16351_0 - 37616^{\frac{1}{2}}$
4700.959	50	4	21266.304	$15618^{\frac{5}{2}} - 36885_4$
4700.772	200	8	21267.150	$10526^{\frac{3}{2}} - 31793_4$
4700.655	2		21267.679	$19713_3 - 40980^{\frac{3}{2}}$
4700.234	8	1	21269.584	$15493_4 - 36762^{\frac{5}{2}}$
4699.602	10	2	21272.445	$18011^{\frac{5}{2}} - 39283_4$
4698.732	25b	3	21276.383	$12114^{\frac{3}{2}} - 33390_1$
4697.600	10	2	21281.510	$17073_1 - 38355^{\frac{3}{2}}$
4697.359	2		21282.602	$19948^{\frac{3}{4}} - 41230_4$
4697.212	10	3	21283.268	$13088_3 - 34371^{\frac{3}{2}}$
4696.697	15b	4b	21285.602	$13297_4 - 34583^{\frac{3}{2}}$
4696.667	25b	8b	21285.738	$13175^{\frac{3}{4}} - 34460_5$
4696.588	2		21286.096	$18699_2 - 39985^{\frac{3}{2}}$
4695.705	1		21290.099	$20737^{\frac{1}{2}} - 42027_2$
4695.456	200	50	21291.228	$15490^{\frac{5}{2}} - 36781_5$
4695.039	300r	100	21293.119	$3687_2 - 24981^{\frac{5}{2}}$
4694.537	5	1	21295.396	$15863_2 - 37159^{\frac{1}{2}}$
4694.478	15	3b	21295.663	$15863_2 - 37159^{\frac{5}{2}}$
4692.465	3	1	21304.798	$17959_4 - 39264^{\frac{3}{2}}$
4691.883	100	8	21307.441	$15493_4 - 36800^{\frac{3}{2}}$
4691.631	300b	50b	21308.586	$6362_2 - 27670^{\frac{5}{2}}$
4691.603	50b	8b	21308.713	$7795^{\frac{3}{4}} - 29104_4$
4691.500	100	15	21309.181	$7280_2 - 28589^{\frac{3}{2}}$
4691.346	100	15	21309.880	$11241^{\frac{5}{2}} - 32551_3$
4690.894	15	2	21311.934	$6362_2 - 27674^{\frac{3}{2}}$
4690.623	300	40b	21313.165	$2869_3 - 24182^{\frac{3}{2}}$
4689.532	4		21318.123	$14481^{\frac{5}{2}} - 35799_6$

TABLE 4. *Classified lines of* Th I—continued

Wavelength (Å)	Intensity		Wavenumber (cm^{-1})	Classification	Wavelength (Å)	Intensity		Wavenumber (cm^{-1})	Classification
	Lamp	Spark				Lamp	Spark		
4689.451	50	5	21318.491	$15166_{3}^{3} - 36485_{2}$	4659.568	200	40	21455.210	$8800_{4} - 30255_{3}^{3}$
4689.252	200l	50b	21319.396	$5563_{1} - 26882_{0}^{0}$	4659.458	5		21455.717	$17501_{0}^{0} - 38956_{4}$
4688.458	5h	2	21323.006	$16783_{4}^{4} - 38106_{5}$	4657.033	1		21466.889	$15618_{3}^{3} - 37085_{4}$
4686.195	500r	50	21333.303	$2869_{3} - 24202_{4}^{4}$	4656.548	50	4	21469.125	$10526_{3}^{3} - 31995_{4}$
4684.634	40	3	21340.412	$18011_{0}^{0} - 39351_{5}$	4655.974	3		21471.771	$20214_{3}^{3} - 41686_{3}$
4684.362	50b	3	21341.651	$13088_{3} - 34430_{3}^{3}$	4655.818	4	1	21472.491	$16346_{4}^{4} - 37819_{4}$
4683.349	200	20	21346.267	$7795_{4}^{4} - 29141_{5}$	4655.328	1		21474.751	$17847_{2}^{2} - 39321_{3}$
4682.728	75	5	21349.098	$15166_{3}^{3} - 36515_{3}$	4655.210	100	20	21475.295	$18431_{3} - 39906_{4}^{4}$
4682.662	3b		21349.399	$17411_{3}^{3} - 38760_{4}$	4655.030	75	10	21476.126	$12847_{3} - 34324_{2}^{2}$
4682.229	150	15	21351.373	$17959_{4} - 39311_{4}^{4}$	4654.002	50	3	21480.869	$13847_{2} - 35328_{1}^{1}$
4681.743	1		21353.590	$11601_{1} - 32954_{2}^{2}$	4652.743	20	2	21486.682	$15166_{3}^{3} - 36653_{2}$
4680.588	50b	10b	21358.859	$11802_{2} - 33161_{1}^{1}$	4651.584	75b		21492.036	$11802_{2} - 33294_{3}^{3}$
4680.387	100	8	21359.776	$8800_{4} - 30160_{4}^{4}$	4651.112	75	5	21494.216	$11802_{2} - 33297_{2}^{2}$
4680.235	200	15	21360.470	$10414_{4}^{4} - 31774_{3}$	4651.062	75b	4	21494.447	$13088_{3} - 34583_{3}^{3}$
4679.919	3		21361.912	$16783_{4}^{4} - 38145_{3}$	4650.628	50	4	21496.453	$18930_{3}^{3} - 40426_{4}$
4679.575	4	2	21363.482	$20214_{3}^{3} - 41578_{2}$	4650.233	100	5	21498.279	$5563_{1} - 27061_{2}^{2}$
4679.390	3		21364.327	$20922_{2}^{2} - 42286_{3}$	4649.975	75	8	21499.472	$17166_{5} - 38665_{0}^{0}$
4679.001	20	1	21366.103	$13962_{1} - 35328_{1}^{1}$	4647.953	100	5	21508.825	$18011_{0}^{0} - 39520_{4}$
4678.358	5	2	21369.040	$7280_{2} - 28649_{1}^{1}$	4647.249	150	20	21512.083	$2869_{3} - 24381_{2}^{2}$
4678.233	150	20b	21369.611	$14206_{4}^{4} - 35576_{3}$	4647.249	150	20	21512.083	$15618_{3}^{3} - 37131_{3}$
4678.145	8	2	21370.012	$19516_{2}^{2} - 40886_{2}$	4647.068	50	2	21512.921	$11877_{1}^{1} - 33390_{1}$
4676.971	150	25b	21375.377	$14206_{4}^{4} - 35582_{5}$	4646.685	150	15	21514.694	$10526_{3}^{3} - 32041_{2}$
4676.248	2		21378.681	$17224_{2}^{2} - 38602_{2}$	4646.538	75b	4	21515.375	$10414_{4}^{4} - 31929_{3}$
4676.248	2		21378.681	$17224_{2}^{2} - 38602_{2}$	4646.505	8b	1	21515.528	$15493_{4} - 37008_{0}^{0}$
4676.056	500r	150	21379.559	$10414_{4}^{4} - 31793_{4}$	4645.186	3		21521.637	$18574_{1} - 40096_{2}^{2}$
4675.375	200	15	21382.673	$7502_{3} - 28884_{3}^{3}$	4644.707	150	50	21523.856	$12847_{3} - 34371_{2}^{2}$
4675.115	3	2	21383.862	$19503_{3}^{3} - 40886_{2}$	4644.495	4		21524.839	$5563_{1} - 27087_{1}^{1}$
4674.006	3		21388.936	$14032_{2}^{2} - 35421_{1}$	4643.557	100	10	21529.187	$14204_{5} - 35733_{4}^{4}$
4673.805	2		21389.856	$9804_{5} - 31194_{3}^{3}$	4643.266	1		21530.536	$16217_{2}^{2} - 37748_{2}$
4673.661	800r	150	21390.515	$2869_{3} - 24259_{4}^{4}$	4642.816	3		21532.623	$13175_{4}^{4} - 34707_{3}$
4673.042	200	25	21393.348	$7280_{2} - 28673_{2}^{2}$	4641.687	5	1	21537.860	$22399_{0}^{0} - 43937_{6}$
4672.632	8	1	21395.225	$15490_{0}^{0} - 36885_{4}$	4641.244	300b	150b	21539.916	$11241_{3}^{3} - 32781_{4}$
4672.436	50	20	21396.123	$7280_{2} - 28676_{3}^{3}$	4641.024	2		21540.937	$20214_{3}^{3} - 41755_{4}$
4672.370	2		21396.425	$17411_{3}^{3} - 38807_{2}$	4640.396	1		21543.852	$16346_{4}^{4} - 37890_{5}$
4672.332	5	1	21396.599	$18699_{2} - 40096_{2}^{2}$	4639.896	75	25	21546.174	$16346_{4}^{4} - 37892_{4}$
4671.091	2		21402.284	$16783_{4}^{4} - 38186_{4}$	4639.857	40b	5	21546.355	$4961_{4} - 26508_{3}^{3}$
4670.942	50	3	21402.966	$10526_{3}^{3} - 31929_{3}$	4639.755	5		21546.828	$18549_{2} - 40096_{2}^{2}$
4670.832	10	1	21403.471	$13088_{3} - 34492_{4}^{4}$	4639.520	200	50	21547.920	$15493_{4} - 37041_{4}^{4}$
4670.059	15b	1	21407.013	$13297_{4} - 34704_{3}^{3}$	4638.686	150	10	21551.794	$2869_{3} - 24421_{3}^{3}$
4669.984	500r	100	21407.357	$8243_{2}^{2} - 29650_{2}$	4638.127	150	10	21554.391	$11241_{3}^{3} - 32796_{3}$
4669.665	75	4	21408.819	$14032_{2}^{2} - 35440_{3}$	4637.191	50	2	21558.742	$21077_{0}^{0} - 42635_{5}$
4668.492	3		21414.198	$17166_{5} - 38580_{4}^{4}$	4636.758	4	1	21560.755	$11601_{1} - 33161_{1}^{1}$
4668.172	800r	150	21415.666	$7502_{3} - 28917_{3}^{3}$	4634.605	8	2	21570.771	$13962_{1} - 35533_{2}^{2}$
4666.797	500r	150	21421.976	$6362_{2} - 27784_{2}^{2}$	4634.227	3		21572.530	$19039_{2}^{2} - 40611_{2}$
4666.515	200	8	21423.270	$4961_{4} - 26384_{4}^{4}$	4633.765	300b	75b	21574.681	$12114_{2}^{2} - 33689_{2}$
4665.713	40	3	21426.953	$14206_{4}^{4} - 35633_{4}$	4633.620	150	8	21575.356	$8111_{4} - 29686_{3}^{3}$
4665.483	5	1	21428.009	$13297_{4} - 34725_{5}^{5}$	4632.294	3		21581.532	$10414_{4}^{4} - 31995_{4}$
4664.968	100	4	21430.375	$7502_{3} - 28932_{4}^{4}$	4632.173	5b	1	21582.096	$14465_{2}^{2} - 36047_{2}$
4664.784	25	2	21431.220	$11877_{1}^{1} - 33309_{2}$	4632.140	8b	2	21582.250	$12847_{3} - 34430_{3}^{3}$
4663.670	5	2	21436.339	$18549_{2} - 39985_{3}^{3}$	4632.038	5	1	21582.725	$16783_{4}^{4} - 38366_{4}$
4663.202	300r	10	21438.490	$2869_{3} - 24307_{2}^{2}$	4631.901	2		21583.363	$17224_{2}^{2} - 38807_{2}$
4662.590	20	2	21441.304	$3865_{1} - 25306_{2}^{2}$	4631.644	100	50	21584.561	$11197_{0}^{0} - 32781_{4}$
4660.254	20	2	21452.052	$14226_{0} - 35678_{1}^{1}$	4631.021	50	3	21587.464	$14206_{4}^{4} - 35794_{4}$
4660.254	20	2	21452.052	$17501_{0}^{0} - 38953_{5}$	4630.640	8	1	21589.241	$13297_{4} - 34886_{0}^{0}$
4660.039	4	1	21453.042	$17354_{1}^{1} - 38807_{2}$	4630.165	5		21591.455	$8243_{2}^{2} - 29835_{3}$

TABLE 4. *Classified lines of* Th I—continued

Wavelength (Å)	Intensity		Wavenumber (cm^{-1})	Classification
	Lamp	Spark		
4629.199	15		21595.961	$17073_1 - 38669^{\frac{5}{2}}_2$
4628.579	15b		21598.854	$10414^{\frac{9}{2}}_4 - 32012_4$
4628.558	75b	40	21598.952	$17411^{\frac{5}{2}}_3 - 39010_3$
4628.202	200	4	21600.613	$8111_4 - 29711^{\frac{5}{2}}_3$
4627.503	3		21603.876	$20423^{\frac{9}{2}}_1 - 42027_2$
4627.298	200	20	21604.833	$7280_2 - 28884^{\frac{5}{2}}_3$
4626.521	5	1	21608.461	$15166^{\frac{5}{2}}_3 - 36775_3$
4625.893	2		21611.395	$18069^{\frac{5}{2}}_3 - 39680_2$
4625.274	100	5	21614.287	$13847_2 - 35462^{\frac{5}{2}}_3$
4624.939	5		21615.852	$13088_3 - 34704^{\frac{5}{2}}_3$
4624.314	75	4	21618.774	$3687_2 - 25306^{\frac{5}{2}}_2$
4623.553	8b	1	21622.332	$8111_4 - 29733^{\frac{5}{2}}_3$
4623.169	10b	1	21624.128	$11802_2 - 33427^{\frac{5}{2}}_2$
4623.118	50b	5	21624.367	$14206^{\frac{9}{2}}_4 - 35831_3$
4621.657	50	2	21631.203	$13945^{\frac{5}{2}}_3 - 35576_3$
4621.165	150	40	21633.506	$8111_4 - 29744^{\frac{5}{2}}_3$
4621.076	50	2	21633.922	$3687_2 - 25321^{\frac{5}{2}}_3$
4620.705	3b		21635.659	$15970_3 - 37605^{\frac{9}{2}}_4$
4620.448	150	10	21636.862	$13088_3 - 34725^{\frac{5}{2}}_3$
4620.241	200	15	21637.832	$7280_2 - 28917^{\frac{5}{2}}_2$
4619.624	50	4	21640.722	$18053^{\frac{9}{2}}_4 - 39694_5$
4619.223	2		21642.600	$19588^{\frac{5}{2}}_5 - 41230_4$
4617.384	3		21651.220	$15166^{\frac{5}{2}}_3 - 36818_2$
4617.295	25	2	21651.637	$14481^{\frac{7}{2}}_4 - 36133_5$
4617.295	25	2	21651.637	$17959_4 - 39611^{\frac{5}{2}}_3$
4616.451	75	100	21655.596	$7502_3 - 29157^{\frac{5}{2}}_3$
4615.669	50	4	21659.265	$12114^{\frac{9}{2}}_2 - 33773_1$
4615.334	150	15	21660.837	$3865_1 - 25526^{\frac{7}{2}}_3$
4615.025	200	40	21662.287	$6362_2 - 28024^{\frac{7}{2}}_3$
4614.538	2		21664.573	$18431_3 - 40096^{\frac{9}{2}}_2$
4614.278	8	2	21665.794	$20054_2 - 41720^{\frac{9}{2}}_2$
4614.162	50	4	21666.339	$15493_4 - 37159^{\frac{5}{2}}_3$
4613.605	150	15	21668.954	$0_2 - 21668^{\frac{7}{2}}_3$
4610.628	300b	50	21682.945	$18011^{\frac{5}{2}}_3 - 39694_5$
4610.532	10	1	21683.397	$18809^{\frac{9}{2}}_4 - 40493_3$
4610.456	2		21683.754	$4961_4 - 26645^{\frac{5}{2}}_3$
4610.307	5	1	21684.455	$15618^{\frac{5}{2}}_3 - 37303_4$
4610.078	100	4	21685.532	$13847_2 - 35533^{\frac{5}{2}}_2$
4609.796	2		21686.859	$15970_3 - 37656^{\frac{5}{2}}_3$
4609.516	2		21688.176	$15618^{\frac{5}{2}}_3 - 37307_3$
4609.439	2		21688.538	$13945^{\frac{5}{2}}_3 - 35633_4$
4608.620	150	8	21692.392	$2869_3 - 24561^{\frac{5}{2}}_3$
4607.935	300	20	21695.617	$7502_3 - 29197^{\frac{5}{2}}_2$
4607.834	50	5	21696.093	$11601_1 - 33297^{\frac{5}{2}}_2$
4607.377	150	50	21698.245	$13175^{\frac{5}{2}}_3 - 34873_4$
4607.224	3		21698.965	$13175^{\frac{5}{2}}_4 - 34874_3$
4605.825	40	2	21705.556	$18549_2 - 40254^{\frac{5}{2}}_3$
4605.425	2		21707.441	$19273_2 - 40980^{\frac{5}{2}}_3$
4603.537	2		21716.344	$13962_1 - 35678^{\frac{7}{2}}_3$
4603.434	1		21716.830	$8800_4 - 30517^{\frac{5}{2}}_3$
4603.143	300b	100b	21718.202	$8243^{\frac{9}{2}}_2 - 29961_1$
4603.113	50b	8b	21718.344	$15166^{\frac{5}{2}}_3 - 36885_4$
4602.795	2		21719.845	$20566^{\frac{9}{2}}_4 - 42286_3$
4602.420	20	2	21721.614	$15490^{\frac{5}{2}}_5 - 37211_5$
4601.347	40	4	21726.680	$19986^{\frac{5}{2}}_3 - 41712_5$
4601.104	4	1	21727.827	$19503^{\frac{5}{2}}_3 - 41230_4$
4600.969	3		21728.464	$11877^{\frac{7}{2}}_3 - 33606_2$
4600.872	100	8	21728.922	$14481^{\frac{7}{2}}_4 - 36210_5$
4599.704	100	10	21734.440	$5563_1 - 27297^{\frac{7}{2}}_3$
4598.939	40	2	21738.055	$0_2 - 21738^{\frac{9}{2}}_2$
4598.888	4	1	21738.296	$19948^{\frac{5}{2}}_4 - 41686_3$
4598.434	50	4	21740.442	$17073_1 - 38814^{\frac{9}{2}}_2$
4597.243	4		21746.075	$16783^{\frac{5}{2}}_4 - 38529_3$
4596.308	200	50	21750.498	$7502_3 - 29252^{\frac{9}{2}}_2$
4596.176	100	8	21751.123	$17501^{\frac{5}{2}}_5 - 39252_5$
4595.902	3		21752.420	$15863_2 - 37616^{\frac{7}{2}}_3$
4595.420	800r	200	21754.701	$3687_2 - 25442^{\frac{5}{2}}_3$
4594.260	2		21760.194	$16346^{\frac{5}{2}}_4 - 38106_5$
4594.046	2		21761.208	$19817^{\frac{7}{2}}_3 - 41578_2$
4593.645	300	150	21763.107	$13088_3 - 34851^{\frac{9}{2}}_2$
4593.524	4	2	21763.681	$17411^{\frac{5}{2}}_3 - 39174_3$
4593.362	8	1	21764.448	$19948^{\frac{5}{2}}_4 - 41712_5$
4592.958	100	5	21766.362	$11197^{\frac{5}{2}}_5 - 32963_5$
4592.877	3		21766.746	$17073_1 - 38840^{\frac{7}{2}}_3$
4592.851	1		21766.869	$15970_3 - 37736^{\frac{9}{2}}_2$
4592.668	500r	150	21767.737	$8243^{\frac{9}{2}}_2 - 30011_3$
4592.519	15	2	21768.443	$10783^{\frac{9}{2}}_2 - 32551_3$
4592.097	8		21770.444	$8111_4 - 29881^{\frac{9}{2}}_4$
4591.972	1		21771.036	$18930^{\frac{5}{2}}_3 - 40701_4$
4591.581	8	1	21772.890	$18809^{\frac{9}{2}}_4 - 40582_5$
4589.526	3		21782.639	$17501^{\frac{5}{2}}_5 - 39283_4$
4589.328	5		21783.579	$13297_4 - 35081^{\frac{5}{2}}_5$
4588.846	8	1	21785.867	$17224^{\frac{5}{2}}_3 - 39010_3$
4588.426	500r	200	21787.861	$10414^{\frac{9}{2}}_4 - 32202_5$
4588.350	100b	25	21788.222	$11802_2 - 33591^{\frac{5}{2}}_3$
4587.332	3		21793.057	$15863_2 - 37656^{\frac{5}{2}}_3$
4586.047	50b	2	21799.163	$14032^{\frac{5}{2}}_3 - 35831_3$
4585.175	2		21803.309	$14243^{\frac{7}{2}}_3 - 36047_2$
4584.300	5	2	21807.470	$19948^{\frac{5}{2}}_4 - 41755_4$
4584.247	10	2	21807.722	$7502_3 - 29310^{\frac{9}{2}}_4$
4583.514	1		21811.210	$11877^{\frac{7}{2}}_3 - 33689_2$
4583.063	5		21813.356	$15490^{\frac{5}{2}}_5 - 37303_4$
4580.981	3		21823.270	$18431_3 - 40254^{\frac{5}{2}}_3$
4580.405	15	2	21826.014	$11601_1 - 33427^{\frac{5}{2}}_2$
4579.829	200	15	21828.759	$4961_4 - 26790^{\frac{9}{2}}_4$
4579.367	75	3	21830.961	$16554_6 - 38385^{\frac{5}{2}}_5$
4578.778	5b		21833.769	$13297_4 - 35131^{\frac{9}{2}}_4$
4577.905	100	3	21837.933	$3865_1 - 25703^{\frac{5}{2}}_2$
4577.823	100s	4	21838.324	$3687_2 - 25526^{\frac{7}{2}}_3$
4577.582	150	5	21839.474	$16346^{\frac{5}{2}}_4 - 38186_4$
4576.964	4		21842.423	$15490^{\frac{5}{2}}_5 - 37332_6$
4576.742	100	2	21843.482	$11877^{\frac{7}{2}}_3 - 33721_2$
4576.542	20	2	21844.437	$19516^{\frac{5}{2}}_3 - 41361_3$
4576.272	8	2	21845.726	$14032^{\frac{5}{2}}_3 - 35877_2$
4575.821	1		21847.879	$19039^{\frac{5}{2}}_3 - 40886_2$
4575.247	200	50	21850.620	$17501^{\frac{5}{2}}_5 - 39351_5$
4574.028	200	20	21856.443	$12847_3 - 34704^{\frac{5}{2}}_3$
4573.574	75	3	21858.613	$14204_5 - 36062^{\frac{9}{2}}_4$
4573.433	3		21859.286	$11802_2 - 33662^{\frac{7}{2}}_3$
4571.959	100	20	21866.334	$9804_5 - 31671^{\frac{9}{2}}_4$

201-606 O - 76 - 13

TABLE 4. *Classified lines of* Th I—continued

Wavelength (Å)	Intensity		Wavenumber (cm^{-1})	Classification
	Lamp	Spark		
4570.972	500r	200	21871.055	$11197^{6}_{6} - 33068_{6}$
4570.655	20h	3	21872.572	$17411^{3}_{3} - 39283_{4}$
4570.551	2		21873.070	$15863_{2} - 37736^{2}_{2}$
4569.736	100	5	21876.971	$7280_{2} - 29157^{1}_{1}$
4569.636	20	2	21877.449	$12847_{3} - 34725^{3}_{3}$
4569.574	5	2	21877.746	$7280_{2} - 29157^{3}_{3}$
4569.148	150	20	21879.786	$10414^{4}_{4} - 32293_{5}$
4568.523	100	10	21882.779	$14206^{4}_{4} - 36089_{4}$
4568.143	200	40	21884.599	$5563_{1} - 27447^{2}_{2}$
4567.856	4	1	21885.974	$13945^{3}_{3} - 35831_{3}$
4567.240	300	100	21888.926	$7795^{4}_{4} - 29684_{5}$
4566.988	10		21890.134	$0_{2} - 21890^{3}_{3}$
4566.713	15	4	21891.452	$18809^{2}_{2} - 40701_{4}$
4565.805	40b	5	21895.806	$11877^{1}_{1} - 33773_{1}$
4565.783	75b	10	21895.911	$17166_{5} - 39062^{6}_{6}$
4564.835	150	10	21900.458	$2869_{3} - 24769^{3}_{3}$
4563.658	400r	200b	21906.106	$8111_{4} - 30017^{3}_{3}$
4562.727	8	1	21910.576	$17411^{3}_{3} - 39321_{3}$
4562.476	75	5	21911.782	$9804_{5} - 31716^{6}_{6}$
4562.081	200	50	21913.679	$17959_{4} - 39873^{6}_{6}$
4561.704	5	2	21915.490	$11802_{2} - 33718^{2}_{2}$
4561.495	200	25	21916.494	$4961_{4} - 26878^{3}_{3}$
4561.397	100b	10	21916.965	$7502_{3} - 29419^{2}_{2}$
4561.348	500r	200	21917.200	$7280_{2} - 29197^{1}_{1}$
4561.228	150	10	21917.777	$7280_{2} - 29197^{2}_{2}$
4560.981	2		21918.964	$15166^{3}_{3} - 37085_{4}$
4560.067	3		21923.357	$13962_{1} - 35885^{2}_{2}$
4559.396	2		21926.583	$14206^{4}_{4} - 36133_{5}$
4559.312	50	5	21926.987	$16351_{0} - 38278^{1}_{1}$
4559.108	1		21927.969	$15166^{3}_{3} - 37094_{2}$
4559.058	100	3	21928.209	$16217^{2}_{2} - 38145_{3}$
4558.346	300	40	21931.634	$10526^{3}_{3} - 32458_{4}$
4555.903	300	150	21943.394	$13297_{4} - 35240^{3}_{3}$
4555.809	500r	100	21943.847	$3865_{1} - 25809^{1}_{1}$
4555.143	100	5	21947.055	$17959_{4} - 39906^{4}_{4}$
4554.415	100	3	21950.563	$16783^{4}_{4} - 38734_{3}$
4553.474	3		21955.099	$21902^{4}_{4} - 43857_{5}$
4552.222	100b	8	21961.138	$7795^{4}_{4} - 29756_{4}$
4552.154	300r	150	21961.466	$8800_{4} - 30761^{3}_{3}$
4551.597	25	5	21964.153	$15166^{3}_{3} - 37131_{3}$
4551.473	200	75	21964.751	$13847_{2} - 35812^{3}_{3}$
4549.833	40	2	21972.669	$7280_{2} - 29252^{2}_{2}$
4549.606	5b		21973.765	$14204_{5} - 36178^{3}_{3}$
4549.052	2		21976.441	$13297_{4} - 35273^{6}_{6}$
4548.979	20	4	21976.794	$16783^{3}_{3} - 38760_{4}$
4548.326	100b	10	21979.949	$15970_{3} - 37950^{4}_{4}$
4547.611	5	1	21983.404	$18069^{3}_{3} - 40052_{4}$
4547.248	200	25	21985.160	$6362_{2} - 28347^{2}_{2}$
4546.675	75		21987.930	$8800_{4} - 30788^{6}_{6}$
4544.729	3b		21997.345	$18614^{1}_{1} - 40611_{2}$
4544.657	20	4	21997.694	$11802_{2} - 33800^{3}_{3}$
4544.422	2		21998.831	$18053^{4}_{4} - 40052_{4}$
4543.412	100b	8b	22003.721	$12847_{3} - 34851^{2}_{2}$
4543.384	20b	5	22003.857	$14206^{4}_{4} - 36210_{5}$
4542.049	8	1	22010.324	$6362_{2} - 28372^{1}_{1}$
4541.501	10	2	22012.980	$10783^{2}_{2} - 32796_{3}$
4541.039	8b		22015.219	$14032^{2}_{2} - 36047_{2}$
4540.999	300r	75	22015.413	$3687_{2} - 25703^{2}_{2}$
4540.566	75	5	22017.513	$11197^{6}_{6} - 33214_{5}$
4540.255	50b	15	22019.021	$17501^{6}_{6} - 39520_{4}$
4540.070	4		22019.918	$16346^{2}_{2} - 38366_{4}$
4537.143	100	3	22034.123	$4961_{4} - 26995^{3}_{3}$
4536.322	2		22038.111	$13847_{2} - 35885^{2}_{2}$
4535.979	100	8	22039.778	$7795^{4}_{4} - 29835_{3}$
4535.546	100	8	22041.882	$13175^{2}_{4} - 35216_{5}$
4535.388	10	3	22042.650	$13088_{3} - 35131^{2}_{2}$
4535.255	300r	150	22043.296	$8243^{2}_{2} - 30286_{1}$
4535.103	2		22044.035	$10414^{4}_{4} - 32458_{4}$
4534.402	50	4	22047.443	$15736^{1}_{1} - 37784_{2}$
4533.717	4		22050.774	$14465^{2}_{2} - 36515_{3}$
4533.071	300	75	22053.916	$7795^{4}_{4} - 29849_{4}$
4531.574	3		22061.202	$11601_{1} - 33662^{1}_{1}$
4531.531	1		22061.411	$19516^{2}_{2} - 41578_{2}$
4530.319	200	100	22067.313	$11241^{3}_{3} - 33309_{2}$
4529.922	40	5	22069.247	$15618^{3}_{3} - 37688_{3}$
4527.115	2l		22082.930	$15970_{3} - 38053^{3}_{3}$
4525.447	40	3	22091.069	$15863_{2} - 37954^{3}_{3}$
4524.129	100	10	22097.505	$17224^{2}_{2} - 39321_{3}$
4523.211	2		22101.990	$13945^{3}_{3} - 36047_{2}$
4522.315	50	4	22106.369	$15863_{2} - 37970^{3}_{3}$
4521.332	15b	4	22111.175	$5563_{1} - 27674^{2}_{2}$
4521.305	150l	20	22111.307	$16554_{6} - 38665^{6}_{6}$
4521.196	500r	75	22111.840	$2869_{3} - 24981^{3}_{3}$
4521.059	50	5	22112.510	$15493_{4} - 37605^{4}_{4}$
4519.259	300	75	22121.317	$3687_{2} - 25809^{1}_{1}$
4518.609	5b		22124.499	$19588^{6}_{6} - 41712_{5}$
4518.342	50		22125.807	$13175^{2}_{4} - 35300_{5}$
4517.725	4b	2	22128.829	$19227^{8}_{8} - 41356_{5}$
4517.680	4b		22129.049	$15618^{3}_{3} - 37748_{2}$
4517.629	8b	3	22129.299	$14206^{4}_{4} - 36336_{3}$
4516.736	3		22133.674	$11601_{1} - 33734^{2}_{2}$
4516.540	40	4	22134.634	$14226_{0} - 36361^{1}_{1}$
4515.629	10	2	22139.100	$7280_{2} - 29419^{2}_{2}$
4515.401	10	2	22140.218	$15166^{3}_{3} - 37307_{3}$
4515.118	300r	50	22141.605	$0_{2} - 22141^{3}_{3}$
4514.548	10	2	22144.401	$13945^{3}_{3} - 36089_{4}$
4514.398	3	1	22145.137	$17166_{5} - 39311^{4}_{4}$
4514.059	75	5	22146.800	$18053^{4}_{4} - 40200_{3}$
4513.681	400r	150	22148.654	$9804_{5} - 31953^{4}_{4}$
4513.224	200	50	22150.897	$6362_{2} - 28513^{2}_{2}$
4512.950	2		22152.242	$13088_{3} - 35240^{3}_{3}$
4510.611	75		22163.729	$15493_{4} - 37656^{3}_{3}$
4510.611	75		22163.729	$17398_{3} - 39562^{2}_{4}$
4510.433	4		22164.604	$13297_{4} - 35462^{3}_{3}$
4509.960	100	8	22166.928	$11241^{3}_{3} - 33408_{3}$
4509.844	20	4	22167.498	$19588^{6}_{6} - 41755_{4}$
4509.461	2		22169.381	$16783^{4}_{4} - 38953_{5}$
4509.390	2		22169.730	$19516^{2}_{2} - 41686_{3}$
4508.715	2		22173.049	$16783^{4}_{4} - 38956_{4}$
4508.035	100	20	22176.394	$11241^{3}_{3} - 33418_{4}$

TABLE 4. *Classified lines of* Th I—continued

Wavelength (Å)	Intensity		Wavenumber (cm^{-1})	Classification
	Lamp	Spark		
4507.639	2		22178.342	$14204_5 - 36382\frac{2}{2}$
4506.549	150	40	22183.706	$12114\frac{2}{2} - 34298_1$
4506.474	200	75	22184.075	$7502_3 - 29686\frac{3}{3}$
4505.607	8	3	22188.344	$14465\frac{2}{2} - 36653_2$
4505.448	2		22189.127	$15863_2 - 38053\frac{3}{3}$
4505.216	500r	100	22190.269	$8800_4 - 30990\frac{3}{3}$
4504.630	100	20	22193.156	$17501\frac{3}{3} - 39694_5$
4503.214	15	3	22200.135	$15618\frac{3}{3} - 37819_4$
4501.177	4	2	22210.181	$19817\frac{1}{1} - 42027_2$
4500.581	20	3	22213.122	$17398_3 - 39611\frac{3}{3}$
4499.984	500	200	22216.069	$7795\frac{2}{4} - 30011_3$
4499.705	50	5	22217.446	$11241\frac{3}{3} - 33459_4$
4499.431	15	3	22218.799	$9804_5 - 32023\frac{3}{3}$
4499.383	20	8	22219.037	$7795\frac{2}{2} - 30014_4$
4498.947	800r	200	22221.190	$5563_1 - 27784\frac{2}{2}$
4498.156	40	3	22225.097	$15863_2 - 38088\frac{2}{2}$
4497.908	150b	50	22226.323	$16783\frac{3}{4} - 39010_3$
4497.908	150b	50	22226.323	$13847_2 - 36074\frac{3}{3}$
4497.888	50b		22226.421	$13962_1 - 36188\frac{2}{2}$
4497.780	3	1	22226.955	$6362_2 - 28589\frac{3}{3}$
4497.125	4	2	22230.192	$13175\frac{3}{4} - 35405_3$
4495.598	15	4	22237.743	$15166\frac{3}{3} - 37404_3$
4494.863	2		22241.380	$14243\frac{1}{1} - 36485_2$
4494.692	100	8	22242.225	$7502_3 - 29744\frac{3}{3}$
4493.763	2		22246.824	$15970_3 - 38216\frac{3}{3}$
4493.568	100	20	22247.789	$3865_1 - 26113\frac{2}{2}$
4493.334	1000r	300	22248.948	$0_2 - 22248\frac{2}{2}$
4492.677	20	5	22252.201	$15490\frac{3}{3} - 37742_6$
4492.573	8	3	22252.716	$19503\frac{3}{3} - 41755_4$
4492.102	200	20	22255.050	$10526\frac{3}{3} - 32781_4$
4490.673	200	4	22262.131	$11197\frac{3}{3} - 33459_4$
4490.524	2		22262.870	$13088_3 - 35351\frac{3}{4}$
4489.664	200	100	22267.134	$14481\frac{3}{3} - 36749_6$
4489.245	2		22269.213	$17411\frac{3}{3} - 39680_2$
4488.554	5	2	22272.641	$18614\frac{1}{1} - 40886_2$
4488.312	200	100	22273.842	$15618\frac{3}{3} - 37892_4$
4486.898	300	100	22280.861	$2558_0 - 24838\frac{1}{1}$
4486.419	8	2	22283.240	$12847_3 - 35131\frac{4}{4}$
4485.898	5	2	22285.828	$11241\frac{3}{3} - 33527_4$
4485.713	150	40	22286.747	$6362_2 - 28649\frac{1}{1}$
4484.038	200		22295.072	$17959_4 - 40254\frac{3}{3}$
4483.346	300	1	22298.513	$4961_4 - 27260\frac{3}{3}$
4482.911	5	2	22300.677	$18930\frac{3}{3} - 41230_4$
4482.855	3	1	22300.955	$8243\frac{3}{3} - 30544_2$
4482.169	400r	100	22304.368	$4961_4 - 27266\frac{4}{4}$
4481.391	20	3	22308.241	$11802_2 - 34111\frac{1}{1}$
4481.226	10	8	22309.062	$14206\frac{4}{4} - 36515_3$
4481.010	8	3	22310.137	$14465\frac{2}{2} - 36775_3$
4480.547	251	10	22312.443	$16217\frac{2}{2} - 38529_3$
4480.308	1		22313.633	$20322\frac{3}{3} - 42635_5$
4480.267	25	3	22313.837	$6362_2 - 28676\frac{3}{3}$
4479.781	15	4	22316.258	$10783\frac{2}{2} - 33099_3$
4479.637	200	75	22316.975	$12114\frac{2}{2} - 34431_3$
4478.594	150	40	22322.172	$2558_0 - 24880\frac{1}{1}$
4478.402	150	40	22323.130	$11241\frac{3}{3} - 33564_3$
4477.865	3		22325.806	$17354\frac{1}{1} - 39680_2$
4477.216	50	8	22329.043	$15490\frac{3}{3} - 37819_4$
4477.037	8		22329.935	$14226_0 - 36556\frac{1}{1}$
4476.977	5	2	22330.235	$12114\frac{2}{2} - 34444_2$
4475.765	75	8	22336.281	$15970_3 - 38306\frac{4}{4}$
4475.410	2		22338.053	$17073_1 - 39411\frac{1}{1}$
4475.410	2		22338.053	$19948\frac{2}{2} - 42286_3$
4475.221	200	40	22338.996	$0_2 - 22338\frac{3}{3}$
4474.819	50	8	22341.003	$8800_4 - 31141\frac{3}{3}$
4474.789	10		22341.153	$13847_2 - 36188\frac{2}{2}$
4474.403	5		22343.080	$14465\frac{2}{2} - 36808_3$
4473.337	2		22348.405	$3687_2 - 26036\frac{3}{3}$
4472.844	200	50	22350.868	$7502_3 - 29853\frac{2}{2}$
4472.620	20	5	22351.987	$13945\frac{3}{3} - 36297_4$
4472.348	3		22353.347	$17847\frac{2}{2} - 40200_3$
4471.871	25	2	22355.731	$4961_4 - 27317\frac{3}{3}$
4471.483	3		22357.671	$18069\frac{3}{3} - 40426_4$
4470.990	200	25	22360.136	$7280_2 - 29640\frac{1}{1}$
4470.990	200	25	22360.136	$15736\frac{1}{1} - 38097_2$
4470.105	5	2	22364.563	$11241\frac{3}{3} - 33606_2$
4469.526	400r	150	22367.460	$10414\frac{2}{2} - 32781_4$
4468.320	200	50	22373.497	$13088_3 - 35462\frac{3}{3}$
4467.188	2		22379.166	$7502_3 - 29881\frac{2}{2}$
4465.975	150	2	22385.245	$15970_3 - 38355\frac{2}{2}$
4465.471	3		22387.771	$16346\frac{3}{3} - 38734_3$
4464.848	50	20	22390.895	$13945\frac{3}{3} - 36336_3$
4464.140	10	3	22394.446	$8800_4 - 31194\frac{2}{2}$
4463.834	200	100	22395.981	$17166_5 - 39562\frac{2}{2}$
4463.668	200	75	22396.814	$0_2 - 22396\frac{1}{1}$
4463.245	4	2	22398.937	$13962_1 - 36361\frac{1}{1}$
4462.757	3		22401.386	$13175\frac{3}{4} - 35576_3$
4461.815	15b		22406.115	$8111_4 - 30517\frac{3}{3}$
4461.789	200b	100	22406.246	$7280_2 - 29686\frac{3}{3}$
4461.602	15		22407.185	$13175\frac{3}{4} - 35582_5$
4461.241	200	100	22408.998	$3687_2 - 26096\frac{3}{3}$
4459.976	15	4	22415.354	$18011\frac{3}{3} - 40426_4$
4458.736	150	75	22421.588	$3865_1 - 26287\frac{1}{1}$
4458.002	600r	200	22425.279	$3687_2 - 26113\frac{2}{2}$
4457.782	2		22426.386	$17411\frac{3}{3} - 39837_3$
4456.809	2		22431.282	$18549_2 - 40980\frac{3}{3}$
4455.867	150	25	22436.024	$13297_4 - 35733\frac{3}{4}$
4455.148	2		22439.645	$18053\frac{3}{4} - 40493_3$
4454.139	75	10	22444.728	$13088_3 - 35533\frac{2}{2}$
4453.860	8	3	22446.134	$15970_3 - 38416\frac{3}{3}$
4452.565	200	100	22452.662	$2869_3 - 25321\frac{3}{3}$
4452.437	50	4	22453.308	$14032\frac{2}{2} - 36485_2$
4451.871	1		22456.162	$17224\frac{2}{2} - 39680_2$
4451.740	20	4	22456.823	$15493_4 - 37950\frac{3}{3}$
4451.359	40	15	22458.745	$13175\frac{3}{4} - 35633_4$
4450.802	100	40	22461.556	$5563_1 - 28024\frac{1}{1}$
4450.238	5		22464.402	$7280_2 - 29744\frac{3}{3}$
4450.066	2		22465.271	$17959_4 - 40425\frac{2}{2}$
4449.437	5	1	22468.446	$16783\frac{3}{4} - 39252_5$
4447.230	150	25	22479.597	$11241\frac{3}{3} - 33721_2$
4446.584	100	15	22482.862	$8800_4 - 31283\frac{3}{3}$

TABLE 4. *Classified lines of* Th I—continued

Wavelength (Å)	Intensity		Wavenumber (cm^{-1})	Classification	Wavelength (Å)	Intensity		Wavenumber (cm^{-1})	Classification
	Lamp	Spark				Lamp	Spark		
4445.901	200	150	22486.316	$2869_3 - 25355^{\circ}_{4}$	4414.486	500d	150	22646.334	$8243^{\circ}_{2} - 30889_1$
4445.447	3	1	22488.612	$16351_0 - 38840^{\circ}_{1}$	4414.216	75	5	22647.719	$18053^{\circ}_{4} - 40701_4$
4445.309	200b	40b	22489.310	$9804_5 - 32294^{\circ}_{4}$	4414.142	15	3	22648.098	$18930^{\circ}_{3} - 41578_2$
4445.032	200	75	22490.712	$10783^{\circ}_{2} - 33273_1$	4413.632	200	25	22650.715	$8111_4 - 30761^{\circ}_{3}$
4444.901	1		22491.375	$15863_2 - 38355^{\circ}_{2}$	4413.589	1		22650.936	$18549_2 - 41200^{\circ}_{2}$
4443.665	150	100	22497.631	$3865_1 - 26363^{\circ}_{2}$	4413.343	10b	3	22652.199	$15166^{\circ}_{3} - 37819_4$
4443.203	4	2	22499.970	$16783^{\circ}_{4} - 39283_4$	4412.565	300b	50b	22656.193	$13175^{\circ}_{4} - 35831_3$
4442.513	20	5	22503.465	$12847_3 - 35351^{\circ}_{4}$	4412.270	25s	2	22657.707	$7502_3 - 30160^{\circ}_{4}$
4441.659	50	4	22507.791	$16554_0 - 39062^{\circ}_{0}$	4411.139	50	5	22663.517	$16346^{\circ}_{4} - 39010_3$
4441.609	100	5	22508.045	$0_2 - 22508^{\circ}_{2}$	4409.899	100	5	22669.889	$0_2 - 22669^{\circ}_{3}$
4441.512	25	3	22508.536	$17398_3 - 39906^{\circ}_{4}$	4408.883	800r	200	22675.113	$3687_2 - 26363^{\circ}_{2}$
4441.198	40	5	22510.128	$11601_1 - 34111^{\circ}_{1}$	4408.481	300	150	22677.181	$8111_4 - 30788^{\circ}_{0}$
4441.149	15	3	22510.376	$19516^{\circ}_{2} - 42027_2$	4408.251	20	2	22678.364	$14206^{\circ}_{4} - 36885_4$
4440.353	300	75	22514.411	$8243^{\circ}_{2} - 30758_2$	4406.472	5	2	22687.520	$19948^{\circ}_{4} - 42635_5$
4440.276	300	75	22514.802	$7502_3 - 30017^{\circ}_{3}$	4405.999	15	3	22689.955	$18011^{\circ}_{5} - 40701_4$
4440.230	2		22515.035	$13297_4 - 35812^{\circ}_{3}$	4404.820	15	3	22696.028	$15490^{\circ}_{5} - 38186_4$
4439.858	100	4	22516.921	$16217^{\circ}_{2} - 38734_3$	4404.474	1		22697.811	$17398_3 - 40096^{\circ}_{2}$
4439.000	8	2	22521.273	$15166^{\circ}_{3} - 37688_3$	4404.113	300	40	22699.672	$15970_3 - 38669^{\circ}_{2}$
4438.746	400	200	22522.562	$6362_2 - 28884^{\circ}_{3}$	4403.425	50	3	22703.218	$18431_3 - 41134^{\circ}_{4}$
4438.092	150	8	22525.881	$10783^{\circ}_{2} - 33309_2$	4402.927	500	150	22705.786	$2869_3 - 25575^{\circ}_{4}$
4437.446	300	20	22529.160	$18053^{\circ}_{4} - 40582_5$	4402.601	75	10	22707.467	$17166_5 - 39873^{\circ}_{0}$
4435.705	4	1	22538.003	$16783^{\circ}_{4} - 39321_3$	4402.448	50	5	22708.256	$13945^{\circ}_{3} - 36653_2$
4435.296	100	10	22540.081	$13945^{\circ}_{3} - 36485_2$	4402.246	200	50	22709.299	$4961_4 - 27670^{\circ}_{3}$
4434.075	150	40	22546.288	$18809^{\circ}_{4} - 41356_5$	4401.581	500	200	22712.729	$7795^{\circ}_{3} - 30508_5$
4433.490	150	50	22549.263	$10414^{\circ}_{4} - 32963_5$	4399.968	150	50	22721.055	$8243^{\circ}_{2} - 30964_3$
4432.252	400	150	22555.561	$6362_2 - 28917^{\circ}_{2}$	4399.583	8	2	22723.044	$11601_1 - 34324^{\circ}_{2}$
4431.416	100	8	22559.816	$15493_4 - 38053^{\circ}_{3}$	4399.453	15	3	22723.715	$15493_4 - 38216^{\circ}_{3}$
4429.979	100	8	22567.134	$15618^{\circ}_{3} - 38186_4$	4399.027	50	15	22725.916	$15166^{\circ}_{3} - 37892_4$
4429.822	200	20	22567.934	$16783^{\circ}_{4} - 39351_5$	4398.272	15	3	22729.817	$14481^{\circ}_{5} - 37211_5$
4429.722	8	2	22568.443	$14206^{\circ}_{4} - 36775_3$	4397.009	200w	40	22736.346	$16783^{\circ}_{4} - 39520_4$
4429.633	200	20h	22568.897	$11802_2 - 34371^{\circ}_{2}$	4396.140	100	10	22740.840	$17166_5 - 39906^{\circ}_{4}$
4428.828	5	2	22572.999	$7280_2 - 29853^{\circ}_{2}$	4395.674	10	2	22743.251	$14032^{\circ}_{2} - 36775_3$
4428.744	100	5	22573.427	$2869_3 - 25442^{\circ}_{3}$	4394.838	50	15	22747.577	$15618^{\circ}_{3} - 38366_4$
4428.553	200	40	22574.400	$14206^{\circ}_{4} - 36781_5$	4393.759	400	150	22753.163	$7502_3 - 30255^{\circ}_{3}$
4427.530	100b	8	22579.616	$13847_2 - 36427^{\circ}_{3}$	4393.131	4	2	22756.416	$18930^{\circ}_{3} - 41686_3$
4427.232	100	15	22581.136	$15166^{\circ}_{3} - 37748_2$	4392.974	400	100	22757.229	$7795^{\circ}_{3} - 30552_4$
4426.019	1		22587.325	$17398_3 - 39985^{\circ}_{3}$	4392.495	100b	10	22759.710	$12114^{\circ}_{2} - 34874_3$
4425.460	200	20	22590.177	$16217^{\circ}_{2} - 38807_2$	4391.531	100	25	22764.706	$17959_4 - 40724^{\circ}_{0}$
4424.836	200b	50	22593.363	$12114^{\circ}_{2} - 34707_3$	4391.390	150	50	22765.437	$13297_4 - 36062^{\circ}_{1}$
4424.661	4	2	22594.257	$13962_1 - 36556^{\circ}_{1}$	4390.613	15	3	22769.466	$19516^{\circ}_{2} - 42286_3$
4424.243	75	5	22596.392	$14204_5 - 36800^{\circ}_{4}$	4389.308	3	1	22776.236	$14032^{\circ}_{2} - 36808_3$
4423.719	400	150	22599.068	$3687_2 - 26287^{\circ}_{1}$	4389.234	8	2	22776.620	$13297_4 - 36074^{\circ}_{3}$
4423.263	100	10	22601.398	$14206^{\circ}_{4} - 36808_3$	4388.569	10	3	22780.071	$11802_2 - 34583^{\circ}_{3}$
4422.048	600	200	22607.608	$10783^{\circ}_{2} - 33390_1$	4388.541	1		22780.216	$21077^{\circ}_{5} - 43857_5$
4420.925	100	8	22613.350	$17224^{\circ}_{2} - 39837_3$	4388.101	50	5	22782.500	$10526^{\circ}_{3} - 33309_2$
4420.782	300b	100b	22614.082	$12847_3 - 35462^{\circ}_{3}$	4387.734	150	40	22784.406	$5563_1 - 28347^{\circ}_{2}$
4420.256	200	20	22616.773	$15490^{\circ}_{5} - 38106_5$	4387.028	100b	40	22788.072	$11802_2 - 34591^{\circ}_{1}$
4420.112	100	10	22617.509	$15166^{\circ}_{3} - 37784_2$	4386.138	3		22792.696	$16217^{\circ}_{2} - 39010_3$
4419.768	100	20	22619.270	$13175^{\circ}_{4} - 35794_4$	4385.753	25	5	22794.697	$6362_2 - 29157^{\circ}_{1}$
4418.554	75	3	22625.484	$10783^{\circ}_{2} - 33408_3$	4384.656	150b	50b	22800.400	$10414^{\circ}_{4} - 33214_5$
4418.201	15	2	22627.292	$11802_2 - 34430^{\circ}_{3}$	4383.872	100	40	22804.478	$14204_5 - 37008^{\circ}_{0}$
4417.229	10	3	22632.271	$18069^{\circ}_{3} - 40701_4$	4383.602	15	3	22805.882	$15863_2 - 38669^{\circ}_{2}$
4416.946	25	3	22633.721	$14204_5 - 36837^{\circ}_{0}$	4382.893	100	15	22809.571	$5563_1 - 28372^{\circ}_{1}$
4416.844	500	100	22634.244	$9804_5 - 32439^{\circ}_{2}$	4382.526	3		22811.481	$15863_2 - 38675^{\circ}_{3}$
4414.767	75	10	22644.892	$13088_3 - 35733^{\circ}_{4}$	4382.205	20	5	22813.152	$15493_4 - 38306^{\circ}_{4}$

TABLE 4. *Classified lines of* Th I—continued

Wavelength (Å)	Intensity		Wavenumber (cm^{-1})	Classification
	Lamp	Spark		
4381.130	2		22818.750	$15970_3 - 38788\frac{5}{6}$
4380.879	4	1	22820.057	$3687_2 - 26508\frac{5}{6}$
4380.716	15		22820.906	$13847_2 - 36668\frac{2}{3}$
4380.289	200	25	22823.131	$10783\frac{2}{3} - 33606_2$
4379.860	20	4	22825.366	$15166\frac{5}{6} - 37992_4$
4378.177	500r	100	22834.140	$2869_3 - 25703\frac{2}{3}$
4378.026	100	3	22834.928	$6362_2 - 29197\frac{1}{2}$
4377.650	8		22836.889	$14204_5 - 37041\frac{1}{4}$
4376.682	8	2	22841.940	$14465\frac{2}{3} - 37307_3$
4376.257	25	5	22844.158	$15970_3 - 38814\frac{2}{3}$
4374.710	8	3	22852.236	$8243\frac{2}{3} - 31095_1$
4374.124	600	150	22855.298	$0_2 - 22855\frac{5}{6}$
4374.013	150	40	22855.878	$7795\frac{3}{4} - 30651_3$
4373.206	40	8	22860.095	$21077\frac{5}{6} - 43937_6$
4372.067	1		22866.051	$15736\frac{1}{2} - 38602_2$
4371.140	75	8	22870.900	$8800_4 - 31671\frac{3}{4}$
4370.980	10	3	22871.737	$17398_3 - 40270\frac{1}{4}$
4370.068	5	2	22876.510	$15490\frac{5}{6} - 38366_4$
4369.876	200	50	22877.515	$0_2 - 22877\frac{1}{2}$
4369.602	50	25	22878.950	$14206\frac{3}{4} - 37085_4$
4369.496	100	25	22879.505	$8111_4 - 30990\frac{5}{6}$
4369.288	50b	25	22880.594	$13297_4 - 36178\frac{3}{4}$
4368.995	20	4	22882.128	$10526\frac{5}{6} - 33408_3$
4368.352	5	2	22885.497	$12847_3 - 35733\frac{1}{4}$
4367.418	100	15	22890.391	$6362_2 - 29252\frac{2}{3}$
4367.287	50	15	22891.077	$4961_4 - 27852\frac{5}{6}$
4367.191	5	2	22891.581	$10526\frac{5}{6} - 33418_4$
4367.113	3	1	22891.989	$15493_4 - 38385\frac{5}{6}$
4365.930	600	150	22898.192	$8243\frac{2}{3} - 31141_3$
4365.302	4	1	22901.486	$11802_2 - 34704\frac{5}{6}$
4365.020	25	8	22902.966	$18809\frac{3}{4} - 41712_5$
4364.506	8	3	22905.663	$16346\frac{5}{6} - 39252_5$
4364.461	5	2	22905.899	$10783\frac{2}{3} - 33689_2$
4364.040	25	4	22908.109	$8111_4 - 31019\frac{3}{4}$
4363.798	2		22909.379	$13962_1 - 36871\frac{2}{3}$
4363.589	1		22910.476	$16783\frac{5}{6} - 39694_5$
4363.500	8	2	22910.944	$15618\frac{5}{6} - 38529_3$
4362.720	15	3	22915.040	$13847_2 - 36762\frac{5}{6}$
4362.472	50	8	22916.343	$8800_4 - 31716\frac{5}{6}$
4361.201	4	1	22923.021	$15493_4 - 38416\frac{5}{6}$
4360.991	5	1	22924.125	$14206\frac{3}{4} - 37131_3$
4360.825	3	1	22924.997	$15863_2 - 38788\frac{5}{6}$
4360.167	100	15	22928.457	$7280_2 - 30208\frac{2}{3}$
4359.836	10	2	22930.198	$15166\frac{5}{6} - 38097_2$
4359.558	15	4	22931.660	$12114\frac{2}{3} - 35046_1$
4359.372	600r	100	22932.638	$10526\frac{5}{6} - 33459_4$
4358.321	500	150	22938.168	$10783\frac{2}{3} - 33721_2$
4358.082	15	5	22939.426	$14465\frac{2}{3} - 37404_3$
4357.974	8	2	22939.995	$13945\frac{5}{6} - 36885_4$
4356.835	3	1	22945.992	$18809\frac{3}{4} - 41755_4$
4356.045	75	20	22950.153	$5563_1 - 28513\frac{2}{3}$
4354.660	5	2	22957.452	$16217\frac{2}{3} - 39174_3$
4354.483	400	100	22958.386	$13175\frac{3}{4} - 36133_5$
4353.449	300b	100b	22963.838	$3687_2 - 26651\frac{2}{3}$
4352.613	150	25b	22968.249	$2558_0 - 25526\frac{1}{2}$
4351.466	100	50	22974.303	$13088_3 - 36062\frac{3}{4}$
4351.274	200	50	22975.317	$7280_2 - 30255\frac{5}{6}$
4351.120	8	3	22976.130	$17224\frac{2}{3} - 40200_3$
4351.017	50	10	22976.673	$15863_2 - 38840\frac{1}{2}$
4350.272	100	10	22980.609	$8800_4 - 31780\frac{5}{6}$
4349.630	40	5	22984.000	$15618\frac{5}{6} - 38602_2$
4349.346	20	4	22985.501	$13088_3 - 36074\frac{5}{6}$
4349.072	400	40	22986.949	$4961_4 - 27948\frac{3}{4}$
4348.828	3	1	22988.239	$19039\frac{2}{3} - 42027_4$
4348.599	400	75	22989.449	$13847_2 - 36837\frac{1}{2}$
4348.498	4	1	22989.983	$11601_1 - 34591\frac{1}{2}$
4348.403	3	1	22990.485	$10783\frac{2}{3} - 33773_1$
4347.638	100	15	22994.531	$10414\frac{3}{4} - 33408_3$
4346.432	500r	200	23000.911	$7280_2 - 30281\frac{1}{2}$
4346.410	15b		23001.028	$10526\frac{5}{6} - 33527_4$
4345.851	150	50	23003.986	$10414\frac{3}{4} - 33418_4$
4345.702	25	10	23004.775	$14206\frac{3}{4} - 37211_5$
4343.744	5		23015.144	$7502_3 - 30517\frac{3}{4}$
4343.381	100	25	23017.068	$3865_1 - 26882\frac{5}{6}$
4342.973	15	4	23019.230	$15166\frac{5}{6} - 38186_4$
4342.674	100	20	23020.815	$17959_4 - 40980\frac{5}{6}$
4342.445	500r	100	23022.029	$8243\frac{2}{3} - 31265_3$
4342.049	50	4	23024.128	$13847_2 - 36871\frac{2}{3}$
4340.896	200	40	23030.244	$8111_4 - 31141\frac{5}{6}$
4339.924	10	2	23035.402	$12114\frac{2}{3} - 35149_2$
4339.449	8	2	23037.923	$12847_3 - 35885\frac{2}{3}$
4339.374	15	3	23038.321	$10526\frac{5}{6} - 33564_3$
4339.069	3	1	23039.941	$17847\frac{2}{3} - 40886_2$
4338.108	400	100	23045.045	$10414\frac{3}{4} - 33459_4$
4337.639	15	4	23047.536	$19588\frac{5}{6} - 42635_5$
4337.277	800r	100	23049.460	$0_2 - 23049\frac{1}{2}$
4336.986	50	10	23051.006	$7502_3 - 30553\frac{2}{3}$
4335.992	5	2	23056.291	$14465\frac{2}{3} - 37521_3$
4335.731	200b	50b	23057.678	$9804_5 - 32862\frac{3}{4}$
4335.347	25b	8	23059.721	$11241\frac{5}{6} - 34301_4$
4333.552	10	3	23069.272	$20867\frac{2}{3} - 43937_6$
4333.284	75	4	23070.699	$15736\frac{1}{2} - 38807_2$
4332.339	150	40	23075.731	$11802_2 - 34878\frac{1}{2}$
4331.582	5	1	23079.764	$10526\frac{5}{6} - 33606_2$
4331.291	4b	2b	23081.314	$15618\frac{5}{6} - 38700_4$
4330.844	300	25	23083.697	$8111_4 - 31194\frac{3}{4}$
4330.565	8b	3	23085.184	$13297_4 - 36382\frac{3}{4}$
4330.412	50	20	23086.000	$5563_1 - 28649\frac{1}{2}$
4328.915	300r	25	23093.983	$0_2 - 23093\frac{5}{6}$
4328.436	3	1	23096.539	$14206\frac{3}{4} - 37303_4$
4327.981	15	3	23098.966	$14032\frac{5}{6} - 37131_3$
4327.715	150	25	23100.386	$13088_3 - 36188\frac{2}{3}$
4327.036	100	25	23104.011	$17166_5 - 40270\frac{1}{4}$
4325.860	150	8	23110.292	$5563_1 - 28673\frac{2}{3}$
4325.274	200	50	23113.423	$10414\frac{3}{4} - 33527_4$
4324.901	20	4	23115.416	$15618\frac{5}{6} - 38734_3$
4323.634	20	5	23122.190	$13175\frac{3}{4} - 36297_4$
4322.181	3		23129.963	$13297_4 - 36427\frac{5}{6}$
4321.224	5	2	23135.085	$15863_2 - 38998\frac{5}{6}$

TABLE 4. *Classified lines of* Th I—continued

Wavelength (Å)	Intensity		Wavenumber (cm^{-1})	Classification	Wavelength (Å)	Intensity		Wavenumber (cm^{-1})	Classification
	Lamp	Spark				Lamp	Spark		
4318.523	20	8	23149.555	$13945\frac{5}{3} - 37094_2$	4288.471	200b	50b	23311.775	$13847_2 - 37159\frac{5}{3}$
4317.838	100	5	23153.227	$8800_4 - 31953\frac{3}{4}$	4287.082	200	40	23319.328	$16554_6 - 39873\frac{6}{5}$
4316.371	25	5	23161.096	$13175\frac{5}{4} - 36336_3$	4286.229	200b	75b	23323.969	$6362_2 - 29686\frac{3}{3}$
4316.218	10	3	23161.917	$18069\frac{3}{3} - 41230_4$	4285.757	3	1	23326.537	$12114\frac{2}{2} - 35440_3$
4316.109	200	50	23162.502	$10526\frac{3}{3} - 33689_2$	4285.398	10	3	23328.491	$13297_4 - 36625\frac{6}{5}$
4315.254	500r	150	23167.091	$2869_3 - 26036\frac{3}{3}$	4283.103	200b	50b	23340.991	$12847_3 - 36188\frac{2}{2}$
4315.052	100	15	23168.176	$11877\frac{1}{1} - 35046_1$	4283.073	50b	20b	23341.155	$15970_3 - 39311\frac{4}{4}$
4314.491	8	3	23171.188	$18549_2 - 41720\frac{2}{2}$	4282.084	150b	50b	23346.546	$7795\frac{4}{4} - 31141_3$
4314.319	300	50	23172.112	$8111_4 - 31283\frac{3}{3}$	4280.568	300r	100	23354.814	$5563_1 - 28917\frac{2}{2}$
4314.279	2		23172.327	$15493_4 - 38665\frac{5}{5}$	4280.322	8	3	23356.156	$18930\frac{3}{3} - 42286_3$
4314.053	20	8	23173.541	$16346\frac{6}{4} - 39520_4$	4279.281	25	3	23361.837	$13945\frac{5}{3} - 37307_3$
4313.778	25	8	23175.018	$17959_4 - 41134\frac{4}{4}$	4279.064	300	40	23363.022	$15166\frac{6}{5} - 38529_3$
4313.335	2		23177.398	$18053\frac{3}{4} - 41230_4$	4278.324	500r	200	23367.063	$14204_5 - 37571\frac{6}{6}$
4312.992	800r	200	23179.241	$2869_3 - 26048\frac{4}{4}$	4275.567	50	4	23382.130	$6362_2 - 29744\frac{3}{3}$
4312.992	800r	200	23179.241	$4961_4 - 28140\frac{4}{4}$	4275.165	15	2	23384.329	$10783\frac{3}{2} - 34167_3$
4311.798	300	100	23185.660	$8243\frac{3}{2} - 31429_1$	4274.817	200	25	23386.233	$13847_2 - 37234\frac{2}{2}$
4311.625	150b	25	23186.590	$13962_1 - 37149\frac{2}{2}$	4273.911	15	3	23391.190	$15618\frac{5}{5} - 39010_3$
4311.576	100b	25	23186.854	$11802_2 - 34989\frac{1}{1}$	4272.875	400r	50	23396.862	$8800_4 - 32197\frac{3}{3}$
4311.062	150	15	23189.618	$11241\frac{3}{3} - 34431_3$	4272.303	300r	100	23399.994	$3687_2 - 27087\frac{1}{1}$
4310.957	75	5	23190.183	$3687_2 - 26878\frac{3}{3}$	4270.734	100	15	23408.591	$14481\frac{3}{3} - 37890_5$
4310.101	15	5	23194.788	$10526\frac{3}{3} - 33721_2$	4269.943	300	75	23412.927	$8111_4 - 31523\frac{3}{3}$
4309.886	150	50	23195.945	$3865_1 - 27061\frac{2}{2}$	4269.272	3	1	23416.607	$16783\frac{4}{4} - 40200_3$
4309.557	25	4	23197.716	$14206\frac{6}{4} - 37404_3$	4269.063	100	5	23417.753	$10414\frac{4}{4} - 33831_4$
4308.599	100b	20	23202.874	$11241\frac{3}{3} - 34444_2$	4266.447	15	3	23432.111	$3865_1 - 27297\frac{1}{1}$
4308.121	300	100	23205.449	$11241\frac{3}{3} - 34447_4$	4264.338	200l	20	23443.700	$7280_2 - 30723\frac{1}{1}$
4307.176	600r	200	23210.540	$11197\frac{8}{8} - 34407_6$	4261.492	150	4	23459.356	$13945\frac{5}{3} - 37404_3$
4305.495	5	2	23219.602	$18011\frac{6}{6} - 41230_4$	4260.984	100	2	23462.153	$12114\frac{2}{2} - 35576_3$
4304.955	150	10	23222.514	$3865_1 - 27087\frac{1}{1}$	4260.802	150	1	23463.155	$15490\frac{6}{6} - 38953_5$
4304.868	8	3	23222.984	$14465\frac{5}{2} - 37688_3$	4260.395	15	1	23465.397	$13297_4 - 36762\frac{3}{3}$
4304.801	8	3	23223.345	$8800_4 - 32023\frac{6}{6}$	4260.332	800r	5	23465.744	$9804_5 - 33270\frac{4}{4}$
4304.290	8	3	23226.102	$12847_3 - 36074\frac{3}{3}$	4260.288	75b	1	23465.986	$11241\frac{3}{3} - 34707_3$
4303.988	75	5	23227.732	$2869_3 - 26096\frac{3}{3}$	4260.138	20		23466.812	$15490\frac{6}{6} - 38956_4$
4300.370	3	1	23247.273	$19039\frac{4}{4} - 42286_3$	4259.494	200	1	23470.360	$7795\frac{4}{4} - 31265_3$
4299.839	500r	100	23250.144	$11197\frac{8}{8} - 34447_4$	4258.521	400	2	23475.723	$7795\frac{4}{4} - 31271_5$
4299.633	200	50	23251.258	$2558_0 - 25809\frac{1}{1}$	4257.496	600r	4	23481.375	$0_2 - 23481\frac{1}{1}$
4298.121	75	5	23259.437	$7502_3 - 30761\frac{3}{3}$	4257.459	10h		23481.579	$7280_2 - 30761\frac{3}{3}$
4297.938	100	20	23260.428	$14481\frac{3}{3} - 37742_6$	4256.254	500r	8	23488.226	$7502_3 - 30990\frac{3}{3}$
4297.307	300b	75	23263.843	$11197\frac{8}{8} - 34460_5$	4256.039	10		23489.413	$14032\frac{2}{2} - 37521_3$
4295.902	2	1	23271.451	$13962_1 - 37234\frac{2}{2}$	4255.795	150b	4	23490.760	$6362_2 - 29853\frac{2}{2}$
4295.816	100	40	23271.917	$11877\frac{1}{1} - 35149_2$	4255.759	50b	3	23490.958	$16346\frac{6}{4} - 39837_3$
4295.584	200	25	23273.174	$7280_2 - 30553\frac{2}{2}$	4255.237	200	3	23493.840	$2869_3 - 26363\frac{2}{2}$
4295.236	25	5	23275.060	$14032\frac{2}{2} - 37307_3$	4254.380	100	1	23498.572	$15970_3 - 39468\frac{5}{5}$
4294.756	75b	25b	23277.661	$11601_1 - 34878\frac{1}{1}$	4253.539	600r	20	23503.218	$13297_4 - 36800\frac{4}{4}$
4294.720	100b	25	23277.856	$6362_2 - 29640\frac{1}{1}$	4253.388	10b		23504.053	$14243\frac{1}{1} - 37748_2$
4293.800	8b	3	23282.844	$14465\frac{5}{2} - 37748_2$	4251.421	5		23514.927	$10783\frac{3}{2} - 34298_1$
4292.681	4	1	23288.913	$18431_3 - 41720\frac{2}{2}$	4251.286	50		23515.674	$2869_3 - 26384\frac{4}{4}$
4292.305	50	10	23290.953	$12114\frac{2}{2} - 35405_3$	4251.077	4		23516.830	$7502_3 - 31019\frac{3}{3}$
4291.810	400	100	23293.639	$8243\frac{3}{2} - 31537_3$	4250.775	100	2	23518.501	$4961_4 - 28480\frac{4}{4}$
4291.635	50	10	23294.589	$15970_3 - 39264\frac{3}{3}$	4250.315	800r	75	23521.046	$0_2 - 23521\frac{3}{3}$
4290.394	200	50	23301.327	$13847_2 - 37149\frac{2}{2}$	4249.476	150	1	23525.690	$11802_2 - 35328\frac{1}{1}$
4289.655	100	40	23305.341	$10526\frac{3}{3} - 33831_4$	4248.518	50	1	23530.995	$8243\frac{3}{2} - 31774_3$
4289.414	8	3	23306.650	$12114\frac{2}{2} - 35421_1$	4248.391	200	3	23531.698	$7795\frac{4}{4} - 31326_4$
4289.204	8	2	23307.791	$3687_2 - 26995\frac{5}{5}$	4248.274	4		23532.346	$17354\frac{1}{1} - 40886_2$
4289.204	8	2	23307.791	$18053\frac{3}{4} - 41361_3$	4248.181	5		23532.861	$7280_2 - 30812\frac{2}{2}$
4288.669	200	75	23310.699	$7502_3 - 30812\frac{2}{2}$	4247.861	150	2	23534.634	$12847_3 - 36382\frac{2}{2}$

TABLE 4. *Classified lines of* Th I—continued

Wavelength (Å)	Intensity		Wavenumber (cm^{-1})	Classification	Wavelength (Å)	Intensity		Wavenumber (cm^{-1})	Classification
	Lamp	Spark				Lamp	Spark		
4247.777	10		23535.099	$20322_{6} - 43857_{5}$	4215.210	4		23716.930	$12114\frac{2}{2} - 35831_{3}$
4246.796	10b		23540.536	$13297_{4} - 36837_{6}$	4214.828	200	4	23719.079	$4961_{4} - 28680\frac{3}{3}$
4246.324	20	1	23543.153	$11877\frac{1}{1} - 35421_{1}$	4213.315	15	1	23727.596	$11601_{1} - 35328\frac{1}{1}$
4245.451	100	3	23547.994	$15863_{2} - 39411\frac{1}{1}$	4213.067	400	5	23728.993	$2558_{0} - 26287\frac{1}{1}$
4244.022	25	1	23555.922	$15618\frac{3}{3} - 39174_{3}$	4212.923	50	1	23729.804	$17501_{6} - 41230_{4}$
4243.261	100	2	23560.147	$8111_{4} - 31671\frac{3}{3}$	4212.653	4		23731.325	$17847\frac{2}{2} - 41578_{2}$
4241.697	4		23568.834	$15493_{4} - 39062_{6}$	4210.923	900r	10	23741.075	$0_{2} - 23741\frac{1}{1}$
4241.096	100	2	23572.173	$3687_{2} - 27260\frac{3}{3}$	4210.765	400	10	23741.965	$7795\frac{4}{4} - 31537_{3}$
4239.791	15		23579.429	$12847_{3} - 36427\frac{3}{3}$	4210.600	2		23742.896	$13945\frac{3}{3} - 37688_{3}$
4239.276	4		23582.293	$3865_{1} - 27447\frac{2}{2}$	4210.455	75	2	23743.713	$13297_{4} - 37041\frac{3}{3}$
4239.276	4		23582.293	$17398_{3} - 40980\frac{3}{3}$	4210.089	75	3	23745.778	$14204_{5} - 37950\frac{1}{1}$
4237.535	10		23591.982	$15970_{3} - 39562\frac{2}{2}$	4208.921	100b	10b	23752.367	$14032\frac{2}{2} - 37784_{2}$
4237.182	20		23593.947	$5563_{1} - 29157\frac{1}{1}$	4208.867	200b		23752.672	$0_{2} - 23752\frac{2}{2}$
4236.049	50	1	23600.258	$13175\frac{4}{4} - 36775_{3}$	4208.750	100b	5	23753.332	$10414\frac{4}{4} - 34167_{3}$
4235.463	600r	5	23603.523	$0_{2} - 23603\frac{2}{2}$	4208.412	150	4	23755.240	$9804_{5} - 33560\frac{4}{4}$
4235.238	20	1	23604.777	$15863_{2} - 39468\frac{3}{3}$	4207.612	25	1	23759.756	$3687_{2} - 27447\frac{2}{2}$
4235.092	50	1	23605.591	$8111_{4} - 31716\frac{6}{6}$	4207.176	20	1	23762.218	$15490\frac{6}{6} - 39252_{5}$
4234.231	50	1	23610.390	$17166_{5} - 40776\frac{4}{4}$	4206.058	10	1	23768.535	$13847_{2} - 37616\frac{1}{1}$
4233.907	50	1	23612.197	$14206\frac{4}{4} - 37819_{4}$	4205.540	10		23771.462	$15493_{4} - 39264\frac{3}{3}$
4232.478	1		23620.169	$16217\frac{2}{2} - 39837_{3}$	4205.012	4		23774.447	$13962_{1} - 37736\frac{2}{2}$
4231.617	10		23624.975	$14481\frac{6}{6} - 38106_{5}$	4204.930	3		23774.911	$10526\frac{3}{3} - 34301_{4}$
4231.136	4		23627.661	$4961_{4} - 28589\frac{3}{3}$	4203.884	75	2	23780.826	$7502_{3} - 31283\frac{3}{3}$
4230.823	150	1	23629.409	$3687_{2} - 27317\frac{5}{5}$	4203.575	15	1	23782.574	$2869_{3} - 26651\frac{2}{2}$
4230.427	500	5	23631.621	$11241\frac{3}{3} - 34873_{4}$	4203.437	4	1	23783.355	$13088_{3} - 36871\frac{2}{2}$
4230.299	15		23632.336	$11241\frac{3}{3} - 34874_{3}$	4203.085	15	1	23785.346	$14206\frac{2}{4} - 37992_{4}$
4229.961	10		23634.224	$5563_{1} - 29197\frac{1}{1}$	4202.266	50	2	23789.982	$15166\frac{3}{3} - 38956_{4}$
4229.864	20		23634.766	$5563_{1} - 29197\frac{2}{2}$	4200.686	2		23798.930	$16783\frac{4}{4} - 40582_{5}$
4229.148	300	4	23638.767	$2869_{3} - 26508\frac{3}{3}$	4200.149	2		23801.973	$17398_{3} - 41200\frac{2}{2}$
4228.761	150b	3	23640.931	$10526\frac{3}{3} - 34167_{3}$	4200.017	2		23802.721	$13945\frac{3}{3} - 37748_{2}$
4228.677	25b	2	23641.400	$15970_{3} - 39611\frac{3}{3}$	4198.936	20	1	23808.849	$3865_{1} - 27674\frac{2}{2}$
4228.418	100	3	23642.848	$16783\frac{4}{4} - 40426_{4}$	4198.876	15	1	23809.189	$13847_{2} - 37656\frac{3}{3}$
4227.387	400	8	23648.614	$7280_{2} - 30928\frac{1}{1}$	4197.317	2		23818.032	$15493_{4} - 39311\frac{3}{3}$
4226.775	100	2	23652.038	$11197\frac{6}{6} - 34849_{5}$	4197.016	2		23819.740	$17411\frac{3}{3} - 41230_{4}$
4226.298	200		23654.708	$6362_{2} - 30017\frac{3}{3}$	4196.846	10s		23820.705	$12847_{3} - 36668\frac{2}{2}$
4226.047	10		23656.113	$14032\frac{2}{2} - 37688_{3}$	4194.936	200	5	23831.551	$7795\frac{4}{4} - 31626_{5}$
4225.489	50l	2	23659.236	$18053\frac{4}{4} - 41712_{5}$	4193.601	1		23839.137	$13945\frac{3}{3} - 37784_{2}$
4225.095	3		23661.443	$10783\frac{2}{2} - 34444_{2}$	4193.518	15	2	23839.609	$17847\frac{2}{2} - 41686_{3}$
4224.871	3		23662.697	$17224\frac{2}{2} - 40886_{2}$	4193.017	600	15	23842.457	$8111_{4} - 31953\frac{4}{4}$
4224.488	3		23664.843	$15618\frac{3}{3} - 39283_{4}$	4192.877	2		23843.253	$15166\frac{3}{3} - 39010_{3}$
4223.589	150b	3	23669.880	$8111_{4} - 31780\frac{3}{3}$	4192.362	150	3	23846.182	$6362_{2} - 30208\frac{2}{2}$
4222.439	20		23676.326	$11197\frac{6}{6} - 34873_{4}$	4191.146	15	1	23853.101	$14243\frac{1}{1} - 38097_{2}$
4221.691	75	2	23680.521	$14465\frac{2}{2} - 38145_{3}$	4191.028	3		23853.772	$16346\frac{4}{4} - 40200_{3}$
4221.151	100	2	23683.550	$14206\frac{4}{4} - 37890_{5}$	4190.813	5	1	23854.996	$17501\frac{6}{6} - 41356_{5}$
4220.730	150	2	23685.913	$8243\frac{2}{2} - 31929_{3}$	4190.620	15	1	23856.095	$5563_{1} - 29419\frac{2}{2}$
4220.730	150	2	23685.913	$14206\frac{4}{4} - 37892_{4}$	4189.633	5	1	23861.715	$15490\frac{6}{6} - 39351_{5}$
4220.570	3		23686.810	$18069\frac{5}{5} - 41755_{4}$	4189.563	100	3	23862.113	$13297_{4} - 37159\frac{3}{3}$
4220.064	200	15	23689.650	$5563_{1} - 29252\frac{2}{2}$	4187.512	1		23873.800	$13945\frac{3}{3} - 37819_{4}$
4219.569	20	1	23692.430	$7502_{3} - 31194\frac{3}{3}$	4187.142	50	3	23875.910	$11802_{2} - 35678\frac{1}{1}$
4217.185	100b	2b	23705.823	$16346\frac{4}{4} - 40052_{4}$	4185.143	50	2	23887.314	$10414\frac{4}{4} - 34301_{4}$
4216.543	3		23709.432	$16783\frac{4}{4} - 40493_{3}$	4184.138	200	4	23893.052	$6362_{2} - 30255\frac{3}{3}$
4216.371	200l	3	23710.399	$7280_{2} - 30990\frac{3}{3}$	4182.933	20	2	23899.934	$14206\frac{2}{4} - 38106_{5}$
4216.205	75	1	23711.333	$13297_{4} - 37008\frac{6}{6}$	4182.707	4		23901.226	$15618\frac{3}{3} - 39520_{4}$
4216.068	300s	5	23712.103	$13088_{3} - 36800\frac{4}{4}$	4182.080	50	2	23904.809	$10526\frac{3}{3} - 34431_{3}$
4215.625	150	1	23714.595	$4961_{4} - 28676\frac{3}{3}$	4181.518	2		23908.022	$11241\frac{3}{3} - 35149_{2}$
4215.383	3		23715.956	$14032\frac{2}{2} - 37748_{2}$	4180.720	10	1	23912.585	$8111_{4} - 32023\frac{6}{6}$

TABLE 4. *Classified lines of* Th I—continued

Wavelength (Å)	Intensity		Wavenumber (cm^{-1})	Classification
	Lamp	Spark		
4180.326	20	2	23914.839	$12847_3 - 36762\frac{5}{2}$
4179.861	1		23917.499	$16783\frac{1}{2} - 40701_4$
4179.760	10	2	23918.077	$10526\frac{5}{2} - 34444_2$
4179.620	200b	5	23918.878	$3865_1 - 27784\frac{2}{2}$
4179.314	100	8	23920.630	$10526\frac{5}{2} - 34447_4$
4179.220	150	3	23921.168	$2869_3 - 26790\frac{5}{2}$
4178.848	200	3	23923.297	$4961_4 - 28884\frac{5}{2}$
4178.624	2		23924.579	$10783\frac{1}{2} - 34707_3$
4177.281	4	1	23932.271	$11601_1 - 35533\frac{3}{2}$
4177.165	100	4	23932.936	$12114\frac{3}{2} - 36047_2$
4176.480	10	1	23936.861	$15970_3 - 39906\frac{3}{2}$
4175.322	4		23943.499	$15736\frac{1}{1} - 39680_2$
4174.620	2		23947.526	$13945\frac{5}{2} - 37892_4$
4173.720	25	1	23952.690	$12847_3 - 36800\frac{3}{4}$
4173.448	50	4	23954.251	$8800_4 - 32754\frac{5}{2}$
4170.533	500b	25	23970.993	$4961_4 - 28932\frac{3}{4}$
4169.762	4		23975.425	$15493_4 - 39468\frac{5}{2}$
4169.085	15	1	23979.319	$7795\frac{3}{4} - 31774_3$
4168.455	50	4	23982.943	$16217\frac{7}{2} - 40200_3$
4167.864	20	1	23986.343	$3687_2 - 27674\frac{3}{2}$
4165.766	800r	15	23998.423	$7795\frac{3}{4} - 31793_4$
4165.496	3		23999.979	$11877\frac{1}{1} - 35877_2$
4164.972	50	3	24002.998	$7280_2 - 31283\frac{5}{2}$
4163.947	100	2	24008.907	$2869_3 - 26878\frac{5}{2}$
4163.827	10	1	24009.599	$11802_2 - 35812\frac{5}{2}$
4162.782	75	5	24015.626	$15970_3 - 39985\frac{5}{2}$
4162.509	400	15	24017.201	$10414\frac{3}{4} - 34431_3$
4162.029	3		24019.971	$11197\frac{5}{5} - 35216_5$
4161.738	150	5	24021.650	$7502_3 - 31523\frac{5}{2}$
4161.344	2		24023.925	$12847_3 - 36871\frac{5}{2}$
4160.272	2b		24030.115	$15490\frac{5}{5} - 39520_4$
4159.764	20	1	24033.049	$10414\frac{3}{4} - 34447_4$
4159.152	75	2	24036.586	$13175\frac{3}{4} - 37211_5$
4158.535	800	20	24040.152	$9804_5 - 33844\frac{5}{5}$
4157.391	150b	3	24046.767	$10414\frac{3}{4} - 34460_5$
4157.363	25b	2b	24046.929	$13945\frac{5}{2} - 37992_4$
4156.481	50b	10b	24052.031	$14226_0 - 38278\frac{1}{1}$
4155.010	5		24060.546	$13088_3 - 37149\frac{3}{2}$
4154.719	200	5	24062.232	$8800_4 - 32862\frac{3}{4}$
4153.573	8	1	24068.870	$15493_4 - 39562\frac{3}{4}$
4153.204	5		24071.009	$13088_3 - 37159\frac{5}{2}$
4152.561	2		24074.736	$18549_2 - 42624\frac{1}{1}$
4152.147	15		24077.137	$5563_1 - 29640\frac{1}{1}$
4152.032	3		24077.803	$11601_1 - 35678\frac{1}{1}$
4151.144	50b	2	24082.954	$11802_2 - 35885\frac{3}{2}$
4150.598	5		24086.122	$8111_4 - 32197\frac{5}{2}$
4150.087	200b	5	24089.088	$4961_4 - 29050\frac{5}{5}$
4148.829	50	3	24096.392	$3687_2 - 27784\frac{2}{2}$
4148.724	100	3	24097.001	$7502_3 - 31599\frac{2}{2}$
4147.538	100	3	24103.892	$11197\frac{5}{5} - 35300_5$
4146.968	15	1	24107.205	$13847_2 - 37954\frac{5}{2}$
4145.858	5b		24113.659	$14032\frac{2}{2} - 38145_3$
4145.296	20	2	24116.928	$15166\frac{3}{3} - 39283_4$
4144.342	40	3	24122.480	$13847_2 - 37970\frac{2}{2}$
4143.711	5		24126.153	$15970_3 - 40096\frac{2}{2}$
4143.648	100	2	24126.520	$2869_3 - 26995\frac{5}{2}$
4143.337	5	1	24128.331	$13175\frac{3}{4} - 37303_4$
4142.325	100	3	24134.225	$7795\frac{3}{4} - 31929_3$
4141.719	100	3	24137.757	$14465\frac{2}{2} - 38602_2$
4138.040	200	3	24159.216	$3865_1 - 28024\frac{1}{1}$
4136.286	300	8	24169.461	$11877\frac{1}{1} - 36047_2$
4136.132	8	1	24170.361	$16554_6 - 40724\frac{5}{5}$
4135.480	300	3	24174.171	$8111_4 - 32285\frac{3}{3}$
4134.323	50	3	24180.936	$14204_5 - 38385\frac{5}{5}$
4134.062	200b	10b	24182.463	$0_2 - 24182\frac{3}{2}$
4133.958	200	10	24183.071	$8111_4 - 32294\frac{3}{4}$
4132.620	150	3	24190.901	$6362_2 - 30553\frac{3}{2}$
4131.710	150	3	24196.229	$4961_4 - 29157\frac{3}{3}$
4131.662	200b	3	24196.510	$9804_5 - 34001\frac{3}{4}$
4131.207	25	2	24199.175	$11241\frac{3}{3} - 35440_3$
4131.002	800	15	24200.375	$7795\frac{3}{4} - 31995_4$
4130.168	10	1	24205.262	$13847_2 - 38053\frac{3}{3}$
4129.073	3		24211.681	$17501\frac{5}{5} - 41712_5$
4128.050	100	2	24217.681	$7795\frac{3}{4} - 32012_4$
4127.345	150b	10	24221.818	$12114\frac{2}{2} - 36336_3$
4126.032	10	1	24229.526	$13175\frac{3}{4} - 37404_3$
4124.105	5b		24240.847	$13945\frac{5}{3} - 38186_4$
4124.043	150	5	24241.211	$13847_2 - 38088\frac{2}{2}$
4123.726	100	3	24243.074	$8800_4 - 33043\frac{5}{3}$
4123.601	150	3	24243.809	$7280_2 - 31523\frac{5}{3}$
4121.744	3		24254.732	$17501\frac{5}{5} - 41755_4$
4120.364	15	1	24262.855	$10783\frac{1}{2} - 35046_1$
4118.490	200	4	24273.895	$13297_4 - 37571\frac{5}{5}$
4118.225	5	1	24275.457	$17411\frac{3}{3} - 41686_3$
4117.698	4b	1	24278.564	$7502_3 - 31780\frac{3}{3}$
4116.635	25b	4b	24284.833	$15970_3 - 40254\frac{3}{3}$
4116.635	25b	4b	24284.833	$11601_1 - 35885\frac{2}{2}$
4115.759	500r	50	24290.002	$5563_1 - 29853\frac{3}{2}$
4113.873	20	1	24301.137	$12847_3 - 37149\frac{2}{2}$
4112.753	600b	15	24307.755	$0_2 - 24307\frac{2}{2}$
4112.713	300b		24307.991	$8243\frac{2}{2} - 32551_3$
4112.665	40b	2	24308.275	$13297_4 - 37605\frac{3}{3}$
4112.104	10	1	24311.591	$12847_3 - 37159\frac{3}{3}$
4110.829	200b	10b	24319.131	$7280_2 - 31599\frac{2}{2}$
4110.317	2		24322.160	$17398_3 - 41720\frac{2}{2}$
4110.174	4		24323.007	$14206\frac{3}{4} - 38529_3$
4109.323	400r	5	24328.044	$8111_4 - 32439\frac{3}{4}$
4108.183	4		24334.794	$11241\frac{3}{3} - 35576_3$
4107.861	100	3	24336.702	$3687_2 - 28024\frac{1}{1}$
4106.522	4		24344.637	$17411\frac{3}{3} - 41755_4$
4106.154	15b	2b	24346.819	$10526\frac{5}{3} - 34873_4$
4106.034	10	1	24347.530	$10526\frac{5}{3} - 34874_3$
4105.894	25b		24348.361	$4961_4 - 29310\frac{3}{4}$
4105.062	25	2	24353.295	$15166\frac{3}{3} - 39520_4$
4103.692	20b	2	24361.425	$6362_2 - 30723\frac{1}{1}$
4102.820	20		24366.603	$10783\frac{1}{2} - 35149_2$
4102.617	400r	3	24367.809	$7502_3 - 31870\frac{2}{2}$
4101.234	5		24376.026	$14204_5 - 38580\frac{3}{4}$
4100.919	40	2	24377.898	$9804_5 - 34182\frac{5}{5}$
4100.341	1000r	20	24381.334	$0_2 - 24381\frac{1}{2}$

TABLE 4. *Classified lines of* Th I—continued

Wavelength (Å)	Intensity		Wavenumber (cm^{-1})	Classification
	Lamp	Spark		
4099.553	100	4	24386.021	$11802_2 - 36188^{\frac{3}{2}}$
4099.553	100	4	24386.021	$12847_3 - 37234^{\frac{3}{2}}$
4098.730	100s	2	24390.917	$2869_3 - 27260^{\frac{5}{2}}$
4097.747	500b	8	24396.768	$2869_3 - 27266^{\frac{3}{2}}$
4097.321	200	8	24399.305	$6362_2 - 30761^{\frac{5}{2}}$
4096.077	150	4	24406.714	$7795^{\frac{3}{2}} - 32202_5$
4094.901	50	3	24413.724	$15493_4 - 39906^{\frac{3}{2}}$
4093.672	40	2	24421.053	$0_2 - 24421^{\frac{5}{2}}$
4091.988	8	1	24431.103	$13847_2 - 38278^{\frac{1}{2}}$
4091.737	40	2	24432.602	$7280_2 - 31712^{\frac{1}{2}}$
4091.590	10	1	24433.479	$15618^{\frac{5}{2}} - 40052_4$
4089.138	400	8	24448.130	$2869_3 - 27317^{\frac{5}{2}}$
4088.728	500	8	24450.582	$6362_2 - 30812^{\frac{3}{2}}$
4088.629	100	3	24451.174	$7502_3 - 31953^{\frac{3}{2}}$
4087.285	200	5	24459.214	$10414^{\frac{3}{2}} - 34873_4$
4087.166	50l	2	24459.926	$10414^{\frac{3}{2}} - 34874_3$
4086.936	15	1	24461.303	$14204_5 - 38665^{\frac{5}{2}}$
4085.434	500	10	24470.296	$8800_4 - 33270^{\frac{3}{2}}$
4085.257	200	8	24471.356	$14481^{\frac{5}{2}} - 38953_5$
4083.469	500	8	24482.071	$3865_1 - 28347^{\frac{3}{2}}$
4081.592	50	2	24493.329	$14206^{\frac{3}{2}} - 38700_4$
4081.368	800	8	24494.673	$8800_4 - 33294^{\frac{3}{2}}$
4080.707	400	20	24498.641	$7795^{\frac{3}{2}} - 32293_5$
4080.359	150	4	24500.730	$7280_2 - 31780^{\frac{5}{2}}$
4079.273	25b	1	24507.253	$3865_1 - 28372^{\frac{1}{2}}$
4078.302	100	2	24513.087	$13175^{\frac{3}{2}} - 37688_3$
4077.623	15	1	24517.169	$13088_3 - 37605^{\frac{3}{2}}$
4075.907	150	5	24527.491	$14206^{\frac{3}{2}} - 38734_3$
4075.503	400r	10	24529.922	$2558_0 - 27087^{\frac{1}{2}}$
4073.960	25	1	24539.213	$12114^{\frac{3}{2}} - 36653_2$
4073.856	200	3	24539.839	$9804_5 - 34344^{\frac{3}{2}}$
4073.007	20	1	24544.954	$14465^{\frac{5}{2}} - 39010_3$
4071.750	200b	15	24552.532	$8243^{\frac{3}{2}} - 32796_3$
4071.731	100b		24552.646	$11241^{\frac{5}{2}} - 35794_4$
4071.553	100	1	24553.719	$14206^{\frac{3}{2}} - 38760_4$
4070.756	100	2	24558.527	$11802_2 - 36361^{\frac{1}{2}}$
4070.238	150	3	24561.652	$0_2 - 24561^{\frac{5}{2}}$
4070.115	25	1	24562.394	$15490^{\frac{5}{2}} - 40052_4$
4070.041	75	1	24562.841	$10526^{\frac{5}{2}} - 35089_3$
4069.901	5		24563.686	$14243^{\frac{1}{2}} - 38807_2$
4069.461	500r	15	24566.342	$6362_2 - 30928^{\frac{1}{2}}$
4069.112	50	2	24568.449	$13847_2 - 38416^{\frac{5}{2}}$
4068.705	75		24570.906	$14032^{\frac{5}{2}} - 38602_2$
4068.470	50	2	24572.325	$16783^{\frac{3}{2}} - 41356_5$
4067.451	400r	5	24578.481	$2869_3 - 27447^{\frac{3}{2}}$
4066.961	50	1	24581.442	$15618^{\frac{5}{2}} - 40200_3$
4066.822	100	2	24582.283	$18053^{\frac{3}{2}} - 42635_5$
4066.435	25		24584.622	$13945^{\frac{5}{2}} - 38529_3$
4065.889	100	3	24587.923	$11601_1 - 36188^{\frac{3}{2}}$
4065.618	100	4	24589.562	$11241^{\frac{5}{2}} - 35831_3$
4065.551	50	1	24589.968	$7280_2 - 31870^{\frac{3}{2}}$
4064.332	400	10	24597.343	$11197^{\frac{5}{2}} - 35794_4$
4063.407	1500r	75	24602.942	$11197^{\frac{5}{2}} - 35799_6$
4061.625	300	3	24613.736	$14226_0 - 38840^{\frac{1}{2}}$
4060.241	5		24622.126	$10783^{\frac{3}{2}} - 35405_3$
4060.062	200	1	24623.211	$10526^{\frac{5}{2}} - 35149_2$
4059.847	200	10	24624.515	$11802_2 - 36427^{\frac{5}{2}}$
4059.253	1500r	20	24628.119	$6362_2 - 30990^{\frac{5}{2}}$
4058.936	75	8	24630.042	$19227^{\frac{5}{2}} - 43857_5$
4057.940	200	2	24636.087	$11241^{\frac{5}{2}} - 35877_2$
4056.718	10		24643.508	$8111_4 - 32754^{\frac{5}{2}}$
4056.636	200	2	24644.006	$13175^{\frac{3}{2}} - 37819_4$
4056.399	100	2	24645.446	$5563_1 - 30208^{\frac{3}{2}}$
4056.007	150	1	24647.828	$3865_1 - 28513^{\frac{3}{2}}$
4055.908	200	1	24648.430	$13088_3 - 37736^{\frac{3}{2}}$
4054.387	200	8	24657.676	$13945^{\frac{5}{2}} - 38602_2$
4054.302	300	8	24658.193	$7502_3 - 32160^{\frac{3}{2}}$
4054.080	20		24659.543	$3687_2 - 28347^{\frac{3}{2}}$
4053.841	40		24660.997	$12114^{\frac{3}{2}} - 36775_3$
4053.527	1000r	75	24662.907	$7795^{\frac{3}{2}} - 32458_4$
4052.240	100b		24670.740	$15166^{\frac{3}{2}} - 39837_3$
4051.913	40		24672.731	$17354^{\frac{1}{2}} - 42027_2$
4051.500	500	15	24675.246	$10414^{\frac{3}{2}} - 35089_3$
4049.944	500	40	24684.726	$3687_2 - 28372^{\frac{1}{2}}$
4049.535	200	25	24687.219	$9804_5 - 34492^{\frac{3}{2}}$
4048.432	800	50	24693.945	$12114^{\frac{3}{2}} - 36808_3$
4048.288	800	40	24694.824	$7502_3 - 32197^{\frac{3}{2}}$
4047.058	50	1	24702.329	$14032^{\frac{5}{2}} - 38734_3$
4046.824	200	15	24703.757	$12114^{\frac{3}{2}} - 36818_2$
4046.252	200	8	24707.249	$13962_1 - 38669^{\frac{5}{2}}$
4045.848	40b	2	24709.717	$14465^{\frac{5}{2}} - 39174_3$
4045.818	50b	3	24709.900	$19227^{\frac{5}{2}} - 43937_6$
4045.226	200	2	24713.516	$6362_2 - 31075^{\frac{5}{2}}$
4044.926	300	8	24715.349	$13175^{\frac{3}{2}} - 37890_5$
4044.515	200b	2	24717.860	$5563_1 - 30281^{\frac{1}{2}}$
4043.394	1000r	50	24724.713	$4961_4 - 29686^{\frac{5}{2}}$
4040.971	100		24739.538	$2558_0 - 27297^{\frac{1}{2}}$
4039.865	800	20	24746.311	$14206^{\frac{3}{2}} - 38953_5$
4039.268	100	2	24749.968	$4961_4 - 29711^{\frac{5}{2}}$
4039.268	100	2	24749.968	$14206^{\frac{3}{2}} - 38956_4$
4039.022	150	1	24751.475	$8111_4 - 32862^{\frac{3}{2}}$
4038.635	100		24753.847	$11802_2 - 36556^{\frac{1}{2}}$
4038.456	300	2	24754.944	$13945^{\frac{5}{2}} - 38700_4$
4038.228	300	10	24756.342	$7795^{\frac{3}{2}} - 32551_3$
4037.993	15		24757.783	$12847_3 - 37605^{\frac{3}{2}}$
4037.663	100	2	24759.806	$8800_4 - 33560^{\frac{3}{2}}$
4037.562	500	15	24760.425	$11601_1 - 36361^{\frac{1}{2}}$
4036.047	2000r	50	24769.719	$0_2 - 24769^{\frac{5}{2}}$
4035.931	200	8	24770.431	$14481^{\frac{5}{2}} - 39252_5$
4035.730	300	1	24771.665	$4961_4 - 29733^{\frac{5}{2}}$
4035.089	100		24775.600	$14032^{\frac{5}{2}} - 38807_2$
4034.878	200	8	24776.896	$15493_4 - 40270^{\frac{3}{2}}$
4033.907	600r	8	24782.860	$4961_4 - 29744^{\frac{3}{2}}$
4033.776	500	8	24783.664	$3865_1 - 28649^{\frac{1}{2}}$
4032.596	600r	200	24790.916	$8800_4 - 33591^{\frac{5}{2}}$
4032.199	20		24793.357	$10783^{\frac{3}{2}} - 35576_3$
4030.842	2000r	50	24801.704	$2869_3 - 27670^{\frac{5}{2}}$
4030.590	20		24803.254	$14206^{\frac{3}{2}} - 39010_3$
4030.292	300	40	24805.088	$2869_3 - 27674^{\frac{3}{2}}$
4030.214	100	1	24805.568	$11241^{\frac{5}{2}} - 36047_2$

201-606 O - 76 - 14

TABLE 4. *Classified lines of* Th I – continued

Wavelength (Å)	Intensity		Wavenumber (cm^{-1})	Classification
	Lamp	Spark		
4030.078	25		24806.405	$15970_3 - 40776^{\frac{3}{4}}$
4029.827	400r	15	24807.951	$3865_1 - 28673^{\frac{1}{2}}$
4029.658	400	15	24808.991	$12847_3 - 37656^{\frac{3}{5}}$
4028.334	200	10	24817.145	$13175^{\frac{5}{4}} - 37992_4$
4027.546	150l	20	24822.000	$13847_2 - 38669^{\frac{1}{2}}$
4027.007	500r	10	24825.322	$3687_2 - 28513^{\frac{1}{2}}$
4026.644	4		24827.560	$13847_2 - 38675^{\frac{3}{5}}$
4024.801	300r	8	24838.929	$0_2 - 24838^{\circ}_{1}$
4023.338	400	10	24847.961	$11241^{\frac{3}{5}} - 36089_4$
4022.728	75	1	24851.729	$13962_1 - 38814^{\frac{1}{2}}$
4022.067	500b		24855.813	$8243^{\frac{3}{2}} - 33099_3$
4021.940	200b	4	24856.598	$14465^{\frac{3}{2}} - 39321_3$
4021.750	200	8	24857.772	$14204_5 - 39062^{\circ}_{5}$
4021.149	300	10	24861.487	$13088_3 - 37950^{\frac{3}{4}}$
4021.007	75	2	24862.365	$13945^{\frac{3}{5}} - 38807_2$
4020.462	100		24865.735	$11802_2 - 36668^{\frac{1}{2}}$
4020.354	500	20	24866.403	$13088_3 - 37954^{\frac{3}{5}}$
4019.787	200	5	24869.911	$14481^{\circ}_{5} - 39351_5$
4018.932	25	2	24875.201	$17411^{\frac{3}{5}} - 42286_3$
4018.354	200	15	24878.779	$10526^{\frac{3}{5}} - 35405_3$
4018.118	50b		24880.241	$0_2 - 24880^{\circ}_{1}$
4018.099	400b	15	24880.358	$7280_2 - 32160^{\frac{1}{2}}$
4017.461	8		24884.309	$16346^{\frac{3}{4}} - 41230_4$
4017.257	100	2	24885.573	$15166^{\frac{3}{5}} - 40052_4$
4017.062	400	5	24886.781	$10414^{\frac{3}{4}} - 35300_5$
4016.896	10		24887.809	$11601_1 - 36488^{\frac{1}{2}}$
4016.112	100	2	24892.668	$11197^{\circ}_{6} - 36089_4$
4014.716	400	10	24901.323	$3687_2 - 28589^{\frac{1}{2}}$
4014.472	40	2	24902.837	$16783^{\frac{1}{4}} - 41686_3$
4012.610	25	2	24914.392	$10526^{\frac{3}{5}} - 35440_3$
4012.495	2000r	150	24915.106	$2869_3 - 27784^{\frac{1}{2}}$
4012.190	150	2	24917.000	$7280_2 - 32197^{\frac{3}{5}}$
4011.739	800r	5b	24919.801	$4961_4 - 29881^{\frac{1}{4}}$
4011.591	500r	40	24920.721	$6362_2 - 31283^{\frac{3}{5}}$
4009.816	400b	10	24931.752	$13175^{\frac{5}{4}} - 38106_5$
4009.783	200b	2	24931.957	$15493_4 - 40425^{\frac{3}{4}}$
4009.724	400	10	24932.324	$8111_4 - 33043^{\frac{3}{5}}$
4009.057	1500r	100	24936.472	$11197^{\circ}_{6} - 36133_5$
4009.012	300r	50	24936.752	$7502_3 - 32439^{\frac{3}{4}}$
4008.443	10		24940.292	$11877^{\circ}_{1} - 36818_2$
4008.312	100		24941.107	$13847_2 - 38788^{\frac{3}{5}}$
4008.210	1500	100	24941.741	$7795^{\frac{3}{4}} - 32737_5$
4005.960	300	8	24955.750	$11601_1 - 36556^{\circ}_{1}$
4005.297	75	1	24959.881	$11802_2 - 36762^{\frac{3}{5}}$
4005.091	500r	10	24961.165	$3687_2 - 28649^{\circ}_{7}$
4004.560	20		24964.474	$13088_3 - 38053^{\frac{3}{5}}$
4004.238	8	1	24966.482	$13847_2 - 38814^{\frac{1}{2}}$
4003.993	4		24968.009	$14206^{\frac{3}{4}} - 39174_3$
4003.574	400	25	24970.622	$13175^{\frac{5}{4}} - 38145_3$
4002.376	75	3	24978.096	$14032^{\frac{3}{2}} - 39010_3$
4001.992	50		24980.493	$12114^{\frac{3}{2}} - 37094_2$
4001.894	300	2	24981.105	$0_2 - 24981^{\frac{3}{5}}$
4001.198	100h		24985.450	$3687_2 - 28673^{\frac{1}{2}}$
4001.058	800r	40	24986.324	$7795^{\frac{3}{4}} - 32781_4$
4000.748	200		24988.261	$3687_2 - 28676^{\frac{3}{5}}$
4000.445	200	3	24990.153	$5563_1 - 30553^{\frac{1}{2}}$
4000.280	800	20	24991.184	$10414^{\frac{3}{4}} - 35405_3$
4000.041	200b		24992.677	$15618^{\frac{3}{5}} - 40611_2$
4000.024	100b		24992.783	$13847_2 - 38840^{\circ}_{1}$
3998.953	600	20	24999.477	$8800_4 - 33799^{\frac{3}{4}}$
3998.800	100b	5	25000.433	$13088_3 - 38088^{\frac{1}{2}}$
3998.733	400b	5	25000.852	$7795^{\frac{3}{4}} - 32796_3$
3998.657	300s	2	25001.327	$7502_3 - 32503^{\frac{1}{2}}$
3998.061	300	5	25005.054	$7280_2 - 32285^{\frac{3}{5}}$
3997.443	15b		25008.920	$13297_4 - 38306^{\frac{3}{4}}$
3997.347	200	4	25009.521	$16346^{\frac{3}{4}} - 41356_5$
3997.172	50	1	25010.615	$15970_3 - 40980^{\frac{3}{5}}$
3997.109	300	5	25011.009	$13175^{\frac{5}{4}} - 38186_4$
3997.019	300	8	25011.573	$13945^{\frac{3}{5}} - 38956_4$
3996.670	500	15	25013.757	$11197^{\circ}_{6} - 36210_5$
3996.508	100	2	25014.771	$16346^{\frac{3}{4}} - 41361_3$
3996.203	300	25	25016.680	$12114^{\frac{3}{2}} - 37131_3$
3994.038	5		25030.240	$8243^{\frac{3}{2}} - 33273_1$
3993.515	200	15	25033.518	$15166^{\frac{3}{5}} - 40200_3$
3993.397	100		25034.258	$11802_2 - 36837^{\circ}_{1}$
3991.731	800r	40	25044.706	$8800_4 - 33844^{\circ}_{5}$
3991.624	300b	40	25045.377	$14206^{\frac{3}{4}} - 39252_5$
3991.289	15		25047.479	$18809^{\frac{3}{4}} - 43857_5$
3990.892	300	15	25049.971	$10526^{\frac{3}{5}} - 35576_3$
3990.809	300	25	25050.492	$5563_1 - 30613^{\circ}_{5}$
3990.492	800r	10	25052.482	$3865_1 - 28917^{\frac{1}{2}}$
3990.020	150b	40	25055.445	$4961_4 - 30017^{\frac{3}{5}}$
3990.002	20b	3	25055.558	$11241^{\frac{3}{5}} - 36297_4$
3988.953	25		25062.147	$17224^{\frac{1}{2}} - 42286_3$
3988.519	25	4	25064.874	$13945^{\frac{3}{5}} - 39010_3$
3988.429	75		25065.440	$8243^{\frac{3}{2}} - 33309_2$
3988.078	10b	8b	25067.646	$11601_1 - 36668^{\frac{1}{2}}$
3987.867	150	2	25068.972	$11802_2 - 36871^{\frac{1}{2}}$
3987.206	200b		25073.128	$7502_3 - 32575^{\frac{1}{2}}$
3986.604	200	25	25076.914	$14206^{\frac{3}{4}} - 39283_4$
3986.215	25		25079.361	$2869_3 - 27948^{\frac{3}{4}}$
3985.815	8		25081.878	$9804_5 - 34886^{\circ}_{5}$
3985.737	4		25082.369	$15618^{\frac{3}{5}} - 40701_4$
3984.879	300	40	25087.769	$13297_4 - 38385^{\circ}_{5}$
3984.095	200		25092.706	$15490^{\circ}_{5} - 40582_5$
3983.815	2		25094.470	$11241^{\frac{3}{5}} - 36336_3$
3983.783	10		25094.671	$10783^{\frac{3}{2}} - 35877_2$
3982.894	200	8	25100.272	$11197^{\circ}_{6} - 36297_4$
3982.607	100	2	25102.081	$12847_3 - 37950^{\frac{3}{4}}$
3981.827	300	100	25106.998	$12847_3 - 37954^{\frac{3}{5}}$
3980.575	15		25114.895	$14206^{\frac{3}{4}} - 39321_3$
3979.956	200	8	25118.801	$13297_4 - 38416^{\frac{3}{5}}$
3979.402	75	2	25122.298	$12847_3 - 37970^{\frac{1}{2}}$
3978.438	50	1	25128.385	$13088_3 - 38216^{\frac{3}{5}}$
3977.434	15		25134.728	$17501^{\circ}_{5} - 42635_5$
3976.152	50b	1	25142.831	$14032^{\frac{3}{2}} - 39174_3$
3975.976	20		25143.944	$16217^{\frac{1}{2}} - 41361_3$
3975.831	150	5	25144.862	$14206^{\frac{3}{4}} - 39351_5$
3975.468	200	20	25147.157	$8243^{\frac{3}{2}} - 33390_1$
3975.008	5s		25150.067	$15736^{\circ}_{1} - 40886_2$

TABLE 4. *Classified lines of* Th I—continued

Wavelength (Å)	Intensity		Wavenumber (cm^{-1})	Classification
	Lamp	Spark		
3974.829	200	4	25151.200	$13847_2 - 38998^{\frac{3}{2}}$
3973.507	25	2	25159.568	$8111_4 - 33270^{\frac{3}{4}}$
3973.333	500	10	25160.669	$5563_1 - 30723^{\frac{1}{2}}$
3973.196	1000r	50	25161.537	$6362_2 - 31523^{\frac{5}{2}}$
3973.063	40b	1	25162.379	$10414^{\frac{3}{4}} - 35576_3$
3972.640	500	75	25165.058	$8243^{\frac{3}{2}} - 33408_3$
3972.230	75	2	25167.656	$8800_4 - 33967^{\frac{3}{2}}$
3972.153	1500r	300	25168.144	$7795^{\frac{3}{4}} - 32963_5$
3972.153	1500r	300	25168.144	$10414^{\frac{3}{4}} - 35582_5$
3969.665	300	15	25183.918	$8111_4 - 33294^{\frac{3}{2}}$
3967.610	200	2	25196.961	$3687_2 - 28884^{\frac{3}{2}}$
3967.392	2000r	300	25198.346	$4961_4 - 30160^{\frac{3}{4}}$
3966.334	200	4	25205.067	$12847_3 - 38053^{\frac{3}{2}}$
3965.483	100	3	25210.476	$19227^{\frac{5}{2}} - 44437_6$
3964.455	75	2	25217.013	$11877^{\frac{1}{2}} - 37094_2$
3964.329	200	3	25217.814	$13088_3 - 38306^{\frac{3}{4}}$
3964.030	300	15	25219.717	$10414^{\frac{3}{4}} - 35633_4$
3962.475	100	3	25229.613	$13945^{\frac{3}{2}} - 39174_3$
3962.420	400r	15	25229.964	$3687_2 - 28917^{\frac{7}{2}}$
3962.371	75	5b	25230.276	$15970_3 - 41200^{\frac{5}{2}}$
3962.197	200	8	25231.384	$15493_4 - 40724^{\frac{5}{2}}$
3960.685	10		25241.015	$12847_3 - 38088^{\frac{3}{2}}$
3960.270	500	50	25243.661	$11241^{\frac{3}{2}} - 36485_2$
3959.300	1000r	100	25249.845	$5563_1 - 30812^{\frac{3}{2}}$
3958.928	200	3	25252.217	$7502_3 - 32754^{\frac{3}{2}}$
3957.736	40		25259.823	$15166^{\frac{3}{2}} - 40426_4$
3957.059	100	20	25264.144	$10783^{\frac{3}{2}} - 36047_2$
3956.481	150	20	25267.835	$10526^{\frac{3}{2}} - 35794_4$
3956.005	400	10	25270.875	$11601_1 - 36871^{\frac{3}{2}}$
3955.891	400	50b	25271.604	$2869_3 - 28140^{\frac{3}{4}}$
3955.477	15		25274.249	$11241^{\frac{3}{2}} - 36515_3$
3955.170	800	40	25276.210	$9804_5 - 35081^{\frac{5}{2}}$
3954.130	100	20	25282.858	$13297_4 - 38580^{\frac{3}{2}}$
3954.068	100	10	25283.255	$15493_4 - 40776^{\frac{3}{4}}$
3953.056	4		25289.727	$14032^{\frac{3}{2}} - 39321_3$
3952.967	75	1	25290.296	$12114^{\frac{3}{2}} - 37404_3$
3952.761	500r	10	25291.614	$3865_1 - 29157^{\frac{1}{2}}$
3952.421	25		25293.790	$4961_4 - 30255^{\frac{3}{2}}$
3950.804	300	8	25304.142	$7795^{\frac{3}{4}} - 33099_3$
3950.707	100s	3	25304.763	$10526^{\frac{3}{2}} - 35831_3$
3950.393	1000r	200	25306.775	$0_2 - 25306^{\frac{3}{2}}$
3948.133	500	40	25321.261	$8243^{\frac{3}{2}} - 33564_3$
3948.029	600r	15	25321.928	$0_2 - 25321^{\frac{5}{2}}$
3947.329	1000r	100	25326.418	$9804_5 - 35131^{\frac{3}{4}}$
3947.136	500	50	25327.656	$13088_3 - 38416^{\frac{5}{2}}$
3946.481	400	10	25331.860	$3865_1 - 29197^{\frac{1}{2}}$
3946.391	300	25	25332.438	$3865_1 - 29197^{\frac{3}{2}}$
3945.206	200	8	25340.046	$16346^{\frac{3}{4}} - 41686_3$
3944.253	500	20	25346.169	$11802_2 - 37149^{\frac{3}{2}}$
3943.605	300	25	25350.333	$6362_2 - 31712^{\frac{1}{2}}$
3943.459	300	40	25351.272	$10526^{\frac{3}{2}} - 35877_2$
3942.907	300	20	25354.821	$13175^{\frac{3}{4}} - 38529_3$
3942.628	100		25356.615	$11802_2 - 37159^{\frac{5}{2}}$
3942.072	500b	50	25360.192	$7502_3 - 32862^{\frac{3}{4}}$
3941.962	10	1	25360.899	$16217^{\frac{3}{2}} - 41578_2$
3941.682	10		25362.701	$8243^{\frac{3}{2}} - 33606_2$
3941.232	100	2	25365.597	$5563_1 - 30928^{\frac{1}{2}}$
3941.137	100	3	25366.208	$16346^{\frac{3}{4}} - 41712_5$
3940.837	200	5	25368.139	$13297_4 - 38665^{\frac{5}{2}}$
3940.705	200	4	25368.989	$12847_3 - 38216^{\frac{3}{2}}$
3940.422	5		25370.811	$7280_2 - 32650^{\frac{1}{2}}$
3939.538	75	2	25376.503	$13945^{\frac{3}{2}} - 39321_3$
3939.318	150	8	25377.921	$13297_4 - 38675^{\frac{3}{2}}$
3938.956	75	2	25380.253	$10414^{\frac{3}{4}} - 35794_4$
3938.614	400b	150	25382.457	$8800_4 - 34182^{\frac{5}{2}}$
3938.152	200	8	25385.434	$7280_2 - 32665^{\frac{1}{2}}$
3937.861	100	2b	25387.310	$3865_1 - 29252^{\frac{3}{2}}$
3934.465	15	1	25409.223	$16346^{\frac{3}{4}} - 41755_4$
3934.060	150	3	25411.838	$11241^{\frac{3}{2}} - 36653_2$
3933.238	400	40	25417.149	$10414^{\frac{3}{4}} - 35831_3$
3933.034	200	5	25418.467	$6362_2 - 31780^{\frac{5}{2}}$
3932.911	1500r	200	25419.262	$7795^{\frac{3}{4}} - 33214_5$
3931.085	150	3	25431.069	$11802_2 - 37234^{\frac{3}{2}}$
3930.252	150	4	25436.459	$14243^{\frac{1}{2}} - 39680_2$
3929.291	300	8	25442.680	$0_2 - 25442^{\frac{5}{2}}$
3928.967	200b	40b	25444.778	$15166^{\frac{3}{2}} - 40611_2$
3928.865	300	50	25445.439	$8243^{\frac{3}{2}} - 33689_2$
3928.308	100	10	25449.046	$8111_4 - 33560^{\frac{3}{4}}$
3927.806	400	10	25452.299	$7502_3 - 32954^{\frac{3}{2}}$
3926.864	200	8	25458.404	$12847_3 - 38306^{\frac{3}{4}}$
3925.596	300	8	25466.628	$2558_0 - 28024^{\frac{1}{2}}$
3925.219	400	50	25469.074	$9804_5 - 35273^{\frac{5}{2}}$
3925.093	1000r	200b	25469.891	$3687_2 - 29157^{\frac{3}{2}}$
3924.404	500l	10	25474.363	$7280_2 - 32754^{\frac{3}{2}}$
3923.799	500r	20	25478.290	$2869_3 - 28347^{\frac{7}{2}}$
3923.510	100	2	25480.167	$8111_4 - 33591^{\frac{3}{2}}$
3922.394	100	8	25487.416	$14206^{\frac{3}{4}} - 39694_5$
3921.782	25	4	25491.394	$13297_4 - 38788^{\frac{3}{2}}$
3921.731	15		25491.725	$13088_3 - 38580^{\frac{3}{4}}$
3920.058	300	10	25502.604	$16783^{\frac{3}{4}} - 42286_3$
3919.275	200	5	25507.699	$6362_2 - 31870^{\frac{5}{2}}$
3919.023	1000r	100	25509.339	$3687_2 - 29197^{\frac{1}{2}}$
3918.934	300	8	25509.919	$3687_2 - 29197^{\frac{3}{2}}$
3917.270	500	50	25520.755	$10526^{\frac{3}{2}} - 36047_2$
3916.597	200	8	25525.140	$13175^{\frac{3}{4}} - 38700_4$
3916.417	500r	25	25526.313	$0_2 - 25526^{\frac{1}{2}}$
3915.848	200	15	25530.022	$8243^{\frac{3}{2}} - 33773_1$
3915.295	300	8	25533.628	$11241^{\frac{3}{2}} - 36775_3$
3915.172	5		25534.430	$15166^{\frac{3}{2}} - 40701_4$
3914.163	200s	8	25541.012	$7502_3 - 33043^{\frac{5}{2}}$
3913.645	200l	5	25544.393	$8800_4 - 34344^{\frac{3}{4}}$
3913.302	75	2	25546.632	$9804_5 - 35351^{\frac{3}{4}}$
3913.082	300	25	25548.068	$11601_1 - 37149^{\frac{3}{2}}$
3912.738	75	3	25550.314	$17073_1 - 42624^{\frac{1}{2}}$
3912.485	75l	1	25551.966	$11197^{\frac{5}{2}} - 36749_6$
3912.211	75	2	25553.756	$3865_1 - 29419^{\frac{3}{2}}$
3911.950	300b	25	25555.460	$4961_4 - 30517^{\frac{5}{2}}$
3911.910	500r	40	25555.722	$4961_4 - 30517^{\frac{7}{2}}$
3911.523	200	3	25558.250	$11601_1 - 37159^{\frac{1}{2}}$
3911.364	15		25559.289	$13175^{\frac{3}{4}} - 38734_3$

TABLE 4. *Classified lines of* Th I—continued

Wavelength (Å)	Intensity		Wavenumber (cm^{-1})	Classification
	Lamp	Spark		
3910.773	300	8	25563.152	$10526\frac{3}{3} - 36089_4$
3910.622	50	2	25564.139	$13847_2 - 39411\frac{1}{1}$
3910.521	100	2	25564.799	$3687_2 - 29252\frac{2}{2}$
3910.251	50	2	25566.564	$11241\frac{3}{3} - 36808_3$
3909.991	100	8	25568.264	$12847_3 - 38416\frac{3}{3}$
3909.139	300	20	25573.837	$12114\frac{2}{2} - 37688_3$
3908.979	300	25	25574.883	$13945\frac{3}{3} - 39520_4$
3908.749	500	15	25576.388	$11241\frac{3}{3} - 36818_2$
3908.014	75	1	25581.198	$13088_3 - 38669\frac{2}{2}$
3907.543	50	5	25584.282	$11197\frac{0}{0} - 36781_5$
3907.352	2		25585.532	$13175\frac{4}{4} - 38760_4$
3907.160	200	10	25586.790	$13088_3 - 38675\frac{3}{3}$
3903.481	300	3	25610.905	$2869_3 - 28480\frac{0}{0}$
3903.315	200	5	25611.994	$15618\frac{3}{3} - 41230_4$
3903.103	1000r	150	25613.385	$7795\frac{4}{4} - 33408_3$
3901.957	20	2	25620.907	$13847_2 - 39468\frac{3}{3}$
3901.662	300	15	25622.844	$7795\frac{4}{4} - 33418_4$
3900.577	600r	50	25629.971	$8800_4 - 34430\frac{3}{3}$
3900.464	40	1	25630.714	$14206\frac{4}{4} - 39837_3$
3898.795	300	100	25641.686	$15493_4 - 41134\frac{4}{4}$
3898.509	300b	100	25643.567	$11241\frac{3}{3} - 36885_4$
3898.438	500r	25	25644.034	$2869_3 - 28513\frac{2}{2}$
3897.778	200	5	25648.376	$14032\frac{2}{2} - 39680_2$
3895.418	2000r	200	25663.914	$7795\frac{4}{4} - 33459_4$
3894.601	8		25669.298	$14204_5 - 39873\frac{0}{0}$
3893.817	200	8	25674.466	$7280_2 - 32954\frac{2}{2}$
3893.651	300	40	25675.561	$10414\frac{3}{3} - 36089_4$
3891.725	400	10	25688.267	$11197\frac{0}{0} - 36885_4$
3891.657	75	1	25688.716	$8111_4 - 33799\frac{4}{4}$
3891.520	300	3	25689.621	$8111_4 - 33800\frac{0}{0}$
3889.906	300	4	25700.279	$13088_3 - 38788\frac{3}{3}$
3889.715	100	2	25701.541	$13297_4 - 38998\frac{3}{3}$
3889.609	150	3	25702.242	$10783\frac{2}{2} - 36485_2$
3889.542	200	8	25702.685	$14204_5 - 39906\frac{4}{4}$
3889.432	15		25703.411	$0_2 - 25703\frac{2}{2}$
3887.220	40		25718.037	$6362_2 - 32080\frac{1}{1}$
3887.019	800r	100	25719.367	$10414\frac{4}{4} - 36133_5$
3886.917	800r	500	25720.042	$2869_3 - 28589\frac{3}{3}$
3886.064	75	25	25725.688	$13088_3 - 38814\frac{2}{2}$
3885.224	200	5	25731.250	$3687_2 - 29419\frac{2}{2}$
3885.066	200	10	25732.296	$7795\frac{4}{4} - 33527_4$
3884.985	25		25732.833	$10783\frac{2}{2} - 36515_3$
3884.629	200	8	25735.191	$13945\frac{3}{3} - 39680_2$
3884.629	200	8	25735.191	$14465\frac{2}{2} - 40200_3$
3883.767	200	15	25740.902	$15490\frac{0}{0} - 41230_4$
3883.536	200	5	25742.433	$15618\frac{3}{3} - 41361_3$
3882.324	200	8	25750.470	$15970_3 - 41720\frac{2}{2}$
3880.404	50	2	25763.211	$7280_2 - 33043\frac{3}{3}$
3880.323	100	3	25763.748	$13847_2 - 39611\frac{3}{3}$
3880.194	300	15	25764.605	$13297_4 - 39062\frac{6}{6}$
3879.644	1000r	200	25768.257	$7502_3 - 33270\frac{4}{4}$
3879.445	400b	10	25769.579	$7795\frac{4}{4} - 33564_3$
3879.269	400	25	25770.748	$10526\frac{3}{3} - 36297_4$
3878.662	400	150	25774.781	$3865_1 - 29640\frac{1}{1}$
3878.160	100	3	25778.117	$13175\frac{4}{4} - 38953_5$
3877.610	500b	15	25781.774	$13175\frac{4}{4} - 38956_4$
3877.462	500	20	25782.758	$8800_4 - 34583\frac{3}{3}$
3875.646	500r	25	25794.838	$7502_3 - 33297\frac{2}{2}$
3875.374	1500r	200	25796.649	$10414\frac{4}{4} - 36210_5$
3875.157	300	2	25798.093	$6362_2 - 32160\frac{2}{2}$
3874.862	1500r	200	25800.057	$4961_4 - 30761\frac{3}{3}$
3874.244	1000r	50	25804.173	$2869_3 - 28673\frac{2}{2}$
3873.821	2000r	500	25806.990	$2869_3 - 28676\frac{3}{3}$
3873.473	500r	50	25809.309	$0_2 - 25809\frac{1}{1}$
3873.421	400b	20	25809.655	$10526\frac{3}{3} - 36336_3$
3873.147	400	10	25811.481	$2869_3 - 28680\frac{1}{1}$
3872.861	200	4	25813.387	$11802_2 - 37616\frac{1}{1}$
3872.672	200b	5	25814.647	$2558_0 - 28372\frac{1}{1}$
3870.891	75		25826.524	$4961_4 - 30788\frac{0}{0}$
3870.763	75	2	25827.378	$12847_3 - 38675\frac{3}{3}$
3869.663	800r	50	25834.720	$6362_2 - 32197\frac{3}{3}$
3868.254	400	10	25844.130	$11241\frac{3}{3} - 37085_4$
3868.040	100	3	25845.559	$14206\frac{4}{4} - 40052_4$
3867.974	100	200	25846.001	$18011\frac{0}{0} - 43857_5$
3867.069	40	10	25852.049	$16783\frac{4}{4} - 42635_5$
3866.907	500b	50	25853.132	$11241\frac{3}{3} - 37094_2$
3866.771	200	2	25854.041	$11802_2 - 37656\frac{3}{3}$
3866.375	100	2	25856.689	$15863_2 - 41720\frac{2}{2}$
3866.338	40	1	25856.937	$8111_4 - 33967\frac{3}{3}$
3864.970	200b	40b	25866.089	$15490\frac{0}{0} - 41356_5$
3862.654	200b	200	25881.597	$7280_2 - 33161\frac{1}{1}$
3862.419	500b	250b	25883.172	$10414\frac{3}{3} - 36297_4$
3861.574	300b	40	25888.835	$11197\frac{0}{0} - 37085_4$
3861.502	300b	40	25889.318	$11241\frac{3}{3} - 37131_3$
3861.351	300	10	25890.331	$8111_4 - 34001\frac{4}{4}$
3861.051	200	2	25892.342	$13945\frac{3}{3} - 39837_3$
3859.289	20		25904.163	$8800_4 - 34704\frac{3}{3}$
3858.927	100b	10	25906.593	$11877\frac{1}{1} - 37784_2$
3858.358	200	150	25910.414	$13088_3 - 38998\frac{3}{3}$
3856.622	300	15	25922.077	$10414\frac{3}{3} - 36336_3$
3856.516	300	50	25922.789	$6362_2 - 32285\frac{3}{3}$
3856.354	400r	40	25923.878	$8243\frac{2}{2} - 34167_3$
3856.222	100	8b	25924.766	$7502_3 - 33427\frac{2}{2}$
3853.985	100	8	25939.813	$16346\frac{4}{4} - 42286_3$
3853.825	200b	15	25940.890	$12847_3 - 38788\frac{3}{3}$
3852.135	800r	50	25952.270	$3687_2 - 29640\frac{1}{1}$
3851.155	300	15	25958.874	$10526\frac{3}{3} - 36485_2$
3851.072	300	20	25959.434	$15618\frac{3}{3} - 41578_2$
3850.058	20		25966.270	$12847_3 - 38814\frac{2}{2}$
3849.910	400	15	25967.269	$13297_4 - 39264\frac{3}{3}$
3847.617	500	10	25982.743	$12114\frac{2}{2} - 38097_2$
3846.886	1000r	100	25987.681	$3865_1 - 29853\frac{2}{2}$
3846.625	400	50	25989.444	$10526\frac{3}{3} - 36515_3$
3846.024	15		25993.505	$14206\frac{4}{4} - 40200_3$
3845.302	100	2	25998.386	$3687_2 - 29686\frac{3}{3}$
3845.092	400	10	25999.805	$13175\frac{4}{4} - 39174_3$
3843.019	300	40	26013.830	$13297_4 - 39311\frac{4}{4}$
3842.898	400r	75b	26014.649	$11197\frac{0}{0} - 37211_5$
3842.803	200	5	26015.292	$11601_1 - 37616\frac{1}{1}$
3842.742	200	4	26015.705	$2869_3 - 28884\frac{3}{3}$

TABLE 4. *Classified lines of* Th I—continued

Wavelength (Å)	Intensity		Wavenumber (cm^{-1})	Classification
	Lamp	Spark		
3842.549	400	40	26017.012	$7280_2 - 33297^{\frac{3}{2}}$
3840.918	25	10	26028.059	$14465^{\frac{3}{2}} - 40493_3$
3840.799	600r	40	26028.866	$4961_4 - 30990^{\frac{3}{2}}$
3840.430	300	250	26031.367	$12114^{\frac{3}{2}} - 38145_3$
3839.898	50	10	26034.973	$10783^{\frac{3}{2}} - 36818_2$
3839.695	800r	200	26036.349	$0_2 - 26036^{\frac{3}{2}}$
3837.875	1500r	200	26048.696	$2869_3 - 28917^{\frac{3}{2}}$
3837.024	200	3	26054.473	$8243^{\frac{3}{2}} - 34298_1$
3836.721	300	20	26056.531	$3687_2 - 29744^{\frac{3}{2}}$
3836.584	800r	100	26057.461	$4961_4 - 31019^{\frac{3}{2}}$
3836.542	1000r	150b	26057.747	$7502_3 - 33560^{\frac{3}{2}}$
3835.960	75	8	26061.700	$11241^{\frac{3}{2}} - 37303_4$
3835.711	200	5	26063.392	$2869_3 - 28932^{\frac{3}{2}}$
3835.414	200	10	26065.410	$11241^{\frac{3}{2}} - 37307_3$
3835.349	200	10	26065.852	$14204_5 - 40270^{\frac{3}{2}}$
3835.077	100	2	26067.700	$15618^{\frac{3}{2}} - 41686_3$
3834.890	100	5	26068.971	$16217^{\frac{3}{2}} - 42286_3$
3834.488	100	75	26071.704	$8111_4 - 34182^{\frac{5}{2}}$
3832.323	75	3b	26086.433	$8800_4 - 34886^{\frac{5}{2}}$
3831.962	100	2	26088.890	$7502_3 - 33591^{\frac{3}{2}}$
3831.640	300	50	26091.083	$2558_0 - 28649^{\frac{1}{2}}$
3830.774	800r	150	26096.981	$0_2 - 26096^{\frac{3}{2}}$
3830.198	50	2	26100.905	$14481^{\frac{5}{2}} - 40582_5$
3830.061	500r	50	26101.839	$10414^{\frac{3}{2}} - 36515_3$
3829.393	50b		26106.392	$11197^{\frac{5}{2}} - 37303_4$
3829.283	150b	4b	26107.142	$13945^{\frac{3}{2}} - 40052_4$
3828.385	3000r	300	26113.265	$0_2 - 26113^{\frac{3}{2}}$
3826.368	400r	75	26127.030	$10526^{\frac{3}{2}} - 36653_2$
3825.132	500r	200	26135.472	$11197^{\frac{5}{2}} - 37332_6$
3824.927	20	2	26136.873	$15618^{\frac{3}{2}} - 41755_4$
3823.527	10		26146.443	$14465^{\frac{3}{2}} - 40611_2$
3823.458	300	25	26146.915	$7280_2 - 33427^{\frac{3}{2}}$
3823.067	500r	100	26149.589	$5563_1 - 31712^{\frac{1}{2}}$
3822.863	300	40	26150.984	$12847_3 - 38998^{\frac{3}{2}}$
3822.709	300	25	26152.038	$11802_2 - 37954^{\frac{3}{2}}$
3821.119	15		26162.920	$11241^{\frac{3}{2}} - 37404_3$
3820.792	600r	75	26165.159	$3687_2 - 29853^{\frac{3}{2}}$
3820.474	300b	10	26167.337	$11802_2 - 37970^{\frac{3}{2}}$
3820.327	200	2	26168.343	$14032^{\frac{3}{2}} - 40200_3$
3819.904	500	100b	26171.241	$13297_4 - 39468^{\frac{3}{2}}$
3819.189	200	10	26176.141	$13088_3 - 39264^{\frac{3}{2}}$
3819.112	300	10	26176.668	$13175^{\frac{3}{2}} - 39351_5$
3818.685	400r	15	26179.595	$4961_4 - 31141^{\frac{5}{2}}$
3817.495	100		26187.756	$8243^{\frac{3}{2}} - 34431_3$
3816.510	15	1	26194.514	$15166^{\frac{3}{2}} - 41361_3$
3815.566	500	50	26200.995	$8243^{\frac{3}{2}} - 34444_2$
3813.815	500r	50	26213.024	$6362_2 - 32575^{\frac{3}{2}}$
3812.905	75	2	26219.280	$11877^{\frac{1}{2}} - 38097_2$
3812.827	15		26219.816	$14206^{\frac{3}{2}} - 40426_4$
3812.667	75	5	26220.917	$14204_5 - 40425^{\frac{3}{2}}$
3812.398	400	40	26222.767	$15490^{\frac{5}{2}} - 41712_5$
3810.995	600r	150	26232.420	$7502_3 - 33734^{\frac{3}{2}}$
3810.906	75	1	26233.033	$4961_4 - 31194^{\frac{3}{2}}$
3808.614	500	20	26248.819	$10526^{\frac{3}{2}} - 36775_3$
3808.430	15		26250.088	$11802_2 - 38053^{\frac{3}{2}}$
3807.700	200	5b	26255.120	$13945^{\frac{3}{2}} - 40200_3$
3807.273	400	50	26258.065	$9804_5 - 36062^{\frac{3}{2}}$
3806.317	100	1	26264.660	$13297_4 - 39562^{\frac{3}{2}}$
3806.153	200	8	26265.791	$15490^{\frac{5}{2}} - 41755_4$
3805.227	200	10	26272.183	$16351_0 - 42624^{\frac{1}{2}}$
3804.127	400	20	26279.779	$11241^{\frac{3}{2}} - 37521_3$
3803.985	600r	150	26280.761	$8800_4 - 35081^{\frac{5}{2}}$
3803.839	400	25	26281.769	$10526^{\frac{3}{2}} - 36808_3$
3803.173	5b	3	26286.371	$14206^{\frac{3}{2}} - 40493_3$
3803.075	3000r	200	26287.049	$0_2 - 26287^{\frac{1}{2}}$
3802.864	500	10	26288.507	$6362_2 - 32650^{\frac{1}{2}}$
3802.589	3		26290.408	$15736^{\frac{1}{2}} - 42027_2$
3802.420	400	25	26291.577	$10526^{\frac{3}{2}} - 36818_2$
3801.571	400r	100	26297.448	$7502_3 - 33799^{\frac{3}{2}}$
3801.443	800r	100	26298.334	$7502_3 - 33800^{\frac{3}{2}}$
3800.745	2		26303.163	$6362_2 - 32665^{\frac{1}{2}}$
3800.197	400	15	26306.956	$5563_1 - 31870^{\frac{3}{2}}$
3799.166	75	1	26314.095	$13297_4 - 39611^{\frac{5}{2}}$
3798.432	200	75	26319.180	$8111_4 - 34430^{\frac{5}{2}}$
3798.103	500r	150	26321.460	$4961_4 - 31283^{\frac{3}{2}}$
3797.205	200	10	26327.684	$9804_5 - 36132^{\frac{5}{2}}$
3796.997	200	10	26329.126	$3687_2 - 30017^{\frac{3}{2}}$
3796.731	500b	20	26330.971	$8800_4 - 35131^{\frac{3}{2}}$
3794.981	200	3	26343.113	$3865_1 - 30208^{\frac{3}{2}}$
3794.697	1500r	100	26345.084	$13175^{\frac{3}{2}} - 39520_4$
3793.097	300	10	26356.197	$17501^{\frac{5}{2}} - 43857_5$
3792.730	400l	75	26358.747	$10526^{\frac{3}{2}} - 36885_4$
3792.371	1000r	100	26361.242	$10414^{\frac{3}{2}} - 36775_3$
3792.104	150	3	26363.098	$0_2 - 26363^{\frac{3}{2}}$
3791.517	300	10	26367.180	$10414^{\frac{3}{2}} - 36781_5$
3791.221	150	8	26369.238	$11601_1 - 37970^{\frac{3}{2}}$
3790.794	1500r	200	26372.209	$7795^{\frac{3}{2}} - 34167_3$
3790.646	100	5	26373.238	$9804_5 - 36178^{\frac{3}{2}}$
3790.269	300	10	26375.861	$14206^{\frac{3}{2}} - 40582_5$
3789.659	50	1	26380.107	$13088_3 - 39468^{\frac{3}{2}}$
3789.529	75	2	26381.012	$8111_4 - 34492^{\frac{3}{2}}$
3789.372	300	10	26382.105	$7280_2 - 33662^{\frac{1}{2}}$
3789.167	500r	100	26383.532	$2869_3 - 29252^{\frac{3}{2}}$
3787.934	300	3	26392.120	$6362_2 - 32754^{\frac{3}{2}}$
3787.638	300	40	26394.182	$10414^{\frac{3}{2}} - 36808_3$
3785.771	100	2	26407.199	$13847_2 - 40254^{\frac{3}{2}}$
3785.154	200	2	26411.503	$15166^{\frac{3}{2}} - 41578_2$
3784.793	300	15	26414.022	$11802_2 - 38216^{\frac{3}{2}}$
3784.574	400	20	26415.551	$3865_1 - 30281^{\frac{1}{2}}$
3784.574	400	20	26415.551	$12114^{\frac{3}{2}} - 38529_3$
3784.406	100	3	26416.723	$12847_3 - 39264^{\frac{3}{2}}$
3783.680	50b		26421.792	$14465^{\frac{3}{2}} - 40886_2$
3781.638	10		26436.059	$17501^{\frac{5}{2}} - 43937_6$
3781.318	300	75	26438.296	$7280_2 - 33718^{\frac{3}{2}}$
3780.966	300r	20b	26440.757	$2869_3 - 29310^{\frac{3}{2}}$
3780.147	200	8	26446.486	$11241^{\frac{3}{2}} - 37688_3$
3778.987	200	3	26454.603	$7280_2 - 33734^{\frac{3}{2}}$
3778.045	300	15	26461.199	$14032^{\frac{3}{2}} - 40493_3$
3777.745	200	40	26463.301	$12847_3 - 39311^{\frac{3}{2}}$
3777.626	50b		26464.134	$8243^{\frac{3}{2}} - 34707_3$

TABLE 4. *Classified lines of* Th I—continued

Wavelength (Å)	Intensity		Wavenumber (cm^{-1})	Classification
	Lamp	Spark		
3777.415	300	40	26465.612	$7502_3 - 33967\frac{3}{3}$
3776.732	10		26470.399	$9804_5 - 36275_6$
3776.622	300	40b	26471.169	$10414\frac{3}{4} - 36885_4$
3776.502	300	8	26472.010	$8111_4 - 34583\frac{3}{3}$
3776.271	600r	150	26473.630	$8800_4 - 35273_6$
3775.937	15		26475.971	$11802_2 - 38278\frac{1}{1}$
3775.157	150	15	26481.442	$13945\frac{3}{3} - 40426_4$
3774.223	50b		26487.995	$11601_1 - 38088\frac{2}{2}$
3774.133	100	8	26488.627	$12114\frac{2}{2} - 38602_2$
3773.306	200	8	26494.432	$14206\frac{3}{4} - 40701_4$
3772.649	400	10	26499.046	$7502_3 - 34001\frac{2}{4}$
3771.629	100b	5	26506.212	$7795\frac{3}{4} - 34301_4$
3771.616	300b	10	26506.303	$11241\frac{3}{3} - 37748_2$
3771.370	1500r	100	26508.032	$0_2 - 26508\frac{3}{3}$
3770.056	1500r	200	26517.271	$5563_1 - 32080\frac{1}{1}$
3769.778	50	1	26519.226	$13175\frac{4}{4} - 39694_5$
3769.697	75	10	26519.796	$15166\frac{3}{3} - 41686_3$
3769.615	200b	40	26520.373	$14204_5 - 40724_6$
3769.592	400b	50	26520.535	$7280_2 - 33800\frac{3}{3}$
3769.101	75	1	26523.990	$10783\frac{2}{2} - 37307_3$
3766.447	300	10	26542.679	$11241\frac{3}{3} - 37784_2$
3766.083	300b	50	26545.244	$11197_6 - 37742_6$
3765.696	200	4	26547.972	$13945\frac{3}{3} - 40493_3$
3765.412	400r	50	26549.975	$2869_3 - 29419\frac{2}{2}$
3765.241	800r	200	26551.181	$8800_4 - 35351\frac{4}{4}$
3765.067	150	2	26552.408	$11802_2 - 38355\frac{2}{2}$
3764.089	4		26559.306	$10526\frac{3}{3} - 37085_4$
3763.668	300	10	26562.277	$4961_4 - 31523\frac{3}{3}$
3762.934	500r	100	26567.458	$3687_2 - 30255\frac{3}{3}$
3762.815	300b	25	26568.298	$10526\frac{3}{3} - 37094_2$
3762.257	200	8	26572.239	$14204_5 - 40776\frac{4}{4}$
3761.704	200	20	26576.145	$13297_4 - 39873_6$
3761.527	200	20	26577.396	$11241\frac{3}{3} - 37819_4$
3761.470	200	25	26577.798	$9804_5 - 36382\frac{4}{4}$
3761.217	200	8	26579.586	$14032\frac{2}{2} - 40611_2$
3759.886	50		26588.995	$15166\frac{3}{3} - 41755_4$
3759.433	500r	75	26592.199	$6362_2 - 32954\frac{2}{2}$
3759.314	200r	100	26593.041	$3687_2 - 30281\frac{1}{1}$
3759.262	300r	100	26593.408	$8111_4 - 34704\frac{3}{3}$
3758.706	400	20	26597.342	$5563_1 - 32160\frac{2}{2}$
3758.467	400r	25	26599.033	$2558_0 - 29157\frac{1}{1}$
3757.694	1000r	200	26604.505	$10526\frac{3}{3} - 37131_3$
3756.451	200	8	26613.308	$11802_2 - 38416\frac{3}{3}$
3756.293	400	25	26614.428	$8111_4 - 34725\frac{3}{3}$
3755.498	25s	3	26620.061	$12114\frac{2}{2} - 38734_3$
3755.211	800r	250	26622.096	$11197_6 - 37819_4$
3754.030	500r	50	26630.471	$8243\frac{2}{2} - 34874_3$
3753.241	300	40	26636.069	$7795\frac{3}{4} - 34431_3$
3752.789	300	8	26639.277	$2558_0 - 29197\frac{1}{1}$
3752.265	10	1	26642.997	$14243\frac{1}{1} - 40886_2$
3751.121	300	25	26651.122	$11241\frac{3}{3} - 37892_4$
3751.021	300r	10	26651.833	$0_2 - 26651\frac{2}{2}$
3749.617	300	20	26661.812	$8800_4 - 35462\frac{3}{3}$
3749.514	300	10	26662.544	$13175\frac{4}{4} - 39837_3$
3749.083	200	25	26665.609	$7795\frac{3}{4} - 34460_5$
3748.820	100	8	26667.480	$15618\frac{3}{3} - 42286_3$
3748.225	20b	5	26671.713	$10414\frac{2}{4} - 37085_4$
3746.929	4		26680.938	$6362_2 - 33043\frac{3}{3}$
3745.176	400l	20	26693.427	$11197_6 - 37890_5$
3744.847	100	5	26695.772	$11197_6 - 37892_4$
3742.923	1000r	100	26709.494	$4961_4 - 31671\frac{2}{2}$
3742.275	200	5	26714.119	$12847_3 - 39562\frac{2}{2}$
3741.884	200	8	26716.910	$10414\frac{2}{4} - 37131_3$
3740.731	40	2	26725.145	$11877\frac{2}{1} - 38602_2$
3737.514	600r	75	26748.147	$3865_1 - 30613_6$
3736.655	100	5	26754.296	$11601_1 - 38355\frac{2}{2}$
3736.566	50	1	26754.933	$4961_4 - 31716_6$
3736.411	5		26756.043	$13945\frac{3}{3} - 40701_4$
3735.827	50b	2	26760.226	$15863_2 - 42624\frac{1}{1}$
3735.363	100	3	26763.550	$12847_3 - 39611\frac{3}{3}$
3733.672	300r	25	26775.671	$8111_4 - 34886_6$
3733.501	10	1	26776.897	$10526\frac{3}{3} - 37303_4$
3732.985	400r	40	26780.599	$10526\frac{3}{3} - 37307_3$
3730.946	50	3	26795.234	$11197_6 - 37992_4$
3730.623	75	4	26797.554	$10414\frac{3}{4} - 37211_5$
3730.368	800r	200l	26799.386	$6362_2 - 33161\frac{1}{1}$
3729.945	400	40	26802.425	$8243\frac{2}{2} - 35046_1$
3727.903	1000r	150	26817.106	$2869_3 - 29686\frac{3}{3}$
3727.725	75	2	26818.386	$13088_3 - 39906\frac{4}{4}$
3727.612	400r	40	26819.199	$4961_4 - 31780\frac{3}{3}$
3727.346	300	40	26821.113	$9804_5 - 36625_6$
3727.251	300	40	26821.797	$7502_3 - 34324\frac{2}{2}$
3725.966	75	2	26831.047	$7280_2 - 34111\frac{1}{1}$
3724.397	100	2	26842.350	$7502_3 - 34344\frac{4}{4}$
3723.921	300s	8	26845.781	$8243\frac{2}{2} - 35089_3$
3722.655	75	2	26854.910	$14032\frac{2}{2} - 40886_2$
3722.591	100b	5	26855.372	$11241\frac{3}{3} - 38097_2$
3722.179	300b	25b	26858.344	$3865_1 - 30723\frac{1}{1}$
3721.881	10b		26860.495	$15166\frac{3}{3} - 42027_2$
3721.219	500r	50	26865.273	$3687_2 - 30553\frac{2}{2}$
3721.003	100	10	26866.833	$11802_2 - 38669\frac{2}{2}$
3720.628	20	15	26869.540	$7502_3 - 34371\frac{2}{2}$
3719.837	400r	40	26875.254	$2869_3 - 29744\frac{3}{3}$
3719.546	300	15	26877.356	$13175\frac{4}{4} - 40052_4$
3719.435	3000	200	26878.158	$0_2 - 26878\frac{3}{3}$
3717.895	50	2	26889.291	$10414\frac{3}{4} - 37303_4$
3717.384	100	3	26892.988	$10414\frac{3}{4} - 37307_3$
3716.992	100b	4	26895.824	$12114\frac{2}{2} - 39010_3$
3716.942	100	2	26896.186	$14465\frac{2}{2} - 41361_3$
3716.808	100	2	26897.155	$13088_3 - 39985\frac{3}{3}$
3715.862	300	20	26904.003	$11241\frac{3}{3} - 38145_3$
3715.561	400	50	26906.182	$8243\frac{2}{2} - 35149_2$
3715.060	100	2	26909.810	$11197_6 - 38106_5$
3714.696	100	3	26912.447	$7795\frac{3}{4} - 34707_3$
3712.299	40	2	26929.824	$11877\frac{1}{1} - 38807_2$
3712.187	25	8	26930.636	$14204_5 - 41134\frac{4}{4}$
3711.926	200	5	26932.530	$6362_2 - 33294\frac{3}{3}$
3711.833	200	15	26933.205	$8800_4 - 35733\frac{4}{4}$
3711.623	600r	50	26934.729	$6362_2 - 33297\frac{2}{2}$
3711.357	75	4b	26936.659	$17501_6 - 44437_6$

TABLE 4. *Classified lines of* Th I—continued

Wavelength (Å)	Intensity		Wavenumber (cm^{-1})	Classification
	Lamp	Spark		
3710.830	100	1	26940.484	$5563_1 - 32503\frac{2}{2}$
3710.665	100l	2	26941.682	$13945\frac{5}{3} - 40886_2$
3710.292	300	8	26944.391	$11241\frac{5}{3} - 38186_4$
3709.861	300	25	26947.521	$3865_1 - 30812\frac{2}{2}$
3708.483	75	2	26957.534	$13297_4 - 40254\frac{3}{3}$
3707.465	200	8	26964.936	$10783\frac{2}{2} - 37748_2$
3706.767	2000r	300	26970.013	$8111_4 - 35081\frac{0}{0}$
3706.402	200	75	26972.669	$13297_4 - 40270\frac{4}{4}$
3704.862	500r	50	26983.880	$2869_3 - 29853\frac{2}{2}$
3704.584	100	5	26985.905	$11802_2 - 38788\frac{3}{3}$
3704.147	200	50	26989.089	$11197\frac{0}{0} - 38186_4$
3703.951	75b		26990.517	$10414\frac{4}{4} - 37404_3$
3703.775	500r	50	26991.800	$4961_4 - 31953\frac{4}{4}$
3703.342	200	2	26994.955	$10526\frac{3}{3} - 37521_3$
3703.230	400r	25	26995.772	$0_2 - 26995\frac{3}{3}$
3702.479	100	2	27001.247	$10783\frac{2}{2} - 37784_2$
3701.594	150b	3	27007.703	$13088_3 - 40096\frac{2}{2}$
3701.099	200	2	27011.315	$11802_2 - 38814\frac{2}{2}$
3700.978	500r	100	27012.198	$2869_3 - 29881\frac{4}{4}$
3699.881	500r	50	27020.207	$8111_4 - 35131\frac{3}{3}$
3699.355	300	5	27024.048	$14206\frac{4}{4} - 41230_4$
3699.182	500	75	27025.312	$13175\frac{4}{4} - 40200_3$
3698.106	1000r	150	27033.176	$9804_5 - 36837\frac{6}{6}$
3697.743	300	10	27035.829	$3687_2 - 30723\frac{1}{1}$
3697.497	300	3	27037.628	$11802_2 - 38840\frac{1}{1}$
3695.288	500r	75	27053.790	$7795\frac{3}{3} - 34849_5$
3694.579	50	2	27058.982	$12847_3 - 39906\frac{4}{4}$
3694.365	300r	50	27060.549	$12114\frac{3}{3} - 39174_3$
3694.246	300r	10	27061.421	$0_2 - 27061\frac{2}{2}$
3694.177	400r	75	27061.926	$4961_4 - 32023\frac{6}{6}$
3693.993	400r	200	27063.274	$3865_1 - 30928\frac{1}{1}$
3693.804	200b	25	27064.659	$6362_2 - 33427\frac{2}{2}$
3693.247	200	10	27068.741	$11601_1 - 38669\frac{2}{2}$
3692.566	1000r	100	27073.733	$3687_2 - 30761\frac{5}{5}$
3691.972	300b	5	27078.088	$7795\frac{3}{3} - 34873_4$
3691.876	400r	100	27078.792	$7795\frac{3}{3} - 34874_3$
3691.613	500r	200	27080.722	$7502_3 - 34583\frac{3}{3}$
3691.411	500r	50	27082.203	$2558_0 - 29640\frac{1}{1}$
3690.649	100b	8b	27087.795	$5563_1 - 32650\frac{1}{1}$
3690.624	600r	4	27087.978	$0_2 - 27087\frac{1}{1}$
3690.115	200	300	27091.715	$7280_2 - 34371\frac{2}{2}$
3688.658	300	20	27102.416	$5563_1 - 32665\frac{1}{1}$
3687.983	400r	75	27107.376	$10414\frac{4}{4} - 37521_3$
3687.193	400l	20	27113.184	$14465\frac{3}{3} - 41578_2$
3686.326	2		27119.560	$15166\frac{3}{3} - 42286_3$
3685.586	300b	10l	27125.005	$3687_2 - 30812\frac{2}{2}$
3685.214	200	4	27127.743	$13297_4 - 40425\frac{3}{3}$
3684.932	300	20	27129.819	$8111_4 - 35240\frac{3}{3}$
3683.856	20		27137.743	$12847_3 - 39985\frac{3}{3}$
3682.759	10b		27145.827	$15490\frac{8}{8} - 42635_5$
3682.486	800r	50	27147.839	$2869_3 - 30017\frac{3}{3}$
3682.295	300	20	27149.247	$14206\frac{4}{4} - 41356_5$
3682.179	300	50	27150.103	$7280_2 - 34430\frac{3}{3}$
3680.605	400r	40	27161.713	$8243\frac{2}{2} - 35405_3$
3680.448	500r	50	27162.871	$8111_4 - 35273\frac{6}{6}$
3679.970	75	2	27166.400	$13088_3 - 40254\frac{3}{3}$
3679.544	400r	150	27169.545	$11197\frac{0}{0} - 38366_4$
3678.478	400r	50b	27177.418	$8243\frac{2}{2} - 35421_1$
3675.960	400	50	27196.034	$11802_2 - 38998\frac{3}{3}$
3675.790	400r	50	27197.292	$8243\frac{2}{2} - 35440_3$
3675.137	500r	50	27202.124	$7502_3 - 34704\frac{3}{3}$
3674.891	300r	50	27203.945	$9804_5 - 37008\frac{6}{6}$
3674.420	50	5	27207.432	$12114\frac{2}{2} - 39321_3$
3674.013	300r	50b	27210.446	$3865_1 - 31075\frac{2}{2}$
3673.639	50	1	27213.216	$11601_1 - 38814\frac{2}{2}$
3672.522	500	25	27221.493	$10526\frac{3}{3} - 37748_2$
3672.522	500	25	27221.493	$14465\frac{3}{3} - 41686_3$
3672.300	500r	50	27223.138	$7502_3 - 34725\frac{3}{3}$
3671.540	600r	150	27228.773	$6362_2 - 33591\frac{3}{3}$
3671.242	75	2	27230.983	$14481\frac{8}{8} - 41712_5$
3670.520	200	4	27236.340	$9804_5 - 37041\frac{4}{4}$
3669.968	2000r	100	27240.436	$8111_4 - 35351\frac{4}{4}$
3668.914	100	4	27248.261	$12847_3 - 40096\frac{2}{2}$
3667.621	500	40	27257.867	$10526\frac{3}{3} - 37784_2$
3667.311	5	1	27260.171	$0_2 - 27260\frac{3}{3}$
3666.981	800r	75	27262.625	$8800_4 - 36062\frac{3}{3}$
3665.476	100b	10b	27273.818	$8800_4 - 36074\frac{3}{3}$
3665.443	150b	500	27274.064	$10414\frac{4}{4} - 37688_3$
3663.543	300	15	27288.208	$11241\frac{5}{3} - 38529_3$
3663.201	1500r	100	27290.756	$2869_3 - 30160\frac{4}{4}$
3662.955	150	15	27292.589	$10526\frac{3}{3} - 37819_4$
3662.750	300r	20	27294.116	$7795\frac{3}{3} - 35089_3$
3662.283	100	3	27297.596	$0_2 - 27297\frac{1}{1}$
3661.982	150	15	27299.840	$6362_2 - 33662\frac{1}{1}$
3661.622	500r	75	27302.524	$3687_2 - 30990\frac{3}{3}$
3661.575	500r	200	27302.874	$7280_2 - 34583\frac{3}{3}$
3660.500	400	25	27310.892	$7280_2 - 34591\frac{1}{1}$
3660.091	200b	4	27313.944	$10783\frac{2}{2} - 38097_2$
3659.629	600r	150	27317.392	$0_2 - 27317\frac{3}{3}$
3658.808	400r	25	27323.522	$4961_4 - 32285\frac{3}{3}$
3657.641	200s	10	27332.240	$8800_4 - 36132\frac{6}{6}$
3657.054	300	20	27336.627	$13088_3 - 40425\frac{3}{3}$
3656.693	500r	50	27339.325	$2869_3 - 30208\frac{2}{2}$
3655.125	300	50	27351.053	$8111_4 - 35462\frac{3}{3}$
3654.915	3		27352.624	$13847_2 - 41200\frac{2}{2}$
3654.461	500r	50	27356.023	$6362_2 - 33718\frac{2}{2}$
3653.586	40		27362.574	$10783\frac{2}{2} - 38145_3$
3653.090	100	2	27366.289	$10526\frac{3}{3} - 37892_4$
365.9284	20	1	27372.328	$6362_2 - 33734\frac{2}{2}$
3650.436	200	50	27386.185	$2869_3 - 30255\frac{3}{3}$
3650.204	300l	2	27387.925	$3687_2 - 31075\frac{2}{2}$
3649.735	1000r	100	27391.445	$5563_1 - 32954\frac{2}{2}$
3647.932	300	50	27404.982	$10414\frac{4}{4} - 37819_4$
3647.662	25		27407.011	$12847_3 - 40254\frac{3}{3}$
3647.575	300	15	27407.665	$13175\frac{4}{4} - 40582_5$
3646.452	15		27416.105	$13945\frac{5}{3} - 41361_3$
3645.706	300	15	27421.715	$7795\frac{3}{3} - 35216_3$
3645.648	200	8	27422.151	$12847_3 - 40270\frac{4}{4}$
3645.365	200b	25b	27424.280	$7280_2 - 34704\frac{3}{3}$
3644.981	200	3	27427.169	$13297_4 - 40724\frac{8}{8}$

TABLE 4. *Classified lines of* Th I—continued

Wavelength (Å)	Intensity		Wavenumber (cm^{-1})	Classification
	Lamp	Spark		
3643.512	600r	50	27438.227	$6362_2 - 33800\frac{3}{3}$
3642.573	500r	50	27445.300	$7280_2 - 34725\frac{3}{3}$
3642.249	2000r	100	27447.741	$0_2 - 27447\frac{2}{2}$
3640.820	10		27458.514	$11241\frac{3}{3} - 38700_4$
3640.390	100	3	27461.757	$11802_2 - 39264\frac{3}{3}$
3639.867	400l	40	27465.703	$10526\frac{3}{3} - 37992_4$
3638.644	500r	50	27474.935	$8800_4 - 36275\frac{6}{6}$
3638.460	40	2	27476.324	$10414\frac{4}{4} - 37890_5$
3638.319	400r	25	27477.389	$4961_4 - 32439\frac{4}{4}$
3638.146	200	4	27478.695	$10414\frac{4}{4} - 37892_4$
3638.097	150	4	27479.066	$13297_4 - 40776\frac{4}{4}$
3638.004	75	4	27479.768	$14206\frac{4}{4} - 41686_3$
3636.295	150	3	27492.682	$11241\frac{3}{3} - 38734_3$
3634.902	200	4	27503.218	$11197\frac{6}{6} - 38700_4$
3634.582	600r	100b	27505.640	$7795\frac{4}{4} - 35300_5$
3634.546	500b	50b	27505.912	$14206\frac{4}{4} - 41712_5$
3633.910	100	3	27510.726	$16346\frac{6}{6} - 43857_5$
3632.830	1000r	100	27518.905	$11241\frac{3}{3} - 38760_4$
3631.863	150	8	27526.231	$13175\frac{4}{4} - 40701_4$
3629.214	15		27546.323	$14032\frac{2}{2} - 41578_2$
3628.867	100	4	27548.956	$14206\frac{4}{4} - 41755_4$
3626.939	300	50	27563.600	$11197\frac{6}{6} - 38760_4$
3626.631	200b	10	27565.941	$11241\frac{3}{3} - 38807_2$
3626.613	50b		27566.078	$12114\frac{2}{2} - 39680_2$
3626.025	50	3	27570.548	$10526\frac{3}{3} - 38097_2$
3625.895	500r	400b	27571.537	$7280_2 - 34851\frac{2}{2}$
3625.150	300	75	27577.203	$12847_3 - 40425\frac{4}{4}$
3625.026	300r	100	27578.146	$10414\frac{4}{4} - 37992_4$
3624.472	300	50	27582.361	$8800_4 - 36382\frac{4}{4}$
3623.773	300	25	27587.681	$8243\frac{2}{2} - 35831_3$
3622.795	600r	50	27595.129	$3687_2 - 31283\frac{3}{3}$
3622.338	500r	20b	27598.610	$5563_1 - 33161\frac{1}{1}$
3621.435	50		27605.492	$6362_2 - 33967\frac{3}{3}$
3620.977	5		27608.983	$11802_2 - 39411\frac{1}{1}$
3620.839	300r	50	27610.035	$7795\frac{4}{4} - 35405_3$
3619.633	100	20	27619.234	$10526\frac{3}{3} - 38145_3$
3619.211	200	40	27622.455	$8111_4 - 35733\frac{4}{4}$
3618.597	200	10	27627.142	$8800_4 - 36427\frac{3}{3}$
3618.363	800r	50	27628.928	$7502_3 - 35131\frac{4}{4}$
3617.818	150	10	27633.090	$13945\frac{3}{3} - 41578_2$
3617.671	300	8	27634.213	$8243\frac{2}{2} - 35877_2$
3616.177	200	8	27645.629	$7795\frac{4}{4} - 35440_3$
3615.849	200	4	27648.137	$2869_3 - 30517\frac{4}{4}$
3615.004	100	5	27654.600	$14032\frac{2}{2} - 41686_3$
3614.352	500r	75	27659.588	$10526\frac{3}{3} - 38186_4$
3613.547	200	5	27665.750	$11802_2 - 39468\frac{3}{3}$
3612.864	600r	5	27670.980	$0_2 - 27670\frac{5}{5}$
3612.427	1500r	75	27674.327	$0_2 - 27674\frac{2}{2}$
3611.257	25	5	27683.293	$13297_4 - 40980\frac{5}{5}$
3611.158	200s	10	27684.052	$2869_3 - 30553\frac{2}{2}$
3610.650	300	20	27687.947	$13088_3 - 40776\frac{4}{4}$
3608.880	300	4	27701.526	$8111_4 - 35812\frac{5}{5}$
3607.819	75		27709.673	$7280_2 - 34989\frac{6}{6}$
3606.090	200	3	27722.958	$2558_0 - 30281\frac{1}{1}$

Wavelength (Å)	Intensity		Wavenumber (cm^{-1})	Classification
	Lamp	Spark		
3604.965	20		27731.609	$10414\frac{4}{4} - 38145_3$
3604.680	600r	40	27733.802	$3865_1 - 31599\frac{2}{2}$
3604.657	100		27733.979	$5563_1 - 33297\frac{2}{2}$
3604.064	200b		27738.542	$7502_3 - 35240\frac{3}{3}$
3603.694	150	4	27741.390	$13945\frac{3}{3} - 41686_3$
3601.770	200	10	27756.208	$11197\frac{6}{6} - 38953_5$
3601.295	300	10	27759.869	$11197\frac{6}{6} - 38956_4$
3600.431	300	50	27766.531	$9804_5 - 37571\frac{6}{6}$
3600.182	100	25	27768.451	$11241\frac{3}{3} - 39010_3$
3599.723	300	20	27771.992	$10414\frac{4}{4} - 38186_4$
3598.523	150	10	27781.252	$7795\frac{4}{4} - 35576_3$
3598.245	75	10	27783.399	$14243\frac{1}{1} - 42027_2$
3598.120	2000r	50	27784.364	$0_2 - 27784\frac{2}{2}$
3597.776	10		27787.020	$7795\frac{4}{4} - 35582_5$
3597.021	75	2	27792.853	$4961_4 - 32754\frac{3}{3}$
3595.975	150	5	27800.937	$9804_5 - 37605\frac{4}{4}$
3595.756	100	10	27802.630	$11877\frac{1}{1} - 39680_2$
3595.617	500r	100	27803.705	$8243\frac{2}{2} - 36047_2$
3594.985	300	20	27808.593	$11802_2 - 39611\frac{3}{3}$
3593.535	15		27819.813	$10783\frac{2}{2} - 38602_2$
3593.352	5		27821.230	$14465\frac{2}{2} - 42286_3$
3592.777	800r	100	27825.682	$8800_4 - 36625\frac{6}{6}$
3591.452	800r	50	27835.948	$3687_2 - 31523\frac{3}{3}$
3591.253	300	50	27837.490	$13297_4 - 41134\frac{4}{4}$
3590.924	400		27840.041	$10526\frac{3}{3} - 38366_4$
3589.992	300	20	27847.268	$3865_1 - 31712\frac{1}{1}$
3589.748	1000r	75	27849.161	$7502_3 - 35351\frac{4}{4}$
3586.703	100		27872.803	$13847_2 - 41720\frac{2}{2}$
3584.175	800r	50	27892.462	$2869_3 - 30761\frac{3}{3}$
3583.100	600r	25	27900.830	$4961_4 - 32862\frac{4}{4}$
3581.754	200	10	27911.315	$3687_2 - 31599\frac{2}{2}$
3579.543	300	50	27928.554	$12847_3 - 40776\frac{4}{4}$
3578.947	400	10	27933.205	$11241\frac{3}{3} - 39174_3$
3577.596	200	10	27943.753	$2869_3 - 30812\frac{2}{2}$
3576.633	300	40	27951.277	$10783\frac{2}{2} - 38734_3$
3576.557	400r	150	27951.871	$8111_4 - 36062\frac{4}{4}$
3576.481	300		27952.465	$10414\frac{4}{4} - 38366_4$
3575.546	50		27959.774	$7502_3 - 35462\frac{5}{5}$
3575.427	100	10	27960.705	$7280_2 - 35240\frac{3}{3}$
3575.301	50b		27961.690	$6362_2 - 34324\frac{2}{2}$
3575.121	500r	50	27963.098	$8111_4 - 36074\frac{3}{3}$
3571.008	300	10	27995.304	$14032\frac{2}{2} - 42027_2$
3570.523	300	10	27999.107	$7795\frac{4}{4} - 35794_4$
3570.357	500	10	28000.408	$8800_4 - 36800\frac{4}{4}$
3569.977	100	5	28003.389	$10526\frac{3}{3} - 38529_3$
3569.820	1000r	25	28004.620	$3865_1 - 31870\frac{2}{2}$
3569.207	75		28009.430	$6362_2 - 34371\frac{2}{2}$
3567.672	200	20	28021.481	$8111_4 - 36132\frac{6}{6}$
3567.264	1000r	50	28024.686	$0_2 - 28024\frac{1}{1}$
3566.459	20	1	28031.011	$7502_3 - 35533\frac{2}{2}$
3565.822	300	15	28036.018	$7795\frac{4}{4} - 35831_3$
3565.604	200	10	28037.732	$8800_4 - 36837\frac{6}{6}$
3565.049	40		28042.097	$11241\frac{3}{3} - 39283_4$
3564.508	100	10	28046.353	$13088_3 - 41134\frac{4}{4}$
3564.235	200	8	28048.501	$7280_2 - 35328\frac{1}{1}$

TABLE 4. *Classified lines of* Th I—continued

Wavelength (Å)	Intensity		Wavenumber (cm^{-1})	Classification
	Lamp	Spark		
3563.375	600r	75b	28055.270	$11197_{5}^{6} - 39252_{5}$
3563.299	300	25	28055.869	$13175_{4}^{4} - 41230_{4}$
3561.879	40		28067.053	$8111_{4} - 36178_{4}^{4}$
3561.780	500r	75	28067.833	$6362_{2} - 34430_{5}^{5}$
3560.688	200	5	28076.441	$10526_{3}^{3} - 38602_{2}$
3560.295	20		28079.540	$14206_{4}^{4} - 42286_{3}$
3560.226	40	5	28080.084	$11241_{3}^{3} - 39321_{3}$
3560.021	300r	50	28081.701	$4961_{4} - 33043_{3}^{3}$
3559.378	200b		28086.774	$11197_{5}^{6} - 39283_{4}$
3558.638	100		28092.614	$8243_{2}^{2} - 36336_{3}$
3558.599	8		28092.922	$3687_{2} - 31780_{3}^{3}$
3557.818	150	5	28099.089	$5563_{1} - 33662_{1}^{1}$
3556.206	8		28111.826	$13088_{3} - 41200_{2}^{2}$
3555.705	500r	50	28115.787	$10414_{3}^{3} - 38529_{3}$
3555.013	1000r	50	28121.259	$2869_{3} - 30990_{3}^{3}$
3551.984	20		28145.239	$9804_{5} - 37950_{4}^{4}$
3551.401	1000r	150	28149.860	$2869_{3} - 31019_{4}^{4}$
3550.878	300	40	28154.006	$14481_{8}^{8} - 42635_{5}$
3550.783	300	40	28154.759	$11197_{5}^{6} - 39351_{5}$
3550.718	100s		28155.274	$5563_{1} - 33718_{2}^{2}$
3549.596	1000r	75	28164.174	$8111_{4} - 36275_{5}^{6}$
3549.396	50	25	28165.761	$2558_{0} - 30723_{1}^{1}$
3548.664	300	8	28171.570	$5563_{1} - 33734_{2}^{2}$
3547.469	150l		28181.060	$13175_{4}^{4} - 41356_{5}$
3547.364	300b		28181.894	$7280_{2} - 35462_{3}^{3}$
3547.338	200b		28182.100	$3687_{2} - 31870_{2}^{2}$
3547.252	100	5	28182.784	$11802_{2} - 39985_{3}^{3}$
3546.809	75		28186.304	$13175_{4}^{4} - 41361_{3}$
3544.250	150	3	28206.654	$2869_{3} - 31075_{2}^{2}$
3544.097	200		28207.872	$10526_{3}^{3} - 38734_{3}$
3544.018	800r	50	28208.500	$8800_{4} - 37008_{5}^{6}$
3543.208	150	3	28214.949	$3865_{1} - 32080_{1}^{1}$
3542.498	500r	50	28220.604	$6362_{2} - 34583_{3}^{3}$
3541.692	40		28227.026	$10783_{2}^{2} - 39010_{3}$
3541.493	150		28228.612	$6362_{2} - 34591_{1}^{1}$
3540.807	2		28234.081	$10526_{3}^{3} - 38760_{4}$
3539.951	8b		28240.908	$8800_{4} - 37041_{4}^{4}$
3539.843	300	25	28241.770	$8243_{2}^{2} - 36485_{2}$
3538.415	3		28253.167	$7280_{2} - 35533_{2}^{2}$
3538.264	15	2	28254.372	$14032_{8}^{8} - 42286_{3}$
3536.009	500r	20	28272.390	$8243_{2}^{2} - 36515_{3}$
3535.250	150b		28278.460	$11241_{3}^{3} - 39520_{4}$
3534.916	15		28281.132	$10526_{3}^{3} - 38807_{2}$
3533.396	40	1	28293.298	$11802_{2} - 40096_{2}^{2}$
3533.181	200b	10	28295.019	$3865_{1} - 32160_{2}^{2}$
3531.450	1000r	50	28308.888	$4961_{4} - 33270_{4}^{4}$
3531.282	200	8	28310.235	$7502_{3} - 35812_{3}^{3}$
3530.514	800r	50	28316.393	$8111_{4} - 36427_{5}^{5}$
3530.030	50	3	28320.276	$10414_{3}^{3} - 38734_{3}$
3529.670	200b	15	28323.164	$11197_{5}^{6} - 39520_{4}$
3529.385	300l	40	28325.451	$2869_{3} - 31194_{4}^{4}$
3528.411	300	50	28333.270	$4961_{4} - 33294_{3}^{3}$
3527.793	200	10	28338.233	$7795_{4}^{4} - 36133_{5}$
3527.434	4s		28341.117	$13945_{3}^{3} - 42286_{3}$
3527.322	200	50	28342.017	$6362_{2} - 34704_{3}^{3}$
3526.764	300		28346.501	$10414_{3}^{3} - 38760_{4}$
3526.634	500r	10	28347.546	$0_{2} - 28347_{2}^{2}$
3526.029	15l	1	28352.410	$12847_{3} - 41200_{2}^{2}$
3525.171	8		28359.310	$8800_{4} - 37159_{3}^{3}$
3524.708	300	8	28363.035	$6362_{2} - 34725_{3}^{3}$
3524.178	300	25	28367.301	$15490_{6}^{6} - 43857_{5}$
3523.758	300	8	28370.682	$2558_{0} - 30928_{1}^{1}$
3523.505	300		28372.719	$0_{2} - 28372_{1}^{1}$
3522.154	100	2	28383.602	$7502_{3} - 35885_{2}^{2}$
3521.141	100	2	28391.767	$10783_{2}^{2} - 39174_{3}$
3521.059	500r	25	28392.428	$3687_{2} - 32080_{1}^{1}$
3520.453	5		28397.315	$14226_{0} - 42624_{1}^{1}$
3520.277	15		28398.735	$7280_{2} - 35678_{1}^{1}$
3518.885	400l	50	28409.969	$8243_{2}^{2} - 36653_{2}$
3518.404	1000r	40	28413.853	$2869_{3} - 31283_{3}^{3}$
3518.197	100	5	28415.524	$7795_{4}^{4} - 36210_{5}$
3516.530	3		28428.994	$14206_{4}^{4} - 42635_{5}$
3515.327	100	40	28438.723	$11241_{3}^{3} - 39680_{2}$
3514.285	200	10	28447.155	$15490_{6}^{6} - 43937_{6}$
3513.682	75s	4	28452.037	$11802_{2} - 40254_{3}^{3}$
3511.157	800r	25	28472.497	$3687_{2} - 32160_{2}^{2}$
3509.784	10		28483.635	$10526_{3}^{3} - 39010_{3}$
3509.089	500	25	28489.276	$6362_{2} - 34851_{2}^{2}$
3508.360	300	3	28495.196	$11601_{1} - 40096_{2}^{2}$
3508.100	300b		28497.307	$11197_{5}^{6} - 39694_{5}$
3507.520	100		28502.020	$7795_{4}^{4} - 36297_{4}$
3506.645	300	5	28509.131	$3687_{2} - 32197_{3}^{3}$
3506.345	150	10	28511.571	$13175_{4}^{4} - 41686_{3}$
3506.132	300	3	28513.303	$0_{2} - 28513_{2}^{2}$
3505.934	10		28514.913	$8111_{4} - 36625_{5}^{6}$
3505.767	150	5	28516.271	$6362_{2} - 34878_{1}^{1}$
3503.863	75		28531.766	$8243_{2}^{2} - 36775_{3}$
3503.786	500r	40	28532.393	$7280_{2} - 35812_{3}^{3}$
3503.130	200	15	28537.736	$13175_{4}^{4} - 41712_{5}$
3503.017	100	5	28538.657	$10783_{2}^{2} - 39321_{3}$
3502.963	200	10	28539.097	$10414_{3}^{3} - 38953_{5}$
3502.739	200b		28540.922	$7795_{4}^{4} - 36336_{3}$
3502.514	100	2	28542.755	$10414_{3}^{3} - 38956_{4}$
3501.866	150b	25	28548.037	$5563_{1} - 34111_{1}^{1}$
3500.326	50	10	28560.596	$7502_{3} - 36062_{3}^{3}$
3499.821	200	5	28564.717	$8243_{2}^{2} - 36808_{3}$
3498.956	200b	20b	28571.779	$7502_{3} - 36074_{3}^{3}$
3498.621	800r	75	28574.514	$8243_{2}^{2} - 36818_{2}$
3497.901	50	10	28580.396	$9804_{5} - 38385_{6}^{6}$
3497.856	50	3	28580.764	$13175_{4}^{4} - 41755_{4}$
3496.811	500r	15	28589.305	$0_{2} - 28589_{3}^{3}$
3496.003	200	10	28595.912	$11241_{3}^{3} - 39837_{3}$
3495.847	15		28597.188	$3687_{2} - 32285_{3}^{3}$
3495.700	800r	25	28598.390	$4961_{4} - 33560_{4}^{4}$
3494.801	100		28605.747	$7280_{2} - 35885_{2}^{2}$
3492.158	25		28627.396	$6362_{2} - 34989_{1}^{1}$
3491.900	500	2	28629.511	$4961_{4} - 33591_{3}^{3}$
3490.848	20	1	28638.139	$3865_{1} - 32503_{2}^{2}$
3489.602	100l	1	28648.364	$10526_{3}^{3} - 39174_{3}$
3489.509	400	2	28649.128	$0_{2} - 28649_{1}^{1}$

TABLE 4. *Classified lines of* Th I—continued

Wavelength (Å)	Intensity		Wavenumber (cm^{-1})	Classification
	Lamp	Spark		
3489.185	500	4	28651.788	$8111_4 - 36762\frac{5}{2}$
3488.834	500	3	28654.670	$2869_3 - 31523\frac{5}{2}$
3487.991	150l	4	28661.596	$13962_1 - 42624\frac{1}{2}$
3486.551	1000r	10b	28673.433	$0_2 - 28673\frac{1}{2}$
3486.269	50	1	28675.752	$7502_3 - 36178\frac{1}{4}$
3486.210	50	1	28676.238	$0_2 - 28676\frac{3}{2}$
3484.943	100	1	28686.663	$7502_3 - 36188\frac{1}{2}$
3484.580	8		28689.651	$8111_4 - 36800\frac{3}{4}$
3480.810	100		28720.723	$7795\frac{3}{4} - 36515_3$
3480.052	500	3	28726.979	$8111_4 - 36837\frac{5}{2}$
3479.684	300	2	28730.017	$2869_3 - 31599\frac{1}{2}$
3479.221	300b	2	28733.840	$11877\frac{1}{2} - 40611_2$
3476.385	200	3	28757.280	$10526\frac{3}{2} - 39283_4$
3475.961	100b		28760.788	$10414\frac{3}{4} - 39174_3$
3475.943	100b		28760.937	$5563_1 - 34324\frac{1}{2}$
3474.717	200	10	28771.084	$8800_4 - 37571\frac{5}{2}$
3474.530	200	3	28772.633	$12114\frac{3}{2} - 40886_2$
3474.188	3		28775.465	$9804_5 - 38580\frac{3}{4}$
3472.989	15b		28785.399	$3865_1 - 32650\frac{1}{2}$
3471.959	500r	50l	28793.938	$7280_2 - 36074\frac{3}{2}$
3471.800	50b		28795.257	$10526\frac{3}{2} - 39321_3$
3471.216	1000r	50b	28800.102	$3865_1 - 32665\frac{1}{2}$
3471.001	300	15	28801.885	$2869_3 - 31671\frac{1}{4}$
3470.568	300	20	28805.479	$8800_4 - 37605\frac{3}{4}$
3470.181	5	2	28808.691	$5563_1 - 34371\frac{1}{2}$
3469.345	1000r	150	28815.633	$3687_2 - 32503\frac{1}{2}$
3466.644	600r	100	28838.083	$4961_4 - 33799\frac{1}{4}$
3466.538	600r	40	28838.965	$4961_4 - 33800\frac{3}{4}$
3465.061	200b	25	28851.258	$8243\frac{1}{2} - 37094_2$
3464.560	25	2	28855.430	$11197\frac{5}{2} - 40052_4$
3463.921	50	2	28860.753	$9804_5 - 38665\frac{5}{2}$
3461.801	8		28878.426	$6362_2 - 35240\frac{3}{4}$
3461.574	200	3	28880.320	$7502_3 - 36382\frac{1}{4}$
3461.215	2000r	75	28883.315	$4961_4 - 33844\frac{5}{2}$
3461.018	1500r	50	28884.959	$0_2 - 28884\frac{3}{4}$
3460.724	75	2	28887.413	$3687_2 - 32575\frac{1}{2}$
3460.724	75	2	28887.413	$8243\frac{1}{2} - 37131_3$
3459.536	50b		28897.333	$10783\frac{1}{2} - 39680_2$
3459.488	75	8	28897.734	$8111_4 - 37008\frac{5}{2}$
3458.299	20		28907.669	$10414\frac{3}{4} - 39321_3$
3457.829	75		28911.598	$2869_3 - 31780\frac{3}{4}$
3457.069	400r	25	28917.954	$0_2 - 28917\frac{1}{2}$
3456.217	2		28925.082	$7502_3 - 36427\frac{3}{4}$
3455.612	200b	10	28930.146	$8111_4 - 37041\frac{1}{4}$
3453.513	300b	10	28947.729	$15490\frac{5}{2} - 44437_6$
3452.207	75	1	28958.680	$11241\frac{3}{4} - 40200_3$
3451.702	800r	100	28962.916	$3687_2 - 32650\frac{1}{2}$
3451.308	100		28966.223	$6362_2 - 35328\frac{1}{2}$
3449.949	200	5	28977.623	$3687_2 - 32665_1$
3448.949	300	10	28986.034	$7795\frac{3}{4} - 36781_5$
3448.891	15h		28986.522	$7502_3 - 36488\frac{1}{2}$
3447.189	40		29000.833	$2869_3 - 31870\frac{1}{2}$
3446.546	300	8	29006.243	$4961_4 - 33967\frac{3}{4}$
3446.200	15		29009.155	$11877\frac{1}{2} - 40886_2$
3443.980	100	8	29027.854	$5563_1 - 34591\frac{1}{2}$
3442.578	800r	20	29039.676	$4961_4 - 34001\frac{1}{4}$
3441.527	200	5	29048.544	$8111_4 - 37159\frac{3}{4}$
3440.827	8		29054.453	$10783\frac{1}{2} - 39837_3$
3439.748	100b		29063.567	$8243\frac{1}{2} - 37307_3$
3439.399	400b	8	29066.516	$3687_2 - 32754\frac{3}{4}$
3437.645	50b	5b	29081.346	$7280_2 - 36361\frac{1}{2}$
3437.307	2000r	75	29084.206	$2869_3 - 31953\frac{1}{4}$
3436.726	1500r	50	29089.122	$3865_1 - 32954\frac{3}{2}$
3436.621	200	4	29090.011	$7795\frac{3}{4} - 36885_4$
3435.487	25l		29099.613	$6362_2 - 35462\frac{3}{2}$
3434.727	200b	2	29106.052	$10414\frac{3}{4} - 39520_4$
3434.103	50b		29111.340	$13175\frac{3}{4} - 42286_3$
3429.871	100b		29147.259	$7280_2 - 36427\frac{3}{2}$
3429.574	200	10	29149.783	$8800_4 - 37950\frac{3}{4}$
3429.086	50		29153.931	$10526\frac{3}{2} - 39680_2$
3428.998	1500r	50	29154.679	$2558_0 - 31712\frac{1}{2}$
3428.714	300r	8	29157.094	$0_2 - 29157\frac{1}{2}$
3428.621	300r	4	29157.885	$0_2 - 29157\frac{3}{2}$
3428.248	50	3	29161.057	$8243\frac{1}{2} - 37404_3$
3427.619	5		29166.408	$7502_3 - 36668\frac{1}{2}$
3427.089	200s		29170.919	$6362_2 - 35533\frac{1}{2}$
3426.285	2		29177.764	$11802_2 - 40980\frac{5}{2}$
3425.435	150	15	29185.004	$11241\frac{3}{4} - 40426_4$
3423.990	1500r	50	29197.320	$0_2 - 29197\frac{1}{2}$
3423.923	200b		29197.891	$0_2 - 29197\frac{3}{2}$
3422.655	1000r	40	29208.708	$7280_2 - 36488\frac{1}{2}$
3421.210	2000r		29221.044	$4961_4 - 34182\frac{5}{2}$
3420.196	100	3	29229.707	$11197\frac{5}{2} - 40426_4$
3418.170	15		29247.032	$12114\frac{3}{2} - 41361_3$
3417.642	100		29251.550	$11241\frac{3}{4} - 40493_3$
3417.498	400r	10	29252.783	$0_2 - 29252\frac{1}{2}$
3416.595	150	3	29260.514	$7502_3 - 36762\frac{3}{2}$
3415.885	500r	75	29266.595	$3687_2 - 32954\frac{1}{2}$
3414.712	200	2	29276.649	$7280_2 - 36556\frac{1}{2}$
3414.565	100b	1	29277.909	$8243\frac{1}{2} - 37521_3$
3414.299	75		29280.190	$10414\frac{3}{4} - 39694_5$
3413.327	100	3	29288.528	$5563_1 - 34851\frac{1}{2}$
3413.086	300b	25	29290.596	$7795\frac{3}{4} - 37085_4$
3413.013	1000r	25	29291.222	$2869_3 - 32160\frac{1}{2}$
3412.422	15		29296.295	$3865_1 - 33161\frac{1}{2}$
3412.181	200		29298.364	$7502_3 - 36800\frac{3}{4}$
3410.699	25		29311.094	$10526\frac{3}{2} - 39837_3$
3410.184	150	3	29315.521	$5563_1 - 34878\frac{1}{2}$
3410.076	300	50	29316.449	$6362_2 - 35678\frac{1}{2}$
3408.750	1000r	25	29327.853	$2869_3 - 32197\frac{3}{2}$
3405.558	1500r	50	29355.341	$3687_2 - 33043\frac{3}{2}$
3403.903	300	8	29369.613	$7502_3 - 36871\frac{1}{2}$
3403.222	15		29375.490	$14481\frac{5}{2} - 43857_5$
3402.354	15		29382.984	$4961_4 - 34344\frac{3}{4}$
3401.711	500r	25	29388.538	$7280_2 - 36668\frac{1}{2}$
3400.680	25		29397.447	$11802_2 - 41200\frac{1}{2}$
3398.545	1500r	50	29415.914	$2869_3 - 32285\frac{3}{2}$
3398.490	150b	4	29416.390	$7795\frac{3}{4} - 37211_5$
3398.457	100b	4	29416.676	$8800_4 - 38216\frac{3}{2}$
3398.162	25		29419.230	$0_2 - 29419\frac{1}{2}$

TABLE 4. *Classified lines of* Th I—continued

Wavelength (Å)	Intensity		Wavenumber (cm^{-1})	Classification
	Lamp	Spark		
3397.516	1500r	50b	29424.823	$2869_3 - 32294^4_4$
3397.306	50	1	29426.642	$5563_1 - 34989^0_1$
3396.727	800r	50	29431.658	$3865_1 - 33297^2_2$
3395.234	20	1	29444.600	$8243^2_2 - 37688_3$
3393.993	200	2	29455.365	$14481^8_8 - 43937_6$
3393.421	150	10	29460.331	$8111_4 - 37571^6_6$
3393.373	4b		29460.747	$13175^4_4 - 42635_5$
3392.993	25		29464.046	$12114^2_2 - 41578_2$
3392.473	100	2	29468.563	$4961_4 - 34430^8_8$
3391.872	400r	40	29473.784	$3687_2 - 33161^1_1$
3390.849	200	8	29482.676	$7280_2 - 36762^5_5$
3389.463	800r	40	29494.731	$8111_4 - 37605^4_4$
3388.348	50		29504.437	$8243^2_2 - 37748_2$
3388.154	150b	5	29506.126	$8800_4 - 38306^4_4$
3388.117	40b	2	29506.448	$9804_5 - 39311^4_4$
3387.920	600r	15	29508.164	$7795^4_4 - 37303_4$
3387.493	50b		29511.883	$7795^4_4 - 37307_3$
3386.291	5		29522.359	$2558_0 - 32080^1_1$
3386.159	15	5	29523.509	$6362_2 - 35885^2_2$
3385.373	4		29530.364	$4961_4 - 34492^4_4$
3384.403	200	4	29538.827	$7502_3 - 37041^4_4$
3384.177	15		29540.800	$8243^2_2 - 37784_2$
3383.586	200	8	29545.959	$8111_4 - 37656^3_3$
3382.310	4		29557.106	$7280_2 - 36837^1_1$
3381.800	2		29561.563	$3865_1 - 33427^2_2$
3380.859	600r	20	29569.790	$2869_3 - 32439^4_4$
3380.571	3		29572.309	$12114^2_2 - 41686_3$
3379.124	10b		29584.973	$8800_4 - 38385^0_0$
3378.348	2		29591.768	$7280_2 - 36871^2_2$
3377.483	100	15	29599.346	$11601_1 - 41200^2_2$
3376.617	25		29606.937	$3687_2 - 33294^3_3$
3376.367	300	1	29609.130	$3687_2 - 33297^2_2$
3375.587	200b		29615.971	$8800_4 - 38416^3_3$
3374.975	1500r	75	29621.341	$4961_4 - 34583^3_3$
3373.493	800r	75	29634.354	$2869_3 - 32503^2_2$
3372.822	400r	100	29640.249	$0_2 - 29640^1_1$
3372.253	10		29645.250	$11241^3_3 - 40886_2$
3372.077	8		29646.798	$7502_3 - 37149^2_2$
3371.664	10		29650.429	$14206^4_4 - 43857_5$
3370.887	200	5	29657.263	$7502_3 - 37159^3_3$
3369.000	200	4	29673.874	$10526^3_3 - 40200_3$
3367.582	400r	10	29686.368	$0_2 - 29686^3_3$
3365.337	400r	50	29706.171	$2869_3 - 32575^2_2$
3364.888	25		29710.135	$10783^2_2 - 40493_3$
3362.443	10b		29731.738	$7502_3 - 37234^2_2$
3361.196	300r	25	29742.768	$4961_4 - 34704^3_3$
3360.997	400r	150	29744.529	$0_2 - 29744^3_3$
3356.986	8		29780.068	$8800_4 - 38580^4_4$
3355.106	500r	10	29796.754	$3865_1 - 33662^1_1$
3351.753	3		29826.561	$6362_2 - 36188^2_2$
3350.352	200	5	29839.033	$8111_4 - 37950^4_4$
3349.800	40b		29843.950	$8111_4 - 37954^3_3$
3348.790	400b		29852.950	$3865_1 - 33718^2_2$
3348.770	1500r	20	29853.129	$0_2 - 29853^2_2$
3347.403	150		29865.319	$8800_4 - 38665^5_5$
3346.992	100	3	29868.987	$7280_2 - 37149^2_2$
3346.966	300	3	29869.219	$3865_1 - 33734^2_2$
3345.851	200r	8b	29879.172	$7280_2 - 37159^1_1$
3345.822	200r	8	29879.431	$7280_2 - 37159^3_3$
3345.170	150	3	29885.255	$2869_3 - 32754^3_3$
3344.310	20	2	29892.940	$7795^4_4 - 37688_3$
3343.499	150	5	29900.190	$10526^3_3 - 40426_4$
3343.281	100b		29902.140	$8243^2_2 - 38145_3$
3343.164	300	5	29903.186	$3687_2 - 33591^3_3$
3342.069	200	10	29912.984	$12114^2_2 - 42027_2$
3341.550	10	2	29917.630	$11802_2 - 41720^2_2$
3340.724	300r	5	29925.026	$4961_4 - 34886^6_6$
3337.505	10		29953.888	$7280_2 - 37234^2_2$
3337.275	200	5	29955.952	$14481^8_8 - 44437_6$
3336.074	150		29966.736	$10526^3_3 - 40493_3$
3335.694	150	4	29970.150	$5563_1 - 35533^2_2$
3335.238	300	5	29974.247	$3687_2 - 33662^1_1$
3333.571	10	1	29989.236	$11241^3_3 - 41230_4$
3333.128	1000r	20b	29993.222	$2869_3 - 32862^4_4$
3332.479	100b	1	29999.062	$6362_2 - 36361^1_1$
3330.976	150	4	30012.598	$10414^3_3 - 40426_4$
3330.477	1500r	40	30017.095	$0_2 - 30017^3_3$
3329.728	400r	75	30023.847	$7795^4_4 - 37819_4$
3328.997	10s		30030.439	$3687_2 - 33718^2_2$
3328.608	4		30033.949	$11197^6_6 - 41230_4$
3327.193	800r	25	30046.721	$3687_2 - 33734^2_2$
3322.945	200b		30085.131	$10526^3_3 - 40611_2$
3322.924	10		30085.321	$2869_3 - 32954^2_2$
3322.093	400r	10	30092.847	$2558_0 - 32650^1_1$
3321.835	5	1	30095.184	$7795^4_4 - 37890_5$
3321.574	300r	40	30097.549	$7795^4_4 - 37892_4$
3321.067	3		30102.143	$9804_5 - 39906^4_4$
3320.879	20		30103.847	$10783^2_2 - 40886_2$
3320.476	400r	25	30107.501	$2558_0 - 32665^1_1$
3319.910	400r	75b	30112.634	$3687_2 - 33800^3_3$
3319.572	50		30115.700	$5563_1 - 35678^1_1$
3319.149	25b		30119.538	$11601_1 - 41720^2_2$
3319.133	300b	40	30119.683	$11241^3_3 - 41361_3$
3318.390	200	5	30126.426	$6362_2 - 36488^2_2$
3315.848	200	2	30149.521	$11877^1_1 - 42027_2$
3314.793	400r		30159.117	$11197^6_6 - 41356_5$
3313.744	20b		30168.663	$10414^4_4 - 40582_5$
3313.647	500r		30169.546	$4961_4 - 35131^4_4$
3313.367	25b		30172.096	$12114^2_2 - 42286_3$
3313.151	5	1	30174.063	$2869_3 - 33043^3_3$
3313.073	300l	40	30174.773	$10526^3_3 - 40701_4$
3310.922	8	2	30194.376	$6362_2 - 36556^1_1$
3310.814	25	4	30195.361	$8111_4 - 38306^4_4$
3310.637	150d	15b	30196.975	$7795^4_4 - 37992_4$
3310.446	200	10b	30198.717	$8800_4 - 38998^3_3$
3309.365	1000r	40	30208.582	$0_2 - 30208^2_2$
3306.506	2b		30234.701	$7502_3 - 37736^2_2$
3305.303	400r	40	30245.705	$3865_1 - 34111^1_1$
3304.238	3000r	200	30255.453	$0_2 - 30255^3_3$
3303.546	20		30261.791	$8800_4 - 39062^6_6$

TABLE 4. *Classified lines of* Th I—continued

Wavelength (Å)	Intensity		Wavenumber (cm^{-1})	Classification
	Lamp	Spark		
3302.192	400r	5	30274.198	$8111_4 - 38385_6^0$
3301.651	1500r	150	30279.159	$4961_4 - 35240_3^3$
3301.570	200	8	30279.902	$3687_2 - 33967_3^3$
3301.449	150	3	30281.011	$0_2 - 30281_1^1$
3300.870	20	4	30286.323	$8243_2^2 - 38529_3$
3300.775	150	4	30287.194	$10414_3^3 - 40701_4$
3298.811	300	8	30305.226	$8111_4 - 38416_3^3$
3298.697	75	4	30306.273	$6362_2 - 36668_2^2$
3298.119	75	3	30311.584	$7795_4^4 - 38106_5$
3298.050	500r	40	30312.218	$4961_4 - 35273_6^0$
3296.901	30h	2	30322.782	$5563_1 - 35885_2^2$
3295.444	25		30336.188	$7280_2 - 37616_1^1$
3292.926	300	4	30359.384	$8243_2^2 - 38602_2$
3292.810	50b	4	30360.454	$10526_3^3 - 40886_2$
3291.037	40l	1	30376.810	$7280_2 - 37656_3^3$
3289.631	150l	10	30389.792	$4961_4 - 35351_4^4$
3289.517	150	10	30390.845	$7795_4^4 - 38186_4$
3288.478	2		30400.447	$6362_2 - 36762_3^3$
3288.387	300r	8	30401.288	$2869_3 - 33270_4^4$
3286.019	20	3	30423.196	$3687_2 - 34111_1^1$
3285.752	800r	20	30425.668	$2869_3 - 33294_3^3$
3285.514	200r	5	30427.872	$2869_3 - 33297_2^2$
3283.671	100	4	30444.949	$11241_3^3 - 41686_3$
3283.369	8	2	30447.749	$7502_3 - 37950_4^4$
3282.837	40	2	30452.683	$7502_3 - 37954_3^3$
3282.385	50	3	30456.877	$7280_2 - 37736_2^2$
3282.198	8	1	30458.612	$3865_1 - 34324_2^2$
3281.189	300	5	30467.978	$7502_3 - 37970_2^2$
3281.049	400r	25	30469.278	$8111_4 - 38580_4^4$
3280.451	20		30474.832	$6362_2 - 36837_1^1$
3278.733	200	25	30490.800	$8243_2^2 - 38734_3$
3277.702	50	3	30500.390	$4961_4 - 35462_3^3$
3277.062	200	4	30506.347	$3865_1 - 34371_2^2$
3276.721	300	5	30509.521	$6362_2 - 36871_2^2$
3276.562	25	3	30511.002	$8800_4 - 39311_4^4$
3276.225	200	8	30514.140	$11241_3^3 - 41755_4$
3276.045	50	5	30515.817	$11197_6^6 - 41712_5$
3272.301	5		30550.730	$7502_3 - 38053_3^3$
3272.027	800r	75	30553.288	$0_2 - 30553_2^2$
3271.892	300r	100	30554.549	$8111_4 - 38665_6^0$
3271.546	50	3	30557.780	$2869_3 - 33427_2^2$
3271.433	2		30558.836	$11197_6^6 - 41755_4$
3270.874	150	10	30564.058	$8243_2^2 - 38807_2$
3270.100	100	5	30571.292	$7795_4^4 - 38366_4$
3269.352	3		30578.286	$10783_2^2 - 41361_3$
3268.453	300	75	30586.697	$7502_3 - 38088_2^2$
3266.635	500r	50	30603.719	$2558_0 - 33161_1^1$
3264.859	40	3	30620.366	$9804_5 - 40425_4^4$
3263.183	400r	20	30636.092	$3687_2 - 34324_2^2$
3259.744	25	2	30668.412	$8800_4 - 39468_3^3$
3259.061	600r	50	30674.839	$7280_2 - 37954_3^3$
3258.744	100	3	30677.823	$8111_4 - 38788_3^3$
3258.274	15	2	30682.248	$13175_4^4 - 43857_5$
3258.103	400r		30683.858	$3687_2 - 34371_2^2$
3257.435	200	75	30690.150	$7280_2 - 37970_2^2$
3257.366	1000r	50	30690.800	$2869_3 - 33560_4^4$
3255.920	200	8	30704.430	$10526_3^3 - 41230_4$
3254.834	8b		30714.674	$7502_3 - 38216_3^3$
3254.067	300r	20	30721.914	$2869_3 - 33591_3^3$
3253.866	300r	50	30723.811	$0_2 - 30723_1^1$
3253.684	300r	40	30725.530	$3865_1 - 34591_1^1$
3251.916	2000r	200	30742.234	$3687_2 - 34430_3^3$
3249.855	800r	25	30761.730	$0_2 - 30761_3^3$
3249.344	50	3	30766.567	$8243_2^2 - 39010_3$
3248.790	3		30771.813	$4961_4 - 35733_4^4$
3247.331	15		30785.639	$11241_3^3 - 42027_2$
3247.218	75	4	30786.710	$6362_2 - 37149_2^2$
3246.319	5	1	30795.235	$10783_2^2 - 41578_2$
3246.144	75	4	30796.895	$6362_2 - 37159_1^1$
3246.116	20	2	30797.161	$6362_2 - 37159_3^3$
3245.994	200	8	30798.319	$5563_1 - 36361_1^1$
3245.386	3	1	30804.088	$7502_3 - 38306_3^3$
3244.883	100	5	30808.863	$7280_2 - 38088_2^2$
3244.628	4		30811.284	$8800_4 - 39611_3^3$
3244.448	1000r	50	30812.994	$0_2 - 30812_2^2$
3244.043	150	10	30816.840	$10414_4^4 - 41230_4$
3243.585	40	2	30821.192	$11802_2 - 42624_1^1$
3242.145	50	15b	30834.880	$10526_3^3 - 41361_3$
3240.644	400r	40b	30849.162	$2869_3 - 33718_2^2$
3240.236	40	3	30853.046	$7502_3 - 38355_2^2$
3238.934	400r	20	30865.448	$2869_3 - 33734_2^2$
3238.287	25	3	30871.615	$6362_2 - 37234_2^2$
3236.573	100	8b	30887.963	$8111_4 - 38998_3^3$
3234.996	400r	20	30903.020	$3687_2 - 34591_1^1$
3234.791	10	2	30904.978	$7795_4^4 - 38700_4$
3233.853	5	2	30913.942	$7502_3 - 38416_3^3$
3233.240	15	2	30919.803	$9804_5 - 40724_6^6$
3232.305	500r	25	30928.747	$0_2 - 30928_1^1$
3232.124	300r		30930.479	$2869_3 - 33799_4^4$
3232.031	200r		30931.368	$2869_3 - 33800_3^3$
3231.461	75		30936.824	$7280_2 - 38216_3^3$
3231.221	5		30939.122	$7795_4^4 - 38734_3$
3230.368	25	2	30947.291	$10414_4^4 - 41361_3$
3228.485	25	3	30965.341	$7795_4^4 - 38760_4$
3227.820	10		30971.720	$9804_5 - 40776_4^4$
3225.863	50	8	30990.509	$0_2 - 30990_3^3$
3225.539	100	8	30993.621	$5563_1 - 36556_1^1$
3225.007	100	5	30998.734	$7280_2 - 38278_1^1$
3223.504	8	2	31013.187	$3865_1 - 34878_1^1$
3223.168	200r	5	31016.420	$3687_2 - 34704_3^3$
3222.475	10l		31023.090	$11601_1 - 42624_1^1$
3220.986	75b		31037.431	$3687_2 - 34725_3^3$
3219.490	20h	4	31051.852	$10526_3^3 - 41578_2$
3217.265	40	2	31073.326	$8800_4 - 39873_6^6$
3216.998	75	3	31075.905	$0_2 - 31075_2^2$
3216.761	40		31078.195	$8243_2^2 - 39321_3$
3214.648	150	5	31098.622	$2869_3 - 33967_3^3$
3214.381	400r	25	31101.205	$4961_4 - 36062_4^4$
3214.076	400r	50	31104.156	$2558_0 - 33662_1^1$
3213.937	8	1	31105.501	$5563_1 - 36668_2^2$

TABLE 4. *Classified lines of* Th I—continued

Wavelength (Å)	Intensity		Wavenumber (cm^{-1})	Classification
	Lamp	Spark		
3213.818	3		31106.653	$8800_4 - 39906^{\frac{3}{2}}$
3211.997	200r	5	31124.288	$3865_1 - 34989^{\circ}$
3211.195	400r	25	31132.061	$2869_3 - 34001^{\frac{1}{2}}$
3210.779	200	5	31136.095	$7280_2 - 38416^{\frac{3}{2}}$
3208.971	15		31153.636	$8111_4 - 39264^{\frac{3}{2}}$
3208.527	100	3	31157.947	$7795^{\frac{1}{2}} - 38953_5$
3208.152	25		31161.589	$7795^{\frac{1}{2}} - 38956_4$
3207.938	100	5	31163.668	$3687_2 - 34851^{\frac{1}{2}}$
3207.548	4		31167.457	$7502_3 - 38669^{\frac{1}{2}}$
3205.696	50	3	31185.462	$8800_4 - 39985^{\frac{3}{2}}$
3205.162	3		31190.658	$3687_2 - 34878^{\circ}$
3202.521	200r	8	31216.379	$4961_4 - 36178^{\frac{1}{2}}$
3199.669	1		31244.202	$10783^{\frac{1}{2}} - 42027_2$
3196.611	20	2	31274.091	$5563_1 - 36837^{\circ}$
3195.688	400r	50	31283.123	$0_2 - 31283^{\frac{3}{2}}$
3194.518	5		31294.580	$6362_2 - 37656^{\frac{3}{2}}$
3194.096	200	5	31298.715	$10414^{\frac{1}{2}} - 41712_5$
3193.781	200r	5	31301.802	$3687_2 - 34989^{\circ}$
3192.586	400r	20	31313.518	$4961_4 - 36275^{\frac{1}{2}}$
3190.895	150b	2	31330.112	$9804_5 - 41134^{\frac{1}{2}}$
3189.711	200	8	31341.741	$10414^{\frac{1}{2}} - 41755_4$
3188.092	8b		31357.656	$8111_4 - 39468^{\frac{3}{2}}$
3186.371	75	2	31374.592	$6362_2 - 37736^{\frac{1}{2}}$
3185.857	1		31379.654	$7795^{\frac{1}{2}} - 39174_3$
3184.843	300	8	31389.644	$7280_2 - 38669^{\frac{1}{2}}$
3184.277	300	15b	31395.223	$7280_2 - 38675^{\frac{3}{2}}$
3181.670	500r	20	31420.947	$4961_4 - 36382^{\frac{1}{2}}$
3180.062	100	5	31436.835	$8243^{\frac{1}{2}} - 39680_2$
3179.858	25	2	31438.851	$11197^{\frac{1}{2}} - 42635_5$
3178.622	200	4	31451.076	$8111_4 - 39562^{\frac{1}{2}}$
3178.244	600r	100	31454.816	$2869_3 - 34324^{\frac{1}{2}}$
3178.018	3		31457.053	$7795^{\frac{1}{2}} - 39252_5$
3177.402	100	2	31463.151	$3865_1 - 35328^{\circ}$
3176.723	4		31469.876	$8800_4 - 40270^{\frac{1}{2}}$
3176.167	200r	5	31475.385	$2869_3 - 34344^{\frac{1}{2}}$
3174.840	200	4	31488.540	$7795^{\frac{1}{2}} - 39283_4$
3174.020	300	8	31496.675	$7502_3 - 38998^{\frac{3}{2}}$
3173.634	2		31500.506	$8111_4 - 39611^{\frac{3}{2}}$
3173.427	500r	50	31502.560	$2869_3 - 34371^{\frac{1}{2}}$
3172.808	8		31508.706	$7280_2 - 38788^{\frac{3}{2}}$
3171.276	500r	75	31523.927	$0_2 - 31523^{\frac{3}{2}}$
3171.015	10	3	31526.521	$7795^{\frac{1}{2}} - 39321_3$
3170.250	5	1	31534.129	$7280_2 - 38814^{\frac{1}{2}}$
3168.342	100	2	31553.118	$2558_0 - 34111^{\circ}$
3165.048	150	3	31585.956	$5563_1 - 37149^{\frac{1}{2}}$
3164.386	25	3	31592.564	$6362_2 - 37954^{\frac{3}{2}}$
3164.239	200	3	31594.031	$8243^{\frac{1}{2}} - 39837_3$
3163.715	200	3	31599.264	$0_2 - 31599^{\frac{1}{2}}$
3162.856	100b		31607.846	$6362_2 - 37970^{\frac{1}{2}}$
3161.364	200	5	31622.762	$2869_3 - 34492^{\frac{1}{2}}$
3161.148	100		31624.923	$8800_4 - 40425^{\frac{1}{2}}$
3159.577	10		31640.647	$3687_2 - 35328^{\circ}$
3157.221	300r	8	31664.257	$4961_4 - 36625^{\frac{3}{2}}$
3156.866	300		31667.818	$3865_1 - 35533^{\frac{1}{2}}$
3152.395	100	3	31712.730	$0_2 - 31712^{\circ}$
3152.295	100	3	31713.736	$2869_3 - 34583^{\frac{3}{2}}$
3151.184	300	5	31724.917	$7795^{\frac{1}{2}} - 39520_4$
3151.017	200		31726.598	$6362_2 - 38088^{\frac{1}{2}}$
3147.449	200	25	31762.562	$8111_4 - 39873^{\frac{3}{2}}$
3146.310	200r	8	31774.060	$3687_2 - 35462^{\frac{3}{2}}$
3145.637	400r	25	31780.858	$0_2 - 31780^{\frac{3}{2}}$
3144.145	100	3	31795.939	$8111_4 - 39906^{\frac{1}{2}}$
3143.632	1		31801.127	$4961_4 - 36762^{\frac{3}{2}}$
3142.422	100	5	31813.372	$3865_1 - 35678^{\circ}$
3140.272	600r	50	31835.152	$2869_3 - 34704^{\frac{3}{2}}$
3139.892	150	100	31839.005	$4961_4 - 36800^{\frac{1}{2}}$
3139.273	150		31845.282	$3687_2 - 35533^{\frac{1}{2}}$
3138.359	40	2	31854.556	$6362_2 - 38216^{\frac{3}{2}}$
3138.200	100	10	31856.170	$2869_3 - 34725^{\frac{3}{2}}$
3136.829	400r	8	31870.093	$0_2 - 31870^{\frac{1}{2}}$
3136.612	10		31872.298	$10414^{\frac{1}{2}} - 42286_3$
3136.216	800r	100	31876.322	$4961_4 - 36837^{\frac{3}{2}}$
3133.980	200	5	31899.064	$7795^{\frac{1}{2}} - 39694_5$
3131.496	20	2	31924.366	$8800_4 - 40724^{\frac{3}{2}}$
3128.314	100	3	31956.838	$8243^{\frac{1}{2}} - 40200_3$
3126.414	200	2	31976.258	$8800_4 - 40776^{\circ}$
3125.812	150	2	31982.416	$2869_3 - 34851^{\frac{1}{2}}$
3125.601	500r	20	31984.575	$7280_2 - 39264^{\frac{3}{2}}$
3124.986	75	2	31990.869	$3687_2 - 35678^{\circ}$
3122.102	15b		32020.419	$3865_1 - 35885^{\frac{1}{2}}$
3120.881	400r	25	32032.946	$2558_0 - 34591^{\circ}$
3119.963	100	20	32042.371	$7795^{\frac{1}{2}} - 39837_3$
3119.504	200r		32047.085	$4961_4 - 37008^{\frac{3}{2}}$
3118.848	15	1	32053.826	$6362_2 - 38416^{\frac{3}{2}}$
3118.266	4		32059.808	$7502_3 - 39562^{\frac{1}{2}}$
3116.352	300r	10	32079.498	$4961_4 - 37041^{\frac{3}{2}}$
3116.263	500r		32080.414	$0_2 - 32080^{\circ}$
3111.982	50	2	32124.544	$3687_2 - 35812^{\frac{3}{2}}$
3111.280	300	8	32131.792	$7280_2 - 39411^{\circ}$
3110.102	200		32143.962	$8111_4 - 40254^{\frac{3}{2}}$
3108.636	200	3	32159.120	$8111_4 - 40270^{\frac{1}{2}}$
3108.504	300r	10	32160.485	$0_2 - 32160^{\frac{1}{2}}$
3107.214	3		32173.837	$5563_1 - 37736^{\frac{1}{2}}$
3105.794	200b		32188.546	$7280_2 - 39468^{\frac{3}{2}}$
3104.966	200r	3	32197.130	$0_2 - 32197^{\frac{3}{2}}$
3104.892	200r	25	32197.897	$4961_4 - 37159^{\frac{3}{2}}$
3102.595	20		32221.734	$10414^{\frac{1}{2}} - 42635_5$
3099.902	20l		32249.725	$8243^{\frac{1}{2}} - 40493_3$
3099.184	100	2	32257.196	$7795^{\frac{1}{2}} - 40052_4$
3098.726	300r	5	32261.963	$2869_3 - 35131^{\frac{1}{2}}$
3096.498	25		32285.176	$0_2 - 32285^{\frac{3}{2}}$
3094.373	2		32307.346	$6362_2 - 38669^{\frac{1}{2}}$
3093.832	4		32312.995	$6362_2 - 38675^{\frac{3}{2}}$
3093.719	200	3	32314.176	$8111_4 - 40425^{\frac{1}{2}}$
3093.102	15		32320.621	$2558_0 - 34878^{\circ}$
3092.828	300r	8	32323.484	$3865_1 - 36188^{\frac{1}{2}}$
3088.567	200r	10	32368.076	$8243^{\frac{1}{2}} - 40611_2$
3088.235	15	1	32371.556	$2869_3 - 35240^{\frac{3}{2}}$
3086.852	50	1	32386.059	$3687_2 - 36074^{\frac{3}{2}}$
3085.084	3b		32404.618	$7502_3 - 39906^{\frac{1}{2}}$

TABLE 4. *Classified lines of* Th I—continued

Wavelength (Å)	Intensity		Wavenumber (cm^{-1})	Classification
	Lamp	Spark		
3085.038	4		32405.101	$7795\frac{5}{4} - 40200_3$
3083.003	75b		32426.490	$6362_2 - 38788\frac{5}{3}$
3082.507	150r	3	32431.707	$2558_0 - 34989\frac{1}{1}$
3080.593	3		32451.857	$6362_2 - 38814\frac{2}{2}$
3078.100	3		32478.139	$6362_2 - 38840\frac{1}{1}$
3077.718	300r	5	32482.170	$2869_3 - 35351\frac{3}{4}$
3077.600	25	1	7502₃ − 39985$\frac{5}{3}$	
3076.410	150	30	32495.980	$3865_1 - 36361\frac{1}{1}$
3075.938	5		32500.966	$3687_2 - 36188\frac{2}{2}$
3075.687	100	3	32503.618	$0_2 - 32503\frac{2}{2}$
3073.589	2		32525.804	$5563_1 - 38088\frac{2}{2}$
3068.908	300r	5	32575.414	$0_2 - 32575\frac{2}{2}$
3067.270	25		32592.809	$2869_3 - 35462\frac{3}{3}$
3067.163	100b		32593.946	$7502_3 - 40096\frac{2}{2}$
3065.683	200r	2	32609.680	$4961_4 - 37571\frac{5}{5}$
3065.314	15b	4	32613.606	$8111_4 - 40724\frac{5}{5}$
3064.396	2		32623.375	$3865_1 - 36488\frac{2}{2}$
3063.637	8b		32631.457	$7795\frac{5}{4} - 40426_4$
3063.157	75b		32636.570	$6362_2 - 38998\frac{5}{5}$
3062.517	100	10	32643.391	$8243\frac{5}{2} - 40886_2$
3062.454	200r	2	32644.062	$4961_4 - 37605\frac{3}{4}$
3061.812	400r	3	32650.907	$0_2 - 32650\frac{1}{1}$
3060.928	100		32660.336	$11197\frac{5}{5} - 43857_5$
3060.582	75		32664.028	$2869_3 - 35533\frac{2}{2}$
3060.440	500r	10	32665.543	$0_2 - 32665\frac{1}{1}$
3059.698	200	1	32673.465	$3687_2 - 36361\frac{1}{1}$
3058.029	200r	2	32691.297	$3865_1 - 36556\frac{1}{1}$
3057.651	100		32695.338	$4961_4 - 37656\frac{3}{3}$
3056.693	150	1	32705.585	$7280_2 - 39985\frac{3}{3}$
3053.536	200	1	32739.397	$3687_2 - 36427\frac{3}{3}$
3053.462	150	1	32740.190	$11197\frac{5}{5} - 43937_6$
3052.296	3		32752.697	$7502_3 - 40254\frac{3}{3}$
3052.128	100	1	32754.500	$0_2 - 32754\frac{3}{3}$
3050.892	4b		32767.769	$7502_3 - 40270\frac{4}{4}$
3050.631	200r	2	32770.572	$2558_0 - 35328\frac{1}{1}$
3049.054	100b		32787.521	$7795\frac{5}{4} - 40582_5$
3048.621	10		32792.177	$5563_1 - 38355\frac{2}{2}$
3047.816	500r	2	32800.838	$3687_2 - 36488\frac{2}{2}$
3046.401	4		32816.073	$7280_2 - 40096\frac{2}{2}$
3041.941	100		32864.185	$2869_3 - 35733\frac{3}{4}$
3041.515	300r	100	32868.788	$3687_2 - 36556\frac{1}{1}$
3041.433	40b		32869.674	$8111_4 - 40980\frac{5}{5}$
3038.417	100l		32902.300	$6362_2 - 39264\frac{3}{3}$
3038.070	100		32906.057	$7795\frac{5}{4} - 40701_4$
3036.518	10b	2	32922.875	$7502_3 - 40425\frac{4}{4}$
3034.639	400r	2	32943.260	$2869_3 - 35812\frac{2}{3}$
3033.595	15		32954.597	$0_2 - 32954\frac{2}{2}$
3032.016	100r	2	32971.758	$3865_1 - 36837\frac{1}{1}$
3031.733	75b		32974.836	$7280_2 - 40254\frac{3}{3}$
3031.195	100r	2	32980.688	$3687_2 - 36668\frac{2}{2}$
3030.487	400r	8	32988.393	$4961_4 - 37950\frac{3}{3}$
3030.035	75		32993.314	$4961_4 - 37954\frac{3}{3}$
3028.830	200	2	33006.439	$3865_1 - 36871\frac{2}{2}$
3027.896	150	3	33016.620	$2869_3 - 35885\frac{2}{2}$
3027.228	200b	15	33023.906	$8111_4 - 41134\frac{3}{3}$
3025.448	200r	2	33043.334	$0_2 - 33043\frac{3}{3}$
3024.883	150		33049.506	$6362_2 - 39411\frac{1}{1}$
3022.567	3	1	33074.829	$3687_2 - 36762\frac{3}{3}$
3021.056	300	1	33091.370	$4961_4 - 38053\frac{3}{3}$
3018.644	100		33117.810	$8243\frac{5}{2} - 41361_3$
3015.785	40	3	33149.205	$3687_2 - 36837\frac{1}{1}$
3014.641	150r	1	33161.784	$0_2 - 33161\frac{1}{1}$
3012.630	150		33183.919	$3687_2 - 36871\frac{2}{2}$
3010.736	200r	2	33204.794	$2869_3 - 36074\frac{3}{3}$
3007.476	100	1	33240.785	$11197\frac{5}{5} - 44437_6$
3006.720	3		33249.143	$6362_2 - 39611\frac{3}{3}$
3006.164	300r	2	33255.292	$4961_4 - 38216\frac{3}{3}$
3004.163	3b		33277.442	$5563_1 - 38840\frac{1}{1}$
3003.605	200	1	33283.624	$3865_1 - 37149\frac{2}{2}$
3002.687	200r	2	33293.799	$3865_1 - 37159\frac{1}{1}$
3002.390	100b	10	33297.092	$0_2 - 33297\frac{2}{2}$
3001.336	50r		33308.785	$2869_3 - 36178\frac{4}{4}$
3000.353	100b		33319.697	$2869_3 - 36188\frac{2}{2}$
2998.103	150b		33344.702	$4961_4 - 38306\frac{4}{4}$
2995.962	100	1	33368.530	$3865_1 - 37234\frac{2}{2}$
2991.032	75b		33423.528	$4961_4 - 38385\frac{5}{5}$
2990.717	75		33427.048	$0_2 - 33427\frac{2}{2}$
2989.272	40l		33443.206	$10414\frac{4}{4} - 43857_5$
2988.255	300r		33454.587	$4961_4 - 38416\frac{3}{3}$
2987.672	300r	2	33461.115	$3687_2 - 37149\frac{2}{2}$
2986.740	100r	2	33471.556	$3687_2 - 37159\frac{3}{3}$
2986.127	2		33478.427	$7502_3 - 40980\frac{3}{3}$
2980.112	200r	2	33545.996	$3687_2 - 37234\frac{2}{2}$
2979.035	100		33558.123	$2869_3 - 36427\frac{5}{5}$
2978.791	75	2	33560.872	$7795\frac{5}{4} - 41356_5$
2978.325	100	1	33566.122	$7795\frac{5}{4} - 41361_3$
2976.103	200r	3	33591.182	$0_2 - 33591\frac{3}{3}$
2973.675	100	1	33618.608	$4961_4 - 38580\frac{3}{4}$
2973.590	15		33619.569	$2869_3 - 36488\frac{2}{2}$
2972.438	10		33632.598	$7502_3 - 41134\frac{3}{4}$
2969.822	200r	4	33662.223	$0_2 - 33662\frac{1}{1}$
2966.662	5		33698.077	$7502_3 - 41200\frac{2}{2}$
2966.441	8		33700.587	$7280_2 - 40980\frac{3}{3}$
2966.150	100l	5	33703.894	$4961_4 - 38665\frac{5}{5}$
2965.290	15		33713.668	$4961_4 - 38675\frac{3}{3}$
2963.521	2		33733.792	$6362_2 - 40096\frac{2}{2}$
2963.442	75		33734.691	$0_2 - 33734\frac{2}{2}$
2959.137	200	2	33783.767	$8243\frac{5}{2} - 42027_2$
2957.767	75	3	33799.414	$2869_3 - 36668\frac{2}{2}$
2957.660	100r	5	33800.637	$0_2 - 33800\frac{3}{3}$
2957.421	10b		33803.368	$2558_0 - 36361\frac{1}{1}$
2955.339	10		33827.181	$4961_4 - 38788\frac{3}{3}$
2953.454	25	1	33848.770	$5563_1 - 39411\frac{1}{1}$
2951.471	50	1	33871.511	$3865_1 - 37736\frac{2}{2}$
2949.736	20	2	33891.433	$7795\frac{5}{4} - 41686_3$
2949.639	50	2	33892.547	$6362_2 - 40254\frac{3}{3}$
2949.551	100r	15b	33893.559	$2869_3 - 36762\frac{3}{3}$
2947.462	100	3	33917.579	$7795\frac{5}{4} - 41712_5$
2947.229	200	25	33920.261	$7280_2 - 41200\frac{2}{2}$
2946.528	100	20	33928.330	$3687_2 - 37616\frac{1}{1}$

TABLE 4. *Classified lines of* Th I—continued

Wavelength (Å)	Intensity		Wavenumber (cm^{-1})	Classification
	Lamp	Spark		
2946.258	200r	50	33931.439	$2869_3 - 36800^{2}_{4}$
2943.729	400	3	33960.589	$7795^{2}_{4} - 41755_4$
2943.095	300r	2	33967.904	$0_2 - 33967^{3}_{5}$
2943.000	300r	20	33969.001	$3687_2 - 37656^{3}_{5}$
2940.432	40h		33998.666	$2558_0 - 36556^{1}_{1}$
2940.088	800r	50	34002.644	$2869_3 - 36871^{2}_{2}$
2937.095	5		34037.292	$4961_4 - 38998^{3}_{5}$
2936.617	150h	3	34042.832	$8243^{2}_{2} - 42286_3$
2936.089	500	5	34048.954	$3687_2 - 37736^{2}_{2}$
2931.663	150b	25	34100.356	$4961_4 - 39062^{0}_{0}$
2931.281	300r	2	34104.800	$3865_1 - 37970^{2}_{2}$
2930.735	4		34111.153	$0_2 - 34111^{1}_{1}$
2925.526	500r	5	34171.887	$2869_3 - 37041^{2}_{4}$
2921.560	15b		34218.273	$7502_3 - 41720^{2}_{2}$
2916.369	500r	10	34279.177	$2558_0 - 36837^{1}_{1}$
2916.313	75b	2	34279.835	$2869_3 - 37149^{2}_{2}$
2916.105	100	2	34282.280	$3687_2 - 37970^{2}_{2}$
2915.424	100	2	34290.287	$2869_3 - 37159^{3}_{5}$
2912.553	100	3	34324.087	$0_2 - 34324^{2}_{2}$
2910.390	150	2	34349.595	$4961_4 - 39311^{0}_{4}$
2909.103	300d	8d	34364.791	$2869_3 - 37234^{2}_{2}$
2909.080	50b	5b	34365.063	$3687_2 - 38053^{3}_{5}$
2908.507	200r	20	34371.833	$0_2 - 34371^{2}_{2}$
2902.714	300	2	34440.426	$7280_2 - 41720^{2}_{2}$
2898.556	100	2	34489.829	$3865_1 - 38355^{2}_{2}$
2898.443	8b		34491.174	$7795^{2}_{4} - 42286_3$
2897.112	40b	20b	34507.019	$4961_4 - 39468^{3}_{5}$
2895.271	150	3	34528.960	$3687_2 - 38216^{3}_{5}$
2890.746	40		34583.007	$0_2 - 34583^{3}_{5}$
2890.078	150r	5	34591.000	$0_2 - 34591^{1}_{1}$
2889.290	150r	15	34600.433	$4961_4 - 39562^{2}_{4}$
2885.169	75		34649.852	$4961_4 - 39611^{3}_{5}$
2883.713	200w	2	34667.346	$3687_2 - 38355^{2}_{2}$
2880.632	200r	3	34704.423	$0_2 - 34704^{3}_{5}$
2878.657	150b		34728.232	$3687_2 - 38416^{3}_{5}$
2877.974	5		34736.473	$2869_3 - 37605^{2}_{4}$
2873.734	75b		34787.722	$2869_3 - 37656^{3}_{5}$
2869.589	2		34837.969	$6362_2 - 41200^{2}_{2}$
2869.374	5		34840.580	$7795^{2}_{4} - 42635_5$
2868.460	300r	10	34851.681	$0_2 - 34851^{2}_{2}$
2867.141	40b		34867.713	$2869_3 - 37736^{2}_{2}$
2866.241	40		34878.661	$0_2 - 34878^{1}_{1}$
2863.510	10		34911.924	$4961_4 - 39873^{0}_{0}$
2860.776	100	2	34945.287	$4961_4 - 39906^{2}_{4}$
2860.491	150	3	34948.769	$3865_1 - 38814^{2}_{2}$
2857.336	10		34987.356	$3687_2 - 38675^{3}_{5}$
2857.138	100	2	34989.781	$0_2 - 34989^{1}_{1}$
2854.342	300	3	35024.054	$4961_4 - 39985^{3}_{5}$
2851.558	50r	4	35058.246	$2558_0 - 37616^{1}_{1}$
2849.725	10	1	35080.796	$2869_3 - 37950^{2}_{4}$
2849.326	100	25	35085.708	$2869_3 - 37954^{3}_{5}$
2848.084	300r	2	35101.007	$2869_3 - 37970^{2}_{2}$
2846.036	150	2	35126.265	$3687_2 - 38814^{2}_{2}$
2843.906	300r	2	35152.572	$3687_2 - 38840^{1}_{1}$
2841.383	150h	2	35183.784	$2869_3 - 38053^{3}_{5}$
2838.483	300r	2	35219.729	$2869_3 - 38088^{2}_{2}$
2836.783	3		35240.834	$0_2 - 35240^{3}_{5}$
2832.568	100		35293.271	$4961_4 - 40254^{3}_{5}$
2831.146	20	4	35310.997	$3687_2 - 38998^{3}_{5}$
2829.732	150r	2	35328.641	$0_2 - 35328^{1}_{1}$
2828.502	200l	4	35344.003	$7280_2 - 42624^{1}_{1}$
2828.206	150r	4	35347.702	$2869_3 - 38216^{3}_{5}$
2821.072	100s	2	35437.086	$2869_3 - 38306^{2}_{4}$
2818.971	15		35463.496	$4961_4 - 40425^{2}_{4}$
2817.180	5		35486.041	$2869_3 - 38355^{2}_{2}$
2813.434	100		35533.287	$0_2 - 35533^{2}_{2}$
2812.395	8b		35546.414	$3865_1 - 39411^{1}_{1}$
2810.002	100		35576.683	$3687_2 - 39264^{3}_{5}$
2805.228	4	1	35637.226	$5563_1 - 41200^{2}_{2}$
2801.957	25		35678.826	$0_2 - 35678^{1}_{1}$
2799.432	100	1	35711.006	$2869_3 - 38580^{2}_{4}$
2798.421	75		35723.907	$3687_2 - 39411^{1}_{1}$
2795.368	100		35762.921	$4961_4 - 40724^{0}_{0}$
2792.433	15	1	35800.508	$2869_3 - 38669^{2}_{2}$
2791.999	50	1	35806.073	$2869_3 - 38675^{3}_{5}$
2791.499	100b		35812.486	$0_2 - 35812^{3}_{5}$
2782.871	100		35923.513	$3687_2 - 39611^{3}_{5}$
2781.209	50		35944.979	$2869_3 - 38814^{2}_{2}$
2775.488	100		36019.067	$4961_4 - 40980^{3}_{5}$
2772.176	4		36062.098	$7795^{2}_{4} - 43857_5$
2771.257	75		36074.056	$0_2 - 36074^{3}_{5}$
2766.988	50		36129.709	$2869_3 - 38998^{3}_{5}$
2763.655	40b		36173.280	$4961_4 - 41134^{2}_{4}$
2762.458	100r		36188.953	$0_2 - 36188^{2}_{2}$
2759.272	8		36230.737	$3865_1 - 40096^{2}_{2}$
2756.912	3		36261.750	$6362_2 - 42624^{1}_{1}$
2755.336	75		36282.490	$2558_0 - 38840^{1}_{1}$
2754.179	8		36297.731	$3687_2 - 39985^{3}_{5}$
2749.351	50	2	36361.468	$0_2 - 36361^{1}_{1}$
2746.786	100		36395.421	$2869_3 - 39264^{3}_{5}$
2744.376	20		36427.381	$0_2 - 36427^{3}_{5}$
2743.274	3		36442.013	$2869_3 - 39311^{0}_{4}$
2739.753	50		36488.844	$0_2 - 36488^{2}_{2}$
2734.661	40	2	36556.783	$0_2 - 36556^{1}_{1}$
2733.900	50		36566.959	$3687_2 - 40254^{3}_{5}$
2726.317	20l		36668.661	$0_2 - 36668^{2}_{2}$
2724.522	25		36692.818	$2869_3 - 39562^{2}_{4}$
2720.857	50		36742.241	$2869_3 - 39611^{3}_{5}$
2719.333	15b		36762.831	$0_2 - 36762^{3}_{5}$
2713.843	75		36837.197	$0_2 - 36837^{1}_{1}$
2712.620	2		36853.804	$2558_0 - 39411^{1}_{1}$
2711.288	5		36871.909	$0_2 - 36871^{2}_{2}$
2699.153	2		37037.670	$2869_3 - 39906^{2}_{4}$
2693.425	50h		37116.433	$2869_3 - 39985^{3}_{5}$
2691.057	200r		37149.091	$0_2 - 37149^{2}_{2}$
2690.319	10		37159.281	$0_2 - 37159^{1}_{1}$
2685.426	3		37226.984	$2869_3 - 40096^{2}_{2}$
2680.688	100r		37292.777	$3687_2 - 40980^{3}_{5}$
2677.666	10		37334.863	$3865_1 - 41200^{2}_{2}$
2674.029	3		37385.640	$2869_3 - 40254^{3}_{5}$

TABLE 4. *Classified lines of* Th I—continued

Wavelength (Å)	Intensity		Wavenumber (cm^{-1})	Classification	Wavelength (Å)	Intensity		Wavenumber (cm^{-1})	Classification
	Lamp	Spark				Lamp	Spark		
2664.996	8		37512.351	$3687_2 - 41200^2_2$	2577.288	75r	3	38788.861	$0_2 - 38788^3_3$
2657.633	3		37616.274	$0_2 - 37616^1_1$	2575.599	3		38814.295	$0_2 - 38814^2_2$
2654.762	4		37656.952	$0_2 - 37656^3_3$	2573.854	3		38840.609	$0_2 - 38840^1_1$
2640.865	10		37855.102	$3865_1 - 41720^2_2$	2563.402	2		38998.967	$0_2 - 38998^3_3$
2633.914	2		37954.997	$0_2 - 37954^3_3$	2546.052	100		39264.707	$0_2 - 39264^3_3$
2632.854	20	1	37970.277	$0_2 - 37970^2_2$	2536.540	25		39411.940	$0_2 - 39411^1_1$
2627.128	5		38053.031	$0_2 - 38053^3_3$	2523.760	25		39611.503	$0_2 - 39611^3_3$
2624.647	100r		38088.999	$0_2 - 38088^2_2$	2500.142	10		39985.674	$0_2 - 39985^3_3$
2623.100	100r		38111.461	$2869_3 - 40980^3_3$	2495.126	10		40066.053	$2558_0 - 42624^1_1$
2615.858	5		38216.966	$0_2 - 38216^3_3$	2493.250	100		40096.198	$0_2 - 40096^2_2$
2611.626	15	2	38278.891	$0_2 - 38278^1_1$	2483.418	50		40254.930	$0_2 - 40254^3_3$
2606.425	20		38355.270	$0_2 - 38355^2_2$	2439.433	150r		40980.707	$0_2 - 40980^3_3$
2602.290	4		38416.212	$0_2 - 38416^3_3$	2345.372	50		42624.104	$0_2 - 42624^1_1$
2585.224	3		38669.796	$0_2 - 38669^2_2$					
2584.851	2		38675.375	$0_2 - 38675^3_3$					

The late Mrs. Ruth L. Peterson carried out the data processing work. It is a pleasure to record recognition of her work. The author is grateful to S. Tomkins and M. Fred for making it possible to observe the Zeeman effect at Argonne National Laboratory; to S. P. Davis for furnishing spectrograms; and to Lucy Hagan, Charles H. Corliss, and William C. Martin for their suggestions and reviewing of the mansucript. The manuscript was typed by Miss Marsha C. Ahalt; her assistance is appreciated.

6. References

Avni, R., and Klein, F. S., Spectrochim. Acta **28B,** 331 (1973).
Brewer, L., J. Opt. Soc. Am. **61,** 1101 (1971).
Charles, G. W., A Compilation of Data on Some Spectra of Thorium, Oak Ridge National Laboratory, ORNL-2319 (1958).
Giacchetti, A., Argonne National Laboratory, Report, ANL-7209 (1966).
Giacchetti, A., and Blaise, J., European Group for Atomic Spectroscopy, Paper 57 (1970).
Giacchetti, A., Blaise, J., Corliss, C. H., and Zalubas, R., J. Res. Nat. Bur. Stand. (U.S.), **78A** (Phys. and Chem.), No. 2, 247–249 (Mar.–Apr. 1947).
Giacchetti, A., Stanley, R. W., and Zalubas, R., J. Opt. Soc. Am. **69,** 474 (1970).
Ionov, N. I., and Mittsev, M. A., Soviet Phys.-JETP **13,** 513 (1961).
Klinkenberg, P. F. A., Physica **16,** 618 (1950).
Lier, J. N., Disertation University of Amsterdam, Holland (1939).
Martin, W. C., J. Opt. Soc. Am. **53,** 1047 (1963).
Meggers, W. F., Corliss, C. H., and Scribner, B. F., Nat. Bur. Stand. (U.S.) Monogr. 32, Part I, 473 pp. (1961).
Moore, B. E., Astrophys. J. **30,** 143 (1909).
Rauh, E. G., and Ackermann, J. Chem. Phys. **60,** 1396 (1973).
Schuurmans, Ph. D. Thesis, Univ. Amsterdam (1946).
Smith, D. H., and Hertel, G. R., J. Chem. Phys. **51,** 3105 (1969).
Steers, E. B. M., Spectrochim. Acta **23B,** 135 (1967).
Stukenbroeker, G. L., and McNally, J. R., Jr., J. Opt. Soc. Am. **43,** 36 (1953).
Sugar, J., private communication (1970).
Sugar, J., J. Chem. Phys. **59,** 788 (1973).
Sugar, J., J. Chem. Phys. **60,** 4103 (1974).
Tech, J. L., private communication (1967).
Trees, R. E., Physica **26,** 353 (1960).
Zalubas, R., J. Res. Nat. Bur. Stand. (U.S.) **63A** (Phys. and Chem.), No. 3, 275–278 (Nov.–Dec. 1959).
Zalubas, R., Nat. Bur. Stand. (U.S.), Monogr. **17,** 130 (1960).
Zalubas, R., J. Opt. Soc. Am. **58,** 1195 (1968).
Zalubas, R., and Corliss, C. H., J. Res. Nat. Bur. Stand. (U.S.), **78A** (Phys. and Chem.), No. 2, 163–249 (Mar.–Apr. 1974).

(Paper 80A2–889)

JOURNAL OF RESEARCH of the National Bureau of Standards — A. Physics and Chemistry
Vol. 80A, No. 2, March-April 1976

Publications of the National Bureau of Standards*

Citations with Selected Abstracts

J. Res. Nat. Bur. Stand. (U.S.), **80A** *(Phys. and Chem.)*, No. 1 (Jan.-Feb. 1976), SD Catalog No. C13.22/sec.A:80/1.

Line strengths and lifetimes of levels in neutral uranium, C. H. Corliss.

Optical properties of nuclear matter, J. S. O'Connell.

A study of the polarization of fluorescence of ordered systems with application to ordered liquid crystals, E. D. Cehelnik, K. D. Mielenz, and R. B. Cundall.

PVT and vapor pressure measurements on ethane, G. C. Straty and R. Tsumura.

Functional equations for the enhancement factors for CO_2-free moist air, L. Greenspan.

Experimental values for the elastic constants of a particulate-filled glassy polymer, J. C. Smith.

Heat capacities of polyethylene IV. High molecular weight linear polyethylene, S. S. Chang.

Computer simulation of metastable fluid states in the Lennard-Jones system, H. J. Raveché and W. B. Streett.

Relative enthalpy of solid beryllium aluminate (chrysoberyl), $BeO \cdot Al_2O_3$, from 1175 to 2025 K, and of liquid beryllium aluminate from 2170 to 2350 K, S. Ishihara and E. D. West.

J. Res. Nat. Bur. Stand. (U.S.), **80B** *(Math. Sci.)*, No. 1 (Jan.-Mar. 1976), SD Catalog No. C13.22/sec.B:80/1.

Non-negative sums of roots of unity, M. Newman.

Plane-wave scattering-matrix theory of antennas and antenna-antenna interactions: formulation and and application, D. M. Kerns.

Optimal facility location for normally and exponentially distributed points, I. N. Katz and L. Cooper.

Real, 3×3, D-stable matrices, B. E. Cain.

Transient solutions for stratified fluid flows, D. W. Fox.

Equivalence of partitioned matrices, R. B. Feinberg.

Tables of binomial coefficients and Sterling numbers, K. Goldberg, F. T. Leighton, M. Newman, and S. L. Zuckerman.

H116. **American National Standard N540; classification of radioactive self-luminous light sources,** Nat. Bur. Stand. (U.S.), Handb. 116, 15 pages (Jan. 1976) SD Catalog No. C13.11:116, $1.10.

Key words: classification; containment; designation; light sources; national standard; radiation source; radioactive; radioluminous products; self-luminous sources; test procedures.

This standard establishes the classification of certain radioactive self-luminous sources according to radionuclide, type of source, activity, and performance requirements. The objectives are to establish minimum prototype testing requirements for radioactive self-luminous light sources, to promote uniformity of marking such sources, and to establish minimum physical performance for such sources. This standard is primarily directed toward assuring adequate containment of the radioactive material. Testing procedures and classification designations are specified for discoloration, temperature, thermal shock, reduced pressure, impact, vibration, and immersion. A range of test requirements is presented according to intended usage and source activity.

SP428. Parts 1, 2, and 3. **Bibliography of infrared spectroscopy through 1960,** C. N. R. Rao, S. K. Dikshit, S. A. Kudchadker, D. S. Gupta, V. A. Narayan, and J. J. Comeford, Nat. Bur. Stand. (U.S.), Spec. Publ. 428/1-3, 2399 pages (Jan. 1976) SD Catalog No. C13.10:428/1-3, $28.50.

Key words: bibliography; data; infrared; inorganic; minerals; organic; ores; polymers; spectroscopy.

This bibliography is based on a systematic search of the literature on infrared spectroscopy up to the end of 1960. It covers, directly or through abstract journals, 121 periodicals. As a general rule, any paper of interest in the field of infrared spectroscopy is included. Substance coverage is provided in four sections: organic compounds, inorganic compounds, polymeric compounds, and minerals and ores. Information provided includes: empirical formula, compound name, range of wavelengths reported, state of material, type of data presented in paper, and literature reference. Issued in three parts.

BSS67. **Abnormal loading on buildings and progressive collapse. An annotated bibliography,** E. V. Leyendecker, J. E. Breen, N. F. Somes, and M. Swatta, Nat. Bur. Stand. (U.S.), Bldg. Sci. Ser. 67, 60 pages (Jan. 1976) SD Catalog No. C13.29/2:67, $1.20.

Key words: abnormal loading; alternate path; annotated bibliography; bibliography; building code; building regulations; collapse; failures; progressive collapse; specific resistance.

This bibliography on the subjects of abnormal loading and progressive collapse is an annotated listing of articles that have appeared in the technical literature from 1948 through 1973. The entries have been arranged chronologically by year and alphabetically within years. Both subject and author indexes have been included. The references listed have been selected as most representative of the historical background and best representing the origin and present state-of-the-art of current practice without undue repetition of data.

References pertaining to characteristics, frequencies, incidents, tests, design procedures, and regulations for many types of abnormal loadings are included. Among these are various types of accidental impacts, construction loads, explosions, faulty practices, and extreme atmospheric loads. Heavy emphasis was placed on referencing applicable building codes and regulations pertaining to the subjects

**Publications with prices and SD Catalog numbers may be purchased directly from the Superintendent of Documents, U.S. Government Printing Office, Washington, D.C. 20402 (foreign: one-fourth additional). Microfiche copies of the above, plus paper copy and microfiche versions of NBS Interagency Reports (NBSIR's), may be purchased from the National Technical Information Service (NTIS), Springfield, Va. 22161. Prices are subject to change. Reprints from the NBS Journal of Research and non-NBS publications may often be obtained directly from the authors.*

201-606 O - 76 - 15

of progressive collapse and abnormal loadings. This bibliography also contains numerous references to contemporary professional opinion as expressed in editorials and discussions of the subject and particularly, on the various regulations proposed. A large number of proposed analysis and design procedures, as well as applicable test results, are referenced. In addition to the general reference material, a careful search was made of the ten most recent years (1964-1973) of *Engineering News Record* to identify and annotate possible progressive collapse examples from building failures reported by that publication.

BSS80. **Safety during construction of concrete buildings—A status report,** H. S. Lew, Nat. Bur. Stand. (U.S.), Bldg. Sci. Ser. 80, 56 pages (Jan. 1976) SD Catalog No. C13.29/2:80, $1.15.

Key words: building; codes; concrete; construction; falsework; formwork; loads; reshoring; safety; shoring; standards.

The current state-of-the-art of safety in concrete building construction is reviewed and summarized. The material presented considers only the technical aspects of the construction safety. Safety of the individual in using equipment and in following construction procedures is not included in this study.

The report presents comparative accident frequencies in concrete construction. Based on reported construction failures, the relative vulnerability of various categories of concrete construction is estimated. The report examines causes of construction failures and reviews major regulatory standards at the federal, state, city and industry level affecting safety in concrete construction.

The factors which affect safety in concrete construction are examined relative to the state-of-the-knowledge and, where appropriate, recommendations are made for areas needing improved standards.

TN674. **Report on the 1975 survey of users of the services of Radio Stations WWV and WWVH,** J. A. Barnes and R. E. Beehler, Nat. Bur. Stand. (U.S.), Tech. Note 674, 91 pages (Oct. 1975) SD Catalog No. C13.46:674, $1.50.

Key words: frequency; questionnaire; standard frequency and time broadcasts; time.

The users of the National Bureau of Standards (NBS) radio stations WWV and WWVH were surveyed by means of a questionnaire. The questionnaire was distributed to the station mailing list, published in some periodicals, and its availability was announced on the stations themselves and publicized in other periodicals. More than 12,000 completed questionnaires were returned, which revealed, among other things, that the 5, 10, and 15 MHz transmissions were the most used frequencies: 25 MHz was the least used. Of the information contained on the broadcasts, the voice time-of-day announcement was the most important, and the DUT1 values the least important. In general the returns were very supportive of the services, with only two of the more than 12,000 responses advocating a complete shutdown of the broadcasts.

TN859. **Literature search: Law enforcement facilities—Planning, design, construction,** R. Kapsch and J. Stroik, Eds., Nat. Bur. Stand. (U.S.), Tech. Note 859, 221 pages (Nov. 1975) SD Catalog No. C13.46:859, $4.15.

Key words: architecture; bibliography; building; construction; design; law enforcement facilities.

Citations and abstracts are provided on literature concerning the planning, design, and construction of law enforcement facilities in the United States and in foreign countries. In addition, plans of 21 select law enforcement facilities are included.

TN895. **An overview of floor slip-resistance research with annotated bibliography,** R. J. Brungraber, Nat. Bur. Stand. (U.S.), Tech. Note 895, 113 pages (Jan. 1976) SD Catalog No. C13.46:895, $2.30.

Key words: building safety; floor surface friction; occupancy safety; slip-resistance; slip-resistance testers; walking friction.

Slips and falls in the home as well as in public buildings have reached serious proportions (8,000,000 accidents per year in the home, resulting in 9,600 deaths and 1,600,000 disabling injuries). This paper reviews the literature relating to this problem. Based on studies of kinesiology and anthropometry, the coefficient of friction between foot surfaces and floor surfaces is found to be a significant parameter controlling slips and falls. A review of the general study of friction and a critical appraisal of methods for determining the coefficient of friction on slip-resistance of floors leads to a guide for selection of slip-resistance criteria. The paper concludes with a discussion of the legal aspects of the problem and the present status of slip-resistance specifications.

TN896. **NBS Reactor: Summary of activities July 1974 to June 1975,** R. S. Carter, Nat. Bur. Stand. (U.S.), Tech. Note 896, 150 pages (Jan. 1976) SD Catalog No. C13.46:896, $2.15.

Key words: activation analysis; crystal structure; diffraction; isotopes; molecular dynamics; neutron; nuclear reactor; radiation.

This report summarizes all those programs which depend on the NBS reactor. It covers the period from July 1974 through June 1975. The programs range from the use of neutron beams to study of the structure and dynamics of materials through nuclear physics and neutron standards to sample irradiations for activation analysis, isotope production and radiation effects studies.

NBSIR 73-264. **Examination of failed one inch black iron pipe natural gas service line, Iowa Public Service Company, Eagle Grove, Iowa,** T. R. Shives, 24 pages (Aug. 30, 1973). Order from NTIS as PB243541, $3.50.

Key words: black iron pipe; dimpled rupture; ductile fracture; gas pipe.

A fractured one inch black iron pipe natural gas service line which connected to a building involved in an explosion and fire in Eagle Grove, Iowa, on February 2, 1973, was examined by the NBS Mechanical Properties Section. The fracture was ductile in nature. There was no evidence found to indicate the presence of a preexisting crack. The fracture appeared to have been due to bending stresses caused by loading from an external source.

NBSIR 74-379. **Completion of the program to evaluate/improve instrumentation and test methods for electroexplosive device safety qualification,** P. A. Hudson, D. G. Melquist, A. R. Ondrejka, and P. E. Werner, 37 pages (June 1974). Order from NTIS as PB247658, $4.00.

Key words: electroexplosive device safety; electromagnetic compatibility; electromagnetic interference; stray energy sensor.

Qualification of weapon and missile systems for electroexplosive device (EED) safety has been a continuing problem in the military services. Quantitative measurement of stray energy in EED's has been hampered by limitations of existing sensors. This report describes a new video diode detector instrumented EED (VIDEED) which responds to both the normal pin-to-pin energy (which would heat an EED bridgewire) and to the pin-to-case voltage (which might cause EED ignition due to arcing).

Also described in this report are the amplifiers, cables, adapters and recorders which make up the rest of the measuring system. Mention is also made of the test procedures used in testing the VIDEED system.

NBSIR 74-507. **Mercurous chloride polarizer material,** R. Forman, W. S. Brower, and H. S. Parker, 31 pages (June 1, 1974). Order from NTIS as ADA000343, $4.00.

Key words: infrared; mercurous chloride; polarizer material; visible.

This contract report covers a feasibility study on the potential use of mercurous chloride crystals for construction of prism polarizers, primarily for the infrared region of the spectrum. In particular, the research has consisted of crystal growth from the vapor phase and optical characterization of the absorption, dichroism, and birefringence.

Crystal growth has been performed in quartz or Vycor ampoules sealed off under a pressure of 10^{-5} torr or better. Crystals are grown in a vertical modified Bridgman furnace by vapor transport. Repeated regrowth has been found to produce a continuous improvement in clarity, the best samples being virtually colorless. The growth rates used of 2 mm/day in tubes of 17 mm inside diameter have been found to be satisfactory for producing the crystals used to date, but strain patterns and a tendency to polycrystallinity indicate that slower growth rates should be attempted. Conditions for growth have not yet been optimized, but reasonably good growing conditions have been delineated.

Single crystal samples have been oriented by Laue back-reflection techniques and measurements made of optical absorption, dichroism, and birefringence. Proper sample handling procedures have been determined to minimize thermal shock and thermal etching. The index of refraction has been measured at selected wavelengths, and calorimetric absorption studies have been performed at AFML on some of the samples produced.

NBSIR 74-518. **Instrumental colorimetry of retroreflective sign materials,** I. Nimeroff and W. A. Hall, 89 pages (Aug. 1974). Order from NTIS as PB239633, $5.00.

Key words: colorimetry; highway signs; photoelectric tristimus colorimeters; photometry of retroreflective materials; retroreflective sign materials.

Because color-coded applications of highway signs increase, specifications of colors and color tolerances are required. In order to assure that the requirements are met within specified regions, a measurement technique needs to be developed and described. To accomplish these goals the U.S. Department of Transportation contracted with the National Bureau of Standards to conduct the required studies and make the necessary recommendations. Having previously performed a study for daytime conditions, the National Bureau of Standards was competent to perform a study for nighttime conditions. The colorimetric properties of 126 samples of retroreflective materials of 7 different colors were measured with 3 telecolorimeters in simulated nighttime conditions. One spectrophotometer was used to measure color of 38 of the samples in simulated daytime conditions. The colors measured were: red, orange, brown, yellow, green, blue and silver (white). Differences of color measured by means of different telecolorimeters on the same samples were evaluated.

As a result of these studies procedures for making colorimetric and photometric measurements were developed and are included in this report. On the basis of the color measurements and their variability tentative recommendations for color boundaries were prepared and are also included in this report.

NBSIR 74-580. **Spectral characteristics of additional Bar Code Readers. II,** J. Cohen, 12 pages (Sept. 1974). Order from NTIS as PB248465, $3.50.

Key words: bar code reader; filters; optical wedge; photodetector; relative spectral output; wavelength.

The spectral characteristics of two bar code readers (submitted by the U.S. Postal Service under Task No. 1, Agreement No. 74-02934 [Mod. No. 1]) have been measured as a function of wavelength in the approximate interval of 450 to 1200 nm.

NBSIR 74-625. **Examination of failed two inch steel pipe natural gas main, Columbia Gas Company, Spring Garden Township, York County, Pennsylvania,** T. R. Shives, 41 pages (Jan. 1975). Order from NTIS as PB243547, $4.00.

Key words: brittle fracture; gas main pipe; impact; low carbon steel; stress corrosion cracking.

The Mechanical Properties Section of the National Bureau of Standards examined a length of a cracked two inch diameter plain carbon, welded steel natural gas main pipe at the request of the Office of Pipeline Safety. The pipe had a transverse crack extending about 85 percent of the circumference. The pipeline had suffered considerable mechanical damage in the vicinity of the failure, and the crack, which propagated in an essentially brittle manner, appeared to have initiated in a gouged area near the bottom of the pipe. There was a considerable amount of corrosion product on the surface of the pipe in the gouged area. The amount and distribution of corrosion product on the fracture surface indicated that the crack had formed in at least two stages, and that a crack was present prior to the time of failure. During the first stage, the crack may have penetrated the entire wall thickness of the pipe in one region opposite the crack origin near the bottom of the pipe. The likely mechanism of fracture for the first stage of the crack appears to be stress corrosion cracking. For the second stage of the crack, either stress corrosion cracking or impact appears to be the likely mechanism of failure.

NBSIR 75-653. **Measurement methodology and supporting documentation for portable air compressor noise,** C. I. Holmer, 48 pages (Jan. 1975). Order from NTIS as PB248097, $4.00.

Key words: acoustics; air compressor; internal combustion engine; noise; sound power level; sound pressure level.

This report presents recommendations and supporting rationale on a measurement methodology for portable air compressors. The methodology provides for the determination of A-weighted sound power level or the equivalent weighted sound pressure level at a reference distance. A-weighted level is used because of its correlation with community response to noise from internal combustion engine noise. It is recommended, however, that the spectra associated with the regulated source be monitored in some manner to insure that the spectra remain similar to those for which A-weighted sound level retains good correlation with community response. The methodology uses weighted sound level measurements at eight positions on a curved surface surrounding the source at a distance of one metre from the surface of the machine. Data recorded at these positions are used to calculate the average weighted sound pressure level of the machine on the measurement surface. This is combined with the area of the measurement surface to give the sound power level of the machine. From this value, a rating sound pressure at a rating distance may be calculated by subtracting a constant value. Procedures which permit the rapid estimation of A-weighted sound level are included. These are applicable for estimation of A-weighted sound level in a variety of circumstances when the sound power or equivalent sound pressure level at a reference distance is known.

NBSIR 75-678. **Analysis of construction systems for the thermal classification of residential buildings,** S. T. Liu, 59 pages (Nov. 24, 1975). Order from NTIS as PB248687, $4.50.

Key words: building classification; building thermal mass; building thermal performance; building thermal time constant; housing systems; industrialized housing; mass per unit area; Operation BREAKTHROUGH; U-value.

This report is the result of a study to classify various kinds of residential buildings in relation to their thermal behavior. A collection of various building data and construction systems taken from the proposals of 18 of the 22 Housing System Producers participating in the Department of Housing and Urban Development (HUD) Opera-

tion BREAKTHROUGH Program is presented. Thermal performance parameters of buildings, such as: U-value, thermal mass, thermal time constant, and mass per unit area were computed and analyzed. The report recommends one way in which construction systems could be classified. Since the housing systems studied represented a cross section of the conventional residential construction systems in the building industry, it is felt that a realistic classification procedure for typical residential buildings can be established and based upon the parameter: mass per unit area. A more refined procedure of subdividing the building within each mass class on the basis of the building thermal time constant is also discussed.

NBSIR 75-706. **Calculations of radiant heat flux in the proposed floor covering flame spread test apparatus,** J. Quintiere and K. Bromberg, 21 pages (Dec. 1975). Order from NTIS as PB248640, $3.50.

Key words: floor covering; heat flux; radiant panel test method.

Calculations have been made to determine the radiant heat flux distribution to the test specimen in the proposed radiant panel flame spread test for floor covering materials. Comparison with measured heat flux indicates a significant heat transfer contribution from the enclosure of the test apparatus. Also, nonuniformities in the temperature of the radiant panel affect the resultant flux distribution. Based on these results, it is expected that two similar test apparatuses would not have identical heat flux profiles along the specimen. Additional calculations were made to illustrate possible heat flux profiles capable with the present apparatus under various panel temperatures and orientations.

NBSIR 75-722. **Closure testing equipment instruction manual,** M. S. Morse, 42 pages (Oct. 1975). Order from NTIS as PB248641, $4.00.

Key words: bottle caps; child protection; closure testing; containers; medicine bottles; poison packaging.

The NBS Closure Testing Equipment is designed to make accurate measurements of the critical parameters of the "childproof" closures required by the Poisoning Prevention Packaging Act of 1971. In general, these parameters are defined as the forces necessary to open these closures, either in the manner by which the closure was designed to be opened, or in an undesired manner. This manual discusses the design and construction of the testing instrument and gives detailed instructions for its operation.

NBSIR 75-742. **Mixed oxides for fuel cell electrodes,** U. Bertocci, M. I. Cohen, W. S. Horton, T. Negas, and A. R. Siedle, 56 pages (Jan. 1976). Order from NTIS as PB248744, $4.50.

Key words: electrocatalysis; fuel cells; mixed oxides; oxygen reduction; phosphoric acid; ternary metal-sulfur arrays; transition elements; triphenylphosphine; tungsten bronze.

Studies of mixed oxides were made in order to determine if such materials could act as oxygen-reducing electrocatalysts in an acid fuel cell. Included were strontium and barium cobaltates and manganates with and without added titanium; lanthanum titanates, with and without calcium or strontium; calcium, strontium, and barium ruthenates; and mixed oxides of the systems Ti-Ta-O, V-Nb-O, Ce-Ta-O, Pr-Ta-O, Ce-Nb-O, and Ce-Pr-Ta-O. Choices were based upon producing variable valence and upon conferring stability at elevated temperatures ($\leq$ 150 °C) in phosphoric acid. Barium ruthenate and the systems Ti-Ta-O, V-Nb-O, V-Ta-O, Ce-Ta-O, were hot-acid stable. The thermal reactions of $CeTaO_{4+x}$ with $0 \leq x \leq 0.5$ were studied in air up to about 1960 °C.

Potentiodynamic and galvanostatic studies are reported on materials from the Ti-Ta-O system, TiO_2 as grown, TiO_2 reduced with hydrogen, TiO_2 with 0.1 percent Nb, lanthanum titanates with and without calcium or strontium, a tungsten bronze, barium ruthenate, and strontium titanate with 0.03 and with 0.15 percent Nb.

Preparation of inorganic compounds with ternary metal-sulfur arrays similar to the arrays in nitrogen reductase was attempted. The following were made: $(Ph_3P)_4Cu_2W_2S_6$, $(Ph_3P)_6Ag_5W_2S_6O_2$, and $[(Ph_3P)_3Ag]_2W_2S_6$, where Ph_3P refers to the triphenylphosphine moiety. Also prepared were $(Ph_3PAu)_2W_2S_4$, $(Ph_3AsAu)_2WS_4$, $(diphos)NiWO_2S_2$, $(diphos)_2Pd_3W_2S_6O_2$, and $(Ph_3P)_3PtW_2S_6O_2$, where "diphos" refers to 1,2-bis(diphenylphosphino)ethane.

NBSIR 75-745. **A model for salmon fishery regulatory analysis,** F. C. Johnson, 33 pages (July 10, 1975). Order from NTIS as PB247657, $4.00.

Key words: fisheries; fishery; fishery modeling; mathematical modeling; regulatory analysis; resource management; salmon fisheries; salmon fishery modeling; simulation; State of Washington; Washington State; Washington State Fisheries.

The salmon fishery modeling project is a joint State-Federal program for the development of improved techniques for analyzing the economic and biological effects of regulatory changes in the Pacific Coast salmon fisheries. This interim report covers the second segment of the project—the implementation of a multi-species, multi-stock fishery analysis model. This segment of the project was sponsored by the Washington State Department of Fisheries under Service Contract No. 588.

NBSIR 75-755. **The CPSC road test of bicycle braking performance—Experimental evaluation,** D. E. Marlowe, 32 pages (Aug. 1975). Order from NTIS as PB248642, $4.00.

Key words: bicycles; braking; consumer safety; handbrake; safety; testing.

The brake performance criteria to be published as part of a mandatory regulation on bicycle safety requirements has been evaluated. Fifteen bicycles were tested in accordance with the regulation. A mathematical adjustment of the actual test speed of the bicycle to 24 km/hr (15 mph) is necessary before the weight allowance can be made to the stopping distance in the evaluation of these tests. A danger of injury to the test rider exists during the tests and future efforts should be made toward replacement of these tests with a simpler laboratory procedure.

NBSIR 75-757. **A technique for the measurement of flash fire potential of polymeric materials,** J. E. Brown and J. J. Comeford, 33 pages (Dec. 1975). Order from NTIS as PB248914, $4.00.

Key words: aircraft fires; fire hazard; flash fire; polyurethane; pyrolysis.

This report summarizes work for the period February-August 1974 on a continuing program to characterize the chemical and physical parameters of importance in a flash fire and to develop laboratory scale methods for measuring the flash fire potential of materials.

Significant modifications have been made to a flash-fire cell developed earlier to measure the flash fire potential of materials by characterizing the condition required to produce an ignitable pyrolyzate-air mixture by thermally degrading a polymer. The furnace temperature, cell geometry and orientation, and sample size are specified. These modifications have resulted in an improved technique, especially in terms of reproducibility, for evaluation of flash fire potential of materials.

Experiments have been conducted on rates of combustible gas formation from flexible polyurethanes to assist in the optimization of the flash-fire cell operating conditions.

In the rate study, two successive major stages of degradation were found for polyurethane as the temperature approached 500° at a rate of about 60 °C/min. It was also found that the products of the second stage appear to be responsible for flash fires in the flash-fire cell. A minimum polyurethane weight to enclosure volume ratio greater than

0.2 g/l and a sample pyrolysis temperature greater than 380 °C were required to produce a flash fire in this apparatus.

NBSIR 75-768. **Reevaluation of the densities of the four NBS silicon crystal standards,** H. A. Bowman, R. M. Schoonover, and C. L. Carroll, 36 pages (Aug. 1975). Order from NTIS as PB247943, $4.00.

Key words: density standard; phase shift; silicon.

There were a few features of our recently completed density standard experiment which were based upon ideas which, we believe, should be changed. This report lists these changes and their justification. The result is to increase the assumed values of the densities of the crystals by about 1.7 ppm. The new assumed values are: X2 = 2.329 1289 g/cm^3; X3 = 2.329 1253 g/cm^3; X4 = 2.329 1228 g/cm^3; X5 = 2.329 1226 g/cm^3.

Additionally, we now believe that the densities of the crystals are stable, and not appreciably changing due to oxidation—a point left unresolved in our published report.

NBSIR 75-769. **Report on an NBS/AID/OAS Workshop on standardization and measurement services in industrializing economies,** H. S. Peiser, R. S. Marvin, M. McNeil, and J. Mejeur, Eds., 227 pages (Sept. 1975). Order from NTIS as PB247978, $8.00.

Key words: AID; assistance; economics; foreign relations; industrializing nations; LDC's; measurement services; OAS; standardization.

On November 3-16, 1974, a Workshop was held at the National Bureau of Standards, Gaithersburg, under the sponsorship of AID and the Organization of American States, the object of which was to give standards officials of industrializing nations insight into the standards and measurement systems in the United States and the role of the National Bureau of Standards, so that these officials might consider what parts of the U.S. system might usefully be adapted to conditions in their home countries. The report contains copies of speeches and presentations by the U.S. hosts and the participants from the other nations. In addition, information is given on the general agenda of discussions, presentations, and tours of laboratories at NBS and other U.S. organizations.

NBSIR 75-775. **Electrical measurement of high voltage pulses in diagnostic x-ray units,** R. E. Hebner, Jr., 62 pages (Nov. 1, 1975). Order from NTIS as PB248684, $4.50.

Key words: calibration; electrical measurements; electro-optics; frequency response; high voltage; Kerr effect; operational amplifier; pulses; radiation; safety; x-ray generators; x rays.

The report describes a method of calibrating dividers used to measure high voltage pulses in diagnostic x-ray units. The experimental development emphasized four areas. These were the divider ratio under direct voltage, the frequency dependence of the ratio, the voltage dependence of the ratio and the effect of self-heating on the device. The results of measurements on approximately fifteen different dividers are summarized.

In addition, this report contains two appendices. The first discusses conventional and electro-optical methods of measuring the high voltage pulses, while the second presents a more detailed analysis of the feasibility of electro-optical measurement of these pulses.

NBSIR 75-782. **Full-scale corridor fire experiment using a glass fiber carpet,** L. H. Breden, 33 pages (Dec. 1975). Order from NTIS as PB248643, $4.00.

Key words: carpet; corridor test; fire testing; flammability; glass fiber.

A corridor fire experiment was carried out using a glass fiber carpet. It was observed that with a fuel loading of 2.7 pounds per square foot of wood in an adjacent fire room, no propagation of the fire occurred down the corridor. The glass fiber carpet in the burn-room became discolored and there was a significant weight loss of the carpet directly in contact with the fire. The carpet did not produce significant levels of smoke and did not spread the fire into the corridor.

NBSIR 75-793. **Microsecond-resolution pulse calorimetry for semiconducting materials at high temperatures (a feasibility study),** A. Cezairliyan and C. W. Beckett, 51 pages (Oct. 1975). Order from NTIS as PB247538, $4.50.

Key words: capacitor discharges; heat capacity; high-speed measurements; high temperature; thermodynamics; uranium dioxide.

A feasibility study is conducted for the applicability of microsecond-resolution pulse heating techniques to the measurement of selected thermodynamic properties of semiconducting substances at high temperatures. The method of pulse heating of the specimen using capacitor discharges is described and general design considerations, including electrical circuitry and various physical, electrical and chemical phenomena, are presented. Measurements of experimental quantities, such as current, voltage, temperature, and pressure are described. The special problems in relation to measurements of heat capacity and vapor pressure of uranium dioxide in the temperature range 2000 to 6000 K are discussed. It is concluded that the capacitor discharge circuitry and the measurement of the experimental quantities, although difficult, are not likely to present major problems. However, problems are likely to stem from the experiment chamber and the specimen. The nature of these problems is discussed, and the performance of some preliminary experiments is suggested.

NBSIR 75-796. **An analysis of the Salmon Statistical Information System,** F. C. Johnson, 20 pages (Sept. 29, 1975). Order from NTIS as PB247656, $3.50.

Key words: Anadromous Fish Catch Record System; catch record system; fisheries statistics; fish record system; fishery management model; fishery modeling; modeling; salmon; salmon fishery; salmon information system; Washington State Fisheries.

This report contains an analysis of the official salmon statistical information system of the Washington State Department of Fisheries relative to the changing data requirements of the Department. Recommendations are given for revising the current system in order to assure the availability of complete, accurate statistics on a timely basis. In addition, the principal requirements are identified for the development of improved procedures for generating input to the hatchery and fishery management models in use by the Department. This project was sponsored by the Washington State Department of Fisheries under Service Contract No. 626.

NBSIR 75-818. **Bibliography of the Electromagnetics Division June 30, 1974 to June 30, 1975,** M. L. Woolley, 27 pages (Sept. 1975). Order from NTIS as PB246439, $4.00.

Key words: antenna parameters; attenuation; automated measurements; EM metrology; field strength; impedance; laser parameters noise; optical electronics; phase; power; pulsed quantities; squids; transmission lines; waveform analysis; waveguides.

This bibliography lists the publications of the NBS Electromagnetics Division between June 30, 1974 and June 30, 1975.

NBSIR 75-820. **Study of cryogenic propellant systems for loading the space shuttle—Part II, Hydrogen systems,** W. G. Steward, 63 pages (Oct. 1975). Order from NTIS as PB246658, $5.00.

Key words: computer modeling; cooldown; cryogenic flow; stresses; two phase flow.

This report covers computer simulation studies of liquid hydrogen fill and vent systems for the space shuttle. The computer programs calculate maximum and minimum permissible flow rates during cooldown as limited by thermal stress considerations, fill line cooldown time, pressure drop, flow rates, vapor content, vent line pressure drop and vent line discharge temperature. The input data for these programs are selected through graphic displays which schematically depict the part of the system being analyzed. The computed output is also displayed in the form of printed messages and graphs. Digital readouts of graph coordinates may also be obtained.

Procedures are given for operation of the graphic display unit and the associated minicomputer and timesharing computer.

NBSIR 75-822. **Study of errors in absolute flux density measurements of Cassiopeia A,** M. Kanda, 34 pages (Oct. 1975). Order from NTIS as PB246933, $4.00.

Key words: accuracy; antenna; calibration; Cassiopeia A; error analysis; flux density; ground station; G/T (system gain/system noise temperature); radio star.

An error analysis for absolute flux density measurements of Cassiopeia A is discussed. The lower-bound quadrature-accumulation error for state-of-the-art measurements of the absolute flux density of Cas A around 7 GHz is estimated to be 1.71 percent for 3σ limits. The corresponding practicable error for the careful but not state-of-the-art measurement is estimated to be 4.46 percent for 3σ limits.

NBSIR 75-823. **Helium research in support of superconducting power transmission,** V. D. Arp, D. E. Daney, N. V. Frederick, M. C. Jones, P. R. Ludtke, W. R. Parrish, and R. L. Powell, 79 pages (Oct. 1975). Order from NTIS as PB246436, $4.50.

Key words: cooling system; cryogenics; helium-cooled electrical leads; helium impurities; microwave cavities; negative differential flow resistance; pressure measurement; system dynamics; thermometers.

This is the first annual report on a program of helium-related research in support of superconducting power transmission. Program areas reported on are concerned with the dynamics of helium cooling systems—theoretical aspects of oscillatory behavior and experiments—and helium related measurements. The latter include pressure measurement, temperature measurement and the problem of impurity levels in the helium refrigerant.

NBSIR 75-910. **The role of chemical kinetics in energy conservation,** H. M. Rosenstock, D. Garvin, J. T. Herron, and W. Tsang, 123 pages (Oct. 1975). Order from NTIS as PB248646, $5.50.

Key words: combustion; data base; energy conservation; estimation schemes; kinetics; modeling; oxidation; pyrolysis.

Many of the technological areas of pertinence to energy independence involve chemical transformation of gas phase materials at high temperatures. The design, control and optimization of such devices and processes have come to depend increasingly on mathematical modeling. Among the most important input data required for these models are information on the detailed chemical mechanisms and the rates of the individual processes. It is concluded that although many resources are available there does not exist at present an adequate, publicly available data base for the modeling of high temperature systems. A detailed program involving a combination of experimentation and compilation, evaluation and dissemination of gas kinetic data is proposed.

NBSIR 75-917. **A multiple-chamber humidity apparatus,** L. Greenspan, 22 pages (Dec. 1975). Order from NTIS as PB247655, $3.50.

Key words: humidity; humdity chamber; microbiological growth; relative humidity; salt solutions; saturated salt.

An apparatus has been developed for studying the growth of microbiological organisms on food under controlled conditions of humidity and temperature. This apparatus contains twenty-eight individual humidity chambers within a temperature controlled bath. A wide range of humidities can be provided within the individual chambers by means of saturated salt solutions. These chambers can be maintained at stable temperatures from 5 to 50 °C with a constancy and uniformity within ±0.02 °C. Individual chambers may be conveniently removed or changed without affecting the other chambers.

NBSIR 75-920. **Distribution of water through a vertical plane from automatic sprinkler heads,** R. L. P. Custer and K. Wahle, 48 pages (Dec. 1975). Order from NTIS as PB248913, $4.00.

Key words: automatic sprinkler; corridor sprinkler systems; discharge patterns; spray distribution; water distribution; water spray.

An investigation was conducted to evaluate the distribution of water through a vertical plane from automatic sprinkler heads as a function of water discharge rate and sprinkler spacing. Tests were conducted to simulate discharging an automatic sprinkler head in a corridor to determine the effectiveness of the sprinkler head in covering a doorway with water spray when positioned at various locations. Major differences in distribution characteristics between sprinkler heads produced by different manufacturers were observed. It was determined that only sprinklers installed on the centerline of the doorway and discharging water at a flow rate of 20 gallons-per-minute or more would cover the top of the doorway.

NBSIR 75-924. **Evaluation, revision and application of the NBS stylus/computer system for surface roughness measurement: Minicomputer software,** E. C. Teague, 79 pages (Apr. 1975). Order from NTIS as PB248686, $5.00.

Key words: amplitude density function; arithmetic average; autocorrelation function; linear least-squares fit; machine language; minicomputer software; surface texture measurement.

A thorough description of all the software used at NBS for characterizing surface texture is given in this report. The description includes flow diagrams and detailed, annotated listings of machine language programs for step-calibrating the system, for acquiring digitized surface profiles and for calculating from these profiles important parameters and statistical functions. Parameters and functions included are the arithmetic average value, mean square value, average wavelength, average slope, amplitude density function and autocorrelation function.

NBSIR 75-952. **An error analysis of failure prediction techniques derived from fracture mechanics,** S. M. Wiederhorn, E. R. Fuller, Jr., J. Mandel, and A. G. Evans, 41 pages (Dec. 1975). Order from NTIS as PB248910, $4.00.

Key words: crack propagation; error analysis; failure prediction; failure prevention; fracture; statistics; strength.

Three principal methods of failure prediction for brittle materials are analyzed statistically. Each method depends on fracture mechanics for its predictive value and hence, the variance of the failure time is found to depend on the scatter in the fracture mechanics data and the scatter in the estimate of the initial size of the strength limiting crack. The variance is used to calculate confidence limits for the prediction of failure for two materials, glass and silicon carbide. Procedures for the collection and analysis of data are discussed, and the implications of the analysis for lifetime prediction are evaluated.

NBSIR 75-955. **Durability and related tests for selected elements and materials used in the exterior envelope of**

buildings, L. W. Masters, E. J. Clark, G. A. Sleater, and A. Hockman, 151 pages (Nov. 1975). Order from NTIS as PB248685, $6.75.

Key words: aging test; building elements and materials; degradation factors; durability; property measurement test; standard test methods.

This report contains a compendium of state-of-the-art methods to aid in the durability testing of selected elements and materials used in the exterior envelope of buildings. The purposes of the report are to identify currently available property measurement tests and aging tests that can be used for durability testing and to identify the degradation factors included in each aging test. The report will form the basis for selecting specific elements and materials for inclusion in subsequent comprehensive durability studies. These additional studies are needed because existing short-term methods are seldom fully adequate for predicting long-term performance.

The sources of the methods include the American Society for Testing and Materials (ASTM), the American National Standards Institute (ANSI), building industry trade associations, Federal Specifications and Federal Standards. Indications are made for each test method to show if the methods described include a property measurement test, an aging test or both. If the method contains an aging test, the degradation factors included in the test are listed.

NBSIR 75-956. **An interference simulator for quantitative determination of the susceptibility of flame detectors to false alarm,** A. Scheidweiler, 16 pages (Nov. 1975). Order from NTIS as PB247654, $3.50.

Key words: false alarms; false alarm simulator; fire detection; fire detector; flame detection; flame detector.

All fire detectors are susceptible to false alarms, i.e., responding to fire-like conditions when no fire is present. Of all the known fire detectors, flame detectors are probably the most false alarm prone of any of the fire detectors, primarily because these detectors are subjected to more environmental influences resembling the detectors' operating mode than any other fire detector.

In this paper, the author describes an investigation into the susceptibility of flame detectors to false alarms. The author describes a test apparatus, constructed and used by his firm, to evaluate the susceptibility of currently-available flame detectors to false alarms. In addition, the apparatus can be used to evaluate prototype flame detectors.

The data developed indicates the false alarm susceptibility of each type of flame sensor. The data also provides a means of selecting a flame detector having the greatest resistance to known or predictable pseudo-fire sources.

NBSIR 75-958. **Simulated precipitation reference materials,** J. K. Taylor, E. R. Deardorff, R. A. Durst, E. J. Maienthal, T. C. Rains, and E. P. Scheide, 25 pages (Oct. 1975). Order from NTIS as PB248743, $3.50.

Key words: chemical analysis; rainwater analysis; reference materials.

The preparation of a series of reference materials for chemical analysis of natural precipitation is described. The materials consist of ampoules of concentrates which can be diluted to simulate naturally collected samples of rainwater. The analytical measurements made to verify the composition of the samples are also described.

NBSIR 75-962. **An outdoor noise monitoring system with automatic calibration and remote digital display,** D. S. Blomquist, J. S. Forrer, and D. M. Corley, 11 pages (Oct. 1975). Order from NTIS as PB247639, $3.50.

Key words: acoustics (sound); environmental acoustics; instrumentation; noise monitoring; outdoor noise.

An Outdoor Noise Monitoring System is described. This system uses a microprocessor for automatic calibration. The design concepts of the system are applicable to other remote noise monitoring systems.

NBSIR 76-982. **Data processing and data analysis procedures for fire load and live load survey program,** R. M. McCabe, C. Culver, L. T. Lee, and J. G. Hirschberg, 344 pages (Dec. 1975). Order from NTIS as PB248699, $10.00.

Key words: buildings; computers; data processing; fire loads; load surveys.

Data collection and data processing procedures utilized in connection with a nationwide fire load and live load survey program are described. The techniques developed for transferring the field survey data to a form suitable for computer processing are discussed. Procedures adopted for data analysis are included. Documentation of the computer programs developed for this purpose is also presented.

This column lists all outside publications by the NBS staff, as soon as possible after issuance as practical. For completeness, earlier references not previously reported may be included from time to time.

Abrams, M. D., **Computer communications network performance measurement (Abstract),** *Proc. Eurocon 1974 Conf. Digest on Electrotechnics, Amsterdam, The Netherlands, Apr. 22-26, 1974,* 2 pages (1974).

Key words: communications; computer; evaluation; measurement; network; performance.

This publication consists of an abstract only which describes computer networks, measures of service, measurement of service delivered, measured effects and applications.

Abrams, M. D., **Consumer-oriented measurement of computer network performance,** *Proc. IEEE National Telecommunications Conf., San Diego, Calif., Dec. 2-4, 1974,* pp. 843-844 (1974).

Key words: computer; consumer; contract; evaluation; network; performance.

This short paper describes measurement of computer network services from the consumer's viewpoint. Two common measures of performance are described. The ICST Network Measurement Machine and its data analysis programs are presented as a prototypical device capable of measuring network service for analysis according to various criteria. Sample results are given. Application of measurement to procurement and contractual obligations is discussed.

Achenbach, P. R., Didion, D. A., **Energy conservation measures in the National Bureau of Standards laboratory complex,** *Proc. Energy Conservation and Energy Management in Buildings, London, England, Nov. 13-14, 1975,* pp. 51-68 (1975).

Key words: building retrofit; building systems; energy conservation in buildings; HVAC automatic control; HVAC systems; measurement of building energy.

Energy conservation measures at the National Bureau of Standards site are being carried out under two separate but interrelated programs; a low-investment, immediate-impact program and a long-range, major retrofit program. The low-investment program has already been implemented and includes lighting reductions, thermostat resettings and nighttime shutdowns of heating, ventilating, air conditioning systems. Data on energy usage before and after this program was instituted are presented. The methodology and analysis of the long-range program are also presented. Various building energy conservation options were considered and evaluated by means of a mathematical model. Quantitative estimates of savings for each are presented. The decision to invest in automatic controls for the air conditioning systems of the laboratory complex and steam/chilled-water power plant is discussed.

Achenbach, P. R., **National Bureau of Standards research in support of energy conservation standards for buildings,** *Proc. 10th Intersociety Energy Conversion Engineering Conf., Newark, Del., Aug. 18-22, 1975*, pp. 667-676 (1975).

Key words: building research; building standards; economics of energy conservation; energy conservation; energy conservation research; energy savings.

Initiation of an energy conservation program for buildings revealed that, until very recently, buildings and the mechanical and electrical equipment installed therein have been designed for low first cost, with little attention given to energy cost. Current efforts to draft energy conservation standards for buildings showed that neither the energy conservation potential nor the life-cycle costs of many well-known energy conservation techniques are established. The research program of the National Bureau of Standards on energy conservation in buildings is presented in overview, and selected projects are discussed in some detail to show the types of information being developed in the laboratory, and in full-scale studies of new and existing buildings. Additional research needs for energy standards purposes are identified.

Allan, D. W., Daams, H., **Picosecond time difference measurement system,** *Proc. 29th Annual Symp. on Frequency Control, Atlantic City, N.J., May 28-30, 1975*, pp. 404-411 (1975).

Key words: atomic clocks; frequency measurements; frequency stability; phase delay; precise time metrology; subpicosecond time difference measurements; time stability.

Recently a time difference measurement system was developed in the Frequency and Time Standards Section of the National Bureau of Standards and independently at the National Research Council which shows more than three orders of magnitude improvement over that which is currently available commercially. Current state-of-the-art time difference measurement devices have specified accuracies of about 1 nanosecond. Measurement precision and potential accuracy of better than 1 picosecond has been demonstrated in this new time difference measuring device. This has significant implications in frequency and time metrology using: state-of-the-art frequency standards and clocks. A brief report was given on this measurement system at the PTTI Planning Meeting at the Naval Research Laboratory on the 5th of December 1974. This paper will give more detailed circuit diagrams necessary to build up such a measurement system.

This particular measurement system has the advantage that it can measure time differences with accuracies of a few picoseconds and with repetition rates ranging from a few milliseconds to as slow a repetition rate as would be desirable, thus expanding convenient measurement of time domain stabilities of frequency and time standards over several decades with only one measurement system. The system is also very amenable to self-calibration and self-noise analysis. Specifically, a fractional frequency stability of about 10^{-16} was measured for the noise of this measurement system at a sample time of 10^3 s.

Allan, D. W., Hellwig, H., Glaze, D. J., **An accuracy algorithm for an atomic time scale,** *Metrologia* **11,** No. 3, 133-138 (1975).

Key words: coordinate time scales; frequency calibration; international frequency comparisons; optimum frequency estimate; primary frequency standards; relativity; SI second; time scale accuracy algorithm; time scale stability.

The accuracy of the rate or frequency of an atomic time scale is the degree to which its unit agrees with the SI second. Primary frequency standards are constructed in such a manner that they provide the most accurate possible physical realization of the SI second. These standards are then used to calibrate or construct an atomic time scale which may also be used as a stable reference standard.

Mathematical models characterizing the performance of both the primary frequency standards and reference standards are developed, and based on these models a current best estimate of the SI second is derived utilizing current and previous calibrations.

The modeling techniques and theory are applied to the NBS primary frequency standards and atomic time scale system and a significant improvement is realized in the accuracy of the frequency estimate so derived. We estimate that the second used by the Bureau International de l'Heure in generating TAI and UTC was too short by about 9 ± 2 parts in 10^{13} during the fall of 1974.

Andrews, J. R., Baldwin, E. E., **Baseband impulse generator useful to 5 GHz,** *Proc. 1975 IEEE Int. Symp. on Electromagnetic Compatibility, San Antonio, Tex., Oct. 7-9, 1975*, pp. 1-4 (1975).

Key words: impulse generator; picosecond; spectrum; spectrum amplitude; step recovery diode.

A baseband impulse generator recently developed at NBS is described. It is completely solid state and features a 100 kHz maximum repetition rate, 50 ohm source impedance, an extremely narrow 100 ps duration impulse of 8 volts amplitude, and a flat spectrum greater than 60 dBμV/MHz up to 5 GHz. The generator was evaluated on the NBS Automatic Pulse Measurement System which measured the time domain waveform with a sampling oscilloscope and computed the spectrum on a minicomputer.

Andrews, J. R., **Directional-coupler technique for triggering a tunnel diode,** *IEEE Trans. Instrum. Meas.* **IM-24,** No. 3, 275-277 (Sept. 1975).

Key words: directional coupler; picosecond; pulse generator; risetime; trigger; tunnel diode.

Present tunnel diode (TD) pulse generators have distortions in the pulse baseline and topline due to feedthrough of the triggering signal. This paper presents a new technique for reducing the trigger-induced distortions. A directional coupler is used to couple the trigger signal to the TD.

Andrews, J. R., Gans, W. L., **Pulsed wavemeter timing reference for sampling oscilloscope calibration,** *IEEE Trans. Instrum. Meas. Short Papers*, **IM-24,** No. 1, 82 (Mar. 1975).

Key words: oscilloscopes; pulsed wavemeter timing.

A pulsed wavemeter technique is described that is useful as a source of microwave frequency sine waves for the time base calibration of sampling oscilloscopes.

Andrews, J. R., Gans, W. L., **Time domain automatic network analyzer,** (Proc. Colloque International sur L'Electronique et la mesure, Paris, France, May 26-30, 1975), Paper in *La Mesure Electrique de Precision*, pp. 258-267 (Le Comité d'Organisation du Colloque International sur L'Electronique et la mesure, Paris, France, 1975).

Key words: attenuation; automated measurement; network analyzer; pulse; S parameters; time domain.

NBS has recently developed a Time Domain Automatic Network Analyzer (TDANA). It measures the S parameters of RF and microwave networks as a function of frequency using pulse measurement techniques. The signal source is typically a tunnel diode pulse generator with a 10-90 percent risetime of less than 20 ps. This generator produces a useful amplitude spectrum extending from dc to beyond 18 GHz. The receiver is a sampling oscilloscope with a 20 ps risetime. The oscilloscope is controlled by a minicomputer. The data measured by the oscilloscope is stored and processed in the minicomputer. The minicomputer averages the data to improve the signal to noise ratio, then Fourier transforms the time domain data into frequency domain data and calculates the S parameters. Exam-

ples of measurements are presented. They include the measurement of 40 dB attenuators to 12.5 GHz.

Ausloos, P., **Pulse radiolysis of alkanes in the gas-phase, ion-molecule reactions and neutralization mechanism of hydrocarbon ions,** (Proc. Symp. on Mechanisms of Hydrocarbon Reactions, Siófok, Hungary, June 5-7, 1973), Paper in *Mechanisms of Hydrocarbon Reactions*, F. Márta and D. Kalló, Eds., *Plenary Lecture* **3**, pp. 603-624 (1975).

Key words: charge recombination rate constants; cobalt gamma radiolysis; hydrocarbons; ion-molecule reaction; neutralization mechanisms; pulse radiolysis.

A discussion is presented of the fate of unreactive hydrocarbon ions in various selected gaseous systems. It is shown that experiments performed with the high radiation dose rates obtained in pulse radiolysis experiments have several advantages over conventional low dose rate experiments for the elucidation of the mechanism of homogeneous neutralization of unreactive hydrocarbon ions. This is so because the charged species has a much shorter life-time with respect to neutralization under high dose rate (pulse radiolysis) conditions, so that the reaction of the ions with minor impurities or accumulated products is much less probable than in low dose rate experiments. It is further shown through a few examples, that quantitative information about the rate constants of neutralization events and ion-molecule reactions can be obtained when the dose rate is high enough for neutralization and chemical reaction to be in competition. Once reliable rate constants for neutralization and ion-molecule reactions are derived, one can obtain a quantitative evaluation of the products which will be formed in the pulse radiolysis of a hydrocarbon gas mixture from a computer calculation.

Beaty, E. C., **Measurements of the energy and angular distribution of secondary electrons,** *Radiat. Res.* **64,** 70-79 (1975).

Key words: cross sections; electron impact; electrons, secondary; ionization.

Measurements have been made of the distribution in energy and angle of secondary electrons from ionizing collisions of electrons with several atoms and molecules. Such data have been published for a wide range of the relevant variables. Some of these measurements have now been repeated in other laboratories. Some recent interpretive efforts also reveal trends in the data that were not previously apparent.

Beers, Y., Howard, C. J., **The microwave spectrum of HO_2 near 65 GHz,** *J. Chem. Phys.* **63,** No. 10, 4212-4216 (Nov. 15, 1975).

Key words: HO_2; hydroperoxyl; microwave.

Using a Zeeman-modulated cavity spectrometer with a 10 sec time constant and a phase locked klystron, we have observed in the products of a discharge-flow system, Zeeman components of the six allowed zero-field lines at 65 070 ± 2, 65 082 ± 2, 65 098 ± 2, 65 373 ± 2, 65 397 ± 2, and 65 401 ± 2 MHz, and of one forbidden zero-field line at 65 369 ± 4 MHz. The Q of the Fabry-Perot cavity is about 10 000, and the magnetic field was swept from 0 − 30 G. Chemical tests indicate that the observed lines are due to HO_2. They have been assigned and least-squares fitted using a simple theoretical model to yield a value of 65 185 ± 2 MHz for the $1_{01} - 0_{00}$ asymmetric rotor transition frequency of HO_2, a value of − 208 ± 2 MHz for the linear combination $(\epsilon_{bb} + \epsilon_{cc})/2$ of elements of the electron spin-molecular rotation interaction tensor, a value of − 28 ± 2 MHz for the nuclear spin-electron spin Fermi contact interaction parameter σ, and a value of +4 ± 2 MHz for the spin-spin tensor interaction parameter λ. These constants are in excellent agreement with three less precise constants obtained from an earlier laser magnetic resonance study and have been confirmed by recent more accurate measurements of Saito.

Bender, P. L., **Laser measurements of the lunar distance,** *Rev. Geophys. Space Phys.* **13,** No. 3, 271-272, 291 (July 1975).

Key words: crustal movements; earth rotation; geophysics; lasers; lunar cartography; lunar gravity; moon; plate tectonics.

Progress since 1971 on laser measurements of the lunar distance is reported. The current status of analysis work based on lunar distance data is described. New lunar and geophysical results which have been obtained by the joint efforts of a number of different institutions are discussed briefly.

Berg, J. L., **Federal Privacy Act countdown—Is the private sector ready?,** *Infosystems* **22,** No. 7, 25-27 (July 1975).

Key words: privacy; privacy legislation; privacy planning.

Reporting on the joint NBS/MITRE workshop, *Planning for Action—the Privacy Mandate*, the article provides, in capsule form, a description of the workshop with specific attention to those comments of use to EDP managers.

Berg, N. J., Lieberman, A. G., **The effects of radiation-induced displacement damage on impurity conduction in gallium arsenide,** *J. Appl. Phys.* **46,** No. 8, 3475-3482 (Aug. 1975).

Key words: activation energy; compensation; epitaxial gallium arsenide; high energy neutron; impurity conduction; reciprocal Hall coefficient; transition regime; ^{60}Co gamma.

The effects of ^{60}Co γ-ray and high-energy neutron displacement damage on impurity conduction in epitaxial gallium arsenide were investigated. The activation energy (ϵ_2) associated with the transition regime of the impurity conduction process was found to increase by a factor of 5 as a result of ^{60}Co γ irradiation, and only by a factor of 1.6 for a comparable neutron irradiation. In addition, the ratio of the Hall carrier density at low and high temperatures, $(n_H)_{4K}/(n_H)_{300K}$, decreased by a larger amount for ^{60}Co γ irradiation than for neutron irradiation. The effects of neutron irradiation are explained in terms of increased compensation. For the case of ^{60}Co γ irradiation, it is postulated that a new donor level is introduced which does not participate in the impurity conduction process, it is found that ϵ_2 is proportional to ϵ_1 (the conduction-band activation energy) and varies inversely with neutral donor spacing in accord with the model proposed by Mikoshiba. Also ρ_{30}, the hopping regime resistivity, is found to vary inversely with the square of the free-carrier concentration and exponentially with the quantity $0.6/N_D^{1/3}a$.

Berger, M. J., Seltzer, S. M., Domen, S. R., Lamperti, P. J., **Stopping-power ratios for electron dosimetry with ionization chambers,** (Proc. Int. Symp. on Advances in Biomedical Dosimetry, Vienna, Austria, Mar. 1975), Paper in *Advances in Biomedical Dosimetry*, pp. 589-609 (International Atomic Energy Agency, Vienna, Austria, 1975).

Key words: absorbed dose; dosimetry; electrons; ionization chambers; standards; stopping power ratio.

In the course of an NBS absorbed-dose standards program, theoretical and experimental determinations have been made of the conversion factor C that relates the absorbed dose from electron beams to the ionization in an air cavity. The average medium/air stopping-power ratio—which is proportional to C—has been calculated as a function of the beam energy (1 to 60 MeV) and of the depth in a water phantom, and similar stopping-power ratios have also been obtained for other phantom materials (carbon, polystyrene, acrylic plastic, muscle). The conversion factor in graphite has been measured at energies between 15 and 50 MeV and depths between 0.9 and 51 g/cm² with the use of a calorimeter and a parallel-plate ionization chamber. These measurements were made with beams broadened by lead scattering foils with various thicknesses from 0.144 to 1.584 g/cm². The extrapolation of the results to zero scattering-foil thickness provided conversion factors that could be compared

with theoretical C-values for broad, parallel, monoenergetic electron beams. The agreement was found to be close (mean difference of 0.3% and r.m.s. difference of 0.8%). Comparisons have also been made with other C-values found in the literature and recommended by medical physics organizations. The overall conclusion can be drawn that the conversion factor is known reliably at the 1 percent level of accuracy.

Berke, J. G., **Procurement—The pull side of technology transfer,** (Proc. ASME 5th Intersociety Conf. on Environmental Systems, San Francisco, Calif., July 21-24, 1975), *75-ENAs-3*, pp. 1-4 (The American Society of Mechanical Engineers, New York, N.Y., 1975).

Key words: innovation; procurement; specifications; standards; technology; transfer.

Public procurement at the federal, state or local levels can be a major influence on the adaptation, implementation and transfer of technology. Through the procurement process, problems can be defined, prototypes can be tested, cost/benefits determined and finally the product can be bought. This final step is what has traditionally been lacking in the technology transfer process. This paper describes ongoing experiments, at the federal, state or local levels, aimed at determining the transfer potential of such market incentives as the use of performance specifications, life cycle costing, value incentive clauses, consensus standards and test methods versus the traditional lowest price for lowest acceptable quality.

Birky, M. M., **Review of smoke and toxic gas hazards in fire environment,** *Proc. Int. Symp. on Fire Safety of Combustible Materials, Edinburgh, Scotland, Oct. 15-17, 1975*, **1**, 231-252 (1975).

Key words: bioassay; combustion products; fire; hazard assessment; toxicity.

Fire statistics show that at least 50 percent of the fire related deaths can be attributed to "smoke inhalation." Detailed investigations of fire fatalities and autopsies of fire victims show that the interaction of carbon monoxide, pulmonary injury, alcohol and cardiovascular disease plays a role in many of these deaths.

The research efforts designed to assess the toxicological effects of products of thermal degradation can be divided into three broad categories: (1) assessment based on extensive chemical analysis, (2) assessment based on analyzing for specific toxicants and (3) assessment based on bioassay techniques frequently combined with analysis for a few selected toxicants.

Assessment categories 1 and 2 have mainly addressed the problem of the gaseous phase of the degradation products, with little consideration given to the particulate phase (smoke). These methodologies illustrate the limitation of basing a hazard assessment on the assumption that the toxicity of the fire environment is due solely to a few known toxicants. In addition, the particulate phase may play a predominant role in the inhalation toxicity that cannot be assessed with chemical analysis. One concludes that due to the complexity of the fire environment, an assessment of this hazard will require the combined efforts of toxicologist, chemists and combustion scientists.

Birmingham, B. W., Smith, C. N., **Cryogenics and the energy crisis,** *Cryogenics* **15**, No. 3, 115-118 (Mar. 1975).

Key words: coal gasification; cryogenics; energy crisis; hydrogen economy; LNG; superconducting electrical equipment and instrumentation.

This paper reviews some of the ways cryogenics can help solve the energy crisis. Five specific areas are covered: the use of LNG, the conversion of coal to fuel gas using oxygen from air separation plants, the use of superconductors in power plants and electrical transmission lines, superconducting instruments for geophysical exploration of new energy resources, and the Hydrogen Economy.

Blanc, R. P., **Availability and useability of computer communication networks,** *Proc. Seventh Int. Conf. on Systems Sciences, Honolulu, Hawaii, Jan. 8-10, 1974*, pp. 10-13 (1974).

Key words: computer networks; computer terminals; networking technology; value-added networks.

The technological characteristics of existing approaches to computer networking technology are reviewed for the purpose of identifying those features which lend themselves particularly well to the interconnection of computers, as well as computer terminals.

Branstad, D. K., **Encryption protection in computer data communications,** *Proc. Fourth Data Communications Symp., Quebec City, Canada, Oct. 7-9, 1975*, pp. 8-1—8-7 (1975).

Key words: communications; computer security; cryptography; data security; encryption; network security; security.

Encryption can be an effective process for protecting data during transmission within distributed computer systems and networks. The degree of protection provided by encryption depends on the encryption algorithm employed, the implementation of the algorithm and the administrative procedures regulating the use of algorithm. Additional security requirements of user identification, access authorization and security auditing may be satisfied by combining encryption technology with a network access control machine in a network security center. This paper presents an encryption algorithm for use in computer data communications and the security requirements that are satisfied by proper use of the algorithm. It also discusses the use of a network access control machine to enforce access restrictions for the network.

Buchbinder, B., Buchbinder, L. B., **The fire hazard analysis process at the National Bureau of Standards,** *Proc. Int. Symp. on Fire Safety of Combustible Materials, Edinburgh, Scotland, Oct. 15-17, 1975*, **1**, 156-161 (1975).

Key words: clothing flammability; fabric flammability; fire hazard; fire investigation; flammability testing; hazard analysis; hazard quantification.

The Office of Information and Hazard Analysis (OIHA) performs its hazard analysis function by means of a multi-faceted program combining in-depth case history investigation of fire accidents, laboratory experimentation, fire testing, and data analysis to identify and characterize specific hazards.

Hazard characterization serves to influence the formulation of basic fire research, to guide test method development for codes and standards, to identify data required to be collected, and to provide input to public education for fire safety. These functions are performed in concert with other United States government agencies, including the National Fire Prevention and Control Administration (NFPCA) in the Department of Commerce with which we have a close working relationship, and the Consumer Product Safety Commission which we support in product standard development.

The main portion of this paper defines the current fire hazard analysis process illustrated by results from the fabric flammability project, describes how this process is evolving into the more quantitative process of the future, and discusses the data needed for future hazard models.

Buchbinder, B., Mathers, W., **Preliminary indications from survey of U.S. household fire experience,** *Proc. 8th Annual Meeting Information Council on Fabric Flammability, New York, N.Y., Dec. 5, 1974*, pp. 174-178 (1975).

Key words: Census Bureau; Consumer Product Safety Commission; data; fire; households; injury; loss; National Fire Data System; National Fire Survey; survey.

A survey of over 33,000 U.S. households was conducted in April, 1974. It was sponsored by the National Bureau of Standards and the Consumer Product Safety Commission. This paper discusses the survey scope and the accuracy of the national estimates. Estimates are presented of the number of household-related fires, classified by such parameters as ignition source and room of origin. Property loss and injury estimates are given.

Buchbinder, B., **Pilot implementation of the Fire Incident System,** *Fire J.* **69,** No. 3, 65-69 (May 1975).

Key words: data; fire; fire incident system; fire service; incident reports; loss; National Fire Data System.

The Fire Incident System (FIS) is based on a data file of individual fire incident reports from the fire services. The pilot implementation of the Fire Incident System is an integral part of the National Fire Data System. This paper examines the objectives of the pilot project, describes the system and its participants, and discusses the project status.

Bussey, H. E., Richmond, J. H., **Scattering by a lossy dielectric circular cylindrical multilayer, numerical values,** *IEEE Trans. Antennas Propag.* **23,** No. 5, 723-725 (Sept. 1975).

Key words: cylinder scattering; electromagnetic scattering; lossy dielectric; multilayer cylinder; reference values; scattering.

The theoretical scattering solution for a plane wave incident normally on a lossy dielectric multilayer circular cylinder of infinite length is outlined. Numerical values of the modal scattering coefficient for TE and TM modes are given for several single and multilayer cylinders. Verifications of the results are described. The values may serve as reference data.

Cabana, A., Laurin, M., Lafferty, W. J., Sams, R. L., **High resolution infrared spectra of the ν_2 and $2\nu_1$ bands of $^{14}N^{16}O_2$,** *Can. J. Phys.* **53,** No. 19, 1902-1926 (1975).

Key words: equilibrium structure; ground state constants; infrared spectrum; nitrogen dioxide, $2\nu_1$ band; nitrogen dioxide, ν_2 band; upper state constants; vibration-rotation interaction constants.

The infrared spectra of two B type bands, ν_2 and $2\nu_1$, of $^{14}N^{16}O_2$ have been recorded under high resolution. Ground state combination differences from these bands have been combined with combination differences obtained in previous studies and eight pure rotational microwave transitions to yield improved ground state rotational constants. Upper state constants and band centers for the ν_2 and $2\nu_1$ bands are also reported. The $2\nu_1$ band contains internal intensity anomalies believed to arise from a weak Coriolis interaction with the much stronger $\nu_1+\nu_3$ band. Equilibrium rotational constants have been calculated. The equilibrium structure of the molecule is: $r_e=1.1945\pm0.0005$ Å and $\Theta_e=133.85\pm0.10°$. For the sake of comparison, effective, substitution, and average structures are also reported.

Cali, J. P., **Reference materials in clinical chemistry,** *Fed. Proc.* **34,** No. 12, 2123-2126 (Nov. 1975).

Key words: accuracy; accurate measurement in clinical chemistry; clinical chemistry; clinical reference materials; standardization.

Reference Materials (RM's) are necessary and critical components of measurement systems, especially useful in helping to achieve compatibility in large laboratory networks, such as those existing in clinical chemistry. What the measurement process is and how RM's fit into this process is discussed. The role of accuracy in helping achieve compatibility is explained and the role of RM's within an accurate measurement system is elucidated. Because RM's are the mechanism for transferring accuracy throughout a measurement network, the criteria for their production and certification are important. They include a knowledge and/or assurance of: purity, homogeneity, stability, continuity and availability of supply and information. Because measurement compatibility in clinical chemistry involves human life, only RM's of highest quality and integrity should be used. Clinical RM's should therefore bear a certificate (or guarantee). Minimal requirements for such certification are discussed.

Currently available clinical RM's from the National Bureau of Standards (NBS) are listed.

Casella, R. C., Rowe, J. M., Trevino, S. F., **Determining the number of independent real parameters in the phonon dynamical matrix,** *Phys. Rev. B* **12,** No. 10, 4573-4574 (Nov. 15, 1975).

Key words: dynamical matrix; matrix, dynamical; phonon dynamical matrix; real parameters.

We apply the algorithm developed earlier by one of us to several illustrative examples and compare with results obtained by Warren and Worlton where difficulties occur as noted by these authors.

Cataland, G., Plumb, H. H., **Fixed points: Superconductive transition temperatures of lead and indium,** *Metrologia* **11,** 161-163 (1975).

Key words: acoustical thermometry; fixed points; lead and indium transition temperatures; low temperature fixed points; low temperature thermometry; superconducting transition temperatures of lead and indium.

This note presents the temperature values for the superconductive transition fixed points (T_c) of lead and indium. Values of T_c derived by interpolations on the NBS P(2-20K) 1965 scale are given. Determinations of isotherms by the NBS acoustical thermometer produced T_c's of 7.199_0 K $\pm$ 1.3 mK for lead and 3.414_2 K $\pm$ 1.3 mK for indium.

Cezairliyan, A., Coslovi, L., Righini, F., Rosso, A., **Radiance temperature of molybdenum at its melting point,** (Proc. Symp. European Conf. on Temperature Measurement, Teddington, England, Apr. 9-11, 1975), Chapter 4 in *Temperature Measurement*, B. F. Billing and T. J. Quinn, Eds., Inst. Phys. Conf. Ser. No. 26, pp. 287-296 (Institute of Physics, London, England, 1975).

Key words: melting point; molybdenum; radiance temperature; wavelength.

Radiance temperature (at two wavelengths, 653 and 995 nm) of molybdenum at its melting point was measured using a subsecond-duration-pulse heating technique. Specimens in the form of strips with initially different surface roughnesses were used. The results do not indicate any dependence of radiance temperature (at the melting point) on initial surface or system operational conditions. The average radiance temperature at the melting point of molybdenum is 2531 K at 653 nm and 2331 K at 995 nm, with a standard deviation of about 0.6 K and a maximum absolute deviation of 1.2 K in both cases. The total inaccuracy in radiance temperature is estimated to be not more than $\pm$8 K.

Cezairliyan, A., McClure, J. L., **A subsecond pulse heating technique for the study of solid-solid phase transformations at high temperatures: Application to iron,** *High Temp. Sci.* **7,** 189-196 (1975).

Key words: high-speed measurement; high temperature; iron; phase transformation; thermodynamics.

A system based on an accurate pulse heating technique is described that can be used for investigations of solid-solid phase transformations at temperatures above 1500 K. The system is capable of heating the specimen from room temperature to its melting point

in less than 1 s and of measuring the pertinent experimental quantities every 0.4 ms with a full-scale signal resolution of approximately one part in 8000. Specimen temperature is measured with a high-speed photoelectric pyrometer and recordings of experimental quantities are made with a high-speed digital data acquisition system. Application of the technique to investigations at the $\gamma \rightarrow \delta$ transformation point of iron is described. Measurements yielded the following results: 1683 K for the transformation temperature, 890 J · mol^{-1} for the transformation energy, and 0.36 for the normal spectral emittance (at 0.65 μm) at the transformation point.

Cezairliyan, A., Righini, F., **Measurement of melting point, radiance temperature (at melting point), and electrical resistivity (above 2,100 K) of zirconium by a pulse heating method,** *Rev. Int. Hautes Temp. Refract.* **12,** No. 3, 201-207 (1975).

Key words: electrical resistivity; high-speed measurements; high temperature; melting point; normal spectral emittance; radiance temperature; zirconium.

A subsecond duration pulse heating method is used to measure the melting point, radiance temperature (at 650 nm) at the melting point, and electrical resistivity (above 2,100 K) of zirconium. The results yield a value of 2,128 K for the melting point on the International Practical Temperature Scale of 1968. The radiance temperature (at 650 nm) of zirconium at its melting point is 1,940 K, and the corresponding normal spectral emittance is 0.367. At 2,100 K electrical resistivity is 128.7×10^{-8} Ωm. Estimated inaccuracy is: 8 K in the melting point and in the radiance temperature, and 3 percent in the normal spectral emittance and in the electrical resistivity.

Chow, L. C., Brown, W. E., **Topical fluoridation of teeth before sealant application,** *J. Dent. Res.* **54,** No. 5, 1089 (Sept.-Oct. 1975).

Key words: dicalcium phosphate dihydrate; fluorapatite; fluoride; pit and fissure sealant; tooth enamel.

Pyrolysis experiments revealed that small amounts of $CaHPO_4 \cdot 2H_2O$ are formed in enamel during conditioning of teeth with 50 percent H_3PO_4 for pit-and-fissure sealants. Unlike the $Ca(HPO_4)_2 \cdot H_2O$ which forms on the surface during the pretreatment, $CaHPO_4 \cdot 2H_2O$ s only sparingly soluble in water and would not be rinsed away in the clinical situation. The presence of $CaHPO_4 \cdot 2H_2O$ in enamel is undesirable because it may slowly dissolve and loosen the sealant. On the other hand, because of its high reactivity with fluoride, the $CaHPO_4 \cdot 2H_2O$ may be converted to $Ca_5(PO_4)_3F$ before sealant application, thereby further reducing caries tendency. Several basic-phosphate-fluoride solutions which had previously been shown to produce $Ca_5(PO_4)_3F$ when reacted with $CaHPO_4 \cdot 2H_2O$ were applied to acid etched enamel samples. Significant enamel-fluoride uptakes were obtained. SEM examinations of the samples show that these fluoride treatments produced no discernible deposits of CaF_2 on the surface which might interfere with sealant penetration and bonding.

Chwirut, D. J., **Tensile creep of angle-plied boron/epoxy laminates,** *J. Test. Eval.* **3,** No. 6, 442-448 (1975).

Key words: angle-plied laminates; boron/epoxy; composite materials; creep; viscoelasticity, linear and nonlinear.

Tensile creep tests were performed at 75 °F (24 °C) and 300 °F (149 °C) on 26 specimens cut from $\pm$30-deg and $\pm$45-deg laminates of boron/epoxy composite material to characterize the creep behavior of these materials. A linear viscoelastic laminate theory proposed by McQuillen was compared with the experimental data for the tests run at 75 °F (24 °C). The predicted creep strains differed greatly from the measured values, indicating that the linear theory is not applicable to laminates with these filament orientations. A general creep equation of the form $\epsilon = k\sigma^m t^n$ was fitted to the experimental data with excellent correlation. The stress exponents m varied from 1.79 to 5.17 for the four series of tests, thus characterizing the nonlinear behavior of boron/epoxy laminates with these filament orientations.

Clifton, J. R., Foster, B. E., Trattner, E., Clevenger, R. A., **Dimensional stability of masonry walls,** *Am. Soc. Test Mater. Spec. Tech. Publ.* **589,** pp. 42-75 (1975).

Key words: brick; dolomitic mineral; masonry; mortars (materials); walls.

To assess the contribution of dolomitic limes to dimensional stability of masonry construction, 65 brick masonry walls, 34 by 40 by 8 in (0.86 by 1.0 by 0.20 m), were constructed. The program involved the following design variables: 6 hydrated limes ranging in autoclave expansion from 0.10 to 15.1 percent; 2 types of brick, one with high water absorption and high autoclave expansion, and the other with low water absorption and insignificant autoclave expansion; and, 2 mortars of cement:lime:sand proportions of 1:1:6 and 1:2:9 by volume. Half of the walls were subjected to temperature and moisture cycles, performed indoors, for 3 1/2 years; the other half were tested outdoors for 14 years. Half of the indoor and outdoor exposed walls were spring loaded at 25 psi ($1.7 \times 10^5 N/m^2$). Observed expansion of the walls was found to be related to the potential expansions (as measured by the autoclave test) of the limes. The largest wall expansion took place with the following combination: high potential expansive lime; stable, low absorption brick; unloaded wall; and, 14 year outdoor exposure. In the 14-year outdoor exposure, loss of bond and resulting damage from freezing were complicating factors. The effects of lime, mortar mix, brick, loading, and exposure on the dimensional instability of the masonry walls are discussed.

Clough, R. B., **The effects of specimen size and microstructure on the Larson-Miller parameter,** *Scr. Metall.* **9,** No. 12, 1325-1329 (1975).

Key words: crack nucleation; elevated temperature; failure prediction; Larson-Miller parameter.

There is a great need for the standardization of methods for predicting elevated temperature material failure. Generally, metallurgical instability limits the accuracy of these methods. Quantitative metallurgical models predicting lifetimes from microscopic parameters are virtually nonexistent. Here an elementary metallurgical model of the well-known Larson-Miller parameter is developed, based on the thermally-activated nucleation of Griffith-type cracks. The concept of the activation volume for fracture is introduced. The analysis permits calculation of the size and surface energy of crack nuclei from stress-rupture curves. These are computed theoretically from stress rupture data of typical high temperature iron- and nickel-base alloys. No independently measured nuclei size data exists, but the surface energies agree with energies obtained from similar alloys by direct measurement. The analysis also predicts that the stress-rupture lifetime is a sensitive function of crack nucleus surface energy, and gives a quantitative rationale for the invariability of the constant in the Larson-Miller parameter predicted from microstructural values.

Cotton, I. W., **Cost-benefit analysis of interactive systems,** *Proc. Second Jerusalem Conf. on Information Technology, Jerusalem, Israel, July 29-Aug. 1, 1974,* pp. 729-746 (1974).

Key words: cost-benefit analysis; cost-effectiveness; economics; interactive systems; performance evaluation.

This report assesses the state-of-the-art in cost-benefit analyses of interactive systems and suggests an approach for developing improved methodology. Cost-benefit analyses are distinguished from analyses of system performance in that the latter are directed at optimizing system performance at a given level of investment, while the former are directed at justifying the investment itself.

Methods of analyzing the performance and costs of computer systems in general and interactive systems in particular are

discussed. With this information it is shown how cost-effectiveness analyses may be performed. The next crucial step is to conduct benefit analysis, an ill-defined art. The results of benefit analysis must be combined with cost-effectiveness analysis in order to perform the desired cost-benefit analysis.

An experimental methodology is suggested for better performing benefit analyses of interactive systems. A more rigorous formulation of the cost-benefit procedure is then outlined. No attempt is made in this report to actually perform such an analysis.

Cotton, I. W., **Remark on stably updating mean and standard deviation of data,** *Commun. ACM* **18,** No. 8, 458 (Aug. 1975).

Key words: data analysis; mean; standard deviation; statistics; updating estimates.

Hanson's article describes an elegant procedure for recomputing the weighted mean and standard deviation of a series of numbers when new values are added. As he observes, in the case of unit weights a considerable simplification occurs; however, he does not present the simplest equations for this case. This remark derives simple results for updating mean and standard deviation in the case of unit weights, when only the previous values of mean, standard deviation, number of occurrences and the new datum are known.

Crawford, E. A., Phelps, A. V., **Formative time lags in CO_2 laser discharges,** *Appl. Phys. Lett.* **25,** No. 1, 59-61 (July 1, 1974).

Key words: CO_2 laser; electrical discharge; gas mixture; time delay.

Time lags for the growth of power input, i.e., formative time lags, have been measured in typical CO_2 laser gas mixtures at pressures from 200 to 760 torr using parallel plane electrodes with the 1- and 2-cm gaps illuminated by a trigger discharge. The measured time lags are about twice the values predicted using a single avalanche growth model and theoretical ionization and attachment coefficients.

Cullen, W. C., **The composite roofing membrane,** *The Roofing Spec.* **3,** No. 5, 17-21 (Sept. 1975).

Key words: application procedures; built-up roofing systems; composite membrane; composition; performance criteria.

The Composite Roofing Membrane is an indispensable component of the built-up roofing system. The paper reviews the functions of the membrane's components and the importance of application procedures on the quality and performance of the membrane. The impact of the development of performance criteria for the composite roofing membrane is described.

Danos, M., **Relativistic nuclear physics, why and how?,** (Proc. Int. Conf. on Interaction Studies in Nuclei, Mainz, Germany, Feb. 17-20, 1975), Paper in *Interaction Studies in Nuclei*, H. Jochim and B. Ziegler, Eds., pp. 885-910 (North-Holland Publishing Co., The Netherlands, 1975).

Key words: axiomatic field theory; composite particles; Haag's theorem; nuclear structure; quantum field theory; relativistic nuclear physics.

It is proposed that by this time the development of physics has progressed to a point where one can tackle the "hydrogen atom" problem of nuclear physics, viz., a description of the deuteron "from first principles." This requires to formulate the problem in terms of strong interaction relativistic field theory. The contemporary work is done instead almost exclusively in terms of the quasi-relativistic framework of effective Lagrangian theory. The inherent inaccuracies of this framework are reviewed. A framework for actually solving the relativistic field theory problem is described. It requires inescapably to consider the composite structure of the deuteron. The nature of the stationary solutions is discussed; their relation to the results of the covariant treatment is explained, and the relevance to certain theorems of field theory is pointed out.

Daywitt, W. C., Kanda, M., **G/T measurement errors with radio stars,** *Proc. IEEE Int. AP-Symp., Urbana/Champaign, Ill., June 2-5, 1975, Session* **20,** pp. 460-463 (1975).

Key words: antenna gain; G/T; radio star; satellite communications.

This talk highlights often-overlooked or poorly treated aspects in G/T error analyses for satellite communication earth terminals. In particular, correction factors due to star size, differential system temperature, antenna pointing, and refractive attenuation used in G/T measurements are discussed in detail.

Drullinger, R. E., Hessel, M. M., Smith, E. W., **New laser measurement techniques for excited electronic states of diatomic molecules,** *Proc. Megeve Laser Spectroscopy Conf., Megeve, France, June 23-27, 1975, Lecture Notes in Physics*, 91-99 (1975).

Key words: diatomic mercury; excimer molecules; fluorescence; lasers; NaK molecule; spectroscopy.

This paper will briefly outline several new laser measurements techniques which we have developed for the analysis of excited electronic states of diatomic molecules. For molecules which have bound ground states, a visible laser is used to selectively excite a single vibration-rotation level in the electronic state of interest. We then use DC Stark effect, RF double resonance and various fluorescence techniques, as discussed in Sections I and II, to obtain excited state dipole moments, lifetimes, quenching cross sections, transition moments as a function of internuclear distance, and other molecular structure data. We have also developed new laser excitation techniques and used optical double resonance methods for excimer molecules which have repulsive ground states and are bound only in their excited states. These techniques, discussed in Sections III and IV, have been used to obtain potential energy curves, *f*-values, lifetimes and various kinetic rates.

Dunn, G. H., **Collision studies with ion storage techniques,** (Proc. Int. Conf. on Atomic Physics, Heidelberg, Germany, July 1974), Paper in *Atomic Physics* **4,** pp. 575-587 (Plenum Press, New York, N.Y., 1975).

Key words: electrons; ion trap; positive molecular ions; recombination.

This paper is a report on recombination measurements made by studying electron-ion collisions in ion traps. We briefly review two-body recombination processes between electrons and ions and the means by which they have previously been measured. The trapping scheme and its realization for collision work is discussed, and results for some recombination measurements are given.

Dziuba, R. F., Field, B. F., Finnegan, T. F., **Cryogenic voltage comparator system for 2e/h measurements,** *IEEE Trans. Instrum. Meas.* **IM-23,** No. 4, 264-267 (Dec. 1974).

Key words: cryogenic resistor; current comparator; Josephson device; microstripline; microwave coupling; SQUID; superconducting switch; tunnel junction; voltage standard.

The design and operation of a cryogenic voltage comparator system for precision 2e/h measurements is described. Major improvements embodied in the new 2e/h system include the use of (1) a single microstripline-coupled Josephson tunnel junction to obtain usable step voltages up to 10 mV at 10.0 GHz, (2) a cryogenic voltage divider comprised of two resistors whose ratio is calibrated with a low temperature dc current comparator, (3) a SQUID null detector, and (4) superconducting switching. The accuracy of the present 196:1 divider system is estimated to be about 2 parts in 10^8 on the basis of preliminary tests and is limited by resistor self-heating during calibration.

Dziuba, R. F., Sullivan, D. B., **Cryogenic direct current comparators and their applications,** *IEEE Trans. Magn.* **MAG-11,** No. 2, 716-719 (Mar. 1975).

Key words: cryogenic resistors; current comparators; low temperature; shielding; SQUID; superconducting shield; superconductivity.

Cryogenic direct current comparators, utilizing superconducting shields and Superconducting QUantum Interference Devices (SQUID's), provide current ratios of up to 100/1 or higher with accuracies of $\leq 1 \times 10^{-9}$ and current resolutions of $\leq 6 \times 10^{-11}$ A. Two types of comparators differing in the shielding arrangement of the ratio windings are described. One type consists of unit windings inside a seamless Pb tube; the other consists of multi-turn ratio winding within an overlapping toroidal superconducting shield. For both shielding configurations, SQUID's serve as flux sensors for the comparators. The application of these comparators to the measurement of resistance ratios is described.

Engen, G. F., **Automated calibration of directional-coupler-bolometer-mount assemblies,** *IEEE Trans. Microwave Theory Tech.* **MTT-23,** No. 12, 984-990 (Dec. 1975).

Key words: automation; calibration; directional coupler; microwave; microwave power.

Although the application of automated methods to power calibration problems in the UHF and microwave region has been described by a number of authors, the primary orientation has been towards the calibration of bolometer mounts and similar items. Little has been published on the problem of calibrating directional-coupler-bolometer-mount assemblies, which also play a major role in the calibration and measurement of UHF and microwave power.

This paper develops a theoretical basis for several different approaches to this measurement problem.

Engen, G. F., **Automated calibration of directional-coupler-bolometer-mount assemblies,** *Proc. IEEE-MTT-S Int. Microwave Symp., Palo Alto, Calif., May 12-14, 1975,* pp. 85-97 (Institute of Electrical and Electronics Engineers, Inc., Piscataway, N.J., May 1975).

Key words: calibration; calibration factor; directional coupler; measurement; microwave; microwave power.

Although the application of automated methods to power calibration problems in the UHF and microwave region has been described by a number of authors, the primary orientation has been towards the calibration of bolometer mounts and similar items. Little has been published on the problem of calibrating directional-coupler-bolometer-mount assemblies, which also play a major role in the calibration and measurement of UHF and microwave power.

This paper describes several approaches to this measurement problem.

Evenson, K. M., **Frequency measurements in the optical region and the speed of light,** (Proc. ICO Conf. Optical Methods in Science and Industrial Measurements, Tokyo, Japan, Aug. 26-30, 1974), *Japan J. Appl. Phys.* **14,** Suppl. 14-1, 1-10 (1975).

Key words: laser frequency measurements; speed of light.

Since the advent of the laser and saturated absorption locking of the laser, the extension of radio frequency technology into the optical region has produced exciting new results, such as a 10 000 fold increase in the resolution of spectroscopy in this region and a new value of the speed of light, 100 times more accurate than the previously accepted value. This paper will describe the techniques and results achieved.

Evenson, K. M., Howard, C. J., **Laser magnetic resonance spectroscopy,** *Laser Spectrosc.*, pp. 535-540 (1975).

Key words: CH; free radical; HCO; HO_2; laser magnetic resonance; OH; pollution.

Laser magnetic resonance spectroscopy provides one of the most sensitive techniques ever devised for the detection of free radicals such as OH, CH, HO_2, and HCO. Paramagnetic molecules inside a laser cavity are Zeeman tuned into coincidence with the laser frequency and a decrease in laser power is detected. With this technique, the reaction rates of free radicals can be measured in a reaction flow system.

Evenson, K. M., Petersen, F. R., **Stabilized lasers and applications,** *Proc. Physics of Quantum Electronics Summer School, Crystal Mountain, Wash., July 8-20, 1973,* pp. 367-436 (1975).

Key words: laser frequency measurements; laser strainmeter; saturated absorption spectroscopy; speed of light; the meter.

Three papers are reproduced which summarize some applications and uses of highly stabilized lasers and applications. Laser frequency measurements, the speed of light, a redefinition of the meter, ultrahigh resolution saturated absorption spectroscopy, the design and operation of a methane absorption stabilized laser strainmeter are all discussed.

Evenson, K. M., Petersen, F. R., Wells, J. S., **Speed of light from direct laser frequency and wavelength measurements: Emergence of a laser standard of length,** *Laser Spectrosc.*, pp. 143-146 (1975).

Key words: laser frequency; laser wavelength; length standard; speed of light.

Recent frequency and wavelength measurements of a methane stabilized laser yield a value of the speed of light 100 times less uncertain than the previously accepted value. Various possibilities using lasers as radiation sources for a new length standard are discussed. One possibility is to fix the value of the speed of light in the redefinition of the meter.

Fechter, J. V., Pezoldt, V. J., Persensky, J. J., Lepkowski, J. R., **Study of the National Standards for Directional and Other Official Signs. Overview of their adequacy,** *Report No. FHWA-RD-75-118,* 75 pages (Available from the National Technical Information Service, Springfield, Va., 22161, Oct. 1975).

Key words: driver information; highway; highway signing; human factors; information displays; standards.

In 1969 the Federal Highway Administration (FHWA) issued National Standards for Directional and Other Official Signs allowing owners of privately-operated scenic and historical sites to erect directional signs in a zone extending from the edge of the right-of-way to a distance 660 ft *(201.2 m)* beyond. Objectors to these Standards sought increases in the height, length, total area, and number of signs allowed. FHWA requested the assistance of the National Bureau of Standards (NBS) to respond to these requests and to evaluate the Standards with respect to the needs of motorists. NBS reviewed pertinent literature and analyzed hypothetical Standards-conforming signs. The analysis showed that the sign dimensions needed to display legible messages vary considerably as the values of each design variable (e.g., vehicle speed) are changed. For many speeds, sign locations, and driver characteristics, Standards-conforming signs are inadequate. The following conclusions were reached: (1) the Standards should require that sign characters be legible at the levels of visual acuity required by state driver licensing regulations, (2) maximum sign size should be specified in terms of the visual angle subtended, rather than as a maximum physical size, and (3) technical material does not support any change to the number of signs allowed to the spacing between signs, or to the spacing from signs to interchanges or exits.

Finnegan, T. F., Toots, J., Wilson, J., **Frequency-pulling and coherent-locking in thin-film Josephson oscillators,** (Proc. 14th Int. Conf. on Low Temperature Physics, Helsinki, Finland, Aug. 14-20, 1975), Paper in *Low Temperature Physics* **LT-14,** N. Krusius and N. Vuorio, Eds., **4,** 184-187 (North Holland Publishing Co., Amsterdam, 1975).

Key words: frequency source; Josephson radiation; Josephson tunnel junction; junction array; microstripline-coupling; thin-film device.

The results of a continuing study of the microwave radiation emitted by pairs of Josephson tunnel junctions simultaneously coupled to each other and an external microwave source are reported. Injection-locking of the junctions was observed and some qualitative features of the phenomenon are discussed.

Fong, E., **A benchmark test approach for generalized data base software,** *Proc. COMPCON fall Conf. Digest, Washington, D.C., Sept. 8-10, 1975,* 7 pages (1975).

Key words: benchmark testing; data base management; performance measurement; test data bases; test transactions.

A benchmark test approach for generalized data base software is described. Although the benchmark test has been designed to experiment on one specific data base management system, the approach is rather general and applicable to many data base management systems that are currently available. The benchmark test consists of the specification of a test data base and the specification of a set of processing transactions to exercise the candidate software on the test data base. This benchmark test can be used both to measure the performance of a data base management system, and as a saturation test. The two parameters to be used in the saturation test are data base size and workload. The data base size is varied by increasing the number of records within the test data base. The workload is varied analytically via a queueing model.

Forman, R. A., Thurber, W. R., Aspnes, D. E., **Second indirect band gap in silicon,** *Solid State Commun.* **14,** No. 10, 1007-1010 (1974).

Key words: band gap; band structure; electronic structure; energy bands; optical properties; silicon.

We report the first observation of the $\Gamma_{25'} \rightarrow L_1$ (second indirect) transition in Si based on optical absorption studies. The energy, (1650 $\pm$ 10) meV, measured for this critical point shows that there remains a large discrepancy between theoretical band structure calculations and experimental results for this material.

Gallagher, A., **Noble-gas broadening of the Li resonance line,** *Phys. Rev. A* **12,** No. 1, 133-138 (July 1975).

Key words: line broadening; lithium; noble gases.

The normalized fluorescence spectrum of the Li 6708-Å resonance line perturbed by the noble gases has been measured for 100 Å either side of the resonance line, at a temperature of 400 $\pm$ 10 °C. The noble-gas pressure range of 100-1800 torr was investigated. It was observed that the line wings scale linearly with this pressure for $2 < |\Delta\lambda| < 100$ Å, and it was demonstrated that a Lorentzian-broadened line core can be observed for this pressure range. The Li density was $\sim 10^{16}/cm^3$ and was varied to establish the fluorescence spectrum in the limit of no radiation entrapment. The central region of the line has been measured with high resolution and compared to calculated profiles due to the various fine structure and isotopic line components, each broadened by a convolution of Lorentz, Doppler, and instrumental profiles. The shift and Lorentz broadening rates, as well as the wavelengths for transition to non-Lorentzian behavior, are reported. In contrast to the heavier alkali-metal-noble-gas cases, no distinctive far-wing features such as satellites or sharp inflections are observed. This is consistent with the much larger collision velocities for the Li case.

Gebbie, K. B., Steinitz, R., **Comparison of Hα and Ca II H and K spectroheliograms as a diagnostic probe,** (Proc. Int. Astronomical Union Symp. on Chromospheric Fine Structure, Surfers' Paradise, Qld. Australia, Sept. 1973), Paper in *Chromospheric Fine Structure,* R. Grant Athay, Ed., No. 56, 55-63 (Reidel Publishing Co., Boston, Mass., 1974).

Key words: Ca II; Hα; solar chromosphere; spectral line formation.

The line formations of Hα and Ca II H and K are compared in order to differentiate the various mechanisms giving rise to observable contrasts in the emergent intensities. Table II summarizes the criteria for distinguishing between horizontal spatial variations in temperature, density, and turbulent velocity.

Glaze, D. J., Hellwig, H., Allan, D. W., Jarvis, S., Jr., Wainwright, A. E., **Accuracy evaluation and stability of the NBS primary frequency standards,** *IEEE Trans. Instrum. Meas.* **IM-23,** 489-501 (Dec. 1974).

Key words: accuracy; accuracy evaluations; cavity phase shift; cesium beam tube; frequency stability; interaction length; phase noise; primary frequency standards; Ramsey cavity.

The National Bureau of Standards has two primary standards for frequency and the unit of time. They are both cesium devices and are designated NBS-4 and NBS-5. The design of NBS-5 is discussed in detail, including its relationship to its predecessor NBS-III, and a brief description of NBS-4 is given. NBS-4 and NBS-5 have been used since January 1973 for a total of twelve calibrations of the NBS Atomic Time Scale.

The application of pulsed microwave excitation, and the use in the accuracy evaluations of frequency shifts due to known changes in the exciting microwave power are discussed. Measurements of the atomic velocity distributions are reported.

A stability of 9×10^{-15} derived from the comparison of NBS-4 and NBS-5 is reported for averaging times of 20 000 s, and data on accuracy are given. Results obtained to date give an evaluated accuracy of $1\text{-}2 \times 10^{-13}$ with indications that this accuracy may be improved in the future.

The bias-corrected frequencies of NBS-4 and NBS-5 agree to within $(1 \pm 10) \times 10^{-13}$ with the value obtained for NBS-III in 1969—which value is preserved in the rate of the NBS Atomic Time Scale.

Goldman, A. J., **The adequacy of management science technology for nonmilitary applications in the Federal Government,** (Proc. Workshop on Management Science in the Federal Government, Washington, D.C., Sept. 18, 1969), Chapter 6 in *Management and Policy Science in American Government,* M. J. White, M. Radnor, and D. A. Tansik, Eds., Part III, pp. 135-170 (Lexington Books, D. C. Heath & Co., Lexington, Mass., 1975).

Key words: management science; mathematical models; numerical analysis; operations research; systems analysis.

The "technology" of management science (MS) is here broadly construed to include physical equipment (e.g., high-speed computers), formal techniques (such as linear programming), paradigms and insights from various disciplines, and at the most basic level the analytical aptitudes of the management scientist. A middle ground is struck between those who consider this technology adequate and sound for the applications in question, and those who regard it as relatively useless for the nonquantitative value-laden problems facing nonmilitary government agencies. The discussion of adequacy and soundness includes the elements of: practical availability of methods and data (the technology's "raw material"); soundness in actual employment; and usefulness in principle when values and/or qualitative considerations are prominent. Some speculative comments are of-

fered concerning the disparity, between promise and actuality, in MS contributions to governmental decision-making and operating procedures. In particular, some principal advantages of MS technology seem subject to considerable negation by typical attributes of large organizations.

Graminski, E. L., **Problems and potentials in paper recycling,** (Proc. National Materials Conservation Symp. on Resource Recovery and Utilization, Gaithersburg, Md., Apr. 29-May 1, 1974), Paper in *Resource Recovery and Utilization*, H. Alter and E. Horowitz, Eds., *Am. Soc. Test. Mater. Spec. Tech. Publ.* **592,** pp. 132-139 (American Society for Testing and Materials, Philadelphia, Pa., 1975).

Key words: market pulp; paper, waste; pulp, secondary; recycled paper; secondary pulp; waste paper.

The U.S. consumed more than 60 million tons of paper and paperboard in 1973, about 20 percent of which was recycled. Steel is the only product that is consumed in larger quantities than paper. The principal disincentives for paper recycling are (1) the ready availability of virgin wood fibers, (2) lack of research on recycling of paper, (3) economics favor the use of virgin fibers, and (4) contaminants in wastepaper present major problems in recycling. In spite of the large amount of wastepaper that is available, a wastepaper shortage occurred in 1973 and has continued into 1974 because of problems in collection, fluctuation of the wastepaper market, and lack of manufacturing capacity. It is anticipated that about 32 million tons of paper and paperboard are available for recycling. About 130 pulp mills with a capacity of 600 tons per day would be needed to recycle this amount of wastepaper, which would produce about 24 million tons of recycled paper. The capital for building these mills is not available, and if a large number of secondary fiber mills were built immediately, it would create chaos in the virgin fiber industry. It is suggested that market pulp mills, located in or near large municipalities, be erected as needed to provide the need for more market pulp. This secondary pulp would be available to many mills that now are not equipped to process wastepaper.

Gravatt, C. C., Allegrini, I., **A new light scattering method for the determination of the size distribution of particulate matter in air,** (Proc. 3rd Int. Clean Air Congress (IUAPPA), Dusseldorf, W. Germany, Oct. 8-12, 1973), Paper in *Proceedings of the 3rd International Clean Air Congress*, pp. C3-C5 (Verlag GMBH, Dusseldorf, W. Germany, 1973).

Key words: air pollution; light scattering; particulate matter.

An instrument has been developed which determines the size distribution of particulate matter in air in essentially real time by a forward lobe light scattering method. The basic concept involves the simultaneous measurement of the intensity of light scattered by a single particle at two small scattering angles. The ratio of the two intensities is a direct measure of the size and is fairly independent of the index of refraction of the particle. Numerical solutions of the Mie equations for spheres have indicated that the sizing error by this method is no greater than 15 percent for the range of particle sizes from 0.1 to 10 μm for essentially all possible indices of refraction. In addition, techniques have been found which extend the lower limit of size determination to 0.05 μm and which may permit some degree of chemical characterization of the particle.

Greenberg, O. W., Nelson, C. A., **Composite models of leptons,** *Phys. Rev. D* **10,** No. 8, 2567-2573 (Oct. 15, 1974).

Key words: composite model of leptons; electron number; leptonic quarks; lorks; muon-electron universality; muon number; neutrino quarks; strong interactions; three triplet model.

We give ten criteria for composite models of leptons, and present two models which satisfy a number of these criteria. Both models use three triplets of leptonic analogs of quarks which we call "leptoquarks"; the first model uses fractionally charged leptoquarks and the second model uses integrally charged ones. In the second model, leptoquarks and quarks could be identical and there is a possibility of unifying the description of leptonic and hadronic phenomena. Both models assign leptons to nonsinglet representations of SU(3)″. A plausible SU(3)″ mass formula allows the known leptons to be less massive than baryons if leptoquarks and quarks are identical.

Greer, S. C., Hocken, R., **Thermal expansion near a critical solution point,** *J. Chem. Phys.* **63,** No. 12, pp. 5067-5072 (Dec. 15, 1975).

Key words: consolute point; critical exponent α; critical phenomena; critical solution point; density; gravity effects; mixture, binary; mixture, liquid; nitroethane; thermal expansion; 3-methylpentane.

We report precise measurements of the density as a function of temperature in the one-phase region near the consolute point in nitroethane + 3-methylpentane. We find evidence of the critical anomaly in the thermal expansion, but are not able to determine a unique value for the critical exponent α. We have performed computer experiments to determine under what conditions α could be extracted from thermal expansion data.

Hamilton, C. A., Phelan, R. J., Jr., Day, G. W., **Pyroelectric radiometers,** *Opt. Spectra* **9,** No. 10, 37-38 (Oct. 1975).

Key words: electrically calibrated; pyroelectric; radiometer.

The performance and detailed operation of an electrically calibrated pyroelectric radiometer are discussed.

Hammond, H. K., Hsia, J. J., **Evaluation of instrument tolerances for 75° gloss,** *Tappi Notes to Editor* **58,** No. 11, 143-144 (Nov. 1975).

Key words: gloss; optical properties; tolerances.

The instrument tolerances of the published TAPPI method for 75° specular gloss are unnecessarily strict. The 1954 report of Zabel and Wink on which the tolerances were based has been re-examined. Improvement in the photometric linearity on instruments and a statistical approach to the combined effect of a number of sources of uncertainty, reveal that if the goal for overall uncertainty is still to be one gloss unit, geometric tolerances could be increased by a factor of 7.

Dimensions and tolerances are all based on the dimension "d" rather than the unit distance of which d is only a part. All dimensions have been rounded to simple figures. The proposed dimensions and tolerances are tabulated.

Hellwig, H., Wainwright, A. E., **Submicrosecond time transport with a rubidium portable clock,** *Proc. 29th Annual Symp. on Frequency Control, Atlantic City, N.J., May 28-30, 1975*, pp. 384-386 (1975).

Key words: clock; frequency stability; frequency standard; time comparison.

Based on a commercially available rubidium standard, the National Bureau of Standards (NBS) developed a portable rubidium clock. Technical modifications which improve the temperature and magnetic environment characteristics allow stabilities in the 10^{-12} range under typical clock transport conditions. The physical size is such that the clock can be carried as hand baggage on commercial airlines allowing up to 18-hours continuous battery operation.

Hessel, M. M., Drullinger, R. E., Broida, H. P., **Chemiluminescent reactions in a heat-pipe oven,** *J. Appl. Phys.* **46,** No. 5, 2317-2318 (May 1975).

Key words: BaO; chemical reactions; chemiluminescent; electronic spectra; heat-pipe ovens; N_2O.

A heat-pipe oven has been used to contain and control the chemiluminescent reaction $Ba + N_2O \rightarrow BaO^* + N_2$. The heat-pipe oven permits Ba vapor to be maintained at any desired pressure. Reactions were easily controlled by varying the flow rate of N_2O or pressure of Ba. A large volume (about 20 cm^3) of chemiluminescence was produced and spectra were taken from 0.1 to 5 torr. In addition to emission from BaO $A^1\Sigma$-$X^1\Sigma$, numerous atomic Ba lines also have been observed. This device is well suited to the study and control of chemical reactions between metal vapors and oxidizers.

Hiza, M. J., Kidnay, A. J., Miller, R. C., **Equilibrium properties of fluid mixtures, a bibliography of data on fluids of cryogenic interest,** Volume in *NSRDS Bibliographic Series,* 160 pages (IFI/Plenum Data Co., New York, N.Y., 1975).

Key words: bibliography; calorimetric measurements; fluid mixtures; Joule-Thomson coefficients; phase equilibria; review.

This bibliography contains references to experimental data for ten equilibria properties of fluid mixtures. The data considered are: solid-liquid, solid-vapor, solid-liquid-vapor, liquid-liquid, liquid-vapor, and gas-gas. In addition, there are sections on liquid mixture densities, gas or vapor mixture densities, Joule-Thomson coefficients, and calorimetric measurement.

Hocken, R., Moldover, M. R., Muth, E., Gerner, S., **Versatile cells for optical studies in fluids,** *Rev. Sci. Instrum.* **46,** No. 12, 1699-1700 (Dec. 1975).

Key words: cell; Kovar; sapphire; temperature; thickness.

We describe high quality optical cells designed for ease of cleaning and accurate definition of optical path length. The cells perform well from liquid nitrogen temperatures to 500 K at pressures up to 11 MPa (112 atm).

Hoer, C. A., Roe, K. C., **Using an arbitrary six-port junction to measure complex voltage ratios,** *IEEE Trans. Microwave Theory Tech.* **MTT-23,** No. 12, 978-984 (Dec. 1975).

Key words: attenuation; automation; detector; insertion loss; microwaves; phase angle; ratio; six-port junction; vector voltmeter; voltage.

An arbitrary six-port junction is analyzed as a microwave vector voltmeter, measuring the amplitudes and phase differences of two input signals in terms of power readings taken at the remaining four ports. The junction may be calibrated for measuring the complex ratio of these two signals using a self-calibration procedure which requires no attenuation or phase standards.

Hoer, C. A., Roe, K. C., **Using an arbitrary six-port junction to measure complex voltage ratios,** *Proc. 1975 IEEE Microwave Theory and Technique Symp. Int., Palo Alto, Calif., May 12-14, 1975,* pp. 98-99 (1975).

Key words: attenuation; microwave; phase angle; ratio; self-calibration; six-port; vector voltmeter; voltage.

An arbitrary six-port junction is analyzed as a microwave vector voltmeter, measuring the amplitudes and phase difference of two input signals in terms of power readings taken at the remaining four ports. The junction may be calibrated for measuring complex voltage ratios using a self-calibration procedure which requires no standards.

Holt, D. R., Nahman, N. S., **Coaxial line pulse-response error due to a planar skin effect approximation,** *Proc. 1972 CPEM Conf. on Precision Electromagnetic Measurement, Boulder, Colo., June 26-29, 1972,* pp. 1-2 (1972).

Key words: coaxial; cylindrical; error; line; loss; response; skin effect; step; time; transition.

The purpose of this paper is to characterize the time domain step response error in the analysis of coaxial lines terminated in their characteristic impedence.

Holton, J. K., Driscoll, P., **Linking research and practice,** *AIA J.,* pp. 67-68 (Apr. 1975).

Key words: AIA/NBS Architect-in-Residence; architectural research; daylight research; National Bureau of Standards; programs for architects; research communication.

There has been a long standing need for more effective interchange between the building community and researchers. The American Institute of Architects and the National Bureau of Standards have established an Architect-in-Residence program to help foster better communications between these groups. The first year of the program is now one-half completed and the activities of the Architect-in-Residence have fallen into three areas: (1) a resource for ongoing research activities at CBT; (2) liaison with the building community; and (3) a personal research project. This latter activity is a study of "The Introduction and Control of Natural Light in Buildings" and exemplifies the objectives of the program, the interrelationship of research work at CBT and the needs and demands of the working building community.

Howe, D. A., Salazar, H. F., **A digital 5.00688 MHz synthesizer and squarewave FM servo system for cesium standards,** *Proc. 29th Annual Symp. on Frequency Control, Atlantic City, N.J., May 28-30, 1975,* pp. 387-393 (1975).

Key words: indirect synthesis; phase noise; squarewave servo.

The cesium clock transition is at 9, 192, 631, 770 Hz by definition. In the design of a cesium frequency standard, it is common to generate a 5-MHz signal which is locked to this transition. Since 5-MHz cannot be directly multiplied to match the exact clock transition frequency, usually another frequency is synthesized and mixed in such a way that the clock transition frequency is produced.

This paper describes a synthesizer using a 5-MHz reference which has an output frequency of 5.00688 MHz which is very nearly an integer submultiple of the cesium clock transition frequency. Indirect synthesis is used in which an internal (number controlled) oscillator is locked at a prescribed frequency offset relative to the reference. Resolution (quantization error) is 1.4 parts in 10^{13}. A frequency stability plot $\sigma_y(\tau)$ of the synthesizer noise is presented. The synthesizer can be made very compact and reliable. Since its output has low phase noise, the signal may be multiplied directly to the cesium clock transition frequency. In a cesium standard, this simplifies the amount of microwave hardware compared to traditional schemes. The design concepts of the synthesizer can easily be extended in order to implement squarewave frequency modulation of the beam tube RF excitation.

Hudson, R. P., Pfeiffer, E. R., **Magnetic susceptibility of single-crystal CMN, 0.002K to 2K,** (Proc. 14th Int. Conf. on Low Temperature Physics, Otaniemi, Finland, Aug. 14-20, 1975), Paper in *Low Temperature Physics* **LT-14,** M. Krusius and M. Vuorio, Eds., **3,** 242-245 (North Holland Publishing Co., Amsterdam, 1975).

Key words: CMN; entropy; magnetic susceptibility; magnetic temperature; thermodynamic temperature.

Correction of a small systematic error present in our earlier measurements leads to a much improved determination of the magnetic temperature (T*) scale for single crystal CMN. These latest results are compared with recently published findings of another laboratory.

Hughes, C. E., Singletary, W. E., **Triadic partial implicational propositional calculi,** *Zeitschr. f. math. Logik und Grundlagen d. Math.* **21,** 21-28 (1975).

Key words: degrees of unsolvability; propositional calculus; recursion theory; undecidability.

201-606 O - 76 - 16

A partial implicational propositional calculus (PIPC) is an inference system having as axioms some finite set of tautologies of the implicational calculus. Its rules of inference are substitution and modus ponens. Its decision problem is the problem of deciding for an arbitrary well-formed formula whether or not it may be inferred. A given PIPC is said to be n-adic if at most n propositional variables appear in any of its well-formed formulas. In this paper we investigate decision problems for triadic (3-adic) PIPC's. The major results presented are: (i) every r.e. many-one degree is represented by the class of decision problems for triadic PIPC's, denoted I_3; (ii) not every r.e. one-one degree is represented by I_3; and (iii) the class of decision problems for partial propositional calculi is many-one equivalent to I_3.

Hughes, E. E., Taylor, J. K., **Accurate gas standards for air pollution analyses,** *Proc. WMO/WHO Tech. Conf. on Observation and Measurement of Atmospheric Pollution, Helsinki, Finland, July 30-Aug. 4, 1973*, pp. 1-13 (World Meteorological Organization, Geneva, Switzerland, 1974).

Key words: air pollution; carbon monoxide; gas analysis; permeation tubes; propane; sulfur dioxide.

The preparation of standards for the measurement of a particular pollutant, either at ambient levels or at source concentrations, requires either an absolute method of preparation or an accurate method of analysis. Few, if any, accurate methods of analysis are applicable at the low concentrations generally associated with air pollution and consequently, most standards have been prepared in this laboratory by a gravimetric technique. The factors which effect the degree of accuracy which can be attained are discussed in detail for the following gases; nitric oxide, nitrogen dioxide, carbon monoxide, carbon dioxide, sulfur dioxide, hydrocarbons, and oxygen. In general, an uncertainty of less than ± 1 percent can be achieved for these substances at concentrations where their mixtures with air or nitrogen are stable. The stability of these mixtures is, therefore, an equally important consideration in the preparation of accurate gas standards. The instability is either due to reaction within the container between the components of the mixture or between a component and the material of the container, or is due to adsorption on the walls of the container. Methods of assessing the degree of instability and methods of preventing it are discussed.

Interrante, C. G., **Report on the ferrous metals workshop,** (Proc. National Materials Conservation Symp. on Resource Recovery and Utilization, Gaithersburg, Md., Apr. 29-May 1, 1974), Paper in *Resource Recovery and Utilization*, H. Alter and E. Horowitz, Eds., *Am. Soc. Test. Mater. Spec. Tech. Publ.* **592,** pp. 146-152 (American Society for Testing and Materials, Philadelphia, Pa., 1975).

Key words: conservation; materials recovery; natural resources; reclamation.

This paper reports the nontechnical and technical findings of the workshop on ferrous metals. Discussions include the technology for the use of municipal ferrous scrap, the economic outlook, and potential markets for ferrous waste. Eight recommendations are suggested for improved recovery of ferrous waste.

Jackson, R. H. F., **Towards algorithmic standardization in mathematical programming: Another step,** *Proc. 1974 Fall UNIVAC Users' Conf., Toronto, Canada, Sept. 1974*, pp. 3-147—3-153 (1974).

Key words: algorithms; mathematical programming standards; testing.

This talk discusses the Mathematical Programming Society's newly formed Working Committee on Algorithms, whose domain of interest includes the accuracy, availability, and transportability of computer codes for the solution of mathematical programming problems. The Committee, it is hoped, will satisfy the pressing need for real achievements in these areas. The discussion will focus on the goals and accomplishments to date of the Committee, and will stress the importance of a good working relationship between it and the O.R. community.

Kamas, G., **TV color frequencies defended as accurate,** *Electron. Design Letter to the Editor* **13,** 7 (June 21, 1975).

Key words: crystal oscillator; frequency calibration; network-originated programs; NBS traceability; phase comparison; television.

This letter is a reply to a previous letter to the editor regarding accuracy of TV color signals to calibrate oscillators.

Kan, P. T., Peterson, G. A., Webb, D. V., Szalata, Z. M., O'Connell, J. S., Fivozinsky, S. P., Lightbody, J. W., Jr., Penner, S., **Electrodisintegration of ^{3}He,** *Phys. Rev. C* **12,** No. 4, 1118-1125 (Oct. 1975).

Key words: continuum; electron scattering; helium-3; monopole state; multipole decomposition; zero range approximation.

The continuum spectra of ^{3}He have been measured up to excitation energies of 40 MeV by means of inelastic electron scattering. Incident electron beam energies between 60 and 120 MeV were used, corresponding to a momentum transfer range of 0.3 fm^{-1} to 1.1 fm^{-1}. Scattered electrons were observed at two angles, 92.6 and 127.7°. The radiation corrected spectra and the form factors are presented, and compared with calculations based on a zero-range approximation. In this model, the sharp rise from the $p+d$ threshold previously reported may be identified as a $^2S \rightarrow {}^2S$ Coulomb monopole transition.

Kanda, M., **Accuracy considerations in the measurement of the power gain of a large microwave antenna,** *IEEE Trans. Antennas Propag.* **AP-23,** No. 3, 407-411 (May 1975).

Key words: calibration; ground antenna; standard antenna gain; three-antenna extrapolation.

Accuracy considerations in the measurement of the power gain of a large microwave antenna are discussed. The analysis indicates that, using the power gain comparison method with a standard antenna of nominally 40-dB gain, a large antenna with a power gain of nominally 60 dB could be calibrated to within an error of 0.17 dB (3σ). The power gain of the standard antenna is considered to be determined via the generalized three-antenna extrapolation method. Individual sources of errors in both the generalized three-antenna extrapolation method and the power gain comparison method are discussed.

Kanda, M., **A measure for the stability of solid state noise sources,** *Proc. 1975 IEEE Microwave Theory and Technique Symp. Int., Palo Alto, Calif., May 12-14, 1975*, pp. 315-317 (1975).

Key words: Allan variance; argon gas noise source; cross correlation; solid state noise source; stability measure.

A measure for the stability of solid state noise sources is discussed. Its applicability is demonstrated. A technique similar to cross correlation is employed to separate the instabilities of the noise source from those of the measurement system.

Kasen, M. B., **Mechanical and thermal properties of filamentary-reinforced structural composites at cryogenic temperatures. 2: Advanced composites,** *Cryogenics* **15,** No. 12, 701-722 (Dec. 1975).

Key words: advanced fiber composites; cryogenics; dynamic mechanical properties; literature review; static mechanical properties; thermal properties.

The low-temperature mechanical and thermal properties of advanced-fiber reinforced structural composites are reviewed. The

magnitude and range of particular properties are discussed with respect to composite type and temperature. A property-material cross reference is given with a 128-entry bibliography. This is Part 2 of a two-part series. Part 1 considered glass-reinforced composites.

King, G. C., Read, F. H., Bradford, R. C., **Structure near autoionizing energies in the excitation of bound states of helium, neon, and argon by electron impact,** *J. Phys. B* **8,** 2210 (1975).

Key words: Ar; atoms; autoionizing; cross sections; electron impact; excitation; He; inelastic; Ne.

Cross sections for the excitation of bound states of atoms by electron impact have been found to contain structures at incident energies near to the energies of short lived autoionizing states of the target atoms. These structures look superficially like resonance structures, but in fact they seem to be caused by a post-collision interaction between inelastically scattered and ejected electrons. Examples are given of these structures in He, Ne, and Ar. A quantum mechanical "shake-down" model to explain these structures is also described and compared with the experimental data.

Koyanagi, R. S., **Development of a low-frequency-vibration calibration system,** *Exp. Mech.* **15,** 443-448 (Nov. 1975).

Key words: accelerometer; calibration; harmonic distortion; low frequency; pickup; vibration; vibration exciter.

The development of the low-frequency-vibration apparatus described in this report was done in response to a need to establish and verify vibration-pickup performance at infrasonic frequencies. The exciter design is an extension of the Dimoff type exciters and, in fact, many of its components are identical.

The motion of such an exciter must have very low distortion and minimal components of motion in all directions other than axial. In addition, the attainable amplitude must be large enough to produce a transducer signal that can be accurately measured. The attainable amplitude and accuracy of transducer calibration on this exciter is limited by transducer size, weight, geometry and vibration sensitivity. Examples of the types of accelerometers which can be calibrated on this exciter are servo or force balance, piezoelectric, piezoresistive and strain gage.

Krauss, M., Neumann, D., **Ion-pair states of O_2,** *J. Chem. Phys.* **63,** No. 12, 5073-5076 (Dec. 15, 1975).

Key words: ion-pair; O_2; photodissociation; predissociation; Rydberg states; valence states.

Valence states of O_2 that correlate adiabatically to the ion pair asymptote, $O^+(^4S) + O^-(^2P)$, have been calculated using the multiconfiguration description of the electronic structure. The production of the ion pair is attributed to valence-Rydberg mixing that predissociates Rydberg states of the excited O_2^+ ion such as those leading to the $b\,^4\Sigma_u^-$ state. The electronic states required the calculation of excited states of a given symmetry. This is possible with the BISON-MC codes if the rigorous restriction on orthogonality to the lower states is relaxed. For homonuclear valence states, in particular, this should be a good approximation.

Krauss, M., Neumann, D., **On the interaction of O(^{1}S) with O(^{3}P),** *Chem. Phys. Lett.* **36,** No. 3, 372-374 (Nov. 15, 1975).

Key words: curve crossing; O(^{1}D); O(^{1}S); quenching rate; spin-orbit coupling; transition probability.

The quenching rate for O(^{1}S) by O(^{3}P) into the O(^{1}D) + O(^{1}D) channel is calculated using a theoretically calculated spin-orbit coupling matrix element. An upper bound to the rate is found to be 2.0×10^{-14} cm^3 s^{-1} which is much smaller than the experimental value. The low value of the rate constant is the result of a spin-orbit coupling matrix element of about 3 cm^{-1} at the relevant curve crossing.

Krauss, M., Neumann, D., **The dipole moment function of CO($a^3\Pi$),** *Mol. Phys.* **30,** No. 4, 1015-1020 (1975).

Key words: $a^3\Pi$; CO; dipole moment; excited state; SCF; vibrational transition intensities.

The dipole moment function of the $a^3\Pi$ state of CO is calculated using the multi-configuration self-consistent-field method of Wahl and Das. Only the dominant valence charge-transfer correlation configurations are mixed with the Hartree-Fock configuration since only the region between the classical turning points of the $v = 1$ vibrational level is considered. The calculated function does not agree with the shape of the fitted dipole moment function of Wicke *et al.* Configurations chosen on the basis of the model of optimized valence configurations do not determine an accurate dipole moment function for an open shell system.

Kunasz, P. B., Hummer, D. G., Mihalas, D., **Theory of extended stellar atmospheres. II. A grid of static spherical models for O stars and planetary nebula nuclei,** *Astrophys. J.* **202,** 92-113 (Nov. 1975).

Key words: emission line stars; line profiles; stellar atmospheres; stellar limb darkening.

Spherical static non-LTE model atmospheres are presented for stars with $M/M_\odot = 30$ and 60 at various points on their evolutionary tracks, and for some nuclei of planetary nebulae at two points of a modified Harman-Seaton sequence. The method of Mihalas and Hummer was employed, which uses a parametrized radiation force multiplier to simulate the force of radiation arising from the entire line spectrum. However, in the present work the density structure computed in the LTE models was held fixed in the calculation of the corresponding non-LTE models; in addition, the opacity of an "average light ion" was taken into account. The effects of sphericity, as distinct from those arising from a density structure modified by a large radiation force, were investigated by computing a few planar models using the same parametrized radiation force multiplier as for the spherical models. These effects were found to be quite significant even though the atmospheric extension never becomes very large. The temperatures for the non-LTE models are generally lower, at a given depth, than for the corresponding LTE models when $T_{eff} <$ 45,000 K, while the situation is reversed at higher temperatures. The continuous energy distributions are generally flattened by extension. The Lyman jump is in emission for extended models of massive stars, but never for the models of nuclei of planetary nebulae (this is primarily a temperature effect). The Balmer jumps are always in absorption. The Lyman lines are in emission and the Balmer lines in absorption; He II λ4686 comes into emission in the most extended models without hydrogen line pumping, showing that it is an indicator of atmospheric extension. Very severe limb darkening is found for extended models, which have apparent angular sizes significantly smaller than expected from the geometrical size of the star. Extensive tables are given of monochromatic magnitudes, continuum jumps and gradients, Strömgren-system colors, monochromatic extensions, and the profiles and equivalent widths of the hydrogen lines for all models, and of the He II lines for some of the 60 $M_\odot$ models.

Lawton, R. A., Andrews, J. R., **Pulsed-laser application to sampling oscilloscope,** *Electron. Lett.* **11,** No. 7, 138 (Apr. 3, 1975).

Key words: GaAs; laser; photoconductor; sampling oscilloscope.

An optically strobed sampling oscilloscope is described in which a GaAs laser diode is used to strobe a GaAs photo-conductive sampling gate.

Lawton, R. A., Scavannec, A., **Photoconductive detector of fast-transition optical waveforms,** *Electron. Lett.* **11,** No. 4, 74-75 (Feb. 20, 1975).

Key words: detector; dye laser; GaAs; photoconductor; picosecond; pulse.

The letter reports the development of a fast-response bulk photoconductor that can be used as a photodetector and as an optically gated switch. The photoconducting material used is semi-insulating, chromium-doped GaAs, a sample of which is mounted in a 50 Ω stripline holder. An estimated detector transition time of 92 ps or less was obtained from tests made with a mode-locked dye laser.

Lee, T. G., Parker, W. J., Tryon, M., **Laboratory fire performance characteristics of a dibromotetrafluoroethane-blown rigid polyurethane foam,** *J. Fire Flammability* **6,** 499-510 (Oct. 1975).

Key words: dibromotetrafluoroethane; fire tests; flame spread index; heat release rate; ignition temperature; rigid urethane foam; smoke.

The fire performance characteristics of a dibromotetrafluoroethane-blown rigid polyurethane foam with a core density of 0.046 g/cm^3 were measured by several laboratory test methods. Measurements included: surface flammability, smoke and gases generated at elevated temperature and during combustion, ignition temperature, rate of heat release, and fire growth. The maximum concentration of the blowing agent in the specimen was approximately 13 wt percent. The release of the blowing agent from the heated specimen began at about 60 °C and reached a rate of about 3 wt percent/hr at 100 °C. The material had a flame spread index (ASTM E 162) of 11 and smoke levels (NFPA 258-T) of 170 and 480, maximum specific optical density under nonflaming and flaming exposures, respectively. The measured rate of heat release was 8.8 W/cm^2, about five times that of a fibrous glass insulation. The measured flash ignition temperature was 530 °C for the material.

Lovas, F. J., **Application of microwave spectroscopy to chemical analysis,** *ISA Trans.* **14,** No. 2, 145-151 (1975).

Key words: applications; chemical analysis; microwave; qualitative analysis; quantitative analysis; rotational spectra.

Traditional analytical techniques have been successfully employed on a great variety of systems for identifying stable reaction products as well as for purity analysis and reaction efficiency. However, most analytical techniques generally can only be applied to "well behaved" chemical systems. Since gas phase reaction products do not always follow the "well behaved" guideline, an alternate analytical tool, such as microwave spectroscopy, could prove beneficial for analyzing such systems and may well provide some new routes to synthetic chemistry. A general review of the present state-of-the-art for applications of microwave techniques to analytical studies will be presented. An attempt will be made to describe the limitations and advantages of microwave spectroscopy for probing chemical systems for product identification and for optimization of the efficiency of gas phase chemical reactions. As an illustration, some recent results obtained in our laboratory on the complex pyrolytic decomposition reactions of ethylamine will be described. Further examples of possible applications will be taken from typical industrial processes that employ vapor phase chemical synthesis techniques.

Lyon, G., Walker, J. C., **On some polynomial search methods for hash tables of prime and composite sizes,** *Proc. Canadian Information Processing Society (CIPS) Nat. Conf., Regina, Sask., Canada, June 25, 1975,* pp. 290-299 (1975).

Key words: collision resolution; hash tables; polynomial search; pseudo-random numbers; scatter storage.

Necessary and sufficient conditions are given for a simple collision resolution polynomial bi**k to search fully a hash table of prime size. Sufficient conditions are then established which ensure a search of all locations of any table using a polynomial bi**k + ai. Observations on special cases for bi**k + ai relate this polynomial to the more simple search bi**k. A final example illustrates a typical pseudo-random sequence generated by a polynomial bi**k + ai.

Masters, L. W., Reichard, T. W., **Evaluation of adhesive-bonded joints in housing components of glass fiber-reinforced polyester laminate,** (Proc. American Society for Testing and Materials Conf. on Composite Reliability, Las Vegas, Nev., Apr. 15-16, 1974). Paper in *Composite Reliability, Am. Soc. Test. Mater. Spec. Tech. Publ.* **580,** pp. 146-156 (American Society for Testing and Materials, Philadelphia, Pa., Aug. 1975).

Key words: adhesive bonding; aging tests (materials); composite materials; glass fibers; housing system; laminates; reinforced plastics; shear strength; sustained loading; tensile strength.

A series of tests was performed on sandwich panel housing components made with glass fiber-reinforced polyester (FRP) laminates. Specifically, long- and short-tests were performed to evaluate the adhesive bonds between the FRP laminate facings and cores of the panels. Specimens of two different FRP laminates were analyzed and their bonding characteristics with two different adhesives were studied. The test data show that the bond strength was significantly affected by the laminate formulation, adhesive formulation, adhesive thickness, sustained loading, and temperature.

Mathey, R. G., Cullen, W. C., **Performance criteria for built-up roofing—Part 2,** *Roofing Siding Insulation* **52,** No. 1, 44-46, 56 (Jan. 1975).

Key words: bituminous roof membranes; performance attributes; performance criteria; physical and engineering properties; test methods.

This report is the last in a series of publications on performance criteria for built-up roof membranes. To remind the reader of the scope of these articles, the authors' introductory remarks for Part I follow. The development of a performance approach to bituminous built-up roof membranes is described and preliminary performance criteria are recommended. A number of test methods have been developed in order to obtain data to evaluate roofing membranes against the recommended criteria. Twenty attributes that affect the performance of roof membranes under service conditions are identified and laboratory tests are described for measuring the engineering properties of the membrane that pertain to many of these attributes. A level of performance is recommended for nine of the identified performance attributes.

May, W. E., Chesler, S. N., Cram, S. P., Gump, B. H., Hertz, H. S., Enagonio, D. P., Dyszel, S. M., **Chromatographic analysis of hydrocarbons in marine sediments and seawater,** *J. Chromatogr. Sci.* **13,** 535-540 (Nov. 1975).

Key words: baseline studies; gas chromatography; gas chromatography-mass spectrometry; hydrocarbon; liquid chromatography; marine sediments; pollution; seawater.

The low concentration of hydrocarbons anticipated in pollution baseline studies necessitates the development of analytical techniques sensitive at the sub-microgram per kilogram concentration level. The method of analysis developed in this laboratory involves dynamic headspace sampling for volatile hydrocarbon components of the sample, followed by coupled-column liquid chromatography for the nonvolatile components. These techniques require minimal sample handling, reducing the risk of sample component loss and/or sample contamination.

Volatile sample components are separated from the matrix in a closed system and concentrated on a TENAX-GC packed precolumn, free from large amounts of solvent and ready for GC/GC-MS analysis. Nonvolatile compounds, such as the benzpyrenes, may be extracted from large volumes of water and concentrated on a Bondapak C18 packed pre-column for coupled-column liquid chromato-

graphic separation and analysis. Results of the application of these techniques to the analysis of samples from sites of known low level hydrocarbon contamination are presented and discussed.

McCaffrey, B. J., Quintiere, J. G., **Fire-induced corridor flow in a scale model study,** *Proc. International Council on Building Research and Documentation (CIB) Symp. on the Control of Smoke Movement in Building Fires, Garston, Watford, England, Nov. 4-5, 1975*, **1**, 34-47 (1975).

Key words: corridors; fire induced flow; recirculating flow; scale-model; smoke movement; stratified flow; theory.

The flow induced by a room fire was studied within a corridor for a scale model configuration. The effect of corridor exit opening was determined for a fixed room door opening and temperature gradient. Velocity and temperature measurements were made. At the room doorway and corridor exit the thermally stratified flow would enter and leave with a sharp boundary between the counter current flows. However, within the corridor the flow was more complex, giving rise to a large recirculating zone traversing the corridor length and trapped between the hot ceiling jet and entering cold flow. Smoke tracer visualization techniques illuminated these complex flow patterns along with mixing caused by shedding vortexes. These flow results are quantitatively presented and their nature is discussed. The measured total mass flow rate induced into the corridor was measured and compared to theoretical results. At this time, the implications of these complex corridor flows in a scale-model must be limited until they are verified in similar full-scale experiments and their nature is more thoroughly understood.

McCamy, C. S., **Specification of geometric and spectral conditions relating to densitometry,** Paper 15.2 in *SPSE Handbook of Photographic Science and Engineering*, W. Thomas, Jr., Ed., pp. 831-840 (John Wiley & Sons, New York, N.Y., 1973).

Key words: modulation; notation; optical density; propagance; reflectance; reflectance factor; symbols; transmittance; transmittance factor.

Reflectance, transmittance, and optical density are regarded as kinds of flux modulation factors. Transmittance is defined as the ratio of transmitted flux to the incident flux, while transmittance factor is here defined for an optical system as the ratio of the emergent flux with the sample in the system to the emergent flux with the sample removed. Transmission density is defined as the negative logarithm of transmittance factor. Reflection, transmission, and fluorescence are considered generically as propagation and generalized modulation terms are given. A coordinate system and functional notation are adopted to systematize the description of optical systems which use or measure modulation. Simplified notation of the form D(g;S:g′S′) describes most cases.

McClintock, W., Linsky, J. L., Henry, R. C., Moos, H. W., Gerola, H., **Ultraviolet observations of cool stars. III. Chromospheric and coronal lines in α Tauri, β Geminorum, and α Bootis,** *Astrophys. J.* **202**, 165-182 (Nov. 1975).

Key words: chromospheres; stellar coronae; stellar ultraviolet.

The ultraviolet spectrometer of the Princeton Experiment Package aboard the *Copernicus* satellite has been used to obtain high-resolution measurements of Lα, the Mg II λ2800 doublet, and upper limits on Si III λ1206 in the K giants α Tau and β Gem. The intensities and line shapes are compared with earlier observations of α Boo. The Lα and Mg II profiles for α Tau resemble those for α Boo, in that they are highly asymmetrical, while β Gem shows much more symmetrical profiles. The asymmetries for all lines except for those of α Boo and the Mg II lines of α Tau could be due to interstellar absorption. In the case of β Gem only, the O V intercombination line at 1218 Å is observed, suggesting a well-developed corona substantially cooler than that of the sun. The Lα profiles of α Tau and β Gem are consistent with the low interstellar hydrogen abundance in the solar neighborhood previously obtained from a similar observation of the α Boo Lα profile. The strength of the Mg II λ2796 line can be used to measure transition region and coronal pressures, and indicates a decrease in both with later spectral type and/or increasing luminosity.

Mighell, A. D., Santoro, A., **Geometrical ambiguities in the indexing of powder patterns,** *J. Appl. Crystallogr.* **8**, Part 3, 372-374 (June 1975).

Key words: ambiguities; geometrical; indexing; patterns; powder diffraction.

There are cases in which different lattices give calculated powder patterns with the identical number of distinct lines in identical 2θ angular positions. The number of planes *(hkl)* contributing to each reflection may differ, however. The lattices having this property are related to each other by transformation matrices with simple rational elements. The resulting ambiguity in indexing of powder patterns is, in these cases, geometrical rather than accidental.

Mighell, A., Santoro, A., Prince, E., Reimann, C., **Neutron diffraction structure determination of dichlorotetra pyrazolecopper(II), $Cu(C_3H_4N_2)_4Cl_2$,** *Acta Crystallogr.* **B31**, Part 10, 2479-2482 (Oct. 15, 1975).

Key words: dichlorotetrapyrazolecopper; neutron diffraction; structure.

The crystal and molecular structure of dichlorotetrapyrazolecopper(II), $Cu(NHN{:}CHCH{:}CH)_4Cl_2$, was determined by single-crystal neutron diffraction techniques. This compound crystallizes in the monoclinic system with $a = 13.657$ (5), $b = 9.200$ (5), $c = 14.900$ (5) Å, $\beta = 118.04$ (1)°, space group $C2/c$, $q_0 = 1.63$ g cm^{-3} and $Z = 4$. The structure was refined by least-squares calculations to a conventional R value of 3 percent for 1143 reflections. The $Cu(C_3H_4N_2)_4Cl_2$ molecule is centrosymmetric with the Cu atom at the center of a distorted octahedron formed by two chlorine atoms and a nitrogen atom from each of four pyrazole rings. The accurate location of the hydrogen atoms shows that the conformation of the complex is due to intramolecular hydrogen bonding. The coordination distances Cu-Cl and Cu-N (2.84 and 2.02, 2.01 Å, respectively) are significantly different from those of the corresponding nickel analog (Ni-Cl and Ni-N 2.51; and 2.10, 2.09 Å, respectively).

Miller, A., Hussmann, E. K., McLaughlin, W. L., **Interferometer for measuring fast changes of refractive index and temperature in transparent liquids,** *Rev. Sci. Instrum.* **46**, No. 12, 1635-1638 (Dec. 1975).

Key words: calorimeter; dosimetry; electron beam; interferometer; radiation chemical kinetics; radiation measurement; refractive index; temperature measurement.

A double-beam interferometer has been designed for detecting changes of refractive index in transparent liquids associated with the absorption of ionizing radiation energy, due to short electron beam pulses from an accelerator. The response time of the interferometer is less than 0.2 μsec, and refractive index changes of the order of 10^{-7} can be measured, corresponding to a temperature change of $\sim 10^{-3}$ °C and an absorbed dose in water of ~ 350 rad. The interferometer can be used as either a real-time or integrating radiation dosimeter, if the temperature coefficient of the refractive index *(dn/dT)* is known for the irradiated liquid in the temperature region of interest.

Mount, G. H., Linsky, J. L., **A new solar carbon abundance based on non-LTE CN molecular spectra,** *Astrophys. J.* **202**, No. 1, L51-L54 (Nov. 15, 1975).

Key words: carbon abundance; molecular spectra; solar photosphere.

A detailed non-LTE analysis of solar CN spectra strongly suggests a revised carbon abundance for the Sun. We recommend a value of

log $A_C = 8.35 \pm 0.15$ which is significantly lower than the presently accepted value of log $A_C = 8.55$. This revision may have important consequences in astrophysics.

Newell, A. C., **Improved polarization measurements using a modified three antenna technique,** *Proc. IEEE Int. AP-Symp., Urbana/Champaign, Ill., June 2-4, 1975, Session* **15,** pp. 337-340 (1975).

Key words: antennas; measurement; polarization.

Absolute polarization parameters have previously been obtained using a 3-antenna measurement technique. By a modification of this approach, the accuracies of the results are significantly increased, and the measurements are easier to perform. This work demonstrates the power and utility of using complex rather than scalar polarization parameters in formulating polarization problems.

Newell, A. C., Yaghjian, A. D., **Study of errors in planar near-field measurements,** *Proc. IEEE Int. AP-Symp., Urbana/Champaign, Ill., June 2-4, 1975, Session* **20,** pp. 470-473 (1975).

Key words: antennas; error analysis; measurements; near-field.

In recent years, planar near-field antenna measurements have been developed and used in a number of applications. One of the primary concerns with this, or any, measurement approach is the accuracy of the results; that is, how do errors in measured near-field quantities affect the accuracies of far-field parameters such as gain, side lobe level, monopulse difference level, beam width, etc. Some efforts have been made in the past to estimate these errors, but the results have been limited in generality and primarily of a qualitative nature.

We have used a two-fold approach to obtain equations giving reasonable upper-bound errors resulting from systematic and random errors in the near-field measurements. The strategy has been to derive error expressions from the equations relating near and farfield quantities and also to simulate errors on actual measured near-field data. The simulation has been given some direction to, and confirmed the results of the analysis. The errors which have been investigated are: truncation of the measurement area, x, y, and z-position errors of the probe, amplitude and phase uncertainties of the measured data, and multiple reflections between the probe and test antenna. The results not only give the effects of errors in a given quantity, but also specify the form of the error (i.e., linear, quadratic, periodic, etc.) which will produce the largest effect. This information is very valuable in designing the measuring equipment so that these types of errors can be avoided or minimized.

Newman, M., Sheingorn, M., **Continuous solutions of a homogeneous functional equation,** *Aequationes Math.* **13,** No. 1/2, 47-59 (1975).

Key words: analytic functions; functional equations; Hurwitz's theorem.

It is shown that the functional equation

$$f(x)+f(ax)+f(bx)=0 \quad , \quad 1<a<b$$

has a nontrivial solution which is continuous for all real x if and only if $b \neq a^2$. Generalizations for the equation

$$\sum_{k=1}^{n} f(a_k x)=0 \quad , \quad 1=a_1<a_2<\ldots<a_n ,$$

are also derived.

Ogburn, F., **Coating thickness—its measurement and its significance,** Chapter 14 in *Properties of Electrodeposits—Their Measurement and Significance,* pp. 229-245 (Electrochemical Society, Princeton, N.J., 1975).

Key words: coating thickness; coating thickness gages; coatings; electrodeposited coatings; electroplated coatings; metal coatings; properties of electrodeposits; thickness gages; thickness measurement.

In addition to dimensional tolerance, thickness is very significant to coating characteristics such as wear, corrosion, porosity, electrical resistance, magnetic properties, ductility, other mechanical properties and monetary value. Many methods of measuring the thickness of electrodeposits are available, and a number of gages are manufactured domestically. These gages are nondestructive, but they are not applicable to all coatings. Measurement accuracies of ± 5 to ± 10 percent are normally expected.

Ogburn, F., **Density of electrodeposited metal, its significance and measurement,** Chapter 5 in *Properties of Electrodeposits Their Measurement and Significance,* R. Sard, H. Leidheiser, Jr., and F. Ogburn, Eds., pp. 71-79 (The Electrochemical Society, Inc., Princeton, N.J., 1975).

Key words: coatings; copper; density; electrodeposited coatings; electrodeposits; metal coatings.

Density of electrodeposits can give information about their soundness and composition. It can be measured by direct determination of the volume and mass of the deposit, but the best measurements are made by conventional hydrostatic techniques. A 2 liquid hydrostatic method of measurement is described. This method involves hydrostatic weighing with a float in a two liquid system. Data obtained by this method are given as an example. These data show a significant density variation between 11 one-half gram samples cut from a 6 gram piece of electrodeposited copper.

Ogburn, F., Johnson, C. E., **Mechanical properties of electrodeposited brass,** *Plating* **62,** 141-148 (Feb. 1975).

Key words: density, brass; ductility, brass; electrical resistivity, brass; electrodeposited brass; electroplated brass; internal stress, brass; mechanical properties, electrodeposited brass: properties, electrodeposited brass; tensile strength, brass; wear rate, brass.

Electrical resistivity, density, hardness, wear rate, tensile strength, internal stress, and ductility of electrodeposited 70-30 brass were measured and microstructures were observed. The deposits were obtained from a high speed cyanide bath designed to deposit 70-30 brass. Included are property data for deposits of other compositions obtained from the same bath under conditions other than normal.

Ott, W. R., Slater, J., Cooper, J., Gieres, G., **H^- shape-resonance studies in an arc plasma,** *Phys. Rev. A* **12,** No. 5, 2009-2016 (Nov. 1975).

Key words: arc; hydrogen; negative ion; plasma; resonance; vacuum ultraviolet.

Calculations by Macek have shown that the H^- photoabsorption cross section should be affected by a shape resonance at 1129.5 Å. This experiment is an attempt to observe the resonance in emission according to the reaction $e + H \rightarrow [H^-]^* \rightarrow H^- + h\nu$. The plasma is in a condition of local thermodynamic equilibrium and is generated by a stationary wall-stabilized hydrogen arc. With an axis temperature of 14 000 K and 1 atm pressure, the H^- free-bound continuum contributes only about 2 percent of the total radiation which is dominated in the 1130-Å region by the Ly-α wing. However, the peak of the shape resonance, according to Macek, should have a cross section about 25 times greater than the continuous free-bound cross section; therefore, it should appear as a very noticeable 50 percent structure superimposed on the Ly-α wing. Except for some small features which are attributed to weak molecular emission, there is no obvious indication of the shape resonance in either deuterium or hydrogen spectra between 1105 and 1135 Å. It is estimated that the minimum feature which could have been detected at 1129 Å was about 2 percent of the total signal.

Parrish, W. R., Steward, W. G., **Vapor-liquid equilibria data for helium-carbon monoxide and helium-nitrous oxide systems,** *J. Chem. Eng. Data* **20,** No. 4, 412-416 (Oct. 1975).

Key words: binary mixture; experimental vapor-liquid equilibria; helium-carbon monoxide system; helium-nitrous oxide system; Henry's constants.

Liquid-vapor data are reported for the helium-carbon monoxide system at 80, 85, 90, 100, and 120K and for the helium-nitrous oxide system at 195, 215, 235, 245, 255, 265, and 285K at pressures up to 138 bars. The data are analyzed for internal consistency using pseudo-Henry's law constants and enhancement factors.

Payne, B. F., Koyanagi, R. S., Federman, C., Jones, E., **Accelerometer calibration at the National Bureau of Standards,** *21st Int. Instrumentation Symp. ASD/TMD, Philadelphia, Pa., May 19-21, 1975,* pp. 1-17 (1975).

Key words: acceleration; automation; calibration; measurements; shakers; standards; transducers; vibration; vibration exciters; vibration pickups.

Accurate calibration of accelerometers requires that accurate measurement techniques be developed and maintained. No single vibration exciter or calibration procedure is adequate for the present calibration frequency range. This paper gives a summary of the various calibration procedures used in calibration of accelerometers and reference exciters at the National Bureau of Standards.

Pella, P. A., Hughes, E. E., Taylor, J. K., **Development of gas-blending systems for calibration: Application to hydrogen fluoride, arsine and phosgene in air,** *Am. Ind. Hyg. Assoc. J.* **36,** No. 10, 755-759 (Oct. 1975).

Key words: arsine; calibration of devices; gas-blending systems; hydrogen fluoride; phosgene.

The calibration of analytical monitoring devices is a prerequisite for making accurate measurements. For this purpose, self-contained gas-blending systems are being constructed and evaluated at the NBS for producing known concentrations of specific industrial contaminants in air from one-half to five times the TLV. This is accomplished by accurate dynamic dilution of a known relatively high concentration of the contaminant (i.e., standardized gas mixture) with air as a diluent to yield the desired range of concentrations. The development and evaluation of systems for producing known concentrations of hydrogen fluoride, arsine, and phosgene in air are reported including the measurement of the stability of these gases, and the determination of the concentrations upon dilution employing specific analytical methods.

Peterlin, A., **Plastic deformation of polymers with fibrous structure,** *Colloid Polym. Sci.* **253,** No. 10, 809-823 (1975).

Key words: fibrous structure; plastic deformation; polymer solids.

The plastic deformation of fibrous material obtains primarily by sliding motion of fibrils. In first approximation the displacement of their centers of mass is well describable by the affine transformation corresponding to the deformation of the bulk sample. Such a sliding motion of fibrils does not affect the morphology of the micro-fibrils. But it smooths by chain unfolding the surface inhomogeneities of the fibrils caused by microfibril ends which act as point defects of the microfibrillar lattice. That makes possible a more perfect lateral contact between adjacent fibrils resulting in a steadily increasing resistance to plastic deformation. The sliding motion of fibrils produces a shearing stress on skewed fibrils yielding a slight shear displacement of microfibrils. But in spite of its smallness, it enormously extends the interfibrillar tie molecules by chain unfolding and this enhances their fraction per amorphous layer.

Peterlin, A., **Structural model of mechanical properties and failure of crystalline polymer solids with fibrous structure,** *Int. J. Fract.* **11,** No. 5, 761-780 (Oct. 1975).

Key words: bond rupture; chain rupture; ESR; fibrils; load-elongation curve; microcracks; microfibrils; radicals.

The failure of an axially strained polymer solid having a fibrous structure is caused by formation, coalescence, and growth of microcracks up to critical size crack, which then propagates catastrophically through the cross-section of the sample. The primary candidates for microcrack formation are the ends of microfibrils where the material connection by tie molecules to the rest of the sample is almost completely interrupted. The opening of microcracks and sliding motion of fibrillar elements ruptures locally the most strained taut tie molecules and, thus, produces radicals detectable by ESR. But, chain rupture is the consequence and not the cause of displacement of the strong fibrillar elements. It also does not substantially affect the load carrying properties of the sample which mainly depend on the lateral autoadhesion of microfibrils and fibrils and on their quasi-viscous resistance to axial displacement. Hence, one has to reject the completely inadequate models trying to base the observed load-elongation curve of such samples on the load carrying properties of those tie molecules which are eventually ruptured upon straining. Some examples of these models are treated explicitly.

Pontius, P. E., **Mass measurement: A study of anomalies,** *Science* **190,** 379-380 (Oct. 24, 1975).

Key words: density of air; mass measurement.

It has always been assumed that the measurement of the difference in mass between two objects would be the same in all laboratories. Recent National Bureau of Standards measurements involving dissimilar objects (effective density ranging from 2.7 to 16.6 grams per cubic centimeter) at a wide variety of pressures (0.5 to 2 atmospheres) have been made with sufficient precision to test this assumption. The results show unsuspected discrepancies which may approach 1 milligram in a kilogram in the assignment of mass values when dissimilar materials are involved. These discrepancies have not been noted in the past because precision comparisons of both like and unlike materials have nearly always been made in a relatively restricted range of environmental conditions. The worldwide mass measurement system is therefore consistent, because similar materials have been used in the construction of weight sets, but possibly offset with respect to the mass unit as embodied in the platinum-iridium defining artifact.

Pyke, T. N., Jr., **Networked minis and micros—Configurations, applications, and standards,** *Proc. Mini Micro Computer Symp., U.S. Naval Academy, Annapolis, Md., Apr. 15, 1975,* pp. 44-46 (1975).

Key words: microcomputers; minicomputers; networks; standards.

Both minis and micros have found their way into extensive use as a part of computer networks. Minicomputers have a head start, but microcomputers will fast catch up in numbers, especially as a part of terminals connected to networks. Mini/micro network configurations can be divided into two categories, local and distributed. Most research-oriented and operational networks can be placed directly into one of these categories. Successful development and operation of these networks employing minis and micros requires a variety of standards, both internally and externally.

Quintiere, J., **The application and interpretation of a test method to determine the hazard of floor covering fire spread in building corridors,** *Proc. Int. Symp. on Fire Safety of Combustible Materials, Edinburgh, Scotland, Oct. 15-17, 1975,* **1,** 355-367 (1975).

Key words: corridor fire; experiments; flame spread; floorcovering; test method; theory.

In recent years, much attention has been given to measuring the potential flame spread hazard of building corridors, in which a floor

covering material is the only combustible present. The intention has been to develop standards for floor coverings which will limit corridor flame spread when the corridor is exposed to a large room fire. Under such circumstances, flame spread along the corridor floor is promoted by radiant heat transfer due to the room fire.

The proposed test method measures the flame spread characteristics of a floor covering material under an external radiant heat flux. One parameter the test measures is the external heat flux at the point of extinguishment. This has been interpreted as the minimum or "critical" radiant heat flux required to support flame spread. A theoretical model was developed to simulate the physical characteristics of the test method and sample materials.

The test method can be applied to measure the potential hazard of building corridors with floor coverings by comparing the critical flux measured for a material with an anticipated corridor heat flux due to a large fire. Results are presented which display corridor floor heat flux for various room fire intensities. These results are compared to theoretical predictions which illustrate the effect of corridor geometry and fire conditions on heat flux to the floor.

Rains, T. C., **Iron, cobalt, and nickel,** Chapter 10 in *Flame Emission and Atomic Absorption Spectrometry*, J. A. Dean and T. C. Rains, Eds., **3,** 216-246 (Marcel Dekker, Inc., New York, N.Y., Nov. 1975).

Key words: atomic absorption; atomic fluorescence; cobalt; interferences; iron; nickel; separations.

A summary is presented of the published work on the determination of iron, cobalt, and nickel by atomic absorption, emission, and fluorescence spectrometery. Optimum conditions for atomization and excitation are described for flame and non-flame methods for the three techniques. Spectral characteristics for wavelength ranges of analytical interest are given for the three elements with their sensitivity and/or detection limits. Interferences encountered under optimum instrumental conditions are minimal; however, separational techniques are described for each element. The paper contains 174 references in which numerous applications are described.

Read, F. H., **Displaced electron energies and the "shake-down" effect,** *Radiat. Res.* **64,** 23-36 (1975).

Key words: atom; autoionizing; collision; cross section; electron; experiment; positive ion; review; Rydberg states.

A brief review is given of the apparent exchanges of energy that can occur sometimes between the outgoing particles in electron-atom impact experiments, when these final particles consist of two electrons receding from a positive ion, and when the incident electron energy is near the energy of an autoionizing state of the target atom. These energy exchanges manifest themselves as changes in the energies of electrons ejected from autoionizing states of atoms excited by near-threshold election impact, displacements of the thresholds for exciting autoionizing states, and structure in the cross sections for exciting Rydberg states of neutral atoms by electron impact at incident energies in the vicinity of autoionizing states. The experimental evidence for these processes is reviewed and qualitative explanations are given. Evidence for analogous effects in other scattering and absorption processes is also discussed.

Rebbert, R. E., Ausloos, P. J., **Photodecomposition of $CFCl_3$ and CF_2Cl_2,** *J. Photochem.* **4,** 419-434 (1975).

Key words: absorption cross section; chlorine atom; dichlorodifluoromethane; freons; photochemistry; quantum yields; stratosphere; trichlorofluoromethane.

The photochemical decomposition of $CFCl_3$ and CF_2Cl_2 has been investigated, using added CH_4 and C_2H_6 as chlorine atom interceptors. From the quantum yields of the stable products formed at 213.9, 184.9, 163.3 and 147 nm, quantum yields of the primary photofragments $CFCl_2$, CF_2Cl, CFCl, CF_2, CF and Cl, were derived. At wavelengths close to the absorption threshold, detachment of one chlorine atom from $CFCl_3$ and CF_2Cl_2 occurs with a quantum yield of 0.95 ± 0.05. As the photon energy increased, there is a rapidly increasing probability that absorption of a photon will lead to the release of two chlorine atoms:

$$CFCl_3 + h\nu \rightarrow CFCl + 2Cl$$

$$CF_2Cl_2 + h\nu \rightarrow CF_2 + 2Cl$$

The CFCl or CF_2 formed in these processes (which are most likely in the ground singlet state) are unreactive towards the parent halocarbons, or alkanes. They combine with other free radicals to form stable products. No evidence was found for the cleavage of C-F bonds, or the elimination of stable chlorine molecules.

In the vicinity of the absorption threshold, the absorption cross-sections of CF_2Cl_2 and $CFCl_3$ diminish sharply with a decrease in temperature.

Rensberger, R. A., **Lead paint hazard abatement,** *Constr. Specifier* **28,** No. 6, 45-46, 48-49 (June 1975).

Key words: abatement; detection; heat-gun; lead paint; materials evaluation; performance specification; rehabilitation; renovation.

The article briefly discusses the history of lead paint poisoning and discusses the safety hazards of lead paint in renovation and rehabilitation work in housing and buildings. Techniques for lead paint detection and methods for abatement are discussed for reference by the specifications writer, architect, design professional, engineer, contractor and other individuals who may be confronted with the hazards of lead paint. The information is from investigations by NBS for the HUD research program on lead paint. A suggested performance specification for lead paint hazard abatement methods is offered as a guideline for materials evaluation. Also a selected bibliography of NBS publications is included for reference by the building community.

Roberts, R. W., **The other face of the measurement base,** *Anal. Chem.* **47,** No. 7, 648A-656A (June 1975).

Key words: length; mass; National Bureau of Standards; reference methods; SI units.

The universal language of measurement is provided by the International System of Units. Progress leading to the present definitions of some of the SI base units, and research that may lead to improved definitions, is described. Work at the National Bureau of Standards that is of interest to analytical chemists, such as atomic weight determinations, standard reference data, physical constants, calibrations, etc., is also described.

Rosasco, G. J., Prask, H. J., **Polarized Raman study of lattice modes in ammonium perchlorate at low temperatures,** *Solid State Commun.* **16,** No. 1, 135-138 (1975).

Key words: ammonium perchlorate; lattice dynamics; Raman scattering; structure.

The Raman spectra of oriented single crystals of ammonium perchlorate have been measured as a function of temperature between 12 and 300 K. The results are consistent with the assignment of NH_4ClO_4 to the D_{2h}^{16} space group at all temperatures. A weak B_{1g} mode at 180 cm^{-1} is assigned as an NH_4^+ libration. Anomalous temperature dependence is observed for low frequency B_{1g} and B_{3g} lattice modes. Detailed results are presented for these modes in the range 18-80 K.

Rosasco, G. J., Simmons, J. H., **Identification of sulfur deposits in bubbles in glass by Raman scattering spectroscopy,** *Am. Ceramic Soc. Bull.* **54,** No. 6, 590-591 (June 1975).

Key words: bubble content analysis; gas analysis; inclusions in glass; Raman spectroscopy of sulfur; sulfur identification.

Raman scattering spectroscopy was conducted on solid deposits in bubbles in glass. Elemental sulfur was identified as forming small spherical deposits, amorphous in appearance. An analysis of the gas contents of the bubbles was also conducted and the changes of concentration with successive heat-treatments provided an estimate of the process of bubble formation.

Rosasco, G. J., Simmons, J. H., **Investigation of gas content of inclusions in glass by Raman scattering spectroscopy,** *Am. Ceramic Soc. Bull.* **53,** No. 9, 626-630 (Sept. 1974).

Key words: gas analysis; inclusions in glass; Raman scattering.

Laser Raman spectroscopy is used to identify the gaseous contents of inclusions in glass. This test is offered as a valuable complement to other analytical techniques. It requires relatively simple specimen preparation, offers good sensitivity to the gases of interest and is a nondestructive test. Further, since the sample is not contained in a confining test apparatus, the temperature of the contents of the bubble may be raised, for example, to vaporize solid deposits for analysis. Spherical bubbles 0.5 mm in diameter have been routinely analyzed without special optics and with good signal-to-noise ratio. The elements of the theory and practice of laser Raman spectroscopy are outlined and their application to the study of the gaseous content of inclusions is discussed in detail.

Rothschild, W. G., Rosasco, G. J., Livingston, R. C., **Dynamics of molecular reorientational motion and vibrational relaxation in liquids. Chloroform,** *J. Chem. Phys.* **62,** No. 4, 1253-1268 (Feb. 15, 1975).

Key words: chloroform; infrared spectra; molecular reorientation; Raman spectra; vibrational relaxation.

Vibrational and rotational (dipole and second-order tensor) correlation functions were obtained by Fourier inversion of infrared and Raman vibrational band contours of the three $\parallel$ and one $\perp$ fundamentals of liquid $CHCl_3$, $CDCl_3$, and isotopically pure $CH^{35}Cl_3$. All correlation functions are nonexponential at short times and approximately for long times. The symmetry axis of the molecule reorients by "free" jumps of about 1/3 rad, turning through a root-mean-square angle of 1 radian within 2 psec by about 13 orientational jumps. Computer simulations show that J diffusion is too fast beyond 1 psec and that M diffusion fits the data up to 4 psec ($\tau_J = 0.12$ psec); thereafter, M diffusion is too slow. The Raman rotational correlation time is approximately equal to the NMR quadrupolar correlation time; the infrared rotational correlation time is only 0.75 of a corresponding dielectric relaxation time. Vibrational relaxation in the symmetric near-infrared carbon-hydrogen stretch is of the same order of importance as rotational relaxation; however, the dynamics of the vibrational relaxation of this mode do not support the presence of "hydrogen bonding" in the neat liquid. In the symmetric far-infrared carbon-chlorine deformation mode, vibrational relaxation is of considerably lesser significance than rotational relaxation throughout the whole time domain, whereas the rate of vibrational relaxation of the symmetric midinfrared carbon-chlorine stretch is intermediate to those of the other two symmetric fundamentals. None of these modes obeys vibrational energy dissipation or resonance vibrational energy transfer mechanisms induced by dipole-dipole interaction. The ratios of the derived polarizability tensor elements, which are required to evaluate the rotational correlation function of the degenerate mode (carbon-hydrogen deformation), were computed from formulations relating them to the bond polarizabilities: It appears that its Raman and infrared correlation functions do not contain the same vibrational correlation function and that the respective contour is determined essentially by nonorientational relaxation processes. An extensive analysis of the experimental errors inherent in our Raman band contour determinations is presented, as well as a critical comparison of our conclusions with previous results in the literature.

Rubin, R. J., Mazur, J., **Ordered spans of unrestricted and self-avoiding random-walk models of polymer chains. I. Space-fixed axes,** *J. Chem. Phys.* **63,** No. 12, 5362-5374 (Dec. 15, 1975).

Key words: Monte Carlo analysis; ordered spans; self-avoiding polymer chains; shape of polymer chains; spans; unrestricted polymer chains.

An N-step random walk on a cubic lattice is adopted as a model of a random polymer chain. The spans, or extents, of each random walk configuration in the principal lattice directions are arranged in order of magnitude, $\xi_3 \geq \xi_2 \geq \xi_1$. In the case of the unrestricted random walk, the average values of the ordered spans $\langle \xi_{i,u} \rangle$ and $\langle \xi_{i,u}^2 \rangle$, $i = 1, 2$, and 3, are calculated analytically in the limit of large N. The limiting relative values of the first moments, $\langle \xi_{i,u} \rangle$ are 1.637: 1.267:1; and the limiting values of the second moments $\langle \xi_{i,u}^2 \rangle$ are 2.710 : 1,600 : 1. In the case of the restricted or self-avoiding walk, the corresponding average spans $\langle \xi_{i,r} \rangle$ and $\langle \xi_{i,r}^2 \rangle$ are estimated for $N \leq 150$ by using a Monte Carlo procedure. The same Monte Carlo procedure is used to estimate the values of $\langle \xi_{i,u} \rangle$ and $\langle \xi_{i,u}^2 \rangle$ for $N \leq 1000$. On the assumption that the rate of approach of the average ordered snaps of the self-avoiding walks to their asymptotic forms is similar to the rate of approach of the average ordered spans of the unrestricted walks to their asymptotic forms, the following estimates are obtained for the ordered spans of the self-avoiding walks: $\langle \xi_{i,r}(N) \rangle = \bar{\xi}_{i,r} N^{0.61}$ for $N \gg 1$ and $\bar{\xi}_{3,r} : \bar{\xi}_{2,r} : \bar{\xi}_{1,r} = 1.75 : 1.31 : 1$. The relative values of the estimates of the second moments of these ordered spans for $N \gg 1$ are $\langle \xi_{3,r}^2 \rangle : \langle \xi_{2,r}^2 \rangle : \langle \xi_{1,r}^2 \rangle = 3.08 : 1.71 : 1$. A simple ellipsoidal model is analyzed in order to obtain estimates of the intrinsic spans of the two kinds of random walks. It is assumed that all random walks have the same intrinsic dimensions and form (ellipsoidal), but that their principal axes are oriented at random. The average ordered spans with respect to a set of orthogonal space-fixed axes of this randomly oriented ensemble of ellipsoids depend uniquely on the principal diameters of the ellipsoid (intrinsic spans). A procedure is devised to solve the inversion problem of determining the relative lengths of the principal diameters which correspond to a given set of relative ordered moments with respect to space-fixed axes. The relative values obtained for the principal diameters of the ellipsoid are 2.59 : 1.61 : 1 in the case of the unrestricted random walk and 3.05 : 1.77 : 1 in the case of the self-avoiding walk.

Rubin, S., **Thermal resistance measurements on monolithic and hybrid Darlington power transistors,** (Proc. 1975 IEEE Power Electronics Specialists Conf., Culver City, Calif., June 9-11, 1975), *PESC 75 Record,* **75-CHO,** 965-4 AES, 252-261 (The Institute of Electrical and Electronics Engineers, New York, N.Y., Sept. 1975).

Key words: Darlington hot spot screen; Darlington thermal resistance; emitter-only switching; hot spot screen for Darlingtons; integrated power Darlington thermal resistance; thermal resistance measurement.

A method for measuring the thermal resistance, R_θ, of integrated power Darlington transistors is described that is based upon the emitter-only switching technique. It is shown that for specified measurement conditions this method can be used to measure the average thermal resistance, $R_{\theta(1+2)}$, of the input and output transistors of the Darlington pair and is therefore applicable to production-line monitoring of the thermal characteristics of the Darlington. It is shown that although a direct measurement of the thermal resistance, $R_{\theta(2)}$, of the output transistor cannot be made for most Darlingtons, an indirect determination of $R_{\theta(2)}$ can be made using the emitter-only switching technique and a simple equation. Comparisons of the differences between the infrared-determined thermal resistance and the electrically-measured thermal resistance of Darlingtons and of discrete power transistors illustrate that the accuracy of the Darlington measurements is comparable with that achievable for discrete

devices. It is also shown that measurements which attempt to use the collector-base voltage of the output transistor of the Darlington as a temperature-sensitive-parameter, either alone or in conjunction with an output commutating diode (when present), are too sensitive to the magnitude of the measuring current to be reliable. Also, the use of the base-current screen for hot spots, as used for discrete transistors, is marginally applicable to integrated Darlingtons, but it is shown that the emitter-base voltage sensed during emitter-only switching is quite effective for detecting hot-spot formation.

Saltman, R. G., **The human side of automating,** *Proc. Association for Computing Machinery and National Bureau of Standards Conf., on The Systems Approach: Key to Successful Computer Applications, Gaithersburg, Md., June 20, 1974*, pp. E.4.1-4.11 (1974); *Cyberdent* **2,** No. 3, 1, 3-4 (1974).

Key words: automation; human relations; job enrichment; organizational development; project management; system integration.

The process of designing and installing an automated system must consider problems of human relations. If the automation will affect the operation of diverse groups within an organization, then the legitimate and conflicting interests of these groups must be recognized, and their cooperation achieved through compromise. Successful automation must include the establishment of a new network of human communications.

The effect of the automation should not be to eliminate or downgrade jobs, but to enrich or increase responsibilities, leaving the repetitive, tedious jobs to the machines. Specialists in job design should be included on the automation team.

Well-designed automation should integrate diverse groups in an organization through improved data flow, but may divorce outside data users completely if their needs are not considered in the design process. An ombudsman with the responsibility of correcting design errors to satisfy outside users' requirements should be provided.

Sanchez, I. C., Eby, R. K., **Thermodynamics and crystallization of random copolymers,** *Macromolecules* **8,** No. 5, 638-641 (Sept.-Oct. 1975).

Key words: comonomer concentration; copolymer; crystallization; defect energy; equilibrium dissolution temperature; equilibrium melting temperature; fold surface energy; growth rate; heat of fusion; lamella thickness; melting.

Equations are developed for the bulk free energy of fusion, melting temperature, crystal thickness, and nucleation rate of copolymer crystals containing an arbitrary concentration of comonomer units. These equations which represent advances over earlier ones are shown to be consistent with experimental data for copolymers of L- and DL-lactides and *cis*- and *trans*-isoprenes. Analysis of the lactide data confirms an earlier prediction that the crystal thickness should increase linearly with increasing small concentrations of the comonomer units for crystallizations carried out at the same temperature. Further, this linear dependence is shown to extend to crystals containing both equilibrium and nonequilibrium concentrations of the comonomer units. The nucleation rate equation is in agreement with the observed linear dependence of the logarithm of the growth rate on the comonomer concentration in isoprene copolymers. The following are consistent with the experimental data for the lactides: 461 K, equilibrium melting temperature of the homopolymer; 403 K, equilibrium dissolution temperature in xylene; 1370 cal/mol of monomer (5730 J/mol) heat of fusion; 26.5 erg/cm² (2.65×10^{-2} J/m²) surface free energy and 585 cal/mol (2447 J/mol) comonomer defect energy. Directions for future research are suggested.

Santoro, A., Choi, C. S., Abel, J. E., **1,5-diacetyl-3,7-dinitro-1,3,5,7-tetraazacyclooctane (DADN),** *Acta Crystallogr.* **B31,** Part 8, 2126-2128 (Aug. 1975).

Key words: crystal structure explosives; least-squares refinement; molecular packing; tetraazacyclooctane derivatives; x rays.

$C_8H_{14}N_6O_6$, monoclinic, $P2_1/c$, $a = 7.422(1)$, $b = 13.253(2)$, $c = 6.156(1)$ Å, $\beta = 103.38(1)°$, $Z = 2$, $D_x = 1.636$, $D_m = 1.63$ gcm^{-3}, $F(000) = 304$. X-ray intensities were measured with Mo $K\alpha$ radiation. The structure was solved by direct methods and refined by full-matrix least-squares calculations to final R and R_w values of 4.1 and 4.8 percent, respectively, for 1149 observed reflections.

Scheide, E. P., Taylor, J. K., **A piezoelectric crystal dosimeter for monitoring mercury vapor in industrial atmospheres,** *Am. Ind. Hyg. Assoc. J.* **36,** No. 12, 897-901 (Dec. 1975).

Key words: air pollution; chemical analysis; dosimeter; industrial hygiene analysis; mercury; personnel monitor; piezoelectric sensor; trace analysis.

A personal dosimeter for mercury vapor in air based on the use of a piezoelectric sensor with a selective coating has been developed and evaluated. The sensor is a gravimetric device which indicates an integrated total exposure to mercury vapor. The mass of the material deposited or adsorbed is determined by measuring the change in oscillation frequency of the crystal. The sensor is small enough to be worn on a worker's clothing and is compatible with existing miniature air pumps. The adsorbed mercury can be desorbed by heating and the sensor can be reused many times. The precision and accuracy of this measurement technique, the effect of sampling flow rate, storage, sample concentration, interferences, sampling period, sensitivity and range, lifetime of the sensor, and other parameters considered in the development of prototype devices are discussed.

Sengers, J. M. H. L., Sengers, J. V., **Universality of critical behavior in gases,** *Phys. Rev. A* **12,** No. 6, 2622-2627 (Dec. 1975).

Key words: air constituents; critical region parameters; ethylene; heavy noble gases; helium; linear model; methane; NBS equation; scaling laws; statistical analysis; steam; universality.

P-V-T data in the critical region of six fluids (^{3}He, ^{4}He, Xe, O_2, CO_2, and H_2O) have been analyzed in terms of two scaled equations of state using the methods of statistical analysis. The results confirm the hypothesis of universality of critical behavior for these gases to within the current experimental accuracy. The results also support the validity of hyperscaling relations between thermodynamic and correlation function exponents for gases. Using the hypothesis of universality we then present critical-region parameters for fourteen fluids in terms of a universal equation of state.

Shank, R., Henderson, M., **Federal Library cooperation,** *Library Trends* **24,** No. 2, 277-292 (Oct. 1975).

Key words: Federal libraries; library cooperation.

Federal support of cooperative library service is influenced by the direct participation of Federal libraries in consortia and various networks. An overview of Federal library activity reveals many instances in which leadership for major cooperative programs was given by librarians in Federal libraries, e.g., the Library of Congress shared cataloging began in 1901. This paper documents trends in cooperation by the more than 2,000 libraries of the Federal Government.

Sibley, E. H., **On the equivalences of data based systems,** *Proc. Association for Computing Machinery SIGMOD Conf., Ann Arbor, Mich., May 1-3, 1974,* **II,** 1-52 (1974).

Key words: data base technology; data manipulation, data structured; data manipulation, relational.

Practitioners of data base technology have been somewhat confused by the many different theories and systems for describing and manipulating data. The two major philosophies which have emerged

may be termed the *relational* or set theoretic approach and the *data structured* or procedural approach. There are obviously differences in these, but there are also similarities.

This paper looks at these approaches from three aspects: (1) The method of describing data and its structure; (2) the methods of manipulating this data; and (3) the time of binding the data name to its operation.

Sibley, E. H., **Summary of CODASYL report on selection and acquisition of data base management systems,** *Digest of Papers, Association for Computing Machinery 1975 Conf., Minneapolis, Minn., Sept. 1974*, 3 pages (1974).

Key words: acquisition; CODASYL; computer; data base management; designers; evaluation; selection; users.

This report presents a method for the selection and acquisition of a data base management system as part of the development of an automated information processing system. It does not attempt to discuss all aspects of information systems, but only those that are pertinent to the utilization of a data base management system. Those issues which relate to information system design, as well as the design and implementation considerations of a data base management system are deferred. This report is the third in a series of CODASYL System Committee reports on its efforts to build up an expertise in and to develop advanced languages for data processing. The report should be of significant value to users and designers of such systems, since it approaches the question of evaluation and selection by relating users needs to system capabilities.

Simiu, E., Filliben, J. J., **Structural safety and the probabilistic definition of design wind speeds,** *Proc. CIB Int. Symp. on the Climatology of Building, Zurich, Switzerland, Sept. 25-27, 1974*, 99 pages (1974).

Key words: building codes; probability distribution function; reliability; risk; statistical analysis; storms; structural engineering; wind loads; wind speeds.

The reliability of the probabilistic approach to the definition of design wind speeds depends upon the extent to which it is possible to model adequately the probabilistic behavior of extreme wind speeds. In this connection, questions arise regarding the type of probability distribution best suited for this purpose and the adequacy of 20-year long wind records, i.e., of such records as have been used as a basis for developing wind maps included in various building codes and standards. With a view to answering these questions, the writers undertook a statistical study of wind speed records taken at 20 U.S. weather stations. The following results were obtained: (1) the assumption currently accepted in the literature that a single probability distribution is universally applicable to all extreme wind data sets, was not confirmed; (2) predictions of 100-year wind speeds based on overlapping 20-year sets of data taken at the same station differed between themselves by as much as 65 percent. These results suggest that extreme caution should be exercised in establishing or using probabilistically defined design wind speeds, particularly if records of sufficient length, considerably in excess of 20 years, do not exist.

Stein, S. R., **Application of superconductivity to precision oscillators,** *Proc. 29th Annual Symp. on Frequency Control, Atlantic City, N.J., May 28-30, 1975*, pp. 321-327 (1975).

Key words: cavity stabilization; frequency multiplication; funnel diode oscillator; parametric oscillator; superconducting oscillator.

Advances in superconducting technology during the last decade have resulted in many experimental applications in the generation of stable frequencies. The properties which make superconducting resonators attractive are their high Q, high frequency, and high operating power level. A variety of techniques can be used to make a superconducting cavity the frequency determining element of an oscillator. They include cavity stabilization via injection locking of a free-running oscillator, negative feedback to a voltage-controlled oscillator, positive feedback around an amplifier, and coupling to a negative resistance amplifier. These techniques are discussed in terms of some of their theoretical and practical limitations with particular emphasis placed on the goal of achieving state-of-the-art frequency stability. The best performance obtained with a superconducting oscillator to date is summarized.

At NBS, work on superconducting oscillators is primarily motivated by the need for a microwave signal which can be multiplied to the infrared and used to measure the frequency of a laser with no loss in precision as compared to the primary cesium standard. The signal source which has been selected for this purpose is the superconducting parametric oscillator. Its principles of operation are discussed along with the reasons why it is expected to have state-of-the-art short-term frequency stability.

Straty, G. C., **Hypersonic velocities in saturated and compressed fluid methane,** *Cryogenics* **15,** No. 12, 729-731 (Dec. 1975).

Key words: compressibility; interferometry; light scattering; methane; sound velocity; specific heat ratio.

Brillouin scattering techniques have been used to measure the velocity of hypersonic waves in gaseous and liquid methane. Measurements were made on the saturated liquid and vapour and along selected isotherms to a maximum pressure of about 17.5 MPa. The data, which agree well with previously measured ultrasonic velocities, have been combined with PVT data to obtain the isentropic compressibility and the ratio of specific heats.

Sugar, J., **Ionization energies of quadruply ionized rare earths,** *J. Opt. Soc. Amer.* **65,** No. 11, 1366-1367 (Nov. 1975).

Key words: atomic spectra; ionization energies; lanthanides; spectra; rare earths.

Values for the ionization energies of four-times-ionized lanthanides are derived from interpolated spectroscopic properties of the $4f^{n-1}ns$ Rydberg series.

Teague, E. C., **Surface finish measurements: An overview,** *Soc. Manuf. Eng. Tech. Pap.* **IQ75-137,** 1-21 (1975).

Key words: electron microscopes; horizontal resolution; optical instruments; stylus instruments; surface texture measurement; surface texture parameters; vertical resolution.

This paper reviews existing methods of surface finish measurement. The methods are considered from the standpoint of measurement systems whose components—specimen surface, measuring instrument, analyzing equipment and data display devices are equally important. Stylus, optical and electron optical instruments are evaluated and compared in terms of peak-to-valley-range, measurement area, vertical resolution, horizontal resolution, and profile measuring capability. Finally, the use of a digital computer as part of a measurement system will be discussed.

Utton, D. B., **The response of phase-sensitive detectors to Lorentzian and Gaussian lineshapes,** *J. Appl. Phys.* **46,** No. 12, 5268-5271 (Dec. 1975).

Key words: Gaussian; lineshapes; Lorentzian; phase sensitive detector.

Calculations are made of the response to Gaussian and Lorentzian lineshapes of a phase-sensitive detector operated at twice the modulation frequency. The modulation traverses the line resonance condition twice each cycle. Sensitivity to variations in linewidth, modulation width, and line center position are discussed. These are compared with the more common operation where small modulation

widths result in signals proportional to the derivatives of the lineshape. A discussion is made of the effects on the phase-sensitive detector output of signals at the harmonics of the modulation frequency.

Vagelatos, N., Rowe, J. M., Rush, J. J., **Lattice dynamics of ND_4I in the NaCl phase (I) at 296°K,** *Phys. Rev. B* **12,** No. 10, 4522-4529 (Nov. 15, 1975).

Key words: acoustic phonons; lattice sodium-chloride; translational dynamics.

Dispersion curves for translational phonons propagating in the high-symmetry directions of sodium-chloride-phase ND_4I have been determined at room temperature by coherent inelastic neutron scattering from single crystals. Acoustic phonons were well defined throughout the Brillouin zone. Optic phonons were considerably more difficult to measure because of the low signal-to-background ratio. The observed phonon energies were fitted to a "simple" and a "breathing" shell model with general repulsive short-range forces out to second neighbors. The results of the model fitting lead to conclusions similar to those reached in previous alkali halide studies. Model predictions of crystal properties are generally in good agreement with observation. The best fit model was used as in interpolation formula to calculate the density of states, $g(\nu)$. The mean-square displacements are in excellent agreement with those derived from the neutron-diffraction results of Seymour and Pryor. The lattice-dynamics results are compared with similar results obtained recently for the NaCl phases of the alkali cyanides.

Ventre, F. T., **Transforming environmental research into regulatory policy,** (6th Annual Meeting of the Environmental Design Research Association (EDRA), Lawrence, Kans., Apr. 23, 1975), Paper in *Responding to Social Change,* pp. 277-284 (Dowden, Hutchinson & Ross, Inc., Stroudsburg, Pa., Apr. 1975).

Key words: applied research; building codes; building design; building standards; diffusion of information; regulation.

Outlines a means enabling environmental design researchers to participate in the formulation of regulatory policies affecting buildings. The standards system is shown to be an underused channel for relaying research findings to building professionals and the regulatory system is shown to be a potential means for directing building technology toward socially-valued ends. Notes include a brief listing of standards- and codes-generating organizations.

Walker, G. R., Minor, J. E., Marshall, R. D., **The Darwin cyclone valuable lesson in structural design,** *Civ. Eng.* **45,** No. 12, 82-86 (Dec. 1975).

Key words: buildings; codes and standards; cyclones; natural disasters; structural engineering; wind damage; wind loads.

Damage to buildings in Darwin, Australia caused by Cyclone Tracy is described. The approximate cyclone track and probable maximum wind speeds are presented along with an assessment of the performance of several types of buildings under extreme wind loading. Australian activities in reconstruction are discussed and it is concluded that what happened at Darwin provides a strong argument for the reassessment of residential construction practices in the United States.

Walls, F. L., DeMarchi, A., **RF spectrum of a signal after frequency multiplication; measurement and comparison with a simple calculation,** *IEEE Trans. Instrum. Meas.* **IM-24,** 210-217 (Sept. 1975).

Key words: frequency multiplication; linewidth; multiplier chain; precision oscillator; rf spectrum; spectral density of phase fluctuations; spectral purity.

A novel experimental technique is introduced and used to measure the effect of frequency multiplication on the RF spectrum of an oscillator. This technique makes it possible to produce the RF spectrum at X band—where measurements are relatively straightforward—that would have been produced by frequency multiplication of the 5-MHz source to any frequency from 9.2 GHz to 100 THz (10^{14} Hz). A simplified theory is developed and shown to reproduce the experimental results for the relative power in the carrier and noise pedestal, and the shape and the width of the carrier and noise pedestal, to within the measurement uncertainty of 2 or 3 dB, from 5 MHz to 10 THz. The calculations are easily made using analytical techniques from the measurement of the spectral density of phase fluctuations of the source, the effective input spectrum density and the bandwidth of the multiplier chain, and the frequency multiplication factor. It is shown that present 5-MHz-crystal-controlled oscillators are useful as a precision source to ~ 500 GHz. Suggestions for extending their range to ~ 100 THz are made.

Walls, F. L., Wainwright, A. E., **Measurement of the short-term stability of quartz crystal resonators and the implications for crystal oscillator design and applications,** *IEEE Trans. Instrum. Meas.* **IM-24,** 15-20 (Mar. 1975).

Key words: crystal controlled oscillator; fast linewidth; quartz crystal resonators; short-term stability; spectral density of frequency fluctuations; time domain stability.

A new technique is presented which makes it possible to measure the inherent short-term stability of quartz crystal resonators in a passive circuit. Comparisons with stability measurements made on crystal controlled oscillators indicate that noise in the electronics of the oscillators very seriously degrades the inherent stability of the quartz resonators for times less than 1 s. A simple model appears to describe the noise mechanism in crystal controlled oscillators and points the way to design changes which should improve their short-term stability by two orders of magnitude. Calculations are outlined which show that with this improved short-term stability it should be feasible to multiply a crystal controlled source to 1 THz and obtain a linewidth of less than 1 Hz. In many cases, this improved short-term stability should also permit a factor of 100 reduction in the length of time necessary to achieve a given level of accuracy in frequency measurements.

Walls, F. L., Wainwright, A. E., **Measurements of the short-term stability of quartz crystal resonators—a window on future developments in crystal oscillators,** *Proc. 6th Annual Precise Time and Time Interval (PTTI) Planning Meeting, Washington, D.C., Dec. 3-5, 1974,* pp. 143-153 (1974).

Key words: crystal controlled oscillator; fast linewidth; quartz crystal resonators; short-term stability; spectral density of frequency fluctuations; time domain stability.

Recent measurements of the inherent short-term stability of quartz crystal resonators will be presented. These measurements show that quartz resonators are much more stable for times less than 1 s than the best available commercial quartz oscillators. A simple model appears to explain the noise mechanism in crystal controlled oscillators and points the way to design changes which should permit more than 2 orders of magnitude improvement in their short-term stability. Stabilities of order 1 part in 10^{12} at. 0.001 s appear obtainable. The achievement of short-term stabilities of this level would in many cases greatly reduce the time necessary to achieve a given level of accuracy in frequency measurements. Calculations show that a reference signal at 1 THz, derived from frequency multiplying a 5 MHz source with the above measured crystal stability, should have an instantaneous or fast linewidth of order 1 Hz. These calculations explicitly include the noise contribution of our present multiplier chains and will be briefly outlined.

Wang, F. W., DiMarzio, E. A., **The dynamics of block-copolymer molecules in solution. The free-draining limit,** *Macromolecules* **8,** No. 3, 356-360 (May-June 1975).

Key words: bead-spring model; block copolymers; concentrated solutions; dynamics; Rouse theory; solution properties; viscoelasticity.

A theory for the viscoelasticity of block-copolymer molecule solutions in the free-draining limit has been developed by modifying the bead-spring model theory of Rouse to take into account the existence of dissimilar segments in block copolymers. The eigenvalue problem encountered in the theory has been solved numerically by matrix computations. Furthermore, for the case of a diblock copolymer, a simple form of the secular equation which is useful for extracting the eigenvalues has been obtained. The applications of the theory have been illustrated with calculations for the viscoelastic properties of poly(styrene-*b*-*cis*-1,4-isoprene) solutions. It is found that the calculated properties for the diblock copolymer are nearly the same as those for the Rouse theory while the calculated properties for the symmetric triblock copolymers deviate from those of the Rouse theory.

Zimmerman, J. E., **Phase slip, dissipation, Bernoulli effect, parametric capacitance, and other curious features of the Josephson effect,** *IEEE Trans. Magn.* **MAG-11,** No. 2, 852-855 (Mar. 1975).

Key words: Josephson effect; phase slip; weak superconductivity.

The details of the Josephson effect in thin metal bridges are difficult to derive quantitatively, and many papers have been written on the subject attempting to describe quantitatively such qualitative features as irreversible phase slip, instantaneous 2π phase slip, variation of order parameter in time and space, Bernoulli effect, and others. It does not seem to be generally recognized that all of these qualitative features are universal attributes of the Josephson effect and occur also in tunnel junctions. In addition, when a steady voltage is impressed across a junction, a term in the electric field is set up (in addition to the Bernoulli field) which has a rather complex temporal and spatial variation.

U. S. GOVERNMENT PRINTING OFFICE : 1976 O - 201-606

NBS TECHNICAL PUBLICATIONS

PERIODICALS

JOURNAL OF RESEARCH reports National Bureau of Standards research and development in physics, mathematics, and chemistry. It is published in two sections, available separately:

- **Physics and Chemistry (Section A)**

Papers of interest primarily to scientists working in these fields. This section covers a broad range of physical and chemical research, with major emphasis on standards of physical measurement, fundamental constants, and properties of matter. Issued six times a year. Annual subscription: Domestic, $17.00; Foreign, $21.25.

- **Mathematical Sciences (Section B)**

Studies and compilations designed mainly for the mathematician and theoretical physicist. Topics in mathematical statistics, theory of experiment design, numerical analysis, theoretical physics and chemistry, logical design and programming of computers and computer systems. Short numerical tables. Issued quarterly. Annual subscription: Domestic, $9.00; Foreign, $11.25.

DIMENSIONS/NBS (formerly Technical News Bulletin)—This monthly magazine is published to inform scientists, engineers, businessmen, industry, teachers, students, and consumers of the latest advances in science and technology, with primary emphasis on the work at NBS. The magazine highlights and reviews such issues as energy research, fire protection, building technology, metric conversion, pollution abatement, health and safety, and consumer product performance. In addition, it reports the results of Bureau programs in measurement standards and techniques, properties of matter and materials, engineering standards and services, instrumentation, and automatic data processing.

Annual subscription: Domestic, $9.45; Foreign, $11.85.

NONPERIODICALS

Monographs—Major contributions to the technical literature on various subjects related to the Bureau's scientific and technical activities.

Handbooks—Recommended codes of engineering and industrial practice (including safety codes) developed in cooperation with interested industries, professional organizations, and regulatory bodies.

Special Publications—Include proceedings of conferences sponsored by NBS, NBS annual reports, and other special publications appropriate to this grouping such as wall charts, pocket cards, and bibliographies.

Applied Mathematics Series—Mathematical tables, manuals, and studies of special interest to physicists, engineers, chemists, biologists, mathematicians, computer programmers, and others engaged in scientific and technical work.

National Standard Reference Data Series—Provides quantitative data on the physical and chemical properties of materials, compiled from the world's literature and critically evaluated. Developed under a world-wide program coordinated by NBS. Program under authority of National Standard Data Act (Public Law 90-396).

NOTE: At present the principal publication outlet for these data is the Journal of Physical and Chemical Reference Data (JPCRD) published quarterly for NBS by the American Chemical Society (ACS) and the American Institute of Physics (AIP). Subscriptions, reprints, and supplements available from ACS, 1155 Sixteenth St. N. W., Wash. D. C. 20056.

Building Science Series—Disseminates technical information developed at the Bureau on building materials, components, systems, and whole structures. The series presents research results, test methods, and performance criteria related to the structural and environmental functions and the durability and safety characteristics of building elements and systems.

Technical Notes—Studies or reports which are complete in themselves but restrictive in their treatment of a subject. Analogous to monographs but not so comprehensive in scope or definitive in treatment of the subject area. Often serve as a vehicle for final reports of work performed at NBS under the sponsorship of other government agencies.

Voluntary Product Standards—Developed under procedures published by the Department of Commerce in Part 10, Title 15, of the Code of Federal Regulations. The purpose of the standards is to establish nationally recognized requirements for products, and to provide all concerned interests with a basis for common understanding of the characteristics of the products. NBS administers this program as a supplement to the activities of the private sector standardizing organizations.

Federal Information Processing Standards Publications (FIPS PUBS)—Publications in this series collectively constitute the Federal Information Processing Standards Register. Register serves as the official source of information in the Federal Government regarding standards issued by NBS pursuant to the Federal Property and Administrative Services Act of 1949 as amended, Public Law 89-306 (79 Stat. 1127), and as implemented by Executive Order 11717 (38 FR 12315, dated May 11, 1973) and Part 6 of Title 15 CFR (Code of Federal Regulations).

Consumer Information Series—Practical information, based on NBS research and experience, covering areas of interest to the consumer. Easily understandable language and illustrations provide useful background knowledge for shopping in today's technological marketplace.

NBS Interagency Reports (NBSIR)—A special series of interim or final reports on work performed by NBS for outside sponsors (both government and non-government). In general, initial distribution is handled by the sponsor; public distribution is by the National Technical Information Service (Springfield, Va. 22161) in paper copy or microfiche form.

Order NBS publications (except NBSIR's and Bibliographic Subscription Services) from: Superintendent of Documents, Government Printing Office, Washington, D.C. 20402.

BIBLIOGRAPHIC SUBSCRIPTION SERVICES

The following current-awareness and literature-survey bibliographies are issued periodically by the Bureau:

Cryogenic Data Center Current Awareness Service

A literature survey issued biweekly. Annual subscription: Domestic, $20.00; foreign, $25.00.

Liquefied Natural Gas. A literature survey issued quarterly. Annual subscription: $20.00.

Superconducting Devices and Materials. A literature survey issued quarterly. Annual subscription: $20.00. Send subscription orders and remittances for the preceding bibliographic services to National Bureau of Standards, Cryogenic Data Center (275.02) Boulder, Colorado 80302.

Electromagnetic Metrology Current Awareness Service Issued monthly. Annual subscription: $24.00. Send subscription order and remittance to Electromagnetics Division, National Bureau of Standards, Boulder, Colo. 80302.

U.S. DEPARTMENT OF COMMERCE
National Bureau of Standards
Washington, D.C. 20234

OFFICIAL BUSINESS
Penalty for Private Use, $300

POSTAGE AND FEES PAID
U.S. DEPARTMENT OF COMMERCE
COM–215

FOURTH CLASS RATE
BOOK

JOURNAL OF RESEARCH of the
A. Physics and Chemistry

o. 2 Mar.-Apr. 1976

Contents

Page

Extinction coefficients of NO_2 and N_2O_4. Arnold M. Bass, Albert E. Ledford, Jr., and Allan H. Laufer. 143

A study of the chemiluminescence of the $Pb + O_3$ reactions. M. J. Kurylo, W. Braun, S. Abramowitz, and M. Krauss. 167

Structure- and solvent-property relationships for the electronic energies of charge-transfer complexes between certain benzene derivatives. Harold Argentar. 173

Bidirectional reflectometry. Part I. A high resolution laser bidirectional reflectometer with results on several optical coatings. Jack J. Hsia and Joseph C. Richmond. 189

Bidirectional reflectometry. Part II. Bibliography on scattering by reflection from surfaces. Joseph C. Richmond and Jack J. Hsia. 207

Energy levels, classified lines, and Zeeman effect of neutral thorium. Romuald Zalubus. 221

Publications of the National Bureau of Standards. 359

Library of Congress Catalog Card Number: 62–37059

For sale by the Superintendent of Documents, U.S. Government Printing Office, Washington, D.C. 20402. (Order by SD Catalog No. C 13.22/sec.A:80/2). Single copy price varies. Subscription price: $17.00 a year; $4.25 additional for foreign mailing.

UNITED STATES GOVERNMENT PRINTING OFFICE, WASHINGTON : 1976